Fisheries and Oceans Canada | Pêches et Océans Canada
Ecosystems and Oceans Science | Sciences des écosystèmes et des océans

Canadian Science Advisory Secretariat (CSAS)

Research Document 2023/070

Pacific Region

Canary Rockfish (*Sebastes pinniger*) stock assessment for British Columbia in 2022

Paul J. Starr[1] and Rowan Haigh[2]

[1]Canadian Groundfish Research and Conservation Society
1406 Rose Ann Drive
Nanaimo, BC V9T 4K8

[2]Fisheries and Oceans Canada
Pacific Biological Station
3190 Hammond Bay Road
Nanaimo, BC V9T 6N7

November 2023

Canada

Foreword

This series documents the scientific basis for the evaluation of aquatic resources and ecosystems in Canada. As such, it addresses the issues of the day in the time frames required and the documents it contains are not intended as definitive statements on the subjects addressed but rather as progress reports on ongoing investigations.

Published by:

Fisheries and Oceans Canada
Canadian Science Advisory Secretariat
200 Kent Street
Ottawa ON K1A 0E6

http://www.dfo-mpo.gc.ca/csas-sccs/
csas-sccs@dfo-mpo.gc.ca

ISSN 1919-5044
ISBN 978-0-660-67546-6 Cat. No. Fs70-5/2023-070E-PDF

Correct citation for this publication:

Starr, P.J. and Haigh, R. 2023. Canary Rockfish (*Sebastes pinniger*) Stock Assessment for British Columbia in 2022. DFO Can. Sci. Advis. Sec. Res. Doc. 2023/070. vi + 293 p.

Aussi disponible en français :

*Starr, P.J. and Haigh, R. 2022. Évaluation du stock de sébaste canari (*Sebastes pinniger*) de la Colombie-Britannique en 2022. Secr. can. des avis sci. du MPO. Doc. de rech. 2023/070. vii + 321 p.*

TABLE OF CONTENTS

LIST OF MAIN TABLES

LIST OF MAIN FIGURES

ABSTRACT

Canary Rockfish (*Sebastes pinniger*, CAR) ranges from the Gulf of Alaska southward to northern Baja California. In British Columbia (BC), the apparent area of highest concentration occurs on the west coast of Vancouver Island and at the heads of the three gullies in Queen Charlotte Sound. This species occurs along the west coast of Graham Island and in the western sections of Dixon Entrance, but the apparent abundance is lower.

In 2007, the Committee on the Status of Endangered Wildlife in Canada (COSEWIC) assessed the coastal population of CAR in British Columbia as 'Threatened', based on an analysis of survey indices and the threat from commercial fishing. As a result, the species was considered for legal listing under the *Species at Risk Act* (SARA). A 2007 stock assessment (also acting as a recovery potential assessment) by Stanley et al. (2009) estimated that CAR was in the 'Cautious Zone' in the DFO Sustainable Fisheries Framework (DFO 2009a) but an update to that assessment conducted in 2009 concluded that CAR was in the 'Healthy Zone' when using a credible steepness value. In 2011, a decision was made not to list Canary Rockfish under Schedule 1 of the SARA. In 2019, Bill-C-68 was enacted to amend the *Fisheries Act* with the Fish Stocks provisions, prompting a national review of the approximately 180 stocks using Sustainability Surveys with the aim to include the majority of those stocks in regulation over the next five years. Canary Rockfish is one of 18 groundfish stocks in the Pacific Region being considered for inclusion. The purpose of this CAR stock assessment is to evaluate the current stock status and provide advice suitable for input to a sustainable fisheries management plan.

This stock assessment evaluated a BC coastwide population harvested by two fisheries: a combined bottom and midwater trawl fishery accounting for over 95% of the catch and an 'other' fishery which combined a range of capture methods but was mostly longline. Midwater trawl catches of CAR were combined with bottom trawl for the purposes of this stock assessment. Analyses of biology and distribution did not support separate regional stocks for CAR. A single coastwide stock was also assumed by Stanley et al. (2009) and the subsequent update.

The assessment used an annual catch-at-age model tuned to six fishery-independent trawl survey series, a bottom trawl catch per unit effort (CPUE) series, annual estimates of commercial catch since 1935, and age composition data from survey series (23 years of data from three surveys) and the commercial fishery (37 years of data). The model started from an assumed equilibrium state in 1935, the survey data covered the period 1967 to 2021 (although not all years were represented) and the CPUE series provided an annual index from 1996 to 2021.

A two-sex model, which estimated M for each sex and the stock-recruitment steepness parameter, was implemented in a Bayesian framework, using the Markov Chain Monte Carlo (MCMC) 'No U-Turn Sampling' (NUTS) procedure. In addition to natural mortality and steepness, the parameters estimated by this model included average recruitment over the period 1950–2012, and selectivity for the three surveys with age frequency (AF) data and the commercial trawl fleet. The survey and CPUE scaling coefficients (q) were determined analytically. Fourteen sensitivity analyses evaluated with MCMC were conducted relative to the base run to test the effect of alternative model assumptions. A further three runs were made with an environment Pacific decadal oscillation (PDO) index series to evaluate the effect of this series on the estimated recruitment trajectory. These models were also evaluated with MCMC.

The base run estimated the CAR spawning population biomass at the end of 2022 (median with 0.05 and 0.95 quantiles) to be 0.78 (0.57, 1.0) relative to B_0 and to be 3.0 (1.9, 4.9) relative to B_{MSY}. This latter result suggested that the 2023 CAR spawning population lay well in the Healthy

zone (with a probability >0.99). Projections predicted that the stock will remain in the Healthy zone up to the end of 2032 at all evaluated catch levels up to 2,000 t/y.

Older female CAR were absent from the AF data (females older than age 40 were rare) while the male CAR AF data extended to above age 60. The previous CAR stock assessment assumed a fixed M = 0.06 for all males and for females up to age 13; females age 14 and older had M = 0.12. This stock assessment approached this problem in three ways: 1) estimating a separate M for males and females to get the best fit to the AF data; 2) estimating separate M values for males and females up to age 13 and then estimating new M values for both sexes from age 14 and higher; 3) while estimating single M values for each age, allowing the female selectivity to the commercial fishery and for five of the six surveys to decline with older ages, creating a cryptic population of female spawners. This assessment found that all three models could fit the data credibly, with the first option being the most parsimonious. This run was selected as the base run. The other two options were more optimistic relative to B_0 and B_{MSY} than was the base run.

The median estimates by the 14 sensitivity runs for B_{2023}/B_0 ranged from 0.62 to 0.97 and for B_{2023}/B_{MSY} ranged from 2.40 to 3.22, indicating that all 14 sensitivity runs lay well in the Healthy zone. These analyses included, higher and lower pre-1996 catch histories, higher and lower recruitment standard deviation (σ_R) assumptions, adding the two hard bottom long line (HBLL) survey series, dropping the CPUE series, substituting an alternative CPUE series, omitting ageing error, adding AF data from the Hecate Strait (HS) and west coast Haida Gwaii (WCHG) synoptic surveys, and using two alternative ageing error functions in addition to the three hypotheses for female natural mortality described above.

Incorporating the environmental PDO index series into the stock assessment resulted in an unsatisfactory conclusion: the degree to which the index series was able to influence the recruitment pattern was dependent on the weight given to the index series. Choosing the weight was arbitrary and higher weights resulted in a deterioration of the fit to the fishery data. This procedure is effectively a correlation analysis because there is no functional link between the index series with the population dynamics.

1. INTRODUCTION

The Committee on the Status of Endangered Wildlife in Canada (COSEWIC) assessed the coastal population of Canary Rockfish (CAR, *Sebastes pinniger*) in British Columbia (BC) as 'Threatened' in 2007 (COSEWIC 2007), based on a review of the available data for this species (Stanley et al. 2005). The primary evidence cited for this evaluation was the combined west coast Vancouver Island shrimp survey and the US National Marine Fisheries Service (NMFS) Triennial survey:

> "*The common slope (combined series) decline is considered to best represent the trend in population abundance. This gives a total decline of 86% over 30 years or 1.0-1.5 generations. Because information on numbers of mature individuals is not available over the entire time period for both surveys, total biomass is used here as a proxy for numbers of mature individuals. Given the apparent loss of older individuals over the period covered (Figure 6), the decline in biomass of mature individuals would probably be steeper than that observed for all individuals.*"
> (pp. 55-56, COSEWIC 2007)

Stanley et al. (2009) assessed the coastwide CAR population using a Bayesian age-structured model based on the Coleraine platform (called Awatea). The 2007 stock assessment assumed a fixed value for M=0.06 for males and females up to age 14, when the female M was increased to 0.12. Two fixed values for steepness[1] h were assumed (0.55, 0.7). This stock assessment concluded that the population was in the 'Cautious zone' (as defined by DFO 2009a: median B_{2008}/B_{MSY} ranged from 0.49-0.73). It also predicted that existing catches (at 750 t/year) would not jeopardise stock status if continued for one or two years while longer term predictions suggested catch reductions would be required. This stock assessment was updated in 2009 (DFO 2010) with two more years of catch data and three additional trawl survey observations. This update included an additional model run (18-u) which estimated h using a prior based on a review of rockfish steepness parameter estimates by Forrest et al. (2010). This updated assessment concluded that CAR stock status was in the Healthy zone for the models with the higher h (run 11-u assumed h = 0.7 and run 18-u estimated mean h = 0.79) while the model with lower fixed steepness (17-u) remained in the Cautious zone. However, catch forecasts concluded that the stock would remain in the Healthy zone up to 2015 at catch levels up to 1200 t/year for the two model runs with higher estimates of h, which were considered more plausible than the model run which used the lower fixed value of 0.55.

In 2011, a decision was made not to list Canary Rockfish under Schedule 1 of the SARA. While DFO will continue to manage this species under the *Fisheries Act*, actions to address conservation concerns were outlined in the order not to list (SI/2011-56, July 6, 2011). In 2019, Bill-C-68 was enacted to amend the *Fisheries Act* with the Fish Stocks provisions, prompting a national review of the approximately 180 stocks using Sustainability Surveys with the aim to include the majority of those stocks in regulation over the next five years. Canary Rockfish are one of 18 groundfish stocks in the Pacific Region being considered for inclusion.

Based on the distribution of catches and CPUE over the period 1996–2021, the bulk of the BC population of CAR was centred in the upper half of the west coast of Vancouver Island, followed by the southern half of the WCVI. Catches of CAR in the three gullies (Goose, Mitchell and Moresby) of Queen Charlotte Sound were also high. There were a few density 'hotspots' off Langara Island (NW corner of Graham Island), but CAR abundance appeared to be lower along the northern BC coast. Analyses showed no strong evidence for stock separation along the BC

[1] See Appendix E: Section E.4.12 for general information on steepness.

coast based on growth and size frequency; therefore, a coastwide population was assessed, as it was in 2007 and 2009.

This stock assessment used the National Oceanic and Atmospheric Administration's (NOAA's) Stock Synthesis 3 (SS3, version 3.30.18, Methot and Wetzel 2013; Methot et al. 2021) software platform, which has been adopted by many United States assessment scientists in the Pacific region. This stock assessment platform has more flexibility in fitting data and provides some useful diagnostics (e.g., retrospective analysis) that were not available in Awatea.

The SS3 statistical catch-at-age software (see Appendix E for equations) was used to model the CAR population. The assessment model included:

- sex-specific parameters;
- abundance indices by year (y):
    - one bottom trawl CPUE series (26y, 1996-2021),
    - four synoptic bottom trawl surveys:
      QCS = Queen Charlotte Sound (11y, spanning 2003 to 2021),
      WCVI = west coast Vancouver Island (9y, spanning 2004 to 2021),
      WCHG = west coast Haida Gwaii (8y, spanning 2006 to 2020),
    - HS = Hecate Strait (9y, spanning 2005 to 2021),
    - two historical bottom trawl surveys:
      NMFS = U.S. National Marine Fisheries Service Triennial (7y, spanning 1980 to 2001),
    - GIG = Goose Island Gully (8y, spanning 1967 to 1994);
- proportions-at-age data (also called age frequencies or 'AF') by year (y), four sets:
    - commercial trawl catch (36y, spanning 1977 to 2017),
    - QCS Synoptic (9y, spanning 2003 to 2021),
    - WCVI Synoptic (8y, spanning 2004 to 2021),
    - NMFS Triennial (6y, spanning 1980 to 2001);
- maximum modelled age of 60 y, with older ages accumulated into the final age class; and
- estimated selectivities for the commercial fishery and for the three sets of survey indices with associated AF data (QCS, WCVI, NMFS).

Process error was added to the CPUE data using the procedure documented in Section E.6.2.1 (Appendix E). The AF weightings were estimable by the model, which offered the Dirichlet-Multinomial distribution to fit the age proportions (Section E.6.2.2).

This stock assessment was conducted at the request of Fisheries and Oceans Canada (DFO) Fisheries Management Branch made to the DFO Science Branch for advice regarding the status of CAR relative to reference points that were consistent with the DFO's *Fishery Decision-Making Framework Incorporating the Precautionary Approach* (DFO 2009), including the implications of various harvest strategies on expected stock status. In the absence of updated science advice, there was uncertainty about the risks posed to the BC CAR stock at current levels of catch. This advice was reviewed at a Canadian Science Advisory Secretariat (CSAS) Regional Peer Review (RPR) meeting that considered the scientific capability of the assessment to inform fisheries management decisions when establishing catch levels for the species. This work also informed and supplemented decisions external to DFO, specifically COSEWIC.

1.1. ASSESSMENT BOUNDARIES

This assessment included Pacific Marine Fisheries Commission (PMFC[2]) major areas (3CD and 5ABCDE) along the BC coast (Figure 1). The available biological data were examined for evidence of stock separation (see Section D.3), comparing data aggregated at the level of north coast (PMFC areas 5D and 5C), central coast (PMFC areas 5A, 5B and 5C), and west coast Vancouver Island (PMFC area 3C and 3D). While some differences (growth, size, and composition taken by gear type) among areas were found, the differences were generally small and not always consistent across years, sexes and regions. Furthermore, CAR catch data were split unevenly from these three areas (mean 1996–2021 total catch percentages 3CD=68%; 5ABC=29%; 5DE=3%). Consequently, the authors elected to make the same single-stock assumption that had been made by Stanley et al. (2009) and DFO (2010).

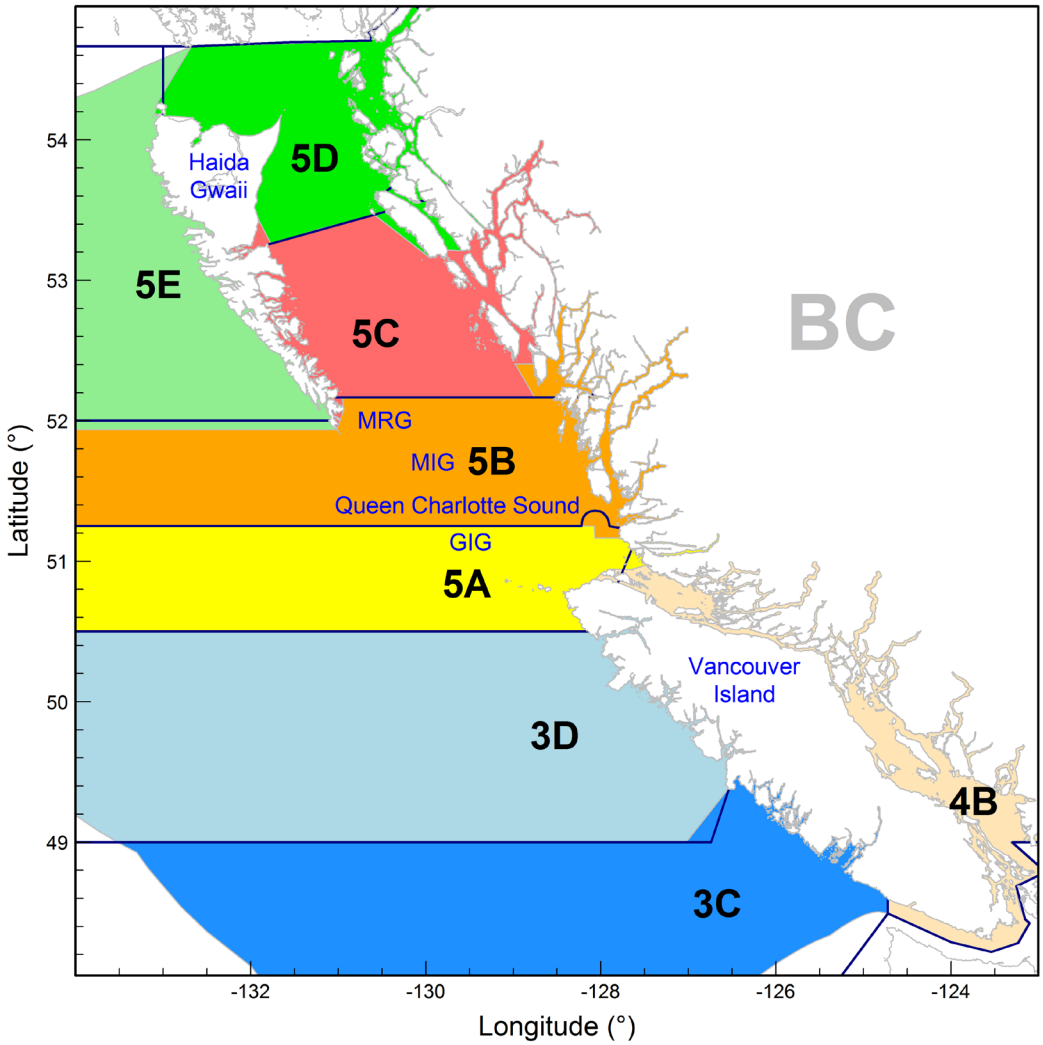

Figure 1. Pacific Marine Fisheries Commission (PMFC) major areas (outlined in dark blue) compared with Groundfish Management Unit areas for CAR (shaded). For reference, the map indicates Moresby Gully (MRG), Mitchell's Gully (MIG), and Goose Island Gully (GIG). This assessment covers one coastwide stock: PMFC 3CD + 5ABCDE.

[2] See Appendix A for historical background on the PMFC.

The PMFC areas are similar but not identical to the management areas used by the Groundfish Management Unit (GMU), which uses combinations of DFO Pacific Fishery Management Areas. This stock assessment did not use GMU management areas for catch reconstruction because catch reporting from these areas was only available since 1996. Although the historical PMFC areas are somewhat different than the GMU areas for CAR, managers can prorate any catch policy using historical catch ratios as outlined in Appendix A, Section A.3.

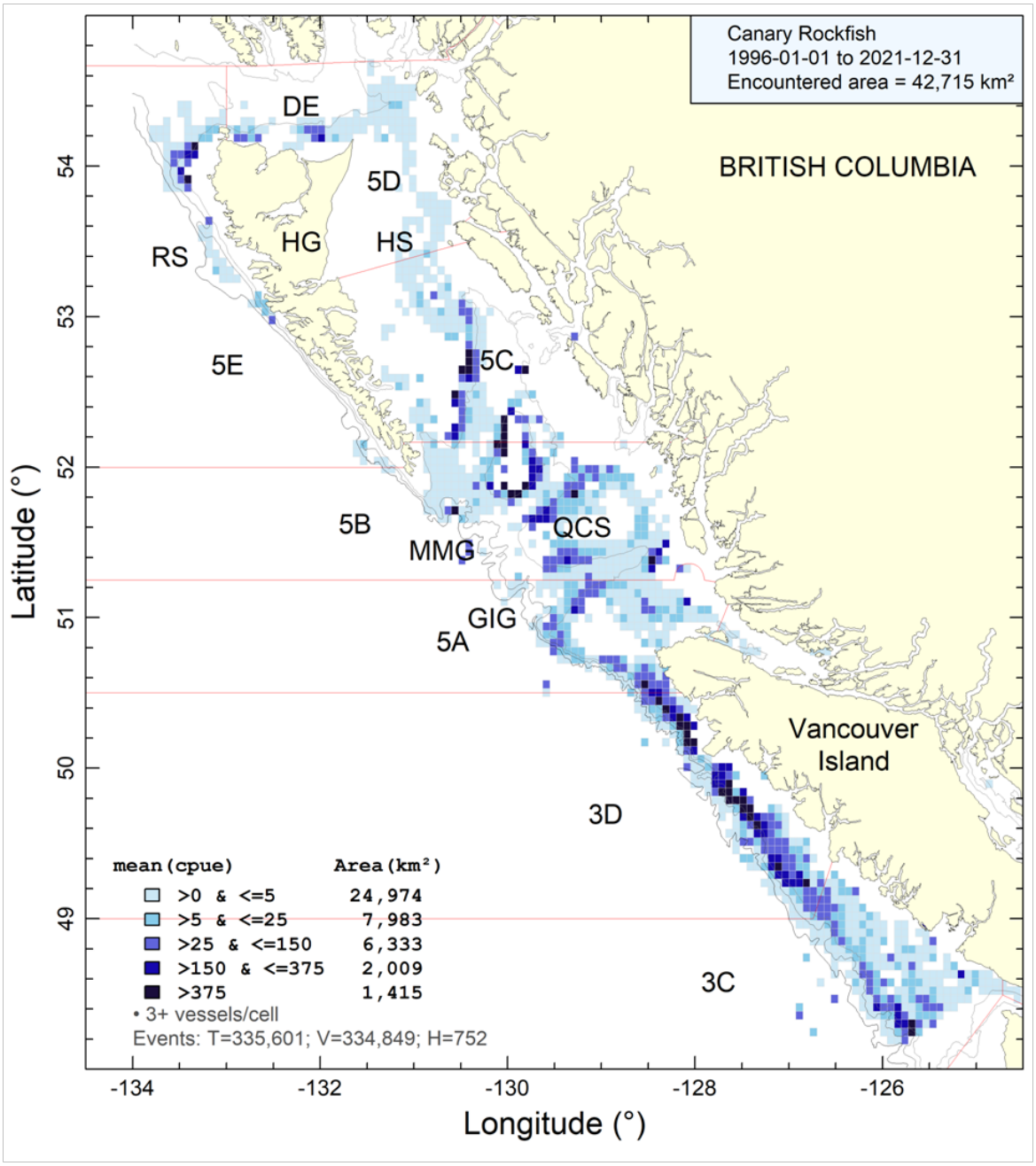

Figure 2. CPUE density of CAR from trawl tows (bottom and midwater) occurring from 1996 to 2021 in grid cells 0.075° longitude by 0.055° latitude (roughly 32 km² each). Isobaths show the 100, 200, 500, and 1000 m depth contours. Cells with <3 fishing vessels are not displayed. DE=Dixon Entrance, GIG=Goose Island Gully, HG=Haida Gwaii, HS=Hecate Strait, MMG=Mitchell's and Moresby Gullies, QCS=Queen Charlottes Sound, RS=Rennell Sound.

1.2. RANGE AND DISTRIBUTION

Canary Rockfish ranges from the Gulf of Alaska southward to northern Baja California, typically at depths between 100 and 230 m (Love et al. 2002). In BC, the apparent area of highest concentration occurred on the west coast Vancouver Island, particularly in the northern part of the west coast (PMFC areas 3D and 3C in Figure 2), but catches were also relatively high in Queen Charlotte Sound (PMFC areas 5A and 5B in Figure 2). This species also occurred at the top end of Graham Island, but the bottom topography in this area precludes much trawling. This species was encountered by the BC bottom trawl fleet over an estimated 42,715 km^2 (Figure 2 top right, based on a roughly 32-km^2 grid size and tow start positions in the commercial fishery, see Appendix G for alternative estimates of occupancy and occurrence), and the bulk of the BC population was captured by the trawl fleet between depths of 68 m and 391 m coastwide (see Appendix G, Figures G.3, G.4 and G.5). Maps of catch hotspots by fishing locality indicated the top three localities to be 'Nootka', 'Esperanza East', and 'Quatsino Sound', all located on the northern part of the west coast Vancouver Island (Figure G.9).

2. CATCH DATA

This stock assessment recognised two commercial fisheries, 'trawl' and 'other', with the first including the combined bottom and midwater trawl fleets and the second combining lesser removals by halibut longline, sablefish trap/longline, lingcod and dogfish troll, and ZN hook and line. Recreational and First Nations CAR catches were assumed to be non-existent or negligible. This second CAR fishery, the sum of all other commercial removals, was included in the stock assessment model to acknowledge that this species was taken in small amounts by hook and line gear. Unfortunately, there were no AF data available from this fishery, so the fishery selectivity for the 'other' fishery had to be assumed. Commercial discards, as reported by full-time observer coverage or electronic monitoring in the trawl fleet since early 1996, were very low, averaging less than 1% over the 26-year period with no evidence of a trend in recent years (see bottom of Table A.3 in Appendix A).

The methods used to reconstruct a catch history for this CAR assessment, along with the full catch history, are presented in detail in Appendix A. Information about species caught concurrently with CAR commercial catches is presented in Appendix G. The average annual CAR catch for the trawl fishery over the most recent five years (2017-2021) was 775 metric tonnes (t) coastwide. The equivalent mean catch for the other fishery was 13 tonnes. Total annual reconstructed trawl catches are presented in Figure 3 for both fisheries.

The catch for 2022 was incomplete (at 275 t by mid-May 2022) so industry was asked for advice on the expected 2022 catch. The 2020 or 2021 catches were not used for guidance because they may have been affected by COVID-19 disruptions (e.g., lockdowns, lack of personnel) as well as changes in market demand. Industry responded with an estimate for the 2022 CAR catch of 780 t, which was split into 767 t for the trawl fishery and 13 t for the other fishery. This current-year catch was added to the model to provide managers with advice that starts at the end of 2022.

A comparison of length and age distributions for bottom and midwater trawl data across years and sexes found some differences in the respective distributions (see Appendix D, Section D.3.2). Occasionally the bottom trawl fishery sampled younger fish than were seen in the midwater trawl fishery (Figure D.19), although there was little difference in the corresponding length distributions (Figure D.18). While these differences may have be sufficient to treat midwater trawl as a separate fishery, there were inadequate age data to fully characterise the midwater fishery across years. Also, this fishery accounted for only 13% of the total annual catch of CAR from 1996 to 2021. Consequently, the authors chose to combine the AF data from

midwater trawl gear with the bottom trawl data and to estimate a single selectivity for this combined fishery.

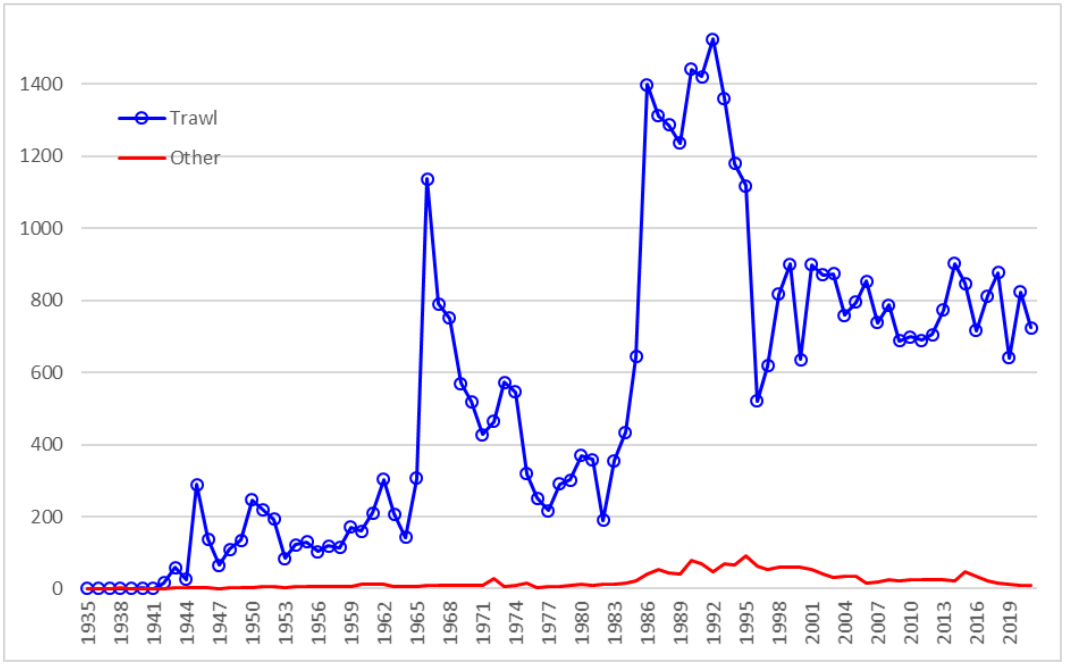

Figure 3. Plots of catch by fishery for CAR from 1935 to 2021 used in the population model. Data values provided in Table A.4.

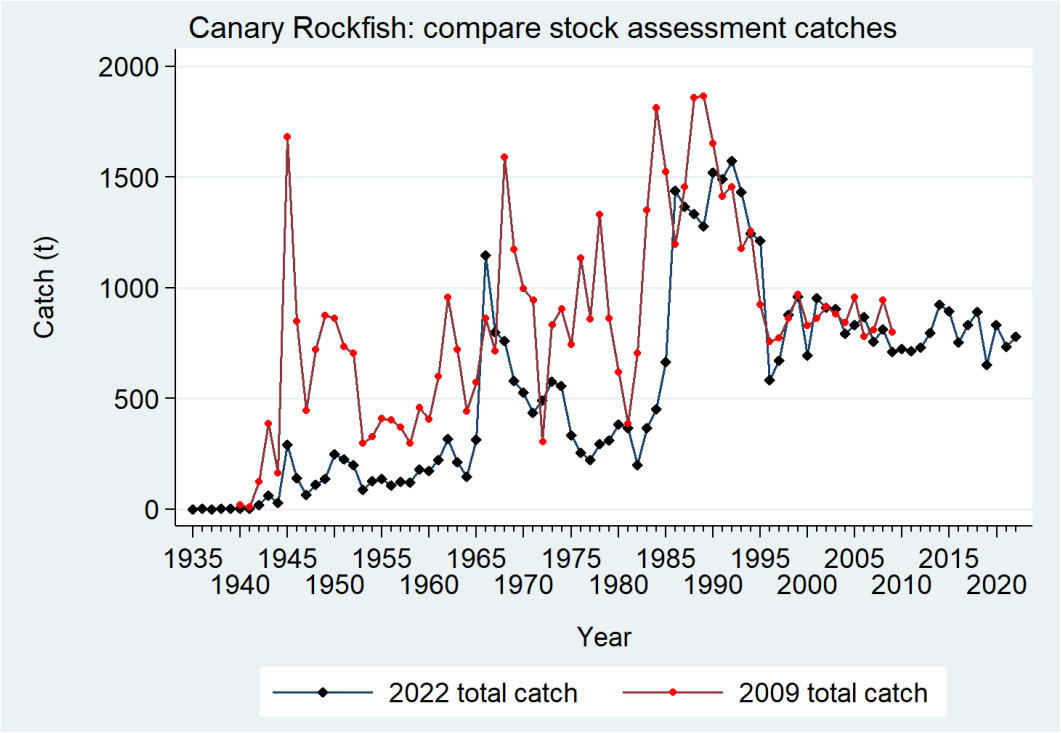

Figure 4. Comparison of the catch trajectory used in the 2009 stock assessment with the reconstructed catch trajectory presented in Figure 3.

The catch trajectory presented in Figure 3 differed substantially from the catch trajectory used in the 2009 CAR stock assessment (Figure 4). The reason for this difference stemmed from the development and evolution of a procedure to reconstruct historical rockfish catches, beginning with the Pacific Ocean Perch (POP) and Yelloweye Rockfish stock assessments in 2010. The procedure used by Stanley et al. (2009) to reconstruct the 2007 and 2009 CAR historical catches was an early version of the more formalised procedure (Haigh and Yamanaka 2011), which has since evolved considerably. Consequently, the differences plotted in Figure 4 reflect cumulative changes in assumptions that are documented in Appendix A as well as making some early decisions which were subsequently dropped[3]. There was also a sensitivity run (S18) which used the 2009 catch reconstruction trajectory.

3. FISHERIES MANAGEMENT

Before 1977, no quotas were in effect for any slope rockfish species. Since then, the groundfish management unit (GMU) at the Department of Fisheries and Oceans (DFO) imposed a combination of species/area quotas, area/time closures, and trip limits on major finfish species. Quotas in the form of total allowable catches (TACs) were first introduced specifically for CAR in 1981 for 3CD, and expanded to also include TACs in 5AB, 5CD and 5E by 1984 (Table A.1, and see Table A.2 for additional management actions taken).

A coastwide CAR stock assessment was conducted in 2007 (Stanley et al. 2009) to address concerns by COSEWIC which listed the species as 'Threatened', with the commercial fishery being the primary threat (COSEWIC 2007). The 2007 stock assessment was updated in 2009 (DFO 2009). The updated stock assessment predicted that the stock would remain in the Healthy zone up to 2015 at catch levels up to 1,200 t/year for the two model runs with higher estimates of steepness (h), which were considered more plausible than the model run which used the lower fixed value of h=0.55.

In 2022, Canary Rockfish had an annual coastwide TAC of 1,100 t, with 965 t (88%) allocated to the bottom trawl fishery and the remaining 135 t (12%) allocated to the ZN hook and line fishery (Appendix A: Table A.1).

4.SURVEY DESCRIPTIONS

Six sets of fishery independent survey indices were used to track changes in the biomass of this population coastwide (Appendix B):

1. **QCS Synoptic** – a random-stratified synoptic (species comprehensive) trawl survey covering all of Queen Charlotte Sound (QCS) and targeting a wide range of finfish species. This survey has been repeated 11 times between 2003 to 2021, using three different commercial vessels (Table B.9) but with a consistent design, including the same net.
2. **WCVI Synoptic** – a random-stratified synoptic trawl survey covering the west coast of Vancouver Island (WCVI). This survey was repeated nine times between 2004 to 2021 using the research vessel FV *Ricker* up to 2016, and was conducted in 2018 and 2021 using the commercial vessel *Nordic Pearl* after the retirement of the *Ricker*. The scheduled 2020 WCVI synoptic survey was delayed until 2021 due to concerns caused by the COVID-19 pandemic. This survey employs a consistent design, including the same net, and targets a wide range of finfish species.

[3] See Appendix A for a more complete discussion of these changes.

3. **WCHG Synoptic** – a random-stratified synoptic trawl survey covering the west coast (WC) of Graham Island in Haida Gwaii (HG) and the western part of Dixon Entrance. This survey has been repeated eight[4] times between 2006 to 2020 using four commercial vessels (Table B.15) and a consistent design, including the same net and targeting a wide range of finfish species. In 2020, during the COVID-19 pandemic, this survey was conducted without any DFO personnel on board, but the data from this survey have been included in this stock assessment. The 2014 survey was omitted from the series because less than ½ of the tows were completed. A random stratified WCHG trawl survey that operated in 1997 under a slightly different design was not included in this series because of the low incidence of CAR in this survey.
4. **HS Synoptic** – a random-stratified synoptic trawl survey covering Hecate Strait, beginning where the QCS survey ends (at its northern boundary), and targeting a wide range of finfish species. This survey has been repeated nine times between 2005 to 2021, using a consistent design and including the same net. Four vessels (Table B.18) have conducted this survey, with commercial vessels in 2005, 2017 and 2019. The research vessel FV *Ricker* was used five times from 2007 to 2015 until it was retired. The replacement research vessel FV *Sir John Franklin* conducted this survey in 2021.
5. **NMFS Triennial** – this survey has operated seven times in Canadian waters over the period 1980 to 2001 (Table B.7), extending variable distances up the west coast of Vancouver Island but never going further north than 49°42′[5]. The survey used a transect design, repeating the transects at 25-nm intervals with a randomised start position in California. Tow locations were selected randomly along the transect. Initially the survey depth ended at 366 m (200 fathoms) but was extended to 500 m in 1995. Ten vessels were used to conduct this survey in Canadian waters, but the information on vessel names was not available. The stratum boundaries changed between the 1983 and 1989 surveys, but the early surveys have been adjusted to ensure a consistent survey index.
6. **GIG Historical** – a composite series of seven indices extending from 1967 to 1984 in Goose Island Gully (GIG). Most of these surveys were performed by the research vessel *G.B. Reed*, but two commercial vessels (*Eastward Ho* and *Ocean Selector*) were used in 1984 and 1994 respectively. Only tows located in Goose Island Gully (GIG) have been used to ensure continuity across all surveys.

The Hecate Strait (HS) multi-species assemblage bottom trawl survey and the two shrimp trawl surveys (WCVI and QCS) have been omitted from this stock assessment (even though the QCS and WCVI shrimp surveys were included in the 2007 and 2009 stock assessments) because either the presence of CAR in these surveys was sporadic or the coverage, spatial or by depth, was incomplete, rendering these surveys poor candidates to provide reliable abundance series for this species. Rockfish stock assessments, beginning with Yellowtail Rockfish (DFO 2015), have explicitly omitted using the WCVI and QCS shrimp surveys because of the truncated depth coverage, which ends at 160 m for the WCVI shrimp survey and at 231 m for the QCS survey. Both surveys have constrained spatial coverage with the WCVI survey confined to the centre of WCVI and the QCS survey only covering the inshore (head) end of Goose Island Gully.

Two hard-bottom longline (HBLL, outside of PMFC area 4B) surveys have been included in this assessment as a sensitivity run (S11, Section 8.2). These are depth-stratified, random design research longline surveys conducted with chartered commercial fishing vessels, which employ standardised longline gear and fishing methods and alternate annually between the northern and

[4] The 2014 West Coast Haida Gwaii survey did not complete and is not usable.

[5] approximately the latitude of the southern tip of Nootka Island

southern portions of BC. These surveys are meant to be complementary to the synoptic trawl surveys by covering habitat that is not available to trawl gear (Doherty et al. 2019) and have been conducted eight times in the North (2006–2021) and seven times in the South (2007–2020) (Table B.21). The reasons these surveys were only included as a sensitivity run (despite relatively high proportions of CAR encountered) were: (i) the survey area covered lay outside of the main concentrations of CAR abundance indicated by trawl records of catch (Figure A.1), and (ii) the age distributions from these surveys were younger than those from the QCS and WCVI synoptic surveys (compare Figure D.14 with Figure D.11).

The relative biomass survey indices were used as data in the models along with the associated relative error for each index value. No process error was added to the survey relative errors because the observation errors were already high (Appendix B).

5. COMMERCIAL CPUE

Commercial catch per unit effort (CPUE) data were used to generate indices of abundance as input to the model fitting procedure (see Appendix C). This series of annual indices, extending from 1996 to 2021, provided a more informative abundance signal to the model than did the six survey series, probably due to the higher relative error within the survey series, the shorter period covered by the surveys, and the greater number of annual index values in the CPUE series. There was concern that using CPUE from a commercial fishery might not reflect abundance well due to contamination by fisher behaviour responses to economic considerations. This concern was addressed in a number of ways. First, the CPUE series was compared with each survey series (see Section C.6 in Appendix C). Although this comparison is equivocal for all surveys because of the large relative errors associated with the survey estimates for this species, none of the comparisons contradicted each other. Second, a sensitivity analysis (S13) that omitted the CPUE series entirely was run, which is reported below in Section 8.2.

The CPUE abundance index series was standardised for changes to vessel configuration, catch timing (seasonality), and location of catch (latitude, DFO locality, and depth) to remove potential biases in CPUE that may result from changes in fishing practices and other non-abundance effects. This procedure was performed in two steps, with one model fitted to the positive catches, assuming a lognormal distribution, and another model fitted to the presence/absence of CAR, assuming a binomial distribution. These two models were then combined using a multiplicative “delta-lognormal” model (Eq. C.4). In these models, abundance was represented as a ‘year effect’ and the explanatory variables were selected sequentially by a General Linear Model, which accounted for variation in the available data. Other factors that might affect the behaviour of fishers, particularly economic factors, do not enter these models due to a lack of applicable data, thus resulting in indices that may not entirely reflect changes in the underlying stock abundance. Appendix C provides details on the CPUE analyses and Appendix F provides one sensitivity to the removing of the CPUE index series and another that uses a CPUE series derived using a Tweedie distribution (Jorgensen 1987; S12, Section 8.2). Process error of 0.178 was added to the observation errors for CPUE derived using the delta-lognormal model (see Appendix E, Section E.6.1 for its derivation).

6. BIOLOGICAL INFORMATION

6.1. BIOLOGICAL SAMPLES

Age proportion samples from 1977 to 2017 were available from commercial trawl (combined bottom and midwater) catches of CAR, with a total of 36 years covered by at least two samples per year. Age frequency (AF) samples were also available from three surveys: QCS (2004-2021

with 9y AF), WCVI (2004-2021 with 8y AF), and the NMFS Triennial (1980-2001 with 6y AF). Additional AF data were available from the WCHG (1997-2018 with 4y AF) and HS (2011-2019 with 5y AF), but initial model fits with these data indicated that these samples showed a lot of inconsistencies with the other AF data. However, these data were included in a sensitivity run (S10, Section 8.2). Only otoliths aged using the 'break and burn' (B&B) method were included in age samples used in this assessment because an earlier surface ageing method was shown to be biased, especially with increasing age (Stanley 1987). However, surface ageing is currently the preferred method for ageing very young rockfish (≤ 3y) by the ageing lab (DFO 2022). Commercial fishery age frequency data were summarised for each quarter year, weighted by the CAR catch weight for the sampled trip. The total quarterly samples were scaled up to the entire year using the quarterly landed commercial catch weights of CAR. See Appendix D (Section D.2.1) for details.

Sampled AFs from bottom and midwater trawl were combined after comparing AF distributions for each gear type by sex and capture year and concluding that the AF series from the two capture methods were variable in this comparison and that there were insufficient data to construct independent midwater trawl AFs (see Section D.3.2). Consequently, the model was run assuming a joint selectivity for these two trawl methods by combining the AFs and the catch data into a single trawl fishery. Three commercial selectivity parameters were estimated in the assessment model using prior means based on the posteriors obtained from the 2007 CAR stock assessment and which assumed a 30% CV on each mean value. There were no ageing data for the other fishery.

Moderate amounts of age frequency data were available from the three survey series used in the model plus two additional surveys (HS and WCHG), which were only used in a sensitivity run. While sample sizes were reasonable, the number of fish aged was marginal (<200 fish by sex per year per survey). The survey AFs were scaled to represent the total survey in a manner similar to that used for the commercial samples: within an area stratum, samples were weighted by the CAR catch density in the sampled tows; stratum samples were then weighted by the stratum areas (section D.2.2). The survey selectivity priors for the three surveys with AF data in the base run were assumed to be the same as the commercial selectivity priors.

6.2. AGEING ERROR

Ageing error is a common issue in most age-structured stock assessments. Figure D.17 (see Section D.2.3 in Appendix D) suggests that CAR ages estimated by the primary readers were reproduced reasonably consistently by secondary readers when performing spot-check analyses, but there were some discrepancies. The base population model for CAR used a smoothed ageing error vector based on the CVs of observed lengths-at-age (Figure D.16). A second ageing error vector, determined from the CVs of otolith ages spot-checked by secondary readers for otoliths previously read by a primary reader, was constructed. This ageing error vector was also smoothed and used in a sensitivity run (S03). A third ageing error vector that assumed a constant 10% error was used in a another sensitivity run (S04). All three ageing error vectors are compared in Figure D.16. Finally, a sensitivity run using no ageing error was performed for comparison (S02).

6.3. GROWTH PARAMETERS

Growth and allometric length-weight parameters were estimated from CAR length and age data using biological samples collected from research/survey trips conducted between 1989 and 2021 (Section D.1.1 in Appendix D). Allometric parameters were similar for females and males: (log α, β) = ♀ (-11.04, 3.01), ♂ (-11.16, 3.04).

Research survey data are preferred over commercial data when estimating allometric and growth parameters because surveys generally capture a wider variety of sizes and ages due to the use of smaller size mesh in the cod ends of the trawl net. Commercial data lack information on smaller fish because the cod ends deliberately exclude small, less marketable fish, while a survey attempts to capture a wide range of sizes. Consequently the growth functions derived from commercial data will be poorly determined at the lower end. There are usually sufficient aged otoliths from the research data alone that there is no need to include commercial data. The stock assessment assumes that CAR has a time invariant set of biological parameters which exist regardless of the gear used to collect the data.

Standard maximum likelihood estimation (MLE) for CAR based on the survey data were used to model growth in this population. Females were larger than males (L_∞: ♀=59.0 cm, ♂=52.7 cm). The estimation of growth models using a Bayesian procedure, with and without ageing error, was not done for this stock assessment because a comparison of these models with the equivalent MLE models in both the Yellowmouth Rockfish (YMR) (Starr and Haigh 2022c) and Bocaccio (BOR) (Starr and Haigh 2022a) stock assessments showed few differences for either sex.

6.4. MATURITY AND FECUNDITY

The proportion mature of CAR were computed from biological samples collected from the commercial fishery and research surveys. Although it is preferable to use research data to estimate biological functions, this was not possible for Canary Rockfish because they spawn in the winter or early spring months, a period not covered by the research surveys (May to September).

Maturity stage was determined macroscopically by either the research technicians on the survey vessels or the commercial fishery observers, partitioning the samples into one of seven maturity stages (Stanley and Kronlund 2000; described in Appendix D, Section D.1.3). Fish assigned to stages 1 or 2 were considered immature while those assigned to stages 3-7 were considered mature. Data representing staged and aged females (using the B&B method) were pooled from research and commercial trips and the observed proportion mature at each age was calculated. All months were used in creating the maturity curve because Canary Rockfish spawn in winter, so winter data were needed to estimate a credible function. A monotonic increasing maturity-at-age vector was constructed by fitting a half-Gaussian function (Equation D.3) to the observed maturity values (Appendix D, Section D.1.3). The ages used in the function fit excluded ages greater than 30 to avoid potentially influential proportions caused by spurious values (due to sparse data). The maturity ogive used in the main model assigned proportions mature to zero for ages 1 to 4, then switched to the fitted monotonic function for ages 5 to 30, all forced to 1.0 (fully mature) from age 19 to age 60 (see Table D.6). This strategy follows previous BC rockfish stock assessments where it was recognised that younger ages are not well sampled, and those that are, tend to be larger and more likely to be mature (e.g., Stanley et al. 2009). Females older than age 10 were estimated to be at least 50% mature.

Fecundity was assumed to be proportional to the female body weight (approximately length cubed); however, researchers have demonstrated that this assumption may have consequences for sustainability. Specifically, if larger and older females produce more eggs of higher quality, the removal of these productive females by fishing will have a disproportionate effect on recruitment (He et al. 2015). Dick et al. (2017) concluded that relative fecundity (eggs per gram body weight) increased with size in *Sebastes*, and estimated the length-fecundity relationship median exponent for POP to be 4.97, which is considerably larger than the cubic length-weight exponents typically used for BC rockfish stock assessments (e.g., Table D.2). Another issue affecting reproductive output is ‘skip spawning’ where some species do not spawn in every year

(Rideout and Tomkiewicz 2011). Conrath (2017) found varying rates of skipped spawning in three deepwater rockfish species. It is not known if CAR exhibit skipped spawning.

6.5. NATURAL MORTALITY

Using the natural mortality estimators of Hoenig (1983) and Gertseva (NOAA, pers. comm. 2018, see Starr and Haigh 2021a), Table D.7 explored the *M* estimate associated with the assumed upper tail of the CAR age distribution (Figure D.9). For ages 40 and above (at 10-y increments), estimates of *M* spanned 0.055 to 0.135. The prior on *M* used in this stock assessment was based on the two lowest values in Table D.8 (0.055 and 0.064), with the prior mean set at 0.06 with an assumed 30% CV.

An important feature of the CAR AF data was the preponderance of older males and the lack of older females. This divergence can be clearly seen in Figure D.9, with the tail of the male age distribution extending well beyond the tail of the female age distribution. The two previous BC CAR stock assessments modelled this divergence by assuming that female natural mortality arbitrarily increased to 0.12 at age 14 (Stanley et al. 2009; DFO 2010). The most recent assessment of CAR in the US assumed a constant *M* [6] for all males. The female *M* was fixed at the same value of *M* as for the males up to age 6. Natural mortality for females for ages 14 and above were estimated, and *M* was interpolated linearly between ages 6 and 14 (Thorson and Wetzel 2016). This stock assessment chose to address this issue in three ways:

1. Base run – estimate a single *M* separately for males and females using the normal prior N(0.06, 0.018)[7].
2. Sensitivity run S01 – estimate a separate *M* for males and females N(0.06, 0.018) up to age 13 and then a second *M* for both sexes from age 14, using the same prior for males but a higher prior for females N(0.12, 0.036), based on prior belief from results in previous CAR surveys. This is a knife-edge assumption. The model allows for breakpoints further apart; however, only two *M* values are estimated. This knife-edge assumption mimics the 2007 and 2009 CAR stock assessments, given the constraints of the SS3 platform.
3. Sensitivity run S09 – estimate *M* separately for males and females using the same prior as well as domed selectivity for females in the trawl fishery and in five of the six survey series, testing the hypothesis that the differential age structure for females is the result of a shift in the selectivity of older aged females.

6.6. STEEPNESS

A Beverton-Holt (BH) stock-recruitment function was used to generate average recruitment estimates in each year based on the biomass of female spawners (Equation E.33). Recruitments were allowed to deviate from this average (Equations E.39 and E.40) in order to improve the fit of the model to the data. The BH function was parameterised using a 'steepness' parameter, *h,* which specified the proportion of the maximum recruitment that was available at 0.2 B_0, where B_0 is the unfished equilibrium spawning biomass (mature females). This parameter was fixed at 0.7 in the 2007 BC CAR stock assessment and for one of the runs in the 2009 updated stock assessment[8]. Another of the 2009 stock assessment runs estimated this parameter, as does this stock assessment. The parameter *h* was estimated in this stock assessment, constrained by a prior developed for west coast rockfish by Forrest et al. (2010) after removing all information for

[6] *M*=0.0521, the median value of a generic prior distribution for *M* in rockfish (Thorson and Wetzel 2016).

[7] In SS3, model priors comprise a distribution, a mean, and a standard deviation about the mean.

[8] The other run using a fixed *h* value set *h*=0.55.

QCS POP (Edwards et al. 2012b). This prior took the form of a beta distribution with equivalent of mean 0.674 and standard deviation 0.168.

7. AGE-STRUCTURED MODEL

A two-sex, age-structured, stochastic model was used to reconstruct the population trajectory of CAR from 1935 to the end of 2022 using NOAA's Stock Synthesis 3 model platform. Ages were tracked from 1 to 60, where 60 acted as an accumulator age category. The population was assumed to be in equilibrium with average recruitment and with no fishing at the beginning of the reconstruction. Female selectivities for the six surveys and the combined bottom and midwater trawl commercial fishery were determined by a flexible selectivity function, parameterised in SS3 using six β parameters (described in Appendix E). For this assessment, only two β parameters were estimated: β_1, equivalent to the μ parameter (age at which selectivity first reaches maximum selectivity) in Awatea, and β_3, equivalent to the log v_L parameter (variance that determines the width of the ascending limb of a double normal curve) in Awatea. The right-hand (descending limb) was assumed to be fixed at the maximum selectivity for the commercial fishery and all surveys to avoid the creation of a cryptic population. Male selectivity was assumed to be the same as the female selectivity except that an offset was estimated relative to the age of maximum selectivity parameter. This parameter (Δ_1) showed very little updating from the initial value of -0.4. The remaining four β parameters ($\beta_{2,4,5,6}$) available in SS3 were only used in a sensitivity run to estimate dome-shaped selectivity for females to test the hypothesis that the lack of older females in the AF data was the result of females becoming less vulnerable to the commercial fishery. The model and its equations are described in Appendix E.

Generally, sample sizes (for composition data) or process error (for abundance data) are used to calculate the variance for a data source and are useful to indicate the relative differences in uncertainty across years within each data source. However, measures of uncertainty may not represent the relative difference in the variance between different data sources (usually abundance vs. composition). Therefore, the relative weights for each data source in an integrated stock assessment should be adjusted to reflect the information content of each, while retaining the relative differences within each data set across years. This can be accomplished by applying adjustment factors to abundance and composition data to their respective data source. This can be an iterative process if one or both data sources are potentially influential.

In a departure from previous stock assessments, reweighting composition data was not employed in this stock assessment using either the Francis (2011) procedure or the McAllister-Ianelli (1997) harmonic mean. Instead, the Dirichlet-Multinomial distribution, as implemented in SS3, was used as a model-based method for estimating effective sample size (Thorson et al. 2017). This distribution incorporates an additional parameter per 'fleet', log (DM θ_g), where g=fleet number, which governs the ratio of nominal ('input') and effective ('output') sample size for each composition data set, accomplishing the weighting as part of the estimation procedure.

The modelling procedure used in this assessment first applied process error to the CPUE series and then determined the best fit, or mode of the posterior distribution (MPD), to the data by minimising the negative log likelihood. Each MPD run was used as the respective starting point for the Markov Chain Monte Carlo (MCMC) simulations. In keeping with the Yellowmouth Rockfish stock assessment (Starr and Haigh 2022c), each run was evaluated using a "No U-Turn Sampling" (NUTS) algorithm (Monnahan and Kristensen 2018; Monnahan et al. 2019) which reduced the evaluation time from days to hours and which employed more efficient search algorithms. For the base run in this assessment, 8,000 NUTS iterations were evaluated by parsing the workload into eight parallel chains (using the R package '`snowfall`', Knaus 2015) of 1,000 iterations each, discarding the first 750 iterations and saving the last 250 samples per

chain. The parallel chains were then merged for a total of 2,000 samples per run for use in the MCMC analyses.

The base run model made the following assumptions:

- assumed two sexes (female, male);
- estimated a single invariant mortality M per sex to represent all ages;
- set accumulator age A = 60 (pooled age for ages $a \geq 60$);
- used six survey abundance index series (QCS Synoptic, WCVI Synoptic, NMFS Triennial, HS Synoptic, WCHG Synoptic, GIG Historical), with the first three surveys having age frequency (AF) data;
- used one commercial fishery abundance index series (bottom trawl CPUE index);
- used a model-derived analytical solution for the abundance series scaling parameters (q_g), where q values are not estimated as active parameters (Methot et al. 2021);
- assumed two fisheries (trawl and other), the first a combined bottom and midwater trawl fishery; the second comprising all remaining non-trawl fisheries, including halibut longline, ZN hook and line, sablefish trap, and dogfish/lingcod troll; this second fishery had no associated AF data while the combined commercial trawl fishery had AF samples for 36 of the 41 year period between 1977 to 2017; there were no commercial AF samples for the period 2018–2021;
- used informed selectivity priors based on MPD values from the 2007 CAR stock assessments. Selectivities were estimated for the commercial trawl fishery and the three surveys with AF data; the remaining fishery and three surveys were fixed at the prior means;
- estimated recruitment deviations from 1950 to 2012 (constraint: sum to zero for the period 1950-2012) and allowed post-2012 recruitments to vary given a data signal;
- applied abundance reweighting: added CV process error to the CPUE index CVs, c_p=0.178 (see Appendix E) and added no process error to the survey indices (relative error was already high for these series);
- used the Dirichlet-Multinomial error distribution (as implemented in SS3) to fit AF data instead of applying composition reweighting;
- fixed the standard deviation of recruitment residuals (σ_R) to 0.9; and
- used an ageing error vector based on CVs of observed lengths-at-age.

Fourteen sensitivity analyses were run (with full MCMC simulations) relative to the base stock assessment run (Run24: M & h estimated, A=60, incorporating ageing error [AE] based on CVs of length-at-age) to test the sensitivity of the outputs to alternate model assumptions:

- S01 (Run25) – split M between ages 13 and 14 (label: “split M ages(13,14)”).
- S02 (Run26) – apply no ageing error (label: “AE1 no age error”).
- S03 (Run27) – use smoothed ageing error from age-reader CVs (label: “AE5 age reader CV”).
- S04 (Run28) – use constant-CV ageing error (label: “AE6 CASAL CV=0.1”).
- S05 (Run29) – reduce commercial catch (1965-95) by 30% (label: “reduce catch 30%”).
- S06 (Run30) – increase commercial catch (1965-95) by 50% (label: “increase catch 50%”).

- S07 (Run31) – reduce σ_R to 0.6 (label: “sigmaR=0.6”).
- S08 (Run32) – increase σ_R to 1.2 (label: “sigmaR=1.2”).
- S09 (Run33) – use female dome-shaped selectivity (label: “female dome select”).
- S10 (Run34) – use AF data from HS & WCHG synoptic surveys (label: “use AF HS WCHG”).
- S11 (Run35) – add HBLL North & South surveys (label: “add HBLL surveys”).
- S12 (Run36) – use CPUE fitted by Tweedie distribution (label: “use Tweedie CPUE”).
- S13 (Run37) – remove commercial CPUE series (label: “remove comm CPUE”).
- S14 (Run49) – use Francis mean-age reweighting (label: “use Francis reweight”).

All sensitivity runs were reweighted once in a manner similar to that described above for the base run. The process error added to the commercial CPUE for all sensitivities (except S04 because Tweedie CPUE standard error was already high) was the same as that adopted in the base run. As for the base run, each sensitivity run was evaluated using the NUTS procedure (described above) to generate 2,000 MCMC samples each, but using 4,000 simulations with a 50% burn-in.

A further four sensitivity runs were made to the MPD level only:

- S15 (Run44) widen period (1935-2015) over which to estimate recruitment deviations (label: “Rdevs 1935-2015”).
- S16 (Run45) use geostatistical synoptic survey indices (label: “geostatistical surveys”).
- S17 (Run46) drop NMFS Triennial and GIG survey series (label: “no historical surveys”).
- S18 (Run48) use Stanley et al (2009) catch history (label: “Stanley et al. catch history”).

These runs were made because they represented potential issues or questions regarding this stock assessment, based on concerns that have been brought up in past stock assessment reviews. They were not pursued further than these MPD runs because it was felt that the best-fit results were sufficient to settle the issues raised.

The “Terms of Reference” for this CAR stock assessment included the task to “7. *Explore environmental effects on the stock assessment, with the understanding that their incorporation at this point is exploratory.*” Incorporating environmental effects into this stock assessment turned out to be more difficult than expected, given the complexities of the SS3 platform and the need to get additional advice from the platform designers. There were several possible ways to implement this task in SS3, but the easiest method (estimating an extra parameter that shifts the recruitment regime by using the environmental index series as perfect knowledge [R. Methot, NOAA, pers. comm., 2022]) had no impact on the assessment results other than some minor adjustments to the recruitment deviations. The most effective approach was to treat the environmental series as if it were another “fleet”[9], allowing the model to estimate a “*q*” scalar and to contribute directly to the likelihood function. However, this implementation raised the issue of relative data weighting, with the impact of the series being dependent on the amount of relative weight assigned to the series.

[9] This “fleet” is not relative biomass, but is a series that is directly applied to the recruitment deviation time series.

The PDO series[10] was selected as the environmental index series that had potential to have an impact on CAR abundance and recruitment. This series was explored in a previous POP stock assessment for possible interaction with POP recruitment (see Appendix F in Haigh et al. 2018). This component of the CAR stock assessment was treated independently of the other sensitivity runs, settling on the following three example runs:

- E01 (Run386) use nominal standard errors from the PDO series (label: “PDO cvpro=0”).
- E02 (Run387) apply a fixed 0.30 process error (label: “PDO cvpro=0.30”).
- E03 (Run388) apply process error estimated using the smoothing procedure described in Section E.6.2.1 (label: “PDO cvpro=0.8258”).

These three runs were taken to the MCMC level and the results are described in Section 8.2.3. PDO was only fitted to recruitment deviates between 1950 and 2012 (the “main” recruitment period in the model). Outside of this period SS3 does not include the environmental index in the model calculation.

8. MODEL RESULTS

8.1. BASE RUN – B1 (R24)

Both natural mortality (M) and steepness (h) were estimated without difficulty, there being only weak correlation between these two parameters (Figure F.1). This eliminated the requirement used in some previous stock assessments where multiple runs using fixed M values were needed to build a composite base case that covered a plausible range of values for this parameter. The MPD for female natural mortality (M = 0.093) shifted much higher than the prior mean value (M = 0.06), while the male MPD remained close to the prior mean (M = 0.065). This divergence between the estimates by sex was driven by the difference in the age frequency data by sex and was required to fit the AF data credibly. Steepness was also estimated to be higher (h=0.88) than the prior mean (h=0.76). The selectivity parameter estimates did not move far from their prior means; however, the estimated age at full selectivity (β_{1g} or μ_g) was lower for the surveys than for the commercial fishery, which is consistent with the surveys using smaller mesh codends. The WCVI μ value was estimated to be near 10 while the QCS and Triennial survey estimates for this parameter were 12.4 and 12.3, respectively, compared to μ=13.3 in the commercial fishery, reflecting the presence of younger fish in the survey data. There was little information in the data to move the male shift parameter away from its initial prior mean of Δ_{1g} = -0.4.

Model fits to the survey abundance indices were generally satisfactory (Figure F.2), although various indices were missed entirely (e.g., 1996 CPUE, 2009 QCS, 2006 WCVI, 1980 NMFS, 2011 & 2021 HS, 2016 WCHG). The fit to the commercial CPUE indices was flat from 1996 to 2002 followed by an upward trend from 2003 to 2021.

[10] Appendix F in Haigh et al. (2018) defined the PDO index series as “*The PDO is the first mode of an Empirical Orthogonal Function (EOF) analysis of gridded sea surface temperature in the North Pacific,(Zhang et al. 1997 and reported in Mantua et al. 1997) and is available from the University of Washington. It represents sea surface temperature and sea surface height anomalies in the North Pacific and is connected to the El Niño Southern Oscillation (ENSO, Alexander et al. 2002; Newman et al. 2003). For this study, we computed the mean values of PDO over the winter months (December to March, Figure F.3f). A negative phase of the PDO is associated with unusual cold temperatures in the eastern North Pacific (Mantua et al. 1997) and a weak Aleutian Low (Di Lorenzo et al. 2010, 2013).*”

Fits to the commercial trawl fishery age frequency data were good, with the model tracking year classes consistently across the 41 year time span represented by the commercial AF data (Figure F.3). Standardised residuals rarely exceeded 1 for the various age classes (Figure F.4), although there were many small negative residuals which may indicate that there was a tendency to underestimate the age proportions. Residuals by sample year show that standardised residuals exceeded 1 only in several years (e.g., 2001, 2004, and 2017). Fits to the survey AFs from the three surveys were fair, with some residuals exceeding 2 (Figures F.5–F.10). As with the commercial AF fits, the survey AF fits also tended to show small negative residuals, again indicating that the model tended to underestimate the age proportions.

Mean ages appeared to be well tracked (Figure F.11), suggesting that the DM θ_g parameters were reweighting effectively. The maturity ogive, generated from an externally fitted model (see Appendix D), was situated to the left of the commercial selectivity fits for all ages up to 11, indicating that younger mature fish were not being heavily harvested by the commercial fishery. This is also true of the QCS and Triennial surveys, while the WCVI survey selectivity ogive sits well to the left of the female maturity ogive, indicating that this survey selects all mature and sub-mature CAR.

The likelihood profile analysis indicated that the age frequency data were the primary contributors of information for the female M parameter (Figure F.16), while both the age data and the biomass data precluded low estimates of log R_0 (Figure F.16). There was not a great deal of information in any of the data sets to constrain the upper bound of log R_0 (Figure F.16).

A retrospective analysis was undertaken using the base run as the initial model. The upper panel of Figure F.17 shows the model adjusting its fit to the CPUE index series as more years are added to the series, while the lower panel shows an increase in the level of the biomass trajectory as some year classes with strong recruitment entered the fishery. This retrospective analysis did not reveal any underlying problems in the model, with between-year shifts explained through the introduction of new information into the model.

The base run was used to calculate a set of parameter estimates (Table 1) and derived quantities at equilibrium and those associated with maximum sustainable yield (MSY) (Table 2). Recruitment of age-0 fish showed fairly even recruitment, with the top four recruitment years being 2010, 2003, 2014, and 2006 (Figure 5). The base run population trajectory from 1935 to 2023 (Figure 6), estimated median spawning biomass[11] B_t in years t = 1935, 2023, and 2033 (assuming a constant catch of 750 t/y) to be 13,908, 10,760, and 11,010 tonnes, respectively. Figure 6 indicates that the median spawning stock biomass will remain above the upper stock reference (USR) for the next 10 years at annual catches equal to all catches used in catch projections. Exploitation (harvest) rates largely stayed below u_{MSY} for much of the history of the fishery (Figure F.25).

A phase plot of the time-evolution of spawning biomass and exploitation rate by the modelled fishery in MSY space (Figure 7) suggests that the stock is firmly in the Healthy zone, with a current position at B_{2023}/B_{MSY} = 3.04 (1.92, 4.89) and u_{2022}/u_{MSY} =0.27 (0.15, 0.47). The current-year stock status figure (Figure F.28) shows the position of the base run in DFO's Healthy zone.

[11] The derived quantity B always refers to mature female spawning stock biomass.

Table 1. Quantiles of the posterior distribution based on 2,000 MCMC samples[12] for the main estimated model parameters for the base run CAR stock assessment. Selectivity parameters are expressed in terms compatible with Awatea; SS counterparts: $\mu_g = \beta_{1g}$, log $v_{Lg} = \beta_{3g}$, $\Delta_g = \Delta_{1g}$ (see Appendix E).

Parameter	5%	25%	50%	75%	95%
log R_0	7.534	7.754	7.933	8.137	8.432
M (Female)	0.08094	0.08841	0.09329	0.09839	0.1063
M (Male)	0.05471	0.06086	0.06543	0.07057	0.07748
BH (h)	0.5659	0.7025	0.7958	0.875	0.9508
μ_1 (TRAWL)	12.05	12.78	13.24	13.75	14.55
log v_{L1} (TRAWL)	1.783	2.16	2.382	2.588	2.884
Δ_1 (TRAWL)	-0.5866	-0.4681	-0.3963	-0.3242	-0.2078
μ_3 (QCS)	10.41	11.47	12.25	13.06	14.36
log v_{L3} (QCS)	1.875	2.357	2.647	2.93	3.307
Δ_3 (QCS)	-0.5892	-0.4712	-0.3931	-0.3124	-0.2022
μ_4 (WCVI)	8.28	9.45	10.33	11.30	13.15
log v_{L4} (WCVI)	2.014	2.478	2.791	3.100	3.545
Δ_4 (WCVI)	-0.5812	-0.4702	-0.3926	-0.3132	-0.2028
μ_5 (NMFS)	9.901	11.15	12.06	13.04	14.52
log v_{L5} (NMFS)	1.642	2.224	2.584	2.926	3.363
Δ_5 (NMFS)	-0.5904	-0.479	-0.4029	-0.3208	-0.2002
log [DM θ_1]	6.088	6.619	6.998	7.480	8.265
log [DM θ_3]	4.873	5.405	5.881	6.393	7.310
log [DM θ_4]	4.636	5.254	5.697	6.267	7.203
log [DM θ_5]	4.048	4.648	5.123	5.716	6.572

[12] Includes four outlier samples with estimated MSY=0 t, h<0.4, and B_{MSY}>12,000 t (well outside the posterior distribution of B_{MSY}).

Table 2. Derived parameter quantiles from the 2,000 samples[13] of the MCMC posterior of the base run. Definitions: B_0 – unfished equilibrium spawning biomass, B_{2023} – spawning biomass at the start of 2023, u_{2022} – exploitation rate (ratio of total catch to vulnerable biomass) in the middle of 2022, u_{max} – maximum exploitation rate (calculated for each sample as the maximum exploitation rate from 1935-2022), B_{MSY} – equilibrium spawning biomass at MSY (maximum sustainable yield), u_{MSY} – equilibrium exploitation rate at MSY. All biomass values (including MSY) are in tonnes. The average catch over the last 5 years (2017-21) was 775 t by trawl and 13.5 t for the 'other' fishery.

Quantity	5%	25%	50%	75%	95%
B_0	10,354	12,218	13,908	15,994	20,295
B_{2023}	7,275	9,071	10,761	12,886	17,637
B_{2023} / B_0	0.5703	0.6848	0.7780	0.8757	1.0450
u_{2022}	0.0134	0.0181	0.0217	0.0256	0.0323
u_{max}	0.0456	0.0572	0.0653	0.0727	0.0836
MSY	948	1,152	1,305	1,496	1,886
B_{MSY}	2,149	2,886	3,580	4,475	5,964
0.4B_{MSY}	860	1,154	1,432	1,790	2,385
0.8B_{MSY}	1,720	2,309	2,864	3,580	4,771
B_{2023} / B_{MSY}	1.9240	2.4680	3.0430	3.7440	4.8860
B_{MSY} / B_0	0.1670	0.2170	0.2593	0.3019	0.3652
u_{MSY}	0.0511	0.0683	0.0812	0.0949	0.1141
u_{2022} / u_{MSY}	0.1514	0.2128	0.2700	0.3419	0.4744

[13] See footnote 11.

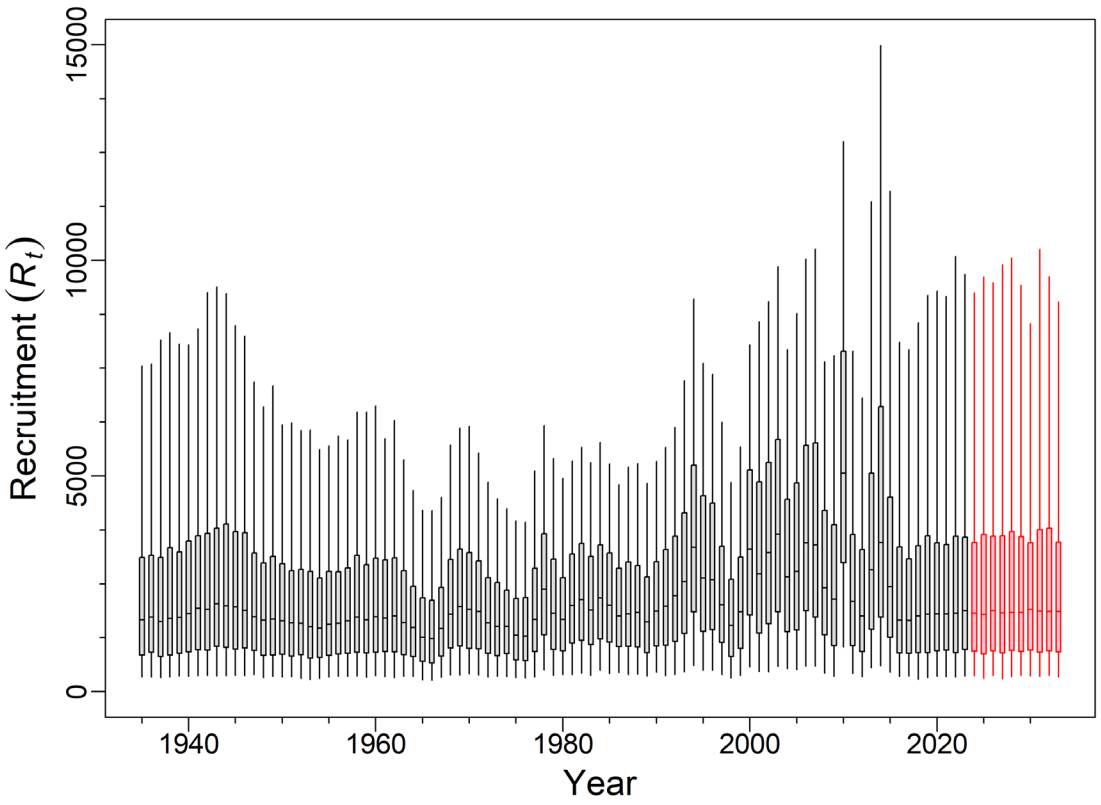

Figure 5. Recruitment trajectory and projection (1000s age-0 fish) for the base run. Boxplots delimit the 0.05, 0.25, 0.5, 0.75, and 0.95 quantiles.

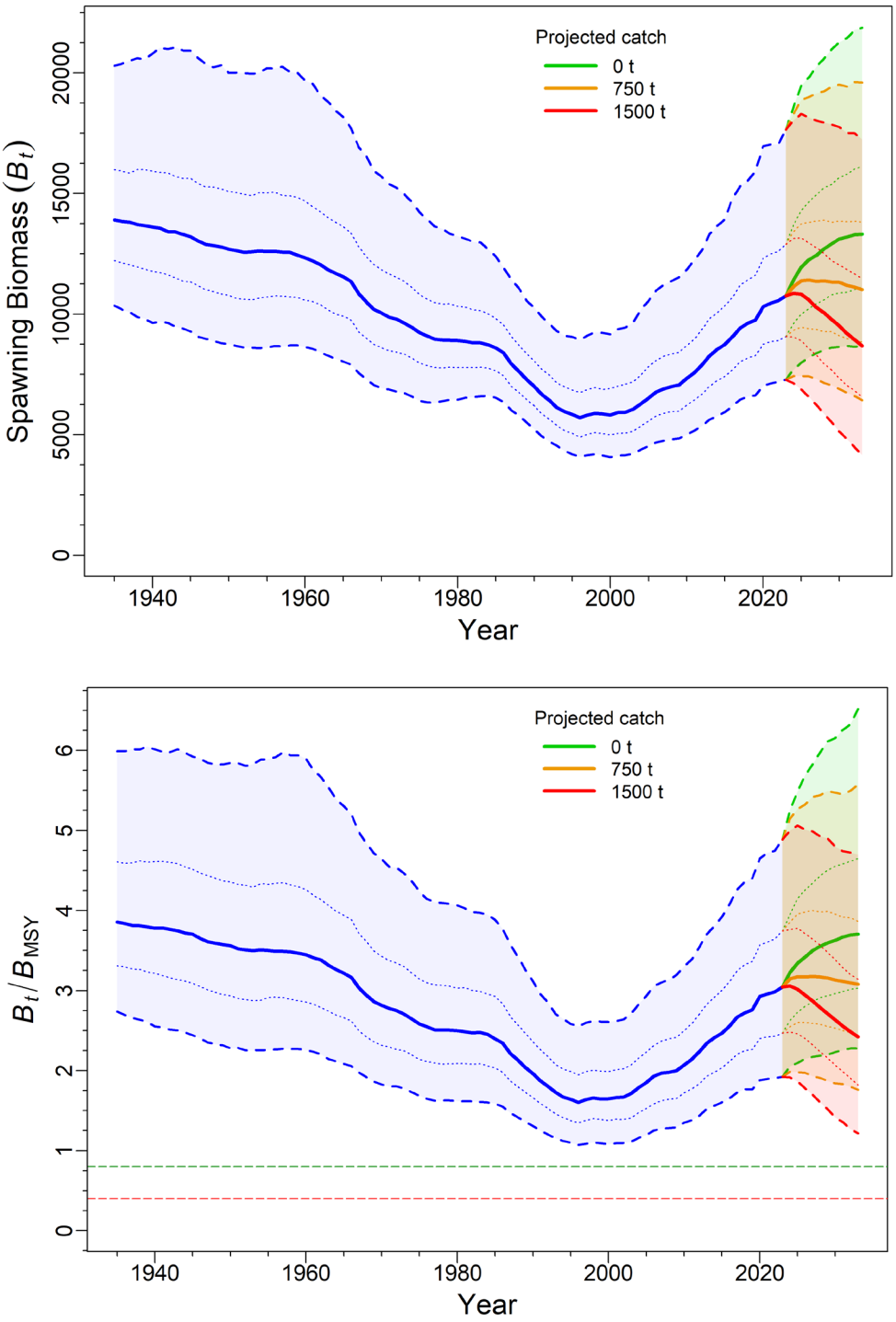

Figure 6. Estimates of spawning biomass B_t (tonnes, top) and B_t relative to B_{MSY} (bottom) for the base run. The median biomass trajectory appears as a solid curve surrounded by a 90% credibility envelope (quantiles: 0.05-0.95) in light blue and delimited by dashed lines for years t=1935-2023; projected biomass (2024-2033) appears for three catch policies: green for no catch (0 t/y), orange for average catch (750 t/y), and red for high catch (1,500 t/y). Also delimited (by dotted lines) is the 50% credibility interval (quantiles: 0.25-0.75). The horizontal dashed lines show the median limit reference point (LRP) = $0.4B_{MSY}$ and USR = $0.8B_{MSY}$.

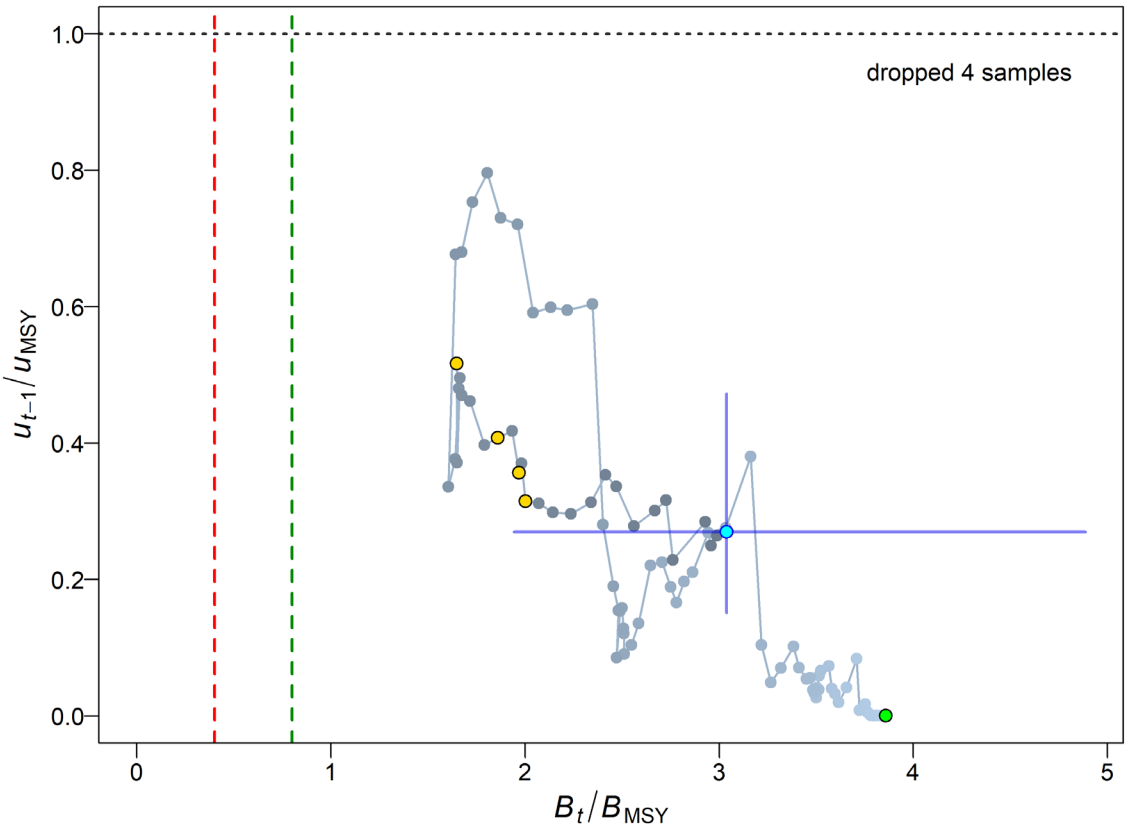

Figure 7. Phase plot through time of the medians of the ratios B_t/B_{MSY} (the spawning biomass at the start of year t relative to B_{MSY}) and fishing pressure relative to u_{MSY} (u_{t-1}/u_{MSY}, where the exploitation rate occurs in the middle of year t-1) for the base run[14]. The filled green circle is the equilibrium starting year (1935). Years then proceed from lighter shades through to darker with the final year (t=2023) as a filled cyan circle, and the blue cross lines represent the 0.05 and 0.95 quantiles of the posterior distributions for the final year. Previous assessment years (1999, 2005, 2007, and 2009) are indicated by gold circles. Red and green vertical dashed lines indicate the PA provisional LRP = $0.4B_{MSY}$ and USR = $0.8B_{MSY}$, and the horizontal grey dotted line indicates u_{MSY}.

[14] Projections for four MCMC samples were undefined because u_{MSY}=0.

8.2. SENSITIVITY ANALYSES

8.2.1. Sensitivity analyses taken to MCMC level

Fourteen primary sensitivity analyses were run (with full MCMC simulations, see Table 3) relative to the base run (Run24: *M and h* estimated) to test the sensitivity of the outputs to alternative model assumptions. The differences among the sensitivity runs (including the base run) are summarised in tables of median parameter estimates (Table F.18-F.19) and median MSY-based quantities (Table F.20).

Table 3. Sensitivity runs used to test a range of base run assumptions. Fourteen primary sensitivity runs were taken to MCMC to generate 2000 samples that were used to generate posterior distributions for all estimated parameters. Four additional sensitivity runs were taken to MPD only.

Sensitivity	Run	Eval	Description
S01	25	MCMC	split *M* between ages 13 and 14 for estimation of *M* for young and mature fish
S02	26	MCMC	apply no ageing error correction
S03	27	MCMC	use smoothed ageing error from age-reader CVs
S04	28	MCMC	use constant-CV ageing error (CV=10%)
S05	29	MCMC	reduce commercial catch (1965-1995; foreign + unobserved domestic) by 30%
S06	30	MCMC	increase commercial catch (1965-1995; foreign + unobserved domestic) by 50%
S07	31	MCMC	reduce sigmaR (σ_R) to 0.6 from 0.9
S08	32	MCMC	increase sigmaR (σ_R) to 1.2 from 0.9
S09	33	MCMC	use female dome-shaped selectivity
S10	34	MCMC	use age frequency data from HS & WCHG synoptic surveys
S11	35	MCMC	add HBLL North and South (longline) surveys
S12	36	MCMC	use CPUE fitted by Tweedie distribution
S13	37	MCMC	remove commercial CPUE series
S14	49	MCMC	use Francis mean-age reweighting instead of using the Dirichlet-Multinomial
S15	44	MPD	widen period (1935-2015) over which to estimate recruitment deviations
S16	45	MPD	use geostatistical synoptic survey indices
S17	46	MPD	drop NMFS Triennial and GIG survey series
S18	48	MPD	use Stanley et al (2009) catch history

MCMC diagnostics were evaluated using the following subjective criteria:

- Good – no trend in traces and no spikes in log (R_0), split-chains align, no autocorrelation;
- Fair – trace trend temporarily interrupted, occasional spikes in log (R_0), split-chains somewhat frayed, some autocorrelation;
- Poor – trace trend fluctuates substantially or shows a persistent increase/decrease, split-chains differ from each other, substantial autocorrelation; and
- Unacceptable – trace trend shows a persistent increase/decrease that has not levelled, split-chains differ markedly from each other, persistent autocorrelation.

The diagnostic plots (Figures F.29 to F.31) suggest that seven sensitivity runs exhibited good MCMC behaviour and seven were fair. None were in the poor or unacceptable categories.

- Good – no trend in traces, no sudden spikes in log (R_0), split-chains align, no autocorrelation
  - S01 (split M ages(13,14)
  - S03 (AE5 age reader CV)
  - S04 (AE6 CASAL CV=0.1)
  - S06 (increase catch 50%)
  - S08 (sigmaR=1.2)
  - S11 (add HBLL surveys)
  - S14 (use Francis reweight)

- Fair – trace trend temporarily interrupted, split-chains somewhat frayed, some autocorrelation
  - S02 (AE1 no age error)
  - S05 (reduce catch 30%)
  - S07 (sigmaR=0.6)
  - S09 (female dome select)
  - S10 (use AF HS WCHG)
  - S12 (use Tweedie CPUE)
  - S13 (remove commercial CPUE)

The trajectories of the B_t medians relative to B_0 (stock depletion, Figure 8) indicate that all sensitivities followed a similar trajectory to the base run trajectory with some variation. The median final-year depletion ranged from a low of 0.622 by S11 (add HBLL) to a high of 0.973 by S01 (split M). As the split-*M* scenario was the most optimistic, with respect to depletion in 2023, the selected base run (first natural mortality hypothesis: single *M*) was considered to be a conservative choice.

Sensitivity S01 (second *M* hypothesis), which emulated the previous CAR stock assessment (Stanley et al. 2009; DFO 2010) by estimating a lower *M* for both males and females and then allowing *M* to increase for females after age 14, resulted in a much more optimistic stock depletion (median estimate B_{2023}/B_0=0.97) than the base run (B_{2023}/B_0=0.78).

The third *M* hypothesis to explain the lack of older females in this population, represented in sensitivity S09, which used female dome-shaped selectivity, resulted in larger biomass (Figure 9) and a more optimistic stock depletion (median estimate B_{2023}/B_0=0.84) than that for the base run (Figure 8). The larger B_0 estimate stemmed from the cryptic biomass that was created by this model run, acting as a reservoir of additional female spawners.

Two of the sensitivity runs resulted in less optimistic estimates of stock depletion. These were S11 (adding the HBLL surveys) and S12 (using Tweedie CPUE). Both these runs provided good MCMC diagnostics and could be considered alternative interpretations for the CAR stock. These runs used different data inputs, either additional survey data or an alternative interpretation of CPUE data. The Tweedie CPUE analysis was credible and represented an alternative interpretation of the catch/effort data. A second Tweedie analysis, using a full interaction model between DFO locality and year, followed quite closely to the delta-lognormal model used in the base run (Figure C.20) and would have returned a model with intermediate results between the base run and S12.

Both CPUE series (delta-lognormal and Tweedie) may have been compromised through changes in the collection procedure of catch-effort data as a result of administrative responses to COVID-19 pandemic. The observer programme was suspended in March 2020 and was replaced by an audited electronic monitoring logbook programme in April 2020. Although individual landings were audited, there has been no overall audit of the post-March 2020 data collection process.

The sensitivity run which omitted the CPUE data entirely (S13) resulted in a less optimistic stock depletion estimate for t=2023 (median B_t/B_0 = 0.67) than in the base run (B_t/B_0 = 0.78) but greater than in the Tweedie sensitivity run (S12, B_t/B_0 = 0.63).

An interesting sensitivity was S10, adding the AF data for the HS and WCHG surveys, data that were not included in the base run because the model did not fit to these data very well. However, the HS survey observed younger ages and sizes (see Figure D.6) compared to the other synoptic surveys. When the model was offered the HS AF data, it estimated a very large year class for 2014 compared to the base run (Figures F.34 and F.35). While this year class may have been as large as the run S10 estimate, it seemed prudent to investigate this possibility as a

sensitivity run without including such an optimistic year class estimate in the base run projections.

Three of the sensitivity runs addressed ageing error issues: S02 dropped ageing error entirely; S03 used an alternative ageing error vector based on the error between alternative reads of the same otolith; and S04 which implemented a constant 10% error term for every age. These alternative ageing error vectors are shown concurrently in Figure D.9. The sensitivity runs employing the alternative ageing error vectors (S03 and S04) resulted in model runs that were almost identical to the base run when plotted as a percentage of B_0 (Figure 8). When plotted as an absolute biomass (Figure 9), sensitivity S04 lay slightly below the base run while sensitivity S03 lay on top of the base run. Sensitivity S02, which dropped ageing error entirely, was less optimistic in terms of percentage B_0 and was considerably larger in terms of absolute B_t (Figure 9) than the base run.

The two sensitivity runs which adjusted early (1965-1995) catches downward (S05) and upward (S06) provided predictable results, with S05 returning a similar B_0 to the base run while S06 proved to be a much larger stock. In terms of percent B_0, S05 returned more optimistic results compared to the base run (especially after about 1990) while S06 was consistently below the base run, returning one of the least optimistic trajectories.

The two sensitivity runs which varied the σ_R parameter (standard deviation of recruitment process error) showed mixed results. Run S07 (sigmaR=0.6) was nearly identical to the base run, apart from estimating a smaller stock (about 10% smaller) but with no difference in terms of stock depletion. Run S08 (sigmaR=1.2) did the opposite: stock size increased (by about 15%; Figure 9) but stock depletion, and consequently the advice, changed very little. The SS3 platform calculates[15] an alternative sigmaR based on the estimated variance of the recruitment deviations. This value was 0.81 for the base run, which aligned well with the sigmaR assumption made by the base run.

The sensitivity run that used Francis reweighting (S14) had good MCMC diagnostics and estimated similar parameter medians as those for the base run, with some divergence in the median estimates for natural mortality: M_{female}=0.097 vs. 0.093 and M_{male}=0.071 vs. 0.065. Estimated age at full selectivity for the trawl fishery was also slightly higher at μ_1=14.0 vs. 13.2. The derived parameters showed more variation with S14 estimating a 12% lower B_0 than that for the base run and a current spawning stock size (B_{2023}) 16% lower. However depletion was very similar between the runs: S14 B_{2023}/B_0 = 0.75, base run B_{2023}/B_0 = 0.78.

Apart from log R_0, there was little variation in the key leading parameter estimates among the fourteen sensitivity runs (Figure F.37) The biggest exception was sensitivity run S01 (split M) because only the M for young (ages 0-13) fish was plotted. The M parameters for young and mature (ages 14+) fish were not comparable to the M values estimated for the other sensitivity runs. Another exception was S14 where the posterior for age at full selectivity for the trawl fishery shifted higher than for all other runs. Derived quantities based on MSY (Figure F.38) exhibited divergences that were consistent with the sensitivity, e.g., high B_0 for S09 (female dome-shaped selectivity) and high $u_{\max}$ for S06 (increased catch in 1965-95).

The stock status (B_{2023}/B_{MSY}) for the sensitivities (Figure 10) were all in the DFO Healthy zone, including the most pessimistic S12 run that used the Tweedie distribution for fitting CPUE index data.

[15] R code: `require(r4ss); replist=SS_output(dir="."); replist$sigma_R_info` (also see Chantel Wetzel, pers. comm. 2015)

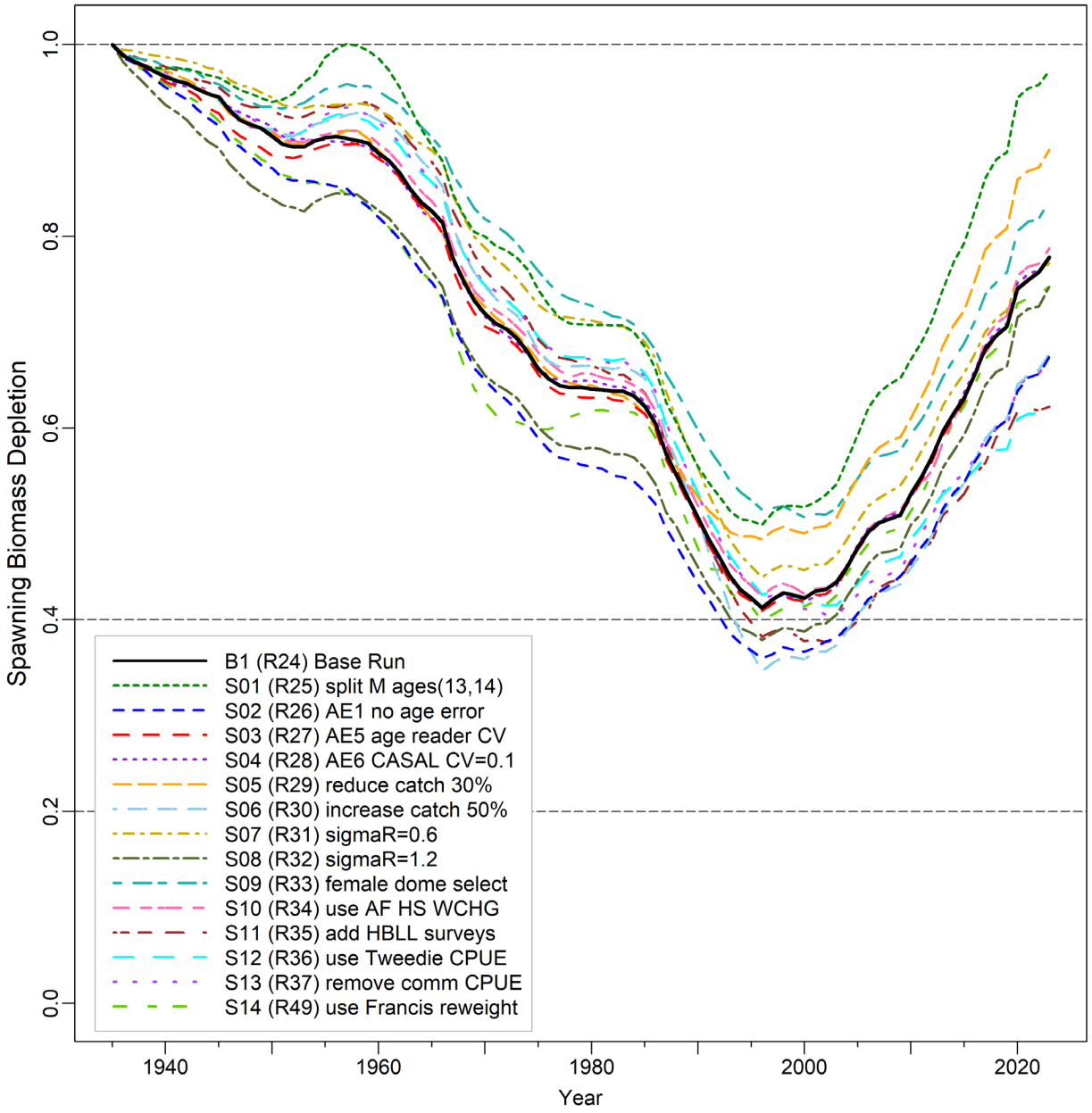

Figure 8. Model median trajectories of spawning biomass as a proportion of unfished equilibrium biomass (B_t/B_0) for the base run and fourteen sensitivity runs (see legend lower left). Horizontal dashed lines show alternative reference points used by other jurisdictions: $0.2B_0$ (~DFO's USR), $0.4B_0$ (often a target level above B_{MSY}), and B_0 (equilibrium spawning biomass).

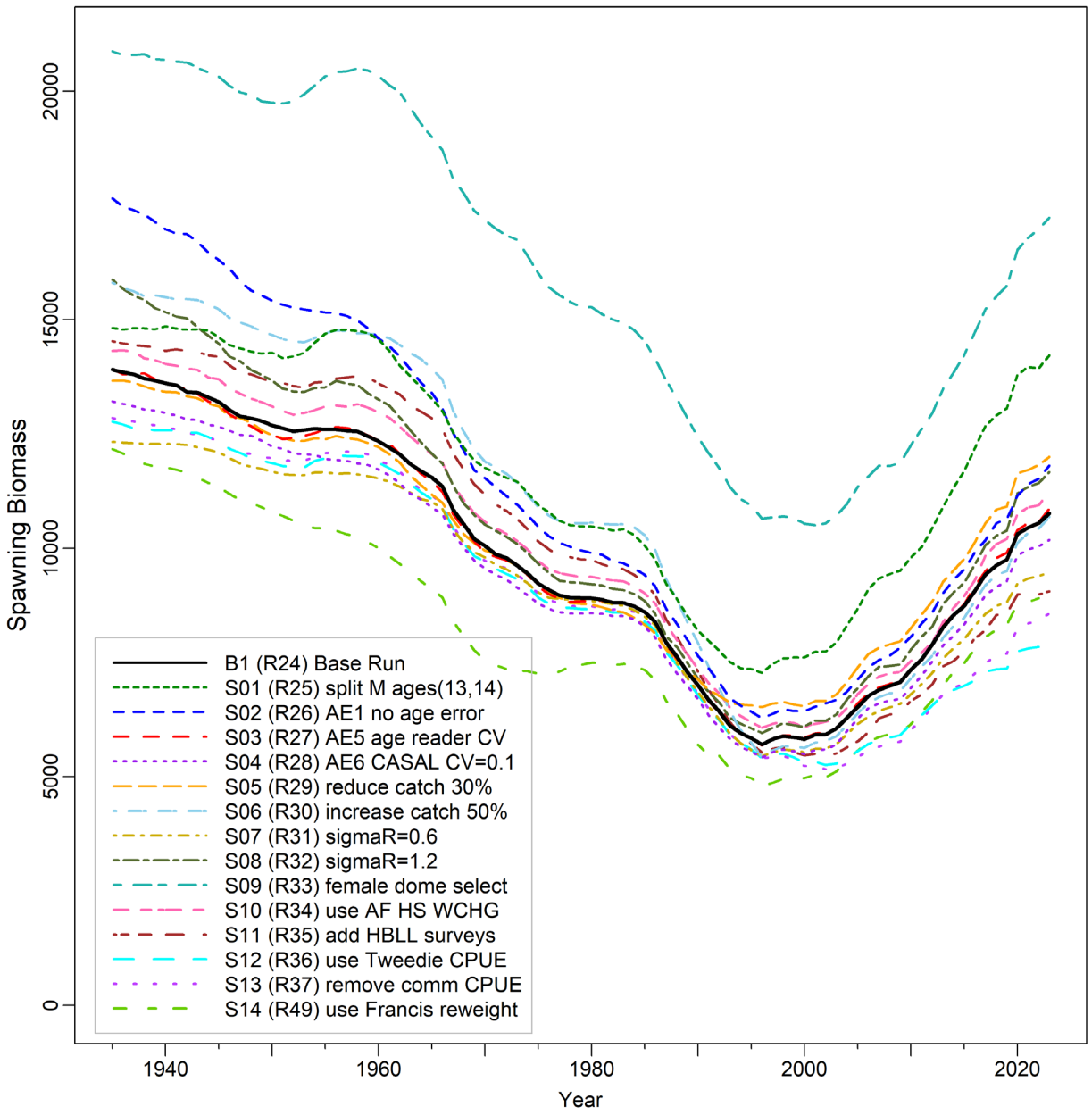

Figure 9. Model median trajectories of spawning biomass (B_t) for the base run and fourteen sensitivity runs (see legend lower left).

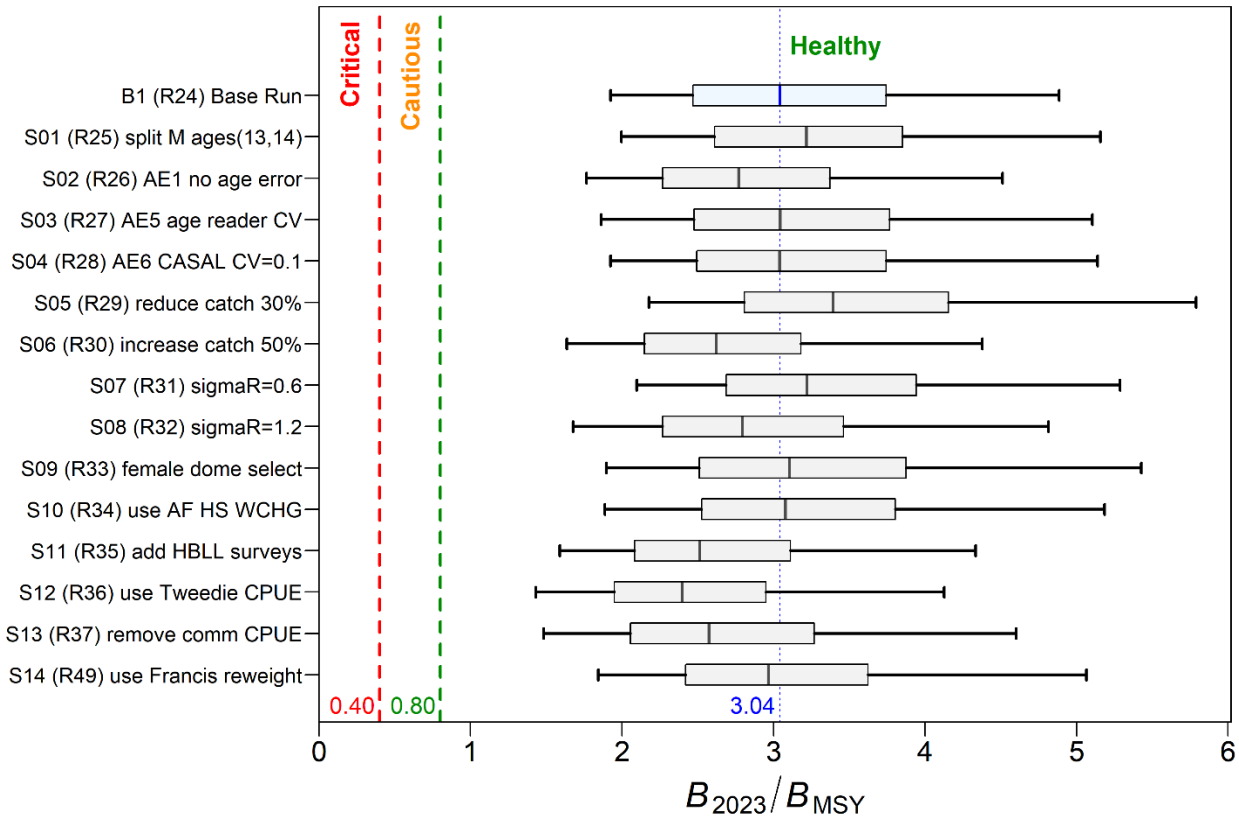

Figure 10. Stock status at beginning of 2023 of the CAR stock relative to the DFO PA provisional reference points of $0.4B_{MSY}$ and $0.8B_{MSY}$ for the base run (B1, M&h estimated) and fourteen sensitivity runs (see y-axis notation and sensitivity descriptions in the main text). Boxplots show the 0.05, 0.25, 0.5, 0.75 and 0.95 quantiles from the MCMC posterior. Appendix F contains the details of these sensitivity runs.

8.2.2. Sensitivity analyses taken to MPD level

Four additional sensitivity analyses were done which were not included in the MCMC set of sensitivity runs (Section 8.2.1) because they were either close variants of the base run (B1, Run24) which would return similar MCMC diagnostics or else an MCMC extension seemed unnecessary. These runs are described in Section 7 and consist of:

- S15 (Run44) widen period for estimation of recruitment deviations to 1935–2015;
- S16 (Run45) use geostatistical synoptic survey indices;
- S17 (Run46) drop NMFS Triennial and GIG survey series; and
- S18 (Run48) use Stanley et al (2009) catch history.

SS3 splits the periods over which recruitment deviations are estimated into three brackets, with only the central period used to estimate R_0 and consequently B_0. Recruitment deviations are estimated for the bracketing periods but are not used to estimate R_0. The base run set this main period to 1950–2012 but sensitivity S15 widened this period to the beginning of the model reconstruction (1935) and extended it to 2015 (thus including the possible strong 2014 year class) to see if there was an impact on the estimates of R_0 and B_0. However, it can be seen that this model returned a very similar estimate of B_0 and stock depletion as did the base run (Table 4).

Previous stock assessment reviews have suggested that a geostatistical analysis of the survey data could be used instead of the swept area design used in this stock assessment (Appendix B). A set of geostatistical survey indices for CAR were obtained for the four synoptic surveys (QCS, WCVI, HS and WCHG; P. English, DFO, pers. comm., 2022). These are documented in Appendix B, along with comparison plots with the swept area indices (Section B.9, Figures B.71–B.74). These indices were used in sensitivity run S16 but, as for S15, the estimates of B_0 and stock depletion were very close to those of the base run (Table 4). The negative log likelihoods for the biomass indices returned by this run are clearly quite different (Table 5) because the index values have changed, but the parameter values in Table 4 are nearly the same as the base run.

While sensitivity run S17 (drop historical surveys) resulted in a larger stock size (both B_0 and total biomass T_0 were increased by about 14% relative to the base run – Table 4), the stock depletion estimates were also larger than for the base run, which was expected, given that the same catch history was removed from a larger stock size. The effect of these early surveys appears to be an anchor on the early catch information, which the authors deemed beneficial.

Replacing the base run catch history with the catch history used in the 2007 and 2009 stock assessments resulted in a run that resembled sensitivity S06 (increase 1965-1995 catches by 50%). The estimates of B_0 and B_{2023}/B_0 for S18 were close to the equivalent S06 estimates (Table 4). This run was not taken to the MCMC level because it duplicated S06. Also, the current catch reconstruction provided a better representation of the historical catch series than that used in the previous stock assessment. This sensitivity run demonstrated that the current selection of sensitivity runs encompassed the catch history used in the previous CAR stock assessment.

Table 5 demonstrates that none of these four sensitivity runs had much impact on the fit to either the biomass index values or to the age composition data. Sensitivity S06 showed a slight improvement to the fit of the historic surveys, which was not apparent in S18 (Stanley et al. 2009 catch history).

Table 4. Selected MPD parameter estimates for the four sensitivity runs that were only taken to MPD level. see text for run descriptions. T_0 and T_{2023}= total biomass

	Leading parameter estimates				Derived state parameters					
Run	M_{female}	M_{male}	LN(R_0)	h	B_{2023}	B_0	B_{2023}/B_0	T_{2023}	T_0	T_{2023}/T_0
Base run	0.093	0.065	7.913	0.877	9,692	13,753	0.705	33,498	44,455	0.754
S15	0.092	0.065	7.894	0.875	9,628	13,635	0.706	33,093	44,073	0.751
S16	0.093	0.065	7.920	0.876	9,727	13,761	0.707	33,604	44,512	0.755
S17	0.093	0.065	8.050	0.866	12,340	15,633	0.789	41,819	50,840	0.823
S18	0.084	0.055	7.807	0.880	9,267	15,441	0.600	32,020	50,299	0.637
S06	0.088	0.060	7.951	0.875	9,690	15,824	0.612	33,888	51,233	0.661

Table 5. Negative log likelihood values for the four sensitivity runs that were only taken to MPD level. see text for run descriptions.

					Biomass indices			Age composition			
Run	CPUE	QCS	WCVI	NMFS	HS	WCHG	GIG	Comm	QCS	WCVI	NMFS
Base run	-24.98	7.933	2.003	13.86	8.634	23.92	8.773	195.8	34.05	26.59	45.69
S15	-25.00	7.935	1.999	13.88	8.631	23.92	8.735	195.9	34.05	26.61	45.66
S16	-25.12	-4.689	0.254	13.84	3.786	5.699	8.773	195.7	34.10	26.63	45.67
S17	-25.28	7.934	2.000	NA	8.648	23.95	NA	194.9	33.78	26.07	NA
S18	-25.16	8.034	2.068	13.19	8.515	23.76	9.231	195.6	33.96	26.31	45.11
S06	-25.36	7.995	2.022	11.87	8.496	23.79	8.170	195.9	33.98	26.42	45.43

8.2.3. Sensitivity analyses fitted to PDO index series

Section 7 describes three sensitivity runs that were fitted to the winter (Dec-Mar) PDO environmental index series, previously used for POP (Haigh et al. 2018) and presented in Section G.4. This implementation treated the index series as if it were data, indexing relative recruitment rather than biomass. A *q*-scalar was estimated and the fit to the series contributed to the total log-likelihood. Three data-weighting scenarios were investigated:

- E01 (R386[16]) use nominal standard errors from the PDO series;
- E02 (R387) apply a fixed 0.30 process error; and
- E03 (R388) apply process error using a smoothing procedure (0.8258, Section E.6.2.1).

All three of the above sensitivity runs were taken to the MCMC level, with E01 having very poor diagnostics (Figure 11). Sensitivities E02 and E03 had good MCMC diagnostics and had clearly converged. It was likely that the poor diagnostics that characterised E01 stemmed from the tight CVs associated with that run (range 0.04 to 0.59; mean=0.20). Table 6 demonstrates the implications of the poor convergence in E01, with the upper 95% percentiles for B_0 and B_{2023} lying well above 3 million tonnes.

The biomass trajectories (Figure 12) for the E01 and E02 environmental sensitivities diverged considerably from the base run trajectory, especially in the final years, while E03 was very close to the base run except in the final three or four years. Table 7 shows that there was a considerable likelihood penalty for E01 and E02 in terms of the best fit to the data with the inclusion of the environmental series. The penalty was much smaller for E03, but E03 also diverged in recent years relative to the base run trajectory. The problem was that there were no commercial AF data after 2017 and the available survey AF data seemed to be insufficient to contradict the PDO prediction.

Figure 13 plots the recruitment deviations for the base run along with the three PDO sensitivities as well as the actual PDO index (all trajectories transformed using exponentiated z-scores and then back-transformed to deviations using the natural log). This plot is instructive because it demonstrates how the PDO dominated in the early part of the series when there were few age data, but all series started to diverge away from the PDO series as more age data entered the model, with the amount of divergence the greatest for E03 and the least for E01. The recruitment deviations after 2000 showed four distinct peaks, only one of which coincided with the PDO series. This conflict between the AF data and the recent observations from the PDO series was the cause of the divergence away from the base run shown in Figure 12.

The primary conclusion that can be taken from these runs is that the degree of impact by this series was attributable to how much weight was applied to the index series. When high weight was used (no added CV, Run E01), there was considerable impact on the outcome of the stock assessment, with the overall median ratio B_0/B_{2023} dropping from 0.78 to 0.59 (Table 6) along with a strong divergence away from the base run trajectory (Figure 12). However, this impact came with a large loss in the quality of the fit to AF and biomass index data (Table 7).

The tail of the E01 stock status distribution dipped into the DFO Cautious zone (0.05 quantile of B_{2023}/B_{MSY} = 0.704, Table 6), but this result should be discounted, given the poor MCMC diagnostics for this simulation (Figure 11). On the other hand, E03 (where the PDO index series was treated in the same manner as the CPUE index series by estimating the process error to add to the series through a spline smoothing exercise – see Section E.6.2) estimated stock size and stock status (relative to B_0 or B_{MSY}) close to the base run estimates. However, the recent

[16] Run 38, version 6

trajectory for E03 differed from the base run and would provide an alternative projection scenario. On balance, it was hard to judge how much credence should be given to these outcomes, particularly with the knowledge that using the PDO series in this manner was effectively a correlation analysis. That is, there was no functional linkage of the PDO index series to the model dynamics and the main determinant of the impact of the series was the amount of arbitrary weight given to it.

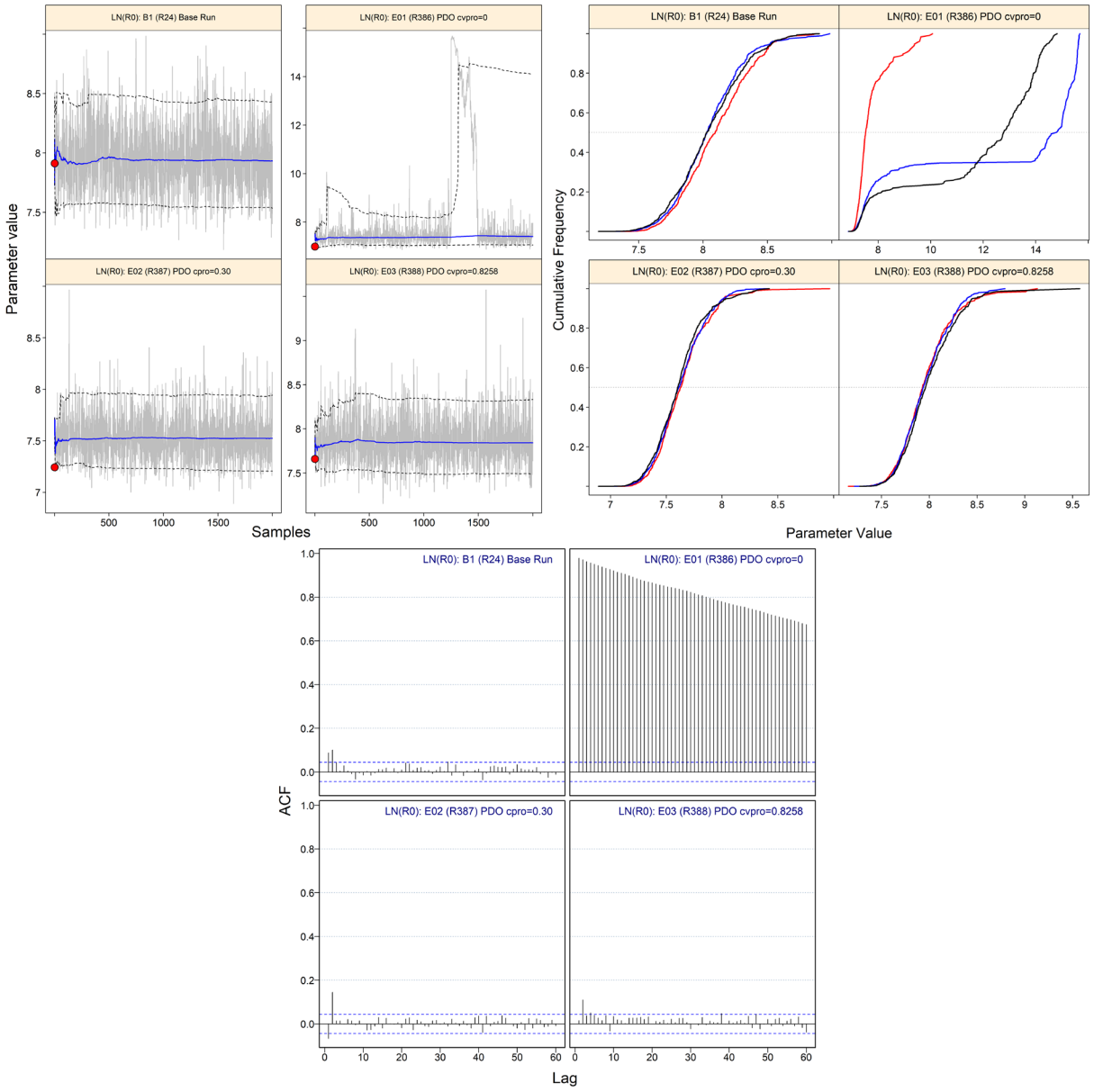

Figure 11. logR_0 MCMC diagnostics for base run and the three sensitivity runs with fitted PDO environmental index series; upper right plot: MCMC traces for the estimated parameters. Grey lines show the 2,000 samples for each parameter, solid blue lines show the cumulative median (up to that sample), and dashed lines show the cumulative 0.05 and 0.95 quantiles. Red circles are the MPD estimates; upper left plot: diagnostic plots obtained by dividing the MCMC chain of 2,000 MCMC samples into three segments, and overplotting the cumulative distributions of the first segment (red), second segment (blue) and final segment (black); lower plot: autocorrelation plots for the estimated parameters from the MCMC output. Horizontal dashed blue lines delimit the 95% confidence interval for each parameter's set of lagged correlations.

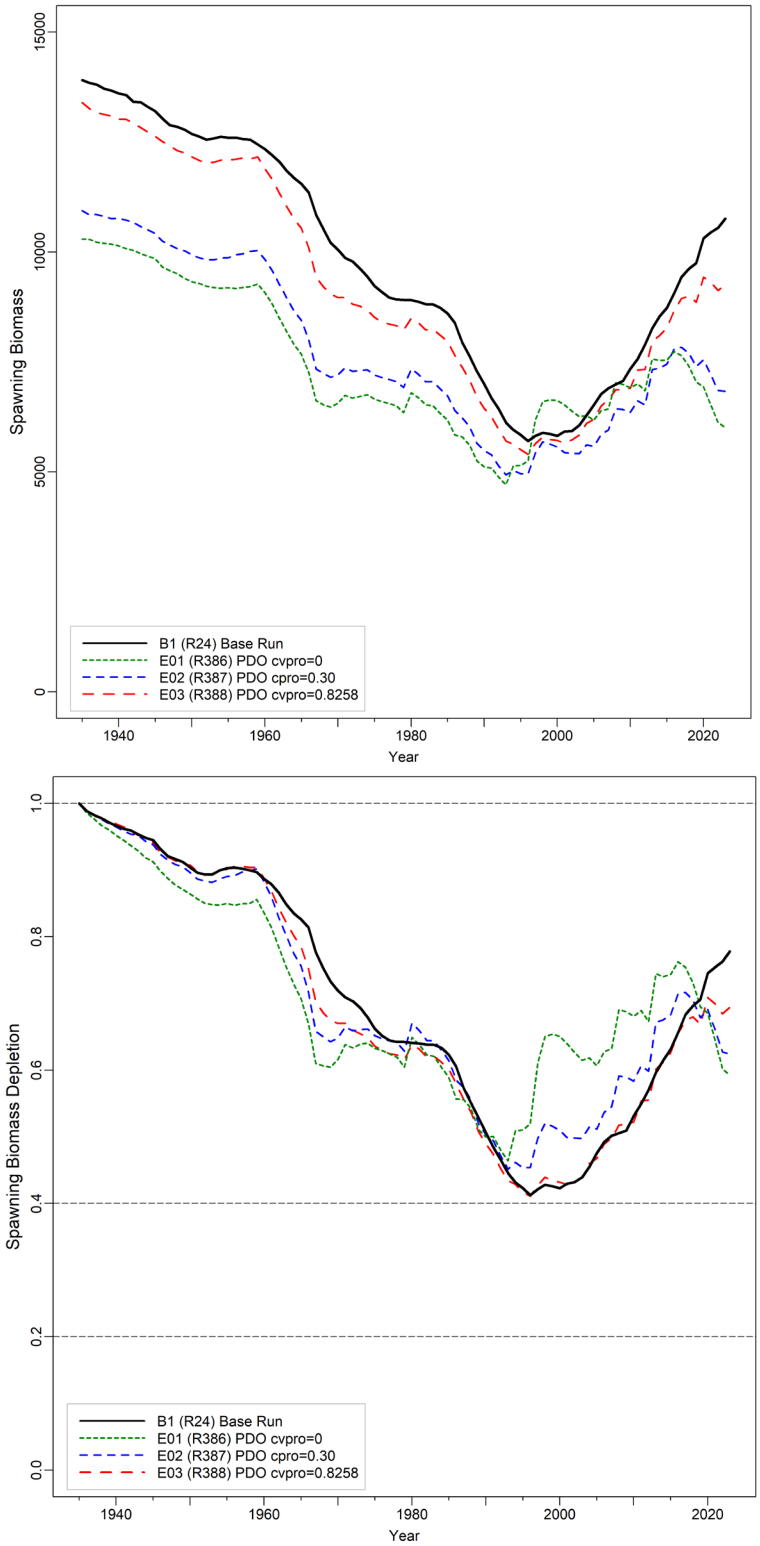

Figure 12. Estimates of the median spawning biomass B_t (tonnes, top) and B_t relative to B_0 (bottom) for the three sensitivity runs with fitted PDO environmental index series compared to the base run.

Table 6. Bayesian distributional statistics calculated from the posterior distributions for six selected derived state parameters from the base run and the three environmental sensitivity runs fitted to the PDO index series.

	Percentiles of the posterior distribution				
	5%	25%	50%	75%	95%
B_0					
Base run	10,351	12,217	13,908	15,995	20,300
E01	8,021	9,226	10,294	12,502	3,832,945
E02	8,670	9,933	10,941	12,228	14,797
E03	10,151	11,817	13,395	15,160	19,058
B_{2023}					
Base run	7,270	9,070	10,761	12,891	17,646
E01	4,158	5,049	6,013	7,800	3,374,335
E02	4,827	5,893	6,835	7,995	10,121
E03	6,378	7,871	9,262	10,989	14,985
B_{2023}/B_0					
Base run	0.5703	0.6847	0.7780	0.8757	1.0455
E01	0.4487	0.5273	0.5926	0.6779	0.9093
E02	0.4708	0.5588	0.6240	0.6996	0.8226
E03	0.5213	0.6173	0.6941	0.7867	0.9278
u_{2022}					
Base run	0.0133	0.0181	0.0217	0.0256	0.0323
E01	0.0001	0.0305	0.0390	0.0466	0.0558
E02	0.0234	0.0294	0.0342	0.0397	0.0483
E03	0.0156	0.0211	0.0252	0.0297	0.0368
B_{2023}/B_{MSY}					
Base run	1.9205	2.4673	3.0428	3.7446	4.8872
E01	0.7037	1.6289	2.0472	2.4910	3.2888
E02	1.6950	2.1649	2.6000	3.1642	4.1184
E03	1.8155	2.3276	2.8063	3.4375	4.6805
u_{2022}/u_{MSY}					
Base run	0.1512	0.2126	0.2696	0.3412	0.4724
E01	0.3515	0.4508	0.5350	0.6379	0.8241
E02	0.2482	0.3279	0.4004	0.4915	0.6513
E03	0.1710	0.2428	0.3021	0.3744	0.5154

Table 7. Negative log likelihood values for the three sensitivity runs that were fitted to the PDO environmental index series. See text for run descriptions.

								Indices				Age composition
Run	CPUE	QCS	WCVI	NMFS	HS	WCHG	GIG	PDO	Comm	QCS	WCVI	NMFS
Base run	-24.98	7.93	2.00	13.86	8.63	23.92	8.77	NA	195.80	34.05	26.59	45.69
E01	-16.19	6.64	3.09	15.68	11.00	27.09	8.13	-84.99	213.10	43.31	34.73	47.58
E02	-22.76	7.29	2.28	14.51	9.70	25.38	8.14	-36.33	201.90	38.70	30.13	46.39
E03	-24.97	7.76	1.97	14.05	8.98	24.35	8.46	8.24	196.60	34.70	26.88	45.68

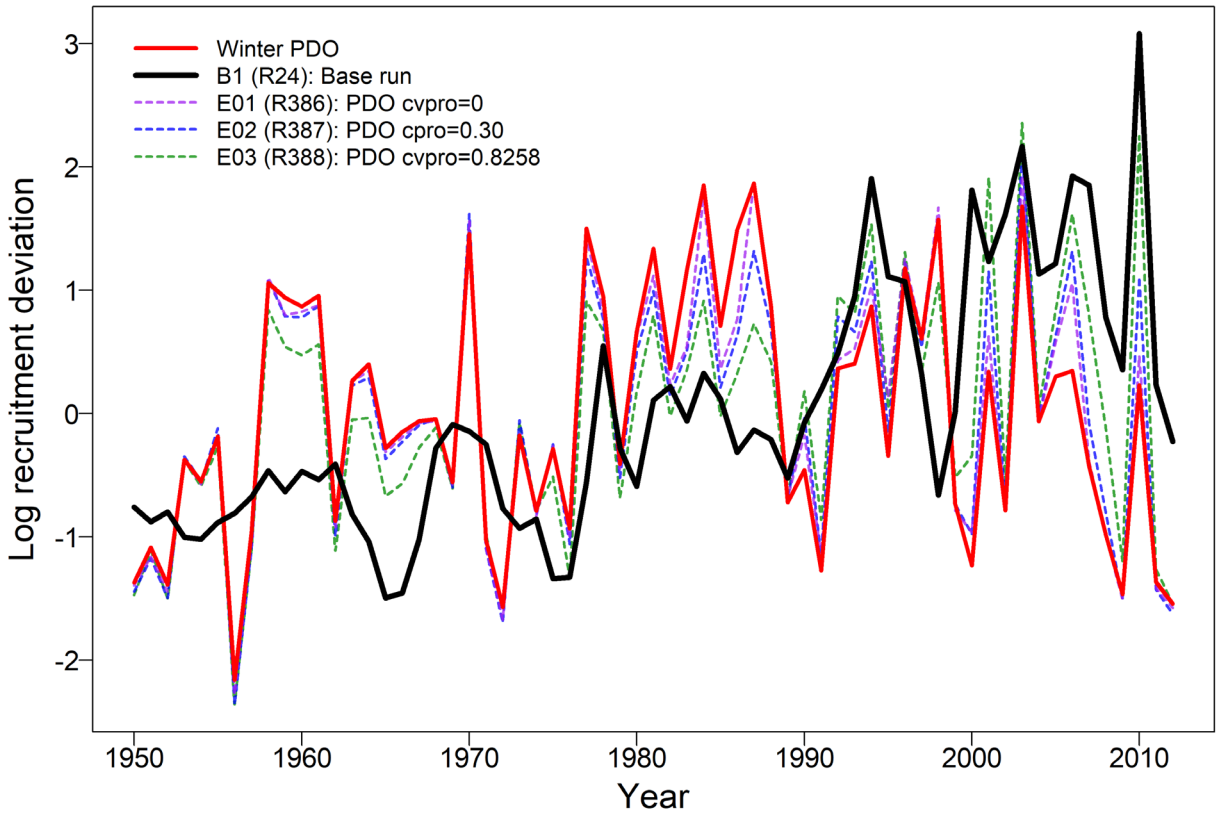

Figure 13. Estimates of the median recruitment deviations for the base run and the three sensitivity runs with fitted PDO environmental index series. Also shown is the PDO series. All trajectories have been transformed using logged exponentiated z-scores.

9. ADVICE FOR MANAGERS

9.1. REFERENCE POINTS

The Sustainable Fisheries Framework (SFF, DFO 2009a) established provisional reference points, which incorporated the 'precautionary approach' (PA), to guide management and assess harvest in relation to sustainability. These reference points are the limit reference point (LRP) of $0.4B_{MSY}$ and the upper stock reference point (USR) of $0.8B_{MSY}$, which have been adopted by previous rockfish stock assessments (Edwards et al. 2012 a,b, 2014 a,b; DFO 2015; Starr et al. 2016; Haigh et al. 2018; Starr and Haigh 2021a,b, 2022 a,b,c) and were used here. Note that to determine the suitability of these reference points for this stock (or any *Sebastes* stock) would require a separate investigation involving simulation testing using a range of operating models.

The zone below $0.4B_{MSY}$ is termed the 'Critical zone' by the SFF, the zone lying between $0.4B_{MSY}$ and $0.8B_{MSY}$ is termed the 'Cautious zone', and the region above the upper stock reference point ($0.8B_{MSY}$) is termed the 'Healthy zone'. Generally, stock status is evaluated as the probability of the spawning female biomass in year t being above the reference points, i.e., $P(B_t > 0.4B_{MSY})$ and $P(B_t > 0.8B_{MSY})$. The SFF also stipulates that, when in the Healthy zone, the fishing mortality (u_t) must be at or below that associated with MSY under equilibrium conditions (u_{MSY}), i.e., $P(u_t < u_{MSY})$. Furthermore, fishing mortality is to be proportionately ramped down when the stock is deemed to be in the Cautious zone, and set equal to zero when in the Critical zone.

The term 'stock status' should be interpreted as 'perceived stock status at the time of the assessment for the year ending in 2022 (i.e., beginning of year 2023)' because the value is

calculated as the ratio of two estimated biomass values (B_{2023}/B_{MSY}) by a specific model using the data available up to 2022. Further, the estimate of B_{MSY} depends on the model assessment of stock productivity as well as the catch split among fisheries (if there are more than one). Therefore, comparisons of stock status among various model scenarios can be misleading because the B_{MSY} space is not the same from one model to the next.

MSY-based reference points estimated within a stock assessment model can be sensitive to model assumptions about natural mortality and stock recruitment dynamics (Forrest et al. 2018). As a result, other jurisdictions use reference points that are expressed in terms of B_0 rather than B_{MSY} (Edwards et al. 2012a; N.Z. Ministry of Fisheries 2011). These reference points, for example, are default values used in New Zealand, with $0.2B_0$ as the 'soft limit', below which management action needs to be taken, and $0.4B_0$ considered a 'target' biomass for low productivity stocks, a mean around which the biomass is expected to vary. The 'soft limit' is equivalent to the upper stock reference (USR, $0.8B_{MSY}$) in the DFO SFF, while a 'target' biomass is not specified by the DFO SFF. Results are also provided comparing projected spawning biomass to B_{MSY} and to current spawning biomass B_{2023}, and comparing projected harvest rate to current harvest rate u_{2022} (Appendix F).

9.2. STOCK STATUS AND DECISION TABLES

In this stock assessment, projections extended to the end of 2032 (beginning of 2033). Projections out to three generations (75 years), where one generation was determined to be 25 years (Appendix D, Section D.1.6), were not computed because the stock status of CAR in the Healthy zone did not warrant such projections.

Stock status for DFO managers is usually defined as the current spawning biomass relative to the estimated spawning biomass required for maximum sustainable yield (MSY). Plots that depict distributions of B_{2023}/B_{MSY} in three zones (Critical, Cautious, Healthy) delimited by $0.4B_{MSY}$ (LRP) and $0.8B_{MSY}$ (USR), show that the CAR base run lay in the Healthy zone with a probability >0.999 in 2023 (Figure F.28, Figure 10). Projections of the base run stock remained above $0.8B_{MSY}$ with a 0.95 probability at all catch policies up to 2,000 t/y out to 2033 (Table 8). However, these projections also predicted that the stock would decline at catch levels above 500 t/y, under the assumption that recruitment was average over that time period (Table F.13).

Stock status plots for sensitivity runs based on the base run (Figure 10) show that all of the sensitivity runs also lay with a high probability in the Healthy zone. Even the most pessimistic sensitivity run (S12) that used the Tweedie distribution for fitting CPUE index data had a probability of >0.99 that this run was in the Healthy zone at the beginning of 2023.

Decision tables for the CAR base run provide advice to managers as probabilities that projected biomass B_t (t = 2024, ..., 2033) will exceed biomass-based reference points (or that projected exploitation rate u_t (t = 2023, ..., 2032) will fall below harvest-based reference points) under constant-catch policies (Table 8). That is, the table presents probabilities that projected B_t using the base run will exceed the LRP and the USR or will be less than the harvest rate at MSY. All decision tables (including those for alternate reference points) for the base run can be found in Appendix F (Tables F8 to F17).

Assuming that a catch of 750 t (close to the recent 5-y mean) will be taken each year for the next 10 years, Table 8 indicates that a manager would be >99% certain that both B_{2028} and B_{2033} lie above the LRP of $0.4B_{MSY}$, >99% certain that both B_{2028} and B_{2033} lie above the USR of $0.8B_{MSY}$, and >99% certain that both u_{2028} and u_{2033} lie below u_{MSY} for the base run. Generally, it is up to managers to choose the preferred catch levels or harvest levels (if available) using their preferred risk levels. For example, it may be desirable to be 95% certain that B_{2033} exceeds an LRP whereas exceeding a USR might only require a 50% probability. Assuming this risk profile,

a catch policy of <=2,000 t/y satisfies the LRP constraint in Table 8. Assuming that u_{MSY} is a target exploitation rate, all catch policies <= 1,250 t/y have a probability greater than 95% of the harvest rate remaining below u_{MSY} in 10 years, whereas catch policies <=2,000 t/y would have a probability greater than 50%.

Table 8. Decision tables for the reference points $0.4B_{MSY}$, $0.8B_{MSY}$, and u_{MSY} for 1-10 year projections for a range of constant catch policies (in tonnes) using the base run (B1, est. M&h). Values are the probability (proportion of 1,996 MCMC samples[17]) of the female spawning biomass at the start of year t being greater than the B_{MSY} reference points, or the exploitation rate of vulnerable biomass in the middle of year t-1 being less than the u_{MSY} reference point. For reference, the average catch over the last 5 years (2017-2021) was 789 t.

Catch policy	Projection year (t): start of year for *B*, middle of previous year for *u*										
	2023	2024	2025	2026	2027	2028	2029	2030	2031	2032	2033
	$P(B_t > 0.4B_{MSY})$										
0	1	1	1	1	1	1	1	1	1	1	1
250	1	1	1	1	1	1	1	1	1	1	1
500	1	1	1	1	1	1	1	1	1	1	1
750	1	1	1	1	1	1	1	1	1	1	1
1000	1	1	1	1	1	1	1	1	1	1	1
1250	1	1	1	1	1	1	1	1	1	1	1
1500	1	1	1	1	1	1	1	1	1	1	1
1750	1	1	1	1	1	1	1	1	1	1	>0.99
2000	1	1	1	1	1	1	1	1	>0.99	>0.99	>0.99
	$P(B_t > 0.8B_{MSY})$										
0	1	1	1	1	1	1	1	1	1	1	1
250	1	1	1	1	1	1	1	1	1	1	1
500	1	1	1	1	1	1	1	1	1	1	1
750	1	1	1	1	1	1	1	1	1	1	1
1000	1	1	1	1	1	1	1	1	1	1	1
1250	1	1	1	1	1	1	1	1	1	1	1
1500	1	1	1	1	1	1	1	1	>0.99	>0.99	>0.99
1750	1	1	1	1	1	1	>0.99	>0.99	>0.99	0.99	0.98
2000	1	1	1	1	1	>0.99	>0.99	0.99	0.99	0.97	0.95
	$P(u_{t-1} < u_{MSY})$										
0	1	1	1	1	1	1	1	1	1	1	1
250	1	1	1	1	1	1	1	1	1	1	1
500	1	1	1	1	1	1	1	1	1	1	1
750	1	1	1	1	1	1	1	1	1	1	1
1000	1	>0.99	>0.99	>0.99	>0.99	>0.99	>0.99	>0.99	>0.99	>0.99	>0.99
1250	1	0.99	0.99	0.99	0.99	0.99	0.98	0.98	0.97	0.97	0.96
1500	1	0.97	0.97	0.96	0.95	0.93	0.92	0.91	0.90	0.88	0.87
1750	1	0.93	0.91	0.89	0.87	0.85	0.83	0.81	0.78	0.75	0.73
2000	1	0.86	0.83	0.79	0.77	0.73	0.70	0.66	0.63	0.60	0.57

Although uncertainty was built into the assessment and its projections by taking a Bayesian approach for parameter estimation, these results depend heavily on the assumed model structure, the informative priors, and data assumptions (particularly the average recruitment assumptions) used for the projections.

[17] Projections for four MCMC samples were undefined because u_{MSY}=0.

Table 9. Decision tables for the reference points $0.2B_0$ and $0.4B_0$ for 1-10 year projections for a range of constant catch policies (in tonnes) using the base run (B1, est. M&h). Values are the probability (proportion of 1,996 MCMC samples) of the female spawning biomass at the start of year t being greater than the B_0 reference points. For reference, the average catch over the last 5 years (2017-2021) was 789 t.

Catch policy	Projection year (t): start of year for *B*										
	2023	2024	2025	2026	2027	2028	2029	2030	2031	2032	2033
	$P(B_t > 0.2B_0)$										
0	1	1	1	1	1	1	1	1	1	1	1
250	1	1	1	1	1	1	1	1	1	1	1
500	1	1	1	1	1	1	1	1	1	1	1
750	1	1	1	1	1	1	1	1	1	1	1
1000	1	1	1	1	1	1	1	1	1	1	1
1250	1	1	1	1	1	1	1	1	1	1	1
1500	1	1	1	1	1	1	1	1	1	>0.99	>0.99
1750	1	1	1	1	1	1	1	>0.99	>0.99	>0.99	0.99
2000	1	1	1	1	1	1	>0.99	>0.99	0.99	0.98	0.96
	$P(B_t > 0.4B_0)$										
0	1	1	1	1	1	1	1	>0.99	1	1	1
250	1	>0.99	1	1	>0.99	>0.99	>0.99	>0.99	>0.99	1	1
500	1	>0.99	1	>0.99	>0.99	>0.99	>0.99	>0.99	>0.99	1	1
750	1	>0.99	>0.99	>0.99	>0.99	>0.99	>0.99	>0.99	>0.99	>0.99	>0.99
1000	1	>0.99	>0.99	>0.99	>0.99	>0.99	>0.99	0.99	0.99	0.98	0.98
1250	1	>0.99	>0.99	>0.99	>0.99	0.99	0.99	0.98	0.97	0.96	0.95
1500	1	>0.99	>0.99	>0.99	0.99	0.99	0.98	0.96	0.94	0.92	0.88
1750	1	>0.99	>0.99	0.99	0.99	0.97	0.95	0.92	0.88	0.84	0.80
2000	1	>0.99	>0.99	0.99	0.98	0.95	0.91	0.86	0.80	0.76	0.70

9.3. STOCK REBUILDING

A rebuilding plan was not required because the CAR stock was assessed to be in the Healthy zone at the end of 2022, and was projected to remain in the Healthy zone up to the end of 2032 at catch levels up to 2,000 t/y under the assumption of average recruitment with a recruitment standard deviation of 0.9.

9.4. ASSESSMENT SCHEDULE

Advice was also requested concerning the appropriate time interval between future stock assessments and, for the interim years between stock updates, potential values of indicators that could trigger a full assessment earlier than usual (as per DFO 2016). The existing synoptic trawl surveys, particularly the QCS and WCVI surveys, should be capable of signalling a major reduction in stock abundance. The next full stock assessment should be scheduled no earlier than 2032, given the currently assessed Healthy state and low exploitation rates. Recruitment appeared to be good and the 2014 year class may have been quite good, if the signal in the HS survey age composition data was credible. *Sebastes* recruitment is known to be episodic, but large recruitment events were less apparent for this species, while recruitment appeared to have been at above average levels since the early 2000s (Figure 5; Figure F.14). Regardless of when a new stock assessment is to be initiated, at least 6-12 months lead time is required before the new stock assessment is initiated to allow for the reading of new ageing structures that will be needed for the interpretation of the population trajectory. Advice for interim years is explicitly included in the decision tables and managers can select another line on the table if stock abundance appears to have changed or if greater certainty of staying above the reference point

is desired. During intervening years the trend in abundance can be tracked by commercial fishery CPUE and, less reliably (because of the high relative error), by the fishery independent surveys used in this stock assessment. The groundfish synopsis report (DFO 2022), updating Anderson et al. (2019), summarised these trends and can be used as a tracking tool.

10. GENERAL COMMENTS

In common with stock assessments for other BC rockfish, this stock assessment depicted a slow-growing, low productivity stock. Unlike several of the more recent BC *Sebastes* stock assessments, this assessment was able to obtain credible estimates for *M*, for both males and females. This was fortunate, because this meant that it was not necessary to construct a complex synthetic composite stock to cover an appropriate range of values for this parameter. This species also exhibited a divergence in the apparent *M* for males from females. This divergence can be seen in Figure D.9, where there is a long tail of male ages past age 60 but the female ages are nearly gone by age 35. The previous BC CAR stock assessment, conducted in 2007 (Stanley et al. 2009) and updated in 2009 (DFO 2010) approached this issue by hypothesizing that female *M* doubled at age 14. The most recent US CAR stock assessment (Thorson and Wetzel 2016) adopted a similar approach by assuming that female *M* increased relative to the male *M*, also at age 14.

This stock assessment used three hypotheses to investigate the problem of differential female *M* in this population.

- The base run (B1, Run24) estimated *M* for both sexes while not allowing the selectivity functions to have descending right-hand limbs. That is, all fish remained fully selected by the fishery or the survey once maximum selectivity was reached. This run estimated the male median *M* to be 0.065 and the median female *M* to be 0.093.
- Sensitivity run S01 emulated the approach used by the 2007 and 2009 BC stock assessments by estimating separate *M* values for both males and females based on age, with the first estimate applied to ages less than or equal to 13 years (young fish) and the second estimate for ages 14 and older (mature fish). Both male and female *M* were stepped because this parameter was estimated independently by sex and SS3 offered no obvious method of stepping only one sex. However, the mature male *M* was estimated to be 0.069 (median), rising from a median estimate of 0.054 for the young males, indicating that the AF data supported similar (and low) *M* values for both male age brackets. The mature female *M* values rose from a median estimate of 0.061 for young females to 0.145, which are similar to the assumed fixed values (0.06 and 0.12) used in the 2007 and 2009 CAR stock assessments.
- Sensitivity run S09 estimated single *M* values for each sex while allowing the right-hand limbs of the fishery and survey selectivities to descend for females. This approach worked well, with the estimated selectivity functions showing pronounced descending right-hand limbs for the trawl fishery and for five of the surveys (Figure 14) while estimating the median *M* for males at 0.069 and for females at 0.086.

The base run hypothesis (single *M*) was the most parsimonious and appeared to fit the AF data nearly as well as either S01 or S09 (compare total AF likelihoods in Table F.21: B1=302; S01=296; S09=295[18]). Because there is no descending right-hand limb to the selectivity function in the base run and run S01, the trawl fishery selects all CAR older than age 14. Those fish are

[18] The use of the Dirichlet-Multinomial distribution with its estimable weighting parameter allows for comparison of the age frequency likelihoods across model runs.

removed from the population and mature females appear to be more heavily impacted than males, given the lack of older females in the population. In run S09, females gradually become less vulnerable to the fishery as they age (Figure 14), forming a cryptic population that is immune to capture. While this scenario has plausibility, there exists no evidence to support it, making it unlikely to be the basis for a management recommendation. Consequently, Run 24 was selected as the base run (B1) because it fit the available AF data and required the fewest assumptions and parameters. While all three runs were well into the Healthy zone (Figure 10), B1 had the lowest stock depletion among the three runs, with the median estimate of B_{2023}/B_0 equalling 0.78 while the median estimates for the same ratio were 0.94 for S01 and 0.84 for S09 (Table F.20).

Foreign fleet effort in 1965-76 along the BC coast targeted offshore rockfish (mostly POP), and CAR catch for these years was estimated as an assumed bycatch; therefore, the magnitude of the foreign fleet removals of CAR was uncertain. Another source of uncertainty in the catch series comes from domestic landings from the mid-1980s to 1995 (pre-observer coverage) which may have misreported lesser rockfish species to bypass quota restrictions on more desirable species like POP (Starr and Haigh 2022a). However, the sensitivity runs on catch (S05: -30%; S06: +50%) showed that catch uncertainty did not have a major effect on the model's biomass trajectory or on the estimates of the relative stock size at the end of 2022 (Figure 8, Table F.20). However, S06 (+50%) resulted in an increase in absolute stock size (Figure 9), which would imply greater productivity than was estimated by the base run.

In the past, the use of commercial CPUE as an index of abundance was generally avoided in BC rockfish stock assessments (primarily due to uncertainty in vessel behaviour in response to regulations). However, CPUE based on the bycatch of the evaluated species in the BC bottom trawl fishery have been used in several recent stock assessments (Starr and Haigh 2017, 2021 a,b, 2022 a,b,c). Yellowmouth Rockfish (Starr and Haigh 2022c) used CPUE, but this is a species that is also frequently targeted. CAR is sometimes a target species as well as a bycatch species, but is more likely to be taken in conjunction with other rockfish and groundfish species. The CPUE models include the incidence of zero tows as well as the tows which captured the species, which should improve the capacity of the model to track abundance. In general, there is confidence that zero tows have been recorded reasonably well as a result of the high level of observer coverage in the BC bottom trawl fishery, at least up until March 2020. However, the shift to electronic monitoring along with the cessation of the observer programme may have led to a change in the reporting of zero tows.

Two runs relating to CPUE were included in the suite of CAR sensitivity runs:

- Sensitivity run S13 dropped the CPUE series and estimated a stock size about 8% smaller than that in the base run. Given that the catch series was the same for the two models, the stock depletion for S13 was lower than for the base run, with the median estimate of B_{2023}/B_0 dropping from 0.78 for B1 to 0.67 for S13 (Table F.20). This run only had fair MCMC diagnostics as it displayed at least one high excursion in the estimates of log R_0 (Figure F29).
- Sensitivity run S12 substituted a CPUE series based on the Tweedie distribution. This model had some differences in the data selection procedure compared to the selection made for the delta-lognormal model (see Section C.7) and handled zero catch observations differently in that they existed alongside positive catch observations in the same distribution (ranging from Poisson to gamma based on a power parameter; Anderson, DFO, pers. comm. 2022). The resulting Tweedie fit differed from the delta-lognormal fit (Figure C.20) and was included as a sensitivity to provide contrast with the delta-lognormal series. S12 also estimated a stock size about 8% smaller than for the base run and an even lower stock depletion estimate than that seen for S13. The median estimate of B_{2023}/B_0 dropped from 0.78 for B1 to 0.63 for S12 (Table F.20). This run was the most pessimistic of all the sensitivity runs with B_{2023}/B_{MSY} = 2.40 (Figure 10, Table F.20).

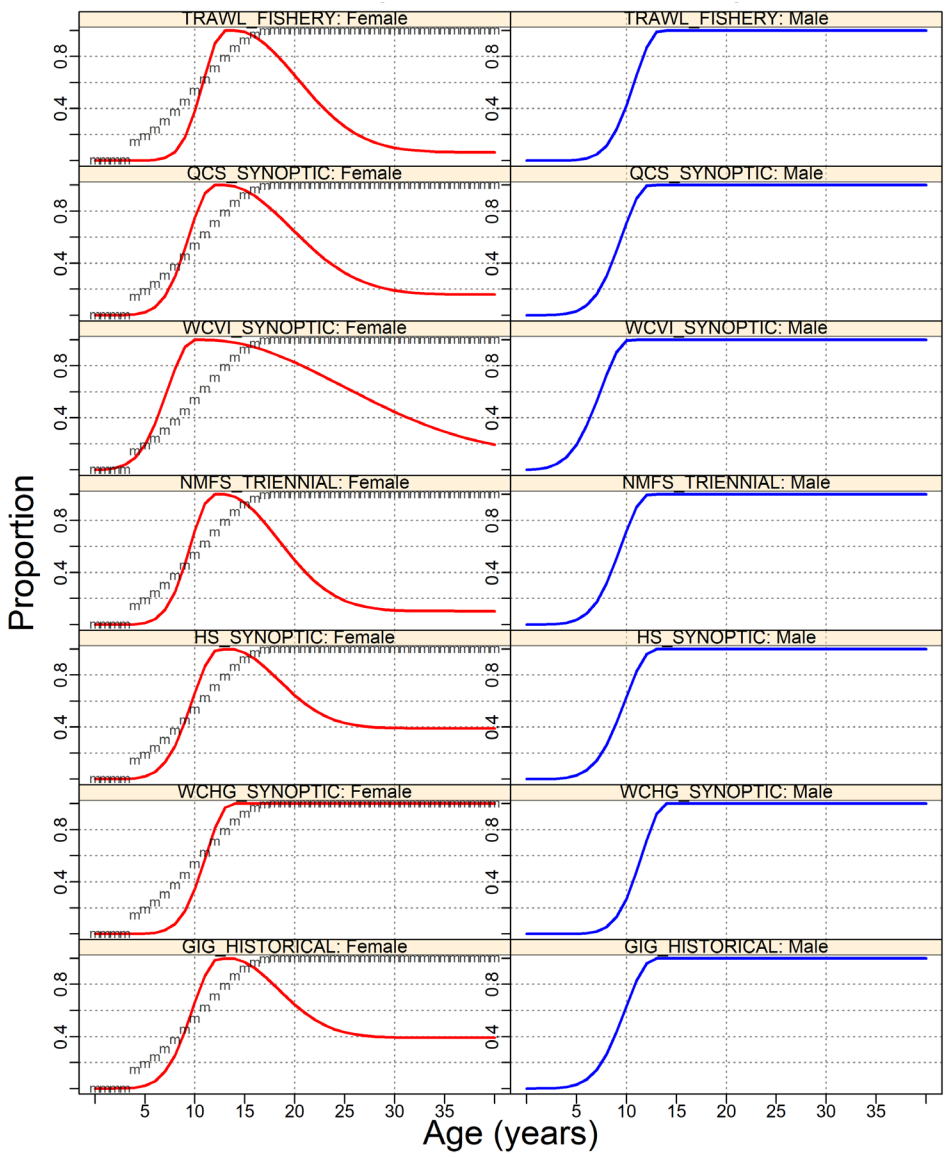

Figure 14. S09 (Run33): Commercial and survey selectivities (all MPD values), with maturity ogive for females indicated by 'm'.

Adding the HBLL longline survey series to the model (S11) also resulted in a more pessimistic run, with the median estimate of B_{2023}/B_0 dropping from 0.78 for B1 to 0.62 for S11 and B_{2023}/B_{MSY} = 2.51 (Table F.20). However, while these surveys may not be monitoring the full range of CAR adults, they may serve as a recruitment and young adult index series if modelled with a descending right-hand selectivity function (Figure B.75 plots the coverage provided by these surveys). This possibility will require an analysis to determine if the hook size used in these surveys reduces the vulnerability of small fish.

More effort was expended on investigating the impact of ageing error in this stock assessment than was done for the YMR stock assessment (Starr and Haigh 2022c), with three sensitivity runs addressing this issue in addition to the base run. In these analyses, ageing error was introduced into the model using a smoothed function rather than the highly variable information based on the individual observations at each age. Figure D.16 plots the smoothed functions along with the underlying age-specific observations.

- The base run (B1) used the AE3 series that resulted from a smoothing function (Figure D.16) of standard deviations (SD) derived from CVs of length-at-age. This function overlapped with the AE5 series (see next bullet) up to age 20, and then stayed high right up to age 60 (Table F.20).
- Sensitivity run S03 implemented the AE5 series (smoothed SD derived from reader error CVs) which dropped away from the AE3 series, reaching zero around age 60. This run was nearly identical to the base run, with the median estimates for B_0, B_{2023} and B_{2023}/B_0 being the same as for B1.
- Sensitivity run S04 implemented a constant 10% error at all ages. This run was also very close to the base run, again with very similar median estimates for B_0, B_{2023} and B_{2023}/B_0 compared to B1 (Table F.20).
- Sensitivity run S02 dropped ageing error entirely. This run diverged from the base run, with B_0 estimated to be 27% greater than for the base run and B_{2023} was 10% greater than for the base run while B_{2023}/B_0 dropped to 0.67 compared to 0.78 for B1 (Table F.20).

While S02 (no ageing error) diverged from the base run, the runs which applied ageing error all returned the same result, perhaps due to the similar standard deviations for younger ages (<25 y). However, even the 'no ageing error' run did not materially change the advice. This result appeared to be quite different than for the YMR stock assessment (Starr and Haigh 2022c).

Raising (S08) or lowering (S07) the standard deviation of recruitment residuals (σ_R) affected the estimate of B_0, where the median estimate rose 13% for S08 and dropped 11% for S07. However, the estimates of B_{2023}/B_0 were similar to the base run, with the median estimate for S07 at 0.77 and at 0.75 for S08 compared to 0.78 for the base run.

The estimates of log(θ) for the Dirichlet-Multinomial were high for all runs where it was used. Parameter estimates above 5 are associated with 99-100% weight with little information in the likelihood about the parameter value (Methot et al. 2021), effectively setting the sample size to the original sample size. Also, the formulation does not allow weights > 1 so this reweighting procedure cannot upweight AF data sets. Sample sizes used in this stock assessment reflected the number of trips or tows sampled; however, the 'maximum realised sample size' of Stewart and Hamel (2014) provides an alternative estimate that attempts to relate both the number of trips/tows and individual fish sampled from those trips/tows. Whether alternative (higher) sample sizes help to improve the fits to log(θ) remains to be explored.

While it appears that it is quite feasible to incorporate environmental index series into a stock assessment, it is hard to evaluate what it means. The degree to which the model uses this information is governed by the relative weight given to the series, which inevitably will be in conflict with some of the model data, leading to a deterioration in the model fit. The series weight will be an arbitrary decision that will depend on how much credence is given to the series and the amount of an effect the analysts judge is sufficient. The main difficulty is that, unlike the equivalent issue between compositional data and biomass data, there is no functional relationship between the data and the model dynamics. Consequently, including these environmental series becomes little more than a correlation analysis. Schirripa et al. (2009) presented a simulation study that evaluated the capacity of two alternative procedures for incorporating environmental data into a stock assessment model. The purpose of the paper was to determine which methodology was superior and it explicitly stated that it did not evaluate how to determine "*...whether the inclusion of the environmental data significantly improves the overall model fit*". They proposed that negative log-likelihoods, with and without the inclusion of the environmental data, could be compared to statistically evaluate the additional parameter(s) used to fit the environmental data. But this comparison will be affected by any change in model data

weighting. In the case of CAR, the weights were changed in each of the three models, with the model having the most weight on the environmental series (E01) being the least credible. However, it is clear from Figure 13 that the resultant recruitment series from all three models indicate that the relationship between recruitment and the PDO series was relatively weak, particularly in the period before 1990 and after 2006.

The recruitment deviation time series suggested a period of below-average recruitment (1935-1995) followed by a period of above-average recruitment (1995 on). While this may have reflected gaps in age composition data, it could also have signalled a regime shift in productivity. The latter was not explored in this stock assessment, but future stock assessments might explore productivity changes through environmental proxies when there appear to be correlated patterns in the recruitment deviations.

The decision tables provide guidance to the selection of short-term catch recommendations and describe the range of possible future outcomes over the projection period at fixed levels of annual catch. The accuracy of the projections was predicated on the model being correct. Uncertainty in the parameters was explicitly addressed using a Bayesian approach but reflected only the specified model and weights assigned to the various data components.

11. FUTURE RESEARCH AND DATA REQUIREMENTS

The following issues should be considered when planning future stock assessments and management evaluations for Canary Rockfish:

1. Continue the suite of fishery-independent trawl surveys that have been established across the BC coast. This includes obtaining age and length composition samples, which will allow the estimation of survey-specific selectivity ogives.
2. Support/improve the collection of additional ageing structures, particularly from the commercial bottom and midwater trawl fisheries. The lack of biological sampling in the commercial fisheries after 2017 was a serious deficiency in this stock assessment.
4. If sufficient midwater trawl fishery biological data become available, consider adding midwater trawl as a separate fishery.
5. Include the HBLL surveys in the base run for the next stock assessment using a descending right-hand selectivity for both sexes. Also request that otoliths be collected from this survey for ageing female and male CAR, along with the usual morphometrics (length, weight, maturity, etc.).
6. Adopt the Tweedie distribution for zero-inflated data common to other DFO CPUE analyses.
7. Explore how hyperallometry in the length relationship influences fecundity (e.g., exponent greater than 3).
8. Consider using constant harvest rates if it is required to project farther than 10 years.
9. Explore the use of a single research survey stock index stitched together using geospatial analysis. Resolve how AF data would be combined to represent this coastwide index if this recommendation is implemented .
10. Explore changes in selectivity over time and how this might be affecting recruitment deviations.
11. The implementation of the PDO index series in this stock assessment was directly linked to the recruitment deviations. It is also possible in SS3 to incorporate such index series as a

pseudo-abundance index that is linked to the model's biomass estimation. This option could be explored in a future CAR stock assessment.

12. Given the unsatisfactory nature of the inclusion of the PDO time series into this stock assessment, it is clear that including this type of information requires more thought. First, a wider range of environmental covariates needs to be identified and the potential effect by each series on fish recruitment evaluated. Then the candidate covariates should be evaluated across a range of species, not just within a single-species stock assessment. It is fairly clear that this approach could create a source document that could be referenced by future stock assessments. If an index series relevant to a species is identified, then the stock assessment will have a more defensible basis on which to include the series.

12. ACKNOWLEDGEMENTS

The principal scientists behind the Stock Synthesis stock assessment platform offered much help and support during the Canary model runs. In particular, the authors thank Richard Methot (NOAA[19]), Ian Taylor (NWFSC[20], NOAA), Chantel Wetzel (NWFSC, NOAA), and Kathryn Doering (NWFSC, NOAA). Additional guidance and data were provided by Dana Haggerty (PBS, DFO), Sean Anderson (PBS, DFO), Philina English (PBS, DFO), Bruce Turris (CGRCS[21]) and Brian Mose (CIC[22] Trawl). The staff in the Sclerochronology Laboratory at the PBS were, as always, quick to process CAR otolith requests. Written peer reviews by Kendra Holt (PBS, DFO) and Aaron Berger (NWFSC, NOAA) provided helpful guidance and discussion during the regional peer review (RPR) meeting. Ben Davis (NWAFC[23], DFO) facilitated the RPR meeting as Chair and Yvonne Muirhead-Vert acted as Rapporteur. Additional feedback by other RPR participants contributed greatly to the process.

13. REFERENCES

Anderson, S.C., Keppel, E.A. and Edwards, A.M. 2019. A reproducible data synopsis for over 100 species of British Columbia groundfish. DFO Can. Sci. Advis. Sec. Res. Doc. 2019/041. vii + 321 p.

Conrath, C.L. 2017. Maturity, spawning omission, and reproductive complexity of deepwater rockfish. Trans. Am. Fish. Soc. 145. 495-507.

COSEWIC. 2007. COSEWIC assessment and status report on the Canary Rockfish *Sebastes pinniger* in Canada. Tech. rep., Committee on the Status of Endangered Wildlife in Canada, Ottawa ON, xi + 49 p.

DFO. 2009a. A fishery decision-making framework incorporating the Precautionary Approach.

DFO. 2010. Stock assessment update for British Columbia Canary Rockfish. DFO Can. Sci. Advis. Sec. Sci. Resp. 2009/019.

DFO. 2015. Yellowtail Rockfish (*Sebastes flavidus*) stock assessment for the coast of British Columbia, Canada. DFO Can. Sci. Advis. Sec. Sci. Advis. Rep. 2015/010.

[19] National Oceanic and Atmospheric Administration, Dept. Commerce, USA

[20] Northwest Fisheries Science Center, Seattle WA

[21] Canadian Groundfish Research and Conservation Society, New Westminster BC

[22] Commercial Industry Caucus, BC

[23] Northwest Atlantic Fisheries Centre, St. John's NL

DFO. 2016. Guidelines for providing interim-year updates and science advice for multi-year assessments. DFO Can. Sci. Advis. Sec. Sci. Advis. Rep. 2016/020.

DFO. 2019. Pacific Region Integrated Fisheries Management Plan – Groundfish: Effective February 21, 2019 (Version 1.1).

DFO. 2022. A data synopsis for British Columbia groundfish: 2021 data update. DFO Can. Sci. Advis. Sec. Sci. Resp. 2022/020.

Dick, E.J., Beyer, S., Mangel, M. and Ralston, S. 2017. A meta-analysis of fecundity in rockfishes (genus *Sebastes*). Fish. Res. 187. 73-85.

Doherty, B., Benson, A. and Cox, S. 2019. Data summary and review of the PHMA hard bottom longline survey in British Columbia after the first 10 years (2006-2016). Can. Tech. Rep. Fish. Aquat. Sci. 3276. ix + 75 p.

Edwards, A.M., Haigh, R. and Starr, P.J. 2012a. Stock assessment and recovery potential assessment for Canary Rockfish (*Sebastes pinniger*) along the Pacific coast of Canada. DFO Can. Sci. Advis. Sec. Res. Doc. 2012/095: iv + 188 p.

Edwards, A.M., Starr, P.J. and Haigh, R. 2012b. Stock assessment for Pacific ocean perch (*Sebastes alutus*) in Queen Charlotte Sound, British Columbia. DFO Can. Sci. Advis. Sec. Res. Doc. 2011/111: viii + 172 p.

Edwards, A.M., Haigh, R. and Starr, P.J. 2014a. Pacific Ocean Perch (*Sebastes alutus*) stock assessment for the north and west coasts of Haida Gwaii, British Columbia. DFO Can. Sci. Advis. Sec. Res. Doc. 2013/092: vi + 126 p.

Edwards, A.M., Haigh, R. and Starr, P.J. 2014b. Pacific Ocean Perch (*Sebastes alutus*) stock assessment for the west coast of Vancouver Island, British Columbia. DFO Can. Sci. Advis. Sec. Res. Doc. 2013/093: vi + 135 p.

Forrest, R.E., McAllister, M.K., Dorn, M.W., Martell, S.J.D. and Stanley, R.D. 2010. Hierarchical Bayesian estimation of recruitment parameters and reference points for Pacific rockfishes (*Sebastes* spp.) under alternative assumptions about the stock-recruit function. Can. J. Fish. Aquat. Sci. 67. 1611–1634.

Forrest, R.E., Holt, K.R. and Kronlund, A.R. 2018. Performance of alternative harvest control rules for two Pacific groundfish stocks with uncertain natural mortality: bias, robustness and trade-offs. Fish. Res. 206. 259–286.

Francis, R.I.C.C. 2011. Data weighting in statistical fisheries stock assessment models. Can. J. Fish. Aquat. Sci. 68(6): 1124–1138.

Haigh, R., Starr, P.J., Edwards, A.M., King, J.R. and Lecomte, J.B. 2018. Stock assessment for Pacific Ocean Perch (*Sebastes alutus*) in Queen Charlotte Sound, British Columbia in 2017. DFO Can. Sci. Advis. Sec. Res. Doc. 2018/038: v + 227 p.

Haigh, R. and Yamanaka, K.L. 2011. Catch history reconstruction for rockfish (*Sebastes* spp.) caught in British Columbia coastal waters. Can. Tech. Rep. Fish. Aquat. Sci. 2943. viii + 124 p.

He, X., Field, J.C., Beyer, S.G. and Sogard, S.M. 2015. Effects of size-dependent relative fecundity specifications in fishery stock assessments. Fish. Res. 165. 54-62.

Hoenig, J.M. 1983. Empirical use of longevity data to estimate mortality rates. Fish. Bull. 82(1): 898-903.

Jorgensen, B. 1987. Exponential dispersion models. J. Royal Stat. Soc. Series B (Methodological) 49(2). 127-162.

Knaus, J. 2015. snowfall: Easier cluster computing (based on snow). R package ver. 1.84-6.1.

Love, M.S., Yoklavich, M. and Thorsteinson, L. 2002. The Rockfishes of the Northeast Pacific. University of California Press, Berkeley and Los Angeles, California.

McAllister, M.K. and Ianelli, J.N. 1997. Bayesian stock assessment using catch-age data and the sampling – importance resampling algorithm. Can. J. Fish. Aquat. Sci. 54(2). 284-300.

Methot, R.D. and Wetzel, C.R. 2013. Stock Synthesis: A biological and statistical framework for fish stock assessment and fishery management. Fish. Res. 142. 86-99.

Methot, R.D., Wetzel, C.R., Taylor, I.G., Doering, K.L., and Johnson, K.F. 2021. Stock Synthesis User Manual, version 3.30.18. October 1, 2021. NOAA Fisheries, Seattle WA. iv + 233 p.

Methot, R.D., Wetzel, C.R., Taylor, I.G., Doering, K.L., and Johnson, K.F. 2022. Stock Synthesis User Manual, version 3.30.20. September 30, 2022. NOAA Fisheries, Seattle WA. iv + 243 p.

Monnahan, C.C., Branch, T.A., Thorson, J.T., Stewart, I.J. and Szuwalski, C.S. 2019. Overcoming long Bayesian run times in integrated fisheries stock assessments. ICES J. Mar. Sci. 76(6). 1477-1488.

Monnahan, C.C. and Kristensen, K. 2018. No-U-turn sampling for fast Bayesian inference in ADMB and TMB: Introducing the adnuts and tmbstan R packages. PLoS ONE 13(5). e0197,954.

New Zealand Ministry of Fisheries. 2011. Operational Guidelines for New Zealand's Harvest Strategy Standard. Ministry of Fisheries, New Zealand.

Rideout, R.M. and Tomkiewicz, J. 2011. Skipped spawning in fishes: More common than you might think. Mar. Coast. Fish. 3. 176-189.

Schirripa, M.J., Goodyear, C.P. and Methot, R.M. 2009. Testing different methods of incorporating climate data into the assessment of US West Coast sablefish. ICES J. Mar. Sci. 66(7). 1605-1613.

Stanley, R.D. 1987. A comparison of age estimates derived from the surface and cross-section methods of otolith reading for Pacific ocean perch (*Sebastes alutus*). In Proceedings of the International Rockfish Symposium, Anchorage, Alaska USA, October 20-22, 1986, Lowell Wakefield Fisheries Symposium, Alaska Sea Grant Rep. No. 87-2, p. 187-196.

Stanley, R.D. and Kronlund, A.R. 2000. Silvergray rockfish (*Sebastes brevispinis*) assessment for 2000 and recommended yield options for 2001/2002. DFO Can. Sci. Advis. Sec. Res. Doc. 2000/173: 116 p.

Stanley, R.D., Starr, P., Olsen, N., Rutherford, K. and Wallace, S.S. 2005. Status report on Canary rockfish *Sebastes pinniger*. DFO Can. Sci. Advis. Sec. Res. Doc. 2005/089. vi + 105 p.

Stanley, R.D., Starr, P. and Olsen, N. 2009. Stock assessment for Canary rockfish (*Sebastes pinniger*) in British Columbia waters. DFO Can. Sci. Advis. Sec. Res. Doc. 2009/013. xxii + 198 p.

Starr, P.J. and Haigh, R. 2017. Stock assessment of the coastwide population of Shortspine Thornyhead (*Sebastolobus alascanus*) in 2015 off the British Columbia coast. DFO Can. Sci. Advis. Sec. Res. Doc. 2017/015: ix + 174 p.

Starr, P.J. and Haigh, R. 2021a. Redstripe Rockfish (*Sebastes proriger*) stock assessment for British Columbia in 2018. DFO Can. Sci. Advis. Sec. Res. Doc. 2021/014. vii + 340 p.

Starr, P.J. and Haigh, R. 2021b. Widow Rockfish (*Sebastes entomelas*) stock assessment for British Columbia in 2019. DFO Can. Sci. Advis. Sec. Res. Doc. 2021/039. vi + 238 p.

Starr, P.J. and Haigh, R. 2022a. Bocaccio (*Sebastes paucispinis*) stock assessment for British Columbia in 2019, including guidance for rebuilding plans. DFO Can. Sci. Advis. Sec. Res. Doc. 2022/001. vii + 292 p.

Starr, P.J. and Haigh, R. 2022b. Rougheye/Blackspotted Rockfish (*Sebastes aleutianus/melanostictus*) stock assessment for British Columbia in 2020. DFO Can. Sci. Advis. Sec. Res. Doc. 2022/022. vii + 385 p.

Starr, P.J. and Haigh, R. 2022c. Yellowmouth Rockfish (*Sebastes reedi*) stock assessment for British Columbia in 2021. DFO Can. Sci. Advis. Sec. Res. Doc. 2022/10. viii + 288 p.

Starr, P.J., Haigh, R. and Grandin, C. 2016. Stock assessment for Silvergray Rockfish (*Sebastes brevispinis*) along the Pacific coast of Canada. DFO Can. Sci. Advis. Sec. Res. Doc. 2016/042: vi + 170 p.

Stewart, I.J. and Hamel, O.S. 2014. Bootstrapping of sample sizes for length- or age-composition data used in stock assessments. Can. J. Fish. Aquat. Sci. 71(4). 581-588.

Thorson, J.T., Johnson, K.F., Methot, R.D. and Taylor, I.G. 2017. Model-based estimates of effective sample size in stock assessment models using the Dirichlet-multinomial distribution. Fish. Res. 192. 84-93.

Thorson, J.T. and Wetzel, C. 2016. The status of canary rockfish (*Sebastes pinniger*) in the California Current in 2015. PFMC groundfish stock assessment documents 2016/05. iv + 678 p.

APPENDIX A. CATCH DATA

A.1. BRIEF HISTORY OF THE FISHERY

Forrester (1969) provides a brief history of the Pacific Marine Fisheries Commission (PMFC), which is reproduced (with some modification) below. Currently, the PMFC is called the Pacific States Marine Fisheries Commission; however, this document retains the acronym 'PMFC' for historical context.

> *The Pacific Marine Fisheries Commission (PMFC) was created in 1947 when the states of Washington, Oregon, and California jointly formed an interstate agreement (called a 'compact') with the consent of the 80th Congress of the USA. In 1956, informal agreement was reached among various research agencies along the Pacific coast to establish a uniform description of fishing areas as a means of coordinating the collection and compilation of otter trawl catch statistics. This work was undertaken by the PMFC with the informal cooperation of the Fisheries Research Board of Canada. Areas 1A, 1B, and 1C encompass waters off the California coast, while Areas 2A-2D involve waters adjacent to Oregon and a small part of southern Washington. The remainder of the Washington coast and the waters off the west coast of Vancouver Island comprise Areas 3A-3D, while United States and Canadian inshore waters (Juan de Fuca Strait, Strait of Georgia, and Puget Sound) are represented by Areas 4A and 4B, respectively. Fishing grounds between the northern end of Vancouver Island and the British Columbia-Alaska boundary are represented by Areas 5A-5E. The entire Alaskan coast is designated as Area 6, but except for a small amount of fishing in inshore channels, this area has not been trawled intensively by North American nationals.*

The early history of the British Columbia (BC) trawl fleet was covered by Forrester and Smith (1972). A trawl fishery for slope rockfish has existed in BC since the 1940s. Aside from Canadian trawlers, foreign fleets targeted Pacific Ocean Perch (POP, *Sebastes alutus*) in BC waters for approximately two decades. These fleets were primarily from the USA (1959–1976), the USSR (1965–1968), and Japan (1966–1976). Consequently, the foreign vessels removed large amounts of rockfish biomass, including species other than POP, in Queen Charlotte Sound (QCS, Ketchen 1976, 1980b), off the west coast of Haida Gwaii (WCHG, Ketchen 1980a,b), and off the west coast of Vancouver Island (WCVI, Ketchen 1976, 1980a,b). All foreign fleets were excluded from Canadian waters inside of 200 nm with the declaration of the Exclusive Economic Zone in 1977. Canadian effort escalated in 1985, and for the next decade, landings by species were often misreported to avoid species-specific trip limits.

The bulk of the BC population of Canary Rockfish is found off the west coast of Vancouver Island and in Queen Charlotte Sound (central BC coast, see Figure A.1), largely in association with the three main gullies – Goose Island, Mitchell's, and Moresby. There are a few 'hotspots' near Langara Spit and in Dixon Entrance (north of Graham Island, Haida Gwaii); however, catch in the northern regions is dwarfed by that from further south. Adults aggregate around pinnacles and other high-relief rock (Love et al. 2002). Preliminary analyses in 2021 showed no strong evidence for stock separation along the BC coast based on growth and size frequencies; therefore, the coastwide population will continue to be assessed as one unit.

In 2012, measures were introduced to reduce and manage the bycatch of corals and sponges by the BC groundfish bottom trawl fishery. These measures were developed jointly by industry and environmental non-governmental organisations (Wallace et al. 2015), and included: limiting the footprint of groundfish bottom trawl activities, establishing a combined bycatch conservation limit for corals and sponges, and establishing an encounter protocol for individual trawl tows when the combined coral and sponge catch exceeded 20 kg. These measures have been

incorporated into DFO's Pacific Region Groundfish Integrated Fisheries Management Plan (Feb 21, 2021, version 1.1) and apply to all vessels using trawl gear in BC.

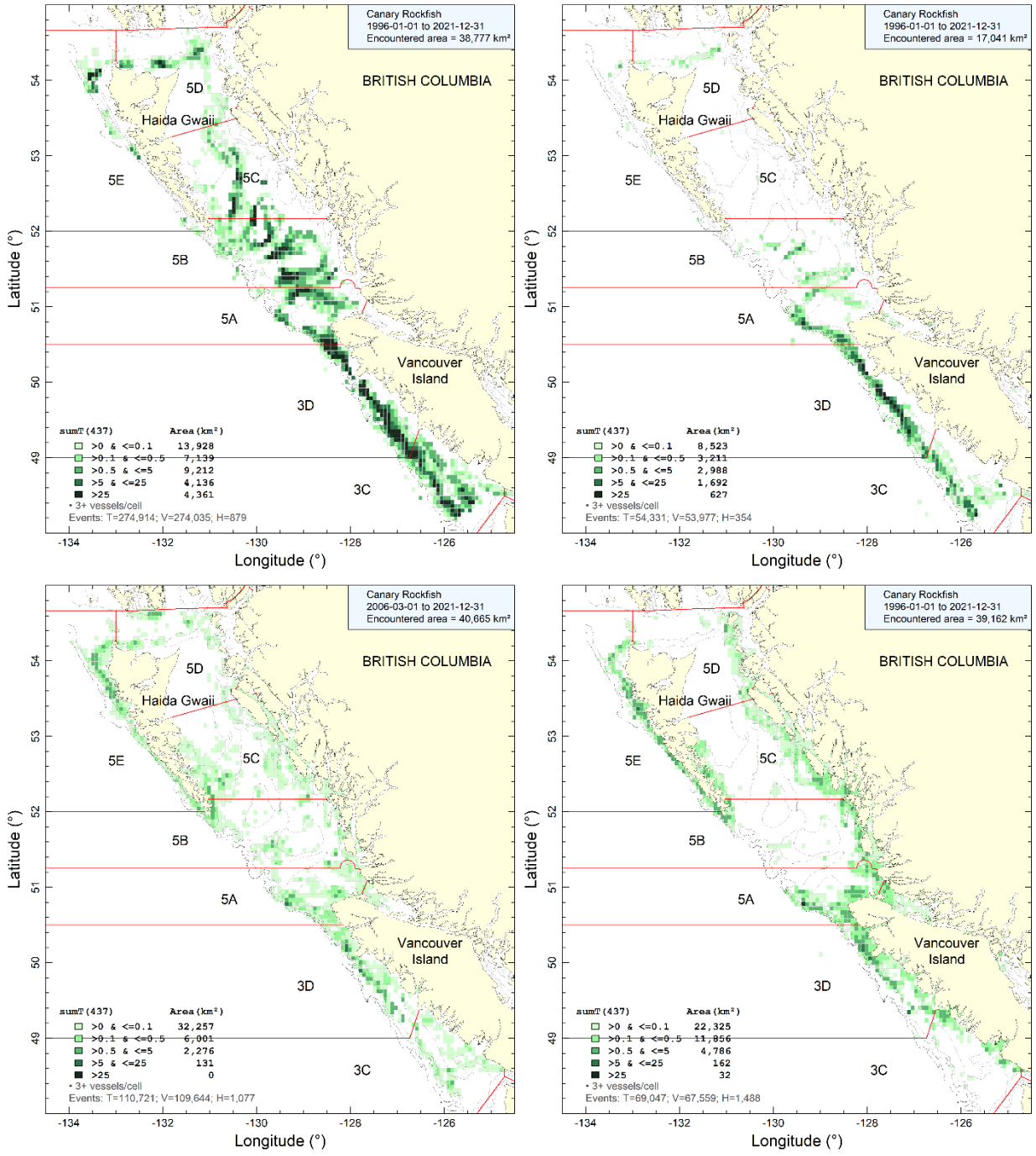

Figure A.1. Aerial distribution of accumulated CAR catch (tonnes) by bottom trawl (upper left), midwater trawl (upper right), halibut fishery (lower left), and outside hook and line fishery (lower right) from 1996 to 2021 in grid cells 0.075° longitude by 0.055° latitude (roughly 32 km²). Isobaths show the 100, 200, 500, and 1200 m depth contours. Note that cells with <3 fishing vessels are not displayed.

Table A.1. Annual Total Allowable Catch (TAC tonnes/year) for CAR caught in BC waters: year can either be calendar year (1993-1996) or fishing year (1997 on). See Table A.2 for details on sector and research allocations, as well as aggregate quotas (e.g., 1994 Trawl coastwide).

			Trawl					Hook & Line					All Sectors				
Year	Start	End	3CD	5AB	5CD	5E	CST	3CD	5AB	5CD	5E	CST	3CD	5AB	5CD	5E	CST
1981	1/1/1981	12/31/1981	350	–	–	–	–	–	–	–	–	–	350	–	–	–	–
1982	1/1/1982	12/31/1982	350	1100	–	–	–	–	–	–	–	–	350	1100	–	–	–
1983	1/1/1983	12/31/1983	600	1100	200	–	–	–	–	–	–	–	600	1100	200	–	–
1984	1/1/1984	12/31/1984	1200	1100	450	950	–	–	–	–	–	–	1200	1100	450	950	–
1985	1/1/1985	12/31/1985	1300	1100	450	950	–	–	–	–	–	–	1300	1100	450	950	–
1986	1/1/1986	12/31/1986	1050	1100	300	750	4100	–	–	–	–	–	1050	1100	300	750	4100
1987	1/1/1987	12/31/1987	1050	1100	300	750	–	–	–	–	–	–	1050	1100	300	750	–
1988	1/1/1988	12/31/1988	1100	1100	300	750	3850	–	–	–	–	–	1100	1100	300	750	3850
1989	1/1/1989	12/31/1989	600	425	300	500	1575	–	–	–	–	–	600	425	300	500	1575
1990	1/1/1990	12/31/1990	–	–	–	250	1475	–	–	–	–	–	–	–	–	250	1475
1991	1/1/1991	12/31/1991	–	–	–	125	1350	–	–	–	–	–	–	–	–	125	1350
1992	1/1/1992	12/31/1992	–	–	–	50	1275	–	–	–	–	–	–	–	–	50	1275
1993	1/1/1993	12/31/1993	–	–	–	–	850	–	–	–	–	–	–	–	–	–	850
1994	1/15/1994	12/31/1994	–	–	–	–	12574	–	–	–	–	–	–	–	–	–	12574
1995	1/1/1995	12/31/1995	–	–	–	–	9716	–	–	–	–	–	–	–	–	–	9716
1996	2/6/1996	3/31/1997	–	–	–	–	2085	–	–	–	–	–	–	–	–	–	2085
1997	4/1/1997	3/31/1998	503	345	81	–	929	–	–	–	–	906	503	345	81	–	1835
1998	4/1/1998	3/31/1999	503	345	81	–	929	–	–	–	–	74	503	345	81	–	1003
1999	4/1/1999	3/31/2000	499	342	80	–	921	–	–	–	–	76	499	342	80	–	997
2000	4/1/2000	3/31/2001	555	277	106	159	1097	–	–	–	–	92.5	555	277	106	159	1190
2001	4/1/2001	3/31/2002	529	265	101	151	1046	–	–	–	–	140	529	265	101	151	1186
2002	4/1/2002	3/31/2003	529	265	101	151	1046	–	–	–	–	140	529	265	101	151	1186
2003	4/1/2003	3/31/2004	529	265	101	151	1046	–	–	–	–	140	529	265	101	151	1186
2004	4/1/2004	3/31/2005	529	265	101	151	1046	–	–	–	–	140	529	265	101	151	1186
2005	4/1/2005	3/31/2006	529	265	101	151	1046	–	–	–	–	140	529	265	101	151	1186
2006	4/1/2006	3/31/2007	529	265	101	151	1046	74	37	14	21	147	604	302	115	173	1193
2007	3/10/2007	3/31/2008	529	265	101	151	1046	74	37	14	21	147	604	302	115	173	1193
2008	3/8/2008	2/20/2009	450	230	90	30	800	57	28	11	16	112	507	258	101	46	912
2009	2/21/2009	2/20/2010	400	145	40	10	595	19	33	15	16	84	419	178	55	26	679
2010	2/21/2010	2/20/2011	569	155	55	10	789	26	43	21	21	111	625	183	66	26	900
2011	2/21/2011	2/20/2013	503	197	79	10	789	26	43	21	21	111	529	240	100	31	900
2012	2/21/2011	2/20/2013	503	197	79	10	789	26	43	21	21	111	529	240	100	31	900
2013	2/21/2013	2/20/2014	503	197	79	10	789	26	43	21	21	111	529	240	100	31	900
2014	2/21/2014	2/20/2015	503	197	79	10	789	26	43	21	21	111	529	240	100	31	900
2015	2/21/2015	2/20/2016	503	197	79	10	789	24	42	19	20	116	527	239	98	30	905
2016	2/21/2016	2/20/2017	503	197	79	10	789	24	42	19	20	116	527	239	98	30	905
2017	2/21/2017	2/20/2018	615	241	97	12	965	31	53	25	26	135	646	294	122	38	1100
2018	2/21/2018	2/20/2019	615	241	97	12	965	31	53	25	26	135	646	294	122	38	1100
2019	2/21/2019	2/20/2020	615	241	97	12	965	31	53	25	26	135	646	294	122	38	1100
2020	2/21/2020	2/20/2021	615	241	97	12	965	31	53	25	26	135	646	294	122	38	1100
2021	2/21/2021	2/20/2022	615	241	97	12	965	31	53	25	26	135	646	294	122	38	1100

Table A.2. Codes to notes on management actions and quota adjustments that appear in Table A.1. Abbreviations that appear under 'Management Actions': Agg = Aggregate, DFO = Department of Fisheries & Oceans, DMP = dockside monitoring program, GTAC =Groundfish Trawl Advisory Committee, H&L = hook and line, IFMP = Integrated Fisheries Management Plan, IVQ = individual vessel quota, MC =Mortality Cap, TAC =Total Allowable Catch, TWL = Trawl. See Archived Integrated Fisheries Management Plans - Pacific Region for further details. Rockfish species codes: BKR=Black, CAR=Canary, CHR=China, CPR=Copper, LST=Longspine Thornyhead, ORF=Other rockfish, POP=Pacific Ocean Perch, QBR=Quillback, RER=Rougheye/Blackspotted, RSR=Redstripe, SCR=Sharpchin, SGR=Silvergray, SKR=Shortraker, SST=Shortspine Thornyhead, TIR=Tiger, WWR=Widow, YMR=Yellowmouth, YTR=Yellowtail.

Year	Management Actions
1981	SRF: Shelf rockfish aggregate is [CAR] for 3D.
1982	SRF: Shelf rockfish aggregates are [CAR] for 3D, [CAR+SGR] for 5AB.
1983	SRF: Shelf rockfish aggregates are [CAR+SGR+YTR] for 3D; [CAR+SGR] for 5AB; [CAR+YTR] for 5CD.
1984	SRF: Shelf rockfish aggregates are [CAR+SGR+YTR] for 3C, 3D, 5E; [CAR+SGR] for 5AB; [CAR+YTR] for 5CD.
1985	SRF: Shelf rockfish aggregates are [CAR+SGR+YTR] for 3C, 3D, 5E; [CAR+SGR] for 5AB; [CAR] for 5CD.
1986	SRF: Shelf rockfish aggregates are [CAR+SGR+YTR] for 3C, 3D, 5E; [CAR+SGR] for 5AB; [CAR] for 5CD; coastwide quota = 4100t; 1986 quotas revised in 1988 MP to exclude YTR.
1987	SRF: Shelf rockfish aggregates are [CAR+SGR] for 3C, 3D, 5AB, 5E; [CAR] for 5CD.
1988	SRF: Shelf rockfish aggregates are [CAR+SGR] for 3C, 3D, 5AB, 5E; [CAR] for 5CD.
1989	CAR: In 1989, quota rockfish comprising Pacific Ocean Perch, Yellowmouth Rockfish, Canary Rockfish and Silvergray Rockfish, will be managed on a coastwide basis.
1990	CAR: Only one half of the 1990 5E South area quotas (250t of CAR and 125t of SGR) have been included in the overall coastwide quotas, due to past underharvesting. Should the area quotas allocated be attained, additional quotas of 250t for CAR and 125t for SGR may be added to the coastwide quotas at a later date.
1991	CAR: For 5E South, 125t of CAR and 125t of SGR have been included in the overall coastwide quotas, due to past underharvesting. Should the allocated area quotas be attained, further tonnages may be added to the applicable coastwide quotas at a later date.
1992	CAR: For 5E South, 50t of CAR and 125t of SGR have been included in the overall coastwide quotas, due to past underharvesting. Should the allocated area quotas be attained, further tonnages may be added to the applicable coastwide quotas at a later date.
1994	TWL: Started a dockside monitoring program (DMP) for the Trawl fleet.
1994	CAR: As a means of both reducing at-sea discarding and simplifying the harvesting regime, rockfish aggregation was implemented. Through consultation with GTAC, the following aggregates were identified: Agg 1= POP, YMR, RER, CAR, SGR, YTR; Agg 2= RSR, WWR; Agg 3= SKR, SST, LST; Agg 4= ORF.
1995	CAR: Trawl aggregates established in 1994 changed: Agg 1= CAR, SGR, YTR, WWR, RER; Agg 2= POP, YMR, RSR; Agg 3= SKR, SST, LST; Agg 4= ORF.
1996	TWL: Started 100% onboard observer program for offshore Trawl fleet.
1996	CAR: Rockfish aggregation will continue on a limited basis in 1996: Agg 1= YTR, WWR; Agg 2= CAR, SGR; Agg 3= POP, YMR; Agg 4= RER, SKR; Agg 5= RSR, SCR; Agg 6= ORF incl. SST, LST
1996	CAR: groundfish equivalent price (GFE) relative to POP = 1.19
1997	TWL: Started IVQ system for Trawl Total Allowable Catch (TAC) species (April 1, 1997)
1997	H&L: All H&L rockfish, with the exception of YYR, shall be managed under the following rockfish aggregates: Agg 1= QBR, CPR; Agg 2= CHR, TIR; Agg 3= CAR, SGR; Agg 4= RER, SKR, SST, LST; Agg 5= POP, YMR, RSR; Agg 6= YTR, BKR, WWR; Agg 7= ORF excluding YYR.
2000	ALL: Formal discussions between the hook and line rockfish (ZN), halibut and trawl sectors were initiated in 2000 to establish individual rockfish species allocations between the sectors to replace the 92/8 split. Allocation arrangements were agreed to for rockfish species that are not currently under TAC. Splits agreed upon for these rockfish will be implemented in the future when or if TACs are set for those species.
2001	ALL: An agreement reached amongst the commercial groundfish industry has established the allocation of the rockfish species between the commercial Groundfish Trawl and Groundfish Hook and Line sectors.
2001	CAR: Sector allocations: T=87.7%, HL=12.3%
2002	TWL: Closed areas to preserve four hexactinellid (glassy) sponge reefs.
2003	CAR: Species at Risk Act (SARA) came into force in 2003.
2006	ALL: Introduced an Integrated Fisheries Management Plan (IFMP) for all directed groundfish fisheries.
2006	H&L: Implemented 100% at-sea electronic monitoring and 100% dockside monitoring for all groundfish H&L fisheries.
2006	CAR: Sector allocations: T=87.7%, ZN=11.77%, L=0.53%
2007	CAR: Research allocation: H&L=7.0t

Year	Management Actions
2008	CAR: Stock status reviewed in Nov 2007; stock declined from original biomass but decline likely arrested; uncertain if recent catch levels will ensure rebuild; TAC for Canary reduced from 1193t to 912t coastwide.
2008	CAR: Research allocation: H&L=7.0t
2009	CAR: TAC for Canary further reduced from 912t to 679t coastwide.
2009	CAR: COSEWIC-designated marine species in Pacific region under consideration for listing under Schedule I of SARA: Canary as 'Threatened'.
2009	CAR: Research allocation: H&L=4.0t
2010	CAR: Stock status reviewed in Dec 2009; stock declined from unfished equilibrium biomass but decline likely arrested; TAC for Canary increased to 900t coastwide; stock expected to rebuild and remain at levels consistent with DFO's Precautionary Approach.
2010	CAR: Research allocation: H&L=6.0t
2011	CAR: Research allocation: H&L=6.0t
2012	TWL: Froze the footprint of where groundfish bottom trawl activities can occur (all vessels under the authority of a valid Category T commercial groundfish trawl license selecting Option A as identified in the IFMP).
2013	TWL: To support groundfish research, the groundfish trawl industry agreed to the trawl TAC offsets to account for unavoidable mortality incurred during the joint DFO-Industry groundfish multi-species surveys in 2013.
2013	CAR: Research allocations: Trawl=2.1t, H&L=6.0t
2014	CAR: Research allocation: H&L=6.0t
2015	ALL: Research allocations were specified starting in 2015 to account for the mortalities associated with survey catches to be covered by TACs.
2015	CAR: Research allocations: Trawl=2.7t, Longline=6.0t, Total=8.7t
2016	CAR: Research allocations: Trawl=3.3t, Longline=6.0t, Total=9.3t
2017	CAR: Research allocations: Trawl=2.3t, Longline=6.0t, Total=8.3t
2018	CAR: Research allocations: Trawl=4.1t, Longline=6.4t, Total=10.5t
2019	CAR: Research allocations: Trawl=2.0t, Longline=1.2t, Total=3.2t
2020	CAR: Research allocations: Trawl=6.2t, Longline=6.5t, Total=12.7t
2021	CAR: Research allocations: Trawl=1.8t, Longline=6.5t, Total=8.3t

A.2. CATCH RECONSTRUCTION

This assessment reconstructs CAR catch back to 1918 but considers the start of the fishery to be 1935 (Figure A.2) before the fishery started to increase during World War II. Prior to this, trawl catches were negligible and halibut fleet catches of CAR were estimated to be <20 tonnes per year. During the period 1950–1975, US vessels routinely caught more rockfish than did Canadian vessels. Additionally, from the mid-1960s to the mid-1970s, foreign fleets (Russian and Japanese) removed large amounts of rockfish, primarily POP. These large catches were first reported by various authors (Westrheim et al. 1972; Gunderson et al. 1977; Leaman and Stanley 1993); however, Ketchen (1980a,b) re-examined the foreign fleet catch, primarily because statistics from the USSR called all rockfish 'perches' while the Japanese used the term 'Pacific ocean perch' indiscriminately. In the catch reconstruction, all historical foreign catches (annual rockfish landings) were tracked separately from Canadian landings, converted to foreign-caught CAR (Section A.2.2), and added to total CAR landings during the reconstruction process.

A.2.1. Data sources

Starting in 2015, all official Canadian catch tables from the databases below (except PacHarv3) have been merged into one table called 'GF_MERGED_CATCH', which is available in DFO's GFFOS database. All groundfish DFO databases are now housed on the DFBCV9TWVASP001 server. CAR catch by fishery sector ultimately comes from the following seven DFO databases:

- PacHarv3 sales slips (1982-1995) – hook and line only;
- GFCatch (1954-1995) – trawl and trap;
- PacHarvHL merged data table (1986-2006) – halibut, Schedule II troll, ZN rockfish;
- PacHarvSable fisherlogs (1995-2005) – Sablefish trap and longline;
- PacHarvest observer trawl (1996-2007) – primarily bottom trawl;
- GFFOS groundfish subset from Fishery Operation System (2006-present) – all fisheries and modern surveys; and
- GFBioSQL joint-venture hake and research survey catches (1947-present) – multiple gear types. GFBioSQL is an SQL Server database that mirrors the GFBio Oracle database.

All data sources other than PacHarv3 were superseded by GFFOS from 2007 on because this latter repository was designed to record all Canadian west coast landings and discards from commercial fisheries and research activities. Reporting changed in GFFOS to reflect fishing 'sectors' that were different for some of the fisheries; primarily, Schedule II became 'Spiny Dogfish' and 'Lingcod' while ZN hook and line became 'Rockfish Inside' and 'Rockfish Outside'.

Prior to the modern catch databases, historical landings of aggregate rockfish – either total rockfish (TRF) or rockfish other than POP (ORF) – are reported by eight different sources (see Haigh and Yamanaka 2011). The earliest historical source of rockfish landings comes from Canada Dominion Bureau of Statistics (1918-1950).

The purpose of this procedure was to estimate the reconstructed catch of any rockfish species (generically designated as RRF) from ratios of RRF/ORF or RRF/TRF, add the estimated discards from the ratio RRF/TAR (where TAR is the target species landed by fishery), to reconstruct the total catch of species RRF.

A.2.2. Reconstruction details

A.2.2.1. Definition of terms

A brief synopsis of the catch reconstruction (CR) follows, with a reminder of the definition of terms:

Fisheries: there are five fisheries in the reconstruction (even though trawl dominates the CAR fishery):

- T = groundfish trawl (bottom + midwater),
- H = Halibut longline,
- S = Sablefish trap/longline,
- DL = Dogfish and Lingcod troll/longline (originally called 'Schedule II'),
- ZN = hook and line rockfish (sector called 'ZN' from 1986 to 2006 and 'Rockfish Outside' and 'Rockfish Inside' from 2007 on).

TRF: acronym for 'total rockfish' (all species of *Sebastes* + *Sebastolobus*)

ORF: acronym for 'other rockfish' (= TRF minus POP), landed catch aggregated by year, fishery, and PMFC (Pacific Marine Fisheries Commission) major area

POP: Pacific Ocean Perch

RRF: Reconstructed rockfish species – in this case, CAR

TAR: Target species landed catch

L & D: L =landed catch, D =releases (formerly called 'discards')

gamma: mean of annual ratios, $\sum_i \mathrm{RRF}_i^L / \mathrm{ORF}_i^L$, grouped by major PMFC area and fishery. For CAR, the reference years were set to 1996-2021 for the trawl fishery and 1996-2021 for the non-trawl fisheries.

delta: mean of annual ratios, $\sum_i \mathrm{RRF}_i^D / \mathrm{TAR}_i$, grouped by major PMFC area and fishery using reference years i = 1997-2006 for the trawl fishery and 2000-2004 for all other fisheries. Observer records were used to gather data on releases.

The stock assessment population model uses calendar year, requiring calendar year catch estimates. Landings were reconstructed before 1996 for the trawl fishery and before 2006 for the non-trawl fisheries. Although reported data existed in earlier time periods, previous TWGs considered that reported catches of less desirable rockfish species from 1985 (start of restrictive trip limits) to 1994 (start of the DMP) were likely inflated, given the incentives for operators to misreport their catch of desirable species during this period.

The reconstruction of Canadian CAR catch estimated landings for years before those with credible records using `gamma` ratios (Table A.3). These ratios were also used to convert foreign landings of ORF to CAR. The ratios were calculated from a relatively modern period (1996-2021 for all fisheries); therefore, an obvious caveat to this procedure is that ratios derived from a modern fishery may not reflect catch ratios during the historical foreign fleet activity or regulatory regimes not using IVQs (individual vessel quotas). Consequently, we use sets of years where gamma does not fluctuate wildly in an attempt to minimise this potential issue.

After CAR landings were estimated, non-retained catch (releases or discards) were estimated and added during years identified by fishery: T = 1954-1995, H = 1918-2005, and S/DL = 1950-2005, and ZN = 1986-2005. The non-retained catch was estimated using the `delta` ratios of CAR discarded by a fishery to fishery-specific landed targets (TAR): T = YMR, H = Pacific Halibut, S = Sablefish, DL = Spiny Dogfish + Lingcod, ZN = YMR (Table A.3).

The current annual CAR catches by trawl fishery and those from the non-trawl fisheries appear in Table A.4 and Figure A.2. The combined fleet catches were used in the population models as plotted in Figure A.4. The catch reconstruction used for CAR was built on May 2, 2022. The 2022 catch was set equal to 780 t after consultation with trawl industry, and apportioned to the two fisheries, 766.7 t to Trawl and 13.3 t to Other, based on ratios of total catch by fishery from 2017 to 2021 to total catch over the same period.

A.2.2.2. Reconstruction results

Table A.3. Estimated 'gamma' (CAR/ORF) and 'delta' (discard) ratios for each fishery and PMFC area used in the catch reconstruction of CAR.

PMFC	Trawl	Halibut	Sablefish	Dogfish/ Lingcod	H&L Rockfish
gamma (proportion CAR/ORF)					
3C	0.05240	0.02032	0.00201	0.05870	0.05827
3D	0.11468	0.02884	0.00246	0.08198	0.05841
5A	0.02733	0.01642	0.00129	0.03549	0.03671
5B	0.05020	0.01221	0.00008	0.03201	0.01492
5C	0.04322	0.02094	0	0.02168	0.02657
5D	0.02794	0.01499	0	0.01118	0.00722
5E	0.00544	0.01241	0.00065	0.04676	0.00965
delta (discard rate)					
3C	0.00426	0.00009	0.00334	0.00061	0.01401
3D	0.00365	0.00020	0.00190	0.00061	0.00478
5A	0.00315	0.00001	0	0.00171	0.00157
5B	0.00200	0.00011	0	0.00048	0.00795
5C	0.00104	0.00019	0	0.00047	0
5D	0.00435	0.00012	0	0.00086	0
5E	0.00184	0.00008	0	0.00613	0

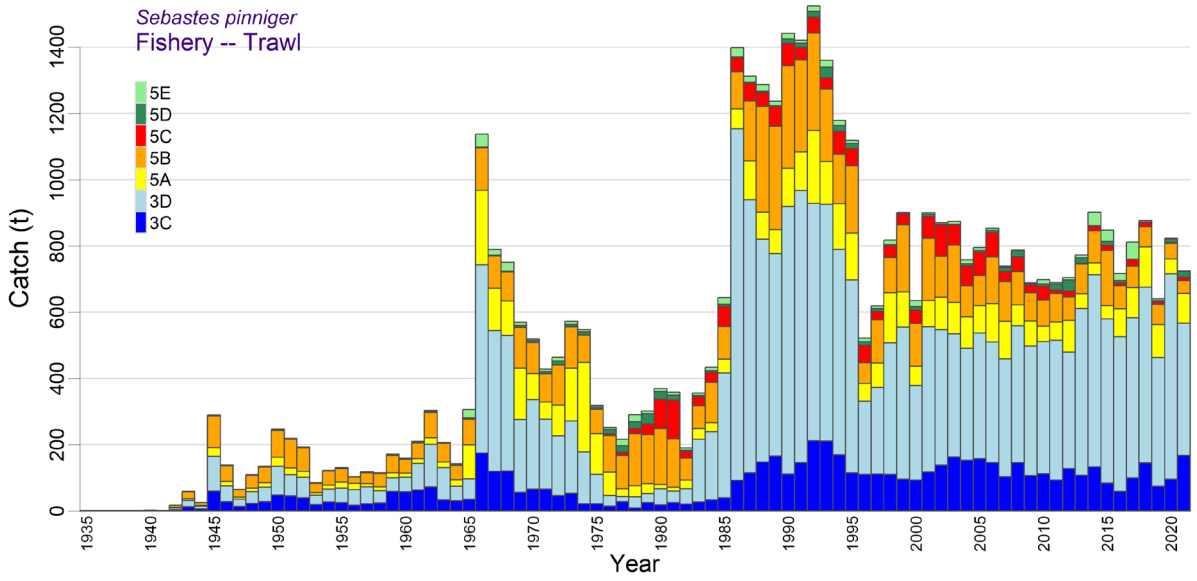

*Figure A.2. Reconstructed total (landed + released) catch (t) for CAR from the **trawl** fishery in PMFC major areas 3C to 5E. Catch in 2022 set to 766.7 tonnes.*

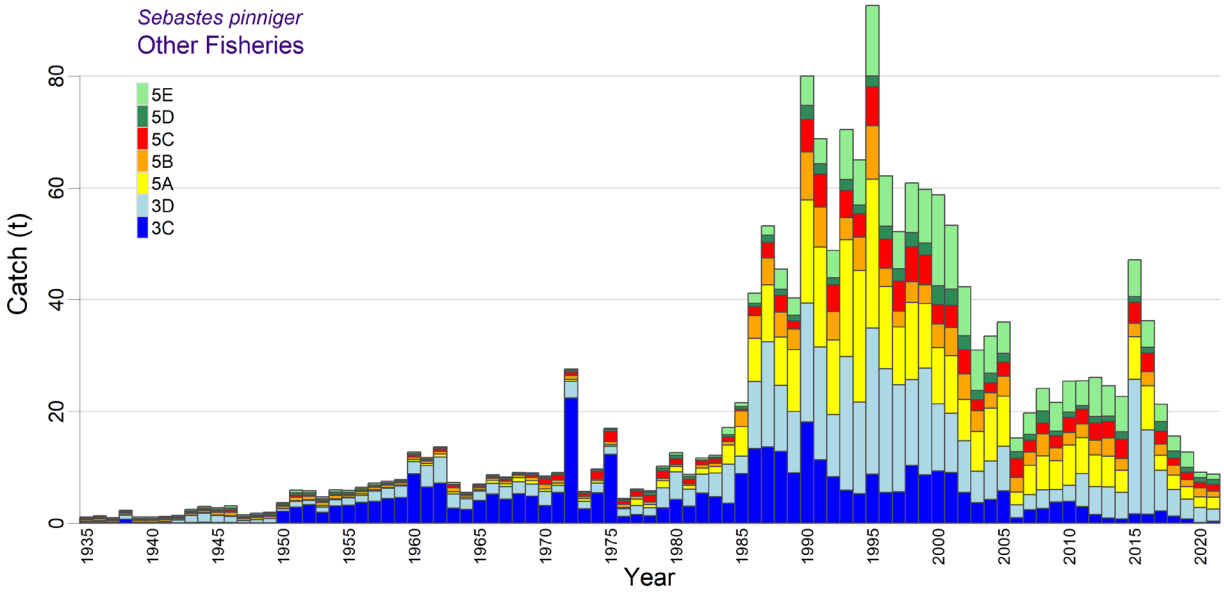

*Figure A.3. Reconstructed total (landed + released) catch (t) for CAR from the **other** fisheries in PMFC major areas 3C to 5E. Catch in 2022 set to 13.3 tonnes.*

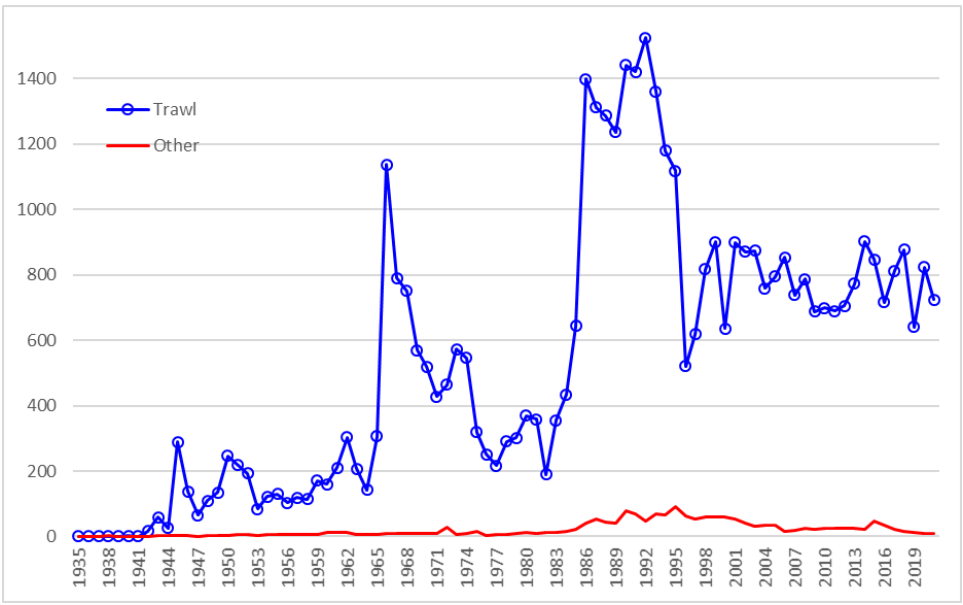

Figure A.4. Plots of catch by fishery for CAR from 1935 to 2021 used in the population model. Data values provided in Table A.4.

Table A.4. Reconstructed catches (in tonnes, landings + releases) of CAR coastwide from trawl and non-trawl fisheries (Halibut, Sablefish, Dogfish/Lingcod, and H&L Rockfish). Shaded columns (marked with an asterisk) indicate catches used in the population model. Coastwide catch for 2022 was set to 780 t after consultation with the trawl industry.

Year	Trawl	Other	Coast*	Year	Trawl	Other	Coast*	Year	Trawl	Other	Coast*
1918	0.368	2.48	2.85	1953	84.9	4.69	89.6	1988	1287	45.4	1332
1919	0.271	2.33	2.60	1954	122	5.95	128	1989	1237	40.3	1277
1920	0.178	2.00	2.18	1955	130	5.83	136	1990	1442	80.0	1522
1921	0.081	1.76	1.84	1956	103	6.42	109	1991	1421	68.8	1490
1922	0.176	2.02	2.20	1957	118	7.17	125	1992	1524	48.8	1573
1923	0.083	1.39	1.47	1958	115	7.45	122	1993	1360	70.5	1431
1924	0.087	1.31	1.39	1959	171	7.81	179	1994	1179	65.0	1244
1925	0.065	1.10	1.16	1960	160	12.7	172	1995	1119	92.6	1211
1926	0.127	1.54	1.66	1961	210	11.7	221	1996	522	62.2	584
1927	0.186	1.71	1.89	1962	303	13.7	317	1997	618	52.2	671
1928	0.160	1.74	1.90	1963	207	7.25	214	1998	817	60.9	878
1929	0.162	1.55	1.71	1964	142	5.52	147	1999	901	59.7	961
1930	0.104	1.19	1.29	1965	306	7.01	313	2000	635	58.8	694
1931	0.078	1.18	1.26	1966	1138	8.61	1146	2001	900	53.3	953
1932	0.046	0.963	1.01	1967	790	8.24	798	2002	870	42.3	912
1933	0.025	0.893	0.918	1968	751	9.07	760	2003	874	31.0	905
1934	0.084	0.945	1.03	1969	570	9.02	579	2004	758	33.4	791
1935	0.543	1.10	1.64	1970	519	8.41	528	2005	795	36.0	831
1936	0.741	1.33	2.07	1971	428	9.07	437	2006	853	15.3	868
1937	0.577	0.987	1.56	1972	464	27.6	491	2007	739	19.7	758
1938	1.09	2.30	3.39	1973	572	5.69	578	2008	787	24.1	811
1939	1.01	1.09	2.09	1974	547	9.66	556	2009	688	21.6	710
1940	2.12	1.07	3.19	1975	319	16.9	336	2010	699	25.4	724
1941	1.26	1.22	2.48	1976	252	4.39	256	2011	689	25.5	714
1942	17.2	1.38	18.6	1977	217	6.09	223	2012	705	26.1	731
1943	58.4	2.47	60.9	1978	291	5.76	297	2013	772	24.6	797
1944	25.6	2.97	28.6	1979	302	10.2	312	2014	902	22.7	924
1945	289	2.77	292	1980	370	12.6	382	2015	847	47.1	895
1946	139	3.09	142	1981	359	8.67	367	2016	717	36.2	753
1947	65.6	1.48	67.0	1982	190	11.7	201	2017	812	21.3	833
1948	109	1.75	111	1983	355	12.1	368	2018	877	15.6	893
1949	134	1.94	136	1984	434	17.1	451	2019	640	12.7	653
1950	247	3.70	251	1985	644	21.6	666	2020	824	9.12	833
1951	219	5.86	225	1986	1398	41.1	1439	2021	724	8.73	733
1952	193	5.79	199	1987	1312	53.2	1366	2022	766.7	13.3	780

A.2.3. Changes to the reconstruction algorithm since 2011

Each stock assessment since Haigh and Yamanaka (2011) has made either permanent changes to the catch reconstruction algorithm or choices specific to the stock being assessed.

A.2.3.1. Pacific Ocean Perch (2012)

In two previous stock assessments for POP in areas 3CD and 5DE (Edwards et al. 2014a,b), the authors documented two departures from the catch reconstruction algorithm introduced by Haigh and Yamanaka (2011). The first dropped the use of trawl and trap data from the sales slip database `PacHarv3` because catches were sometimes reported by large statistical areas that could not be clearly mapped to PMFC areas. In theory, `PacHarv3` should report the same catch as that in the `GFCatch` database (Rutherford 1999), but area inconsistencies cause catch inflation when certain large statistical areas cover multiple PMFC areas. Therefore, only the `GFCatch` database for the trawl and trap records from 1954 to 1995 were used, rather than trying to mesh `GFCatch` and `PacHarv3`. The point is somewhat moot as assessments since 2015 by the Offshore Rockfish Program use the merged-catch data table (Section A.2.1). Data for the H&L fisheries from `PacHarv3` are still used as these do not appear in other databases.

The second departure was the inclusion of an additional data source for BC rockfish catch by the Japanese fleet reported in Ketchen (1980a).

A.2.3.2. Yellowtail Rockfish (2014)

The Yellowtail Rockfish assessment (DFO 2015) selected offshore areas that reflected the activity of the foreign fleets' impact on this species to calculate `gamma` (RRF/ORF) and `delta` ratios (RRF/TAR). This option was not used in the CAR reconstruction.

A.2.3.3. Shortspine Thornyhead (2015)

The Shortspine Thornyhead assessment (Starr and Haigh 2017) was the first to use the merged catch table (`GF_MERGED_CATCH` in `GFFOS`). Previous assessments required the meshing together of caches from six separate databases: `GFBioSQL` (research, midwater joint-venture Hake, midwater foreign), `GFCatch` (trawl and trap), `GFFOS` (all fisheries), `PacHarvest` (trawl), `PacHarvHL` (hook and line), and `PacHarvSable` (trap and longline). See Section A.2.1 for further details.

A.2.3.4. Yelloweye Rockfish Outside (2015)

The Yelloweye Rockfish (YYR) assessment (Yamanaka et al. 2018) introduced the concept of depth-stratified `gamma` and `delta` ratios; however, this functionality has not been used for offshore rockfish to date.

Also in the YYR assessment, rockfish catch from seamounts was removed (implemented in all subsequent reconstructions, including the CAR one), as well as an option to exclude rockfish catch from the foreign fleet and the experimental Langara Spit POP fishery (neither were excluded from the CAR reconstruction). The latter option is more likely appropriate for inshore rockfish species because they did not experience historical offshore foreign fleet activity or offshore experiments.

A.2.3.5. Redstripe Rockfish (2018)

The Redstripe Rockfish assessment (Starr and Haigh 2021a), introduced the use of summarising annual `gamma` and `delta` ratios from reference years (Section A.2.2) by calculating the geometric mean across years instead of using the arithmetic mean. This choice reduces the influence of single anomalously large annual ratios. The geometric mean was used in the CAR reconstruction.

Also new in 2018 was the ability to estimate RRF (using `gamma`) for landings later than 1996, should the user have reason to replace observed landings with estimated ones. For CAR, observed landings by fishery were used starting in 1996 for the trawl fishery and 2006 for the non-trawl fisheries; prior to these years, landings were estimated using `gamma`.

Another feature introduced in 2018 was the ability to specify years by fishery for discard regimes, that is, when discard ratios were to be applied. Previously, these had been fixed to 1954-1995 for the trawl fishery and 1986-2005 for the non-trawl fisheries. For CAR, discard regimes by fishery were set to T = 1954-1995, H = 1918-2005, S/DL = 1950-2005, and ZN = 1986-2005. As previously, years before the discard period assume no discarding, and years after the discard period assume that discards have been reported in the databases.

A.2.3.6. Widow Rockfish (2019)

The Widow Rockfish (WWR) assessment (Starr and Haigh 2021b) found a substantial amount of WWR reported as foreign catch in the database `GFBioSQL` that came from midwater gear off WCVI. Subsequently, the catch reconstruction algorithm was changed to assign GFBio foreign catch to four of the five fisheries based on gear type:

- bottom and midwater trawl gear assigned to the T fishery,
- longline gear assigned to the H fishery,
- trap and line-trap mix gear assigned to the S fishery, and
- h&l gear assigned to the ZN fishery.

The assignment only happens if the user chooses to use foreign catch in the reconstruction (see Section A.2.3.3). These foreign catches occurred well after the foreign fleet activity between 1965 and the implementation of an exclusive economic zone in 1977. CAR foreign catches in GFBio occurred primarily in 1987-1989 (23 t).

A.2.3.7. Bocaccio (2019)

The Bocaccio rockfish (BOR) assessment (Starr and Haigh 2022a) used advice from the technical working group, which identified specific reference years for the calculation of `gamma`: 1990-2000 for trawl (to capture the years before decreasing mortality caps for BOR were placed on the trawl fleet) and 2007-2011 for non-trawl (to capture years after some form of observer program like electronic monitoring was applied to the hook and line fleets). The catch reconstruction algorithm was previously coded to only allow one set of reference years to be applied across all fisheries. The algorithm was changed so that a user can now specify separate reference years for each fishery.

Once the merged catch table (`GF_MERGED_CATCH` in `GFFOS`) was introduced (Section A.2.3.3), catch from all databases other than `PacHarv3` have been reconciled so that caches are not double counted. In the BOR assessment, the remaining two catch data sources (GFM and PH3, for brevity) were re-assessed by comparing ORF data, and the CR algorithm was changed in how the data sources were merged for the categories RRF landed, RRF discarded, ORF landed, POP landed, and TRF landed:

- GFM catch is the only source needed for FID 1 (Trawl fishery), as was previously assumed;
- GFM and PH3 catches appear to supplement each other for FIDs 2 (Halibut fishery), 3 (Sablefish fishery), and 4 (Dogfish/Lingcod fishery), and the catches were added in any given year up to 2005 (electronic monitoring started in 2006 and so the GFFOS database was reporting all catch for these fisheries by then); and
- GFM and PH3 catches appear to be redundant for FID 5 (H&L Rockfish fishery), and so the maximum catch was used in any given year.

Also new in the BOR assessment was the introduction of historical Sablefish (SBF) and Lingcod (LIN) trawl landings from 1950 to 1975 (Ketchen 1976) for use in calculating historical discards for FIDs 3 and 4 during this period. These landings could not be used directly because they were taken by the trawl fleet; therefore, an estimation of SBF and LIN landed catch by FIDs 3 and 4, respectively, relative to SBF and LIN landed catch by FID 1 (trawl) was calculated from GFM. Annual ratios of SBF_3/SBF_1 and LIN_4/LIN_1 from 1996-2011 were chosen to calculate a geometric mean; the ratios from 2012 on started to diverge from those in the chosen period. The procedure yielded average ratios: $SBF_3/SBF_1 = 10.235$ and $LIN_4/LIN_1 = 0.351$, which were used to scale the 1950-75 trawl landings of SBF and LIN, respectively. From these estimated landings, discards of YMR were calculated by applying `delta` (see Section A.2.2.1).

Another departure was the re-allocation of PH3 records to the various catch reconstruction fisheries based on data from 1952-95 (see the 2019 Bocaccio stock assessment by Starr and Haigh 2022a, Section A.2.3.7).

A.2.3.8. Rougheye/Blackspotted Rockfish (2020)

During the Rougheye/Blackspotted Rockfish (REBS) catch reconstruction, a close look at annual gammas revealed large fluctuations from 1991 to 2019 (Starr and Haigh 2022b). Based on these findings, the reference years chosen to calculate a geometric mean gamma by fishery were: 1997:2005 for Trawl and 2007:2009 for non-trawl. These intervals were selected to reflect times of credible data: (i) reconciled observer logs with DMP landings in PacHarvest for the trawl fishery, and (ii) least volatility in GFFOS for the non-trawl fisheries.

A.2.3.9. Yellowmouth Rockfish (2021)

During the YMR catch reconstruction, the annual gammas only experienced moderate fluctuations from 1996 to 2019 (Starr and Haigh 2022c). Based on these figures, the reference years chosen to calculate a geometric mean gamma by fishery were: 1996:2019 for Trawl and 1996:2019 for the non-trawl fisheries. Normally, intervals are selected to reflect times of credible data (see Section A.2.3.8); however, all available years were chosen because no management changes had occurred for YMR since the inception of the Trawl observer program, and the other fisheries were largely irrelevant for this species.

A.2.3.10. Canary Rockfish (2022)

During the CAR catch reconstruction, the annual gammas for the trawl fishery experienced moderate fluctuations from 1996 to 2021 (Figure A.5). Annual gammas for the other fisheries showed some noise (Figure A.6) but the running geometric means were fairly stable. Based on these figures, the reference years chosen to calculate a geometric mean gamma by fishery were 1996:2021 for all fisheries. Normally, intervals are selected to reflect times of credible data (see Section A.2.3.8); however, all available years were chosen because no management changes had occurred for CAR since the inception of the trawl observer program, and the other fisheries were largely irrelevant for this species.

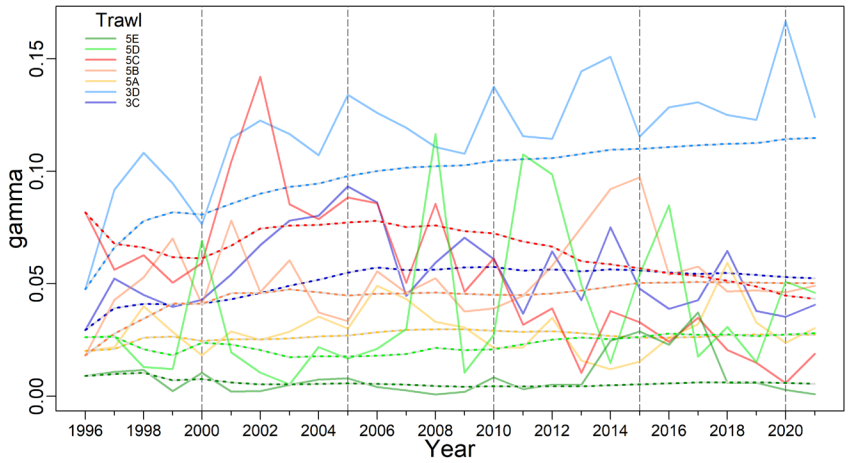

Figure A.5. Annual gamma ratios (CAR/ORF) for the trawl commercial groundfish fishery (solid lines). Dotted lines trace the running geometric mean. Vertical dashed lines delimit 5-yr intervals.

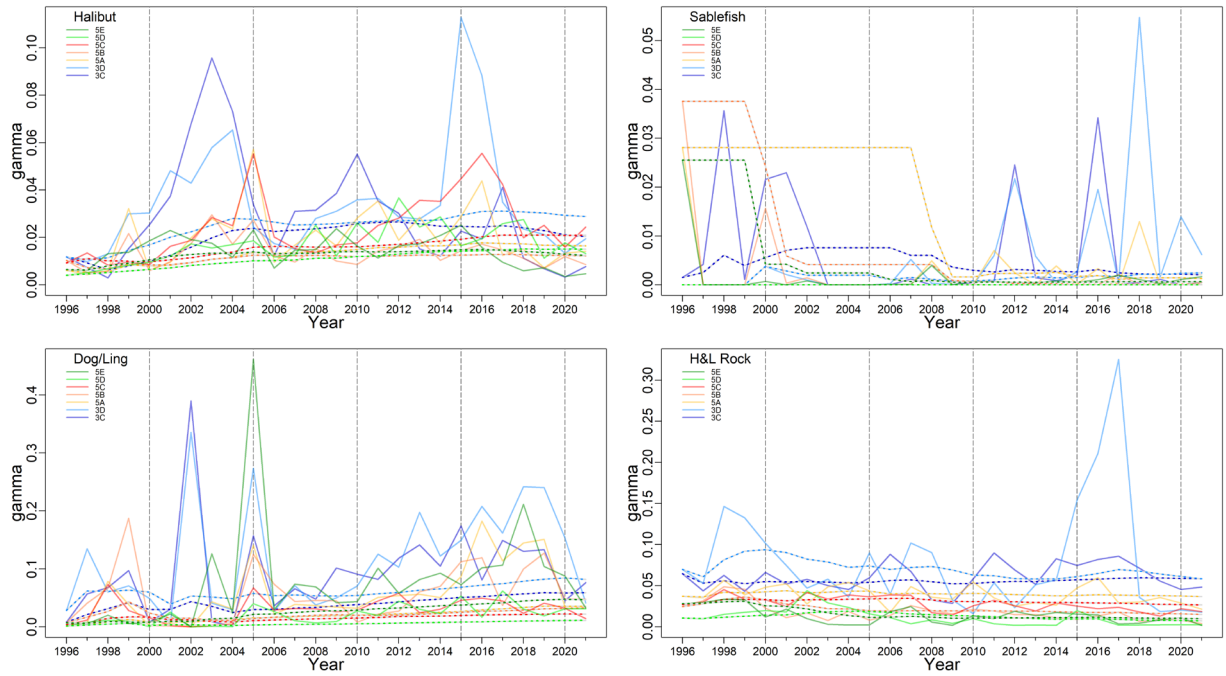

Figure A.6. Annual gamma ratios (CAR/ORF) for the four non-trawl commercial groundfish fisheries.

A.2.4. Comparison with catches used in the 2007 and 2009 CAR assessments

The catch trajectory presented in Figure A.4 differs substantially from the catch trajectory used in the previous CAR stock assessments (Figure A.7). The reason for this difference lies in the development of a standardised procedure to reconstruct historical catches, beginning with the Yelloweye Rockfish and POP in 2011. The procedure used to reconstruct the 2007 and 2009 CAR historical catches was an early version of the 2011 procedure (Stanley et al. 2009, Appendix B), which has evolved considerably since then. The primary difference was the 2009 calculation of the ratio CAR/ORF of 0.46 in 3CD and 0.16 in 5AB, values considerable higher than equivalent geometric means of 0.078 and 0.037 of the gamma values used in this assessment (see Table A.3). Therefore, the differences plotted in Figure A.7 reflect the consequences of cumulative changes in assumptions that are documented in the above paragraphs.

A.1.1. Caveats

The available catch data before 1996 (first year of onboard observer program) present difficulties for use in a stock assessment model without some form of interpretation, both in terms of misreporting (i.e., reporting catches of one species as another) or misidentifying species. There is also the possible existence of at-sea discarding due to catches exceeding what was permitted for retention. Although there were reports that fishermen misreported the location of catches, this issue is not a large problem for an assessment of a coastwide stock. Additionally, there was a significant foreign fishery for rockfish in BC waters, primarily by the United States, the Soviet Union and Japan from 1965 to 1976. These countries tended to report their catches in aggregate form, usually lumping rockfish into a single category. These fisheries ceased after the declaration of the 200 nm exclusive economic zone by Canada in 1977.

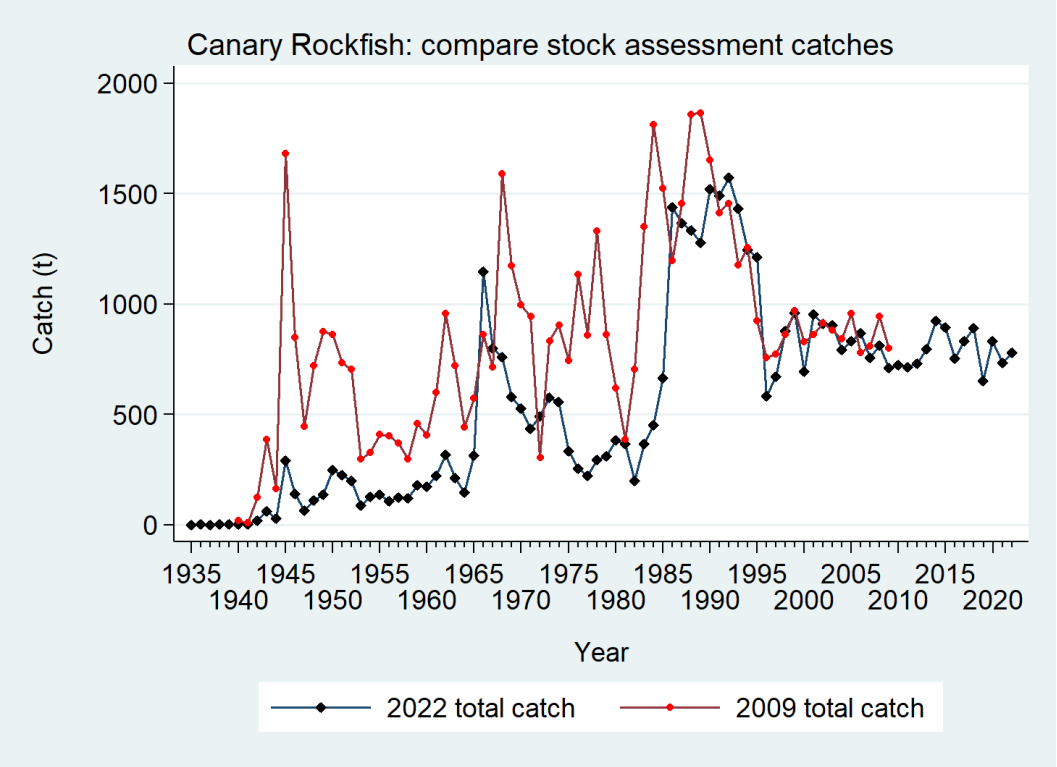

Figure A.7. Comparison of the catch trajectory used in the 2009 stock assessment with the reconstructed catch trajectory presented in Figure A.4.

The accuracy and precision of reconstructed catch series inherently reflect the problems associated with the development of a commercial fishery:

- trips offloading catch with no area information,
- unreported discarding,
- recording catch of one species as another to avoid quota violations,
- developing expertise in monitoring systems,
- shifting regulations,
- changing data storage technologies, etc.

Many of these problems have been eliminated through the introduction of observer programs (onboard observers starting in 1996 for the offshore trawl fleet, electronic monitoring starting in 2006 for the H&L fleets), dockside [observer] monitoring, and tradeable individual vessel quotas (starting in 1997) that confer ownership of the resource to the fishing sector.

The catch reconstruction procedure does not rebuild catch by gear type (e.g., bottom trawl vs. midwater trawl, trap vs. longline). While adding this dimension is possible, it would mean splitting catches back in time using ratios observed in the modern fishery, which likely would not accurately represent historical activity by gear type (see Section A.2.2 for similar caveats regarding the use of modern catch ratios to reconstruct the catch of one species from a total rockfish catch). In this assessment, we combined the catches of CAR by bottom and midwater trawl because the biological data (Appendix D) by gear did not support two fleets in the population model and it was inconclusive whether there was a demonstrable difference in selectivity. Table A.5 and Figure A.8 show the reported coastwide catch (landings plus non-

retained) by gear type. Note that the catch reconstruction allocates catch of RRF from unknown areas to PMFC areas proportionally by known catch in PMFC areas to reflect all potential removals of biomass from BC waters. Consequently, reported catches by area are often less than the reconstructed catches by area.

The catch for 2022 was incomplete and so we used a catch of 780 t that the trawl industry believed to be feasible under current-year conditions (economic and regulatory). This amount was higher than the 2021 catch but similar to the 5-year (2017-2021) average mean catch. Twenty tonnes were added to this total to cover the 2022 'other' catch for a total of 800 t.

Table A.5. Reported catch (tonnes) by gear type, sector, and fishery for the BC CAR coastwide starting when trawl fleet activity was monitored by onboard observers. BT=bottom trawl, MW=midwater trawl, HL=hook and line, GFT=groundfish trawl, ZN=license for hook and line, RO=HL rockfish outside, H=halibut longline, S=sablefish trap, HS=halibut + sablefish, DL=dogfish/lingcod.

	Gear				Sector						Fishery				
Year	BT	MW	HL	Trap	GFT	ZN	RO	H	HS	S	T	H	S	DL	HL
1996	453	64.2	49.7	–	517	48.5	–	1.27	–	–	517	1.27	–	–	48.5
1997	527	88.3	33.0	–	616	31.2	–	0.957	–	–	616	0.957	–	0.807	31.2
1998	731	84.3	58.2	–	816	54.6	–	3.11	–	0.005	816	3.11	0.005	0.515	54.6
1999	729	171	60.5	–	901	55.7	–	3.74	–	–	901	3.74	–	1.13	55.7
2000	522	113	43.3	–	634	36.6	–	6.74	–	–	634	6.74	–	–	36.6
2001	854	45.6	47.5	–	899	36.2	–	11.2	–	–	899	11.2	–	0.081	36.2
2002	799	69.5	31.6	–	868	18.6	–	12.6	–	–	868	12.6	–	0.357	18.6
2003	801	72.3	28.2	–	873	13.1	–	13.1	–	0.212	873	13.1	0.212	1.76	13.1
2004	693	62.9	32.7	–	756	18.9	–	12.8	–	–	756	12.8	–	0.982	18.9
2005	747	46.4	34.3	–	793	15.4	–	16.5	–	0.005	793	16.5	0.005	2.41	15.4
2006	791	61.1	14.7	–	852	2.97	2.79	7.04	1.18	0.012	852	8.22	0.012	0.728	5.76
2007	631	106	18.2	0.002	738	–	6.67	6.86	1.97	0.169	738	8.83	0.169	2.48	6.72
2008	645	142	22.4	–	787	–	6.87	10.7	2.60	0.237	787	13.3	0.237	1.95	6.87
2009	644	40.9	20.4	–	685	–	6.17	7.70	3.23	–	685	10.9	–	3.27	6.17
2010	632	66.3	24.4	0.003	698	–	10.3	8.19	4.00	0.032	698	12.2	0.032	1.84	10.3
2011	618	69.6	24.8	–	688	–	10.1	8.52	3.48	0.351	688	12.0	0.351	2.32	10.1
2012	667	37.5	24.3	–	704	–	7.70	8.28	5.60	0.665	704	13.9	0.665	2.07	7.72
2013	689	64.7	24.4	–	754	–	6.27	9.48	5.88	0.343	754	15.4	0.343	2.33	6.41
2014	752	149	21.8	0.030	901	–	7.46	8.57	4.63	0.081	901	13.2	0.110	1.05	7.50
2015	776	69.2	46.5	0.036	845	–	13.3	15.8	15.0	0.105	845	30.8	0.137	2.20	13.4
2016	620	87.4	34.7	0.003	708	–	10.4	13.1	8.21	0.397	708	21.3	0.400	2.51	10.5
2017	706	104	19.9	0.003	811	–	5.09	6.20	6.00	0.103	811	12.2	0.107	2.49	5.12
2018	663	192	15.3	0.002	855	–	3.26	5.93	2.28	1.01	855	8.21	1.01	2.78	3.26
2019	443	190	12.4	–	633	–	3.33	5.04	1.39	0.066	633	6.42	0.066	2.61	3.34
2020	605	214	9.01	–	819	–	1.72	4.98	0.596	0.689	819	5.58	0.689	1.03	1.72
2021	413	303	8.02	0.003	716	–	1.69	4.03	1.72	0.146	716	5.75	0.148	0.423	1.71

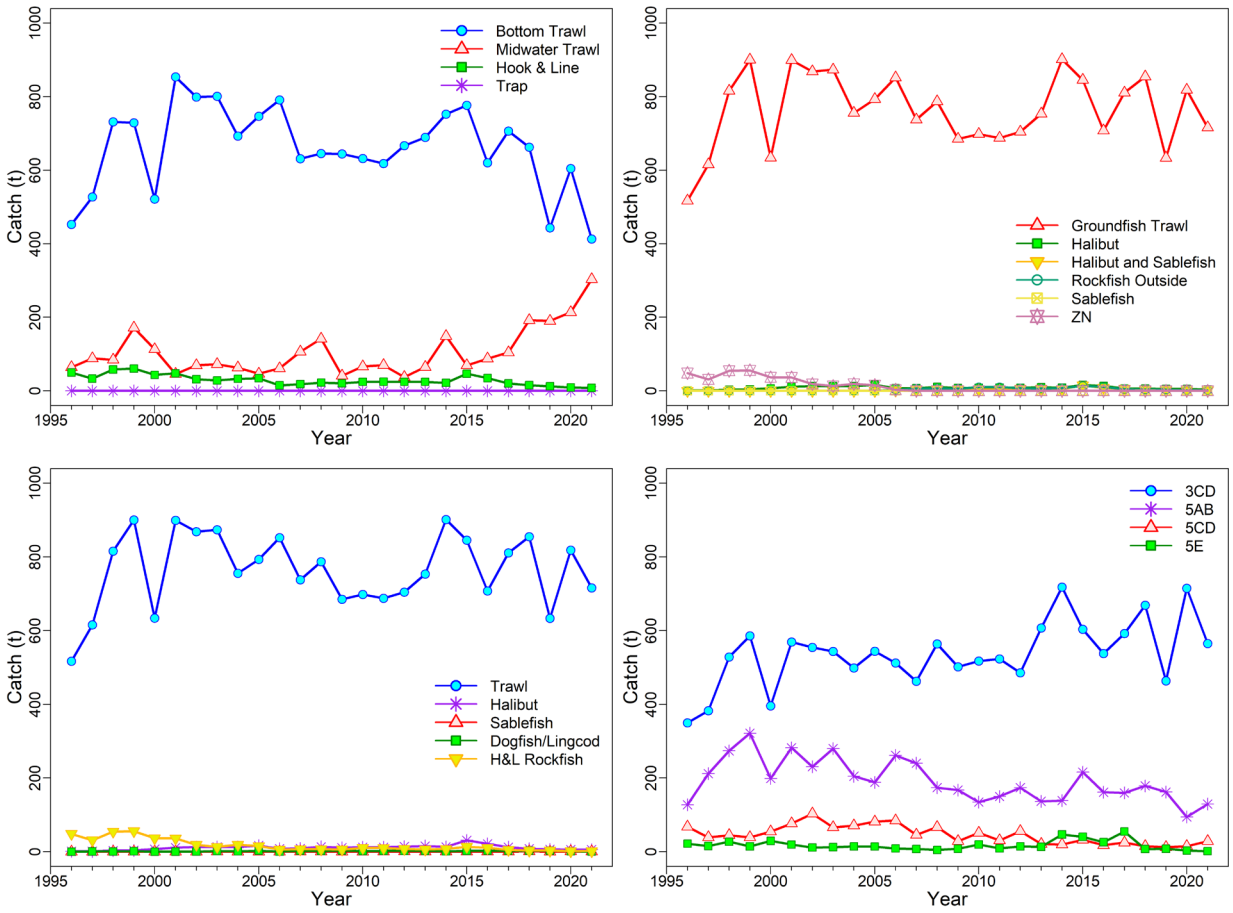

Figure A.8. Reported CAR catch (landings + released) by gear (top left), by sector (top right), by fishery (bottom left), and by groundfish management area (bottom right) since the implementation of the trawl fishery onboard-observer program in 1996.

A.2. SCALING CATCH POLICY TO GMU AREA TACS

The area definitions used by DFO Groundfish Science (PMFC areas) differ somewhat from those used by the DFO Groundfish Management, which uses Pacific Fishery Management Areas (PFMA). The reasons for these discrepancies vary depending on the species, but they occur to address different requirements by Science and Management. For Science, there is a need to reference historical catch using areas that are consistently reported across all years in the databases and catch records. The PMFC and GMU areas, while similar but not identical (Figure 1), address current management requirements.

As this assessment covers a coastwide stock, and GMU issues four area-specific TACs, a catch policy for the coastwide stock could be allocated to PMFC areas using the average 5-year proportional catch ratios in Table A.6. For example, a catch policy of 1000 tonnes/year of CAR would be allocated as follows:

- 3CD = 782 t/y (0.1477 + 0.6339) * 1000 t/y
- 5AB = 188 t/y (0.1147 + 0.0729) * 1000 t/y
- 5CD = 21 t/y (0.0137 + 0.0077) * 1000 t/y
- 5E = 9 t/y 0.0094 * 1000 t/y

Table A.6. Catch of CAR from the combined fishery in PMFC areas from the last 5 years of complete catch statistics. Annual proportions of catch by area are shown in rows marked by year. Area-specific 5-year geometric means of annual proportions (normalised) are shown in the final row.

Year	3C	3D	5A	5B	5C	5D	5E	BC
Catch(t)								
2017	101.640	491.209	92.870	67.362	22.408	2.585	55.037	752.787
2018	145.767	536.088	123.845	62.036	14.363	2.957	7.469	833.111
2019	74.793	392.576	101.058	63.016	9.042	3.991	8.188	892.524
2020	95.813	622.080	47.244	48.767	3.770	11.805	3.174	652.664
2021	167.454	402.108	91.431	40.550	11.149	18.424	1.724	832.653
Proportion								
2017	0.1350	0.6525	0.1234	0.0895	0.0298	0.0034	0.0731	1
2018	0.1750	0.6435	0.1487	0.0745	0.0172	0.0035	0.0090	1
2019	0.0838	0.4398	0.1132	0.0706	0.0101	0.0045	0.0092	1
2020	0.1468	0.9531	0.0724	0.0747	0.0058	0.0181	0.0049	1
2021	0.2011	0.4829	0.1098	0.0487	0.0134	0.0221	0.0021	1
GeoMean	0.1423	0.6108	0.1105	0.0703	0.0132	0.0074	0.0090	0.9636
Normalise	0.1477	0.6339	0.1147	0.0729	0.0137	0.0077	0.0094	1

A.3. REFERENCES – CATCH

Canada Dominion Bureau of Statistics. 1918-1950. Fisheries Statistics of Canada (British Columbia). Tech. rep., Canada Dominion Bureau of Statistics, Ottawa, ON.

DFO. 2015. Yellowtail Rockfish (*Sebastes flavidus*) stock assessment for the coast of British Columbia, Canada. DFO Can. Sci. Advis. Sec. Sci. Advis. Rep. 2015/010.

Edwards, A.M., Haigh, R. and Starr, P.J. 2014a. Pacific Ocean Perch (*Sebastes alutus*) stock assessment for the north and west coasts of Haida Gwaii, British Columbia. DFO Can. Sci. Advis. Sec. Res. Doc. 2013/092: vi + 126 p.

Edwards, A.M., Haigh, R. and Starr, P.J. 2014b. Pacific Ocean Perch (*Sebastes alutus*) stock assessment for the west coast of Vancouver Island, British Columbia. DFO Can. Sci. Advis. Sec. Res. Doc. 2013/093: vi + 135 p.

Forrester, C.R. 1969. Results of English Sole tagging in British Columbia waters. Bull. Pac. Mar. Fish. Comm. 7: 1-10.

Forrester, C.R. and Smith, J.E. 1972. The British Columbia groundfish fishery in 1971, some aspects of its investigation and related fisheries. Fish. Res. Board Can. Tech. Rep. 338: 67 p.

Gunderson, D.R., Westrheim, S.J., Demory, R.L. and Fraidenburg, M.E. 1977. The status of Pacific Ocean Perch (*Sebastes alutus*) stocks off British Columbia, Washington, and Oregon in 1974. Fish. Mar. Serv. Tech. Rep. 690: iv + 63 p.

Haigh, R. and Yamanaka, K.L. 2011. Catch history reconstruction for rockfish (*Sebastes* spp.) caught in British Columbia coastal waters. Can. Tech. Rep. Fish. Aquat. Sci. 2943: viii + 124 p.

Ketchen, K.S. 1976. Catch and effort statistics of the Canadian and United States trawl fisheries in waters adjacent to the British Columbia coast 1950-1975. Fisheries and Marine Service, Nanaimo, BC, Data Record 6.

Ketchen, K.S. 1980a. Assessment of groundfish stocks off the west coast of Canada (1979). Can. Data Rep. Fish. Aquat. Sci. 185: xvii + 213 p.

Ketchen, K.S. 1980b. Reconstruction of Pacific Ocean Perch (*Sebastes alutus*) stock history in Queen Charlotte sound. Part I. Estimation of foreign catches, 1965–1976. Can. Manuscr. Rep. Fish. Aquat. Sci. 1570: iv + 46 p.

Leaman, B.M. and Stanley, R.D. 1993. Experimental management programs for two rockfish stocks off British Columbia, Canada. In S. J. Smith, J. J. Hunt and D. Rivard, eds., Risk evaluation and biological reference points for fisheries management, p. 403-418. Canadian Special Publication of Fisheries and Aquatic Sciences 120.

Love, M.S., Yoklavich, M. and Thorsteinson, L. 2002. The Rockfishes of the Northeast Pacific. University of California Press, Berkeley and Los Angeles, California.

Rutherford, K.L. 1999. A brief history of GFCatch (1954-1995), the groundfish catch and effort database at the Pacific Biological Station. Can. Tech. Rep. Fish. Aquat. Sci. 2299: v + 66 p.

Stanley, R.D., Starr, P. and Olsen, N. 2009. Stock assessment for Canary Rockfish (*Sebastes pinniger*) in British Columbia waters. DFO Can. Sci. Advis. Sec. Res. Doc. 2009/013. xxii + 198 p.

Starr, P.J. and Haigh, R. 2017. Stock assessment of the coastwide population of Shortspine Thornyhead (*Sebastolobus alascanus*) in 2015 off the British Columbia coast. DFO Can. Sci. Advis. Sec. Res. Doc. 2017/015: ix + 174 p.

Starr, P.J. and Haigh, R. 2021a. Redstripe Rockfish (*Sebastes proriger*) stock assessment for British Columbia in 2018. DFO Can. Sci. Advis. Sec. Res. Doc. 2021/014: vii + 340 p.

Starr, P.J. and Haigh, R. 2021b. Widow Rockfish (*Sebastes entomelas*) stock assessment for British Columbia in 2019. DFO Can. Sci. Advis. Sec. Res. Doc. 2021/039: iv + 238 p.

Starr, P.J. and Haigh, R. 2022a. Bocaccio (*Sebastes paucispinis*) stock assessment for British Columbia in 2019, including guidance for rebuilding plans. DFO Can. Sci. Advis. Sec. Res. Doc. 2022/001. vii + 292 p.

Starr, P.J. and Haigh, R. 2022b. Rougheye/Blackspotted Rockfish (*Sebastes aleutianus/melanostictus*) stock assessment for British Columbia in 2020. DFO Can. Sci. Advis. Sec. Res. Doc. 2022/022. vii + 385 p.

Starr, P.J. and Haigh, R. 2022c. Yellowmouth Rockfish (*Sebastes reedi*) stock assessment for British Columbia in 2021. DFO Can. Sci. Advis. Sec. Res. Doc. 2022/10. viii + 288 p.

Wallace, S., Turris, B., Driscoll, J., Bodtker, K., Mose, B. and Munro, G. 2015. Canada's Pacific groundfish trawl habitat agreement: A global first in an ecosystem approach to bottom trawl impacts. Mar. Pol. 60: 240-248.

Westrheim, S.J., Gunderson, D.R. and Meehan, J.M. 1972. On the status of Pacific Ocean Perch (*Sebastes alutus*) stocks off British Columbia, Washington, and Oregon in 1970. Fish. Res. Board Can. Tech. Rep. 326: 48 p.

Yamanaka, K.L., McAllister, M.M., Etienne, M.P., Edwards, A.M. and Haigh, R. 2018. Assessment for the outside population of Yelloweye Rockfish (*Sebastes ruberrimus*) for British Columbia, Canada in 2014. DFO Can. Sci. Advis. Sec. Res. Doc. 2018/001: ix + 150 p.

APPENDIX B. TRAWL SURVEYS

B.1. INTRODUCTION

This appendix summarises the derivation of relative abundance indices for Canary Rockfish (CAR) from the following bottom trawl surveys:

- a set of historical surveys operated in the Goose Island Gully of Queen Charlotte Sound (Section B.3);
- National Marine Fisheries Service (NMFS) Triennial survey operated off the lower half of Vancouver Island (Section B.4);
- Queen Charlotte Sound (QCS) synoptic survey (Section B.5);
- West coast Vancouver Island (WCVI) synoptic survey (Section B.6);
- West coast Haida Gwaii (WCHG) synoptic survey (Section B.7);
- Hecate Strait (HS) synoptic survey (Section B.8);
- alternative geostatistical survey index series for the four synoptic surveys (B.9); and
- Hard-bottom longline (HBLL) surveys (B.10).

Only surveys used in the CAR stock assessment are presented in this appendix. The Hecate Strait multi-species survey and the WCVI shrimp and Queen Charlotte Sound shrimp surveys have been omitted because the presence of CAR in these surveys has been either sporadic or the coverage, either spatial or by depth, has been incomplete, rendering these surveys poor candidates to provide abundance series for this species. Rockfish stock assessments, beginning with Yellowtail Rockfish (DFO 2015), have explicitly omitted using the two shrimp surveys because of the truncated depth coverage, which ends at 160 m for the WCVI shrimp survey, and the constrained spatial coverage of the QC Sound shrimp survey as well as its truncated depth coverage, which ends at 231 m. The International Pacific Halibut Commission (IPHC) hook and line survey was not considered because the mean positive sets per year were very low for this species (Anderson et al. 2019), indicating an expectation that this survey will not provide reliable abundance indices. Canary Rockfish is captured frequently in the outside (excluding PMFC area 4B) Hard Bottom Longline (HBLL) surveys, warranting inclusion in a sensitivity analysis.

B.2. ANALYTICAL METHODS

Catch and effort data for strata i in year y yield catch per unit effort (CPUE) values U_{yi}. Given a set of data $\{C_{yij}, E_{yij}\}$ for tows $j = 1,\ldots,n_{yi}$,

Eq. B.1 $$U_{yi} = \frac{1}{n_{yi}} \sum_{j=1}^{n_{yi}} \frac{C_{yij}}{E_{yij}},$$

where C_{yij} = catch (kg) in tow j, stratum i, year y;

E_{yij} = effort (h) in tow j, stratum i, year y;

n_{yi} = number of tows in stratum i, year y.

CPUE values U_{yi} convert to CPUE densities δ_{yi} (kg/km^2) using:

Eq. B.2 $$\delta_{yi} = \frac{1}{vw} U_{yi},$$

where v = average vessel speed (km/h);
w = average net width (km).

Alternatively, if vessel information exists for every tow, CPUE density can be expressed

Eq. B.3 $$\delta_{yi} = \frac{1}{n_{yi}} \sum_{j=1}^{n_{yi}} \frac{C_{yij}}{D_{yij} w_{yij}},$$

where C_{yij} = catch weight (kg) for tow j, stratum i, year y;
D_{yij} = distance travelled (km) for tow j, stratum i, year y;
w_{yij} = net opening (km) for tow j, stratum i, year y;
n_{yi} = number of tows in stratum i, year y.

The annual biomass estimate is then the sum of the product of CPUE densities and bottom areas across m strata:

Eq. B.4 $$B_y = \sum_{i=1}^{m} \delta_{yi} A_i = \sum_{i=1}^{m} B_{yi},$$

where δ_{yi} = mean CPUE density (kg/km^2) for stratum i, year y;
A_i = area (km^2) of stratum i;
B_{yi} = biomass (kg) for stratum i, year y;
m = number of strata.

The variance of the survey biomass estimate V_y (kg^2) follows:

Eq. B.5 $$V_y = \sum_{i=1}^{m} \frac{\sigma_{yi}^2 A_i^2}{n_{yi}} = \sum_{i=1}^{m} V_{yi},$$

where σ_{yi}^2 = variance of CPUE density (kg^2/km^4) for stratum i, year y;
V_{yi} = variance of the biomass estimate (kg^2) for stratum i, year y.

The coefficient of variation (CV) of the annual biomass estimate for year y is

Eq. B.6 $$CV_y = \frac{\sqrt{V_y}}{B_y}.$$

B.3. EARLY SURVEYS IN QUEEN CHARLOTTE SOUND GOOSE ISLAND GULLY (GIG)

B.3.1. Data selection

Tow-by-tow data were available from a series of 12 historical trawl surveys spanning the period from 1965 to 1995. The first two surveys, in 1965 and 1966, were wide-ranging, with the 1965 survey extending from near San Francisco to halfway up the Alaskan Panhandle (Westrheim 1966a, 1967b). The 1966 survey was only slightly less ambitious, ranging from the southern US-Canada border in Juan de Fuca Strait into the Alaskan Panhandle (Westrheim 1966b, 1967b). It was apparent that the design of these two early surveys was exploratory and that these surveys would not be comparable to the subsequent Queen Charlotte Sound (QCS) surveys which were much narrower in terms of area covered and which had a much higher density of tows in the Goose Island Gully (GIG). This can be seen in the small number of tows used by the first two surveys in GIG (Table B.1). As a consequence, these surveys were not included in this series.

The 1967 (Figure B.1, left panel) and 1969 (Figure B.2, left panel) surveys (Westrheim 1967a, 1969; Westrheim et al. 1968) also performed tows on the west coast of Vancouver Island, the west coast of Haida Gwaii and SE Alaska, but both of these surveys had a reasonable number of tows on the GIG grounds (Table B.1). The 1971 survey (Figure B.3, left panel) was entirely confined to GIG (Harling et al. 1971) while the 1973 (Figure B.4, left panel), 1976 (Figure B.5, left panel) and 1977 (Figure B.6, left panel) surveys covered both Goose Island and Mitchell Gullies in QCS (Harling et al. 1973; Westrheim et al. 1976; Harling and Davenport 1977).

A 1979 survey (Nagtegaal and Farlinger 1980) was conducted by a commercial fishing vessel (*Southward Ho*, Table B.1), with the distribution of tows being very different from the preceding and succeeding surveys (plot not provided; see Figure C5 in Edwards et al. 2012). As well, the distribution of tows by depth was also different from the other surveys (Table B.2). These observations imply a substantially different survey design and consequently this survey was not included in the time series.

The 1984 survey was conducted by two vessels: the *G.B. Reed* and the *Eastward Ho* (Nagtegaal et al. 1986). Part of the design of this survey was to compare the catch rates of the two vessels (one was a commercial fishing vessel and the other a government research vessel – G. Workman, DFO, pers. comm.), thus they both followed similar design specifications, including the configuration of the net. Unfortunately, the tows were not distributed similarly in all areas, with the *G.B. Reed* fishing mainly in the shallower portions of the GIG, while the *Eastward Ho* fished more in the deeper and seaward parts of the GIG (Figure B.7, left panel) although the two vessels fished more contiguously in Mitchell Gully (immediately to the north). When the depth-stratified catch rates for Pacific Ocean Perch (the main design species of the surveys) of the two vessels were compared within the GIG only (using a simple ANOVA), the *Eastward Ho* catch rates were significantly higher ($p=0.049$) than those observed for the *G.B. Reed*. However, the difference in catch rates was no longer significant when tows from Mitchell's Gully were added to the analysis ($p=0.12$). Given the lack of significance when the full suite of available tows was compared, along with the uneven spatial distribution of tows among vessels within the GIG (although the ANOVA was depth-stratified, it is possible that the depth categories were too coarse), the most parsimonious conclusion was that there was no detectable difference between the two vessels. Consequently, all the GIG tows from both vessels were pooled for this survey year.

The 1994 survey, also conducted by a commercial vessel (the *Ocean Selector*, Table B.2), was modified by the removal of 19 tows which were part of an acoustic experiment and therefore

were not considered appropriate for biomass estimation (they were tows used to estimate species composition for ensonified schools). Although this survey was designed to emulate as closely as possible the previous *G.B. Reed* surveys in terms of tow location selection (same fixed tow locations, G. Workman, DFO, pers. comm.), the timing of this survey was about two to three months earlier than the previous surveys (starting in mid-June rather than August or September, Table B.3).

A 1995 survey, conducted by two commercial fishing vessels: the *Ocean Selector* and the *Frosti* (Table B.2), used a random stratified design with each vessel duplicating every tow (G. Workman, DFO, pers. comm.). This type of design was entirely different from the fixed station (based on Loran coordinates) used in the previous surveys. As well, the focus of this survey was on Pacific Ocean Perch (POP), with tows optimised to capture this species. Given the difference in design (random stations rather than fixed locations), this survey was not used in the stock assessment.

Table B.1. Number of tows in GIG and in other areas (Other) by survey year and vessel conducting the survey for the 12 historical (1965 to 1995) surveys. Survey years in grey and marked with an asterisk were not used in the assessment.

Survey	GB Reed		Southward Ho		Eastward Ho		Ocean Selector		Frosti	
Year	Other	GIG	Other	GIG	Other	GIG	Other	GIG	Other	GIG
1965*	76	8	–	–	–	–	–	–	–	–
1966*	49	15	–	–	–	–	–	–	–	–
1967	17	33	–	–	–	–	–	–	–	–
1969	3	32	–	–	–	–	–	–	–	–
1971	3	36	–	–	–	–	–	–	–	–
1973	13	33	–	–	–	–	–	–	–	–
1976	23	33	–	–	–	–	–	–	–	–
1977	15	47	–	–	–	–	–	–	–	–
1979*	–	–	20	59	–	–	–	–	–	–
1984	19	42	–	–	15	27	–	–	–	–
1994	–	–	–	–	–	–	2	69	–	–
1995*	–	–	–	–	–	–	2	55	1	57

Table B.2. Total number of tows by 20-fathom depth interval (in metres) in GIG and in other areas (Other) by survey year for the 12 historical (1965 to 1995) surveys. Survey years in grey and marked with an asterisk were not used in the assessment. Some of the tows in the GIG portion of the table have usability codes other than 0,1,2, or 6.

Survey	20 fathom depth interval (m)									Total
Year	66-146	147-183	184-219	220-256	257-292	293-329	330-366	367-402	440-549	Tows
Areas other than GIG										
1965	3	15	26	17	6	6	1	1	1	76
1966	3	11	18	8	2	1	3	2	1	49
1967	1	–	6	1	2	1	1	4	–	16
1969	–	1	–	1	–	1	–	–	–	3
1971	–	–	–	–	–	–	–	–	–	–
1973	–	–	4	3	2	2	2	–	–	13
1976	–	–	4	4	4	4	4	–	–	20
1977	–	–	3	2	2	3	2	–	–	12
1979	11	2	1	5	1	–	–	–	–	20
1984	–	–	4	10	7	7	6	–	–	34
1994	–	–	–	–	–	–	–	–	–	–
1995	–	–	–	–	–	–	–	–	–	–
GIG										
1965*	–	2	4	1	1	–	–	–	–	8
1966*	3	2	3	5	2	–	–	–	–	15
1967	1	6	11	6	10	–	–	–	–	34
1969	–	9	11	6	6	–	–	–	–	32
1971	–	5	15	9	10	–	–	–	–	39

Survey Year	20 fathom depth interval (m)									Total Tows
	66-146	147-183	184-219	220-256	257-292	293-329	330-366	367-402	440-549	
1973	–	7	11	7	8	–	–	–	–	33
1976	–	7	15	8	6	–	–	–	–	36
1977	1	12	14	14	9	–	–	–	–	50
1979*	23	12	18	6	–	–	–	–	–	59
1984	–	13	25	17	13	1	–	–	–	69
1994	–	15	18	20	18	–	–	–	–	71
1995*	2	23	47	22	15	6	–	–	–	115

Given that the only area that was consistently monitored by these surveys was the GIG grounds, tows lying between 50.9°N and 51.6°N latitude from the seven acceptable survey years, covering the period from 1967 to 1994, were used to index the CAR population (Table B.1).

The original depth stratification of these surveys was in 20 fathom (36.1 m) intervals, ranging from 36 fathoms (66 m) to 300 fathoms (549 m). These depth strata were combined for analysis into three ranges which encompassed most rockfish: 120–183 m, 184–218 m and 219–300 m, for a total of 332 tows from the eight accepted survey years (Table B.3).

Table B.3. Number of tows available by survey year and depth stratum for the analysis of the historical GIG trawl survey series. Survey year in grey and marked with an asterisk was not used in the CAR stock assessment.

Survey Year	Depth stratum			Total	Start Date	End Date
	120-183 m (70–100 fm)	184-218 m (100–120 fm)	219-300 m (120–160 fm)			
1967	7	11	15	33	07-Sep-67	03-Oct-67
1969	8	11	12	31	14-Sep-69	24-Sep-69
1971	4	15	17	36	14-Oct-71	28-Oct-71
1973	7	11	15	33	07-Sep-73	24-Sep-73
1976	7	13	13	33	09-Sep-76	26-Sep-76
1977	13	14	20	47	24-Aug-77	07-Sep-77
1984	13	23	33	69	05-Aug-84	08-Sep-84
1994	10	16	24	50	21-Jun-94	06-Jul-94
1995*	22	45	45	112	11-Sep-95	22-Sep-95

A doorspread density (Eq. B.3) was calculated for each tow based on the catch of CAR, using a fixed doorspread value of 61.6 m (Yamanaka et al. 1996) for every tow and the recorded distance travelled. Unfortunately, the speed, effort and distance travelled fields were not well populated for these surveys. Therefore, missing values for these fields were filled in with the mean values for the survey year. This resulted in the majority of the tows having distances towed near 3 km, which was the expected result given the design specification of ½ hour tows at an approximate speed of 6 km/h (about 3.2 knots).

B.3.2. Results

Maps showing the locations where CAR were caught in the Goose Island Gully (GIG) indicate that this species is generally found along the 200 m contour on both sides of the gully, although in variable amounts. This species was present in every year, although in appreciable amounts only in 1971, 1977 and 1984 (see Figure B.1 to Figure B.8). CAR was taken relatively frequently, but in small amounts, with 109 of the 332 (33%) valid tows capturing CAR with a median catch weight of 4.5 kg. The largest valid CAR tow in terms of catch weight was 2,092 kg in 1984. CAR were mainly taken at depths from 157 to 240 m (5% and 95% quantiles of the starting depth empirical distribution), with the minimum and maximum observed CAR catch weights at starting tow depths of 148 and 282 m respectively (Figure B.9).

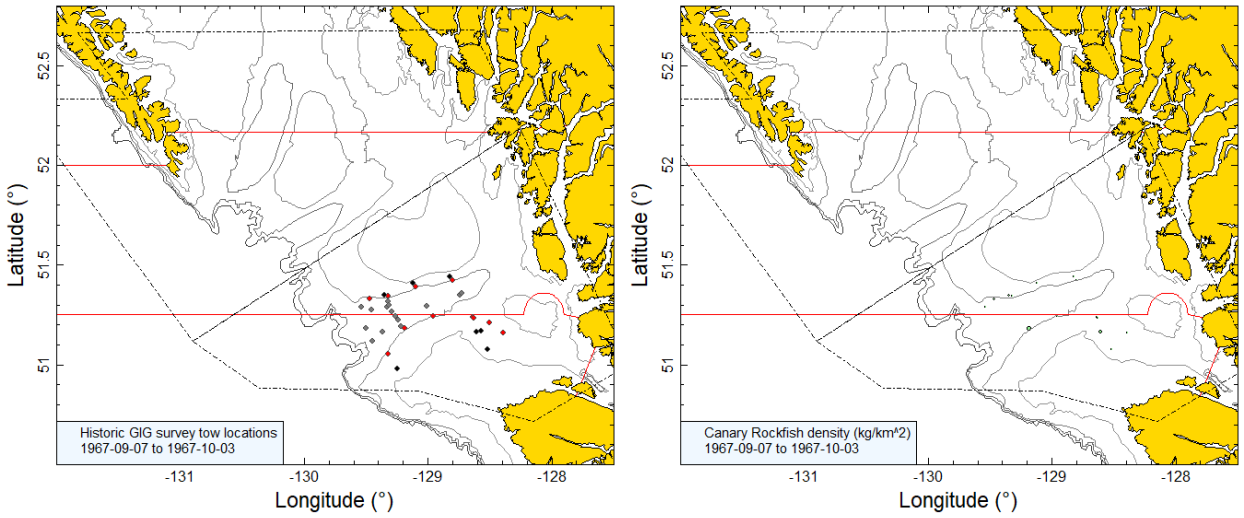

Figure B.1. Valid tow locations and density plots for the historic 1967 Goose Island Gully (GIG) survey. Tow locations are colour-coded by depth range: black=120–183 m; red=184-218 m; grey=219-300 m. Circle sizes in the right-hand density plot scaled across all years (1967, 1969, 1971, 1973, 1976, 1977, 1984, and 1994), with the largest circle = 2,420 kg/km^2 in 1971. Black boundary lines show the extent of the modern Queen Charlotte Sound synoptic survey and the red solid lines indicate the boundaries between PMFC areas 5A, 5B and 5C. Depth contours denote 100 m, 200 m, 300 m, 500 m.

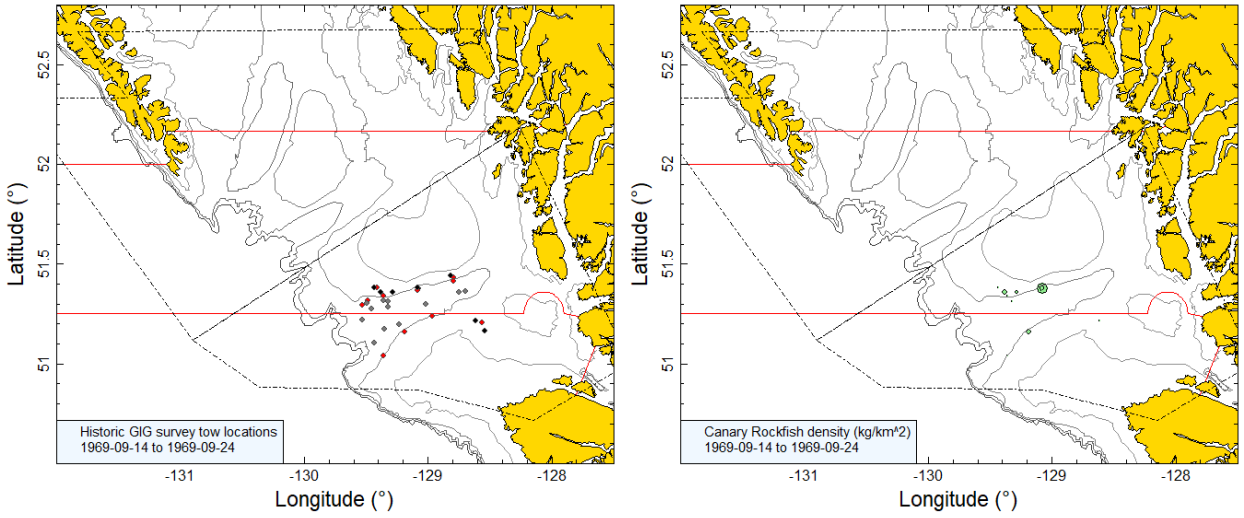

Figure B.2. Tow locations and density plots for the historic 1969 Goose Island Gully (GIG) survey (see Figure B.1 caption).

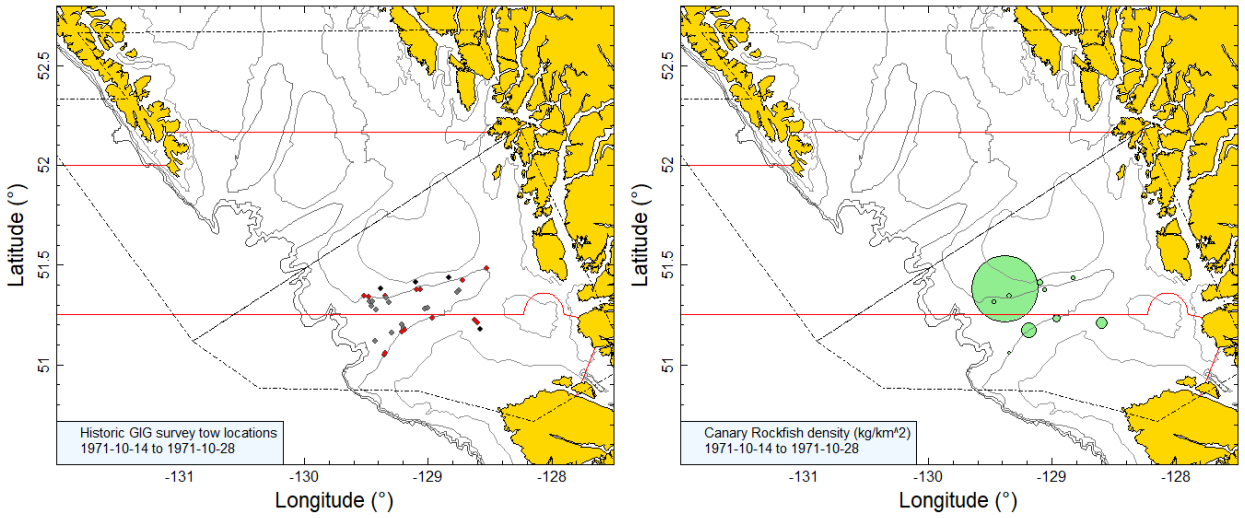

Figure B.3. Tow locations and density plots for the historic 1971 Goose Island Gully (GIG) survey (see Figure B.1 caption).

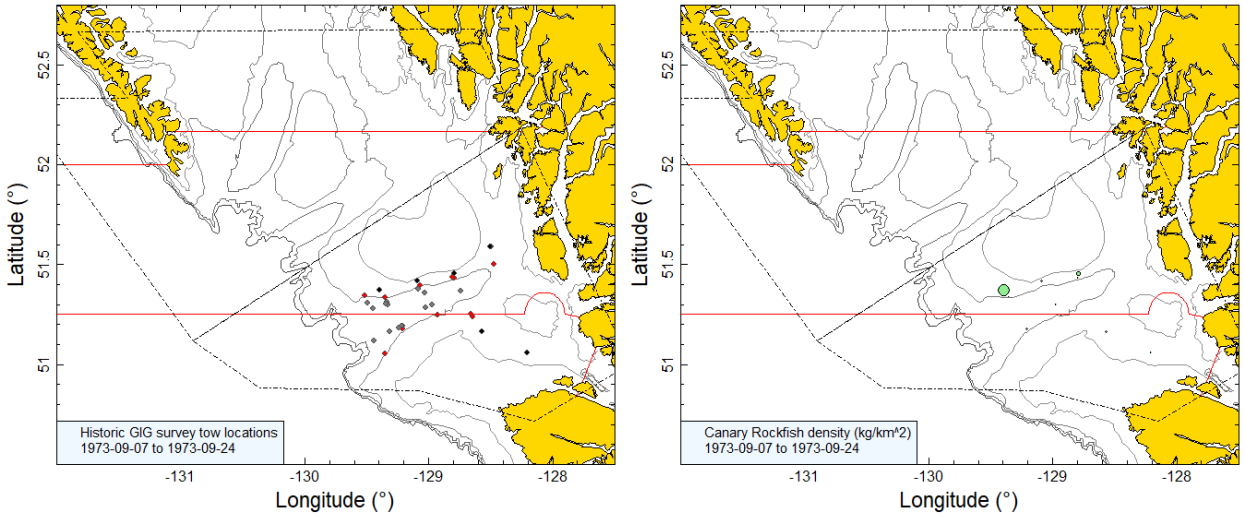

Figure B.4. Tow locations and density plots for the historic 1973 Goose Island Gully (GIG) survey (see Figure B.1 caption).

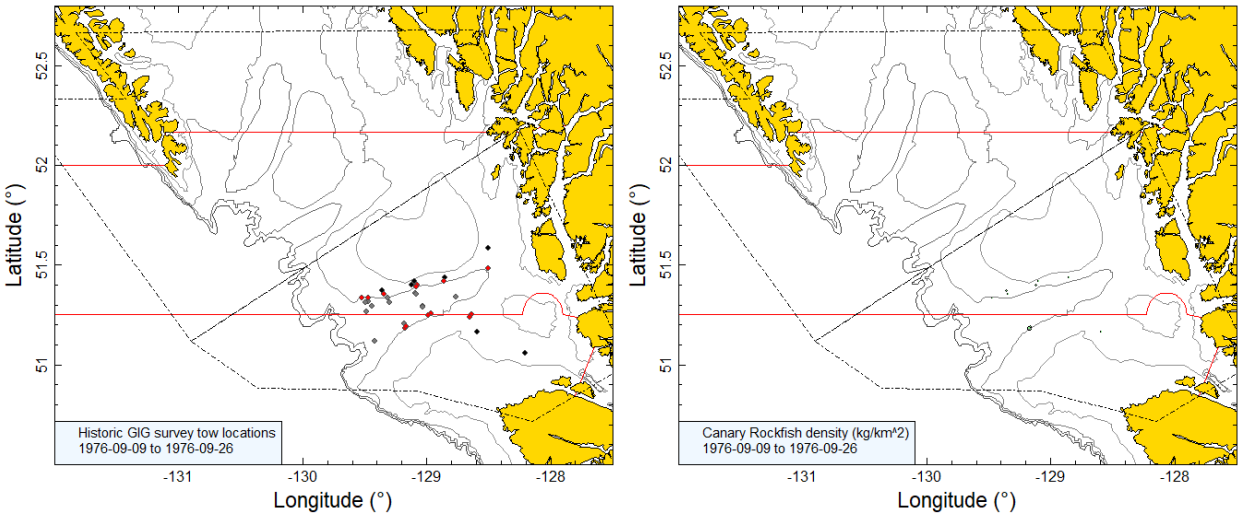

Figure B.5. Tow locations and density plots for the historic 1976 Goose Island Gully (GIG) survey (see Figure B.1 caption).

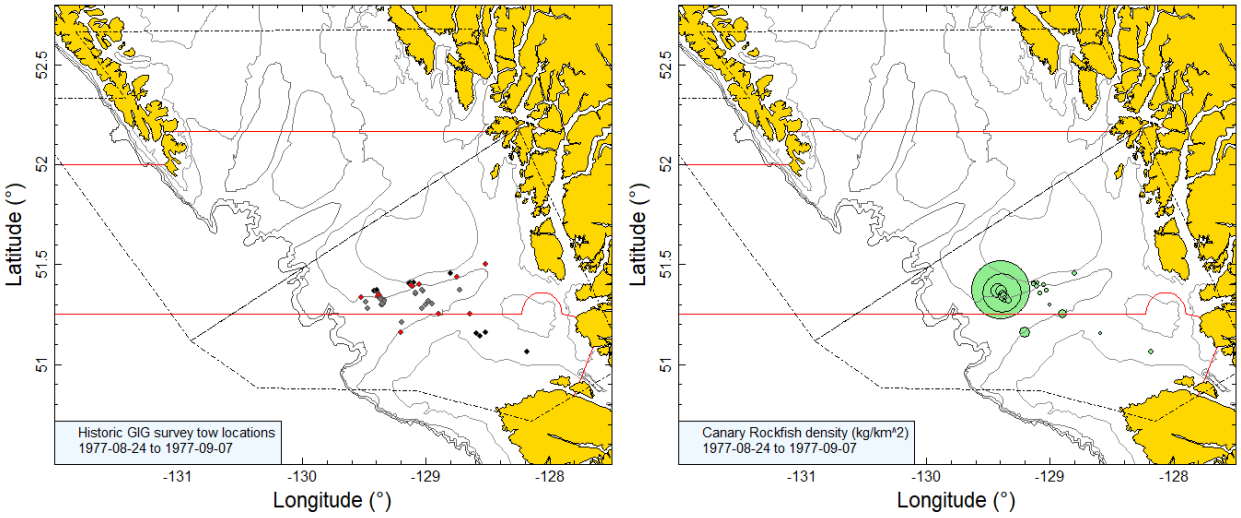

Figure B.6. Tow locations and density plots for the historic 1977 Goose Island Gully (GIG) survey (see Figure B.1 caption).

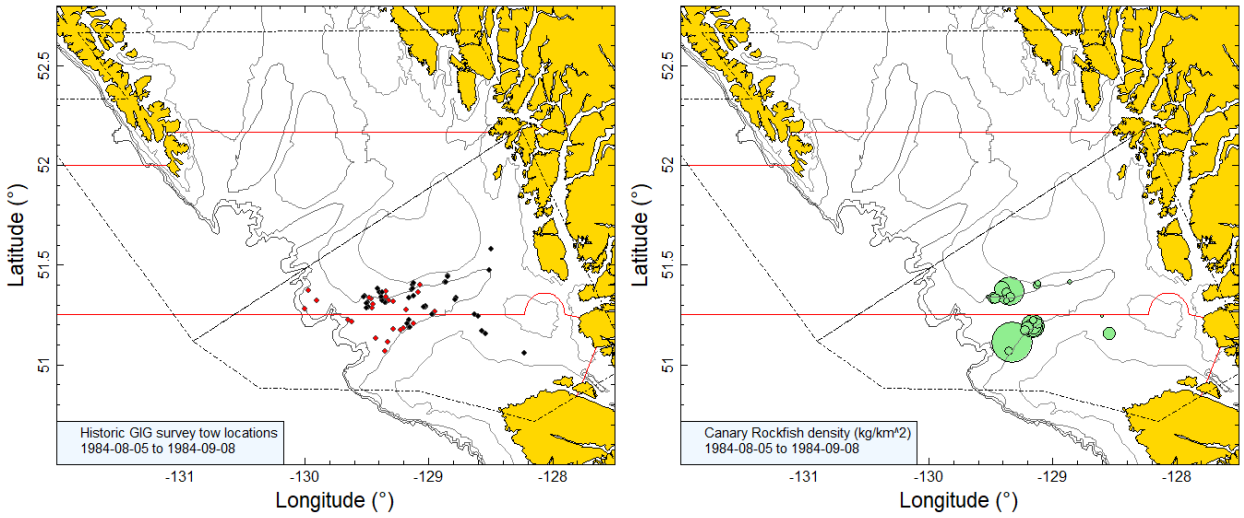

Figure B.7. [left panel]: Tow location colours indicate the vessel fishing rather than depth: black=G.B. Reed; red=Eastward Ho; [right panel]: density plot for the historic 1984 Goose Island Gully (GIG) survey (see Figure B.1 caption).

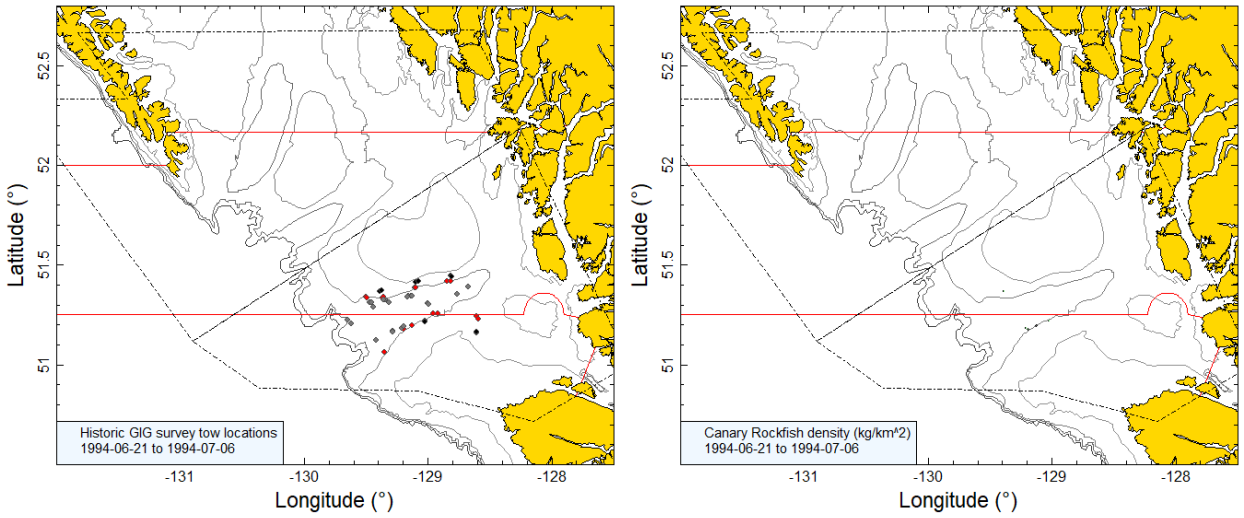

Figure B.8. Tow locations and density plots for the Ocean Selector 1994 Goose Island Gully (GIG) survey (see Figure B.1 caption).

Estimated biomass levels in the GIG for Canary Rockfish from the historical GIG trawl surveys were variable, with the maximum biomass recorded in 1971 (at 1,327 t) and the minimum biomass in 1994 (at 35 t) (Figure B.10; Table B.4). Survey relative errors were variable and very high for this species, ranging from a low of 0.32 in 1967 to 1.00 in 1971 (Table B.4). The proportion of tows which caught CAR ranged between 10% in 1994 and 51% in 1977 (Figure B.11). Overall, 109 tows from a total 332 valid tows (33%) contained CAR.

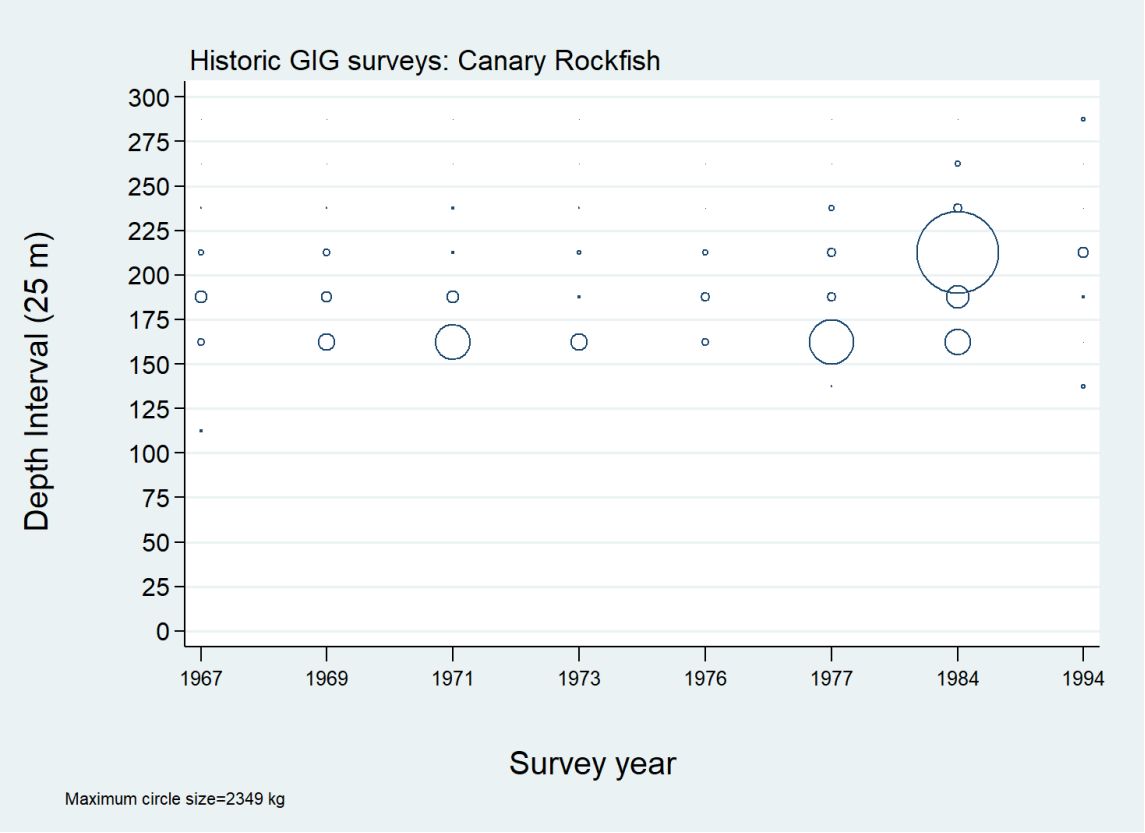

Figure B.9. Distribution of observed catch weights of Canary Rockfish (CAR) for the historic Goose Island Gully (GIG) surveys (Table B.3) by survey year and 25 m depth zone. Depth zones are indicated by the mid point of the depth interval and circles in the panel are scaled to the maximum value (2349 kg) in the 200–225 m interval in 1984. The 1% and 99% quantiles for the CAR empirical start of tow depth distribution = 151 m and 240 m respectively.

Table B.4. Biomass estimates for Canary Rockfish from the historical Goose Island Gully trawl surveys for the years 1967 to 1994. Biomass estimates are based on three depth strata (Table B.3), assuming that the survey tows were randomly selected within these areas. Bootstrap bias corrected confidence intervals and CVs are based on 1000 random draws with replacement.

Survey Year	**Biomass (t)** (Eq. B.4)	**Mean bootstrap biomass (t)**	**Lower bound biomass (t)**	**Upper bound biomass (t)**	**Bootstrap CV**	**Analytic CV** (Eq. B.6)
1967	100.7	101.8	49.7	174.7	0.322	0.325
1969	187.4	183.4	51.2	447.2	0.545	0.554
1971	1,326.9	1,260.7	30.2	5,168.1	1.000	0.963
1973	174.3	180.1	23.0	482.8	0.713	0.713
1976	64.6	64.6	20.9	124.0	0.403	0.413
1977	589.0	582.9	88.7	1,533.7	0.600	0.621
1984	394.3	397.0	169.7	748.3	0.379	0.377
1994	35.0	34.9	8.2	80.0	0.501	0.494

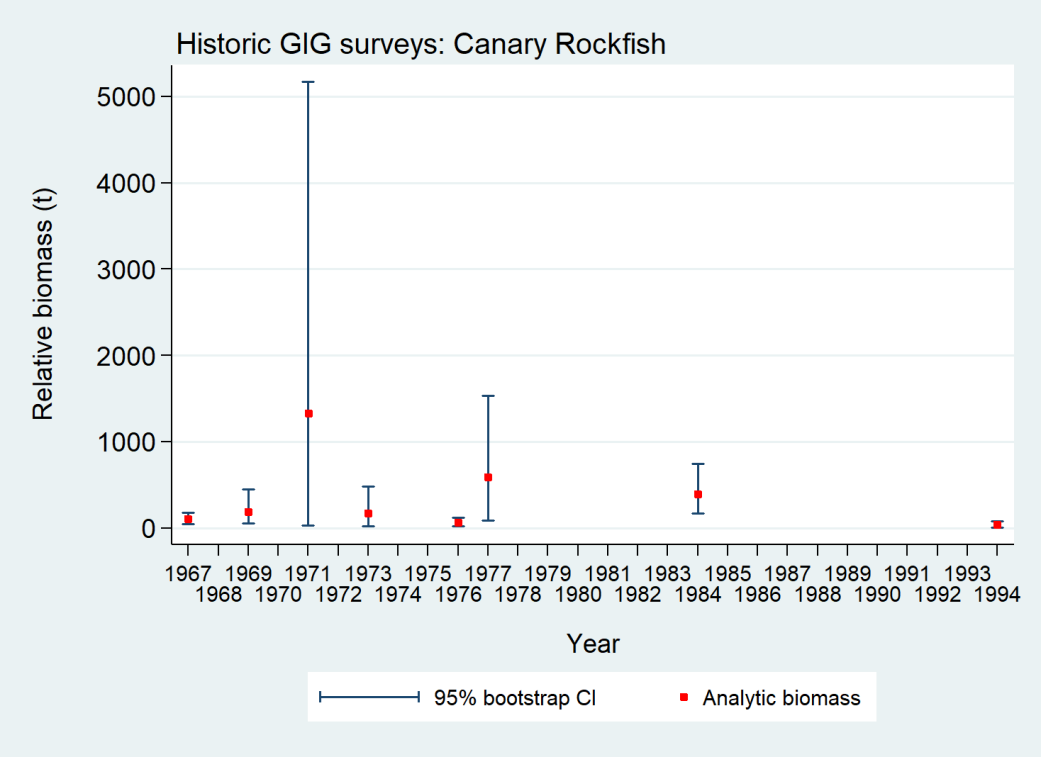

Figure B.10. Plot of biomass estimates for the CAR historic Goose Island Gully (GIG) surveys: 1967 to 1994 (values provided in Table B.4). Bias corrected 95% confidence intervals from 1000 bootstrap replicates are plotted.

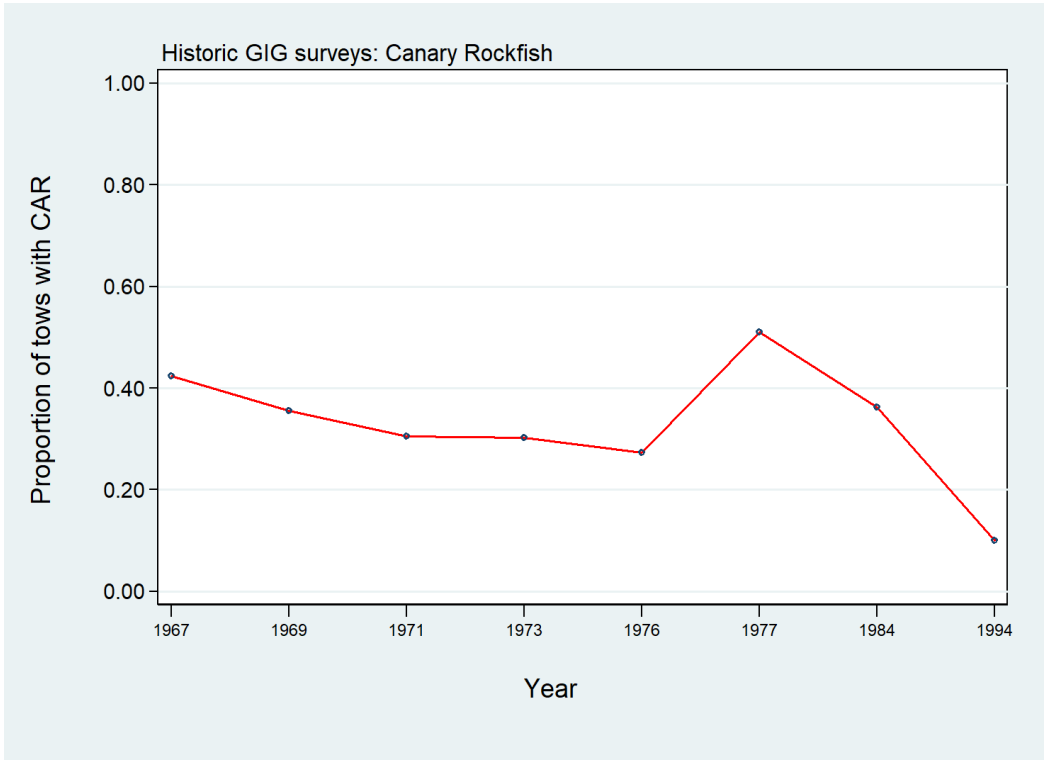

Figure B.11. Proportion of tows by year which contain CAR from the historic Goose Island Gully (GIG) surveys: 1967 to 1994.

B.4. NMFS TRIENNIAL TRAWL SURVEY

B.4.1. Data selection

Tow-by-tow data from the US National Marine Fisheries Service (NMFS) triennial survey covering the Vancouver INPFC (International North Pacific Fisheries Commission) region were provided by Mark Wilkins (NMFS, pers. comm., 2008) for the seven years that the survey operated in BC waters (Table B.5; 1980: Figure B.12; 1983: Figure B.13; 1989: Figure B.14; 1992: Figure B.15; 1995: Figure B.16; 1998: Figure B.17; 2001: Figure B.18). These tows were assigned to strata by the NMFS, but the size and definition of these strata have changed over the life of the survey (Table B.6). The NMFS survey database also identified in which country the tow was located. This information was plotted and checked against the accepted Canada/USA marine boundary: all tows appeared to be appropriately located with respect to country, based on the tow start position (Figure B.12 to Figure B.18). The NMFS designations were accepted for tows located near the marine border. Note that the data provided did not include the dates of the tows, so it is not possible to provide the dates on which these surveys operated.

Table B.5. Number of tows by stratum and by survey year for the NFMS triennial survey. Strata coloured grey and marked with an asterisk have been excluded from the analysis due to incomplete coverage across the seven survey years or were from locations outside the Vancouver INPFC area (Table B.6).

Stratum	1980		1983		1989		1992		1995		1998		2001	
No.	CDN	US	CDN	US	CDN	US	CDN	US	CDN	US	CDN	US	CDN	US
10	–	17	–	7	–	–	–	–	–	–	–	–	–	–
11	48	–	–	39	–	–	–	–	–	–	–	–	–	–
12	–	–	38	–	–	–	–	–	–	–	–	–	–	–
17N	–	–	–	–	–	8	–	9	–	8	–	8	–	8
17S*	–	–	–	–	–	27	–	27	–	25	–	26	–	25
18N*	–	–	–	–	1	–	1	–	–	–	–	–	–	–
18S	–	–	–	–	–	32	–	23	–	12	–	20	–	14
19N	–	–	–	–	58	–	53	–	55	–	48	–	33	–
19S	–	–	–	–	–	4	–	6	–	3	–	3	–	3
27N	–	–	–	–	–	2	–	1	–	2	–	2	–	2
27S*	–	–	–	–	–	5	–	2	–	3	–	4	–	5
28N*	–	–	–	–	1	–	1	–	2	–	1	–	–	–
28S	–	–	–	–	–	6	–	9	–	7	–	6	–	7
29N	–	–	–	–	7	–	6	–	7	–	6	–	3	–
29S	–	–	–	–	–	3	–	2	–	3	–	3	–	3
30	–	4	–	2	–	–	–	–	–	–	–	–	–	–
31	7	–	–	11	–	–	–	–	–	–	–	–	–	–
32	–	–	5	–	–	–	–	–	–	–	–	–	–	–
37N*	–	–	–	–	–	–	–	–	–	1	–	1	–	1
37S*	–	–	–	–	–	–	–	–	–	2	–	1	–	1
38N*	–	–	–	–	–	–	–	–	1	–	–	–	–	–
38S*	–	–	–	–	–	–	–	–	–	2	–	–	–	3
39*	–	–	–	–	–	–	–	–	6	–	4	–	2	–
50	–	5	–	1	–	–	–	–	–	–	–	–	–	–
51	4	–	–	10	–	–	–	–	–	–	–	–	–	–
52	–	–	4	–	–	–	–	–	–	–	–	–	–	–
Total	59	26	47	70	67	87	61	79	71	68	59	74	38	72

All usable tows had an associated median net width (with 1-99% quantiles) of 13.4 (11.3-15.7) m and median distance travelled of 2.8 (1.4-3.5) km, allowing for the calculation of the area swept by each tow. Biomass indices and the associated analytical CVs for Canary Rockfish were calculated for each of the Canadian and US Vancouver sub-regions, using appropriate area estimates for each stratum and year (Table B.6). Strata that were not surveyed

consistently in all seven years of the survey were dropped from the analysis (Table B.5; Table B.6), allowing the remaining data to provide a comparable set for each year (Table B.7).

The stratum definitions used in the 1980 and 1983 surveys were different than those used in subsequent surveys, particularly in Canadian waters (Table B.7). Therefore, the 1980 and 1983 Canadian indices were scaled by the ratio (9166 km^2 / 7399 km^2 = 1.24) of the total stratum areas relative to the 1989 and later surveys so that the coverage from the first two surveys would be comparable to the surveys conducted from 1989 onwards. Correspondingly, the 1980 and 1983 US indices were scaled down slightly (4699 km^2 /4738 km^2 = 0.99) in the same manner. The tow density was much higher in US waters although the overall number of tows was approximately the same for each country (Table B.7). This occurred because the size of the total area fished in the INPFC Vancouver area was about twice as large in Canadian waters than in US waters (Table B.7). Note that the northern extension of the survey varied from year to year (see Figure B.12 to Figure B.18), but this difference has been compensated for by using a constant survey area for all years and assuming that catch rates in the unsampled areas were the same as in the sampled area.

Table B.6. Stratum definitions by year used in the NMFS triennial survey to separate the survey results by country and by INPFC area. Stratum definitions in grey and marked with an asterisk are those strata which have been excluded from the final analysis due to incomplete coverage across the seven survey years or because the locations were outside the Vancouver INPFC area.

Year	Stratum No.	Area (km^2)	Start	End	Country	INPFC area	Depth range
1980	10	3537	47°30	US-Can Border	US	Vancouver	55-183 m
1980	11	6572	US-Can Border	49°15	CDN	Vancouver	55-183 m
1980	30	443	47°30	US-Can Border	US	Vancouver	184-219 m
1980	31	325	US-Can Border	49°15	CDN	Vancouver	184-219 m
1980	50	758	47°30	US-Can Border	US	Vancouver	220-366 m
1980	51	503	US-Can Border	49°15	CDN	Vancouver	220-366 m
1983	10	1307	47°30	47°55	US	Vancouver	55-183 m
1983	11	2230	47°55	US-Can Border	US	Vancouver	55-183 m
1983	12	6572	US-Can Border	49°15	CDN	Vancouver	55-183 m
1983	30	66	47°30	47°55	US	Vancouver	184-219 m
1983	31	377	47°55	US-Can Border	US	Vancouver	184-219 m
1983	32	325	US-Can Border	49°15	CDN	Vancouver	184-219 m
1983	50	127	47°30	47°55	US	Vancouver	220-366 m
1983	51	631	47°55	US-Can Border	US	Vancouver	220-366 m
1983	52	503	US-Can Border	49 °15	CDN	Vancouver	220-366 m
1989&after	17N	1033	47°30	47°50	US	Vancouver	55-183 m
1989&after*	17S	3378	46°30	47°30	US	Columbia	55-183 m
1989&after*	18N	159	47°50	48°20	CDN	Vancouver	55-183 m
1989&after	18S	2123	47°50	48°20	US	Vancouver	55-183 m
1989&after	19N	8224	48°20	49°40	CDN	Vancouver	55-183 m
1989&after	19S	363	48°20	49°40	US	Vancouver	55-183 m
1989&after	27N	125	47°30	47°50	US	Vancouver	184-366 m
1989&after*	27S	412	46°30	47°30	US	Columbia	184-366 m
1989&after*	28N	88	47°50	48°20	CDN	Vancouver	184-366 m
1989&after	28S	787	47°50	48°20	US	Vancouver	184-366 m
1989&after	29N	942	48°20	49°40	CDN	Vancouver	184-366 m
1989&after	29S	270	48°20	49°40	US	Vancouver	184-366 m
1995&after*	37N	102	47°30	47°50	US	Vancouver	367-500 m
1995&after*	37S	218	46°30	47°30	US	Columbia	367-500 m
1995&after*	38N	66	47°50	48°20	CDN	Vancouver	367-500 m
1995&after*	38S	175	47°50	48°20	US	Vancouver	367-500 m

Table B.7. Number of usable tows performed and area surveyed in the INPFC Vancouver region separated by the international border between Canada and the United States. Strata 18N, 28N, 37, 38 and 39 (Table B.6) were dropped from this analysis as they were not consistently conducted over the survey period. All strata occurring in the Columbia INPFC region (17S and 27S; Table B.6) were also dropped. Thirty-three "water hauls" are separately listed in this table.

	Tows: Canada waters			Tows: US waters			All Tows			Coverage (km^2)		
Year	Usable tows	Water hauls	Total	Usable tows	Water hauls	Total	Usable tows	Water hauls	Total	Canada waters	US waters	Total
1980	48	11	59	23	3	26	71	14	85	7,399	4,738	12,137
1983	39	8	47	65	5	70	104	13	117	7,399	4,738	12,137
1989	63	2	65	54	1	55	117	3	120	9,166	4,699	13,865
1992	59	–	59	47	3	50	106	3	109	9,166	4,699	13,865
1995	62	–	62	35	–	35	97	–	97	9,166	4,699	13,865
1998	54	–	54	42	–	42	96	–	96	9,166	4,699	13,865
2001	36	–	36	37	–	37	73	–	73	9,166	4,699	13,865
Total	361	21	382	303	12	315	664	33	697	–	–	–

Six hundred and ninety-seven tows across seven survey years remained in the data set after the inconsistently surveyed strata identified in Table B.6 were removed (Table B.7). A further 33 tows were identified as "water hauls" (Table B.7) after a reviewer from NOAA for the 2014 Yellowtail Rockfish stock assessment (DFO 2015) pointed out that a number of the early Triennial survey tows had been so designated because they caught no fish or invertebrates and recommended that they should be discarded from the estimation procedure.

B.4.2. Methods

The data were analysed using the equations in Section B.1. When calculating the variance for this survey, it was assumed that the variance and CPUE within any stratum were equal, even for strata that were split by the Canada/USA border. The total biomass $\left(B_{y_i}\right)$ within a stratum that straddled the border was split between the two countries $\left(B_{y_{i_c}}\right)$ by the ratio of the relative area within each country:

Eq. B.7 $$B_{y_{i_c}} = B_{y_i} \frac{A_{y_{i_c}}}{A_{y_i}},$$

where $A_{y_{i_c}}$ = area (km^2) within country *c* in year *y* and stratum *i*.

The variance $V_{y_{i_c}}$ for that part of stratum *i* within country *c* was calculated as being in proportion to the ratio of the square of the area within each country *c* relative to the total area of stratum *i*. This assumption resulted in the CVs within each country stratum being the same as the CV in the entire stratum:

Eq. B.8 $$V_{y_{i_c}} = V_{y_i} \frac{A^2_{y_{i_c}}}{A^2_{y_i}}.$$

The partial variance $V_{y_{ic}}$ for country *c* was used in Eq. B.5 instead of the total variance in the stratum V_{y_i} when calculating the variance for the total biomass in Canadian or American waters. CVs were calculated as in Eq. B.6.

The biomass estimates Eq. B.4 and the associated standard errors were adjusted to a constant area covered using the ratios of area surveyed provided in Table B.7. This was required to adjust the Canadian biomass estimates for 1980 and 1983 to account for the smaller area surveyed in those years compared to the succeeding surveys. The 1980 and 1983 biomass estimates from Canadian waters were consequently multiplied by the ratio 1.24 (= 9166 km^2 / 7399 km^2) to make them equivalent to the coverage of the surveys from 1989 onwards.

Biomass estimates were bootstrapped using 1000 random draws with replacement to obtain bias-corrected (Efron 1982) 95% confidence intervals for each year and for the two regions (Canadian-Vancouver and US-Vancouver) based on the distribution of biomass estimates and using the above equations.

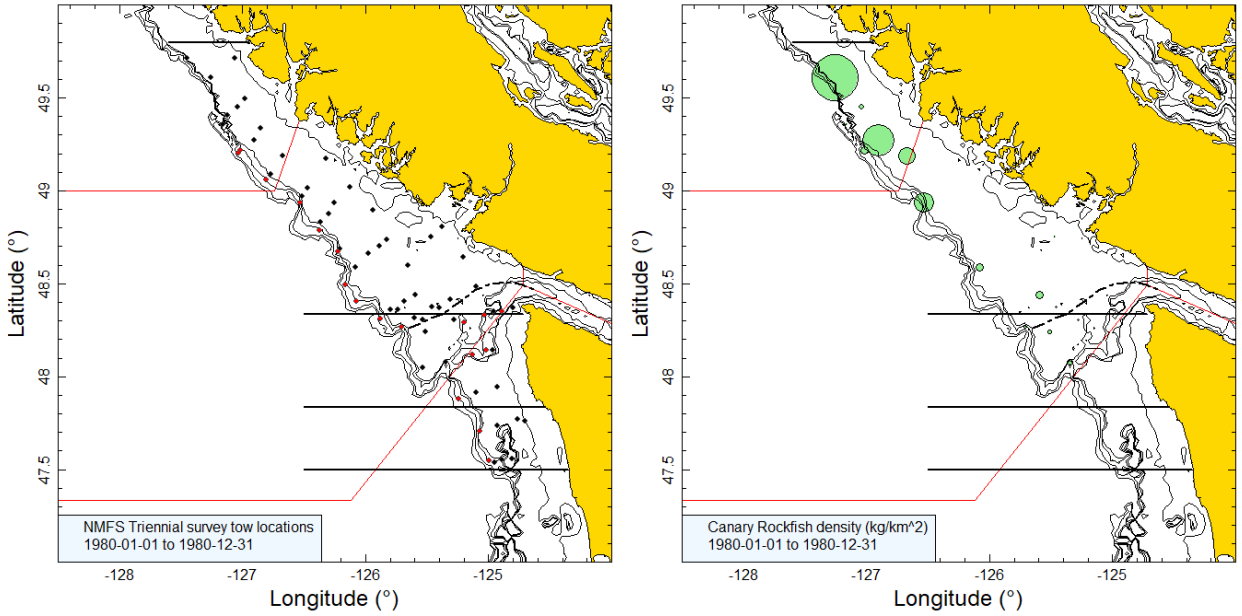

Figure B.12. [left panel]: plot of tow locations in the Vancouver INPFC region for the 1980 NMFS triennial survey in US and Canadian waters. Tow locations are colour-coded by depth range: black=55–183 m; red=184-366 m. Dashed line shows approximate position of the Canada/USA marine boundary. Horizontal lines are the stratum boundaries: 47°30', 47°50', 48°20' and 49°50'. Tows south of the 47°30' line were not included in the analysis. [left panel]:water hauls (Table B.7) have been excluded; [right panel]: circle sizes in the density plot are scaled across all years (1980, 1983, 1989, 1992, 1995, 1998, and 2001), with the largest circle = 44,379 kg/km^2 in 1983 (US waters). The red solid lines indicate the boundaries between PMFC areas 3B, 3C and 3D. Depth contours denote 50 m, 200 m, 300 m, 400 m, 500 m. Note that survey dates were not available so only the survey year can be identified.

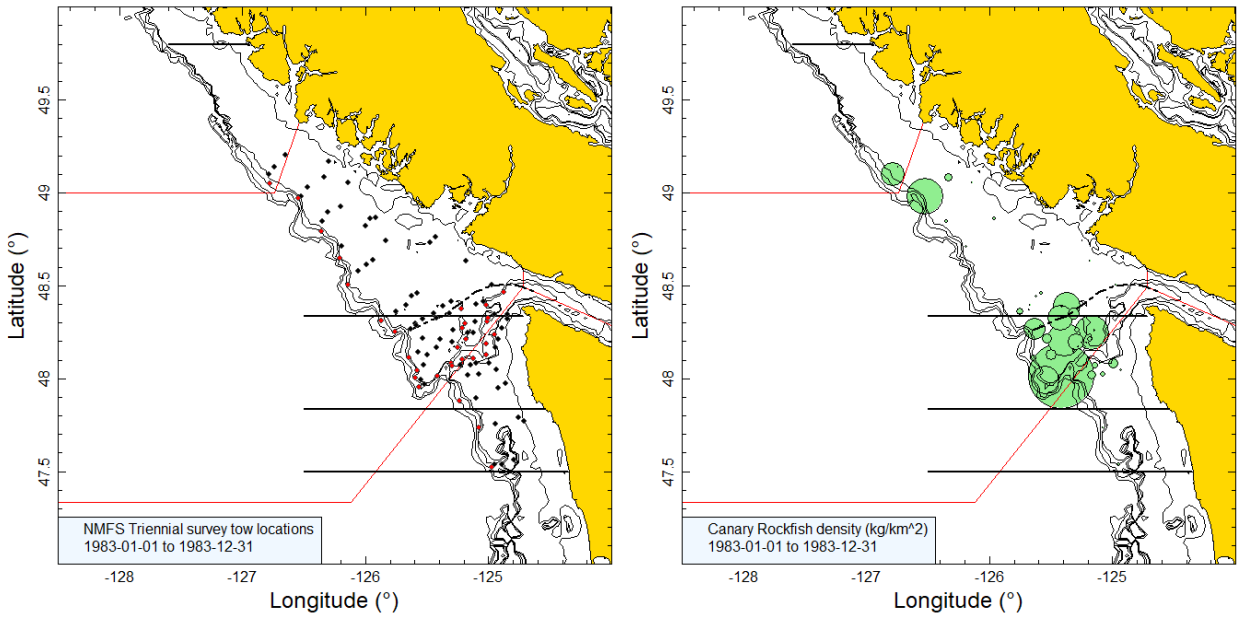

Figure B.13. Tow locations and density plots for the 1983 NMFS triennial survey in US and Canadian waters (see Figure B.12 caption).

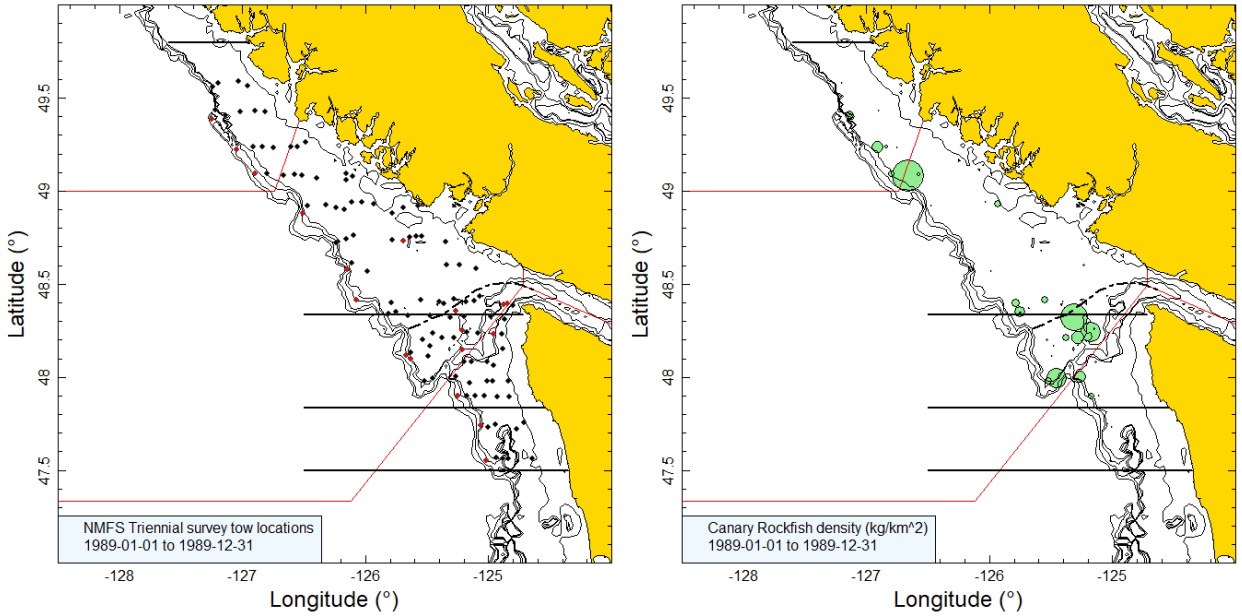

Figure B.14. Tow locations and density plots for the 1989 NMFS triennial survey in US and Canadian waters (see Figure B.12 caption).

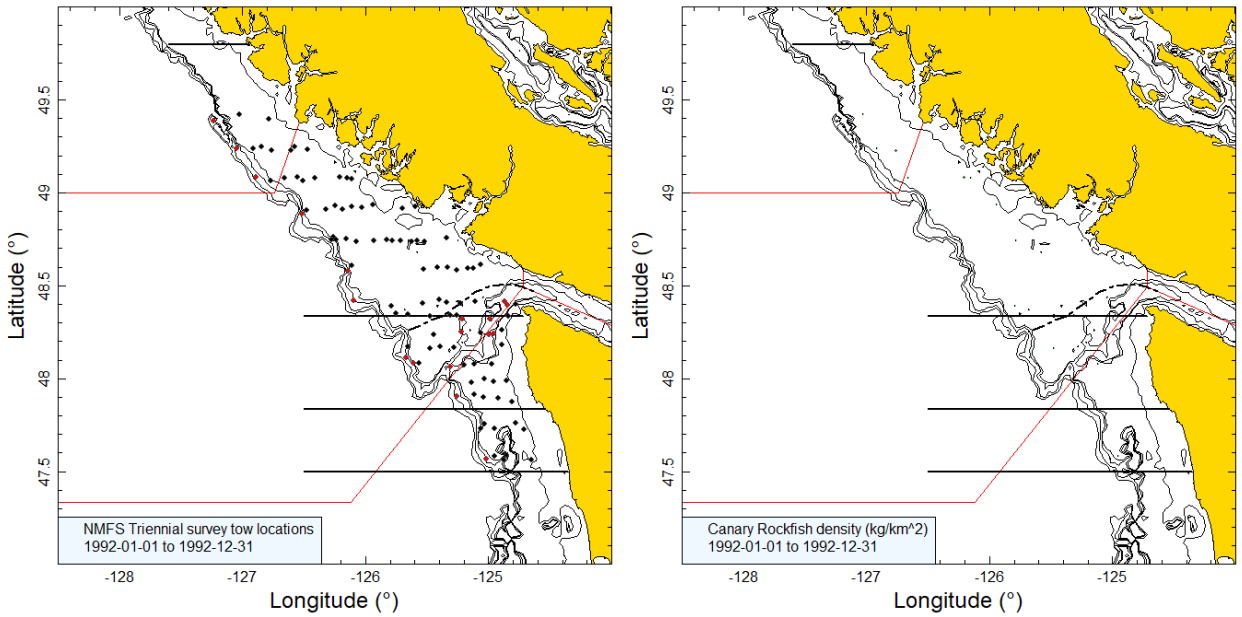

Figure B.15. Tow locations and density plots for the 1992 NMFS triennial survey in US and Canadian waters (see Figure B.12 caption).

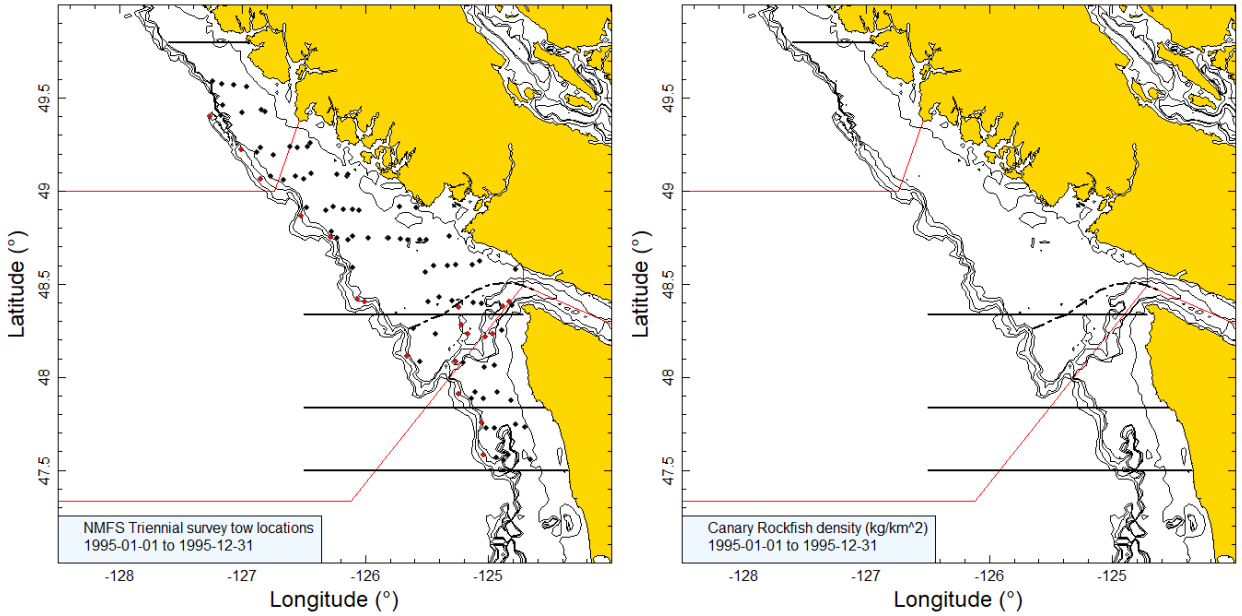

Figure B.16. Tow locations and density plots for the 1995 NMFS triennial survey in US and Canadian waters (see Figure B.12 caption).

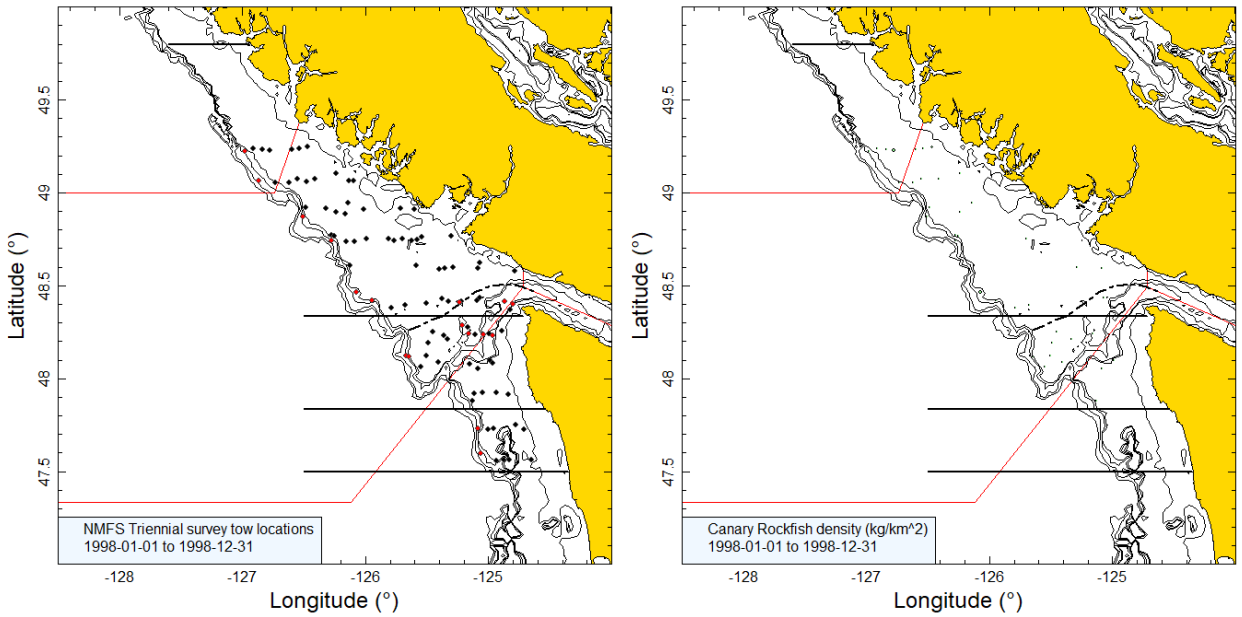

Figure B.17. Tow locations and density plots for the 1998 NMFS triennial survey in US and Canadian waters (see Figure B.12 caption).

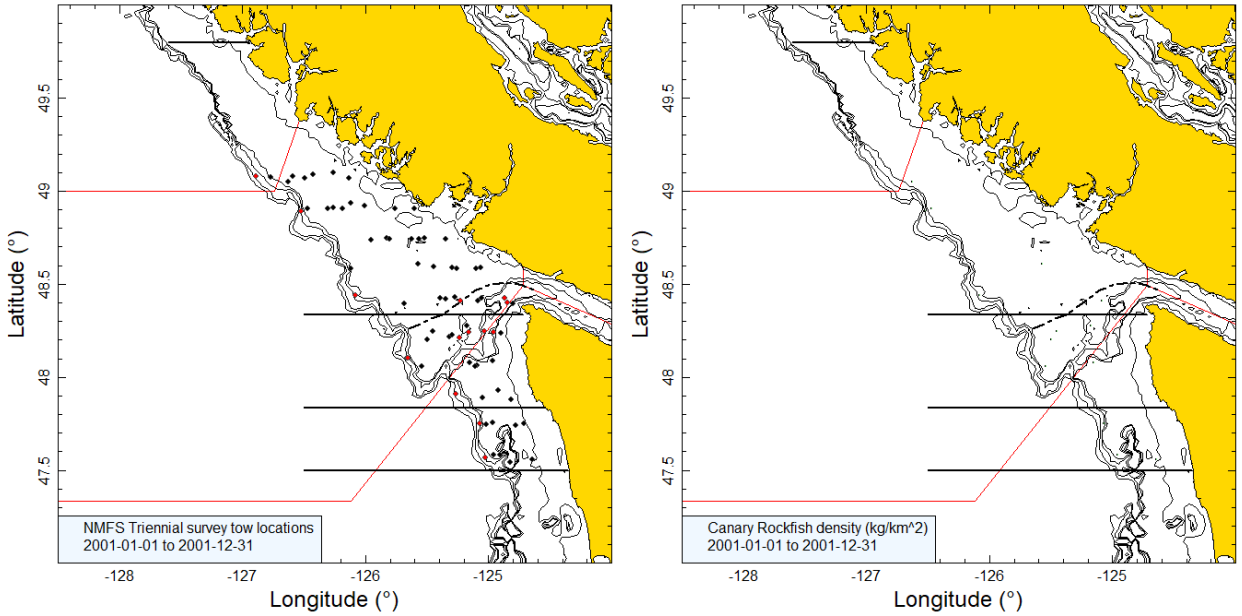

Figure B.18. Tow locations and density plots for the 2001 NMFS triennial survey in US and Canadian waters (see Figure B.12 caption).

B.4.3. Results

The occurrence of Canary Rockfish (CAR) in this survey was variable, with the median catch weight for the tows catching CAR at 6.4 kg while there were 16 tows (from 192 tows which captured CAR and were used for biomass estimation) which caught more than 100 kg of CAR. Three tows among the 192 tows captured more than 1000 kg. Only the first three surveys caught appreciable amounts of CAR (1980, 1983, 1989), with the following four surveys (1992, 1995, 1998, 2001) only catching small amounts of this species. It is not known why this species

figured so little in these surveys, but the WCVI synoptic survey (see Section B.6) indicates that this species tends to favour the more northern sections of the Vancouver Island coast (above the northern limit of this survey) and is found less frequently in the more southern part of the coast. Figure B.19 shows that this species was mainly captured between 100 and 225 m (the 10 and 90% quantiles of [bottom_depth] were 108 m and 200 m respectively), with the deepest observation at 241 m, indicating that this survey encompassed the full depth range for this species.

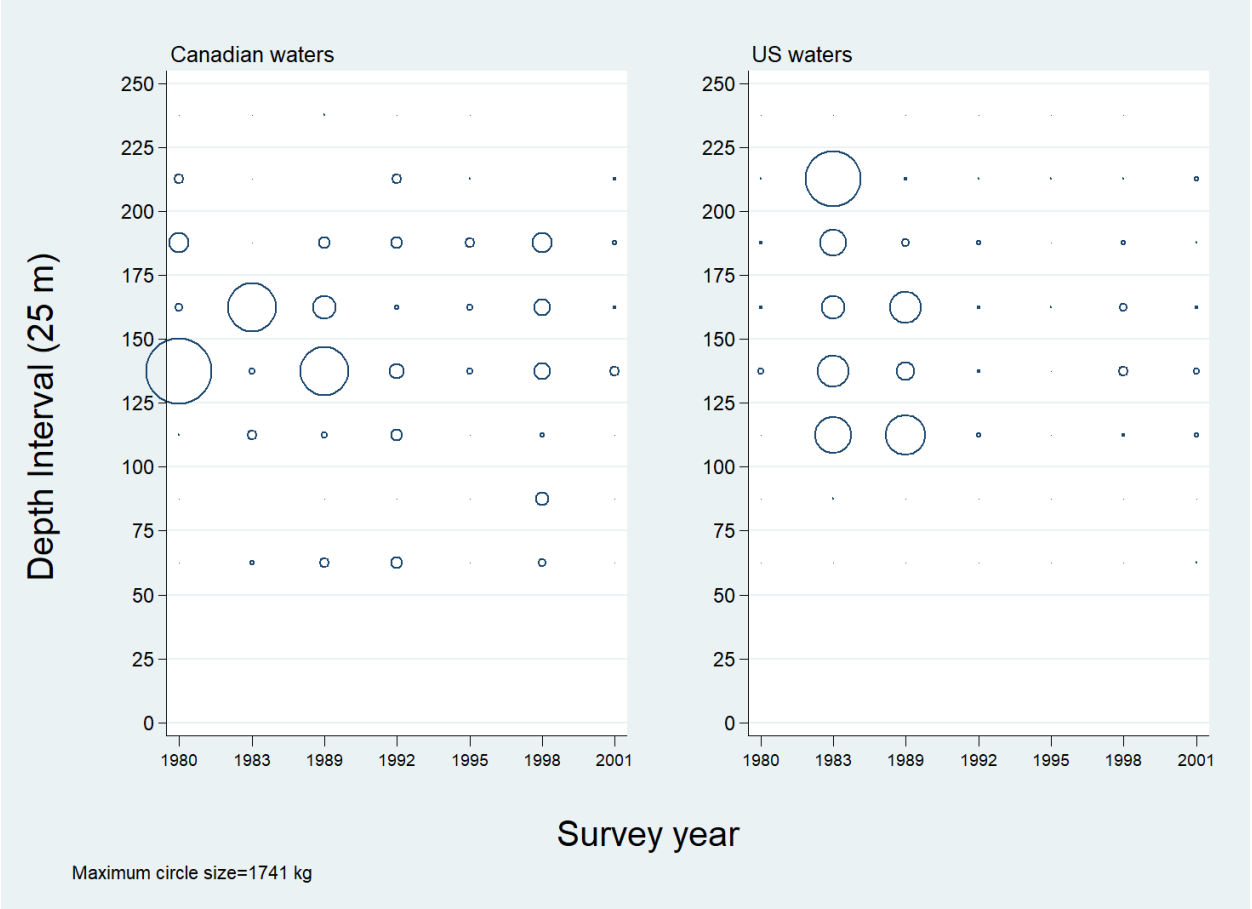

Figure B.19. Distribution of Canary Rockfish catch weights for each survey year summarised into 25 m depth intervals for all tows (Table B.7) in Canadian and US waters of the Vancouver INPFC area. Catches are plotted at the mid-point of the interval.

The biomass estimates for the first three surveys (1980, 1983, 1989) were much larger than the following biomass estimates and were associated with very large relative errors (0.62, 0.53, 0.61)(Figure B.20; Table B.8). This results in an apparent declining trend for CAR in the Canadian series when coupled with the low biomass estimates after the 1989 survey. This trend should be viewed with caution given that this survey is only covering a small portion of the available CAR habitat on the Canadian west coast. Note that the bootstrap estimates of relative error do not include any uncertainty with respect to the ratio expansion required to make the 1980 and 1983 survey estimates comparable to the 1989 and later surveys. Therefore, it is likely that the true uncertainty for this series is greater than estimated.

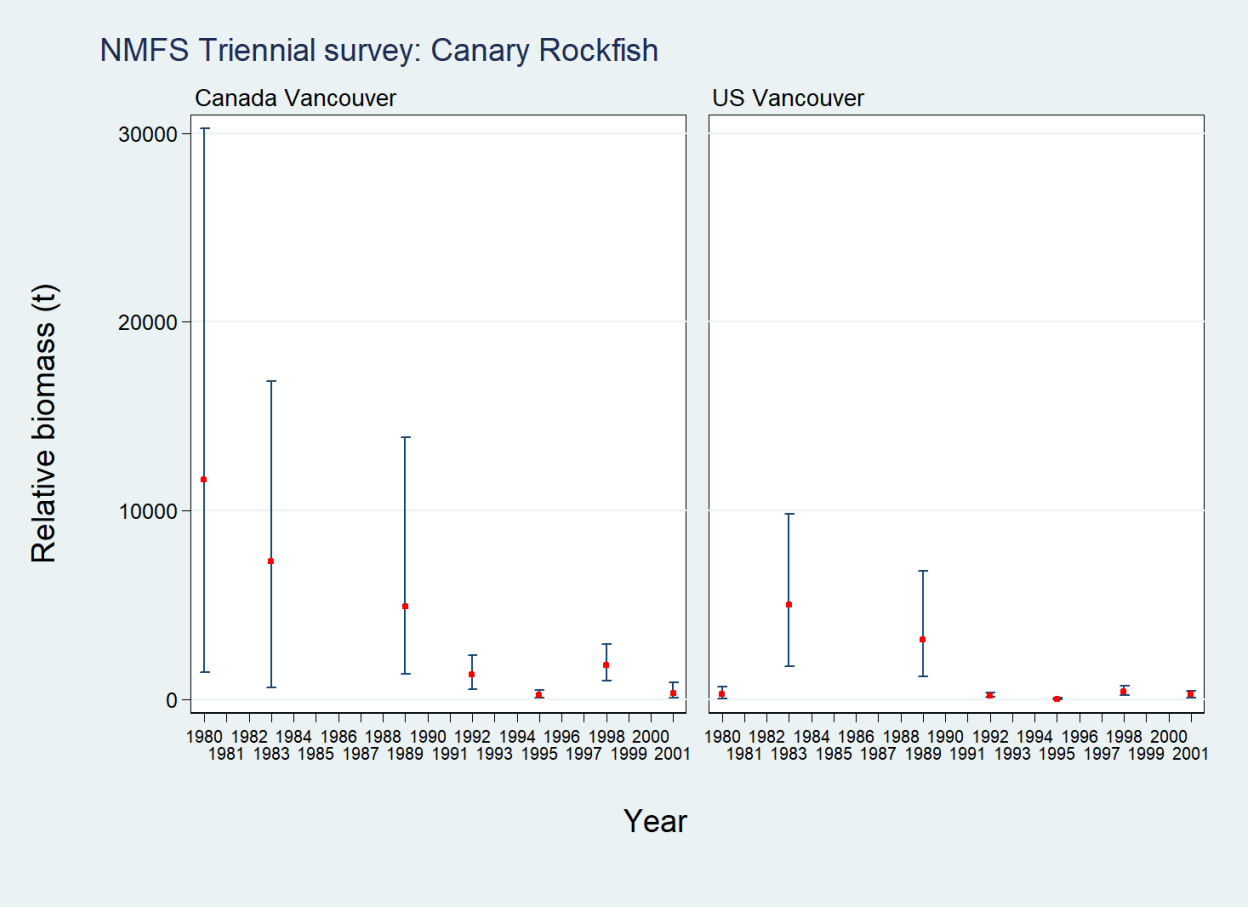

Figure B.20. Biomass estimates for Canary Rockfish in the INPFC Vancouver region (Canadian waters only, US waters only) with 95% error bars estimated from 1000 bootstrap random draws with replacement.

Table B.8. Two sets of biomass estimates for Canary Rockfish in the Vancouver INPFC region (Canadian waters; US waters) with 95% confidence bounds based on the bootstrap distribution of biomass. Bootstrap estimates were based on 1000 random draws with replacement.

Estimate series	Year	Biomass (Eq. B.4)	Mean bootstrap biomass	Lower bound biomass	Upper bound biomass	CV bootstrap	CV Analytic (Eq. B.6)
Canada Vancouver	1980	11,629.6	11,792.3	1,432.3	30,234.4	0.624	0.629
	1983	7,340.1	7,426.5	639.7	16,858.7	0.528	0.552
	1989	4,941.4	4,785.4	1,378.3	13,876.9	0.609	0.608
	1992	1,309.1	1,324.7	536.2	2,364.3	0.348	0.363
	1995	252.8	256.9	94.7	488.7	0.393	0.413
	1998	1,802.7	1,820.6	1,012.6	2,920.0	0.274	0.281
	2001	349.6	346.2	78.4	900.9	0.566	0.566
US Vancouver	1980	272.5	271.0	59.6	666.7	0.550	0.553
	1983	5,045.8	5,112.9	1,779.6	9,813.9	0.380	0.388
	1989	3,156.4	3,074.9	1,231.4	6,811.1	0.428	0.420
	1992	210.0	195.2	121.3	352.0	0.289	0.281
	1995	42.1	41.6	11.3	96.3	0.539	0.534
	1998	438.0	433.0	246.0	717.9	0.277	0.271
	2001	271.4	268.7	98.4	474.2	0.373	0.391

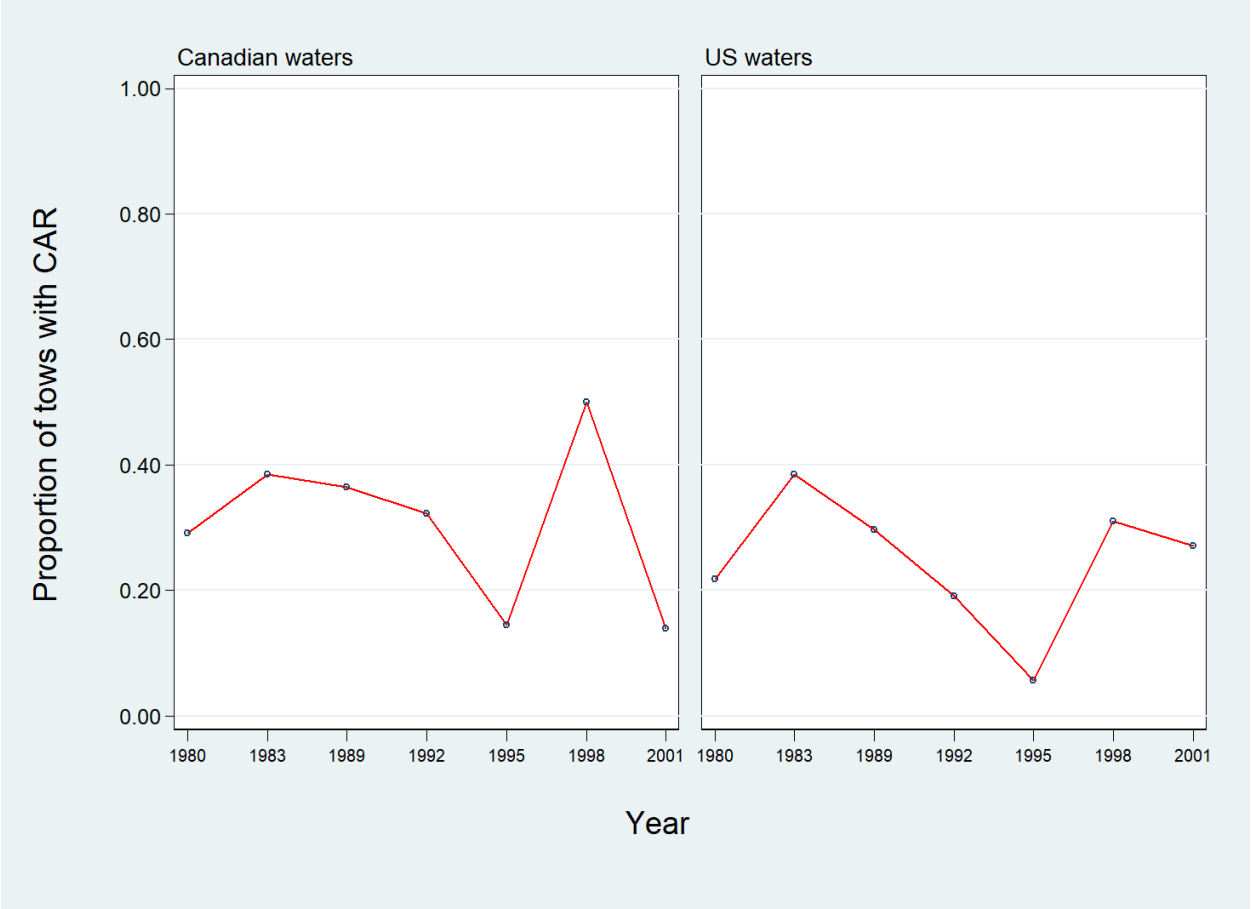

Figure B.21. Proportion of tows with Canary Rockfish by year for the Vancouver INPFC region (Canadian and US waters).

The proportion of tows which contained Canary Rockfish ranged between 14% and 50% in Canadian waters while the range was less wide in US waters (19% to 38%)(Figure B.21). The overall mean was 31% in Canadian waters and 25% in US waters. The incidence of CAR in Canadian waters for this survey is somewhat lower than the synoptic survey operating in the 2000s off the west coast of Vancouver Island, with the latter survey having a mean incidence of 37% (range: 29-43%) of the tows containing CAR.

The seven Triennial survey indices from the Canada Vancouver region, spanning the period 1980 to 2001, were used as abundance indices in the stock assessment model (described in Appendix F).

B.5. QUEEN CHARLOTTE SOUND SYNOPTIC TRAWL SURVEY

B.5.1. Data selection

This survey has been conducted eleven times over the period 2003 to 2021 in the Queen Charlotte Sound (QCS), which lies between the top of Vancouver Island and the southern portion of Moresby Island and extends into the lower part of Hecate Strait between Moresby Island and the mainland. The design divided the survey into two large areal strata which roughly correspond to the PMFC regions 5A and 5B while also incorporating part of 5C (all valid tow starting positions are shown by survey year in Figure B.22 to Figure B.32). Each of these two

areal strata was divided into four depth strata: 50–125 m; 125–200 m; 200–330 m; and 330–500 m (Table B.9).

Table B.9. Number of usable tows for biomass estimation by year and depth stratum for the Queen Charlotte Sound synoptic survey over the period 2003 to 2021. Also shown is the area of each stratum for the 2021 survey and the vessel conducting the survey by survey year.

		South depth strata				North depth strata				Total
Year	Vessel	50-125	125-200	200-330	330-500	50-125	125-200	200-330	330-500	tows[1]
2003	*Viking Storm*	29	56	29	6	5	38	46	19	228
2004	*Viking Storm*	42	48	30	8	20	38	37	6	229
2005	*Viking Storm*	29	60	28	8	8	43	37	8	221
2007	*Viking Storm*	33	61	24	7	19	56	48	7	255
2009	*Viking Storm*	34	60	27	8	10	43	42	6	230
2011	*Nordic Pearl*	38	67	23	8	10	51	43	8	248
2013	*Nordic Pearl*	32	65	29	10	9	45	41	5	236
2015	*Frosti*	30	65	26	4	12	49	44	8	238
2017	*Nordic Pearl*	36	57	28	8	12	51	40	7	239
2019	*Nordic Pearl*	35	62	26	9	15	52	35	8	242
2021	*Nordic Pearl*	24	53	28	3	5	40	37	3	193
Area (km^2)[2]		5,012	5,300	2,640	528	1,740	3,928	3,664	1,236	24,048[2]

[1] GFBio usability codes=0,1,2,6 [2] Total area (km^2) for 2019 synoptic survey

Table B.10. Number of missing doorspread values by year for the Queen Charlotte Sound synoptic survey over the period 2003 to 2021 as well as showing the number of available doorspread observations and the mean doorspread value for each survey year.

Year	Number tows with missing doorspread [1]	Number tows with doorspread observations [2]	Mean doorspread (m) used for tows with missing values [2]
2003	13	236	72.1
2004	8	267	72.8
2005	1	258	74.5
2007	5	262	71.8
2009	2	248	71.3
2011	30	242	67.0
2013	42	226	69.5
2015	0	249	70.5
2017	1	264	64.7
2019	8	264	62.9
2021	8	202	65.5
Total	118	2,718	69.4

[1] valid biomass estimation tows only [2] includes tows not used for biomass estimation

A doorspread density value (Eq. B.3) was generated for each tow based on the catch of CAR from the mean doorspread for the tow and the distance travelled. [`distance travelled`] is a database field which is calculated directly from the tow track. This field is used preferentially for the variable D_{yij} in Eq. B.3. A calculated value ([`vessel speed`] X [`tow duration`]) was used for this variable if [`distance travelled`] is missing, but there were only two instances of this occurring in the eleven trawl surveys. Missing values for the [`doorspread`] field were filled in with the mean doorspread for the survey year (118 values over all years, Table B.10).

B.5.2. Results

An examination of the spatial plots provided from Figure B.22 to Figure B.32shows that most CAR were caught in the mid-region of QC Sound with very low captures along the western shelf edge along the drop-off to deeper water (e.g., Figure B.26). CAR were found in tows at moderate depth, with the 1% to 99% quantiles ranging from 93 m to 205 m (Figure B.33). The CAR biomass estimates ranged from 500 to 3,300 t, with the relative error ranging from 23% to

71% (Table B.11, Figure B.34). While the relative error is generally high for this species, it doesn't appear to be associated with the high catch years. An examination of the density plots shows that this species is relatively widely dispersed across the shelf, with small catches in many tows.

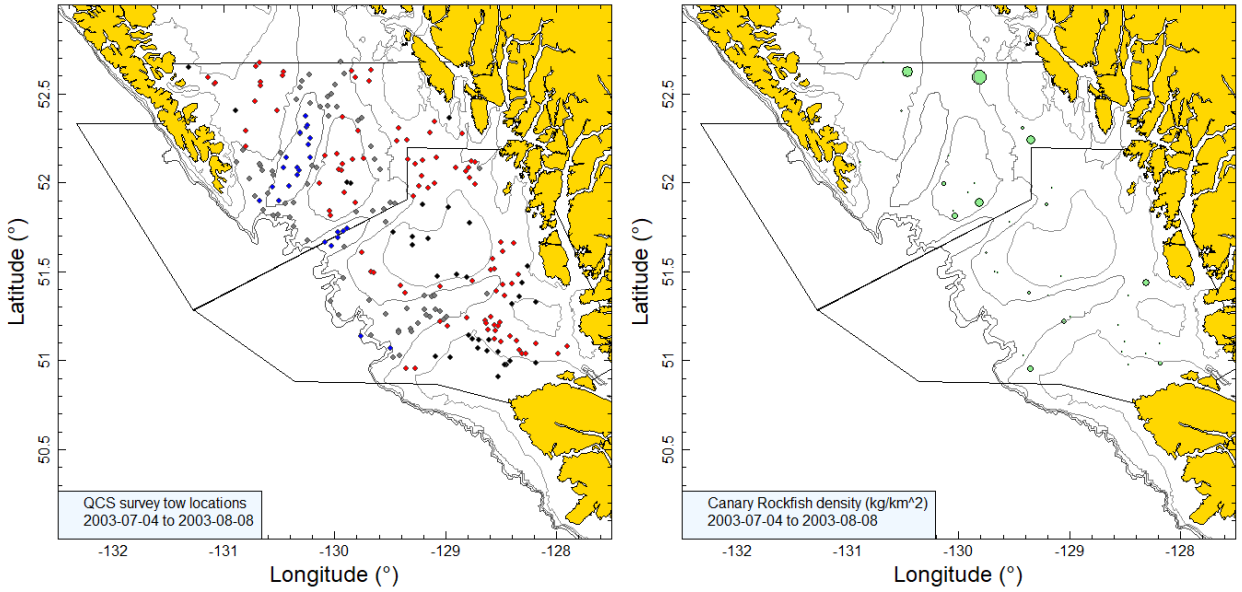

Figure B.22. Valid tow locations (50-125m stratum: black; 126-200m stratum: red; 201-330 m stratum: grey; 331-500m stratum: blue) and density plots for the 2003 QC Sound synoptic survey. Circle sizes in the right-hand density plot scaled across all years (2003–2005, 2007, 2009, 2011, 2013, 2015, 2017, 2019, 2021), with the largest circle = 12,431 kg/km^2 in 2019. Boundaries delineate the North and South areal strata.

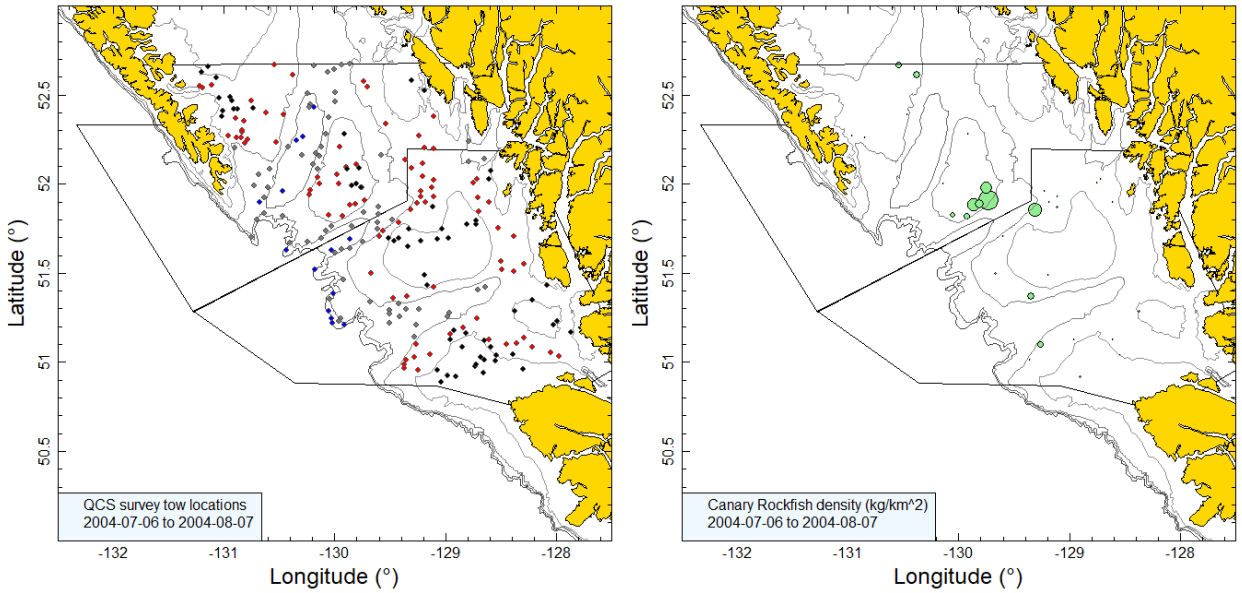

Figure B.23. Tow locations and density plots for the 2004 Queen Charlotte Sound synoptic survey (see Figure B.22 caption).

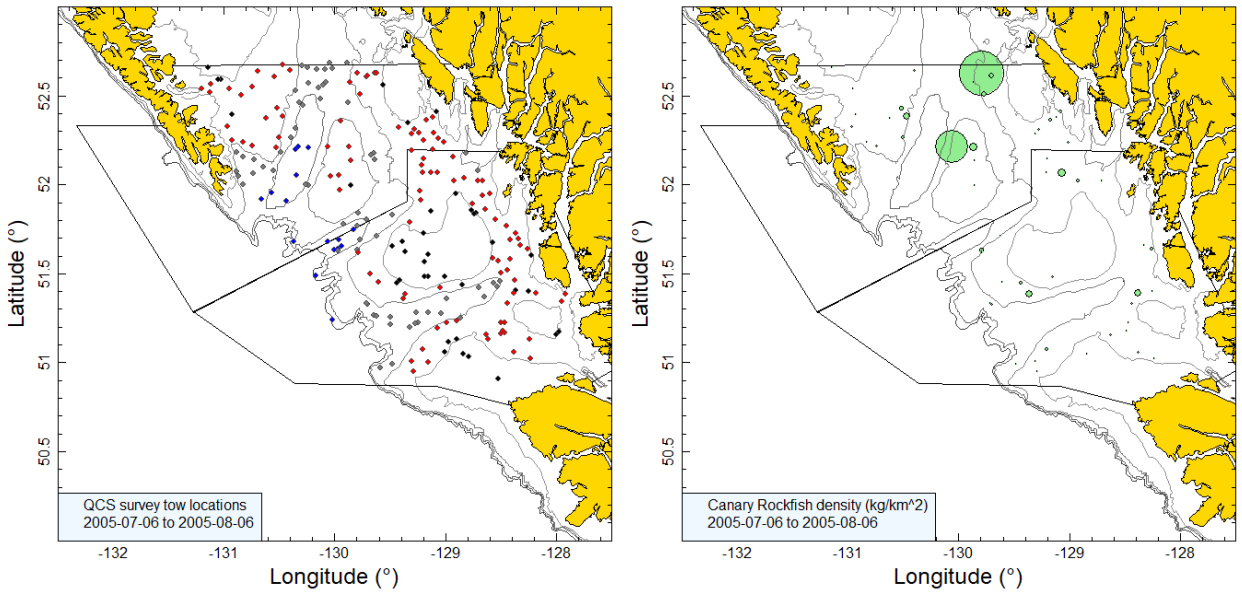

Figure B.24. Tow locations and density plots for the 2005 Queen Charlotte Sound synoptic survey (see Figure B.22 caption).

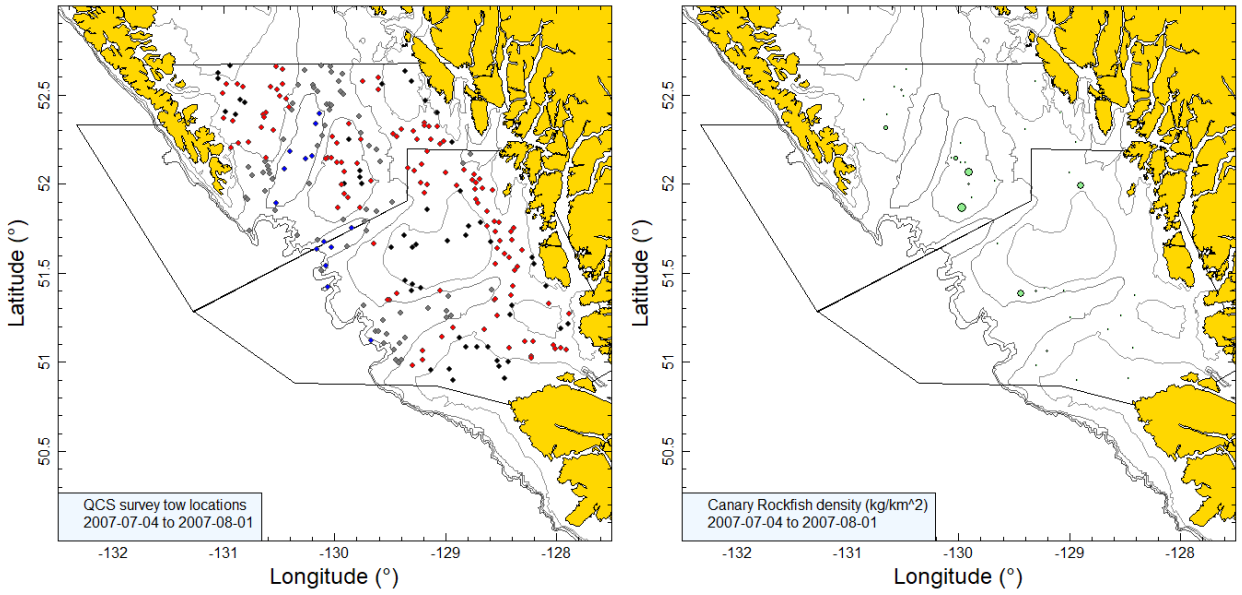

Figure B.25. Tow locations and density plots for the 2007 Queen Charlotte Sound synoptic survey (see Figure B.22 caption).

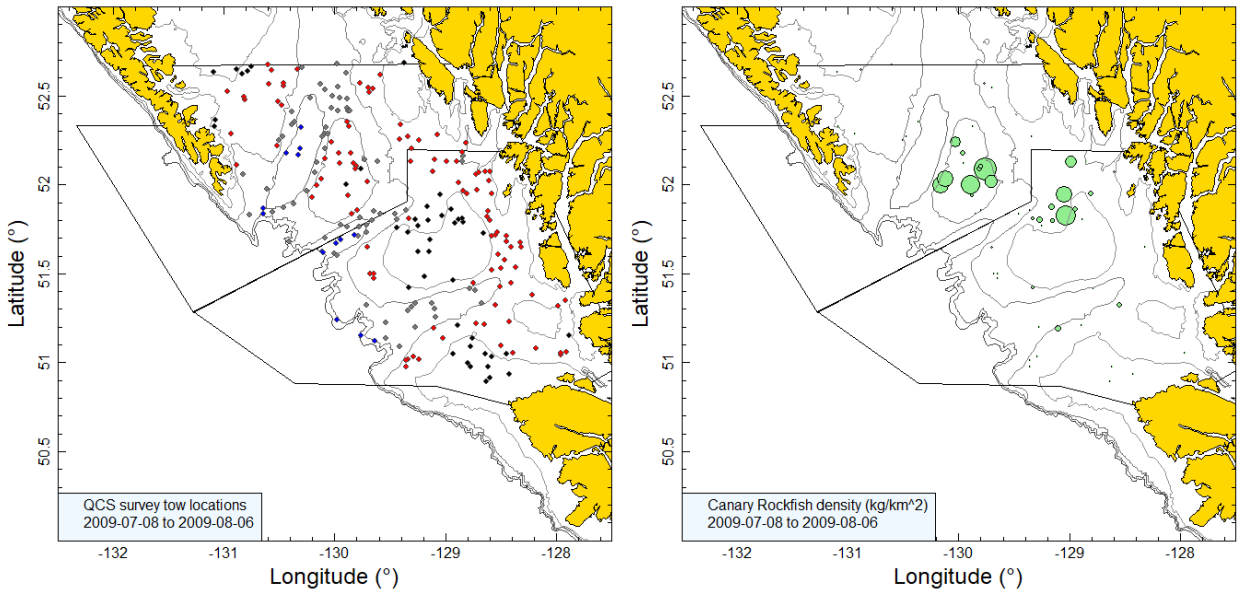

Figure B.26. Tow locations and density plots for the 2009 Queen Charlotte Sound synoptic survey (see Figure B.22 caption).

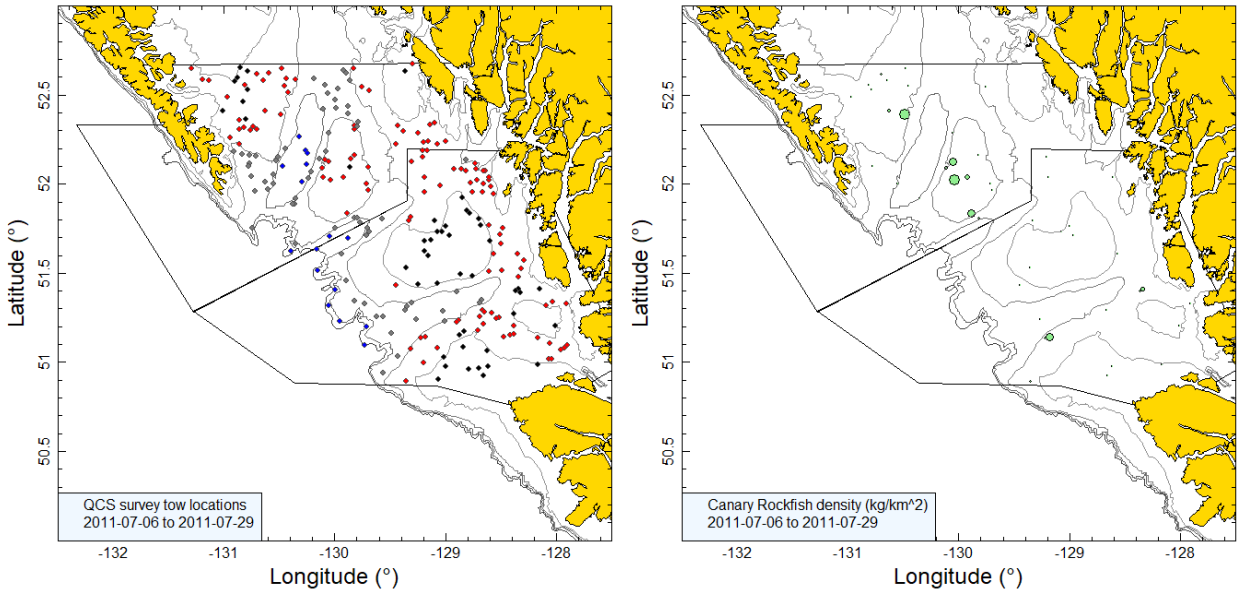

Figure B.27. Tow locations and density plots for the 2011 Queen Charlotte Sound synoptic survey (see Figure B.22 caption).

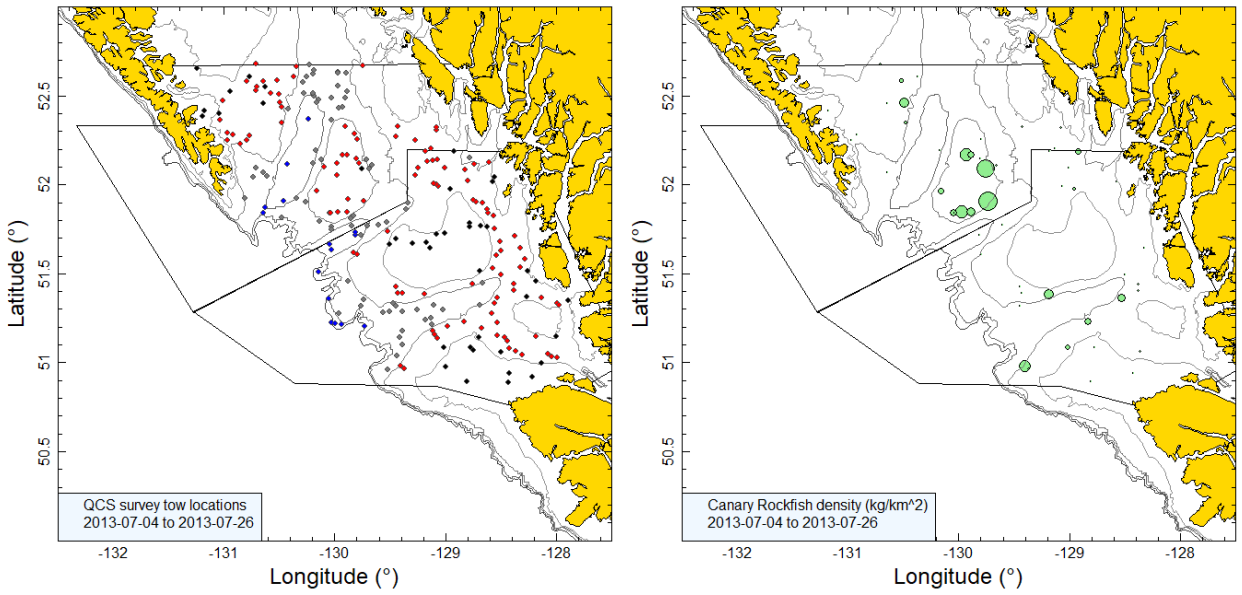

Figure B.28. Tow locations and density plots for the 2013 Queen Charlotte Sound synoptic survey (see Figure B.22 caption).

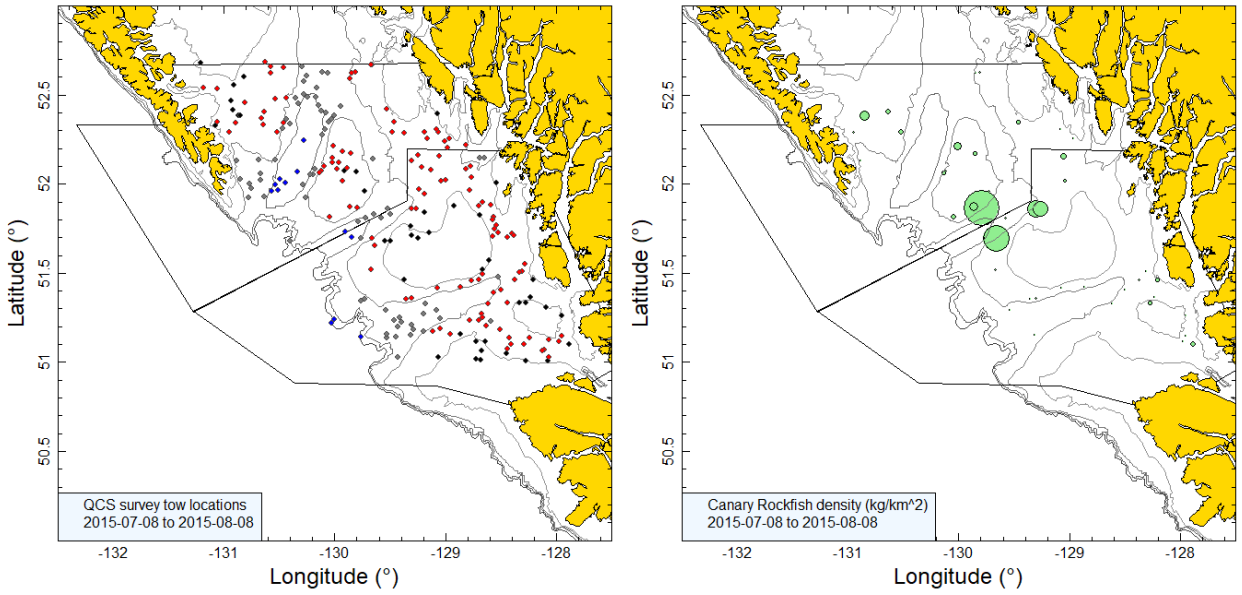

Figure B.29. Tow locations and density plots for the 2015 Queen Charlotte Sound synoptic survey (see Figure B.22 caption).

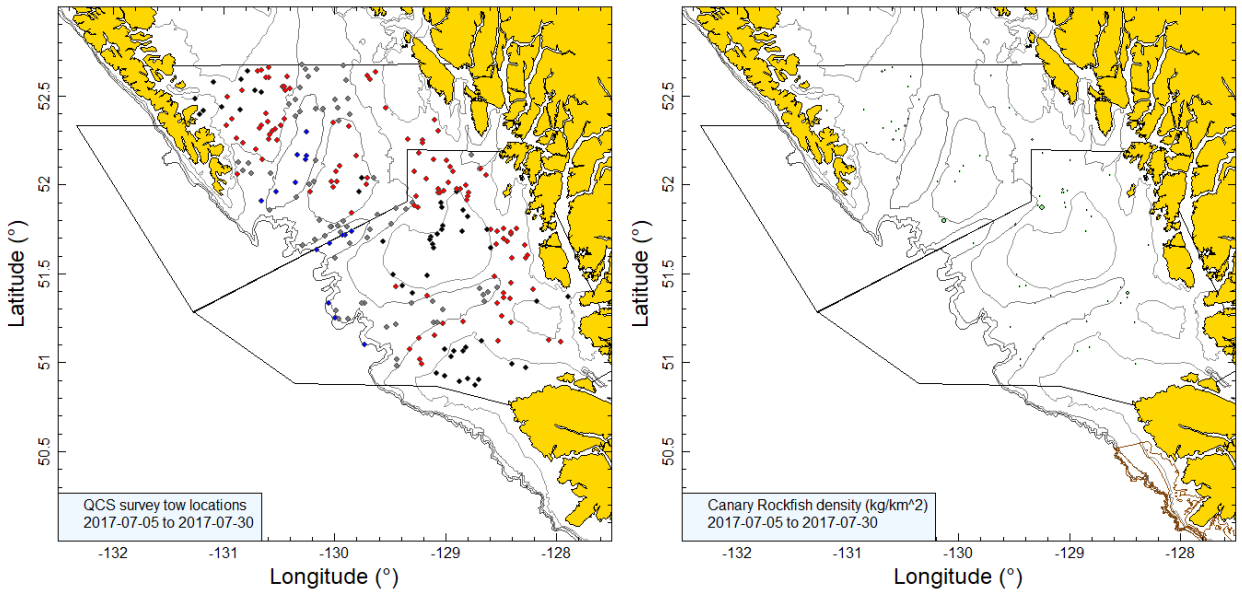

Figure B.30. Tow locations and density plots for the 2017 Queen Charlotte Sound synoptic survey (see Figure B.22 caption).

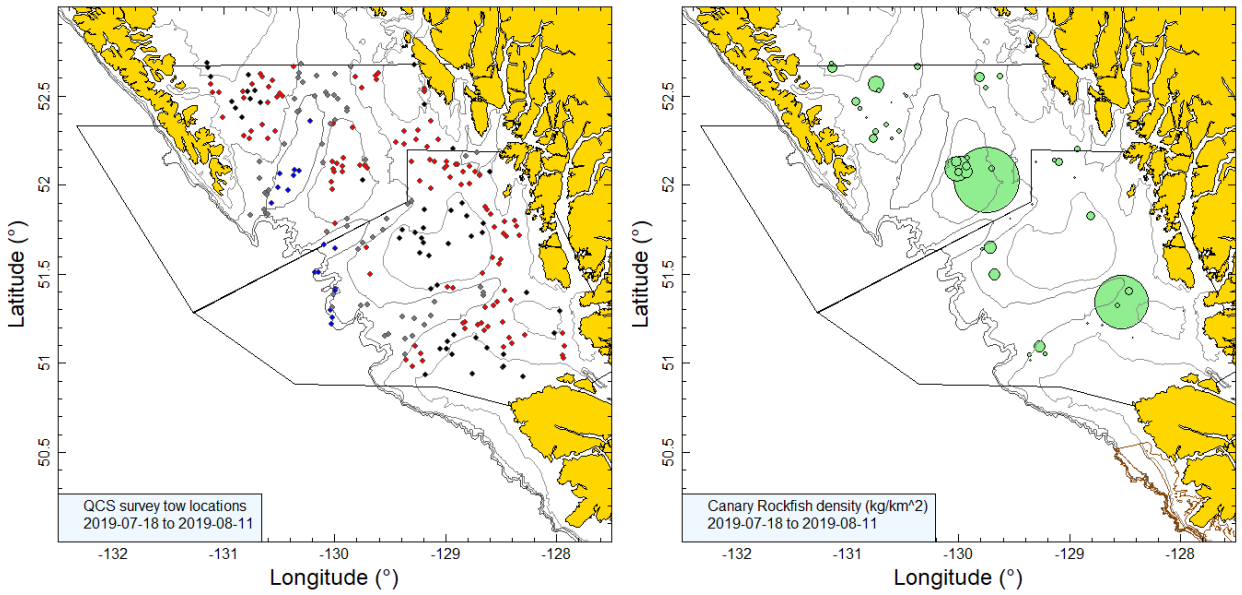

Figure B.31. Tow locations and density plots for the 2019 Queen Charlotte Sound synoptic survey (see Figure B.22 caption).

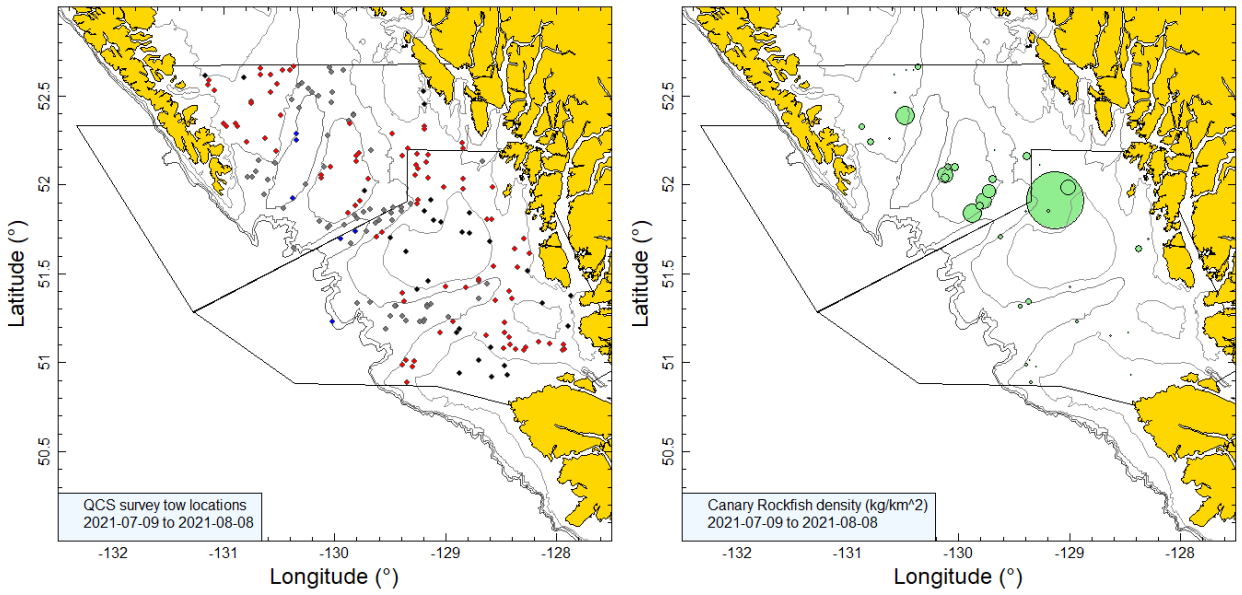

Figure B.32. Tow locations and density plots for the 2021 Queen Charlotte Sound synoptic survey (see Figure B.22 caption).

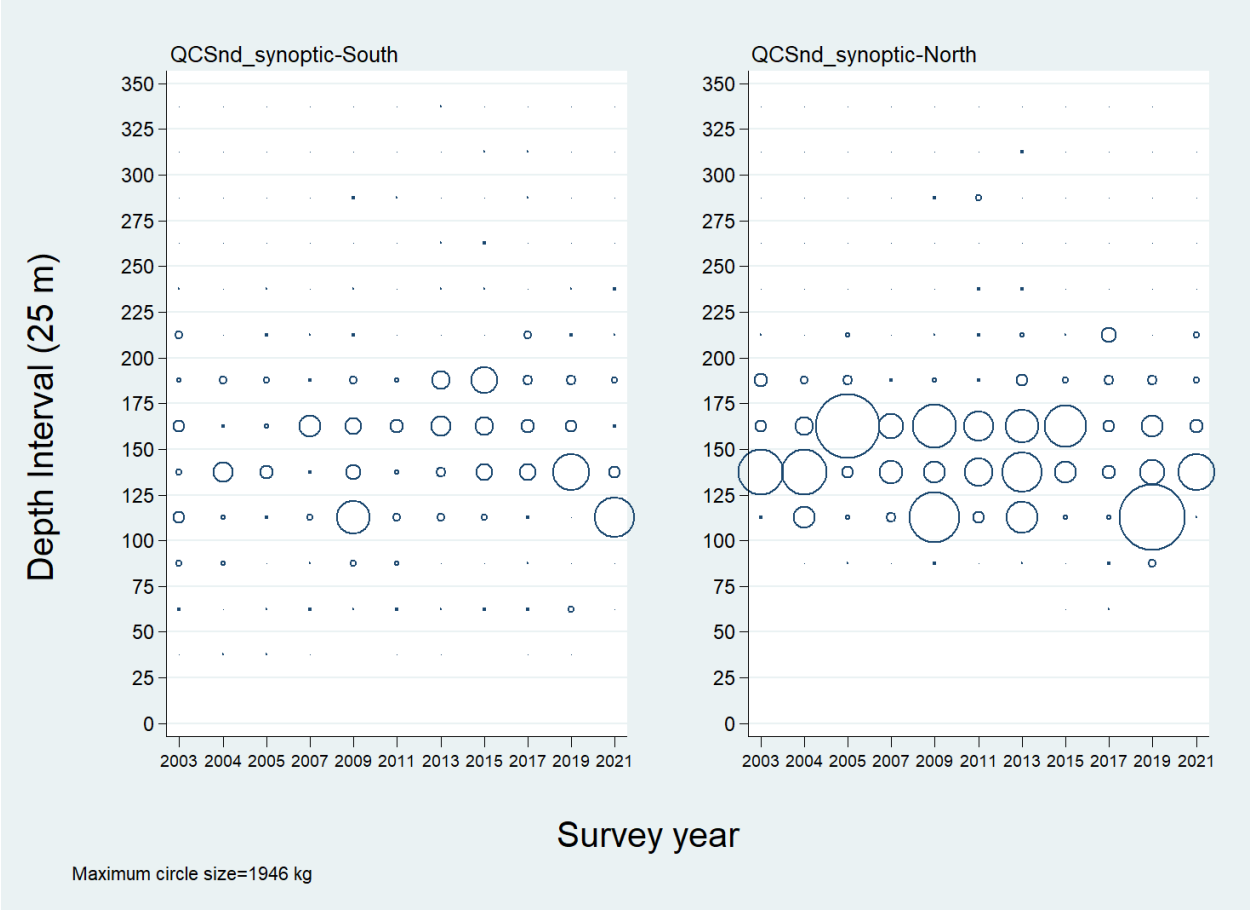

Figure B.33. Distribution of observed catch weights for tows used in biomass estimation for CAR in the two main Queen Charlotte Sound synoptic survey areal strata (Table B.9) by survey year and 25 m depth zone. Catches are plotted at the mid-point of the interval and circles in the panel are scaled to the

maximum value (1946 kg) in the 100–125 m interval in the 2019 northern stratum. The 1% and 99% quantiles for the CAR start of tow depth distribution= 93 m and 205 m respectively.

Table B.11. Biomass estimates for CAR from the Queen Charlotte Sound synoptic trawl survey for the survey years 2003 to 2021. Bootstrap bias corrected confidence intervals and CVs are based on 1000 random draws with replacement.

Survey Year	Biomass (t) (Eq. B.4)	Mean bootstrap biomass (t)	Lower bound biomass (t)	Upper bound biomass (t)	Bootstrap CV	Analytic CV (Eq. B.6)
2003	1,141.0	1,123.7	579.3	2,180.5	0.343	0.334
2004	1,257.1	1,261.8	470.8	2,351.4	0.378	0.386
2005	1,466.5	1,476.8	264.7	3,722.9	0.575	0.591
2007	597.9	588.1	277.4	1,092.1	0.344	0.349
2009	3,299.5	3,272.1	1,425.1	5,899.4	0.350	0.338
2011	801.2	805.8	357.1	1,424.0	0.326	0.330
2013	2,118.5	2,098.7	997.1	4,410.0	0.390	0.368
2015	1,421.4	1,438.1	462.3	2,901.6	0.431	0.450
2017	553.6	561.9	332.0	828.4	0.230	0.245
2019	2,923.8	2,906.1	651.4	6,671.7	0.544	0.551
2021	3,231.0	3,231.6	569.7	8,960.2	0.711	0.708

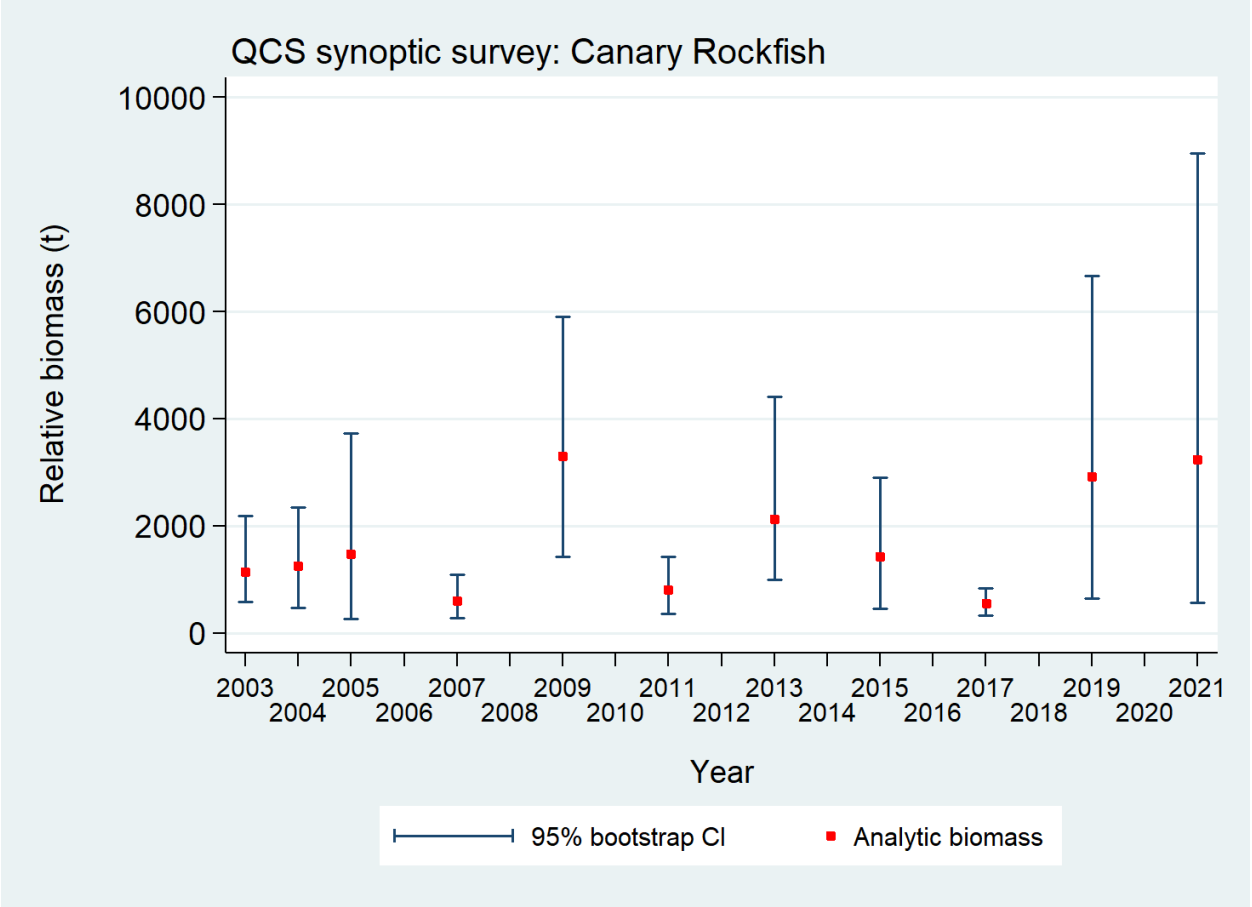

Figure B.34. Plot of biomass estimates for CAR (values provided in Table B.11) from the Queen Charlotte Sound synoptic survey over the period 2003 to 2021. Bias corrected 95% confidence intervals from 1000 bootstrap replicates are plotted.

On average, CAR were captured in about 20% of tows across both areal strata, ranging from 13% to 30% of the tows in the South strata and 13% to 27% of the tows in the North strata

(Figure B.35). Overall, 522 of the 2,559 valid survey tows (20.4%) contained CAR. The median catch weight for positive tows used in biomass estimation was 4.8 kg/tow across the eleven surveys, and the maximum catch weight in a tow was 1,750 kg in the 2019 survey.

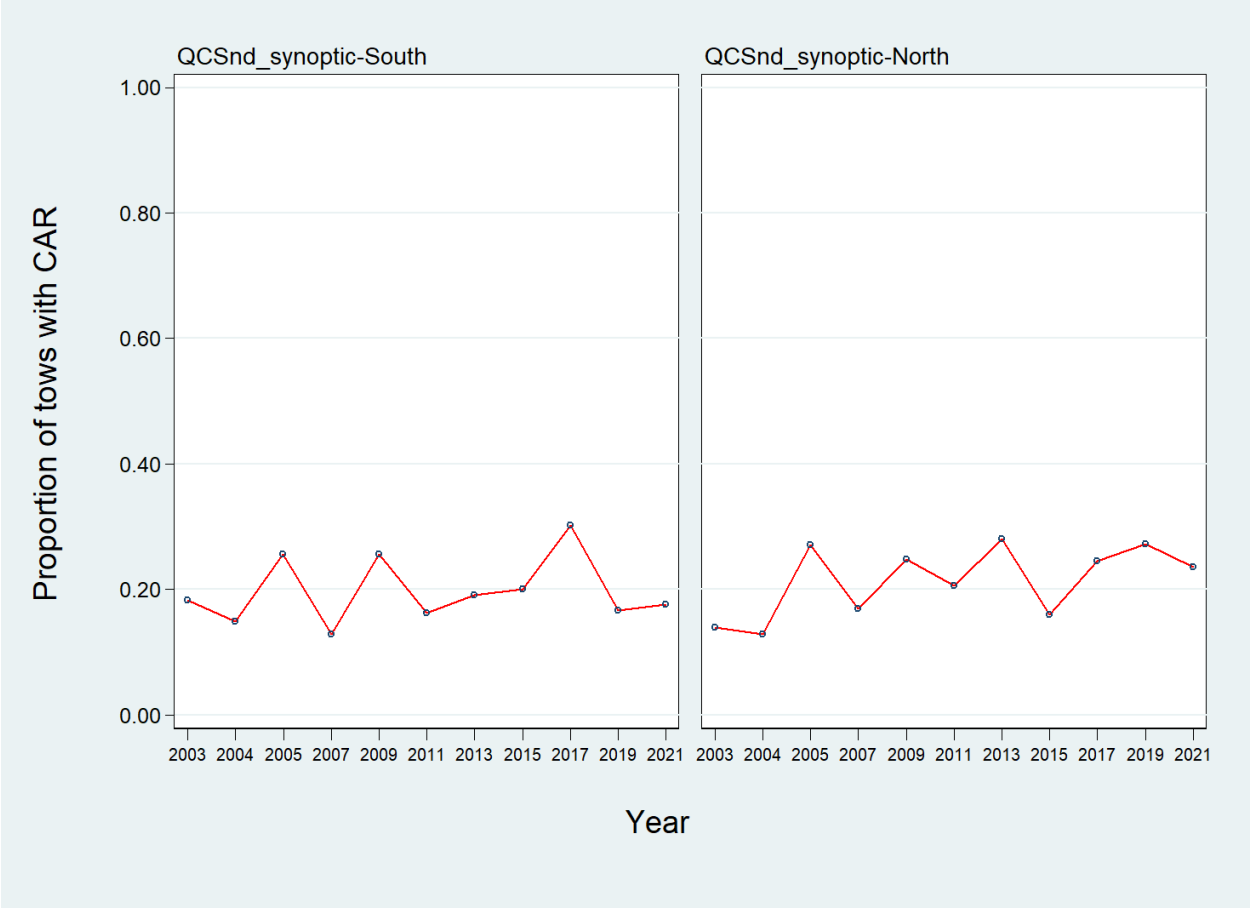

Figure B.35. Proportion of tows by stratum and year which contain CAR from the Queen Charlotte Sound synoptic survey over the period 2003 to 2021.

B.6. WEST COAST VANCOUVER ISLAND SYNOPTIC TRAWL SURVEY

B.6.1. Data selection

This survey was conducted seven times over the period 2004 to 2016 off the west coast of Vancouver Island by the RV *W.E. Ricker*. However, due to the decommissioning of the *W.E. Ricker* in 2017, two subsequent surveys in 2018 and 2021 were conducted by the RV *Nordic Pearl*. The 2020 survey was rescheduled to 2021 due to restrictions on the deployment of government vessels imposed by Canadian policy pertaining to the ongoing COVID-19 epidemic. This survey comprises a single areal stratum, separated into four depth strata: 50-125 m; 125-200 m; 200-330 m; and 330-500 m (Table B.12). Approximately 150 to 200 2-km^2 blocks are selected randomly among the four depth strata when conducting each survey (Olsen et. al. 2008).

A “doorspread density” value was generated for each tow based on the catch of CAR, the mean doorspread for the tow and the distance travelled (Eq. B.3). The distance travelled was provided as a data field, determined directly from vessel track information collected during the tow. There were only two missing values in this field (in 2004 and 2010) which were filled in by multiplying

the vessel speed by the time that the net was towed. There were a large number of missing values for the doorspread field in the first five surveys, which were filled in using the mean doorspread for the survey year or a default value of 64.0 m for the three years with no doorspread data (Table B.13). The default value is based on the mean of the observed doorspread from the net mensuration equipment, averaged across the years with doorspread estimates.

Table B.12. Stratum designations, number of usable and unusable tows, for each year of the west coast Vancouver Island synoptic survey. Also shown is the area of each depth stratum in 2018 and the start and end dates for each survey.

Survey Year	Stratum depth zone				Total Tows[1]	Unusable tows	Start date	End date
	50-125 m	125-200 m	200-330 m	330-500 m				
2004	34	34	13	8	89	17	26-May-04	09-Jun-04
2006	61	62	28	13	164	12	24-May-06	18-Jun-06
2008	54	50	32	23	159	19	27-May-08	21-Jun-08
2010	58	47	22	9	136	8	08-Jun-10	28-Jun-10
2012	60	46	25	20	151	6	23-May-12	15-Jun-12
2014	55	49	29	13	146	7	29-May-14	20-Jun-14
2016	54	41	26	19	140	7	25-May-16	15-Jun-16
2018	69	64	36	21	190	12	19-May-18	12-Jun-18
2021	60	57	31	21	169	6	16-May-21	08-Jun-21
Area (km^2)	5,716	3,768	708	572	10,764[2]	–	–	–

[1] GFBio usability codes=0,1,2,6
[2] Total area (km^2) for 2021 synoptic survey

Table B.13. Number of tows with and without doorspread measurements by survey year for the WCVI synoptic survey. Mean doorspread values for those tows with measurements are provided.

Survey Year	Number tows		Mean doorspread (m)
	Without doorspread	With doorspread	
2004	89	0	–
2006	96	69	64.3
2008	58	107	64.5
2010	136	0	–
2012	153	0	–
2014	14	139	64.3
2016	0	147	65.5
2018	0	202	64.3
2021	2	173	61.6
All surveys	546	837	64.0

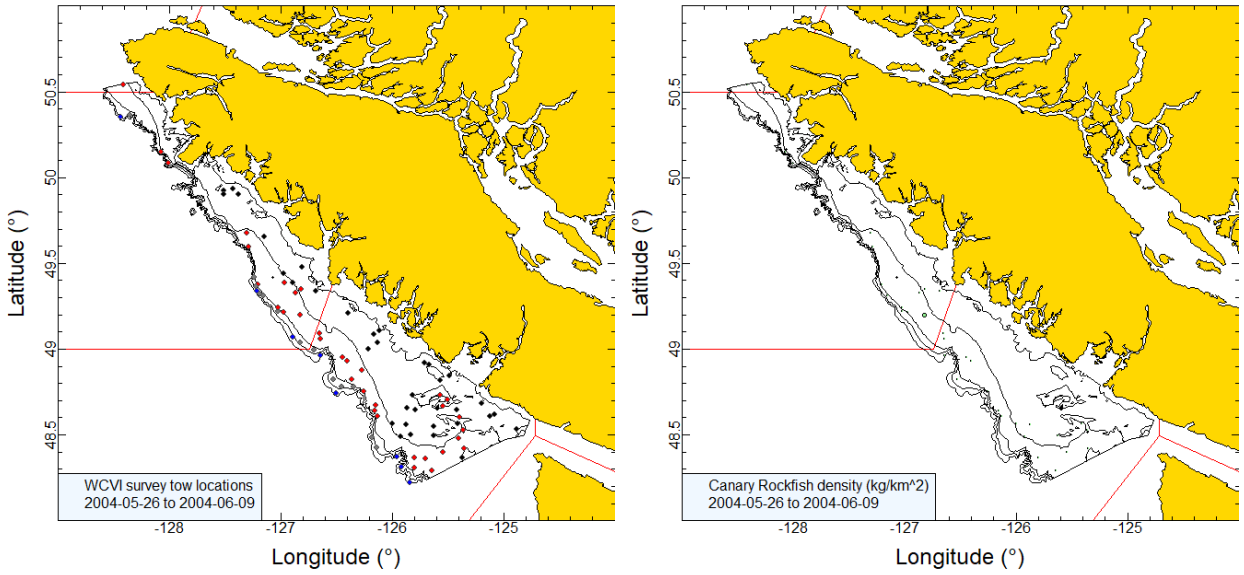

Figure B.36. Valid tow locations (50-125 m stratum: black; 126-200 m stratum: red; 201-330 m stratum: grey; 331-500 m stratum: blue) and density plots for the 2004 west coast Vancouver Island synoptic survey. Circle sizes in the right-hand density plot scaled across all years (2004, 2006, 2008, 2010, 2012, 2014, 2016, 2018, 2021), with the largest circle = 36,036 kg/km^2 in 2006. The red solid lines indicate the boundaries for PMFC areas 3C, 3D and 5A.

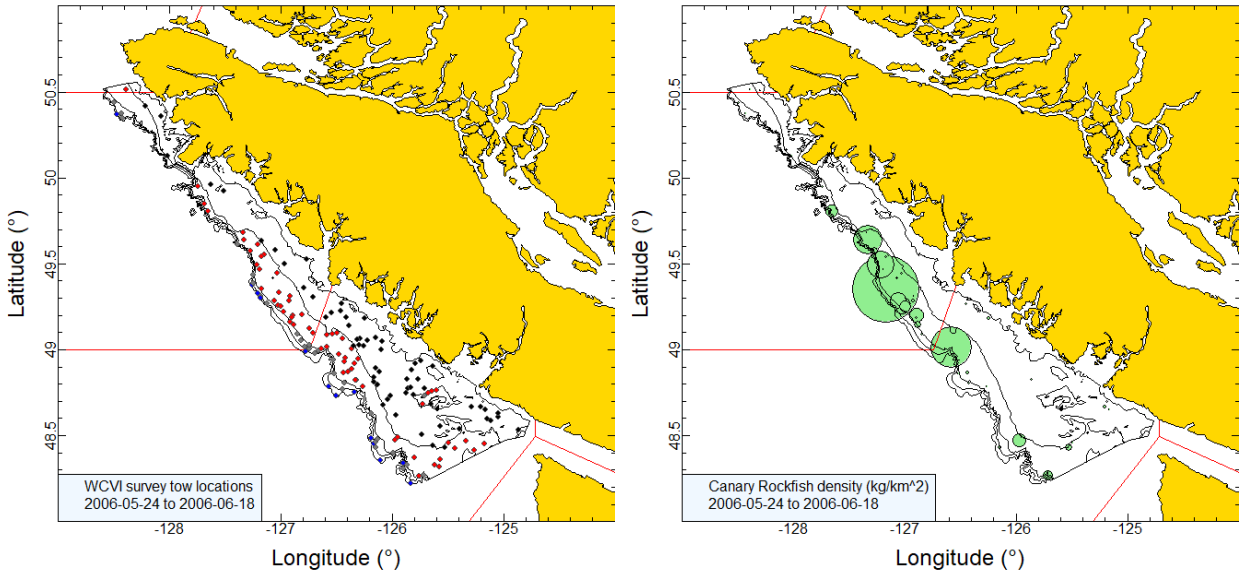

Figure B.37. Tow locations and density plots for the 2006 west coast Vancouver Island synoptic survey (see Figure B.36 caption).

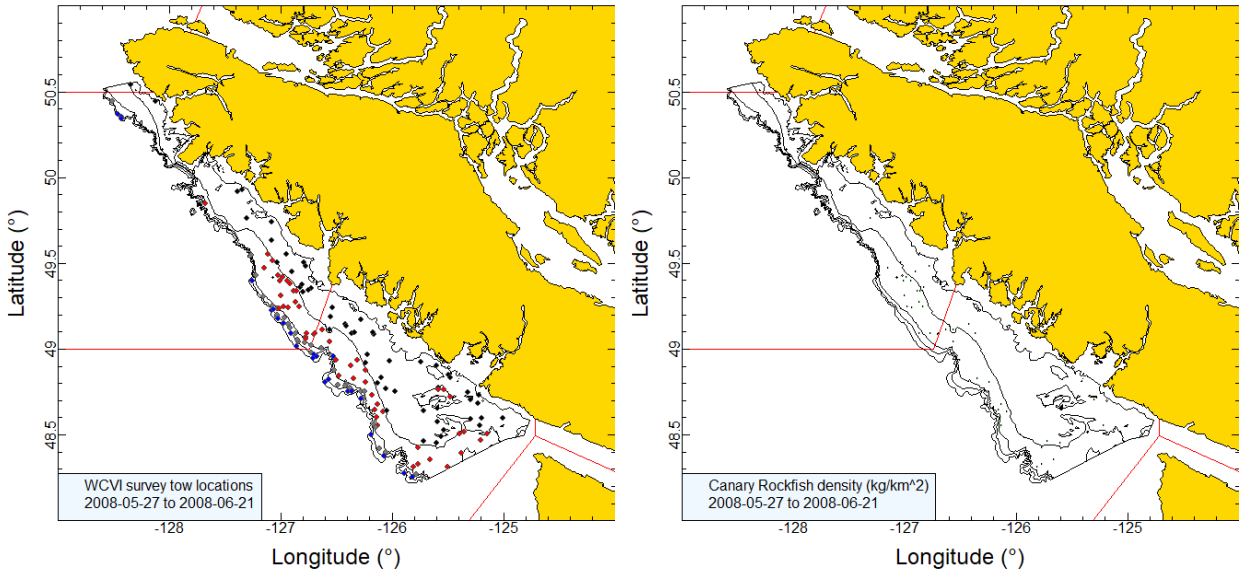

Figure B.38. Tow locations and density plots for the 2008 west coast Vancouver Island synoptic survey (see Figure B.36 caption).

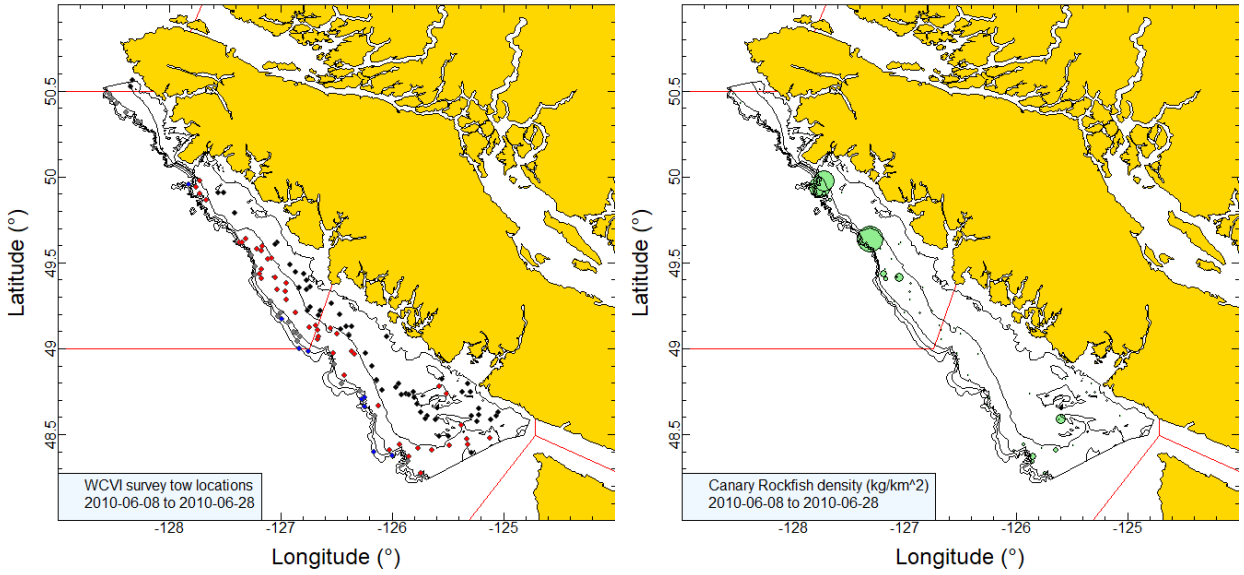

Figure B.39. Tow locations and density plots for the 2010 west coast Vancouver Island synoptic survey (see Figure B.36 caption).

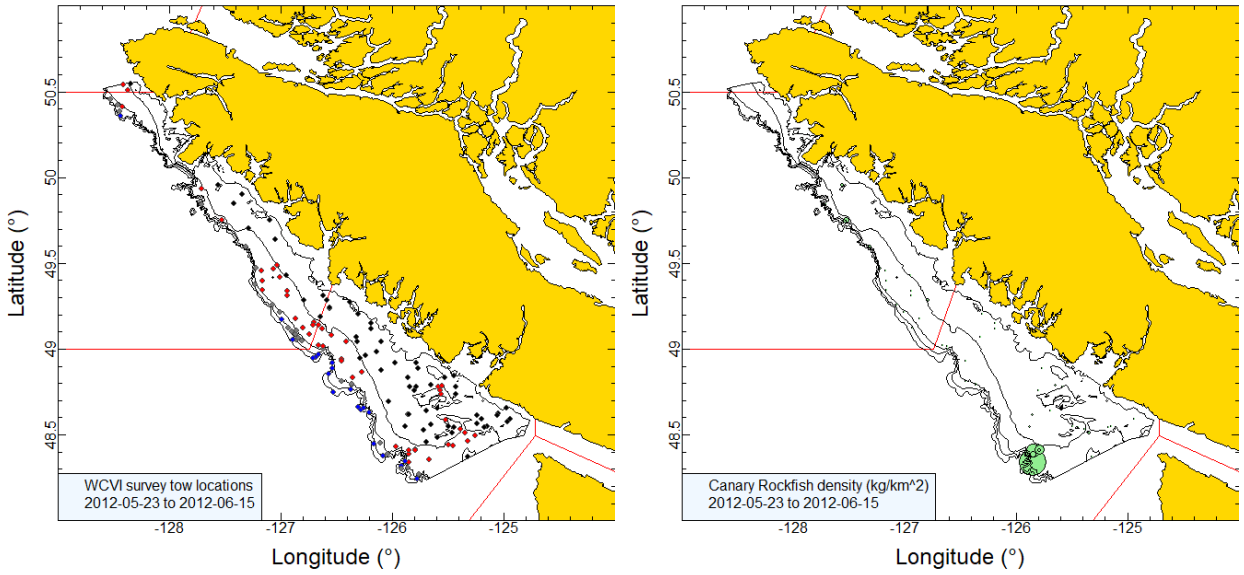

Figure B.40. Tow locations and density plots for the 2012 west coast Vancouver Island synoptic survey (see Figure B.36 caption).

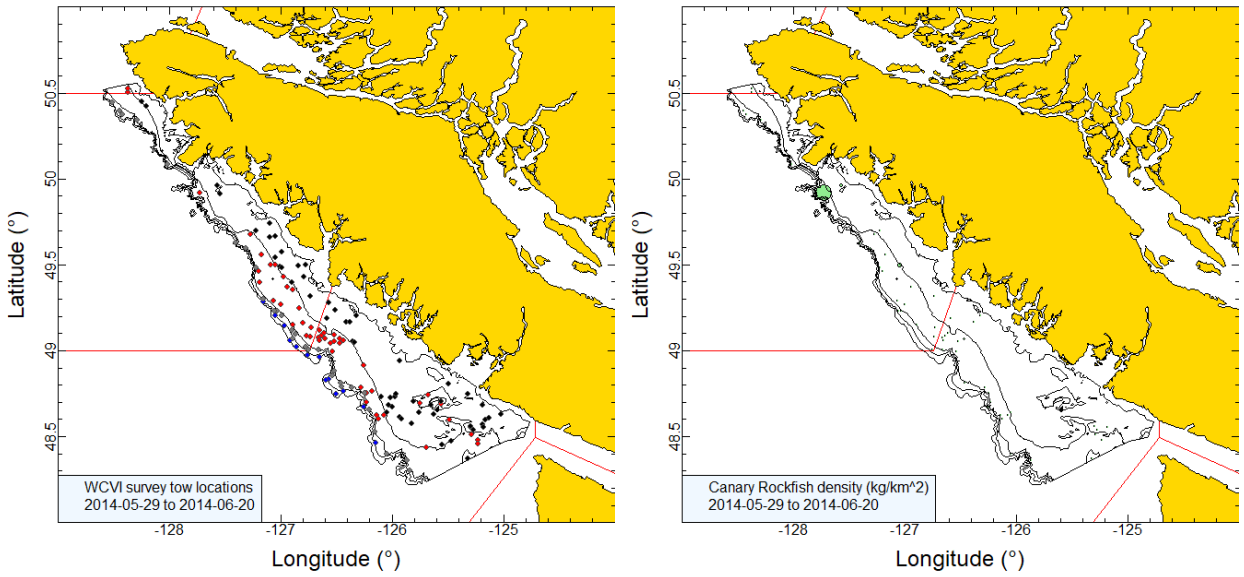

Figure B.41. Tow locations and density plots for the 2014 west coast Vancouver Island synoptic survey (see Figure B.36 caption).

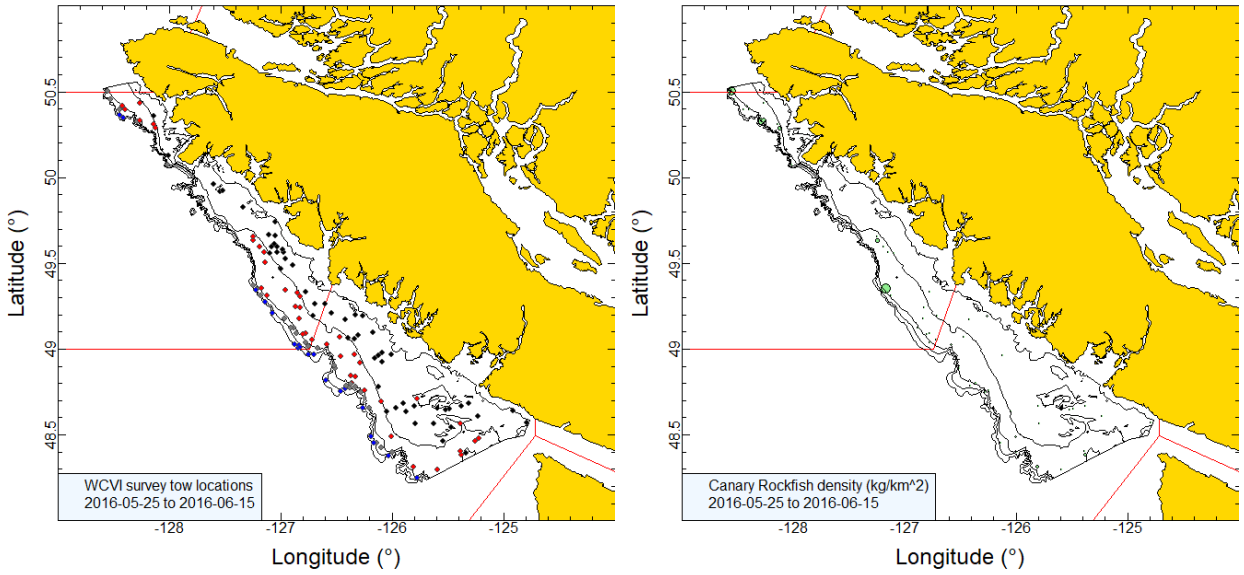

Figure B.42. Tow locations and density plots for the 2016 west coast Vancouver Island synoptic survey (see Figure B.36 caption).

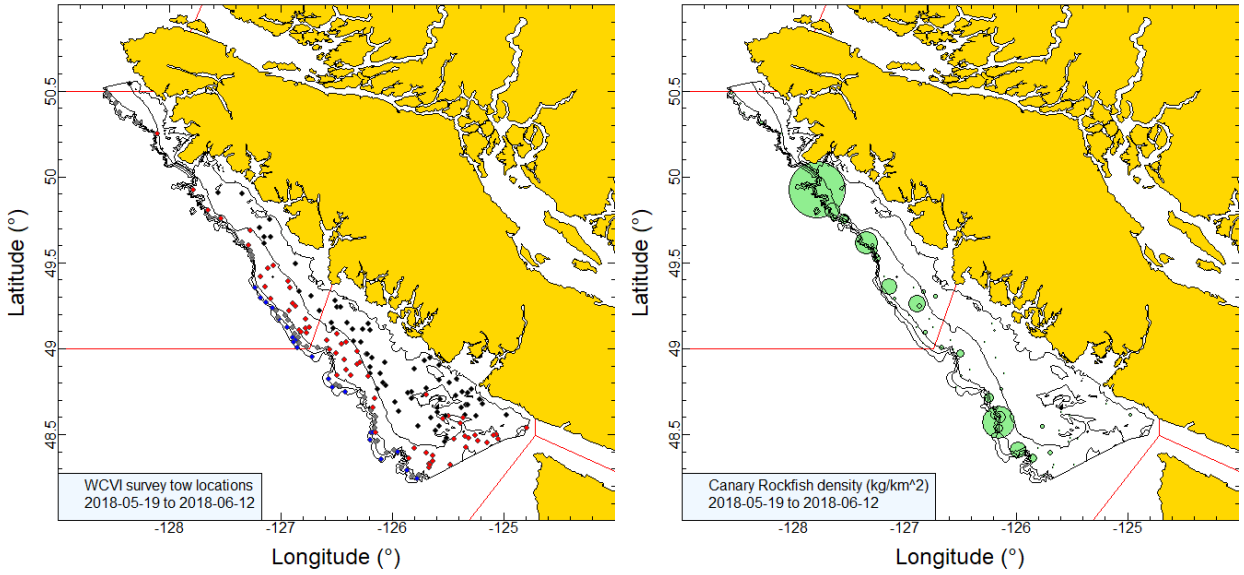

Figure B.43. Tow locations and density plots for the 2018 west coast Vancouver Island synoptic survey (see Figure B.36 caption).

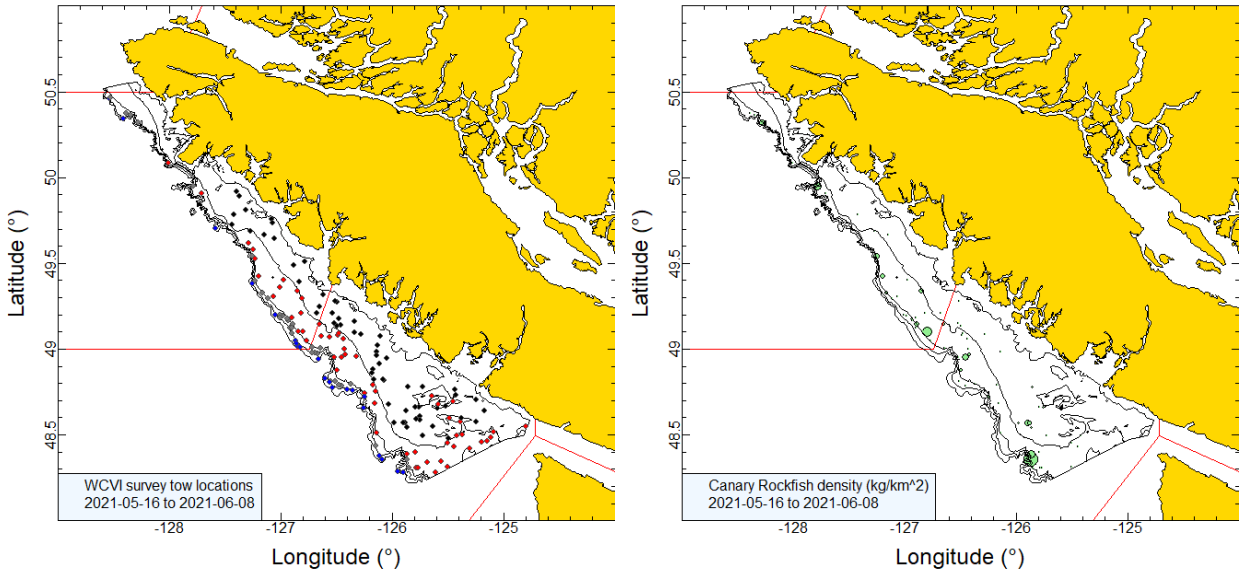

Figure B.44. Tow locations and density plots for the 2021 west coast Vancouver Island synoptic survey (see Figure B.36 caption).

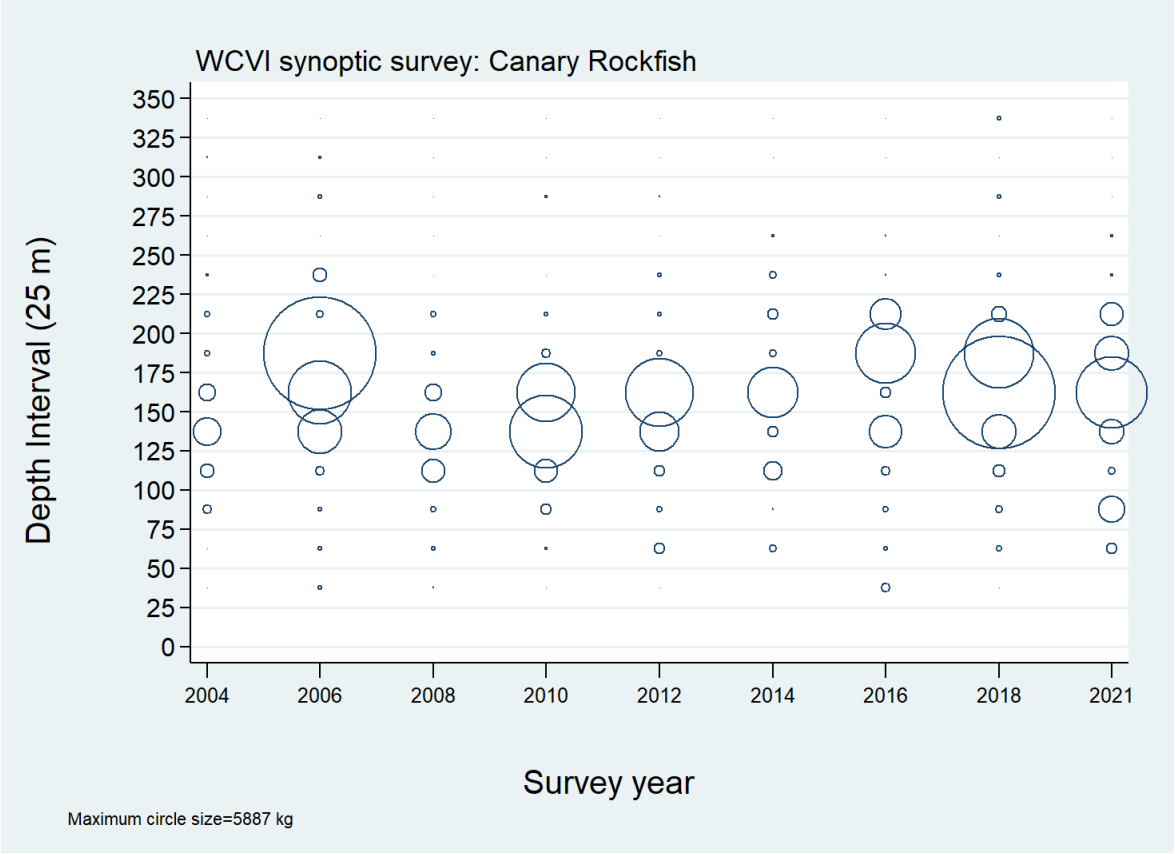

Figure B.45. Distribution of observed weights of CAR by survey year and 25 m depth zone. Catches are plotted at the mid-point of the interval and circles in the panel are scaled to the maximum value (5,887 kg) in the 175-200 m interval in 2006. The 1st and 99th percentiles for the CAR start of tow depth distribution = 78 m and 212 m, respectively.

B.6.2. Results

CAR were taken primarily along the shelf edge from near the US border to the most northern section of the survey, well above Brooks Peninsula near the top of Vancouver Island (Figure B.36 to Figure B.44). The distribution appeared to predominate in the lower two-thirds of Vancouver Island, with the highest density tows taken in the central section of the coast. CAR were mainly taken in the relatively narrow depth range, from about 125 to 200 m (5–95 percentiles=124 to 198 m) (Figure B.45). Relative biomass levels for CAR from this trawl survey were reasonable but variable, ranging from 720 to 4600 t, with variable relative errors, which ranged from 0.27 to 0.68 (Figure B.46; Table B.14). There is evidence from the distributional plots that there is variability in catchability, with successive survey years showing high and low densities. For instance, the year with the highest biomass estimate (2006, Figure B.37) in the series was followed by the year with the lowest biomass estimate (2008, Figure B.38) in the series. However, there were subsequent years which showed good levels of biomass (e.g., 2010 and 2018), so the low biomass estimates more likely reflected changes in catchability, not depletion.

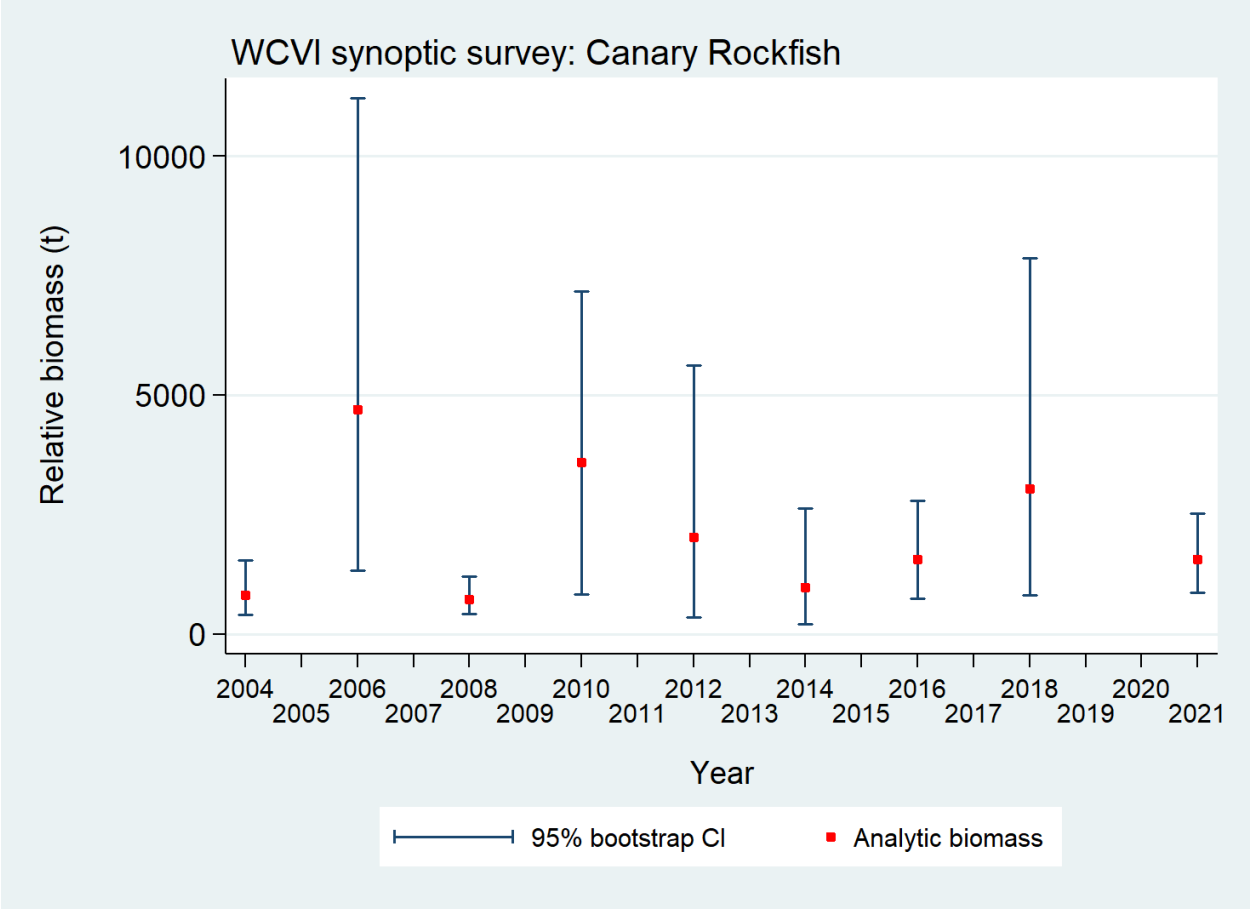

Figure B.46. Plot of biomass estimates for CAR from the 2004 to 2021 west coast Vancouver Island synoptic trawl surveys (Table B.14). Bias-corrected 95% confidence intervals from 1000 bootstrap replicates are plotted.

The proportion of tows capturing CAR was consistently near 40%, and showed relatively little year-to-year variation, ranging between 29 and 43% over the nine surveys and with a mean value of 37% (Figure B.47). Four hundred ninety-seven of the 1344 usable tows (37%) from this

survey contained CAR, with a median catch weight for positive tows of 6 kg/tow. Two tows caught more than 4000 kg of CAR, one in 2006 and the other in 2018.

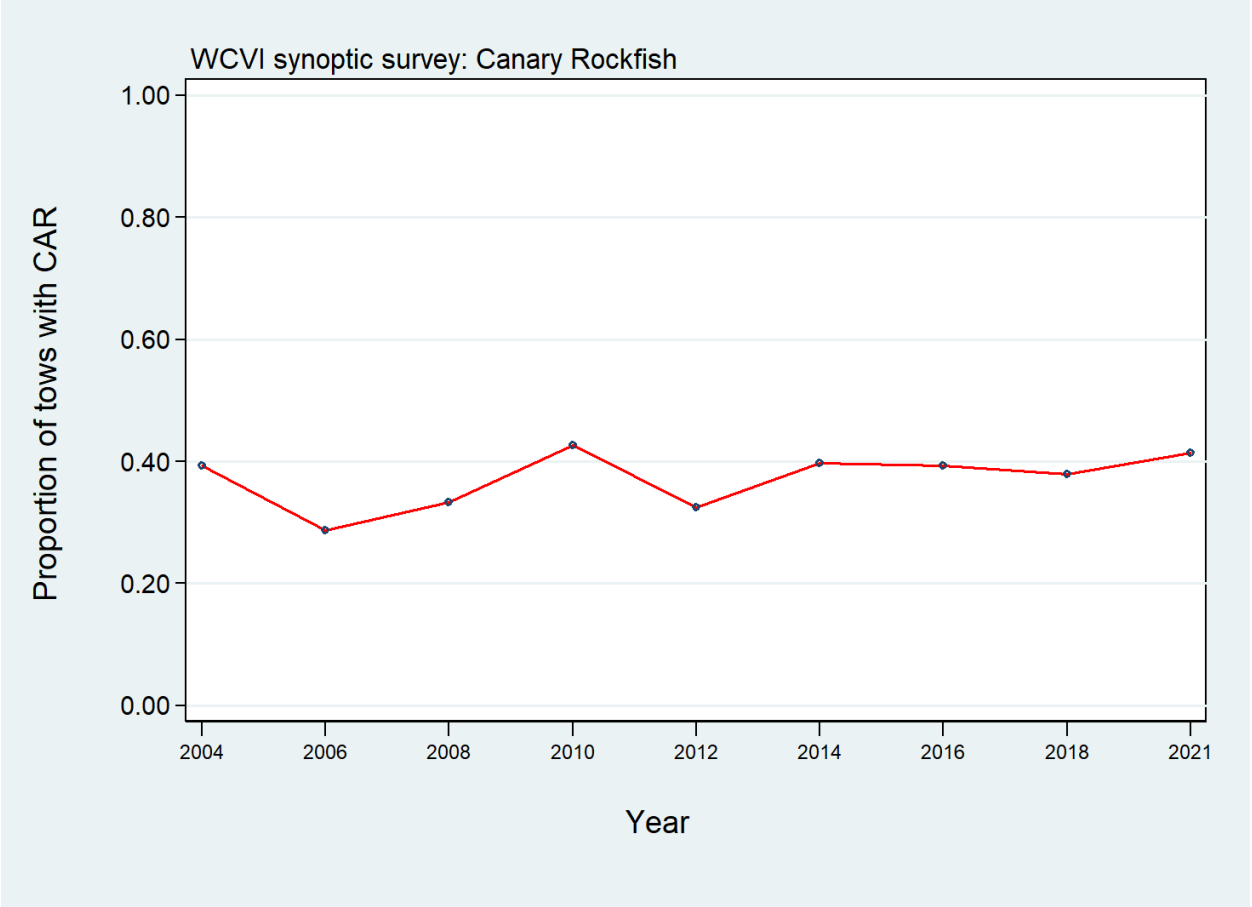

Figure B.47. Proportion of tows by stratum and year capturing CAR in the WCVI synoptic trawl surveys, 2004–2021.

Table B.14. Biomass estimates for CAR from the WCVI synoptic trawl survey for the survey years 2004 to 2021. Bootstrap bias-corrected confidence intervals and CVs are based on 1000 random draws with replacement.

Survey Year	Biomass (t) (Eq. B.4)	Mean bootstrap biomass (t)	Lower bound biomass (t)	Upper bound biomass (t)	Bootstrap CV	Analytic CV (Eq. B.6)
2004	818.1	812.5	395.3	1,541.8	0.347	0.351
2006	4,695.3	4,648.9	1,331.5	11,213.5	0.519	0.507
2008	721.5	723.6	420.8	1,209.0	0.265	0.261
2010	3,603.2	3,688.0	828.9	7,178.7	0.442	0.432
2012	2,018.6	2,075.3	358.2	5,626.6	0.639	0.630
2014	973.8	976.0	212.3	2,623.8	0.682	0.697
2016	1,558.5	1,561.7	747.3	2,797.4	0.341	0.350
2018	3,050.5	3,114.3	814.4	7,869.9	0.587	0.599
2021	1,565.1	1,558.0	868.6	2,531.5	0.266	0.260

B.7. WEST COAST HAIDA GWAII SYNOPTIC TRAWL SURVEY

B.7.1. Data selection

The west coast Haida Gwaii (WCHG) survey has been conducted nine times over the period 2006 to 2020 off the west coast of Haida Gwaii. This includes a survey conducted in 2014 which did not complete a sufficient number of tows for it to be considered comparable to the remaining surveys and which is consequently omitted from Table B.15. An earlier survey, conducted in 1997, also using a random stratified design similar to the current synoptic survey design along with an Atlantic Western II box trawl net (Workman et al. 1998), has not been included in this time series because of the low incidence of CAR in this survey. The current design of this survey comprises a single areal stratum extending from 53°N to the BC-Alaska border and east to 133°W (Olsen et al. 2008) stratified into four depth strata: 180–330 m; 330–500 m; 500–800 m; and 800–1300 m (Table B.15). Tows are assigned to a stratum based on the mean of the beginning and end depths of each tow. The 2006 synoptic survey used a different depth stratification (150–200 m, 200–330 m, 330–500 m, 500–800 m, and 800–1300 m) and has been re-stratified to conform to the stratification adopted beginning in 2007. Tows S of 53°N from this survey have been dropped. Plots of the locations of all valid tows by year and stratum are presented in Figure B.48 (2006), Figure B.49 (2007), Figure B.50 (2008), Figure B.51 (2010), Figure B.52 (2012), Figure B.53 (2016), Figure B.54 (2018) and Figure B.55 (2020). Note that the range of the depth stratum boundaries for this survey differ from those used for the Queen Charlotte Sound (Edwards et al. 2012) and west coast Vancouver Island (Edwards et al. 2014) synoptic surveys due to the considerable difference in the seabed topography of the area being surveyed. The deepest stratum (800–1300 m) has been omitted from this analysis because of lack of coverage in 2007.

Table B.15. Stratum designations, vessel name, number of usable and unusable tows, for each completed year of the west coast Haida Gwaii synoptic survey. Also shown are the dates of the first and last survey tow in each year.

		Depth stratum							
Survey year	Vessel	180-330 m	330-500 m	500-800 m	800-1300 m	Total tows[1]	Unusable tows	Minimum date	Maximum date
2006	*Viking Storm*	54	26	14	54	94	14[2]	30-Aug-06	22-Sep-06
2007	*Nemesis*	67	33	8	67	108	8	14-Sep-07	12-Oct-07
2008	*Frosti*	70	31	8	70	109	10	28-Aug-08	18-Sep-08
2010	*Viking Storm*	81	28	11	81	120	5	28-Aug-10	16-Sep-10
2012	*Nordic Pearl*	75	28	9	75	112	13	27-Aug-12	16-Sep-12
2016	*Frosti*	67	28	5	67	100	10	28-Aug-16	24-Sep-16
2018	*Nordic Pearl*	67	30	10	67	107	12	05-Sep-18	20-Sep-18
2020	*Nordic Pearl*	65	26	3	65	94	16	29-Aug-20	18-Sep-20
Area (km^2)		1,076	1,004	952	2,248	5,280[3]	–	–	–

[1] GFBio usability codes=0,1,2,6 and omitting the 800-1300 m stratum; [2] excludes 2 tows S of 53°N; [3] Total area in 2020 (km^2)

Table B.16. Number of valid tows with doorspread measurements, the mean doorspread values (in m) from these tows for each survey year and the number of valid tows without doorspread measurements.

Year	Tows with doorspread	Tows missing doorspread	Mean doorspread (m)
2006	93	30	77.7
2007	113	3	68.5
2008	123	4	80.7
2010	129	2	79.1
2012	92	49	73.8
2016	105	15	74.1
2018	130	0	67.0
2020	107	5	67.5
Total/Average	1,000	108	73.0[1]

[1] average 2007–2020: all observations

A doorspread density (Eq. B.3) was generated for each tow based on the catch of CAR from the mean doorspread for the tow and the distance travelled. [`distance travelled`] is a database field which is calculated directly from the tow track. This field is used preferentially for the variable D_{yij} in Eq. B.3. A calculated value ([`vessel speed`] X [`tow duration`]) is used for this variable if [`distance travelled`] is missing, but there were no instances of this occurring in the eight trawl surveys. Missing values for the [`doorspread`] field were filled in with the mean doorspread for the survey year (103 values over all years, Table B.16).

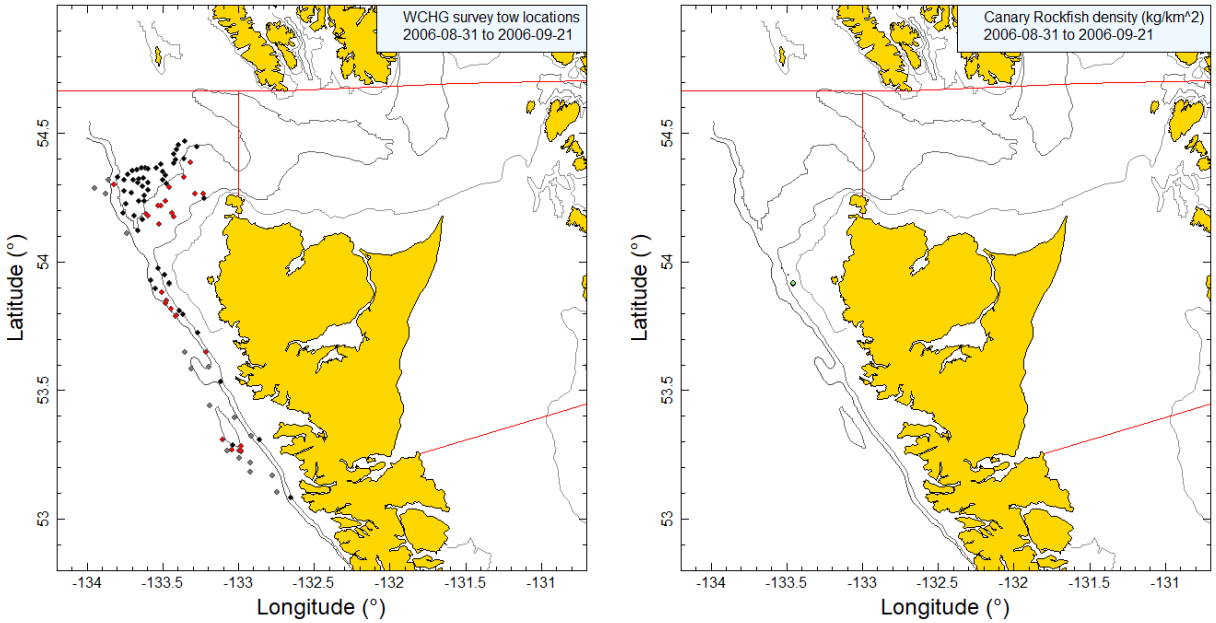

Figure B.48. Valid tow locations by stratum (180-330 m: black; 330-500 m: red; 500-800 m: grey; 800-1300 m: blue) and density plots for the 2006 Viking Storm synoptic survey. Circle sizes in the right-hand density plot scaled across all years (2006–2020), with the largest circle =19,837 kg/km^2 in 2016. The red lines show the Pacific Marine Fisheries Commission 5E and 5D major area boundaries. Depth contour lines denote 100, 300 and 500 m.

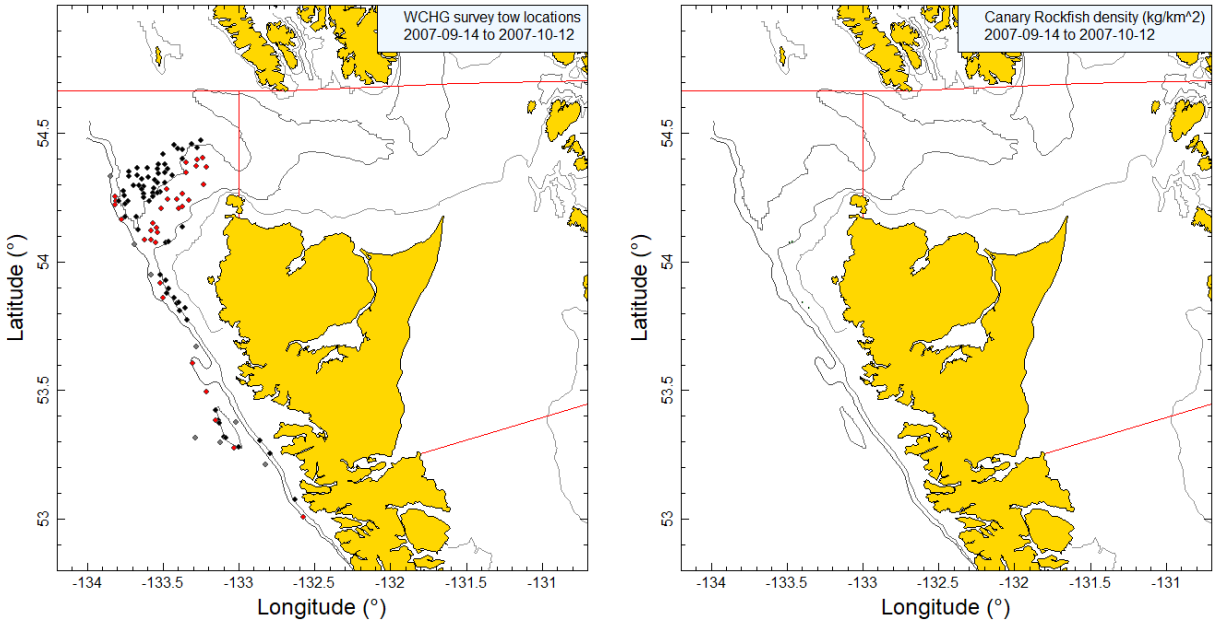

Figure B.49. Tow locations and density plots for the 2007 Nemesis synoptic survey (see Figure B.48 caption).

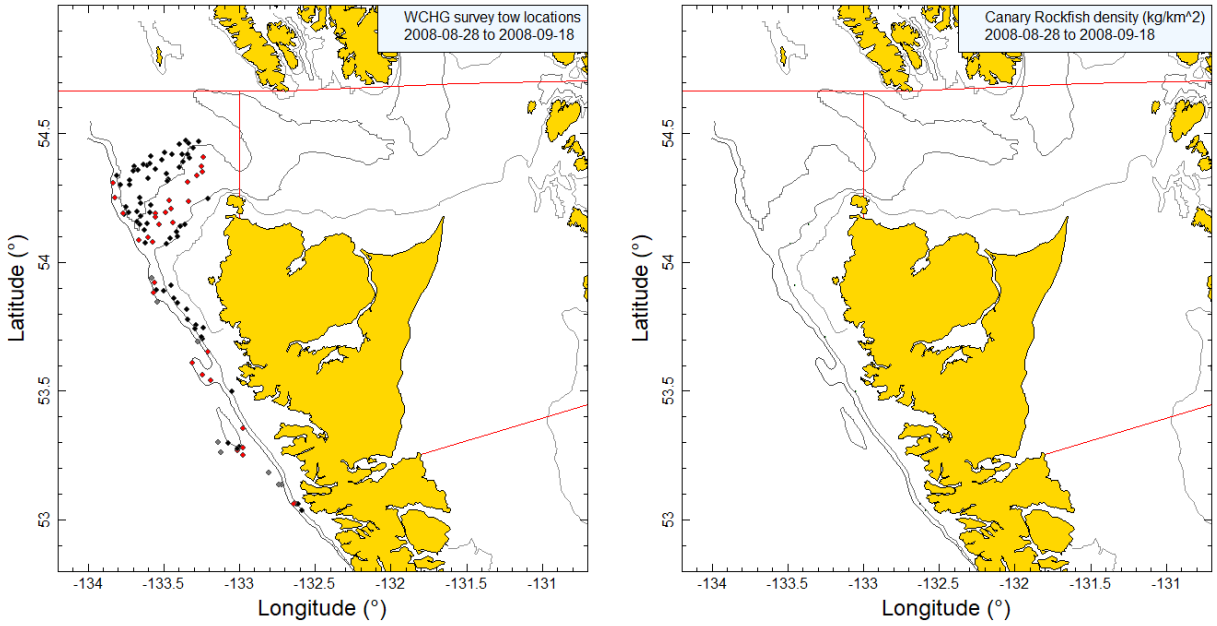

Figure B.50. Tow locations and density plots for the 2008 Frosti synoptic survey (see Figure B.48 caption).

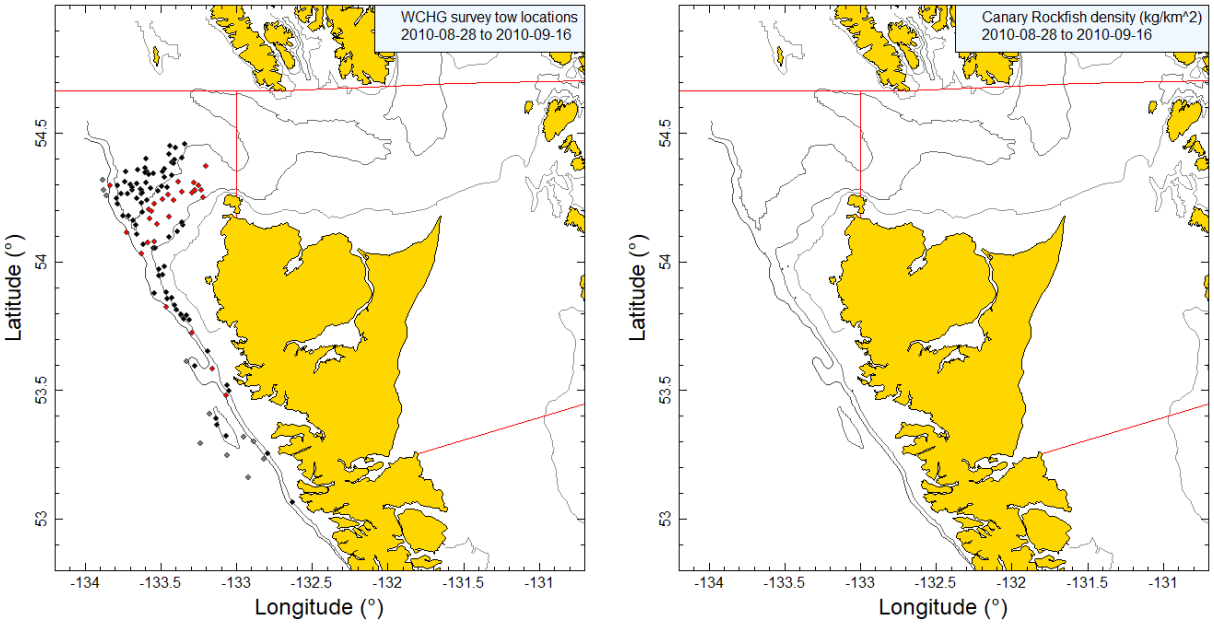

Figure B.51. Tow locations and density plots for the 2010 Viking Storm synoptic survey (see Figure B.48 caption).

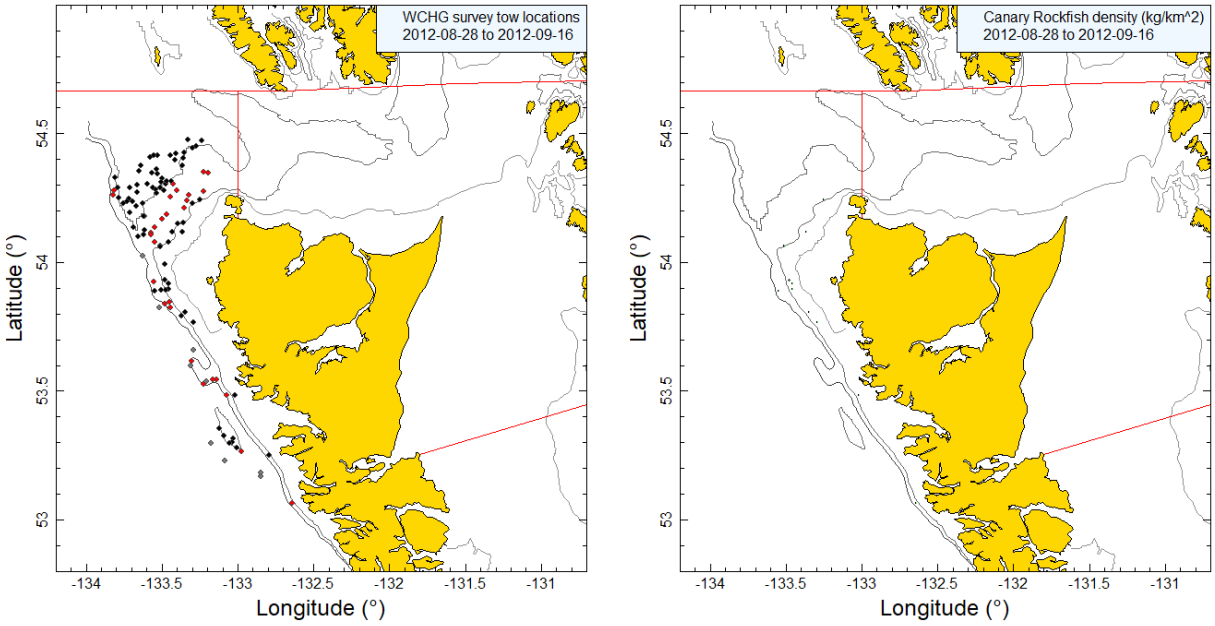

Figure B.52. Tow locations and density plots for the 2012 Nordic Pearl synoptic survey (see Figure B.48 caption).

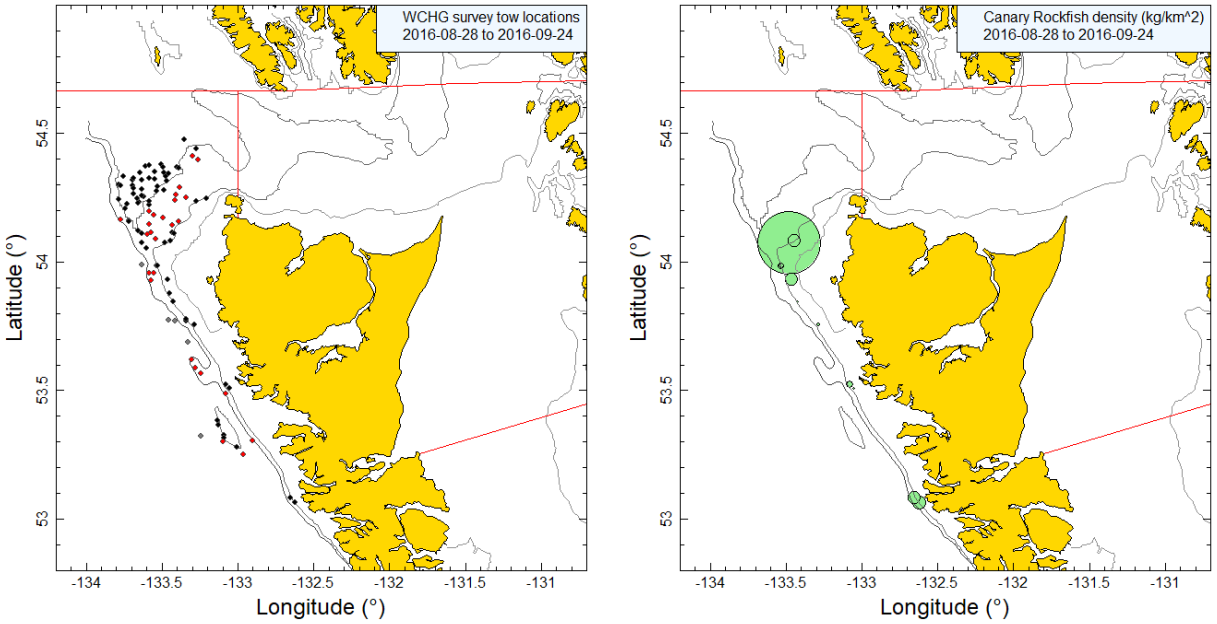

Figure B.53. Tow locations and density plots for the 2016 Frosti synoptic survey (see Figure B.48 caption).

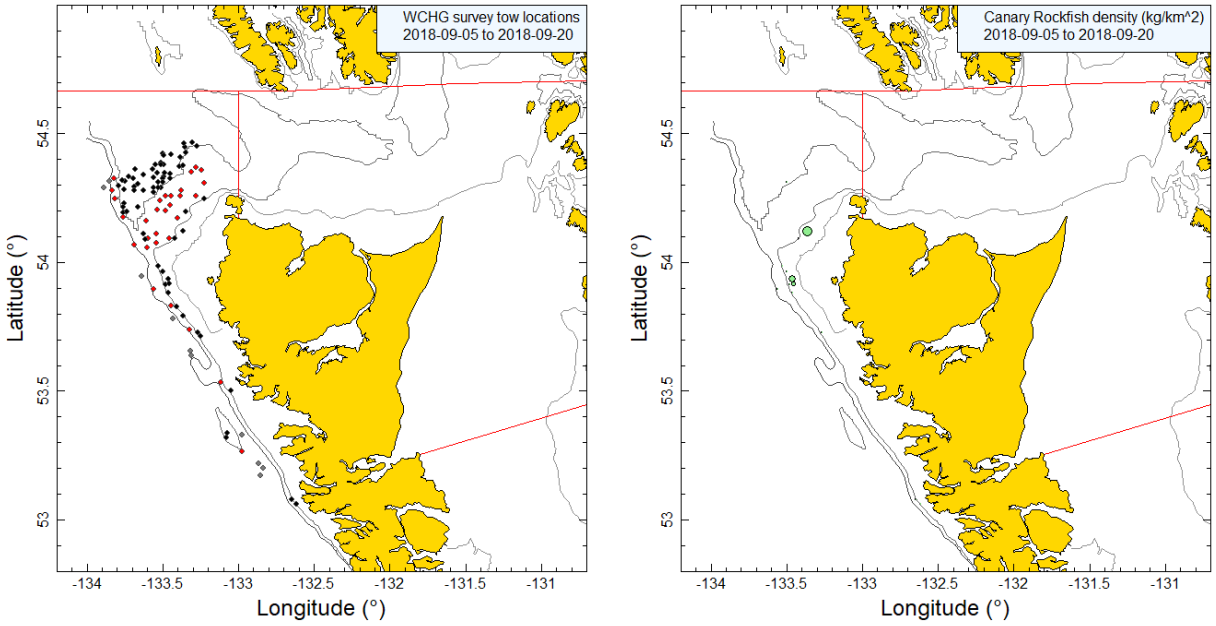

Figure B.54. Tow locations and density plots for the 2018 Nordic Pearl synoptic survey (see Figure B.48 caption).

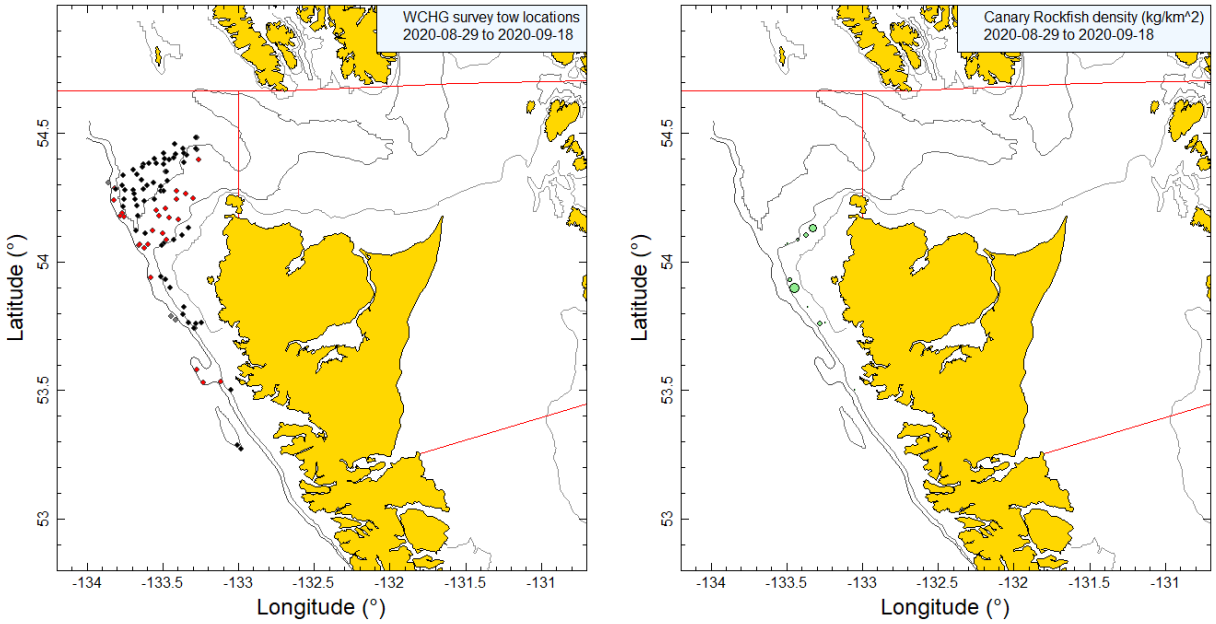

Figure B.55. Tow locations and density plots for the 2020 Nordic Pearl synoptic survey (see Figure B.48 caption).

B.7.2. Results

These eight surveys have taken CAR along a narrow depth band between 200 and 225 m on the north and west coasts of Graham Island (Figure B.48 to Figure B.55). This species is clearly not well represented in this survey, given the considerable biomass of this species that is present between 180 m and 100 m in the WCVI and QCS synoptic surveys (see Figure B.33 and Figure B.45), depths which are not covered by this survey due to the extreme bottom topography on this part of the coast. In this survey, CAR were mainly taken at in a narrow depth range around 200 m, which is near the lower depth boundary of this survey (5 to 95% quantiles of the starting tow depth=173–225 m) (Figure B.56).

The incidence of this species in this survey is low, with the proportion of tows that captured CAR averaging at 8% (68 of 846 tows) and ranging from 4% to 12% of tows over the eight survey years (Figure B.58). The median CAR catch weight for positive tows was 7.5 kg/tow and the maximum catch weight across the eight surveys was a single tow of 2,223 kg in 2016 (the next largest tow was 438 kg).

Table B.17. Biomass estimates for CAR from the eight west coast Haida Gwaii synoptic surveys used in the stock assessment. Bootstrap bias-corrected confidence intervals and coefficients of variation (CVs) are based on 1000 random draws with replacement.

Survey Year	Biomass (t) (Eq. B.4)	Mean bootstrap biomass (t)	Lower bound biomass (t)	Upper bound biomass (t)	Bootstrap CV	Analytic CV (Eq. B.6)
2006	73.7	72.5	5.2	192.6	0.644	0.647
2007	9.5	9.8	0.4	21.8	0.540	0.544
2008	2.4	2.4	0.9	5.1	0.431	0.416
2010	12.0	12.1	0.7	38.4	0.769	0.769
2012	36.3	36.4	11.8	72.8	0.423	0.421
2016	374.0	378.8	39.9	1,295.8	0.820	0.821
2018	87.9	89.2	10.9	232.4	0.611	0.618
2020	133.9	134.1	40.6	287.5	0.462	0.487

Estimated biomass levels for CAR from these trawl surveys were low, with only two of the biomass estimates exceeding 100 t and the largest estimate at less than 400 t in 2016 due to a single large tow (Figure B.57; Table B.17). The estimated relative errors (RE) for these surveys are variable and large, ranging from 0.42 in 2012 to 0.82 in 2016 (Table B.17).

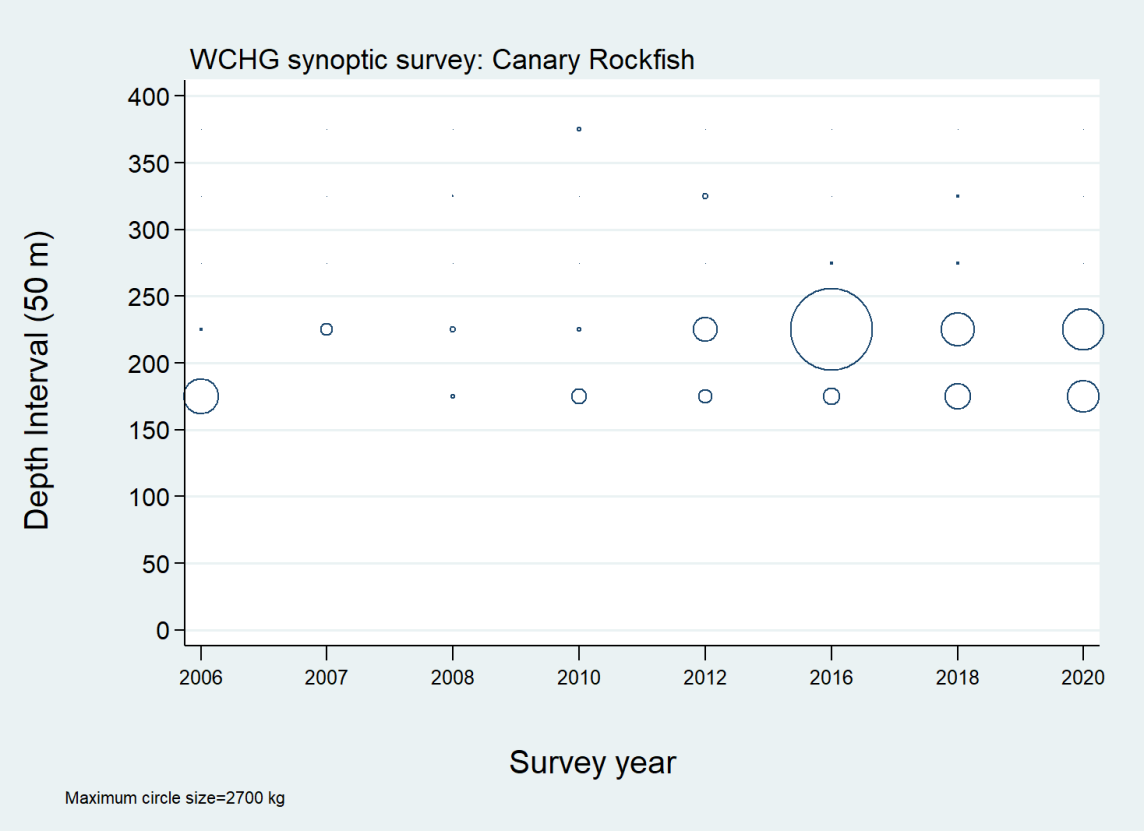

Figure B.56. Distribution of observed weights of CAR by survey year and 25 m depth zone intervals. Catches are plotted at the mid-point of the interval and circles in the each panel are scaled to the maximum value (4,136 kg – 200-225 m interval in 2020). Minimum and maximum depths observed for CAR: 157 m and 558 m, respectively.

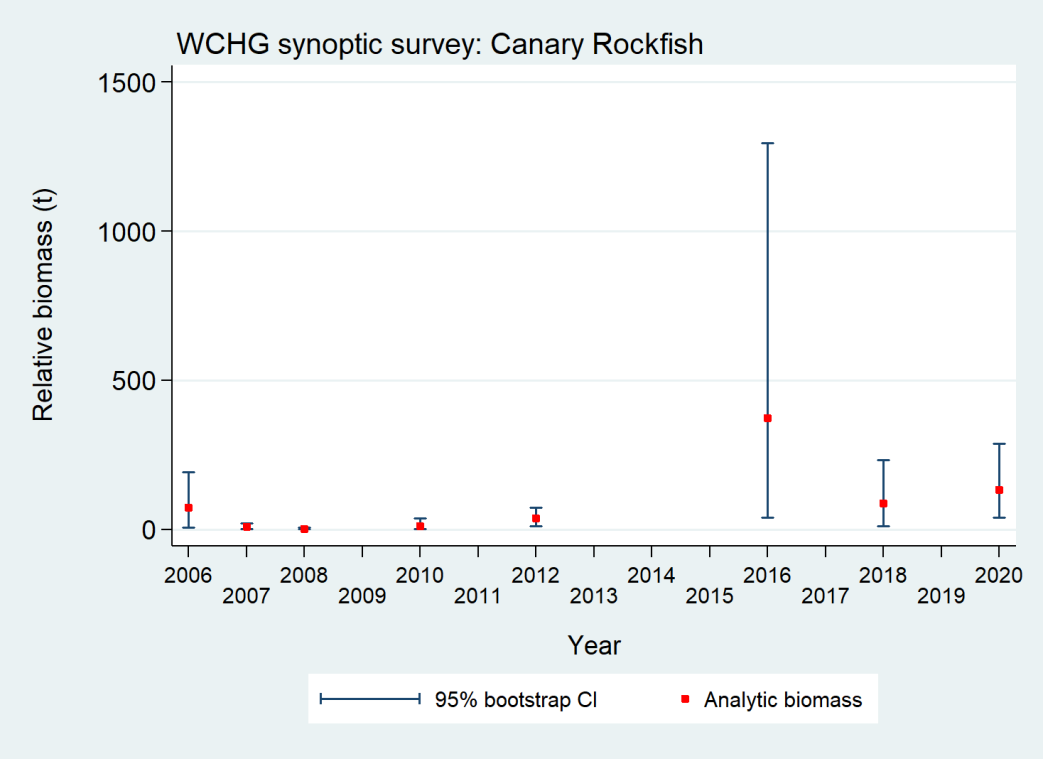

Figure B.57. Biomass estimates for CAR from the 2006 to 2020 west coast Haida Gwaii synoptic surveys (Table B.17). Bias-corrected 95% confidence intervals from 1000 bootstrap replicates are plotted.

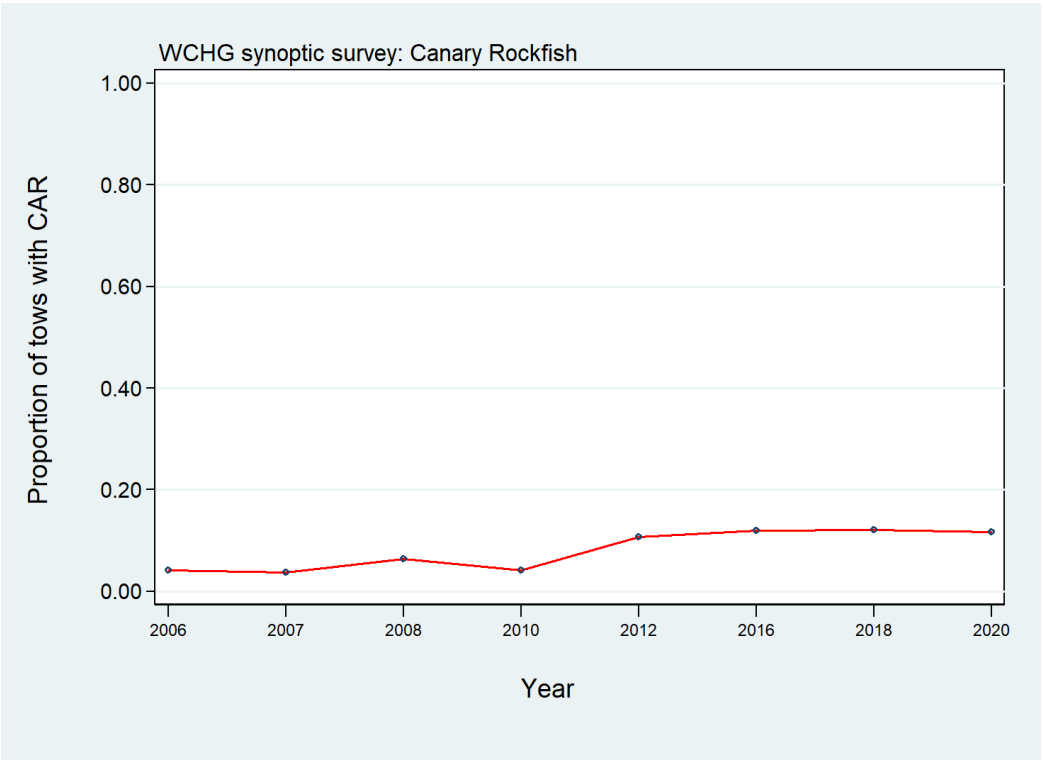

Figure B.58. Proportion of tows by year that contain CAR for the eight west coast Haida Gwaii synoptic surveys.

B.8. HECATE STRAIT SYNOPTIC SURVEY

B.8.1. Data selection

This survey has been conducted in nine alternating years over the period 2005 to 2021 in Hecate Strait (HS) between Moresby and Graham Islands and the mainland and in Dixon Entrance at the top of Graham Island (all valid tow starting positions by survey year are shown in Figure B.59 to Figure B.66). This survey treats the full spatial coverage as a single areal stratum divided into four depth strata: 10–70 m; 70–130 m; 130–220 m; and 220–500 m (Table B.18).

Table B.18. Number of usable tows for biomass estimation by year and depth stratum for the Hecate Strait synoptic survey over the period 2005 to 2021. Also shown is the area of each depth stratum, the vessel conducting the survey by survey year, the number of unusable tows and the beginning and end dates for each survey year. The final dates are the minimum and maximum start and end dates among all the survey years.

		Depth stratum (m)				Total	Unusable	Minimum	Maximum
Year	Vessel	10-70	70-130	130-220	220-500	tows[1]	tows	date	date
2005	Frosti	77	86	26	9	198	38	27-May-05	27-Jun-05
2007	W.E. Ricker	47	42	36	7	132	24	24-May-07	16-Jun-07
2009	W.E. Ricker	53	43	47	12	155	8	28-May-09	18-Jun-09
2011	W.E. Ricker	70	51	49	14	184	18	26-May-11	18-Jun-11
2013	W.E. Ricker	74	42	43	16	175	0	30-May-13	21-Jun-13
2015	W.E. Ricker	47	46	40	15	148	4	28-May-15	20-Jun-15
2017	Nordic Pearl	47	44	38	9	138	14	21-May-17	12-Jun-17
2019	Nordic Pearl	40	44	37	14	135	11	19-May-19	07-Jun-19
2021	Sir John Franklin	44	34	30	8	116	12	20-May-21	10-Jun-21
Area (km^2)		5,958	3,011	2,432	1,858	13,259[2]	–	19-May	27-Jun

[1] GFBio usability codes=0,1,2,6
[2] Total area (km^2) for 2021 synoptic survey

Table B.19. Number of missing doorspread values by year for the Hecate Strait synoptic survey over the period 2005 to 2021 as well as showing the number of available doorspread observations and the mean doorspread value for the survey year.

Year	Number tows with missing doorspread [1]	Number tows with doorspread observations [2]	Mean doorspread (m) used for tows with missing values [2]
2005	7	217	64.4
2007	97	37	59.0
2009	93	70	54.0
2011	13	186	54.8
2013	6	169	51.7
2015	0	151	59.4
2017	2	150	64.2
2019	5	141	59.2
2021	0	128	54.4
Total	223	1,249	58.3

[1] valid biomass estimation tows only
[2] includes tows not used for biomass estimation

A doorspread density value (Eq. B.3) was generated for each tow based on the catch of CAR from the mean doorspread for the tow and the distance travelled. [`distance travelled`] is a database field which is calculated directly from the tow track. This field is used preferentially for the variable D_{yij} in Eq. B.3. A calculated value ([`vessel speed`] X [`tow duration`]) is used for this variable if [`distance travelled`] is missing, but there were no instances of this occurring

among the valid tows in the nine trawl surveys. Missing values for the [doorspread] field were filled in with the mean doorspread for the survey year (223 values over all years: Table B.19).

B.8.2. Results

Canary Rockfish have only been notably present in this survey in four of the nine survey years: 2011, 2013, 2015 and 2021 (Figure B.59 to Figure B.66). When present, CAR tend to be in the upper sections of Mitchell Gully (upper Hecate Strait). Canary Rockfish are also occasionally present in the western parts of Dixon Entrance, just east of Langara Island. There is little presence of CAR in the eastern parts of Dixon Entrance or the top section of Hecate Strait. Canary Rockfish are not abundant in the region covered by this survey, with only four tows in nine years exceeding 100 kg of CAR catch and with a median catch of 2.3 kg for positive tows. Canary Rockfish are found in relatively shallow depths in this survey (66-146 m=25-75% empirical depth observations) (Figure B.68). There is evidence from the age frequency data the CAR taken in this survey are quite young (compare the age distributions from the QC Sound survey with the HS survey in Figure D.11: there are relatively very few older CAR in the HS survey data). Perhaps the high incidence of CAR in the 2021 survey (Figure B.67) may be indicative of good recruitment in some of the recent year classes.

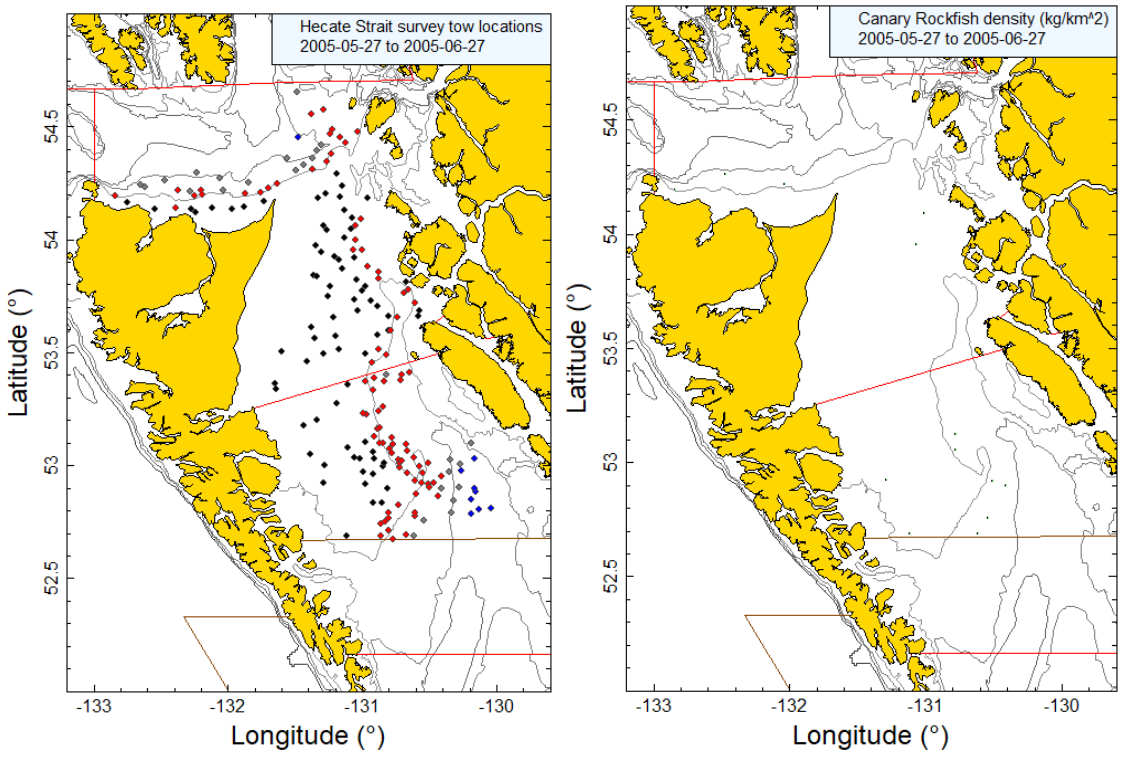

Figure B.59. Valid tow locations (10-70m stratum: black; 70-130m stratum: red; 130-220m stratum: grey; 220-500m stratum: blue) and density plots for the 2005 Hecate Strait synoptic survey. Circle sizes in the right-hand density plot scaled across all years (2005, 2007, 2009, 2011, 2013, 2015, 2017, 2019, 2021), with the largest circle = 3117 kg/km^2 in 2021. Red lines indicate boundaries for PMFC major statistical areas 5C, 5D and 5E. Brown lines indicate the upper boundary of the QC Sound survey. Depth contour lines denote 100, 200, 300 and 500 m.

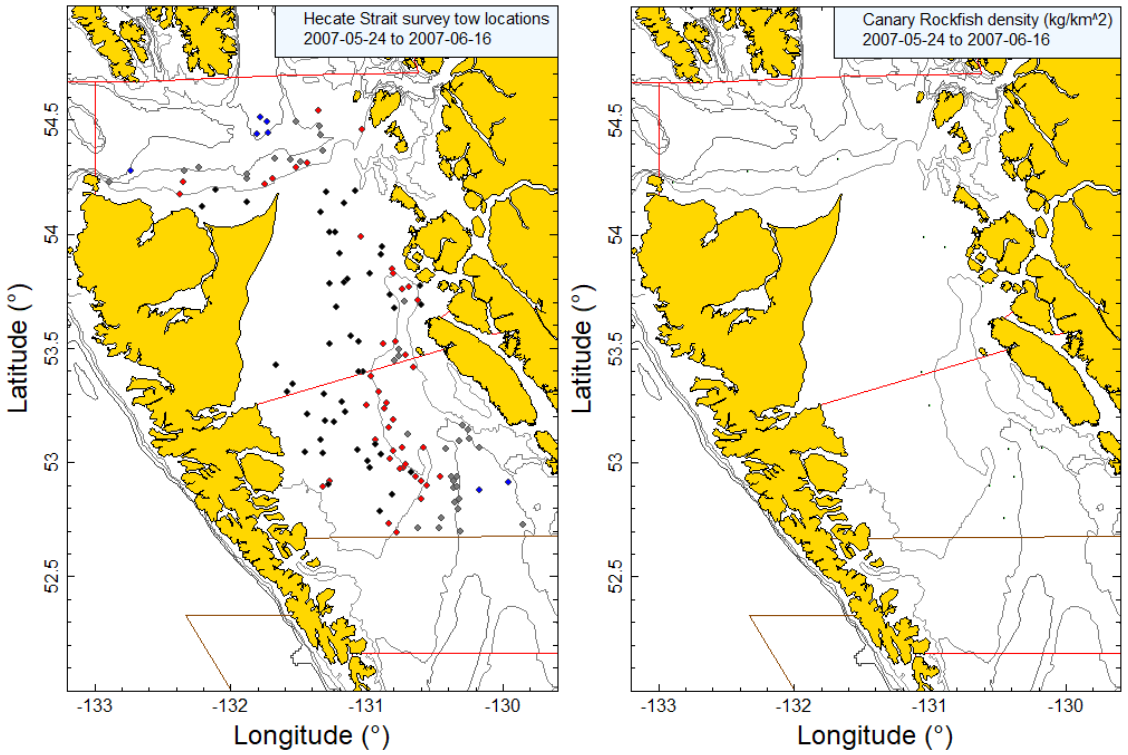

Figure B.60. Tow locations and density plots for the 2007 Hecate Strait synoptic survey (see Figure B.59 caption).

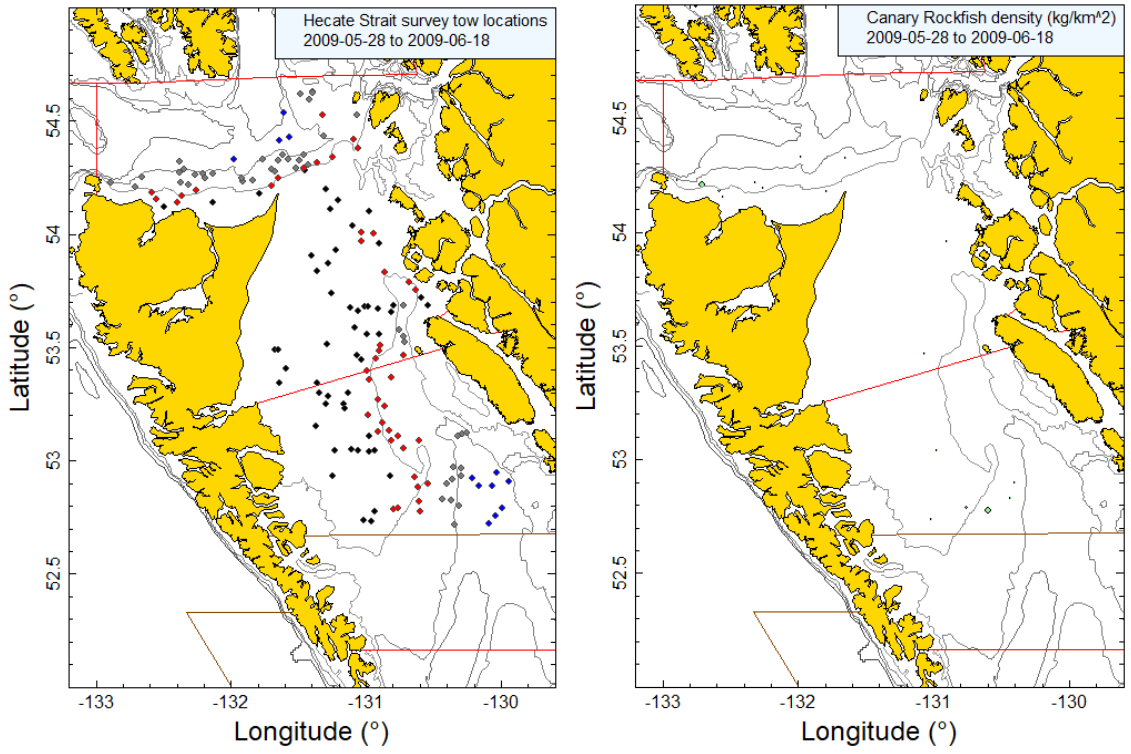

Figure B.61. Tow locations and density plots for the 2009 Hecate Strait synoptic survey (see Figure B.59 caption).

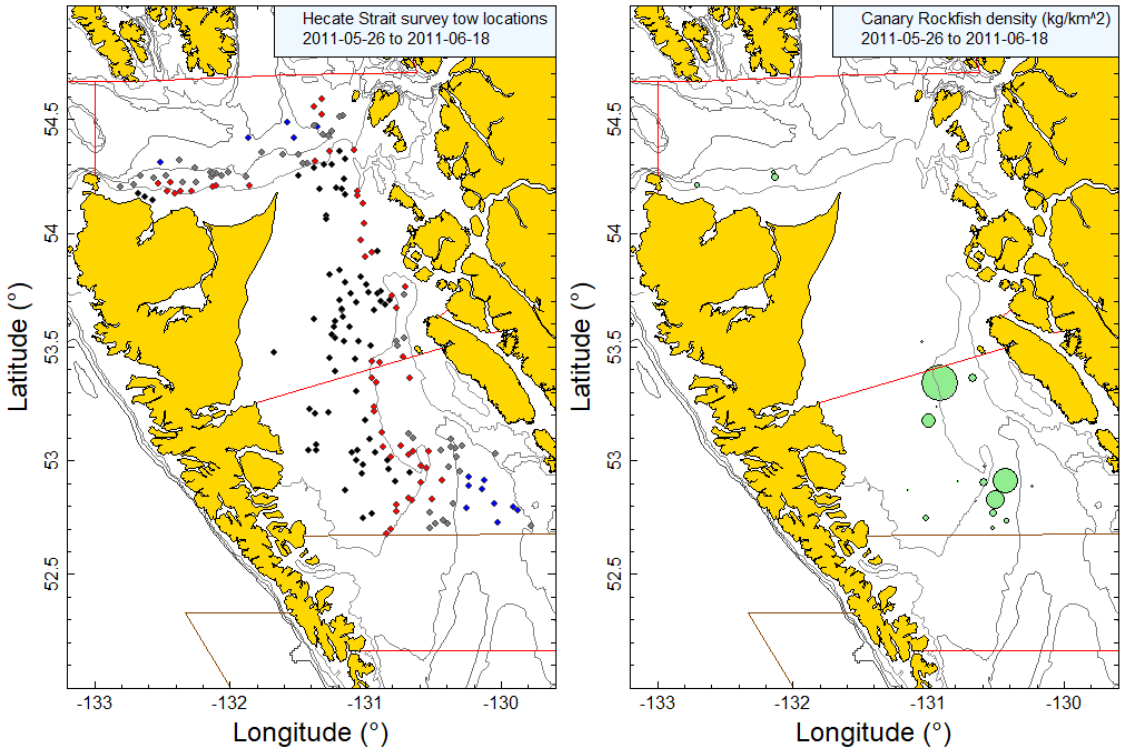

Figure B.62. Tow locations and density plots for the 2011 Hecate Strait synoptic survey (see Figure B.59 caption).

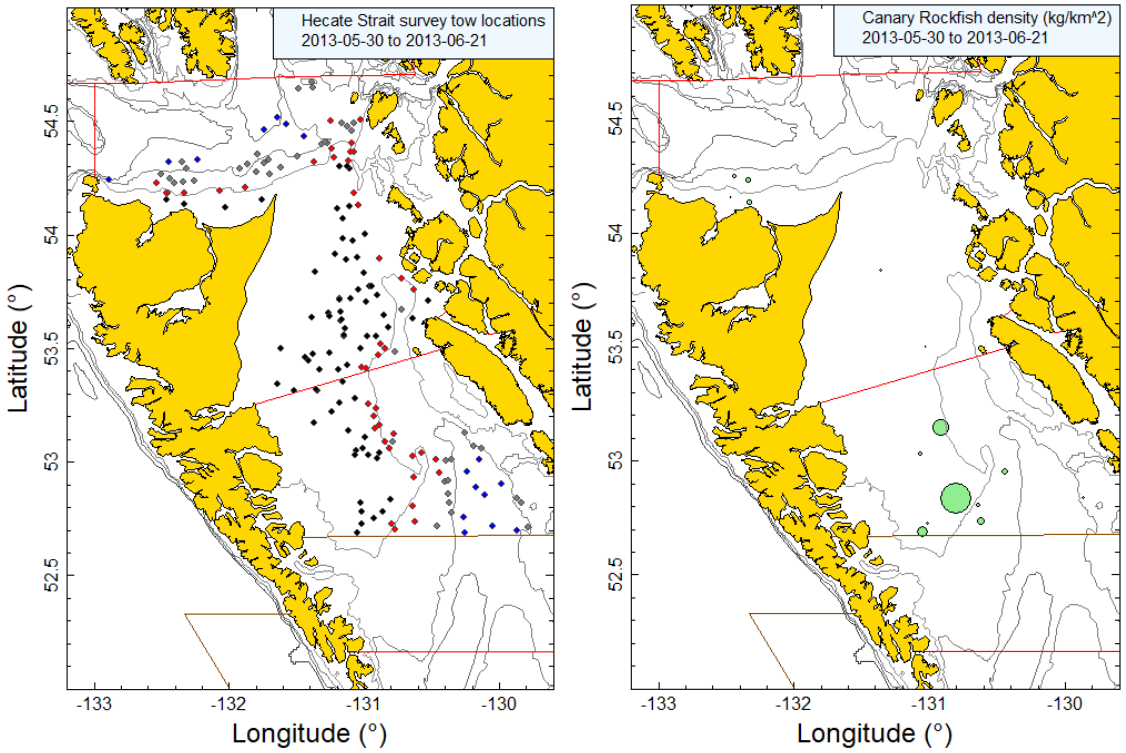

Figure B.63. Tow locations and density plots for the 2013 Hecate Strait synoptic survey (see Figure B.59 caption).

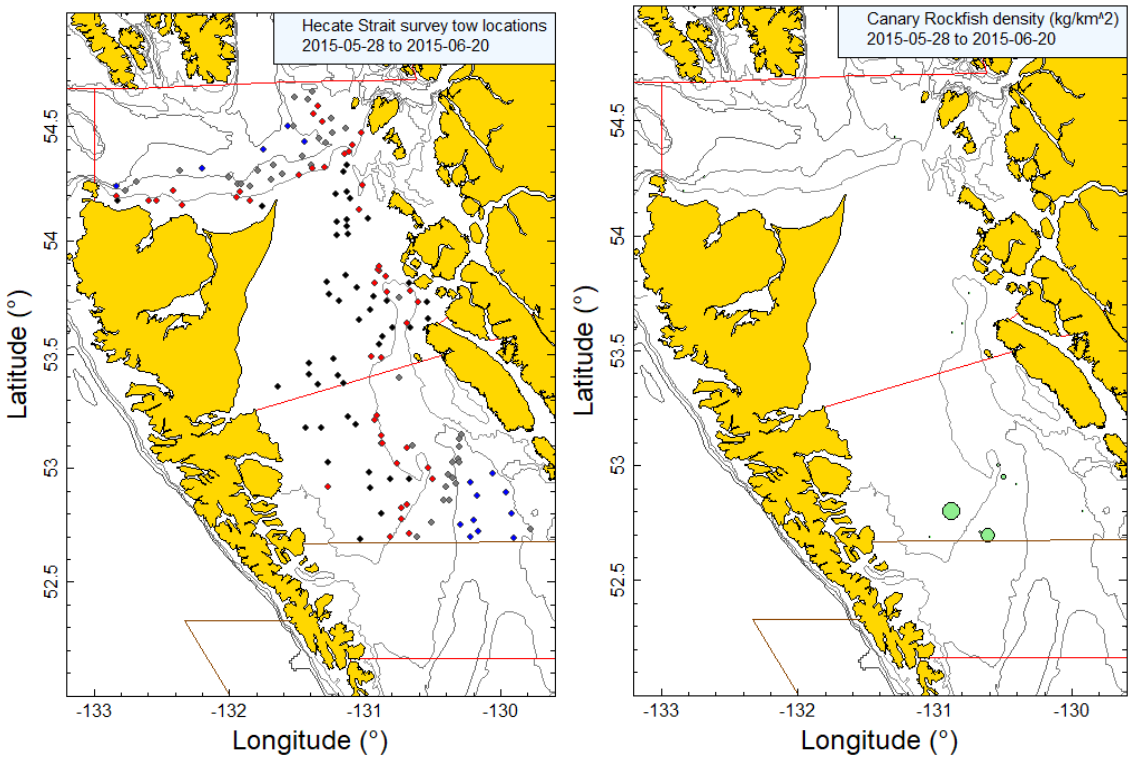

Figure B.64. Tow locations and density plots for the 2015 Hecate Strait synoptic survey (see Figure B.59 caption).

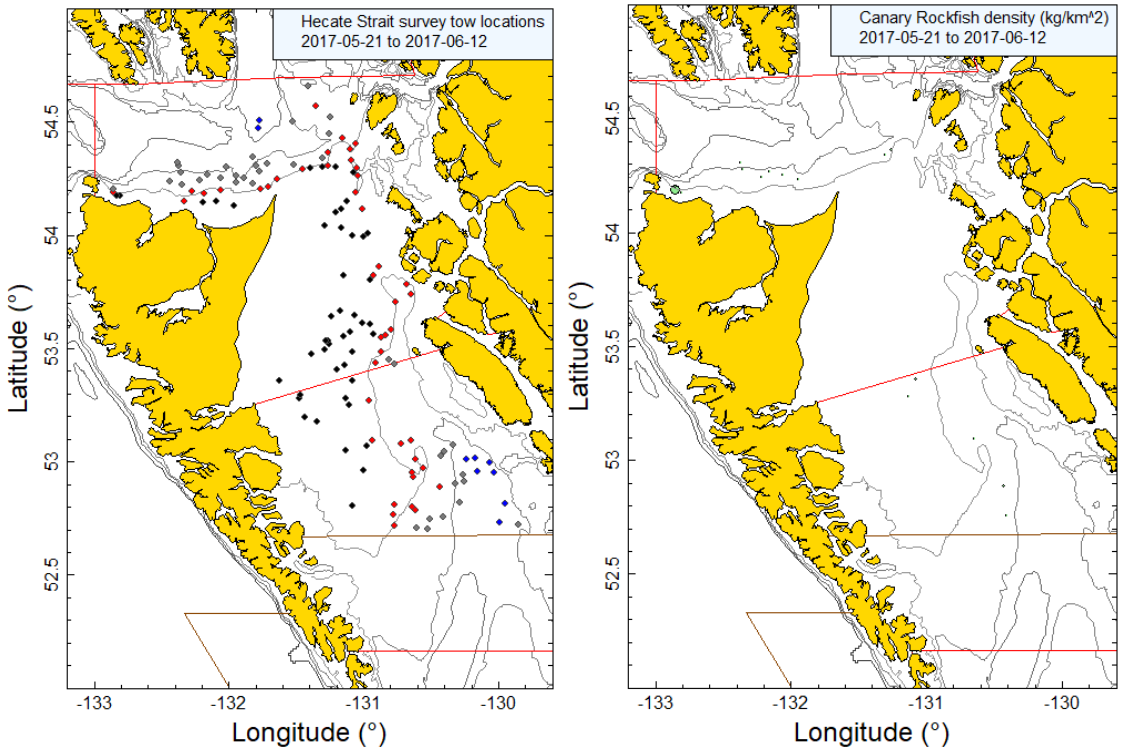

Figure B.65. Tow locations and density plots for the 2017 Hecate Strait synoptic survey (see Figure B.59 caption).

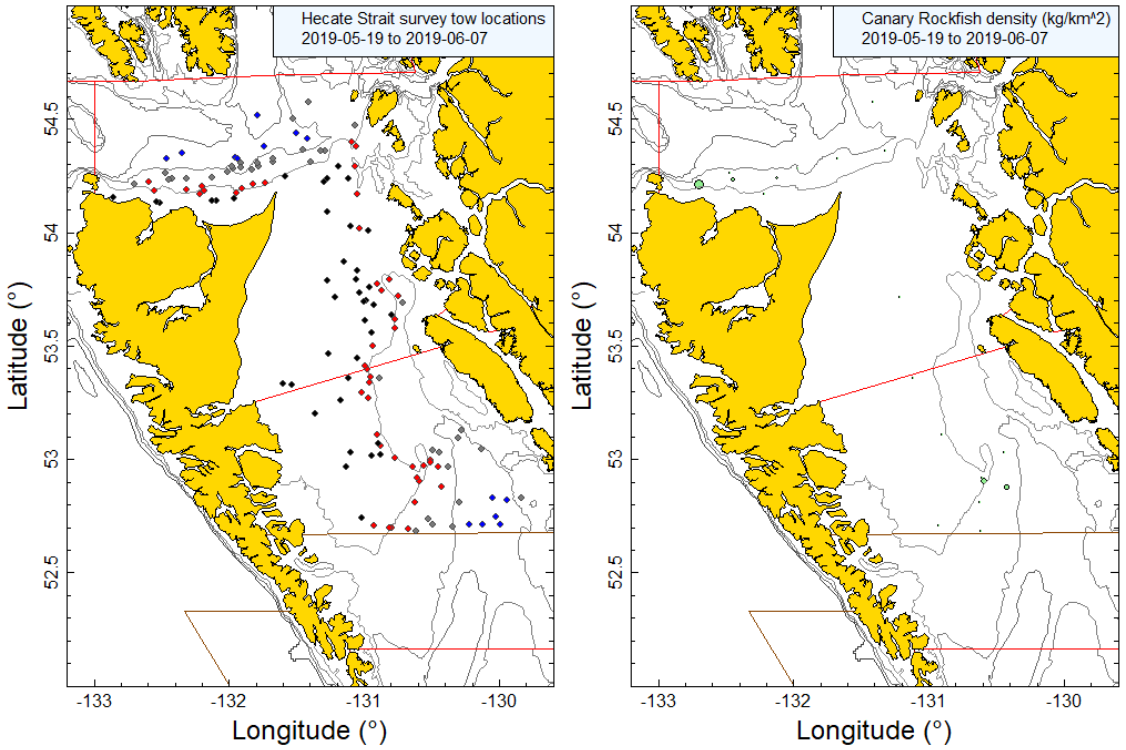

Figure B.66. Tow locations and density plots for the 2019 Hecate Strait synoptic survey (see Figure B.59 caption).

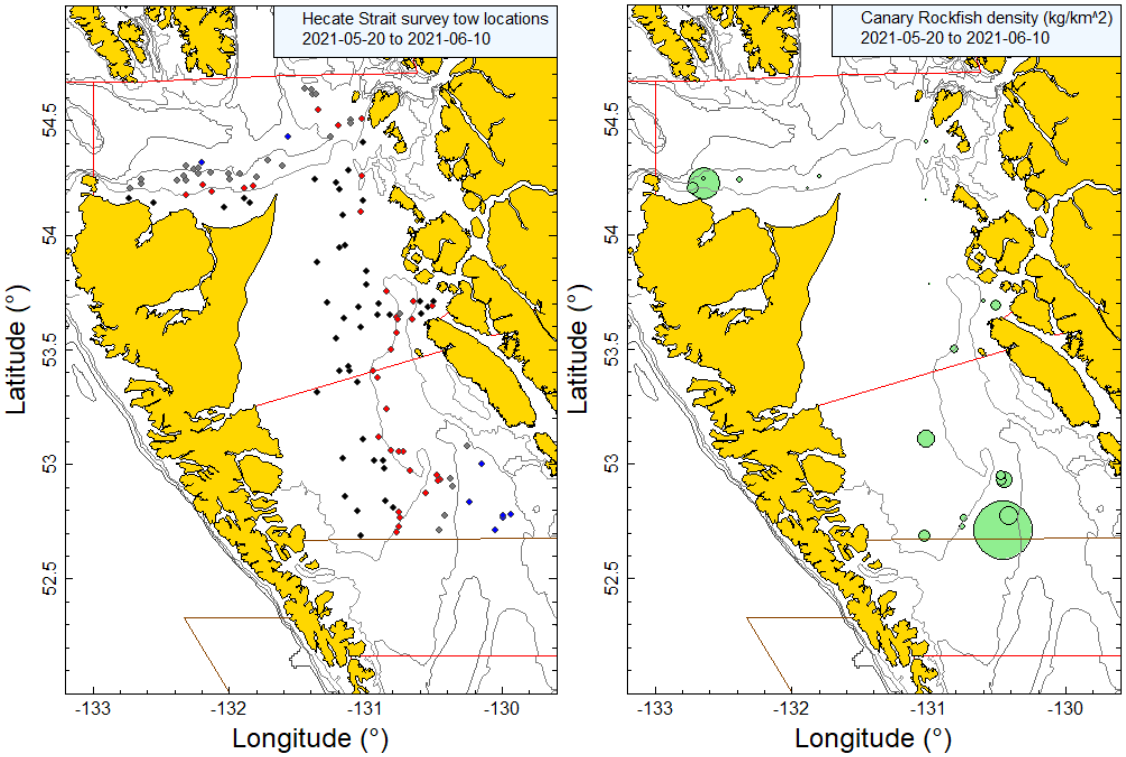

Figure B.67. Tow locations and density plots for the 2021 Hecate Strait synoptic survey (see Figure B.59 caption).

Estimated CAR doorspread biomass indices from this trawl survey showed no overall trend over the period 2005 to 2019, but with a strong relative increase observed in 2021 (Table B.20; Figure B.69). The estimated relative errors associated with these surveys were high, ranging from 0.35 to 0.68 (Table B.20). The incidence of CAR in this survey was low, with an average occurrence of 11% of tows capturing this species, ranging from 7% (2005) to 19% (2021) (Figure B.70). Overall, 151 (11%) of the 1,381 usable survey tows contained CAR.

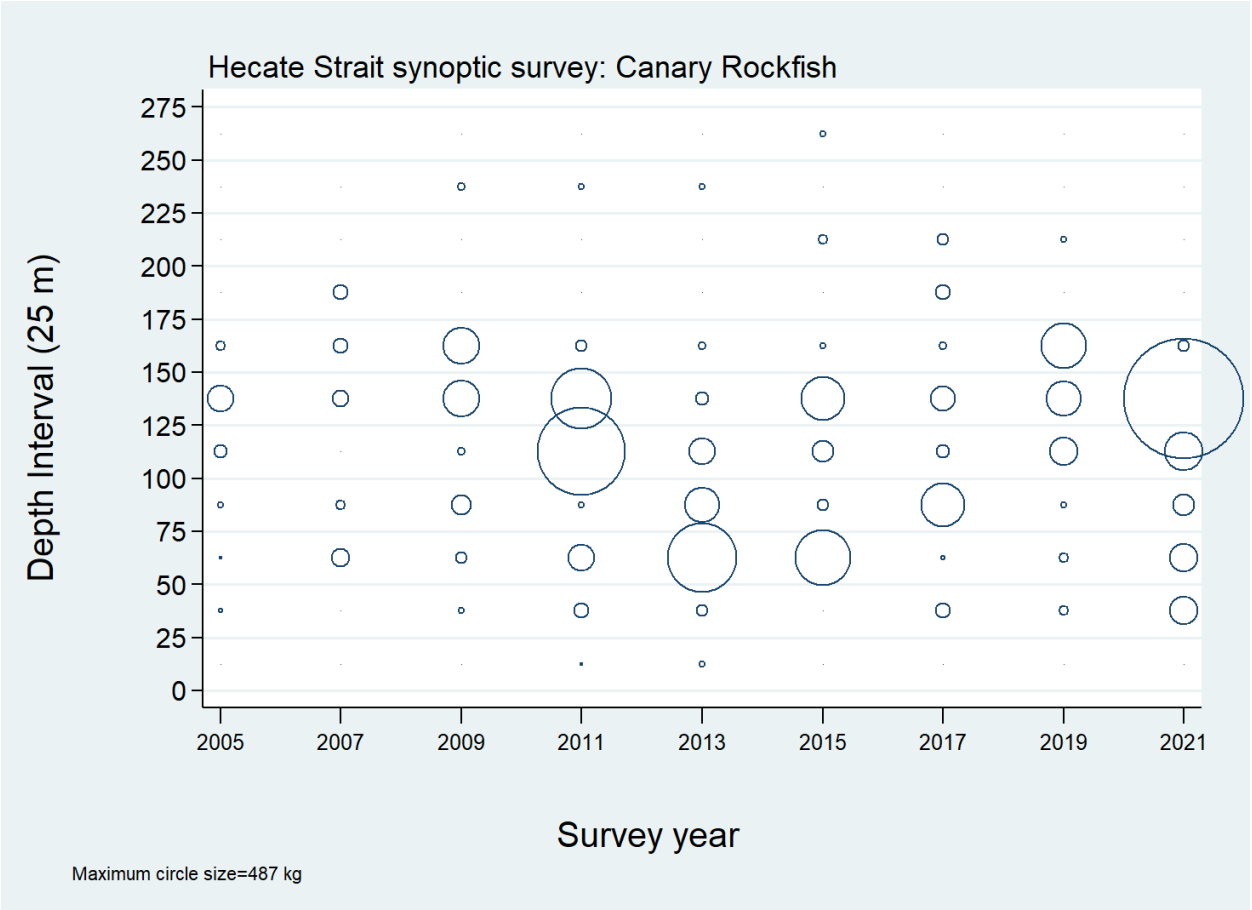

Figure B.68. Distribution of observed catch weights of Canary Rockfish for the Hecate Strait synoptic survey (Table B.18) by survey year and 25 m depth zone. Catches are plotted at the mid-point of the interval and circles in the panel are scaled to the maximum value (487 kg) in the 125-150 m interval in 2021. The 1% and 99% quantiles for the CAR empirical start of tow depth distribution= 42 m and 194 m respectively.

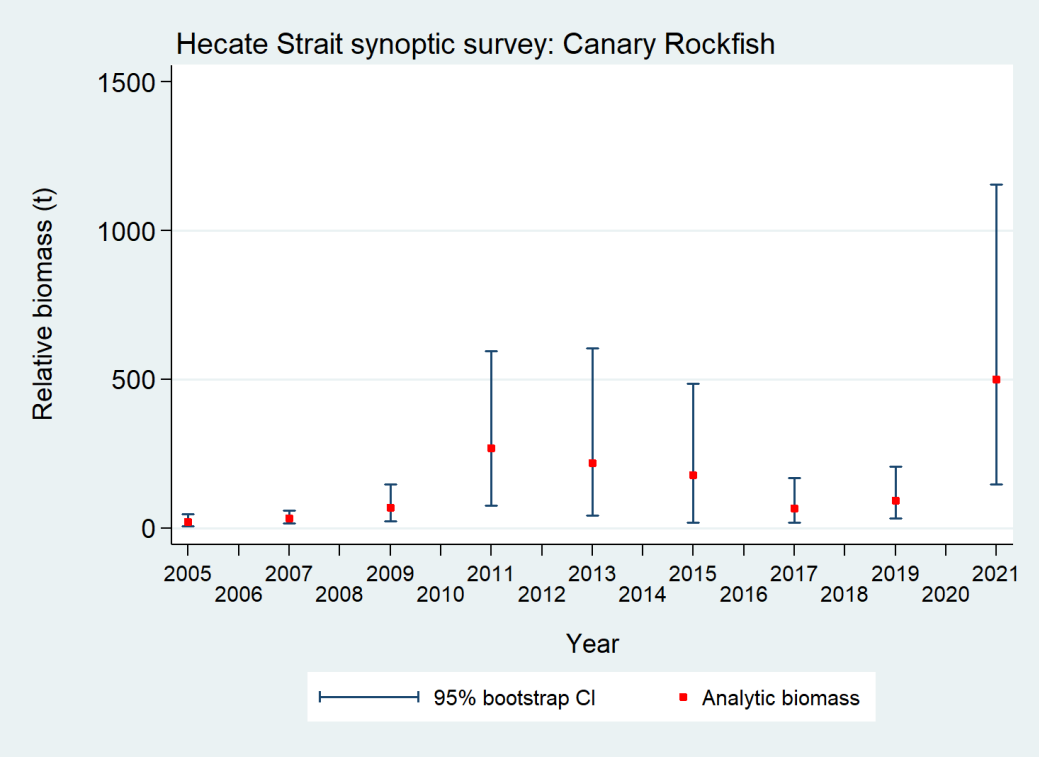

Figure B.69. Plot of biomass estimates for Canary Rockfish values provided in Table B.20 from the Hecate Strait synoptic survey over the period 2005 to 2021. Bias corrected 95% confidence intervals from 1000 bootstrap replicates are plotted.

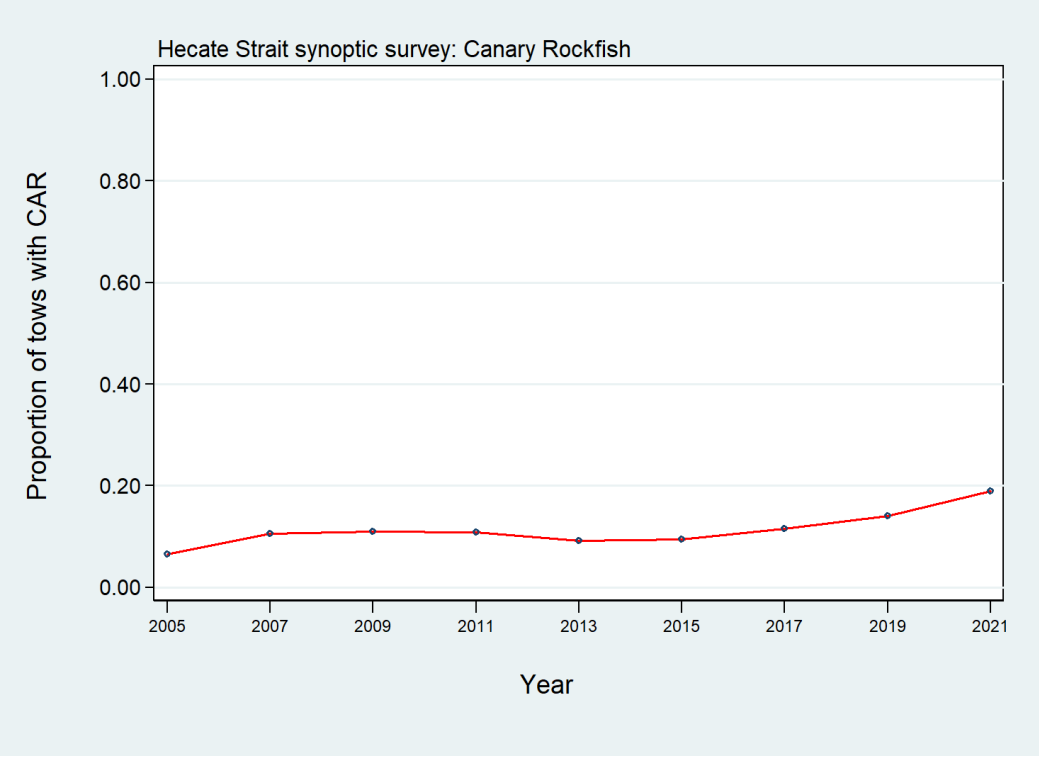

Figure B.70. Proportion of tows by year which contain Canary Rockfish from the Hecate Strait synoptic survey over the period 2005 to 2021.

Table B.20. Biomass estimates for Canary Rockfish from the Hecate Strait synoptic trawl survey for the survey years 2005 to 2021. Bootstrap bias corrected confidence intervals and CVs are based on 1000 random draws with replacement.

Survey Year	Biomass (t) (Eq. B.4)	Mean bootstrap biomass (t)	Lower bound biomass (t)	Upper bound biomass (t)	Bootstrap CV	Analytic CV (Eq. B.6)
2005	21.4	21.7	6.6	46.3	0.459	0.464
2007	33.6	33.2	15.4	58.5	0.346	0.350
2009	67.7	67.9	23.8	148.0	0.448	0.450
2011	267.8	261.4	75.7	594.8	0.493	0.498
2013	218.2	218.2	42.8	603.5	0.630	0.629
2015	177.7	180.7	17.1	485.6	0.678	0.709
2017	66.8	66.6	19.2	168.9	0.564	0.553
2019	93.4	95.9	31.4	206.3	0.451	0.454
2021	500.7	494.7	146.4	1,156.3	0.526	0.532

B.9. GEOSTATISTICAL SYNOPTIC SURVEY ESTIMATES

The equations presented in Section B.2 represent an approach which takes advantage of the random design of the surveys by assuming that fish density is constant within each stratum. However, this is a strong assumption that is unlikely to be correct, given the considerable habitat heterogeneity that is inherent in the marine environment and the relatively large size of the component strata. Anderson et al. (2019) proposed an alternative procedure for analysing the synoptic survey data that models the data geostatistically by predicting density as a continuous process affected by constant spatial processes (such as depth) and processes that vary both spatially and temporarily (such as temperature). This methodology is described in Appendix E of Anderson et al. (2019) and is applied to the four synoptic surveys in Appendix F of the same report.

While the survey estimates generated from the random swept area design are used in the base case stock assessment, it was proposed to use equivalent biomass estimates generated from a geostatistical analysis in a sensitivity run. Two sets of geostatistically-based biomass indices for each of the four synoptic surveys were provided for this purpose (P. English, DFO, pers. comm., July 5, 2022). One set was generated without consideration of depth as a covariate and the other included depth. The two geostatistical series are compared with the swept area surveys series, including the estimated error distribution, in Figure B.71 (WCVI synoptic survey), Figure B.72 (QCS synoptic survey), Figure B.73 (HS synoptic survey) and Figure B.74 (WCHG synoptic survey). In general, the correspondence between the three survey estimates is good, with only a few departures between the swept area estimates and the geostatistical estimates. Unusually, it appears that the uncertainty generated from the bootstrap procedure often exceeds the geostatistical uncertainty in many of the comparisons.

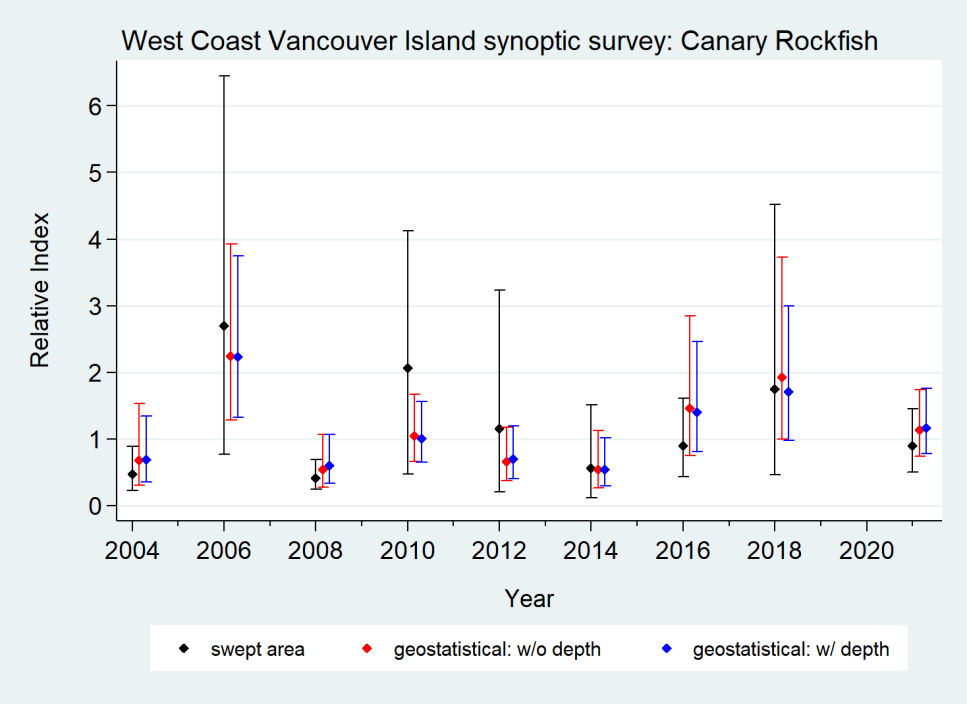

Figure B.71. Comparison of WCVI synoptic survey Canary Rockfish biomass indices estimated using three different procedures: a) the swept area method described in Section B.2; b) geostatistical model (Anderson et al. 2019) without including depth; c) geostatistical model which includes depth. All series have been standardised to a geometric mean of 1.0.

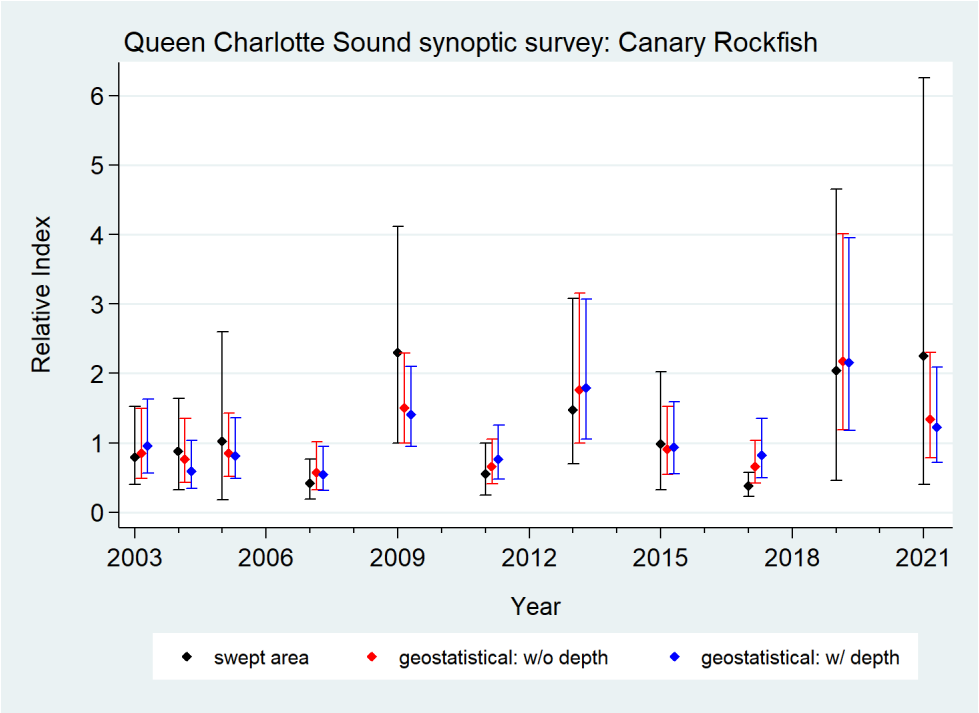

Figure B.72. Comparison of QCS synoptic survey Canary Rockfish biomass indices estimated using three different procedures: a) the swept area method described in Section B.2; b) geostatistical model (Anderson et al. 2019) without including depth; c) geostatistical model which includes depth. All series have been standardised to a geometric mean of 1.0.

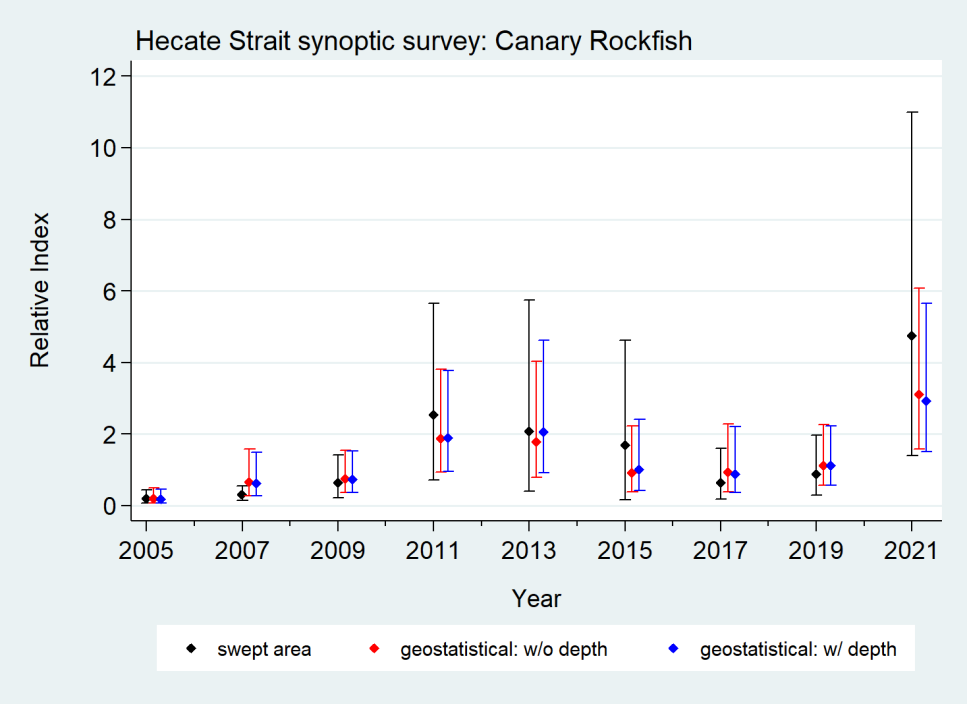

Figure B.73. Comparison of HS synoptic survey Canary Rockfish biomass indices estimated using three different procedures: a) the swept area method described in Section B.2; b) geostatistical model (Anderson et al. 2019) without including depth; c) geostatistical model which includes depth. All series have been standardised to a geometric mean of 1.0.

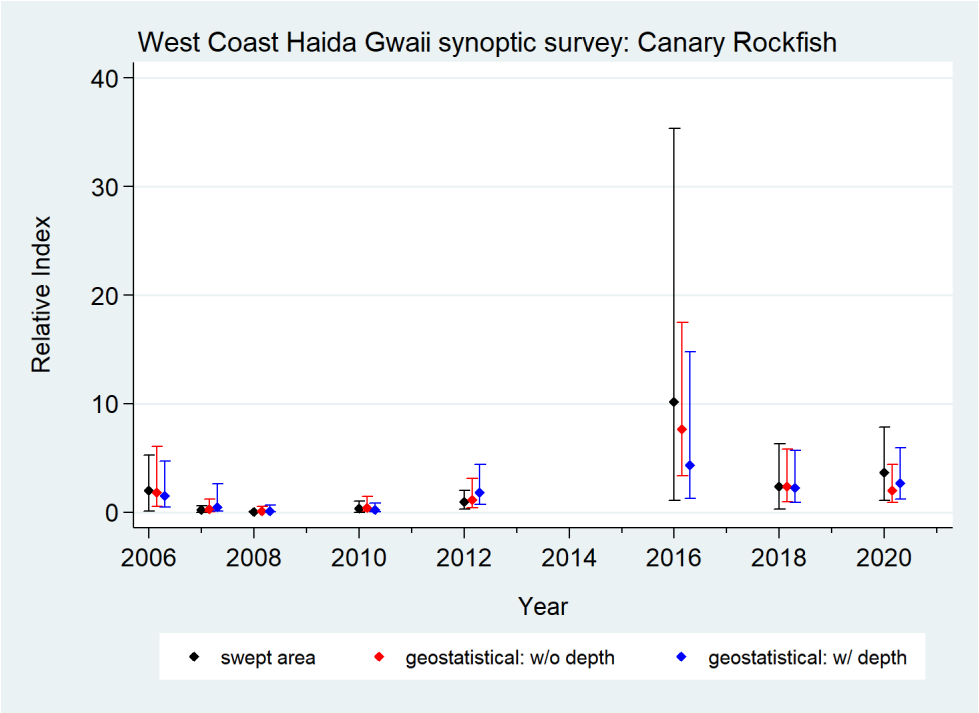

Figure B.74. Comparison of WCHG synoptic survey Canary Rockfish biomass indices estimated using three different procedures: a) the swept area method described in Section B.2; b) geostatistical model (Anderson et al. 2019) without including depth; c) geostatistical model which includes depth. All series have been standardised to a geometric mean of 1.0.

B.10. HARD BOTTOM LONGLINE SURVEYS

The Hard Bottom Longline (HBLL) outside (excluding PMFC area 4B) surveys are depth-stratified, random-design research longline surveys conducted with chartered commercial fishing vessels which employ standardised longline gear and fishing methods and alternate annually between the northern and southern portions of BC. These surveys provide catch rates and biological samples of rockfish from the outside coastal waters of BC which are meant to be complementary to the synoptic trawl surveys by covering habitat that is not available to trawl gear (Figure B.75) (Doherty et al. 2019). Code to extract CAR survey index series was provided (D. Haggarty, DFO, pers. comm., April 11, 2022) for inclusion in the stock assessment in a sensitivity analysis. The code included an algorithm for hook competition adjustment which produced estimates of fish density (pieces per km^2) which could be used along with stratum areas to bootstrap relative abundance.

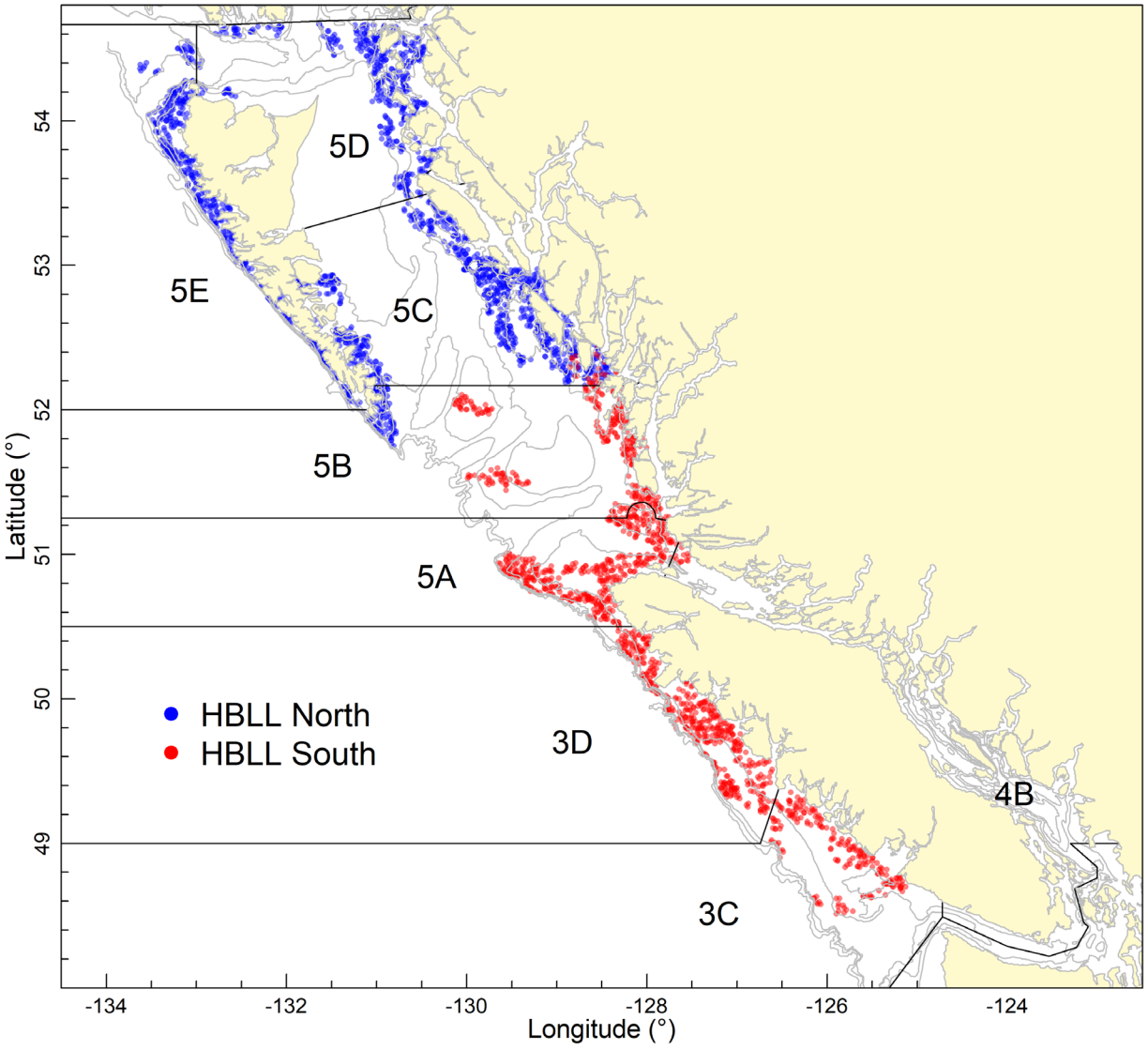

Figure B.75. Extent of the coverage by the North and South Hard Bottom longline surveys.

These survey indices show relatively little contrast with no overall trend (Figure B.76; Table B.21). However, survey relative errors are low compared to the synoptic trawl survey indices, ranging from 0.15 to 0.32 across the two surveys (Table B.21). Although CAR is not often reported commercially from longline gear, the proportion of sets which capture CAR in this survey is higher than the comparable synoptic survey (Figure B.77), with 35% of the sets in the North capturing CAR (over eight surveys) and 44% in the South (over seven surveys) capturing this species. The equivalent values for the synoptic surveys are: HS (11%), QCS (20%) WCVI (37%). The age composition of the CAR catch from these surveys is presented in Figure D.14, showing fewer older CAR than in the WCVI or QCS surveys which may point to this survey sampling mostly juvenile and early adult individuals.

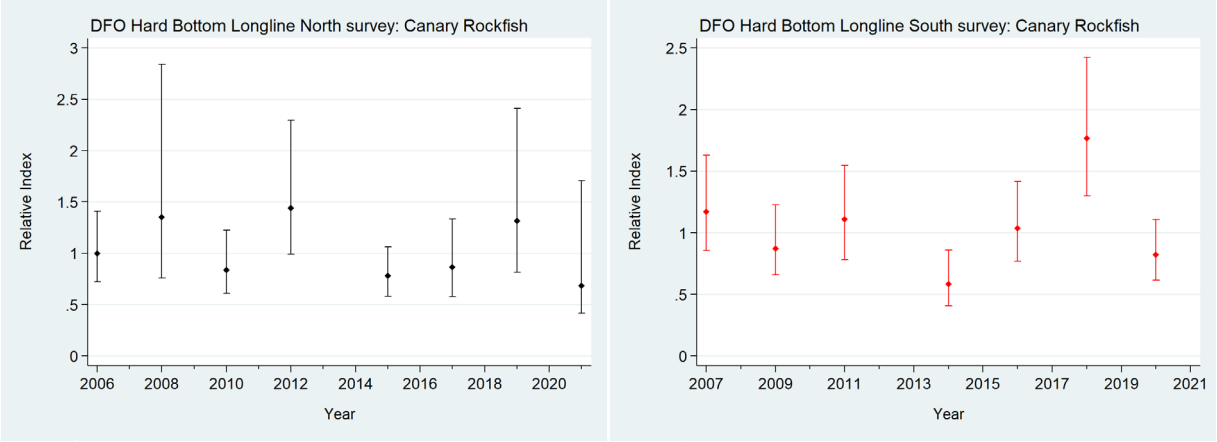

Figure B.76. Biomass estimates for Canary Rockfish from the two Hard Bottom Longline surveys with 95% error bars estimated from bootstrap random draws with replacement. Each series has been normalised to a geometric mean=1.0.

Table B.21. Biomass estimates for Canary Rockfish from the two Hard Bottom Longline surveys with 95% confidence bounds based on the bootstrap distribution of biomass estimates.

Survey	Year	Biomass (Eq. B.4)	Mean bootstrap biomass	Lower bound biomass	Upper bound biomass	CV bootstrap	CV Analytic (Eq. B.6)
HBLL North	2006	6,634.6	6,629.2	4,793.1	9,377.4	0.169	0.170
	2008	9,012.2	8,986.9	5,041.9	18,908.9	0.322	0.329
	2010	5,569.2	5,552.3	4,053.8	8,157.7	0.182	0.183
	2012	9,598.5	9,646.9	6,595.6	15,269.7	0.223	0.222
	2015	5,201.9	5,199.9	3,871.4	7,080.7	0.153	0.151
	2017	5,764.8	5,781.2	3,834.3	8,856.9	0.209	0.209
	2019	8,759.6	8,862.2	5,427.1	16,037.7	0.270	0.294
	2021	4,572.7	4,507.2	2,769.8	11,352.6	0.325	0.328
HBLL South	2007	7,970.7	8,071.6	5,814.5	11,083.7	0.165	0.168
	2009	5,935.1	5,854.6	4,469.3	8,364.2	0.163	0.167
	2011	7,561.8	7,593.3	5,332.7	10,510.8	0.167	0.167
	2014	3,973.8	3,930.8	2,758.8	5,845.5	0.193	0.188
	2016	7,059.1	7,049.6	5,228.8	9,637.2	0.154	0.154
	2018	12,022.0	12,044.6	8,835.1	16,496.6	0.151	0.151
	2020	5,588.0	5,568.7	4,184.1	7,542.4	0.152	0.154

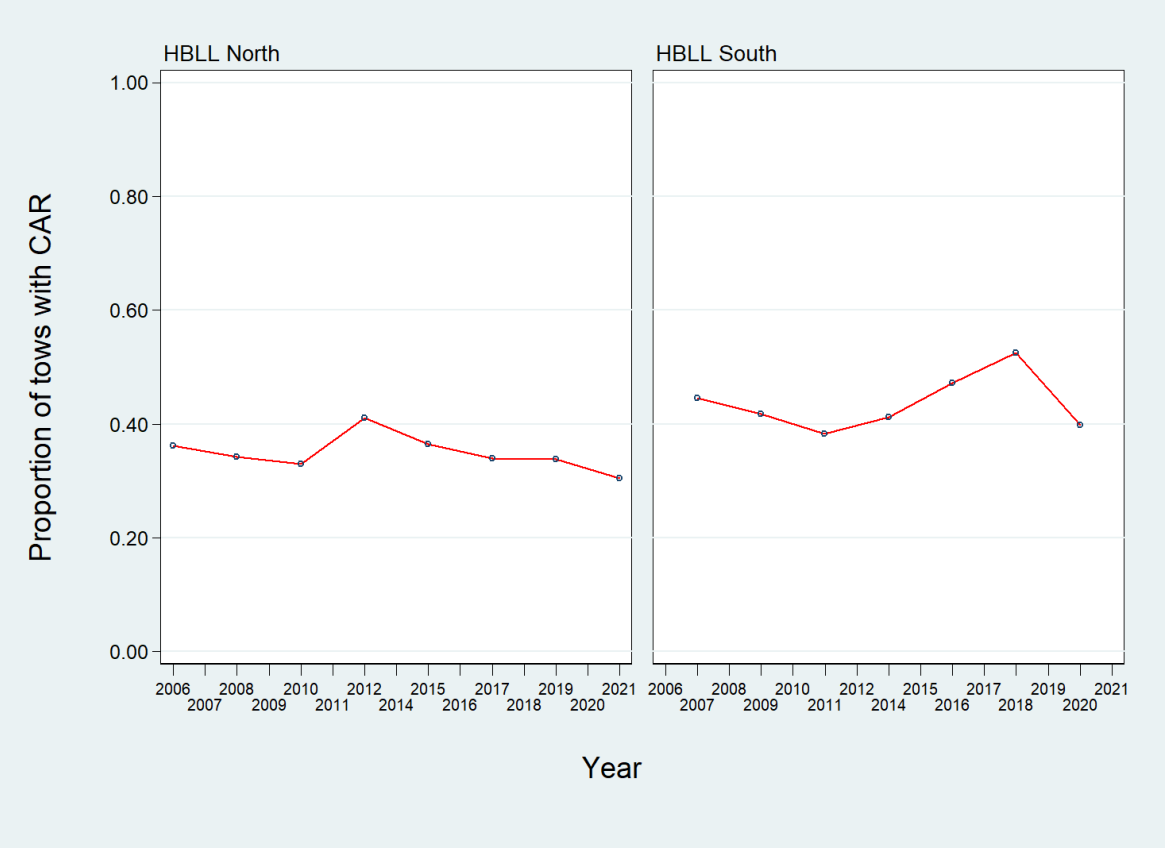

Figure B.77. Proportion of tows by year which contain Canary Rockfish from the two Hard Bottom Longline surveys over the period 2006 to 2021.

B.11. REFERENCES – SURVEYS

Anderson, S.C., Keppel, E.A. and Edwards, A.M. 2019. A reproducible data synopsis for over 100 species of British Columbia groundfish. DFO Can. Sci. Advis. Sec. Res. Doc. 2019/041. vii + 321 p.

DFO. 2015. Proceedings of the Pacific regional peer review on Stock assessment for Yellowtail Rockfish (*Sebastes flavidus*) in British Columbia; November 18-19, 2014. DFO Can. Sci. Advis. Sec. Proceed. Ser. 2015/020.

Doherty, B., Benson, A.J., and Cox, S.P. 2019. Data summary and review of the PHMA hard bottom longline survey in British Columbia after the first 10 years (2006-2016). Can. Tech. Rep. Fish. Aquat. Sci. 3276: ix + 75 p.

Edwards, A.M., Haigh, R. and Starr, P.J. 2014. Pacific Ocean Perch (*Sebastes alutus*) stock assessment for the west coast of Vancouver Island, British Columbia. DFO Can. Sci. Advis. Sec. Res. Doc. 2013/093: vi + 135 pp.

Edwards, A.M., Starr, P.J. and Haigh, R. 2012. Stock assessment for Pacific ocean perch (*Sebastes alutus*) in Queen Charlotte Sound, British Columbia. DFO Can. Sci. Advis. Sec. Res. Doc. 2011/111: viii + 172 pp.

Efron, B. 1982. The Jackknife, the Bootstrap and Other Resampling Plans. No. 38 in CBMS-NSF Regional Conference Series in Applied Mathematics. Society for Industrial and Applied Mathematics.

Harling, W.R. and Davenport, D. 1977. *G.B. Reed* Groundfish Cruise No. 77-3 August 22 to September 8, 1977. Fish. Mar. Serv. Data Rep. 42: iii + 46 pp.

Harling, W.R., Davenport, D., Smith, H.S., Wowchuk, R.H. and Westrheim, S.J. 1971. *G.B. Reed* Groundfish Cruise No. 71-3, October 1-29, 1971. Fish. Res. Board Can. Tech. Rep. 290: 35 pp.

Harling, W.R., Davenport, D., Smith, M.S., Phillips, A.C. and Westrheim, S.J. 1973. *G.B. Reed* Groundfish Cruise No. 73-2, September 5-25, 1973. Fish. Res. Board Can. Tech. Rep. 424: 37 pp.

Nagtegaal, D.A. and Farlinger, S.P. 1980. Catches and trawl locations of the M/V *Southward Ho* during a rockfish exploration and assessment cruise to Queen Charlotte Sound, September 7-27, 1979. Can. Data Rep. Fish. Aquat. Sci. 216: iii + 95 pp.

Nagtegaal, D.A., Leaman, B.M. and Stanley, R.D. 1986. Catches and trawl locations of R/V *G.B. Reed* and M/V *Eastward Ho* during the Pacific Ocean Perch assessment cruise to Queen Charlotte Sound, August-September, 1984. Can. Data Rep. Fish. Aquat. Sci. 611: iii + 109 pp.

Olsen, N., Rutherford, K.L. and Stanley, R.D. 2008. West Coast Queen Charlotte Islands groundfish bottom trawl survey, August 25th to September 21st , 2008. Can. Manuscr. Rep. Fish. Aquat. Sci. 2858: vii + 50 pp.

Westrheim, S.J. 1966a. Report on the trawling operations of the Canadian Research Vessel *G.B. Reed* from Queen Charlotte Sound, British Columbia to Cape Spencer, Alaska, August 23 to September 7, 1965. Fish. Res. Board Can. Manuscr. Rep. 890: 27 pp.

Westrheim, S.J. 1966b. Report on the trawling operations of the Canadian Research Vessel *G.B. Reed* from Queen Charlotte Sound, British Columbia to Sitka Sound, Alaska, August 24 to September 15, 1966. Fish. Res. Board Can. Manuscr. Rep. 891: 27 pp.

Westrheim, S.J. 1967a. Report on the trawling operations of the Canadian Research Vessel *G.B. Reed* off British Columbia and Southeastern Alaska, September 6 - October 4, 1967. Fish. Res. Board Can. Manuscr. Rep. 934: 8 pp.

Westrheim, S.J. 1967b. *G.B. Reed* groundfish cruise reports, 1963-66. Fish. Res. Board Can. Tech. Rep. 30: ii + 286 pp.

Westrheim, S.J. 1969. Report of the trawling operations of the Canadian Research Vessel *G.B. Reed* off British Columbia, September 1969. Fish. Res. Board Can. Manuscr. Rep. 1063: 6 pp.

Westrheim, S.J., Harling, W.R. and Davenport, D. 1968. *G.B. Reed* Groundfish Cruise No. 67-2, September 6 to October 4, 1967. Fish. Res. Board Can. Tech. Rep. 46: 45 pp.

Westrheim, S.J., Leaman, B.M., Harling, W.R., Davenport, D., Smith, M.S. and Wowchuk, R.M. 1976. *G.B. Reed* Groundfish Cruise No. 76-3, September 8-27, 1976. Fish. Mar. Serv. Data Rec. 21: 47 pp.

Workman, G.D., Olsen, N. and Rutherford, K.L. 2007. West Coast Queen Charlotte Islands groundfish bottom trawl survey, August 28th to September 25th , 2006. Can. Manuscr. Rep. Fish. Aquat. Sci. 2804: vii + 44 pp.

Yamanaka, K.L., Richards, L.J. and Workman, G.D. 1996. Bottom trawl survey for rockfish in Queen Charlotte Sound, September 11 to 22, 1995. Can. Manuscr. Rep. Fish. Aquat. Sci. 2362: iv + 116 pp.

APPENDIX C. COMMERCIAL TRAWL CPUE

C.1. INTRODUCTION

Commercial catch and effort data have been used to generate indices of abundance in several ways. The simplest indices are derived from the arithmetic mean or geometric mean of catch divided by an appropriate measure of effort (Catch Per Unit Effort or CPUE) but such indices make no adjustments for changes in fishing practices or other non-abundance factors that may affect catch rates. Consequently, methods to standardise changes to vessel configuration, the timing or location of catch and other possible effects have been developed to remove potential biases to CPUE that may result from such changes. In these models, abundance is represented as a "year effect" and the dependent variable is either an explicitly calculated CPUE represented as catch divided by effort, or an implicit CPUE represented as catch per tow or catch per record. In the latter case, additional effort terms can be offered as explanatory variables, allowing the model to select the effort term with the greatest explanatory power. It is always preferable to standardise for as many factors as possible when using CPUE as a proxy for abundance. Unfortunately, it is often not possible to adjust for factors that might affect the behaviour of fishers, particularly economic factors, resulting in indices that may not entirely reflect the underlying stock abundance.

C.2. METHODS

C.2.1. Arithmetic and Unstandardised CPUE

Arithmetic and unstandardised CPUE indices provide potential measures of relative abundance, but are generally considered unreliable because they fail to take into account changes in the fishery, including spatial and temporal changes as well as behavioural and gear changes. They are frequently calculated because they provide a measure of the overall effect of the standardisation procedure.

Arithmetic CPUE (Eq. C.1) in year y was calculated as the total catch for the year divided by the total effort in the year using Eq. C.1:

Eq. C.1 $$\hat{A}_y = \sum_{i=1}^{n_y} C_{i,y} \Big/ \sum_{i=1}^{n_y} E_{i,y}$$

where $C_{i,y}$ is the field name `[catch]` and $E_{i,y}$ is the field name `[tows]` or `[hours_fished]` in the data object for record i in year y; n_y is the number of records in year y.

Unstandardised (geometric) CPUE assumes a log-normal error distribution. An unstandardised index of CPUE (Eq. C.2) in year y was calculated as the geometric mean of the ratio of catch to effort for each i in year y, using Eq. C.2:

Eq. C.2 $$\hat{G}_y = \exp\left[\frac{1}{n_y}\sum_{i=1}^{n_y}\ln\left(\frac{C_{i,y}}{E_{i,y}}\right)\right].$$

C.2.2. Standardised CPUE

These models are preferred over the unstandardised models described above because they can account for changes in fishing behaviour and other factors which may affect the estimated abundance trend, as long as the models are provided with adequate data. In the models described below, catch per record is used as the dependent variable and the associated effort is treated as an explanatory variable.

C.2.2.1. Lognormal Model

Standardised CPUE often assumes a lognormal error distribution, with explanatory variables used to represent changes in the fishery. A standardised CPUE index (Eq. C.3) is calculated from a generalised linear model (GLM) (Quinn and Deriso 1999) using a range of explanatory variables including `[Year]`, `[month]`, `[depth]`, `[vessel]` and other available factors:

Eq. C.3 $$\ln\left(I_i\right) = B + Y_{y_i} + \alpha_{a_i} + \beta_{b_i} + ... + f\left(\chi_i\right) + f\left(\delta_i\right) + ... + \varepsilon_i$$

where I_i = C_i or catch;

B = the intercept;

Y_{y_i} = year coefficient for the year corresponding to record i;

α_{a_i} and β_{b_i} = coefficients for factorial variables a and b corresponding to record i;

$f\left(\chi_i\right)$ and $f\left(\delta_i\right)$ are polynomial functions (to the 3rd order) of the continuous variables χ_i and δ_i corresponding to record i;

ε_i = an error term.

The actual number of factorial and continuous explanatory variables in each model depends on the model selection criteria and the nature of the data. Because each record represents a single tow, $C_{i,y}$ has an implicit associated effort of one tow. Hours fished for the tow is represented on the right-hand side of the equation as a continuous (polynomial) variable.

Note that calculating standardised CPUE with Eq. C.3, while assuming a lognormal distribution and without additional explanatory variables, is equivalent to using Eq. C.2 as long as the same definition for $E_{i,y}$ is used.

Canonical coefficients and standard errors were calculated for each categorical variable (Francis 1999). Standardised analyses typically set one of the coefficients to 1.0 without an error term and estimate the remaining coefficients and the associated error relative to the fixed coefficient. This is required because of parameter confounding. The Francis (1999) procedure rescales all coefficients so that the geometric mean of the coefficients is equal to 1.0 and calculates a standard error for each coefficient, including the fixed coefficient.

Coefficient-distribution-influence (CDI) plots are visual tools to facilitate understanding of patterns which may exist in the combination of coefficient values, distributional changes, and annual influence (Bentley et al. 2012). CDI plots were used to illustrate each explanatory variable added to the model.

C.2.2.2. Binomial Logit Model

The procedure described by Eq. C.3 is necessarily confined to the positive catch observations in the data set because the logarithm of zero is undefined. Observations with zero catch were modelled by fitting a logit regression model based on a binomial distribution and using the

presence/absence of the species being modelled as the dependent variable (where 1 is substituted for ln(I_i) in Eq. C.3 if it is a successful catch record and 0 if it is not successful) and using the same data set. Explanatory factors are estimated in the model in the same manner as described in Eq. C.3. Such a model provides an alternative series of standardised coefficients of relative annual changes that is analogous to the series estimated from the lognormal regression.

C.2.2.3. Combined Model

A combined model (sometimes termed a "hurdle" model), integrating the two sets of relative annual changes estimated by the lognormal and binomial models, can be estimated using the delta distribution, which allows zero and positive observations (Fletcher et al. 2005). Such a model provides a single index of abundance which integrates the signals from the positive (lognormal) and binomial series.

This approach uses the following equation to calculate an index based on the two contributing indices, after standardising each series to a geometric mean=1.0:

Eq. C.4 $$ {}^{C}Y_{y} = {}^{L}Y_{y}\,{}^{B}Y_{y} $$

where ${}^{C}Y_{y}$ = combined index for year y,

${}^{L}Y_{y}$ = lognormal index for year y,

${}^{B}Y_{y}$ = binomial index for year y

Francis (2001) suggests that a bootstrap procedure is the appropriate way to estimate the variability of the combined index. Therefore, confidence bounds for the combined model were estimated using a bootstrap procedure based on 100 replicates, drawn with replacement, operated by re-estimating each component model and then repeating Eq. C.4 for each bootstrap replicate.

The index series plots below present normalised values, i.e., each series is divided by its geometric mean so that the series is centred on 1. This facilitates comparison among series.

C.3. PRELIMINARY INSPECTION OF THE DATA

The analyses reported in this Appendix are based on tow-by-tow total catch (landings + discards) data collected over the period 1996–2021 for which detailed positional data for every tow are available. Each tow has an estimate of retained and discarded catch because of the presence of an observer on board the vessel[1]. These data are held in the DFO PacHarvTrawl (PacHarvest) and GFFOS databases (Fisheries and Oceans Canada, Pacific Region, Groundfish Data Unit).

[1] The observer programme was suspended after March 2020 because of COVID-19 restrictions and lack of available personnel. From April 2020, the observer programme was replaced by an electronic monitoring (EM) programme whereby all tows were video recorded with high definition cameras. Operators provided estimates of catch and discard by species and every trip was subject to an audit of at least 10% of tows (randomly selected) which checked these estimates. Note that total landings by species continued to be monitored at dockside. From late 2019, all discards of rockfish species at sea have been prohibited.

Tow-by-tow catch and effort data for Canary Rockfish (CAR) from the BC trawl fishery operating from Juan de Fuca Strait to the Dixon Entrance from 1996 to 2021 were selected using the following criteria:

- Tow start date between 1 January 1996 and 31 December 2021;
- Bottom trawl type (includes 'unknown' trawl gear);
- Fished in PMFC regions: 3C, 3D, 5A, 5B, 5C, 5D or 5E;
- Fishing success code <=1 (code 0= unknown; code 1= useable);
- Catch of at least one fish or invertebrate species (no water hauls or inanimate object tows);
- Valid depth field;
- Valid latitude and longitude co-ordinates;
- Valid estimate of time towed that was > 0 hours and <= 6 hours.

Each record represented a single tow, which resulted in equivalency between the number of records and number of tows. Catch per record can therefore be used to represent CPUE because each record (tow) has an implicit effort component.

The catch and effort data for CAR were treated as a single area (BC) representing all catch outside of the Strait of Georgia, upper Johnstone Strait and Juan de Fuca Strait, based on the declared distribution of trawl catches (see Appendix A). Only bottom trawl data were used as this is by far the most prevalent capture method for this species. Figure C.1 plots the distribution of depth for all successful CAR bottom trawl tows in the designated region. A depth range for this analysis was selected from this plot and is summarised in Table C.1.

Table C.1. Depth bins used in CPUE analyses of stock by gear.

Analysis	Trawl Gear	First year	Depth range (m)	Upper bound effort (h)	Minimum bin + records	N depth bins	N latitude bins	N locality bins
BC (3CD5ABCDE)	Bottom trawl[1]	1996	50–350	6	140	12	46	40

[1] codes used: gear==0|1|17|18 or gear==unknown

Vessel qualification criteria for the bottom trawl fisheries were based on number of trips per year and number of years fishing to avoid including vessels which only occasionally captured CAR. The vessel qualification criteria used in this analysis appear in Table C.2 and the distribution of tows by vessel and year is presented in Figure C.2. Once a vessel was selected, all data for the qualifying vessel were included, regardless of the number of trips in a year. Table C.2 shows the number of vessels used in this analysis and the fraction (93%) of the total catch represented in the core fleet. There was good vessel overlap across years (Figure C.2) in the fishery, where 26 of the 46 core vessels participated in the fishery for at least 20 years of the analysis.

Table C.2. Vessel qualification criteria used in CPUE analyses of stock by gear.

		Vessel selection criteria				Data set characteristics			
Analysis	Trawl Gear	N years	N trips	Minimum positive Records	N vessels	% total catch[1]	catch (t)	Total records	Positive records
BC (3CD5ABCDE)	Bottom	5	10	140	46	93	15,426	135,702	66,335

[1] total catch calculated with all filters applied except for the vessel and depth restrictions

Table C.3 reports the explanatory variables offered to the model, based on the tow-by-tow information in each record, with the number of available categories varying as indicated in Table C.1, Table C.2 and Table C.3. Table C.4 summarises the core vessel data used in the analysis by calendar year, including the number of records (tows), the total hours fished and the associated CAR catch. This table also tracks the annual proportion of tows which did not report CAR.

Table C.3. Explanatory variables offered to the CPUE model, based on the tow-by-tow information.

Variable	Data type
Year	26 categories (calendar years)
Hours fished	continuous: 3rd order polynomial
Month	12 categories
DFO locality	Fishing locality areas identified by Rutherford (1999) (includes a final aggregated category, Table C.1)
Latitude	Latitude aggregated by 0.1° bands starting at 48°N (includes a final aggregated category, Table C.1)
Vessel	See Table C.2 for number of categories by analysis (no final aggregated category)
Depth	See Table C.1 for number of categories by analysis (no final aggregated category)
PFMC major area	7 categories: PMFC areas 3C, 3D, 5A, 5B, 5C, 5D, 5E

Table C.4. Summary data for the CAR bottom trawl fishery in BC (3CD5ABCDE) by year for the core data set (after applying all data filters and selection of core vessels).

Year	Number vessels[1]	Number trips[1]	Number tows[1]	Number records[1]	Number records[2]	% zero records[2]	Total catch (t)	Total hours[1]	CPUE (kg/h) (Eq. C 1)
1996	44	311	1,380	1,380	5,958	76.8	172.4	2,682	64.3
1997	43	419	2,166	2,166	7,826	72.3	344.5	4,290	80.3
1998	40	506	2,665	2,665	8,896	70.0	538.5	5,591	96.3
1999	41	558	3,153	3,153	10,152	68.9	589.3	6,928	85.1
2000	42	619	3,130	3,130	12,190	74.3	463.2	6,131	75.5
2001	42	604	2,971	2,971	10,377	71.4	759.2	5,615	135.2
2002	41	648	3,483	3,483	12,117	71.3	725.9	6,704	108.3
2003	40	673	3,586	3,586	11,528	68.9	755.5	6,808	111.0
2004	41	656	3,371	3,371	10,996	69.3	653.6	6,067	107.7
2005	41	730	4,170	4,170	11,438	63.5	695.4	8,162	85.2
2006	38	588	3,179	3,179	9,386	66.1	754.9	6,262	120.5
2007	37	493	3,072	3,072	8,280	62.9	587.8	6,107	96.2
2008	35	456	2,700	2,700	6,868	60.7	584.5	5,250	111.3
2009	35	466	2,545	2,545	7,959	68.0	566.6	4,849	116.8
2010	34	454	2,606	2,606	7,900	67.0	581.5	5,218	111.4
2011	35	473	2,505	2,505	7,848	68.1	610.3	4,998	122.1
2012	35	420	2,349	2,349	7,118	67.0	628.2	4,543	138.3
2013	30	409	2,075	2,075	6,834	69.6	681.3	3,995	170.5
2014	30	407	2,338	2,338	5,817	59.8	724.6	4,606	157.3
2015	29	412	2,643	2,643	6,020	56.1	700.1	5,188	134.9
2016	25	390	2,363	2,363	5,430	56.5	597.7	4,710	126.9
2017	27	419	2,433	2,433	5,326	54.3	662.6	4,739	139.8
2018	23	313	2,122	2,122	4,502	52.9	615.5	4,031	152.7
2019	19	288	1,451	1,451	4,162	65.1	431.9	2,603	165.9
2020	22	197	990	990	3,442	71.2	601.2	1,696	354.5
2021	19	223	889	889	3,667	75.8	400.5	1,693	236.6

[1] calculated for tows with CAR catch >0; [2] calculated for all tows

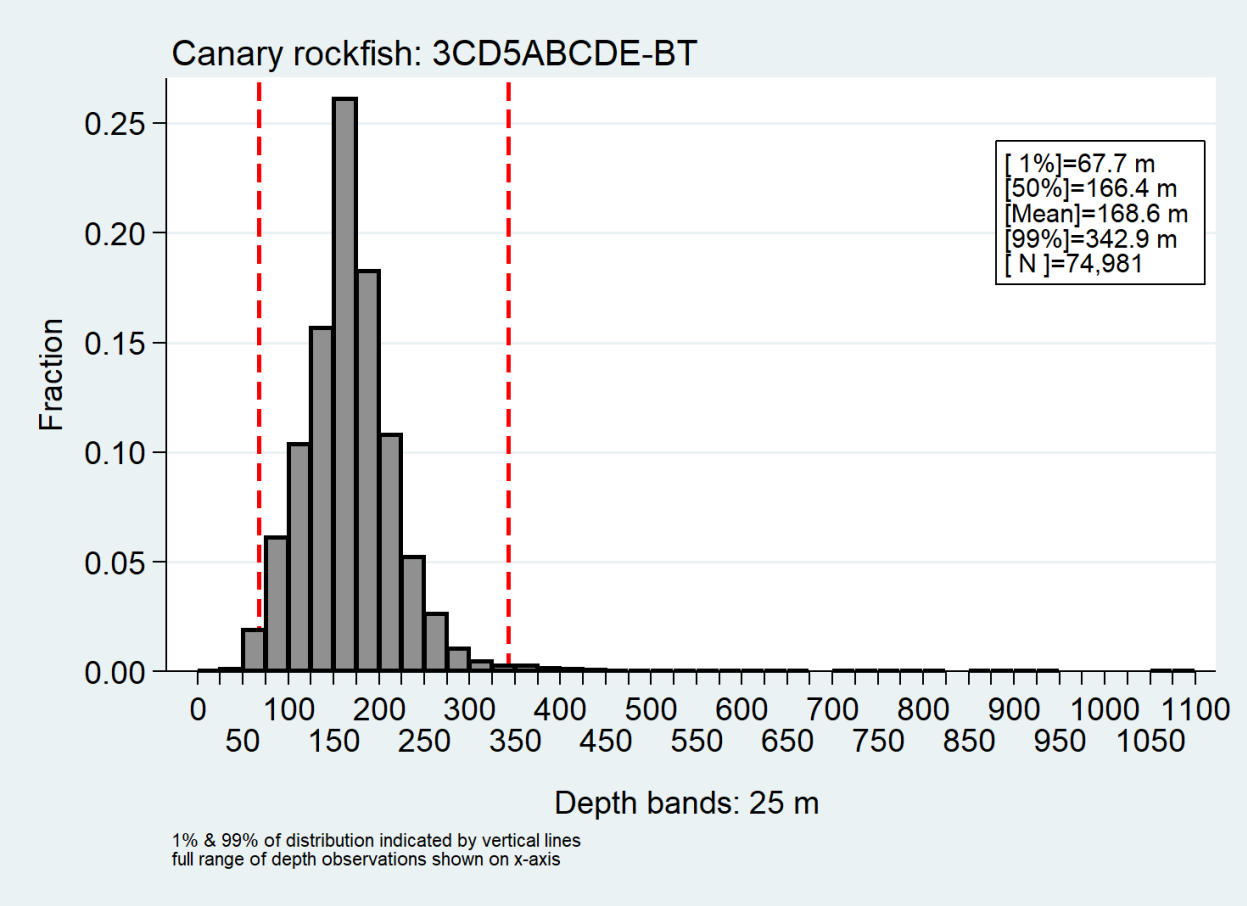

Figure C.1. Depth distribution of tows capturing CAR for the BC (3CD5ABCDE) bottom trawl (BT) GLM analyses from 1996 to 2021 using 25 m intervals (each bin is labelled with the upper bound of the interval). Vertical lines indicate the 1% and 99% percentiles.

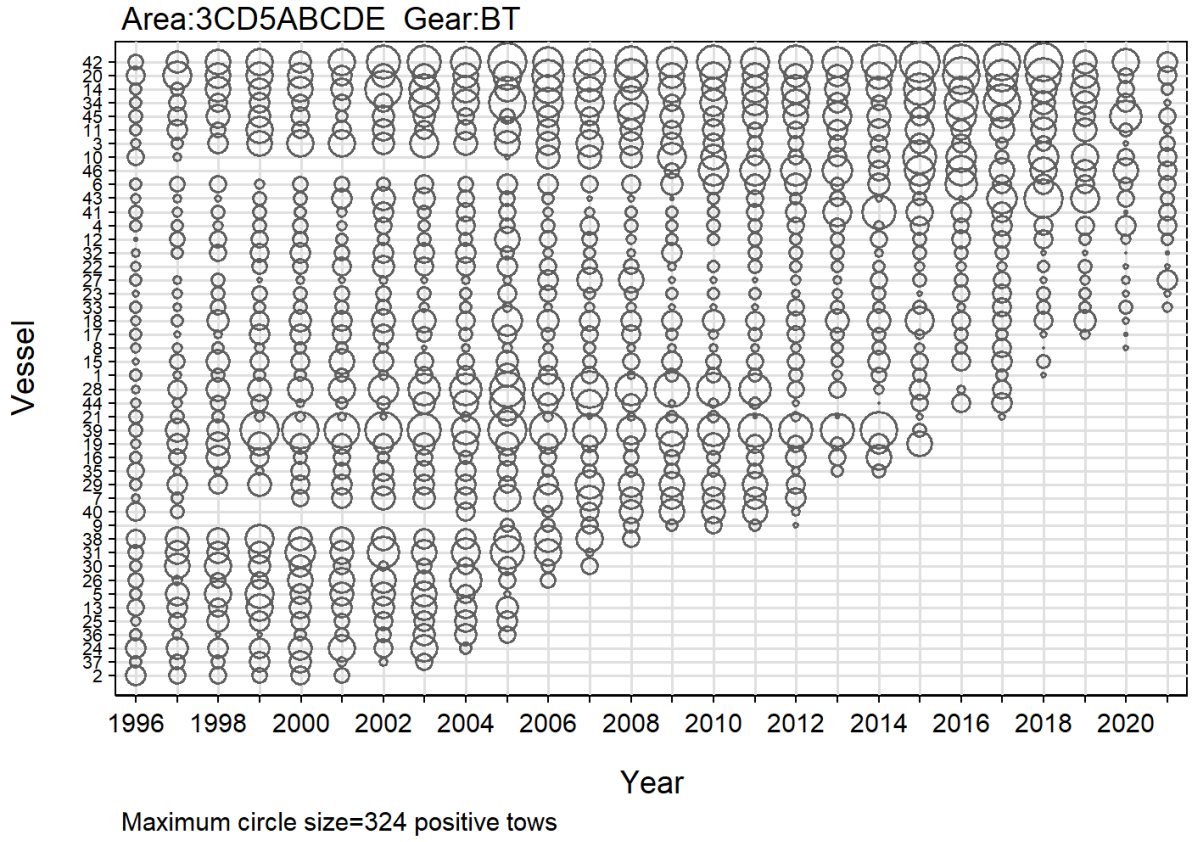

Figure C.2. Bubble plot showing vessel participation (number positive tows) by the core fleet in the BC (3CD5ABCDE) BT GLM analyses. Vessels are coded in ascending order total effort by year.

C.4. RESULTS

C.4.1. Coastwide BC (3CD5ABCDE)

C.4.1.1. Bottom trawl fishery: positive lognormal model

A standardised lognormal General Linear Model (GLM) analysis was performed on positive catch records from the bottom trawl tow-by-tow data set generated as described in Section C.3. Eight explanatory variables (Table C.3) were offered to the model and `ln(catch)` was used as the dependent variable, where catch is the total by weight of landed plus discarded CAR in each record (tow) (Eq. C.3). The resulting CPUE index series is presented in Figure C.3.

The `[Year]` categorical variable was forced to be the first variable in the model without regard to its effect on the model deviance. The remaining seven variables were offered sequentially, with the stepwise acceptance of the remaining variables with the best AIC. This process was continued until the improvement in the model R^2 was less than 1% (Table C.5). This model selected four of the seven remaining explanatory variables, including `[DFO locality]`, `[Depth]`, `[0.1°Latitude_bands]`, and `[Vessel]` in addition to `[Year]`. The final lognormal model accounted for 29% of the total model deviance (Table C.5), with the year variable explaining 1.1% of the model deviance.

Model residuals showed a satisfactory fit to the underlying lognormal distributional assumption, with only some skewness in the body of the distribution and few deviations in the tails outside of +/- 2 standard errors (Figure C.4).

A stepwise plot showing the effect on the year indices as each explanatory variable was introduced into the model shows that the standardisation procedure made downward adjustments to the unstandardised series in the final two years of the series and a small upward adjustment in 1999 with the introduction of the [DFO locality] variable (Figure C.5). Further downward adjustments occurred with the introduction of the [vessel] variable. Apart from these adjustments, the standardisation procedure had little impact on the initial series.

*Table C.5. Order of acceptance of variables into the lognormal model of positive total mortalities (verified landings plus discards) of CAR BC (3CD5ABCDE) bottom trawl fishery with the amount of explained deviance (R^2) for each variable. Variables accepted into the model are identified in bold with an *. [Year] was forced as the first variable.*

Variable	1	2	3	4	5	6
Year*	**0.0113**	–	–	–	–	–
DFO locality*	0.1690	**0.1789**	–	–	–	–
Depth bands*	0.1403	0.1508	**0.2538**	–	–	–
0.1° Latitude bands*	0.1614	0.1726	0.2157	**0.2767**	–	–
Vessel*	0.0426	0.0509	0.1988	0.2719	**0.2937**	–
PFMC major area	0.1086	0.1200	0.1942	0.2691	0.2848	0.3022
Hours fished	0.0048	0.0159	0.1797	0.2553	0.2788	0.2946
Month	0.0157	0.0262	0.1816	0.2572	0.2795	0.2956
Improvement in deviance	0.0000	0.1676	0.0749	0.0229	0.0170	0.0084

CDI plots of the four explanatory variables introduced to the model in addition to [Year] show impacts in final two years of the series with very little adjustment to the unstandardised series in the remaining years (Figure C.5). CDI plots are presented for the successive variables [DFO locality] (Figure C.6), [Depth_bands] (Figure C.7), [0.1°Latitude_bands] (Figure C.8), and [vessel] (Figure C.9).

The lognormal year indices show almost no trend from the beginning of the series to 2019, followed by a sharp uptick in the final two years of the series (Figure C.3). It is notable that this increase remains in the series in spite of the standardisation effect which severely downgraded this increase. This model has reasonable diagnostics and the changes from the unstandardised series in 2020 and 2021 result from the preponderance of high catch rate [DFO locality] as well as the presence of [vessel] with high catch rate coefficients.

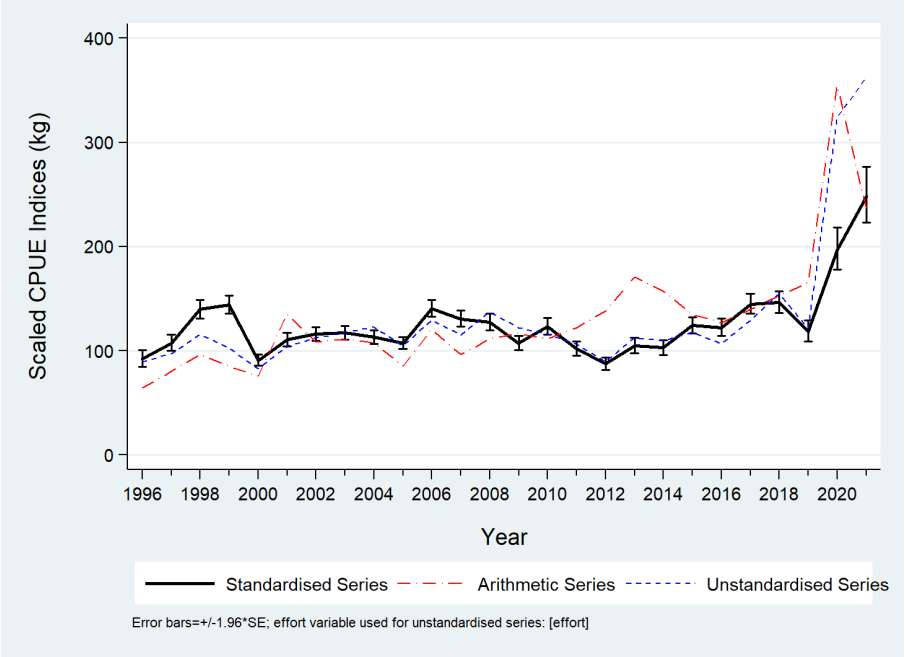

Figure C.3. Three positive catch CPUE series for CAR from 1996 to 2021 in the BC (3CD5ABCDE) bottom trawl fishery. The solid line is the standardised CPUE series from the lognormal model (Eq. C.3). The arithmetic series (Eq. C.1) and the unstandardised series (Eq. C.2) are also presented. All three series have been scaled to same geometric mean.

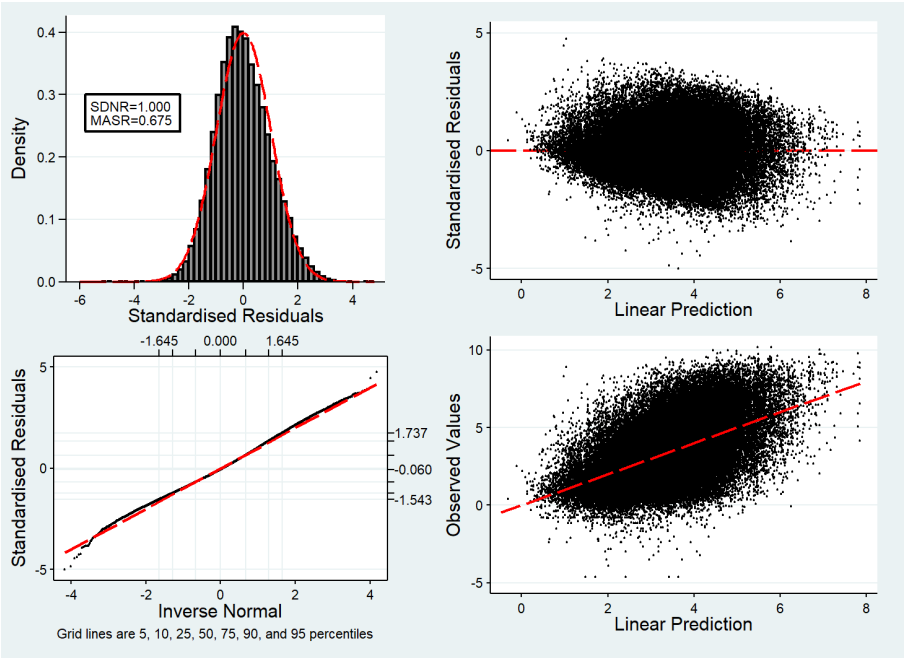

Figure C.4. Residual diagnostic plots for the GLM lognormal analysis for CAR in BC (3CD5ABCDE) bottom trawl fishery. Upper left: histogram of the standardised residuals with overlaid lognormal distribution (SDNR = standard deviation of normalised residuals. MASR = median of absolute standardised residuals). Lower left: Q-Q plot of the standardised residuals with the outside horizontal and vertical lines representing the 5th and 95th percentiles of the theoretical and observed distributions. Upper right: standardised residuals plotted against the predicted CPUE. Lower right: observed CPUE plotted against the predicted CPUE.

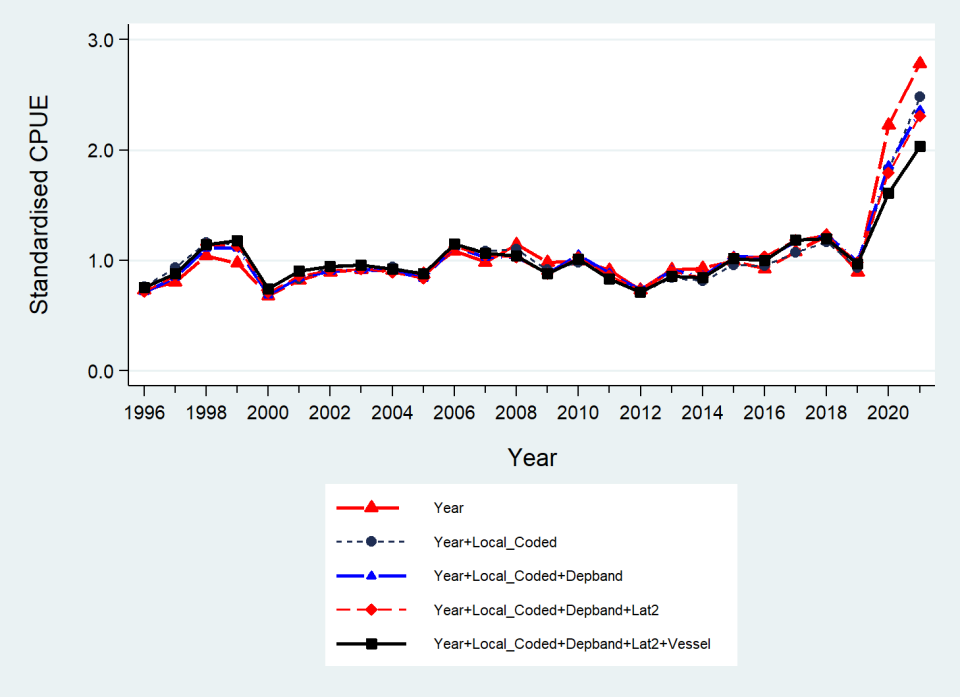

Figure C.5. Plot showing the year coefficients after adding each successive term of the standardised lognormal regression analysis for CAR in the BC (3CD5ABCDE) bottom trawl fishery. The final model is shown with a thick solid black line. Each line has been scaled so that the geometric mean equals 1.0.

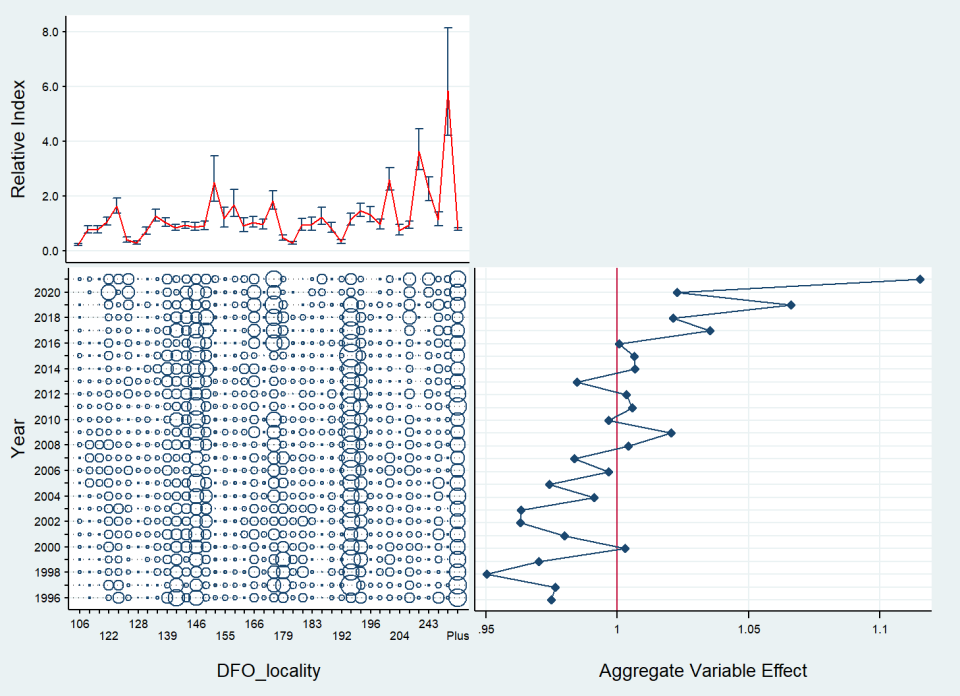

Figure C.6. CDI plot showing the effect of introducing the categorical variable [DFO locality] to the lognormal regression model for CAR in the BC (3CD5ABCDE) bottom trawl fishery. Table C.6 provides the definitions for the coded values used for each locality in the above plot. Each plot consists of subplots showing the effect by level of variable (top left), the relative distribution by year of variable records (bottom left), and the cumulative effect of variable by year (bottom right).

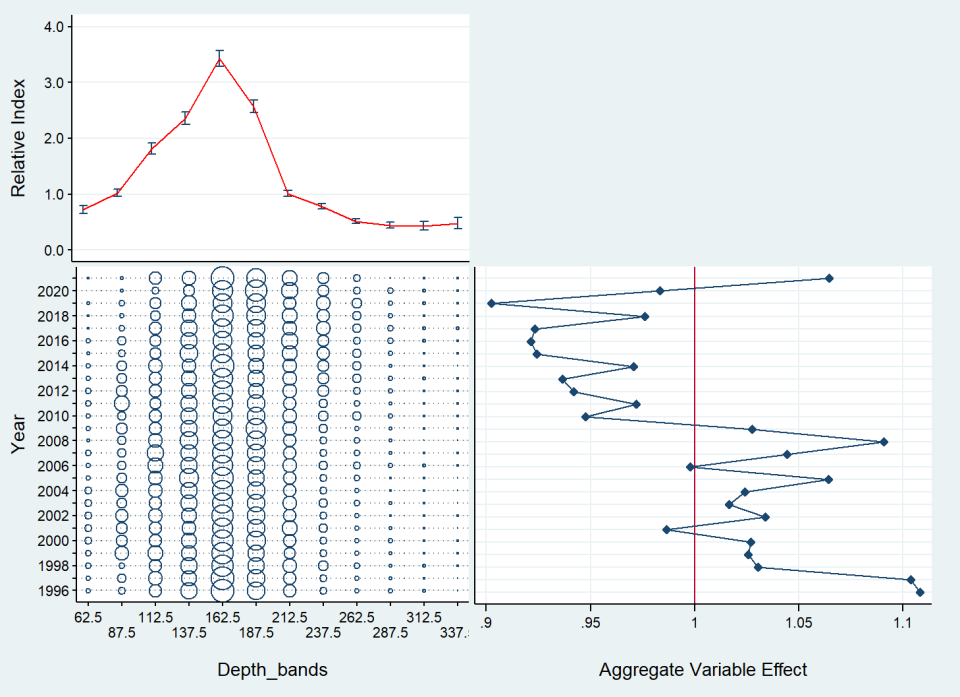

Figure C.7. CDI plot showing the effect of introducing the categorical variable [`Depth bands`] to the lognormal regression model for CAR in the BC (3CD5ABCDE) bottom trawl fishery. Each plot consists of subplots showing the effect by level of variable (top left), the relative distribution by year of variable records (bottom left), and the cumulative effect of variable by year (bottom right).

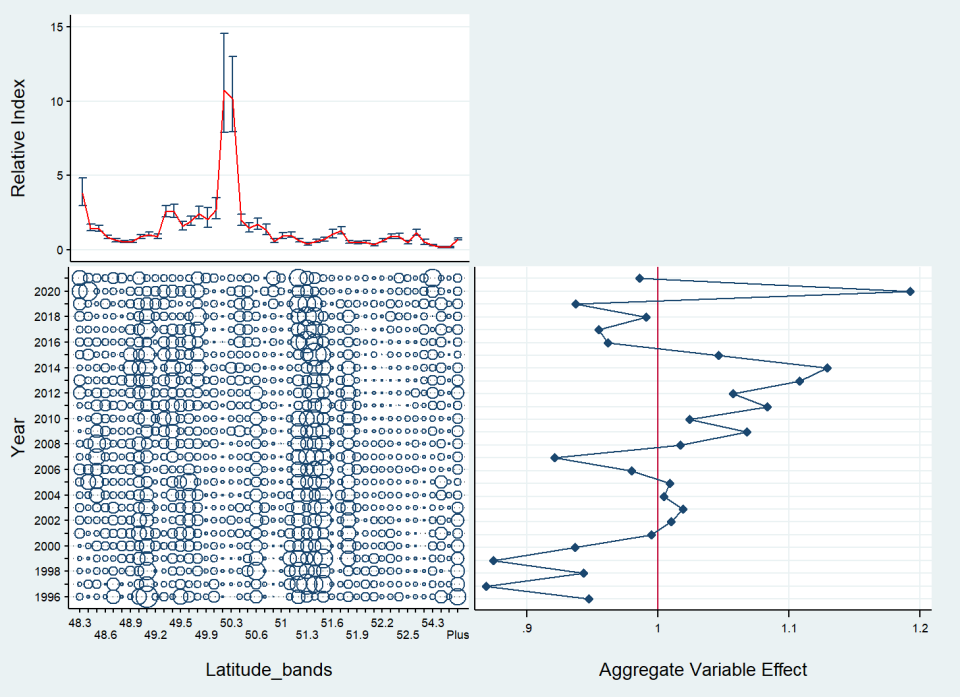

Figure C.8. CDI plot showing the effect of introducing the categorical variable [`0.1°Latitude bands`] to the lognormal regression model for CAR in the BC (3CD5ABCDE) bottom trawl fishery. Each plot consists of subplots showing the effect by level of variable (top left), the relative distribution by year of variable records (bottom left), and the cumulative effect of variable by year (bottom right).

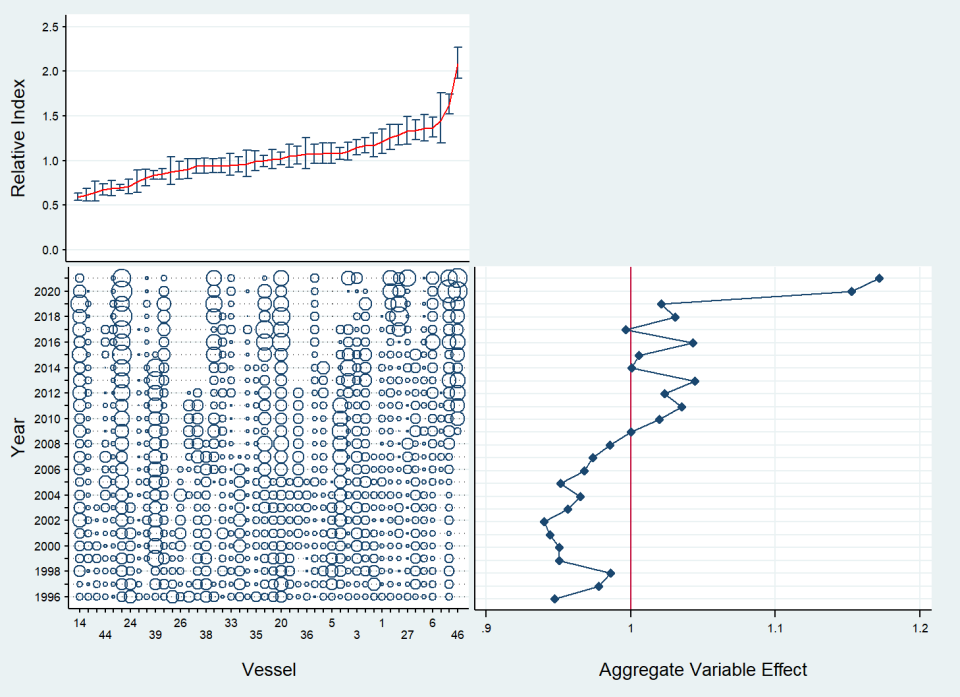

Figure C.9. CDI plot showing the effect of introducing the categorical variable [vessel] to the lognormal regression model for CAR in the BC (3CD5ABCDE) bottom trawl fishery. Each plot consists of subplots showing the effect by level of variable (top left), the relative distribution by year of variable records (bottom left), and the cumulative effect of variable by year (bottom right).

Table C.6. Definition of locality codes used in Figure C.6.

Code	PFMC Major	DFO Minor	Minor Name	Locality Name	Lognormal Index
106	3	21	Southeast Of Big Bank	Swiftsure	0.2263
110				South Finger	0.7710
118				Fingers	0.7694
122				Deep Big Bank/Barkley Canyon	1.0736
124	3	23	Big Bank	Ucluelet/Loudon Canyons	1.6370
125				Nitinat Canyon	0.4015
128				Barkley Hake	0.2928
133				Lennard I./Tofino	0.7217
138	3	24	Clayoquot Sd.	Father Charles Canyon	1.2861
139				Clayoquot Canyon	1.0384
140				South Estevan	0.8455
145				North Estevan	0.9364
146	4	25	Estevan-Esperanza Inlet	Nootka	0.8793
147				Esperanza East	0.9194
153				Lookout Island	2.5111
155	4	26	Kyuquot Sd.	Kyuquot Sd (>100 fm)	1.1822
157				Crowther Canyon	1.6869
165	4	27	Quatsino Sd.	West Cape Cook	0.9132
166				Quatsino Sound	1.0368
177				Unknown	0.9636
178				Triangle	1.8262
179				Cape Scott Spit	0.4748
180	5	11	Cape Scott-Triangle	Mexicana	0.2849
181				Topknot	0.9424
183				South Scott Islands	0.9588
187				South Triangle	1.2362
188				Pisces Canyon	0.8333
192				NE Goose	0.3353
193				SE Goose	1.1366
195				SW Goose	1.4742
196	6	8	Goose Island Bank	Mitchell's Gully	1.3171
197				SE Cape St. James	0.9654
202				SW Middle Bank	2.5942
204				West Virgin Rocks	0.7503
212	7	2	2B-East	South Morseby	0.9364
218				NW Middle Bank	3.6326
243	8	3	1 East-Dixon Entrance	McIntyre Bay	2.2278
251	8	4	4-Two Peaks-Dundas Is.	Two Peaks	1.1419
294	9	35	1 West - Langara	N Fred-Langara (Deep)	5.8539

C.4.1.2. Bottom trawl fishery: binomial logit model

The same explanatory variables used in the lognormal model were offered sequentially to this model, beginning with the year categorical variable, until the improvement in the model R^2 was less than 1% (Table C.7). A binary variable which equalled 1 for positive catch tows and 0 for zero catch tows was used as the dependent variable. The final binomial model accounted for 31% of the total model deviance, with the year variable explaining about 1% of the model deviance. This model showed an increasing trend from the beginning of the series to 2018, followed by a strong drop in the final three years (Figure C.10). The stepwise plot (Figure C.11), which shows the effect of adding each successive explanatory variable, indicates that there was little change to the unstandardised occurrence series through the standardisation procedure.

*Table C.7. Order of acceptance of variables into the binomial model of presence/absence of verified landings plus discards of CAR in BC (3CD5ABCDE) bottom trawl fishery with the amount of explained deviance (R^2) for each variable. Variables accepted into the model are marked in bold with an *. Year was forced as the first variable.*

Variable	1	2	3	4	5
Year*	**0.0113**	–	–	–	–
Depth bands*	0.1906	**0.2032**	–	–	–
DFO locality*	0.1806	0.1884	**0.2841**	–	–
0.1° Latitude bands*	0.1692	0.1776	0.2827	**0.3050**	–
Vessel	0.0642	0.0756	0.2351	0.2925	0.3101
Hours fished	0.0001	0.0115	0.2041	0.2846	0.3062
Month	0.0158	0.0280	0.2143	0.2897	0.3093
PFMC major area	0.1245	0.1337	0.2651	0.3022	0.3093
Improvement in deviance	0.0000	0.1919	0.0810	0.0209	0.0051

The selected explanatory variables included [Depth_bands] (Figure C.12), [DFO locality] (Figure C.13), and [0.1°Latitude_bands] (Figure C.14), in addition to [Year].

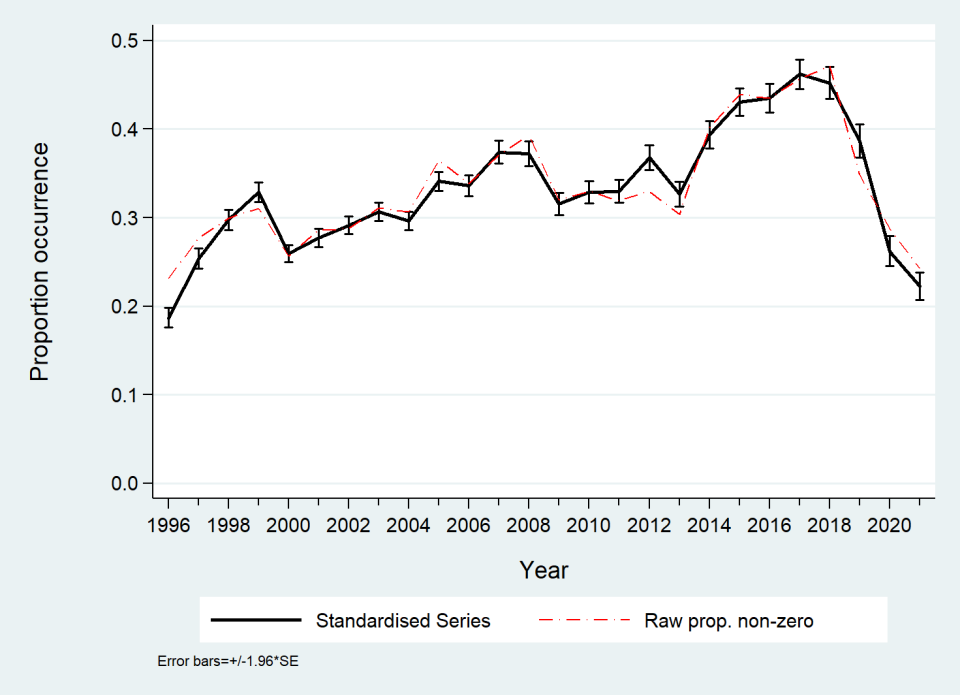

Figure C.10. Binomial index series for the CAR BC (3CD5ABCDE) bottom trawl fishery analysis, also showing the trend in proportion of non-zero tows from the same data set.

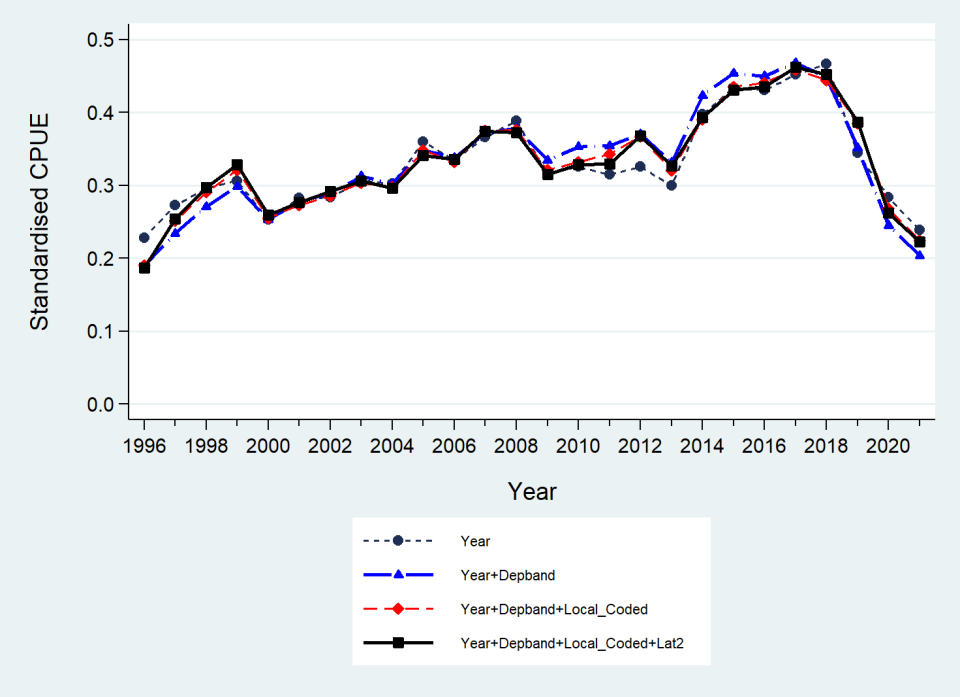

Figure C.11. Plot showing the year coefficients after adding each successive term of the standardised binomial regression analysis for CAR in the BC (3CD5ABCDE) bottom trawl fishery. The final model is shown with a thick solid black line. Each line has been scaled so that the geometric mean equals 1.0.

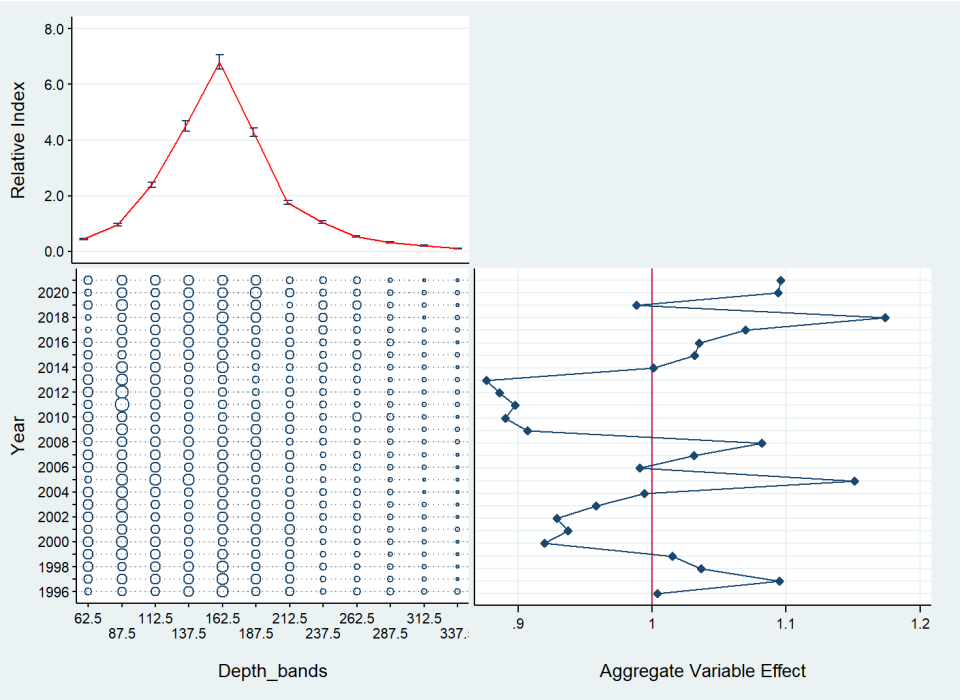

Figure C.12. CDI plot showing the effect of introducing the categorical variable [Depth bands] to the binomial regression model for CAR in the BC (3CD5ABCDE) bottom trawl fishery. Each plot consists of subplots showing the effect by level of variable (top left), the relative distribution by year of variable records (bottom left), and the cumulative effect of variable by year (bottom right).

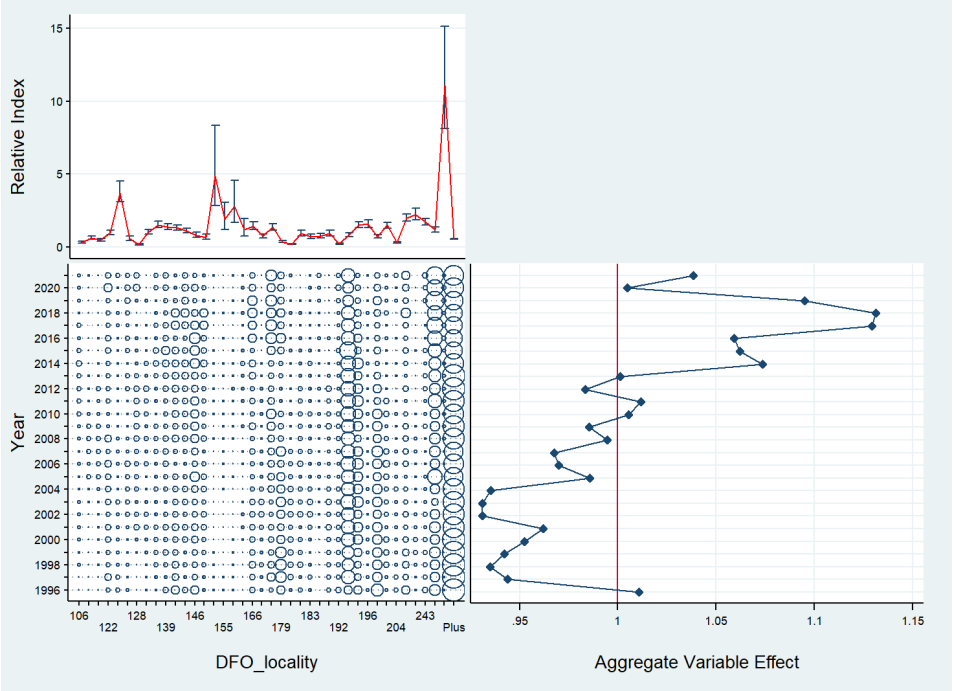

Figure C.13. CDI plot showing the effect of introducing the categorical variable [DFO locality] to the binomial regression model for CAR in the BC (3CD5ABCDE) bottom trawl fishery. Table C.8 provides the definitions for the coded values used for each locality in the above plot. Each plot consists of subplots showing the effect by level of variable (top left), the relative distribution by year of variable records (bottom left), and the cumulative effect of variable by year (bottom right).

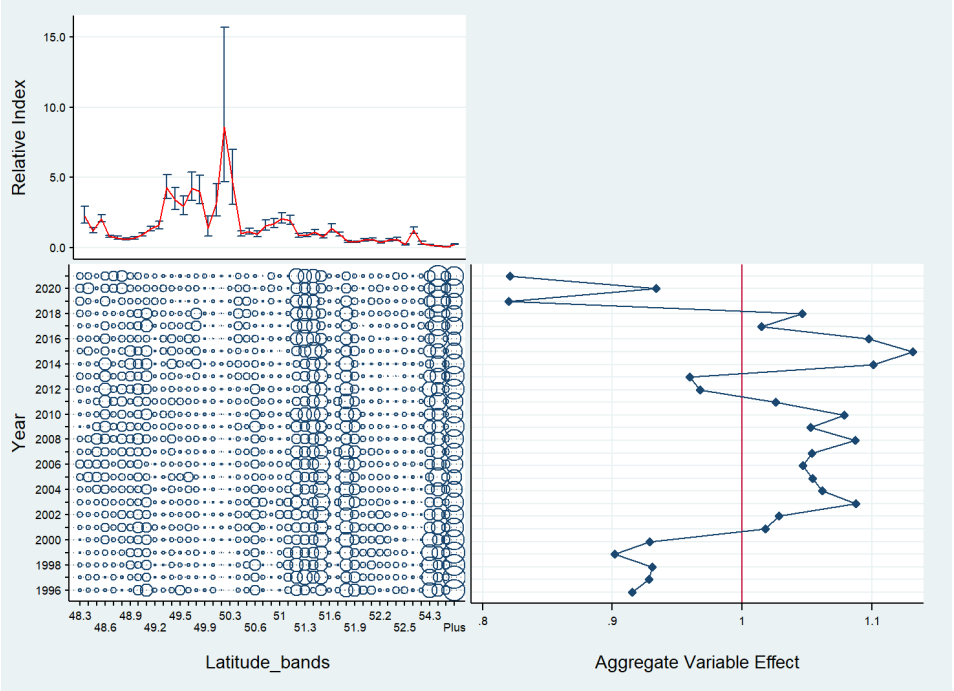

Figure C.14. CDI plot showing the effect of introducing the categorical variable [0.1°Latitude bands] to the binomial regression model for CAR in the BC (3CD5ABCDE) bottom trawl fishery. Each plot consists of subplots showing the effect by level of variable (top left), the relative distribution by year of variable records (bottom left), and the cumulative effect of variable by year (bottom right).

Table C.8. Definition of locality codes used in Figure C.13.

Code	PFMC Major	DFO Minor	Minor Name	Locality Name	Binomial Index
106	3	21	Southeast Of Big Bank	Swiftsure	0.3280
110				South Finger	0.6285
118				Fingers	0.4933
122				Deep Big Bank/Barkley Canyon	0.9894
124	3	23	Big Bank	Ucluelet/Loudon Canyons	3.7432
125				Nitinat Canyon	0.5863
128				Barkley Hake	0.1769
133				Lennard I./Tofino	1.0275
138	3	24	Clayoquot Sd.	Father Charles Canyon	1.5231
139				Clayoquot Canyon	1.3953
140				South Estevan	1.3212
145				North Estevan	1.1143
146	4	25	Estevan-Esperanza Inlet	Nootka	0.8056
147				Esperanza East	0.6730
153				Lookout Island	4.8793
155	4	26	Kyuquot Sd.	Kyuquot Sd (>100 Fm)	1.9216
157				Crowther Canyon	2.7897
165	4	27	Quatsino Sd.	West Cape Cook	1.2212
166				Quatsino Sound	1.4424
177				Unknown	0.7468
178				Triangle	1.3797
179				Cape Scott Spit	0.3661
180	5	11	Cape Scott-Triangle	Mexicana	0.2013
181				Topknot	0.9441
183				South Scott Islands	0.7044
187				South Triangle	0.7623
188				Pisces Canyon	0.9472
192				NE Goose	0.2395
193				SE Goose	0.8350
195				SW Goose	1.5292
196	6	8	Goose Island Bank	Mitchell's Gully	1.5775
197				SE Cape St. James	0.7286
202				SW Middle Bank	1.4896
204				West Virgin Rocks	0.3013
212	7	2	2B-East	South Morseby	2.0077
218				NW Middle Bank	2.2216
243	8	3	1 East-Dixon Entrance	Mcintyre Bay	1.7127
251	8	4	4-Two Peaks-Dundas Is.	Two Peaks	1.1831
294	9	35	1 West - Langara	N Fred-Langara (Deep)	11.0797

C.4.1.3. Bottom trawl fishery: combined model

While the lognormal and binomial models show relatively similar overall trends over most of the period, the multiplicative nature of the combined model equation (Eq. C.4) results in an overall increasing trend to a two year peak in 2017 and 2018, followed by a drop in 2019 and a gradual rise to 2021 (Figure C.15). However, the binomial and lognormal series trend in opposite directions in the final two years (2020 and 2021), implying alternative incentives. One possible explanation is that operators were severely constrained in their CAR catch, so the reduction in the occurrence of CAR reflects the avoidance of this species. While the strong upward trend in the positive catch model reflects an overall improvement in the catch of this species when encountered.

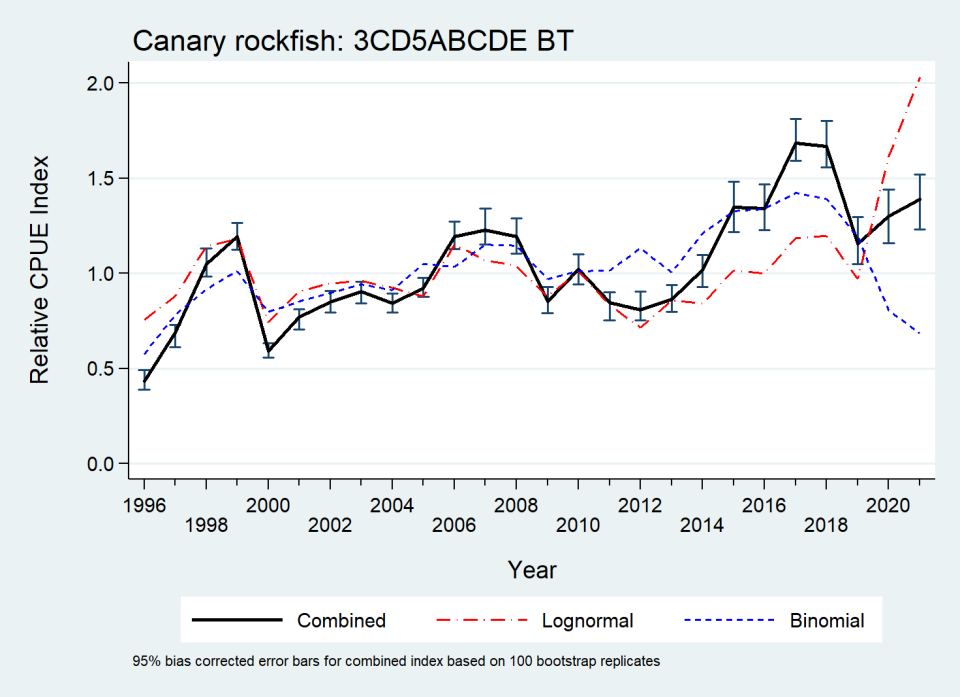

Figure C.15. Combined index series (Eq. C.4) for the BC (3CD5ABCDE) bottom trawl fishery also showing the contributing lognormal and binomial index series. Confidence bounds based on 100 bootstrap replicates.

C.5. RELATIVE INDICES OF ABUNDANCE

Table C.9 summarises the suite of relative abundance indices and associated standard errors derived from this CAR CPUE analysis. The CPUE indices used in the age-structured stock assessment model appear as the delta-lognormal (combined) indices from the bottom trawl data (Figure C.15, Table C.9). The associated bootstrap standard errors (SE) were used as the initial CVs when fitting the stock assessment model.

Table C.9. Relative indices of annual CPUE from the arithmetic, unstandardised, lognormal models of non-zero bottom trawl catches of CAR in BC (3CD5ABCDE). Also shown are the indices from the binomial model of presence/absence in this fishery and the combined delta-lognormal model (Eq. C.4). All indices are scaled so that their geometric means equal 1.0. Upper and lower 95% analytic confidence bounds and associated standard error (SE) are presented for the lognormal model, while bootstrapped (100 replicates) upper and lower 95% confidence bounds and the associated SE are presented for the combined model.

	Arithmetic	Geometric	Lognormal (Eq. C.3)				Binomial	Combined (Eq. C.4)			
Year	Index (Eq. C.1)	Index (Eq. C.2)	Index	Lower bound	Upper bound	SE	Index (Eq. C.3)	Index	Lower bound	Upper bound	SE
1996	0.526	0.730	0.756	0.693	0.824	0.0443	0.575	0.435	0.390	0.492	0.0269
1997	0.657	0.796	0.879	0.820	0.943	0.0357	0.781	0.687	0.614	0.729	0.0276
1998	0.788	0.946	1.143	1.073	1.218	0.0324	0.916	1.048	0.984	1.131	0.0380
1999	0.696	0.839	1.179	1.112	1.251	0.0300	1.012	1.193	1.124	1.265	0.0350
2000	0.618	0.678	0.743	0.700	0.788	0.0300	0.798	0.593	0.559	0.635	0.0197
2001	1.106	0.852	0.906	0.853	0.962	0.0307	0.853	0.772	0.704	0.813	0.0280
2002	0.886	0.919	0.948	0.897	1.002	0.0284	0.897	0.851	0.796	0.908	0.0271
2003	0.908	0.960	0.960	0.909	1.014	0.0280	0.943	0.905	0.842	0.956	0.0283
2004	0.881	1.006	0.925	0.874	0.978	0.0289	0.913	0.844	0.795	0.895	0.0263
2005	0.697	0.856	0.880	0.836	0.926	0.0263	1.050	0.924	0.876	0.978	0.0251
2006	0.986	1.060	1.152	1.087	1.220	0.0294	1.035	1.192	1.129	1.272	0.0375
2007	0.787	0.942	1.068	1.007	1.132	0.0301	1.151	1.229	1.152	1.340	0.0453
2008	0.911	1.124	1.041	0.978	1.108	0.0318	1.146	1.194	1.104	1.290	0.0465
2009	0.956	1.000	0.879	0.824	0.937	0.0328	0.971	0.853	0.792	0.930	0.0315
2010	0.912	0.949	1.010	0.948	1.076	0.0324	1.012	1.022	0.942	1.099	0.0391
2011	0.999	0.871	0.834	0.782	0.890	0.0330	1.015	0.846	0.755	0.900	0.0324
2012	1.131	0.732	0.715	0.669	0.764	0.0339	1.132	0.810	0.754	0.905	0.0361
2013	1.395	0.922	0.858	0.799	0.920	0.0360	1.005	0.862	0.799	0.941	0.0384
2014	1.287	0.897	0.841	0.787	0.900	0.0343	1.211	1.019	0.929	1.096	0.0417
2015	1.104	0.965	1.016	0.954	1.083	0.0323	1.326	1.348	1.217	1.481	0.0593
2016	1.038	0.874	1.001	0.936	1.070	0.0341	1.340	1.341	1.226	1.468	0.0533
2017	1.144	1.058	1.185	1.110	1.266	0.0336	1.423	1.686	1.592	1.812	0.0653
2018	1.249	1.266	1.197	1.115	1.286	0.0362	1.392	1.667	1.556	1.803	0.0653
2019	1.357	0.992	0.971	0.892	1.057	0.0432	1.190	1.155	1.050	1.296	0.0589
2020	2.900	2.651	1.611	1.455	1.784	0.0520	0.807	1.300	1.159	1.441	0.0758
2021	1.935	2.962	2.031	1.824	2.262	0.0549	0.685	1.391	1.233	1.520	0.0738

C.6. COMPARISON OF CPUE SERIES WITH SYNOPTIC SURVEYS

C.6.1. Queen Charlotte Sound survey

Figure C.16 compares the BC (3CD5ABCDE) combined CPUE series (Figure C.15, Table C.9) with the relative biomass series from the Queen Charlotte Sound synoptic survey (see Appendix B, Section B.5). This comparison seems reasonable, in spite of the very large error bars associated with this survey, with the CPUE series intersecting the range between survey error bars in nine of the eleven indices (apart from the 2007 and 2017 indices). There is general agreement between the two series, given the high level of variability that is associated with this survey.

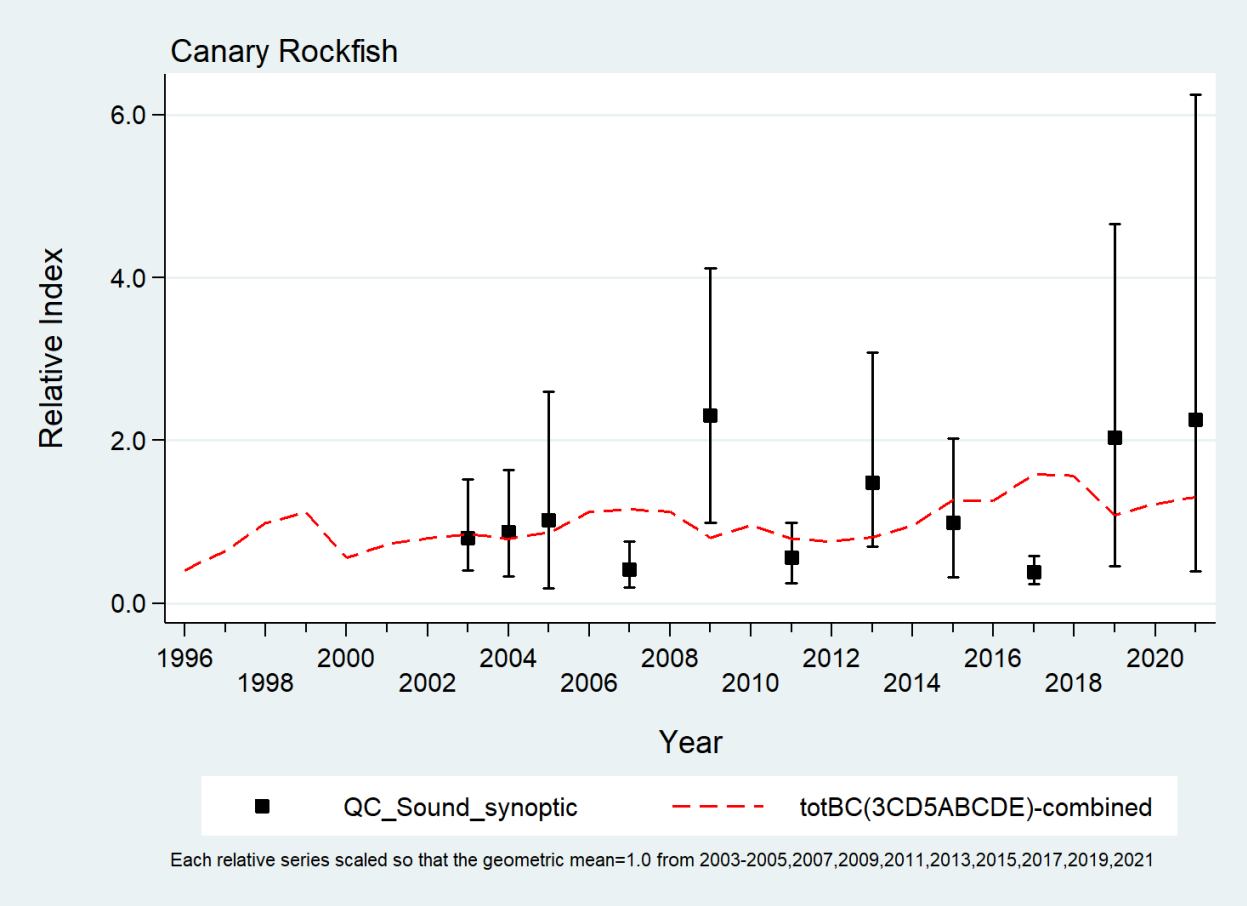

Figure C.16. Comparison of the Queen Charlotte Sound synoptic survey series with the CPUE index series (Eq. C.4) for the BC (3CD5ABCDE) bottom trawl fishery. Survey confidence bounds based on 1000 bootstrap simulations.

C.6.2. West coast Vancouver Island survey

Figure C.17 compares the BC (3CD5ABCDE) combined series (Figure C.15, Table C.9) with the relative biomass series from the west coast Vancouver Island synoptic survey (see Appendix B, Section B.6). This comparison seems poorer than for the QC Sound survey, with the 2006 to 2014 indices showing a descending trend while the CPUE series shows no trend. All but one of the survey index values intersect the CPUE series with their error bars. This series appears to be a only a moderate match to the CPUE series, perhaps because of considerable interannual variation in availability.

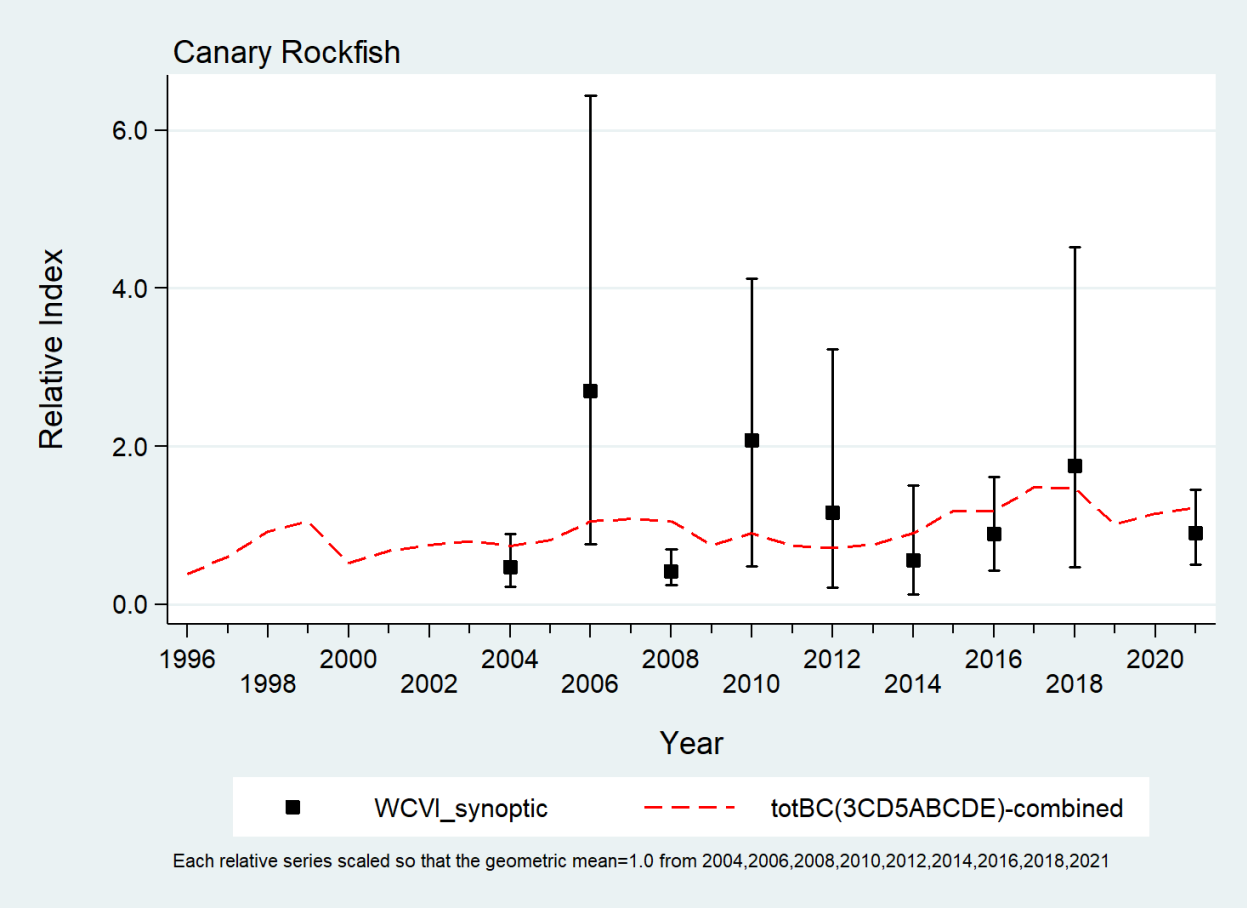

Figure C.17. Comparison of the west coast Vancouver Island synoptic survey series with the CPUE index series (Eq. C.4) for the BC (3CD5ABCDE) bottom trawl fishery. Survey confidence bounds based on 1000 bootstrap simulations.

C.6.3. West coast Haida Gwaii survey

Figure C.18 compares the BC (3CD5ABCDE) combined series (Figure C.15, Table C.9) with the relative biomass series from the west coast Haida Gwaii synoptic survey (see Appendix B, Section B.7). This comparison is swamped by the very high relative index observed in 2016 along with its high relative error. The remaining indices follow the trajectory, but this species is not very prevalent in this part of the BC coast and there appears to be a large amount of variation between years in the availability of this species to the survey. This comparison, as with the previous two surveys, is hampered by the very large relative errors associated with CAR.

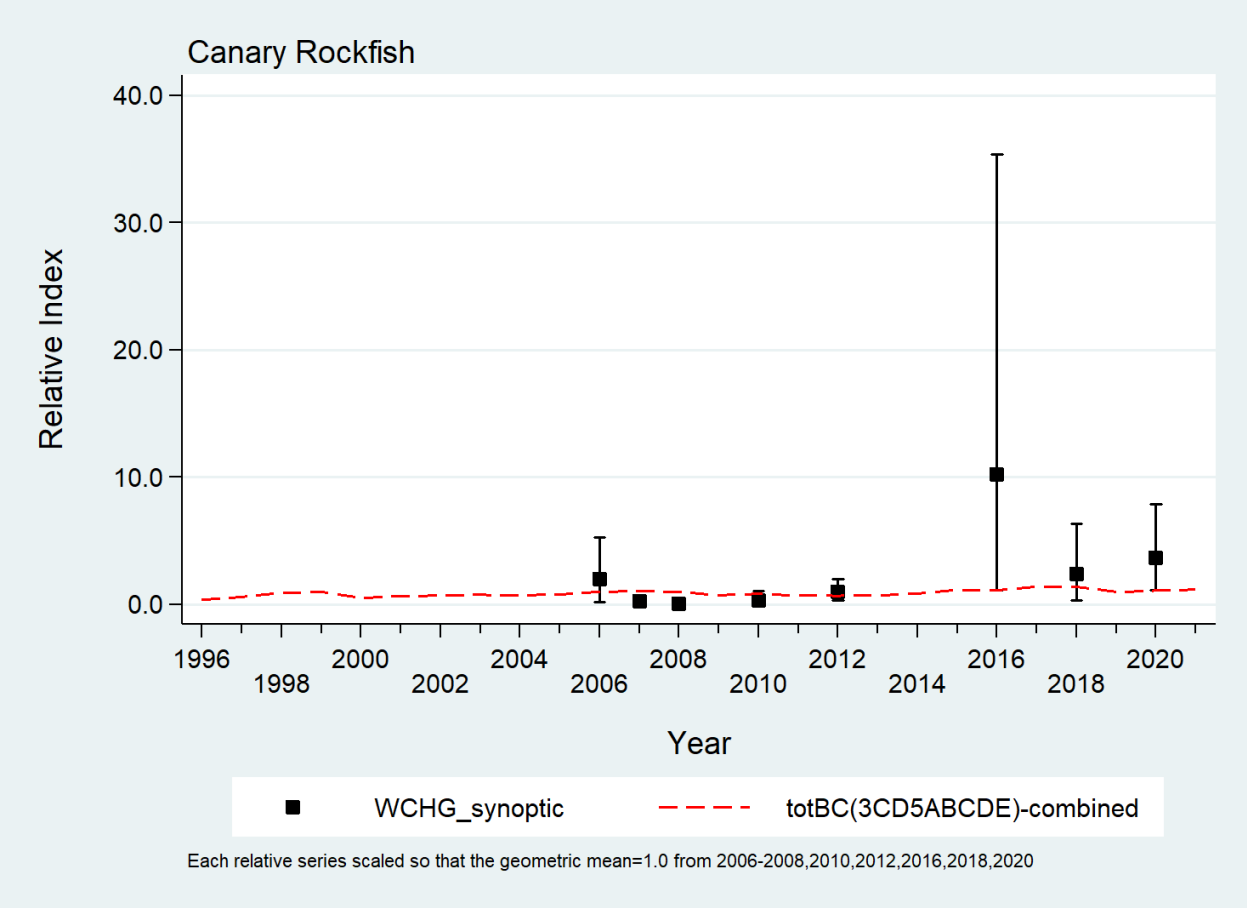

Figure C.18. Comparison of the west coast Haida Gwaii synoptic survey series with the CPUE index series (Eq. C.4) for the BC (3CD5ABCDE) bottom trawl fishery. Survey confidence bounds based on 1000 bootstrap simulations.

C.6.4. Hecate Strait survey

Figure C.19 compares the BC (3CD5ABCDE) combined series (Figure C.15, Table C.9) with the relative biomass series from the Hecate Strait synoptic survey (see Appendix B, Section B.8). As with the WCHG survey, this species does not appear to be especially abundant in the region covered by the survey, so there will be considerable interannual variation. Figure D.6 (Appendix D), which compares the length distributions captured by the four synoptic surveys, indicates that CAR captured by this survey are consistently smaller than from the other three surveys. This may be evidence that CAR from this survey are new recruits from a 2014 year class, so the resulting index is tracking recruitment rather than the adult biomass represented in the CPUE series. If this interpretation is correct, the strong index observed for 2021 may be indicative of a strong upcoming year class in this population.

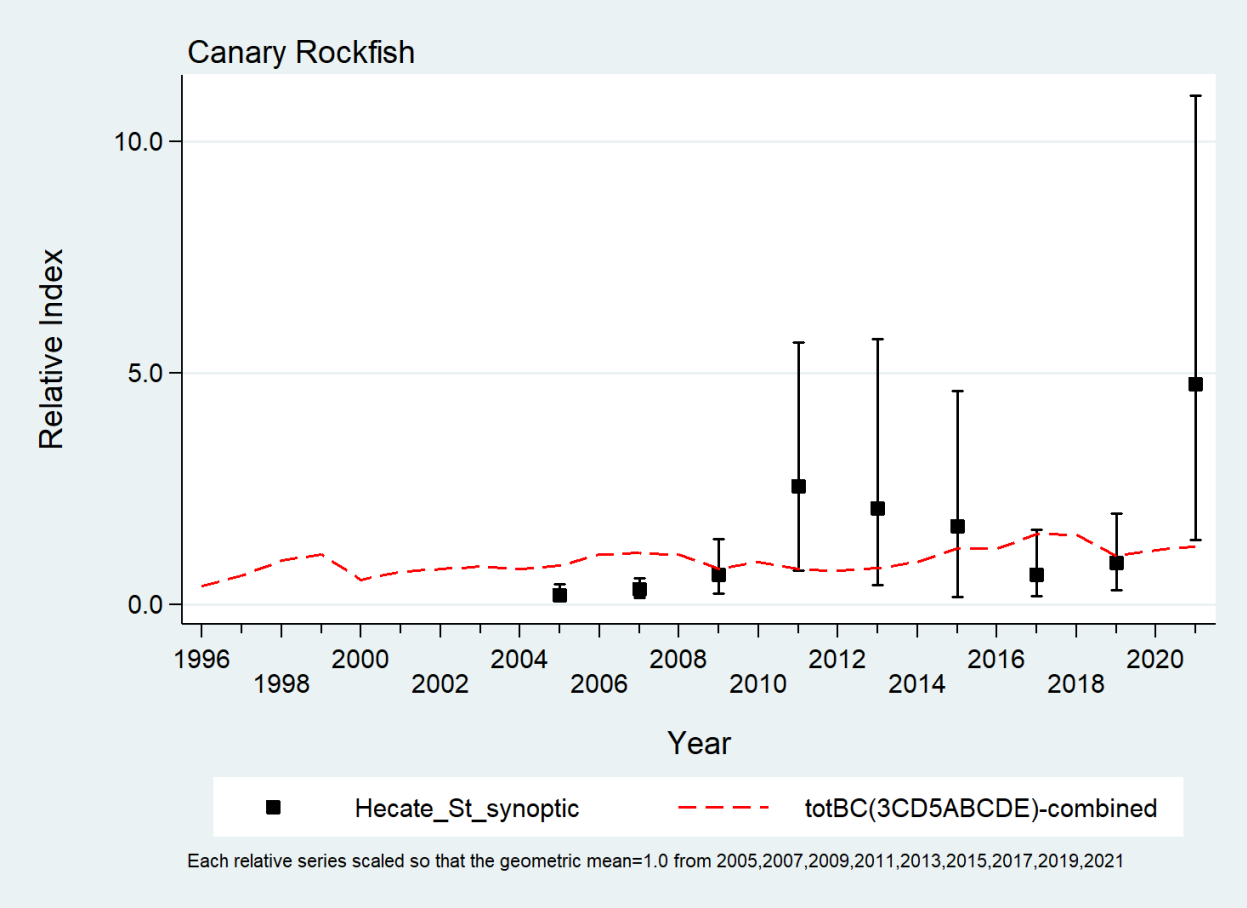

Figure C.19. Comparison of the Hecate Strait synoptic survey series with the CPUE index series (Eq. C.4) for the BC (3CD5ABCDE) bottom trawl fishery. Survey confidence bounds based on 1000 bootstrap simulations.

C.7. COMPARISON OF CPUE SERIES WITH TWEEDIE CPUE MODEL

Two analyses of the coastwide CAR catch/effort data using an alternative model structure (compared to the model described in Section C.2.2) were prepared for use in the CAR stock assessment (Sean Anderson, DFO Pacific Biological Station, pers. comm., 2022). These models were based on the Tweedie distribution which can accommodate zero and positive tows in the same model, thus eliminating the necessity to estimate separate positive and logit models which were then combined using the delta-lognormal procedure (Eq. C.4). The procedure followed by the Tweedie model is documented in Anderson et al. (2019, Section D.3).

The Tweedie model is based on a similar set of filters as described in Section C.3, and consisted as follows:

- area = "3CD5ABCDE"
- year_range = c(1996, 2021)
- lat_range = c(48, Inf)
- min_positive_tows = 100
- min_positive_trips = 10
- min_yrs_with_trips = 5
- lat_band_width = 0.1

- depth_band_width = 25
- gear = "bottom trawl"

This set of filters resulted in a slightly different data set than that summarised in Table C.4, with 44 vessels compared to 46 as listed in Table C.2. The Tweedie models also excluded “unknown” trawl which was included in the delta/lognormal data set.

The “`no[locality x year]`” Tweedie model used random intercepts for vessel and locality while the delta-lognormal model treated these variables as factors. A second Tweedie model (`[full]`) included a year-DFO locality interaction term, also treated as a random effect. These two series are plotted (with error bars) along with the delta/lognormal combined model (Table C.9) in Figure C.20. The stock assessment sensitivity run S12 used the Tweedie series without [`locality x year`] interactions for consistency with the selection made for the YMR stock assessment (Starr and Haigh 2022) and because it differed more from the delta/lognormal model than did the Tweedie(`[full]`) model. The selected Tweedie model appears to reflect the binomial component of the delta-lognormal model (Section C.2.2.2) more than the lognormal component (Section C.2.2.1).

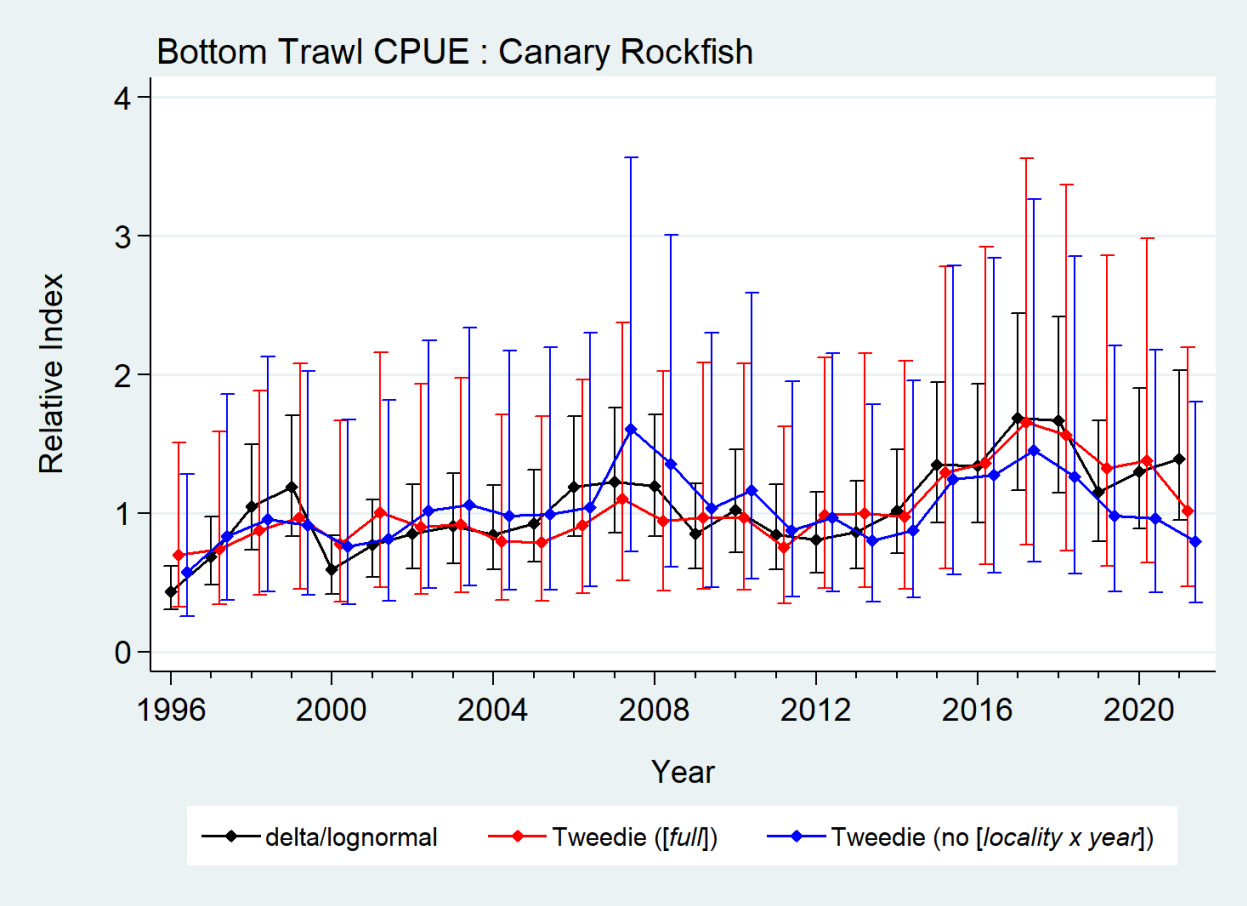

Figure C.20. Comparison of the delta-lognormal series (BC(3CD5ABCDE)) with two Tweedie models (Sean Anderson, DFO, pers. comm., 2022): one which omits the [locality x year] interaction term and the other ([full]) which includes it. The Tweedie [no [locality x year] series was used in Sensitivity run S12. Note that the delta/lognormal error bars have been widened to include 0.178 process error as specified in Section E.6.2.1 (Appendix E).

C.8. REFERENCES – CPUE

Anderson, S.C., Keppel, E.A., and Edwards, A.M. 2019. A reproducible data synopsis for over 100 species of British Columbia groundfish. DFO Can. Sci. Advis. Sec. Res. Doc. 2019/041. vii + 321 p.

Bentley, N., Kendrick, T.H., Starr, P.J., and Breen, P.A. 2012. Influence plots and metrics: tools for better understanding fisheries catch-per-unit-effort standardizations. ICES J. Mar. Sci. 69(1): 84-88.

Fletcher, D., Mackenzie, D. and Villouta, E. 2005. Modelling skewed data with many zeros: A simple approach combining ordinary and logistic regression. Environmental and Ecological Statistics12, 45–54.

Francis, R.I.C.C. 1999. The impact of correlations on standardised CPUE indices. N.Z. Fish. Ass. Res. Doc. 99/42: 30 pp. (Unpublished report held in NIWA library, Wellington, NZ)

Francis, R.I.C.C. 2001. Orange roughy CPUE on the South and East Chatham Rise. N.Z. Fish. Ass. Rep. 2001/26: 30 pp.

Quinn, T.R. and R.B. Deriso. 1999. Quantitative Fish Dynamics. Oxford University Press. 542 pp.

Rutherford, K.L. 1999. A brief history of GFCatch (1954-1995), the groundfish catch and effort database at the Pacific Biological Station. Can. Tech. Rep. Fish. Aquat. Sci. 2299: v + 66 p.

Starr, P.J. and Haigh, R. 2022. Yellowmouth Rockfish (*Sebastes reedi*) stock assessment for British Columbia in 2021. DFO Can. Sci. Advis. Sec. Res. Doc. 2022/10. viii + 288 p.

APPENDIX D. BIOLOGICAL DATA

This appendix describes analyses of biological data for Canary Rockfish (CAR) along the British Columbia (BC) coast. These analyses follow the methods adopted in previous rockfish stock assessments (e.g., Starr and Haigh 2021a), including length-weight relationships, von Bertalanffy growth models, maturity schedules, natural mortality, and age proportions for use in the CAR catch-at-age stock assessment model (Sections D.1 and D.2). As well, the data were investigated for possible differences among northern (5DE), central (5ABC), and southern (3CD) regions (Section D.3) to determine if there was evidence that these regions should be treated as separate stocks. All biological analyses are based on CAR data extracted from the Fisheries and Oceans Canada (DFO) Groundfish database GFBioSQL on 2021-11-23 (60,332 records). Results from some analyses were used for input to the model platform Stock Synthesis 3 (SS3, see Appendix E). General data selection criteria for most analyses are summarised in Table D.1, although data selection sometimes varied depending on the analysis.

Table D.1. Data selection criteria for analyses of biological data for allometric and growth analyses.

Field	Criterion	Notes
Trip type	`[trip_type] == c(2,3)`	Definition of research observations
	`[trip_type] == c(1,4,5)`	Definition of commercial observations
Sample type	`[sample_type] == c(1,2,6,7,8)`	Only random or total samples.
Ageing method	`[agemeth] == c(3, 17) or == (0 & [year]>=1980) or == 1 for ages 1:3`	Break & burn|bake method unknown from 1980 on (assumed B&B) surface readings for young fish
Species category code	`[SPECIES_CATEGORY_CODE]==1 (or 3)`	1 = Unsorted samples 3 = Sorted (keeper) samples
Sex code	`[sex] == c(1,2)*`	Clearly identified sex (1=male or 2=female)
Area code	`[stock]` select stock area (coastwide)	PMFC major area codes 3:9

*GFBioSQL codes for `sex` (1=male, 2=female) are reversed in SS3 (1=female, 2=male).

D.1. LIFE HISTORY

D.1.1. Allometry – Weight vs. Length

A log-linear relationship with additive errors was fit to females (*s*=2), males (*s*=1), and combined to all valid weight and length data pairs i, $\{W_{is}, L_{is}\}$:

$$\ln\left(W_{is}\right) = \alpha_s + \beta_s \ln\left(L_{is}\right) + \varepsilon_{is}, \quad \varepsilon \sim N(0,\sigma^2) \tag{D.1}$$

where α_s and β_s are the intercept and slope parameters for each sex s.

Survey and commercial samples, regardless of gear type, were used independently to derive length-weight parameters for consideration in the model (Table D.2); however, only survey data coastwide were adopted for model use (Figure D.2). Commercial fishery weight data were not as abundant as those from research surveys and tended to represent a restricted range of weights compared to those from surveys (compare minimum, maximum and mean weights in Table D.2). It is also possible that the commercial weights were less precise than the survey weight data.

*Table D.2. Length-weight parameter estimates, standard errors (SE) and number of observations (n) for CAR (females, males, and combined) from survey and commercial samples, regardless of gear type from 1989 to 2021. W_i = weight (kg) of specimen i, W_{pred} = predicted weight from fitted data set. (**S**): survey data; (**C**): commercial data.*

Stock	Sex	n	ln(*a*)	SE ln(*a*)	*b*	SE *b*	mean W_i	SD W_i	min W_i	max W_i	mean W_{pred}
CAR	F	5,288	-11.040	0.017	3.009	0.004	1.712	0.861	0.022	4.340	1.808
Coast	M	6,407	-11.157	0.014	3.043	0.004	1.562	0.718	0.024	3.792	1.661
(**S**)	F+M	11,699	-11.100	0.011	3.027	0.003	1.629	0.789	0.022	4.340	1.726
CAR	F	1,045	-10.864	0.079	2.973	0.020	2.224	0.665	0.381	4.903	2.173
Coast	M	1,647	-10.392	0.063	2.848	0.016	1.913	0.472	0.427	4.192	2.021
(**C**)	F+M	2,697	-10.672	0.049	2.922	0.013	2.033	0.576	0.381	4.903	2.080
CAR	F	556	-10.878	0.070	2.971	0.018	2.319	0.818	0.104	4.294	2.341
5DE	M	677	-11.212	0.065	3.055	0.017	2.029	0.627	0.048	3.792	2.049
(**S**)	F+M	1,234	-11.056	0.048	3.015	0.012	2.160	0.733	0.048	4.294	2.184
CAR	F	117	-11.237	0.200	3.069	0.051	2.170	0.738	0.796	4.903	2.560
5DE	M	152	-10.732	0.193	2.937	0.050	1.944	0.488	0.963	3.212	2.180
(**C**)	F+M	270	-11.032	0.139	3.015	0.036	2.042	0.617	0.796	4.903	2.308
CAR	F	2,412	-10.987	0.027	2.993	0.007	1.634	0.818	0.040	4.322	1.661
5ABC	M	2,983	-11.155	0.022	3.040	0.006	1.577	0.703	0.029	3.660	1.615
(**S**)	F+M	5,396	-11.077	0.017	3.018	0.005	1.602	0.757	0.029	4.322	1.636
CAR	F	541	-10.904	0.106	2.980	0.027	2.181	0.684	0.540	4.442	2.028
5ABC	M	863	-10.521	0.077	2.878	0.020	1.914	0.522	0.427	4.192	1.966
(**C**)	F+M	1,407	-10.724	0.063	2.932	0.016	2.016	0.604	0.427	4.442	1.990
CAR	F	2,316	-11.073	0.024	3.020	0.006	1.647	0.856	0.022	4.340	1.822
3CD	M	2,749	-11.198	0.020	3.056	0.005	1.429	0.706	0.024	3.375	1.648
(**S**)	F+M	5,065	-11.134	0.015	3.038	0.004	1.529	0.786	0.022	4.340	1.724
CAR	F	386	-10.567	0.134	2.902	0.034	2.297	0.606	0.381	4.480	2.298
3CD	M	631	-10.019	0.118	2.754	0.030	1.904	0.390	0.488	3.195	2.065
(**C**)	F+M	1,020	-10.425	0.088	2.862	0.023	2.053	0.519	0.381	4.480	2.157

D.1.2. Growth – Length vs. Age

Otolith age data were available from both surveys and commercial fishing trips; however, data from the surveys were used in determining the growth function used in the model. Of the 20,426 records with age data, 20,309 records had concurrent lengths, and 5,322 records were suitable for growth analysis after qualifying by sex (female|male), trip type (research|surveys), sample type (random), and ageing methodology. The majority of these ages were determined using the break-and-burn (B&B) method (MacLellan 1997). Table D.3 summarises the availability of all CAR otoliths.

Growth was formulated as a von Bertalanffy model where lengths by sex, L_{is}, for fish $i = 1,\ldots,n_s$ are given by:

$$L_{is} = L_{\infty s}\left[1 - e^{-\kappa_s(a_{is}-t_{0s})}\right] + \varepsilon_{is}, \quad \varepsilon \sim N\left(0,\sigma^2\right) \tag{D.2}$$

where for each sex s,

$L_{\infty s}$ = the average length at maximum age of an individual,

κ_s = growth rate coefficient, and

t_{0s} = age at which the average size is zero.

The negative log likelihood for each sex s, used for minimisation is:

$$\ell\left(L_\infty,\kappa,t_0,\sigma\right)=n\ln\left(\sigma\right)+\frac{\sum_i^n\left(L_i-\hat{L}_i\right)^2}{2\sigma^2},\qquad i=1,\ldots,n$$

D.1.2.1. Maximum Likelihood Estimation

Various maximum likelihood estimation (MLE) fits were made for the length vs. age data. One growth model (von Bertalanffy) was used on the full set of research|survey data (Figure D.3), three regions (Figure D.4), and the four primary synoptic surveys (Figure D.5). See Table D.4 for all parameter fits. Figure D.6 shows cumulative length frequencies the synoptic surveys using 4-year periods. The HS survey tended to capture smaller fish than the other surveys.

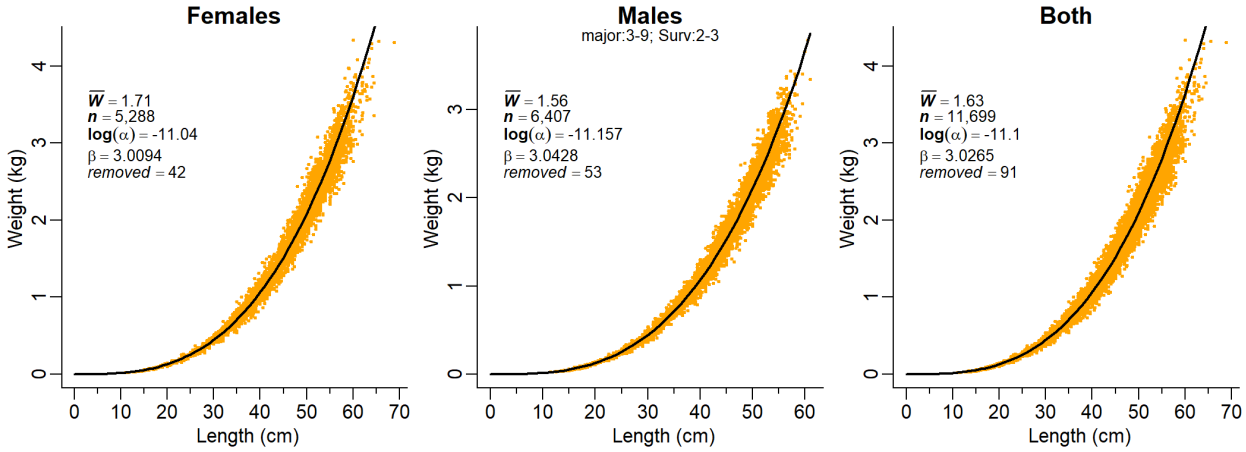

Figure D.1. Length-weight relationship for CAR derived from all research and survey data for BC coastwide. Records with absolute value of standardised residuals >3 (based on a preliminary fit) were dropped.

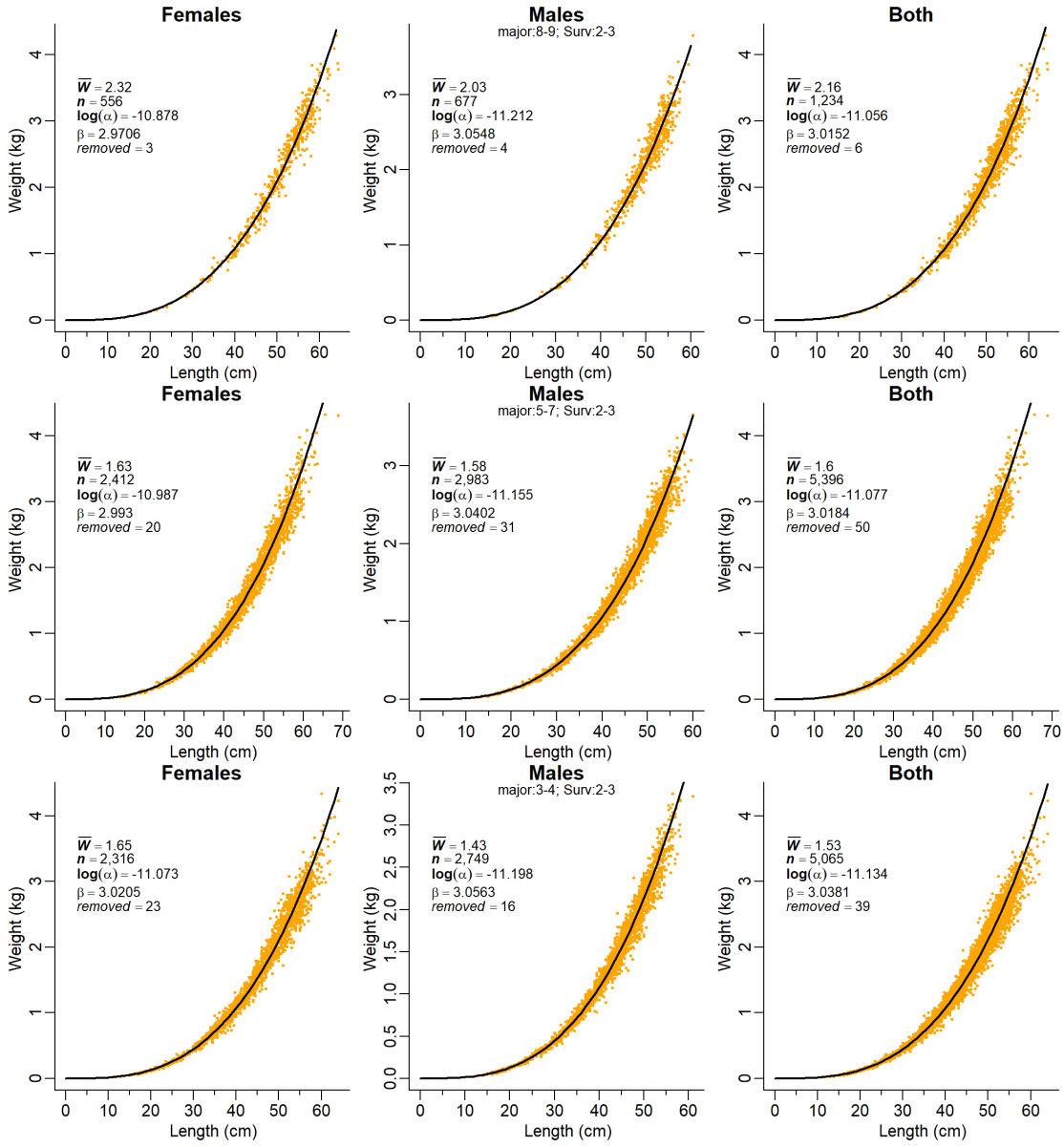

Figure D.2. Length-weight relationship for CAR by area derived from all research and survey data – (top) BC north 5DE, (middle) BC central 5ABC, and (bottom) BC south 3CD. Records with absolute value of standardised residuals >3 (based on a preliminary fit) were dropped.

Table D.3. Number of CAR specimen otoliths aged by various methods. Number of samples appear in parentheses and are not additive between the sexes (i.e., otoliths in a sample usually come from both sexes). The 'Charter' samples are from research surveys conducted on commercial vessels. These otoliths were collected over the period 1967 to 2021.

Trip Type	Activity	Age method	Female	Male	Unknown
Non-obs domestic	commercial	break & burn	1645 (69)	3066 (70)	–
Research	survey	surface read	2 (1)	15 (3)	–
Research	survey	break & burn	718 (111)	794 (108)	2 (2)
Charter	survey	unknown	352 (39)	624 (36)	–
Charter	survey	break & burn	2161 (421)	2459 (383)	13 (7)
Obs domestic	commercial	unknown	1 (1)	–	–
Obs domestic	commercial	break & burn	3907 (208)	6281 (210)	291 (18)

Table D.4. Age-length parameter estimates for CAR (females, males, and both combined) from fits using the von Bertalanffy growth model (Quinn and Deriso 1999) using specimens from research and surveys combined for the BC coast and PMFC areas (north=5DE, central=5ABC, south=3CD), as well as for synoptic surveys (north to south: WCHG = west coast Haida Gwaii, HS = Hecate Strait, QCS = Queen Charlotte Sound, WCVI = west coast Vancouver Island).

MLE Model	Data Source	Sex	n	Linf (cm)	K	t_0 (cm)
CAR Coast	research+survey	Female	2,490	59.0	0.1403	0.22
		Male	2,783	52.7	0.1658	0.13
		Both	5,288	54.4	0.1666	0.40
CAR 5DE	research+survey	Female	334	60.9	0.1339	-0.52
		Male	368	54.4	0.1344	-2.62
		Both	705	55.3	0.1910	0.81
CAR 5ABC	research+survey	Female	1,034	58.9	0.1288	-0.48
		Male	1,201	52.5	0.1618	-0.25
		Both	2,240	53.9	0.1597	-0.10
CAR 3CD	research+survey	Female	1,123	58.1	0.1495	0.58
		Male	1,216	52.2	0.1704	0.39
		Both	2,343	54.2	0.1696	0.63
CAR WCHG	synoptic survey	Female	165	63.4	0.0827	-7.68
		Male	228	54.6	0.0997	-8.15
		Both	396	54.6	0.2299	1.63
CAR HS	synoptic survey	Female	112	61.5	0.1206	-0.35
		Male	142	53.5	0.1648	0.12
		Both	254	55.1	0.1546	0.04
CAR QCS	synoptic survey	Female	511	58.7	0.1251	-1.03
		Male	830	52.6	0.1455	-1.46
		Both	1,345	53.5	0.1560	-0.67
CAR WCVI	synoptic survey	Female	585	57.2	0.1479	-0.04
		Male	697	51.4	0.1655	-0.45
		Both	1,286	53.2	0.1690	0.02

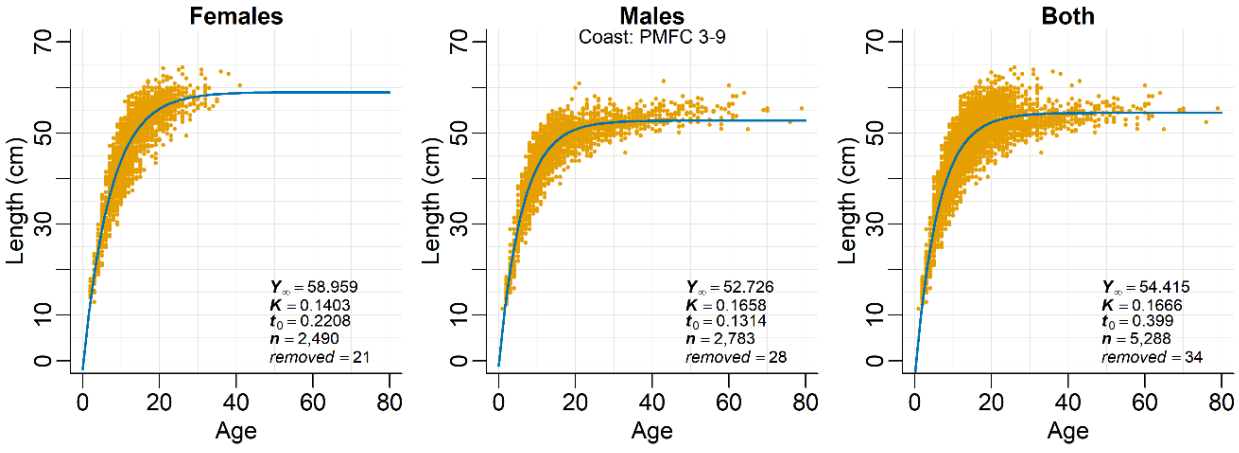

Figure D.3. Growth specified by age-length relationship: von Bertalanffy fits to CAR coastwide using data from research and surveys. Ages were determined by break-and-burn otoliths and surface-read otoliths from ages 1 to 3. Records with absolute value of standardised residuals >3 (based on a preliminary fit) were dropped.

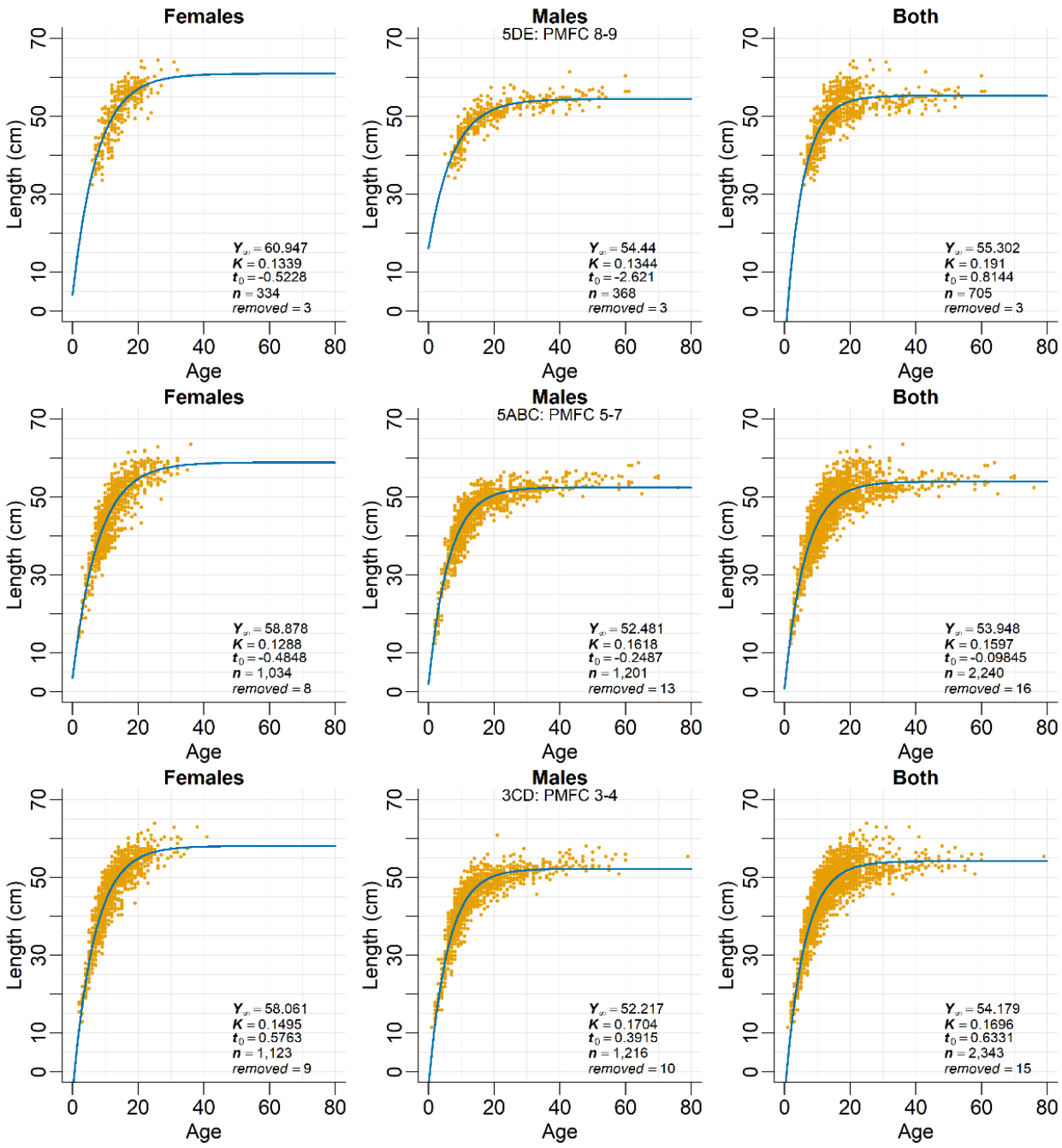

Figure D.4. Growth specified by age-length relationship: von Bertalanffy fits to CAR using data from research and surveys – (top) BC north 5DE, (middle) BC central 5ABC, and (bottom) BC south 3CD. See caption in Figure D.3 for additional details.

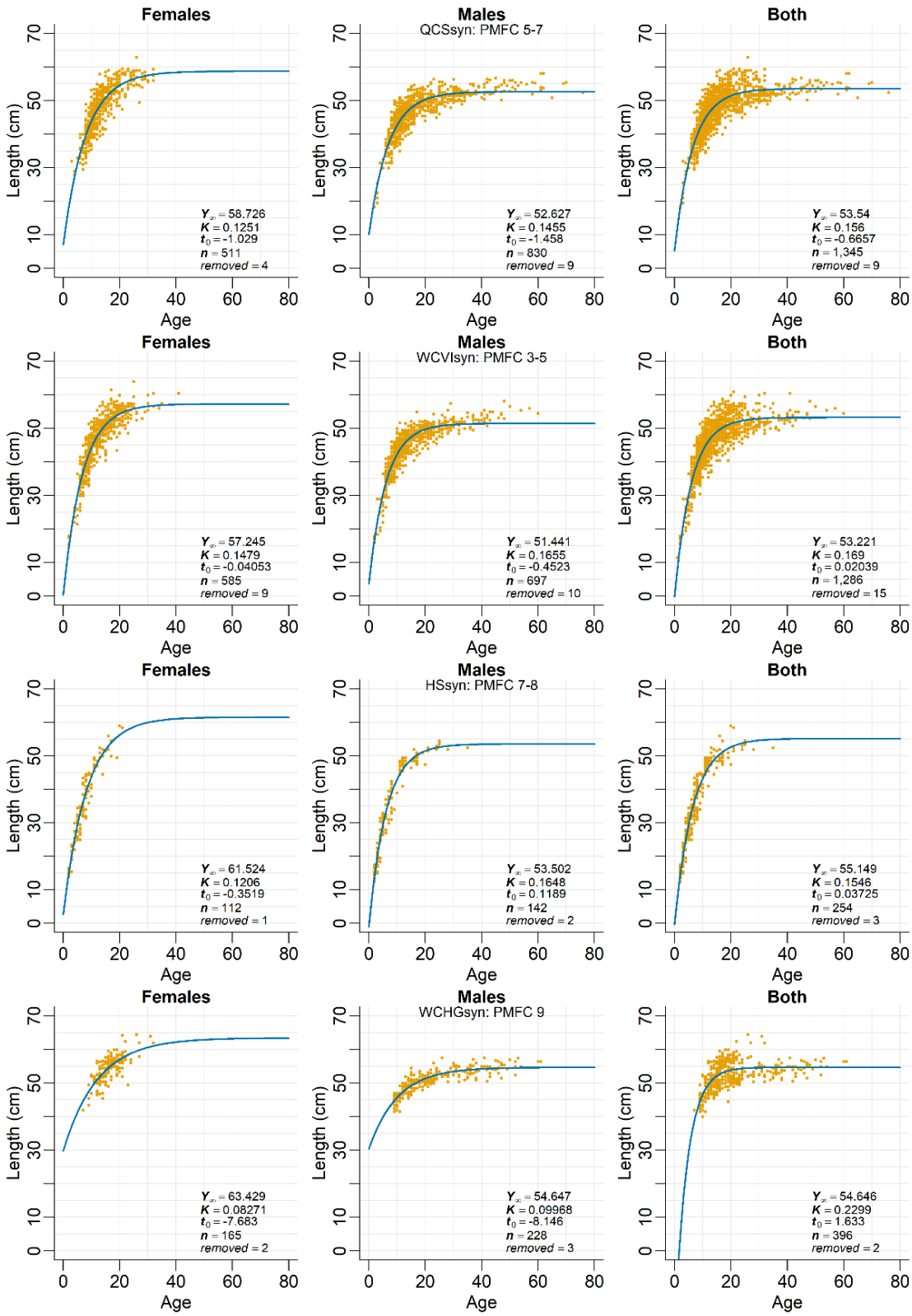

Figure D.5. Growth specified by age-length relationship: von Bertalanffy fits to CAR from four surveys: QCS synoptic, WCVI synoptic, HS synoptic, and WCHG synoptic. See caption in Figure D.3 for additional details.

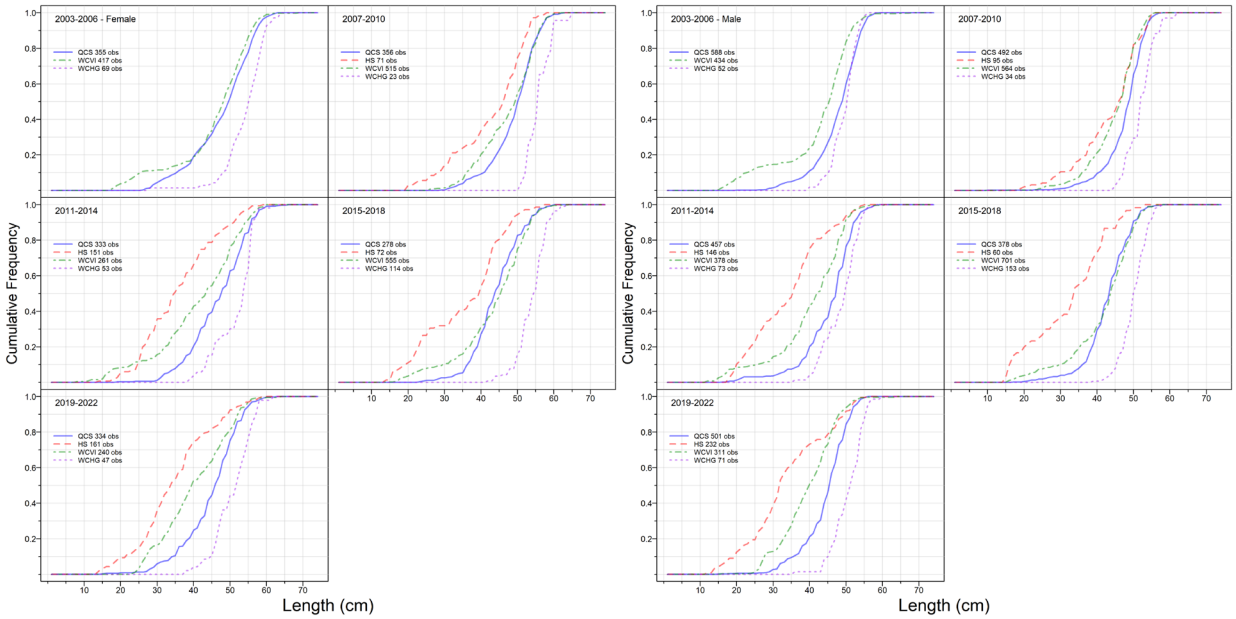

Figure D.6. Cumulative length frequencies for CAR females (left) and males (right) comparing synoptic surveys over 4-year blocks. QCS = Queen Charlotte Sound, HS = Hecate Strait, WCVI = west coast Vancouver Island, WCHG = west coast Haida Gwaii.

D.1.3. Maturity

This analysis was based on all (research, survey, and commercial combined) "staged" (examined for maturity status) females and males in the DFO GFBioSQL database. Maturity codes for CAR in the database (Table D.5) come from `MATURITY_CONVENTION_CODE = 1`, which describes seven maturity conditions for Rockfish (1977+).

Table D.5. GFBio maturity codes for rockfish, including BC rockfish.

Code	Female	Male
1	Immature - translucent, small	Immature - translucent, string-like
2	Maturing - small yellow eggs, translucent or opaque	Maturing - swelling, brown-white
3	Mature - large yellow eggs, opaque	
4	Fertilized - large, orange-yellow eggs, translucent	Mature - large white, easily broken
5	Embryos or larvae - includes eyed eggs	Ripe - running sperm
6	Spent - large flaccid red ovaries; maybe a few larvae	Spent - flaccid, red
7	Resting - moderate size, firm, red-grey ovaries	Resting - ribbon-like, small brown

Mature (stage 3) CAR females start appearing in July and are most abundant during the months of November through January, with fertilised females peaking in February followed by embryo-bearing fish also in February (Figure D.7, left). Ideally, lengths- and ages-at-maturity are calculated at times of peak development stages (males: insemination season, females: parturition season; Westrheim 1975). However, all months were used in creating the maturity curve because these data provided cleaner fits than using a subset of months. This required combining commercial and research data because most of the research/survey data do not extend into the late autumn, winter and early spring months.

The proportion female (Figure D.7, right) coastwide ranged from 0.29 in August to 0.47 in September, although this may be an artifact of sampling. The proportion female in samples tends to be low in winter and slightly higher in summer across the three regions (north=5DE,

central=5ABC, south=3CD). Generally, females appear to occur less frequently than males in BC waters and rarely account for more than 40% of the samples by sex.

For the maturity analysis, all stages 3 and higher were assumed to be mature, and a maturity ogive was fit to the filtered data using a double-normal model:

$$m_{as} = \begin{cases} e^{-(a-v_s)^2/\rho_{sL}}, & a \le v_s \\ 1, & a > v_s \end{cases} \quad \text{(D.3)}$$

where, m_{as} = maturity at age a for sex s (combined),

v_s = age of full maturity for sex s,

ρ_{sL} = variance for the left limb of the maturity curve for sex s.

To estimate a maturity ogive, the biological data records (recs) were qualified as follows:

• stocks – CAR coastwide	`major = 3:9`	`60,007 recs`
• ageing method (*see below)	`ameth = c(0,1*,3,17)`	`20,389 recs`
• years	`year = 1996:2021`	`14,892 recs`
• sample type – total catch/random	`stype = c(1,2,6,7)`	`14,718 recs`
• sex – females|males	`sex = c(2,1)`	`6,123|8,595 recs`
• maturity codes for rockfish	`mats = c(1:7)`	`4,192|5,580 recs`
• ogive age limits	`age = c(0,30)`	`4,145|4,800 recs`
• trip type – survey + commercial	`ttype = 1:5`	`4,145|4,800 recs`
• month – all months	`month = 1:12`	`4,145|4,800 recs`

Generally, rockfish biological analyses use ages from otoliths processed and read using the 'break and burn' procedure (`ameth=3`) or coded as 'unknown' (`ameth=0`) but processed in 1980 or later. There is also a method termed 'break and bake' (`ameth=17`); however, no CAR were processed using this technique. Additionally, rockfish otoliths aged 1-3 y are sometimes processed using surface readings (`ameth=1`) because the ageing lab finds this technique more reliable than B&B for very young fish; however, the protocol is usually applied to flatfish and hake only (S. Wischniowski, DFO, pers. comm, June 21, 2018).

The above qualification yielded 4,145 CAR female specimens from research surveys and the commercial fishery with maturity readings and valid ages. Mature specimens comprised those coded 3 to 7 for rockfish (Table D.5). The empirical proportion of mature females|males at each age was calculated (Figure D.8). A double-normal function (Eq. D.3) was fitted to the observed proportions mature at ages 1 to 30[1] to smooth the observations and determine an increasing monotonic function for use in the stock assessment model (Figure D.8). Additionally, a logistic function used by Vivian Haist (VH) for length models in New Zealand rock lobster assessments (Haist et al. 2009) was used to compare with the double normal model.

Following a procedure adopted by Stanley et al. (2009) for Canary Rockfish (*S. pinniger*), the proportions mature for young ages fitted by Eq. D.3 were not used because the fitted line may overestimate the proportion of mature females (Figure D.8). Therefore, the maturity ogive used in the stock assessment models (columns marked 'Mod m_a' in Table D.6) set proportion mature

[1] The ages used for fitting exclude ages greater than 30 to avoid potentially influential proportions caused by spurious values (due to sparse data).

to zero for ages 1 to 4, then switched to the fitted monotonic function for ages 5 to 18. All ages from 19 were forced to 1 (fully mature). This strategy follows previous BC rockfish stock assessments where it was recognised that younger ages are not well sampled and those that are, tend to be larger and more likely to be mature. The function of this ogive in the stock assessment model is to calculate the spawning biomass used in the Beverton-Holt stock recruitment function, and is treated as a constant known without error. The ages at 50% and full maturity are estimated from the double-normal fit at 10.6 y and 18.8 y, respectively for females, and 8.8 and 14 y for males, respectively.

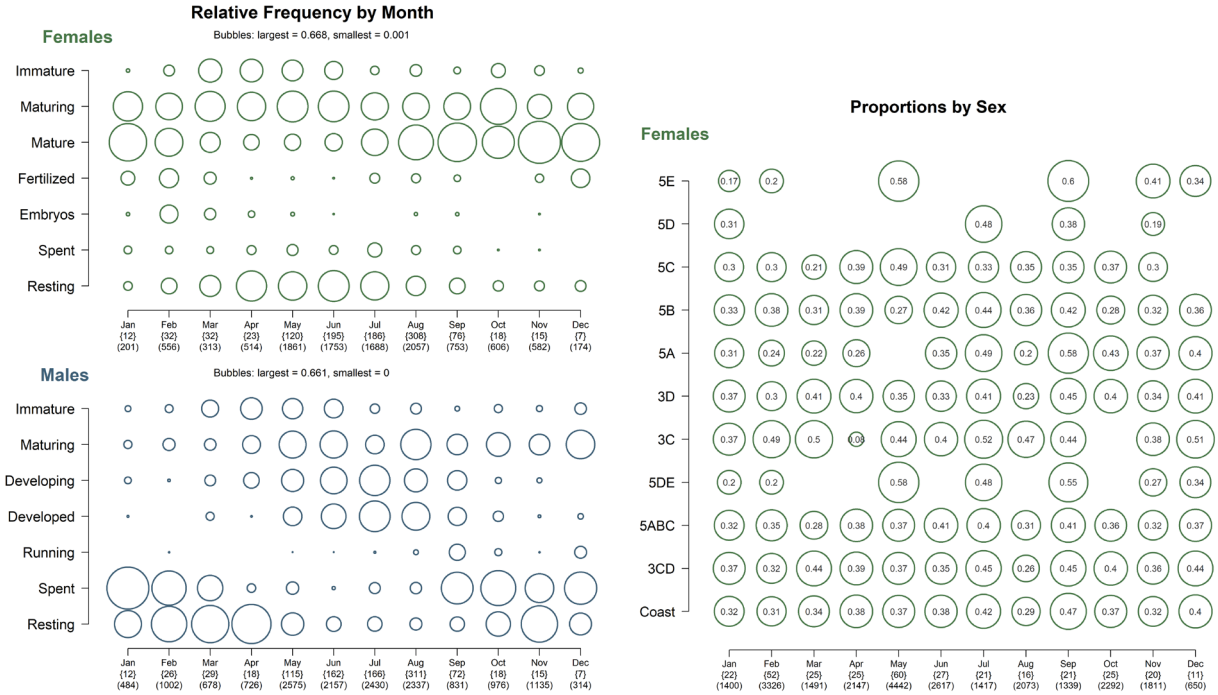

Figure D.7. Relative frequency of maturity codes by month (left) for CAR females and males. Data include maturities from commercial and research specimens. Frequencies are calculated among each maturity category for every month. Proportion CAR females by area and month (right) using commercial data.

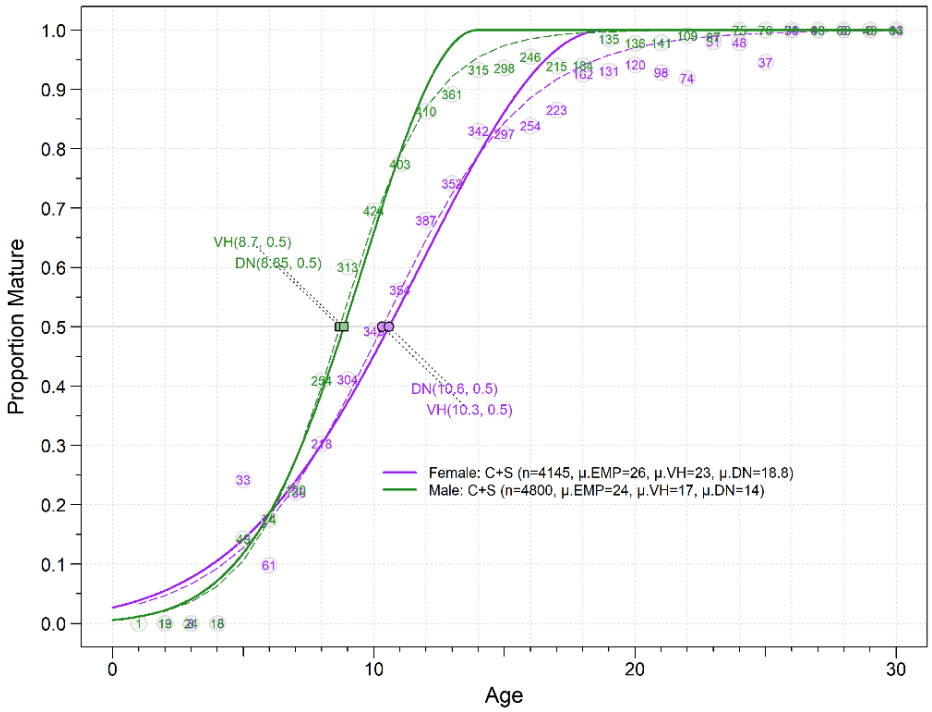

Figure D.8. Maturity ogives for CAR females (purple) and males (green). Solid line shows double-normal (DN) curve fit; dashed line shows logistic model fit (VH = Vivian Haist); numbers in circles denote number of specimens used to calculate the input proportions-mature (EMP =empirical). Estimated ages at 50% maturity are indicated near the median line; ages at full maturity (µ.VH, µ.DN) are displayed in the legend. Maturity data were limited to years from 1996 to 2021.

Table D.6. Proportion CAR females mature by age (m_a) used in the catch-age model ('Mod' column). Maturity stages 1 and 2 were assumed to be immature fish and all other staged fish (stages 3 to 7) were assumed to be mature. EMP = empirical, BL = binomial logit, VH =logistic used by Vivian Haist, DN = double normal (Eq.D.3), Mod = used in population model.

Age	# Fish	EMP m_a	BL m_a	VH m_a	DN m_a	Mod m_a
1	0	–	0.0537	0.0334	0.0389	0
2	13	0	0.0721	0.0472	0.0554	0
3	8	0	0.0961	0.0663	0.0774	0
4	15	0	0.1270	0.0925	0.1059	0
5	33	0.2424	0.1660	0.1276	0.1419	0.1419
6	61	0.0984	0.2141	0.1735	0.1864	0.1864
7	136	0.2206	0.2715	0.2314	0.2398	0.2398
8	218	0.3028	0.3378	0.3017	0.3023	0.3023
9	304	0.4112	0.4111	0.3827	0.3734	0.3734
10	349	0.4928	0.4885	0.4708	0.4518	0.4518
11	354	0.5621	0.5665	0.5607	0.5356	0.5356
12	387	0.6796	0.6414	0.6469	0.6221	0.6221
13	352	0.7415	0.7099	0.7244	0.7079	0.7079
14	342	0.8304	0.7700	0.7904	0.7892	0.7892
15	297	0.8249	0.8209	0.8440	0.8620	0.8620
16	254	0.8386	0.8625	0.8859	0.9225	0.9225
17	223	0.8655	0.8956	0.9176	0.9671	0.9671
18	162	0.9259	0.9215	0.9411	0.9933	0.9933
19	131	0.9313	0.9414	0.9582	1	1
20	120	0.9417	0.9565	0.9705	1	1
25	37	0.9459	0.9906	0.9950	1	1
30	13	1	0.9980	0.9992	1	1

D.1.4. Natural Mortality

In the previous stock assessment for CAR (Stanley et al., 2009), natural mortality (*M*) was fixed at 0.06 for males and 0.06 for females up to age 13 then 0.12 for ages 14 and older. The reasons cited were that US assessments found the best fit when female *M* was allowed to increase coincident with reproductive maturation.

The Hoenig (1983) estimator describes an exponential decay LN(*k*) = -*Z* t_L, where *Z* = natural mortality, t_L = longevity of a stock, and *k* = proportion of animals that are still alive at t_L. Quinn and Deriso (1999) popularised this estimator by re-arranging Hoenig's equation and setting *k*=0.01 (as originally suggested by Hoenig):

$$M = -\ln(0.01) \,/\, t_{\max} \tag{D.4}$$

Then et al. (2015) revisited various natural mortality estimators and recommended the use of an updated Hoenig estimator based on nonlinear least squares:

$$M = 4.899 t_{\max}^{-0.916} \tag{D.5}$$

where t_{max} = maximum age.

During the review process for Redstripe Rockfish (DFO 2022a), one of the principal reviewers, Vladlena Gertseva (Northwest Fisheries Science Center, NOAA, pers. comm., 2018), noted that Then et al. (2015) did not consistently apply a log transformation. In real space, one might expect substantial heteroscedasticity in both the observation and process errors associated with the relationship of *M* to t_{max}. Re-evaluating the data used in Then et al. (2015) by fitting the one-parameter t_{max} model using a log-log transformation (such that the slope is forced to be -1 in the transformed space, as in Hamel 2015), Gertseva recalculated the point estimate for *M* as:

$$M = 5.4 \,/\, t_{\max} \tag{D.6}$$

In past CSAS Regional Peer Review meetings, participants have been averse to adopting a maximum age that comes from a single, usually isolated individual, preferring instead to observe the tail distribution of ages (Figure D.9). For CAR, we set t_{max} = 99% quantile of the age data by sex: female t_{max}=33 y, male t_{max}=58 y. Using Hoenig (1983) and Gertseva/Hamel estimators, female *M*=0.140 and 0.164, respectively, while male *M*=0.079 and 0.093, respectively. These values exceed what we deemed plausible for a fish that lives to 84 y, which would yield a low *M* of 0.055 and 0.064, respectively. Table D.7 calculates possible *M* values based on the two estimators. In this assessment, the base run estimates *M* using a normal prior N(0.06, 0.018) without splitting *M* by maturity for females (but see Sensitivity section F.2.3. in Appendix F).

Table D.7. Estimates of CAR natural mortality M using equations based on fish longevity (males and females combined). Various ages > 0.95 quantile up to the observed t_{max} = 84y (males) are used to illustrate the variability in M based on alternative 'maximum' ages. Empirical cumulative distribution function in R [function(x,pc) ecdf(x)(pc)] was used to estimate quantiles for various ages.

Age	Quantile from `ecdf`	Hoenig (1983) `M=-LN(0.01)/tmax`	Gertseva/Hamel `M=5.4/tmax`
40	0.9519	0.115	0.135
50	0.9804	0.092	0.108
60	0.9956	0.077	0.090
70	0.9993	0.066	0.077
80	0.9999	0.058	0.068
84	1	0.055	0.064

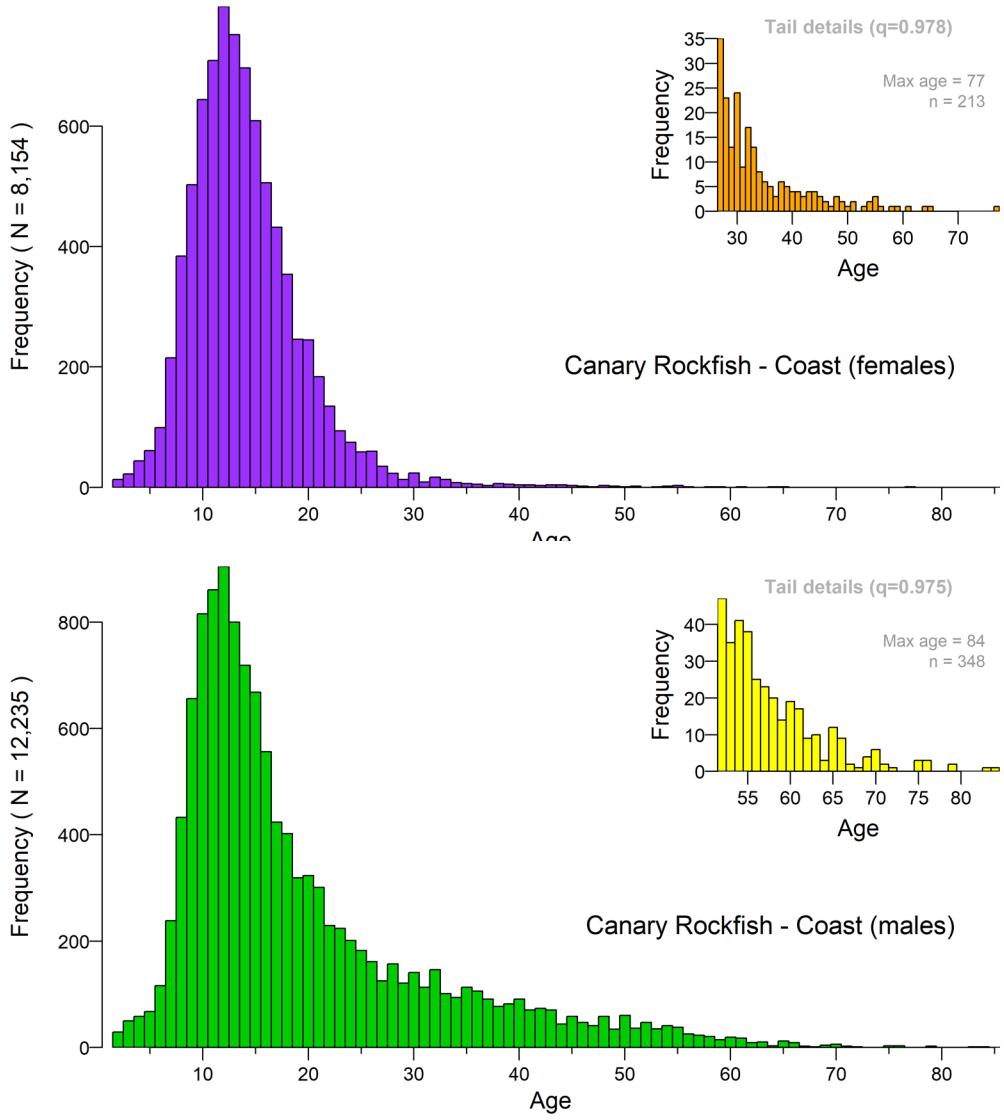

Figure D.9. Distribution of CAR female (top) and male (bottom) ages; insets shows details for female ages >=27 y and male ages >=47 y old, which are the 0.975 quantiles of the age data set by sex.

D.1.5. Generation Time

Generation time t_G is assumed to be the average age of adults (males and females) in the population, approximated by the age of first reproduction plus the inverse of adult natural mortality[2], and takes the form:

[2] This equation assumes that natural mortality after the age of first reproduction is well known, and mortality and fecundity do not change with age after the age of first reproduction (i.e., there is no senescence). For species that exhibit senescence (mortality increasing and fecundity decreasing) with age, this formula will overestimate generation time (Section 4.4, option 2 of IUCN Standards and Petitions Committee 2022).

$$t_G = k + \frac{1}{e^M - 1} \quad \text{(D.7)}$$

where k = age at 50% maturity,
M = instantaneous rate of natural mortality.

Using a Taylor expansion, $e^M = 1 + M + M^2/2$, COSEWIC adopts a rough approximation to generation time for small values of M:

$$t_G = k + \frac{1}{M} \quad \text{(D.8)}$$

From Section D.1.3, k = 10.6 y for CAR females. If we assume that M = 0.064 (using age=84 in Table D.7), then the COSEWIC estimate of generation time (D.8) t_G = 26 y for the coastwide stock. For simplicity, we adopt t_G = 25 years, which was close to the generation time of 22.8 years (M~0.09) for a 2005 US assessment (Methot and Stewart 2005).

D.2. WEIGHTED AGE PROPORTIONS

This section summarises a method for representing commercial and survey age structures in the stock assessment model for a given species (herein called 'target') through weighting observed age frequencies x_a or proportions x'_a by catch‖density in defined strata (h). (Throughout this section, the symbol '‖' is used to delimit parallel values for commercial and survey analyses, respectively, as the mechanics of the weighting procedure are similar for both. The symbol can be read 'or', e.g., catch or density.) For commercial samples, these strata comprise quarterly periods within a year, while for survey samples, the strata are defined by longitude, latitude, and depth boundaries unique to each survey series. A two-tiered weighting system is used as follows:

Within each stratum h, commercial age samples were identified by trip (usually one sample per trip[3]) and the age frequencies per trip were weighted by the target catch weight (tonnes) of the tows that were sampled to yield one weighted age frequency per stratum (quarter). For each year, the quarterly age frequencies were then weighted by the quarterly fishery catch of the target. If a quarter had not been sampled, it was not used in the weighting for the year. For example, if samples of the target were missing in Oct-Dec of a particular year, only the first three quarters of target catch would be used to prorate three quarterly age frequencies in that year, resulting in a single age frequency for the year.

Annual survey ages were weighted similarly. Each sampled tow in a survey stratum was weighted by the tow's target catch density (t/km^2) to yield a single weighted age frequency per stratum. As above, not all survey strata had age samples and so weighted age frequencies by sampled stratum were weighted by the appropriate stratum area (km^2). For example, if only shallow strata were sampled for age, the deep strata areas were not used to prorate the shallow-strata age frequencies. As for commercial ages, the two-tiered weighting scheme yielded one age frequency per survey year.

Ideally, sampling effort would be proportional to the amount of the target caught, but this is not usually the case. Personnel can control the sampling effort on surveys more than on board commercial vessels, but the relative catch among strata over the course of a year or survey

[3] Samples were combined, weighted by the tow weight, for trips with more than one sample to give a single age frequency for each trip.

cannot be known with certainty until the events have occurred. Therefore, the stratified weighting scheme outlined above and detailed below attempts to adjust for unequal sampling effort among strata.

For simplicity, the weighting of age frequencies x_a is used for illustration, unless otherwise specified. The weighting occurs at two levels: h (quarters for commercial ages, strata for survey ages) and i (years if commercial, total stratum area if survey). Notation is summarised in Table D.8.

Table D.8. Equations for weighting age frequencies or proportions; (c) = commercial, (s) = survey.

Symbol	Description
	Indices
a	age class (1 to A, where A is an accumulator age-class)
d	(c) trip ID as sample unit (usually one sample per trip) (s) sample ID as sample unit (usually one sample per survey tow)
h	(c) calendar year quarter (1 to 4), 91.5 days each (s) survey stratum (area-depth combination)
i	(c) calendar year (1977 to present) (s) single survey ID in survey series (e.g., 2003 QCS Synoptic)
	Data
x_{adhi}	observations-at-age a for sample unit d in quarter‖stratum h of year‖survey i
x'_{adhi}	proportion-at-age a for sample unit d in quarter‖stratum h of year‖survey i
C_{dhi}	(c) commercial catch (tonnes) of the target for sample unit d in quarter h of year i (s) density (t/km^2) of the target for sample unit d in stratum h of survey i
C'_{dhi}	C_{dhi} as a proportion of total catch‖density $C_{hi} = \sum_d C_{dhi}$
y_{ahi}	weighted age frequencies at age a in quarter‖stratum h of year‖survey i
K_{hi}	(c) total commercial catch (t) of the target in quarter h of year i (s) stratum area (km^2) of stratum h in survey i
K'_{hi}	K_{hi} as a proportion of total catch‖area $K_i = \sum_h K_{hi}$
p_{ai}	weighted frequencies at age a in year‖survey i
p'_{ai}	weighted proportions at age a in year‖survey i

For each quarter‖stratum h, sample unit frequencies x_{ad} are weighted by sample unit catch‖density of the target species. (For commercial ages, trip is used as the sample unit, though at times one trip may contain multiple samples. In these instances, multiple samples from a single trip will be merged into a single sample unit.) Within any quarter‖stratum h and year‖survey i there is a set of sample catches‖densities C_{dhi} that can be transformed into a set of proportions:

$$C'_{dhi} = C_{dhi} \Big/ \sum_d C_{dhi} \ . \tag{D.9}$$

The proportion C'_{dhi} is used to weight the age frequencies x_{adhi} summed over d, which yields weighted age frequencies by quarter‖stratum for each year‖survey:

$$y_{ahi} = \sum_{d} \left(C'_{dhi} x_{adhi} \right). \tag{D.10}$$

This transformation reduces the frequencies x from the originals, and so y_{ahi} is rescaled (multiplied) by the factor

$$\sum\nolimits_a x_{ahi} \Big/ \sum\nolimits_a y_{ahi} \tag{D.11}$$

to retain the original number of observations. (For proportions x' this is not needed.) Although this step is performed, it is strictly not necessary because at the end of the two-step weighting, the weighted frequencies are transformed to represent proportions-at-age.

At the second level of stratification by year‖survey i, the annual proportion of quarterly catch (t) for commercial ages or the survey proportion of stratum areas (km^2) for survey ages is calculated

$$K'_{hi} = K_{hi} \Big/ \sum\nolimits_h K_{hi} \tag{D.12}$$

to weight y_{ahi} and derive weighted age frequencies by year‖survey:

$$p_{ai} = \sum_{h} \left(K'_{hi} y_{ahi} \right). \tag{D.13}$$

Again, if this transformation is applied to frequencies (as opposed to proportions), it reduces them from the original, and so p_{ai} is rescaled (multiplied) by the factor

$$\sum\nolimits_a y_{ai} \Big/ \sum\nolimits_a p_{ai} \tag{D.14}$$

to retain the original number of observations.

Finally, the weighted frequencies are transformed to represent proportions-at-age:

$$p'_{ai} = p_{ai} \Big/ \sum\nolimits_a p_{ai}\,. \tag{D.15}$$

If initially we had used proportions x'_{adhi} instead of frequencies x_{adhi}, the final transformation would not be necessary; however, its application does not affect the outcome.

The choice of data input (frequencies x vs. proportions x') can sometimes matter: the numeric outcome can be very different, especially if the input samples comprise few observations. Theoretically, weighting frequencies emphasises our belief in individual observations at specific ages while weighting proportions emphasises our belief in sampled age distributions. Neither method yields inherently better results; however, if the original sampling methodology favoured sampling few fish from many tows rather than sampling many fish from few tows, then weighting frequencies probably makes more sense than weighting proportions. In this assessment, age frequencies x are weighted.

D.2.1. Commercial Ages

For the CAR stock, sampled age frequencies (AF) from the trawl fishery were combined; the shrimp trawl data were not used. Therefore, the model was run assuming a joint selectivity for all trawl gear types (bottom and midwater). The commercial trawl AF dataset spans years 1977

to 2017, but drops years 1981, 1989, and 2014 because these years were only represented by one sample each (Table D.9, Figure D.10). The remaining trawl AF dataset included 36 years.

The 2018 stock assessment of Redstripe Rockfish (Starr and Haigh 2021a) did not separate sorted (by size or sex) and unsorted samples when introducing proportions-at-age into the model. This practice was also followed for the 2019 BOR stock assessment after exploratory runs using only sorted and only unsorted samples were examined. Usually the sorted samples occur earlier in the time series than do the unsorted samples. Consequently, dropping sorted samples loses information about early recruitment strength. This stock assessment uses combined sorted and unsorted samples for CAR AFs.

Table D.9. Commercial trip quarterly data from the 'Trawl' fishery used to weight CAR proportions-at-age: number of sampled trips, CAR catch (t) by sampled trip and by all trips.

Year	# Trips | # Samples				Sampled catch (t)				Fishery catch (t)			
	Q1	Q2	Q3	Q4	Q1	Q2	Q3	Q4	Q1	Q2	Q3	Q4
REBS north Trawl Fishery												
1977	–	3 | 3	–	–	–	65.74	–	–	11	180	136	30
1978	–	2 | 2	4 | 4	3 | 3	–	17.34	52.31	43.43	9	139	210	91
1979	1 | 1	1 | 1	1 | 1	1 | 1	7.29	3.57	26.99	15.62	20	276	183	87
1980	1 | 1	–	1 | 1	1 | 1	19.51	–	11.34	18.14	54	269	212	79
1981	1 | 1	–	–	–	6.80	–	–	–	32	131	101	118
1982	1 | 1	2 | 2	–	–	5.94	54.43	–	–	53	276	192	232
1983	–	2 | 3	–	–	–	106.60	–	–	23	765	349	225
1984	–	2 | 3	–	–	–	68.04	–	–	127	906	609	148
1985	1 | 1	–	–	1 | 1	27.22	–	–	22.68	213	729	188	369
1988	–	–	–	2 | 2	–	–	–	13.61	112	542	754	414
1989	–	1 | 1	–	–	–	12.25	–	–	103	655	619	435
1990	3 | 3	2 | 2	1 | 1	2 | 2	32.21	14.06	4.31	4.54	366	602	455	218
1991	7 | 7	1 | 1	–	–	39.33	6.35	–	–	327	502	389	151
1992	1 | 1	2 | 2	–	–	3.63	5.94	–	–	279	559	347	242
1993	–	1 | 1	–	3 | 3	–	1.59	–	5.90	187	489	259	211
1994	1 | 1	2 | 2	3 | 3	5 | 5	6.80	5.31	9.66	19.51	166	398	308	325
1995	1 | 1	1 | 1	3 | 3	–	7.03	0.91	12.48	–	153	262	434	12
1996	–	2 | 3	4 | 4	–	–	3.56	7.57	–	41	207	166	102
1997	–	–	1 | 1	7 | 8	–	–	0.13	16.73	192	135	120	170
1998	12 | 13	6 | 6	3 | 3	3 | 3	34.95	32.84	6.96	18.07	266	212	180	158
1999	5 | 5	5 | 5	3 | 4	2 | 2	27.58	15.16	23.20	1.48	210	254	248	188
2000	7 | 9	3 | 3	1 | 1	–	54.32	6.36	0.08	–	219	110	119	186
2001	5 | 6	2 | 2	3 | 3	–	61.40	3.91	10.42	–	355	191	187	166
2002	2 | 2	2 | 2	3 | 3	1 | 1	22.68	15.42	13.89	0.19	249	237	170	212
2003	4 | 4	2 | 3	3 | 3	1 | 1	6.62	11.22	9.03	2.49	252	217	193	212
2004	7 | 8	4 | 4	1 | 2	1 | 1	21.23	7.05	8.02	1.47	212	215	158	170
2005	2 | 2	9 | 9	1 | 1	5 | 5	6.21	25.79	1.00	13.24	234	264	153	142
2006	5 | 5	6 | 6	3 | 3	2 | 3	22.73	27.45	9.75	16.24	332	284	137	99
2007	–	1 | 1	1 | 1	2 | 2	–	1.85	3.27	3.72	237	220	154	127
2008	–	1 | 1	2 | 2	3 | 3	–	10.02	13.77	20.65	225	177	172	213
2009	–	–	2 | 2	1 | 1	–	–	1.25	2.27	277	202	102	105
2010	7 | 7	2 | 2	1 | 1	–	24.83	6.80	0.05	–	283	211	91	114
2011	3 | 4	1 | 1	1 | 1	1 | 1	36.44	0.17	5.90	1.59	225	205	111	146
2012	2 | 2	1 | 1	1 | 1	1 | 1	6.56	2.81	12.08	5.68	218	202	180	105
2013	3 | 3	3 | 3	–	–	21.00	17.15	–	–	252	218	136	147
2014	–	–	–	1 | 1	–	–	–	2.24	291	272	170	168
2015	–	1 | 1	1 | 1	–	–	6.69	2.36	–	318	277	133	117
2016	–	3 | 3	–	–	–	4.88	–	–	224	240	128	115
2017	4 | 4	1 | 1	2 | 2	–	6.27	0.62	3.02	–	299	264	155	93

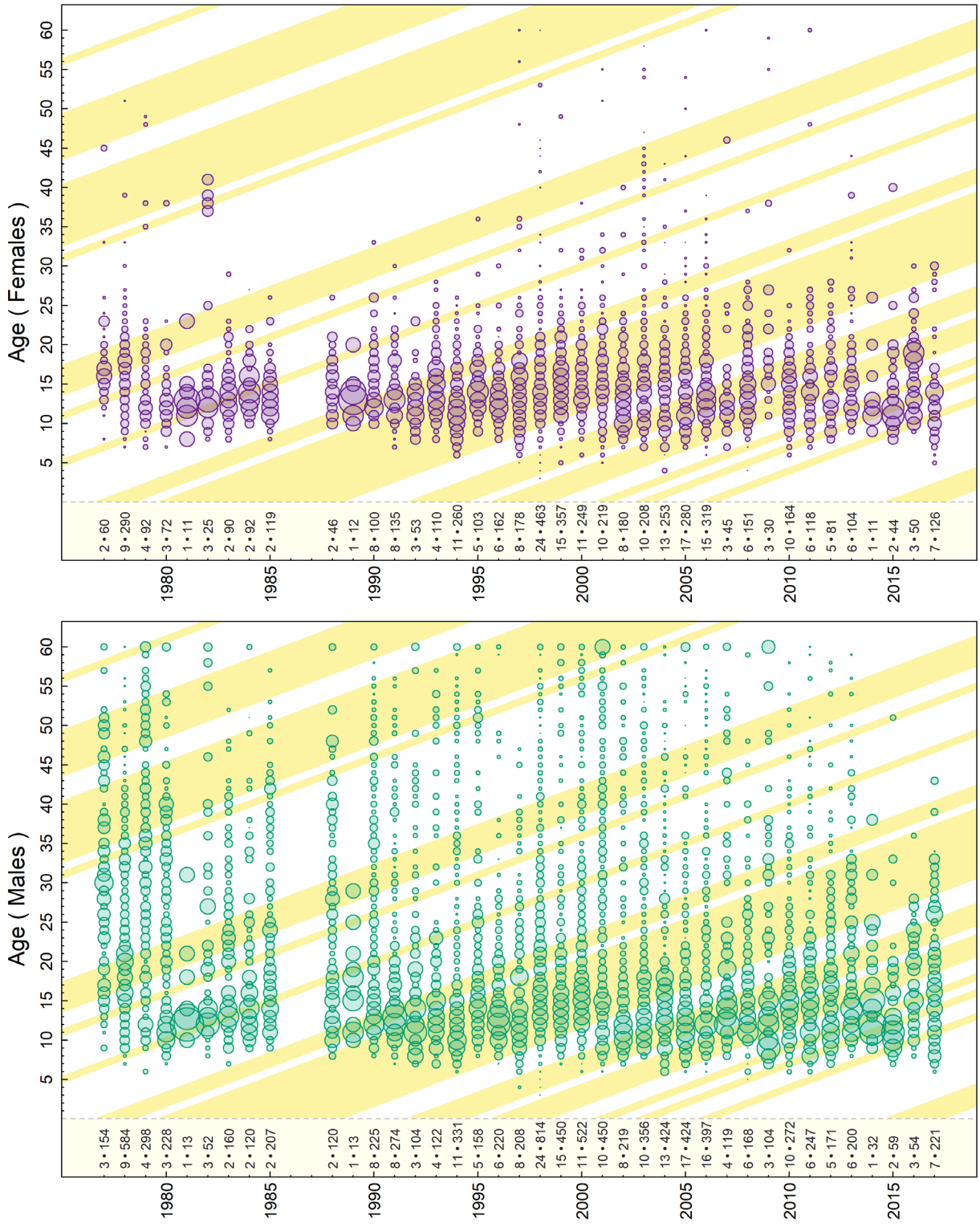

Figure D.10. Proportions-at-age for CAR caught along the coast of BC by commercial trawl gear calculated as age frequencies weighted by trip catch within quarters and commercial catch within years. Diagonal shaded bands indicate year when the mean winter (Dec-Mar) Pacific Decadal Oscillation was positive. Numbers displayed along the bottom axis indicate number of samples and number of fish aged (bullet delimited) by year.

D.2.2. Research/Survey Ages

Age data for CAR from the surveys cover years from 1977 to 2019 (Table D.10). Age cohort patterns are typically obscure in survey data.

The coastwide CAR stock is covered by several surveys with AF data (Figure D.11 to Figure D.14), but only the following three AF series were used in the base model run:

- QCS Synoptic (9 y AF) from 2004-2021;
- WCVI Synoptic (8 y AF) from 2004-2021;
- NMFS Triennial (6 y AF) from 1980-2001.

Sensitivity analyses explored the inclusion of these surveys:

- HS Synoptic (5 y AF) from 2011-2019 (2009 dropped, one sample only);
- WCHG Synoptic (4 y AF) from 1997 to 2018 (2006 & 2010 dropped, one sample each);
- HBLL North (5 y AF) from 2006-2015;
- HBLL South (5 y AF) from 2007-2016.

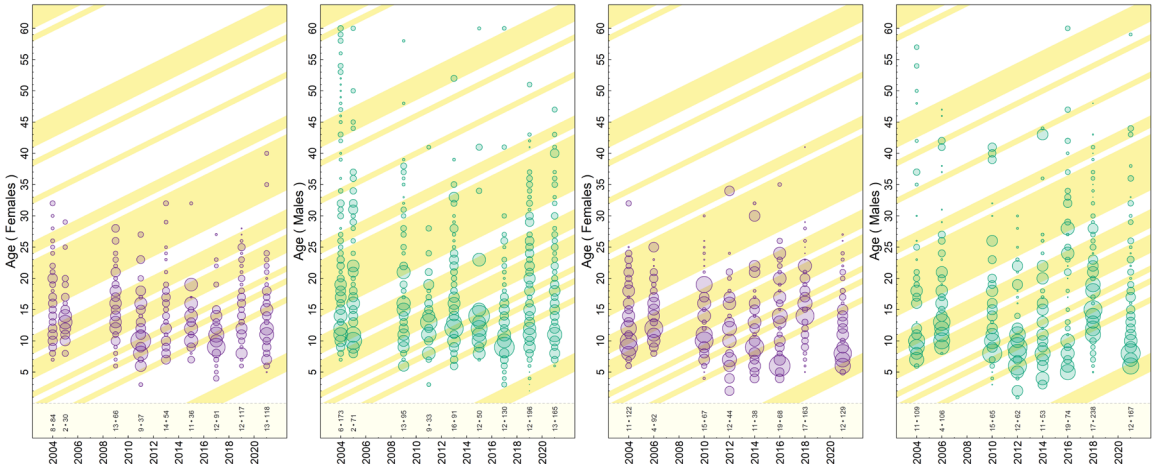

Figure D.11. QCS Synoptic (left) and WCVI Synoptic (right) – proportions-at-age based on age frequencies weighted by mean fish density within strata and by total stratum area within survey (Table D.10). See Figure D.10 for details on diagonal shaded bands and displayed numbers.

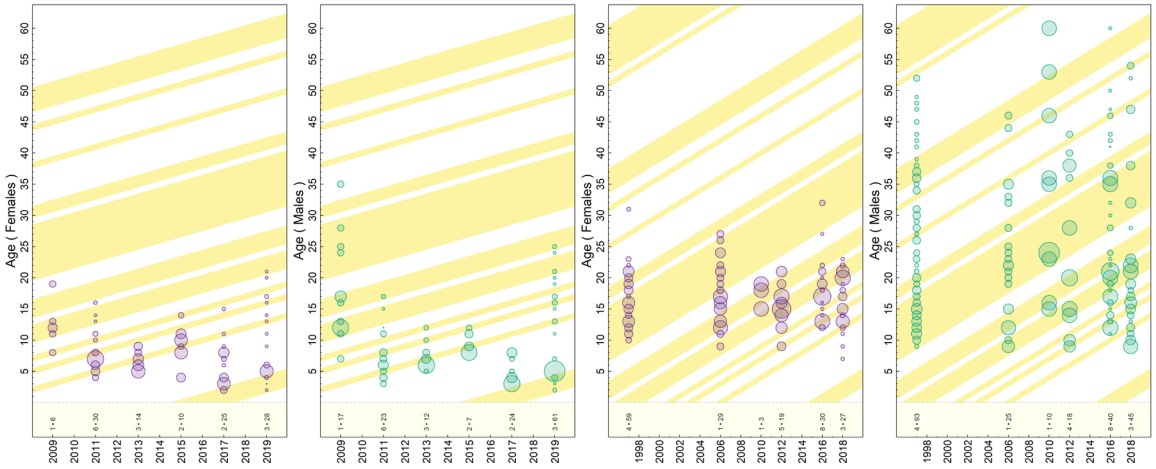

Figure D.12. HS Synoptic (left) and WCHG Synoptic (right) – proportions-at-age based on age frequencies weighted by mean fish density within strata and by total stratum area within survey (Table D.10). See Figure D.10 for details on diagonal shaded bands and displayed numbers.

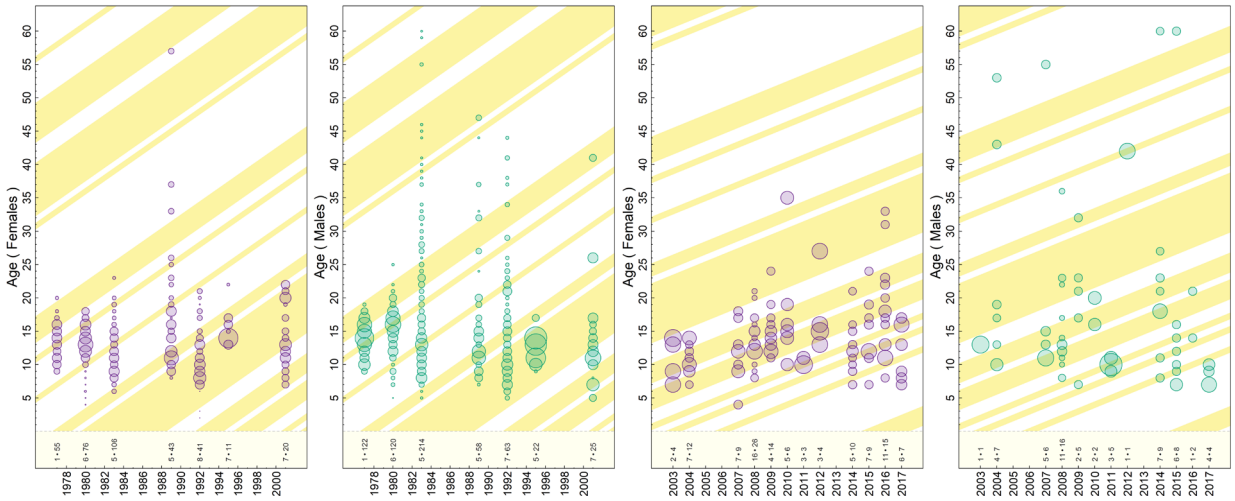

Figure D.13. NMFS Triennial (left) and IPHC Longline (right) – proportions-at-age based on age frequencies weighted by mean fish density within strata and by total stratum area within survey (Table D.10). See Figure D.10 for details on diagonal shaded bands and displayed numbers.

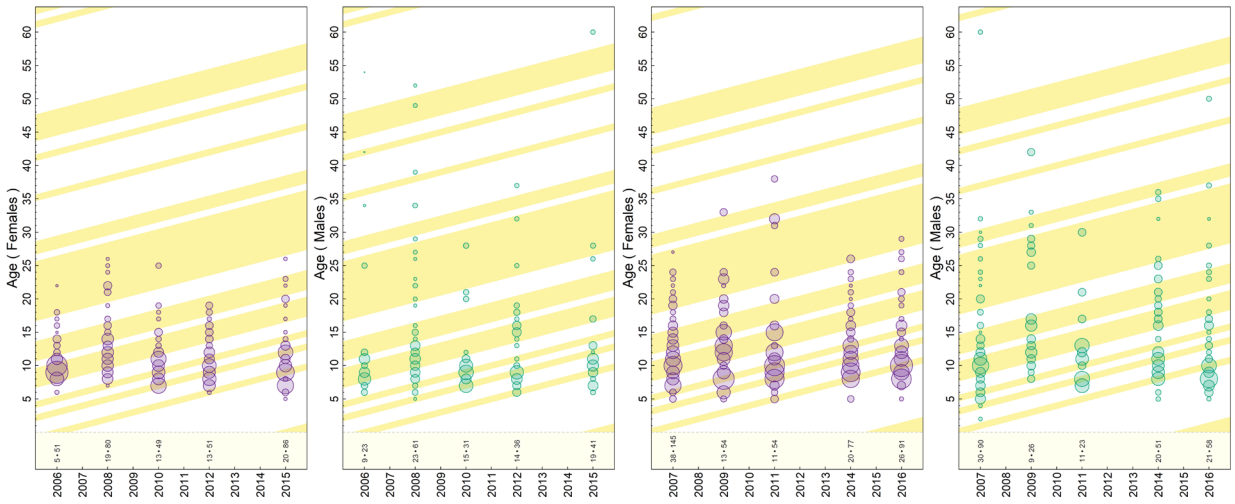

Figure D.14. HBLL Outside North (left) and HBLL Outside South (right) – proportions-at-age based on age frequencies weighted by mean fish density within strata and by total stratum area within survey (Table D.10). See Figure D.10 for details on diagonal shaded bands and displayed numbers.

Table D.10. Number of CAR age samples (s) collected from trawl surveys used in base run and CAR density (d=kg/km^2) by survey stratum identifier (h); stratum area is shown in parentheses.

Year	Survey Strata								
QCS	h=18 (5,012 km^2)	h=19 (5,300 km^2)	h=20 (2,640 km^2)	h=22 (1,740 km^2)	h=23 (3,928 km^2)	h=24 (3,664 km^2)	–	–	–
2004	–	s=3, d=0.606	–	s=1, d=1.328	s=4, d=1.587	–	–	–	–
2005	–	–	–	–	s=2, d=6.500	–	–	–	–
2009	s=2, d=2.889	s=3, d=0.600	–	s=2, d=3.735	s=6, d=1.231	–	–	–	–
2011	s=2, d=0.203	s=1, d=1.058	–	–	s=6, d=1.148	–	–	–	–
2013	s=2, d=0.338	s=3, d=1.015	–	s=1, d=3.413	s=10, d=1.057	–	–	–	–
2015	s=1, d=0.111	s=4, d=1.724	–	s=1, d=0.576	s=6, d=1.312	–	–	–	–
2017	s=1, d=0.065	s=4, d=0.512	s=2, d=0.172	s=1, d=0.079	s=3, d=0.224	s=1, d=0.649	–	–	–
2019	–	s=3, d=3.043	–	s=3, d=4.322	s=6, d=0.730	–	–	–	–
2021	s=1, d=10.866	s=1, d=0.831	–	s=1, d=0.591	s=9, d=0.577	s=1, d=0.154	–	–	–
WCVI	h=65 (5,716 km^2)	h=66 (3,768 km^2)	h=67 (708 km^2)	h=68 (572 km^2)	–	–	–	–	–
2004	s=3, d=0.446	s=8, d=0.523	–	–	–	–	–	–	–
2006	–	s=4, d=13.404	–	–	–	–	–	–	–
2010	s=4, d=0.645	s=10, d=3.749	–	s=1, d=0.275	–	–	–	–	–
2012	s=5, d=0.149	s=6, d=3.738	s=1, d=0.209	–	–	–	–	–	–
2014	s=4, d=0.186	s=4, d=2.465	s=3, d=0.176	–	–	–	–	–	–
2016	s=4, d=0.204	s=11, d=0.963	s=4, d=2.141	–	–	–	–	–	–
2018	–	s=9, d=4.547	s=8, d=2.239	–	–	–	–	–	–
2021	s=2, d=1.207	s=5, d=1.963	s=5, d=2.851	–	–	–	–	–	–
NMFS	h=475 (12,405 km^2)	h=476 (12,405 km^2)	h=477 (12,405 km^2)	h=479 (12,405 km^2)	h=480 (12,405 km^2)	h=482 (12,405 km^2)	h=483 (12,405 km^2)	h=485 (12,405 km^2)	h=497 (12,405 km^2)
1977	–	–	–	–	–	–	–	–	s=1, d=49.320
1980	s=1, d=0.126	s=5, d=0.877	–	–	–	–	–	–	–
1983	–	s=1, d=0.295	s=3, d=1.864	–	–	–	–	s=1, d=9.273	–
1989	–	–	–	s=3, d=0.713	s=1, d=4.615	–	s=1, d=0.155	–	–
1992	–	–	–	s=1, d=0.316	s=4, d=0.191	–	s=3, d=0.130	–	–
1995	–	–	–	–	s=6, d=0.038	–	s=3, d=0.068	–	–
2001	–	–	–	s=4, d=0.041	s=2, d=0.101	s=1, d=0.068	s=1, d=0.065	–	–

D.2.3. Ageing Error

Accounting for ageing error in stock assessments helps to identify episodic recruitment events. Figure D.15 suggests that CAR ages determined by primary readers are produced fairly consistently by secondary readers when performing spot-check analyses; however, there are some large deviations which become more extreme at older ages. Therefore, the population model for CAR uses an ageing error (AE) vector based on standard deviations that are calculated from the CV of observed lengths-at-age (AE2, Figure D.16, Table D.11). Explicitly, the ageing error vector used was the standard deviation for each age determined as the CV of lengths-at-age multiplied by the corresponding age a:

$$\mathrm{AE}_2 = \sigma_a = a\ \mathrm{CV}_{L_a}, \text{ where } \mathrm{CV}_{L_a} = \sigma_{L_a} / \mu_{L_a}.$$

Based on feedback during the Yellowmouth Rockfish assessment of 2021 (DFO 2022b), AE2 was loess-smoothed to produce AE3, which was used in the current CAR assessment's base case.

Additionally, ageing error can be determined from the CVs of otolith ages spot-checked by secondary readers for otoliths previously read by a primary reader (counting of otolith rings):

$$\mathrm{AE}_4 = \sigma_a = a\ \mathrm{CV}_{A_a}, \text{ where } \mathrm{CV}_{A_a} = \sigma_{A_a} / \mu_{A_a}.$$

Similarly, AE5 is the loess-smoothed vector of AE4.

Lastly, AE6 describes a CASAL-style (constant CV, Bull et al. 2012) ageing error where the standard deviation used in SS3 was directly proportional to age (Figure D.16). Essentially,

$$\mathrm{AE}_6 = \sigma_a = a\ \mathrm{CV}_{A_a}, \text{ where } \mathrm{CV}_{A_a} = 0.1$$

Alternative AE vectors (AE1: no ageing error, AE5, and AE6), were explored in sensitivity analyses.

In the SS3 data file, ages start at 0 and end at *A* (60 for CAR), which means A+1 entries are needed. In the ageing error section of the data file, we specified ages 0.5 to 60.5 with the entries of σ_a from Table D.11 for ages 1 to 61.

Ageing error can also be estimated using statistical models that use multiple age readings from individual fish to derive a classification matrix that defines the probability of assigning an observed age to a fish based on its true age (Richards et al. 1992). True ages are not known but can be considered the most probable value for the observed ages with a degree of imprecision depicted using normal, exponential, or age reader error (Richards et al. 1992).

Table D.11. Calculating ageing error (AE) vector for use in SS3 from CVs of observed lengths-at age L_a or CVs of primary age readers' ages spot-checked by secondary readers A_a, where n_{La}/n_{Aa} = number of lengths observed at each age a, $\mu_{La}/\mu A_a$ = mean length at age, σ_{La}/σ_{Aa} = standard deviation of mean length at age, and CV=σ/μ.

a	n_{La}	μ_{La}	σ_{La}	CV_{La}	n_{Aa}	μ_{Aa}	σ_{Aa}	CV_{Aa}	AE2	AE3	AE4	AE5	AE6
1	1	11.5	0.000	0.200	0	0.0	0	0.2	0.200	0.340	0.200	0.360	0.1
2	31	15.6	1.576	0.101	6	2.5	0.548	0.219	0.202	0.395	0.438	0.424	0.2
3	32	20.6	3.607	0.175	10	3.2	0.422	0.132	0.525	0.449	0.395	0.488	0.3
4	31	26.1	3.868	0.148	14	4.0	0.392	0.098	0.594	0.503	0.392	0.550	0.4
5	71	30.8	4.064	0.132	11	5.5	0.820	0.148	0.659	0.558	0.740	0.611	0.5
6	154	34.2	4.199	0.123	37	6.0	0.499	0.084	0.736	0.613	0.502	0.672	0.6
7	255	37.2	3.923	0.106	48	7.1	0.577	0.082	0.739	0.667	0.571	0.733	0.7
8	418	39.6	3.786	0.096	74	8.1	0.792	0.098	0.765	0.722	0.787	0.792	0.8
9	456	41.5	3.700	0.089	82	9.0	1.159	0.128	0.802	0.777	1.155	0.851	0.9
10	493	43.7	3.488	0.080	94	10.1	1.274	0.126	0.798	0.833	1.261	0.911	1
11	553	45.1	3.495	0.077	116	11.1	0.997	0.090	0.852	0.888	0.986	0.969	1.1
12	501	46.6	3.559	0.076	118	12.0	1.237	0.103	0.916	0.943	1.236	1.025	1.2
13	423	47.7	3.512	0.074	98	13.0	1.585	0.122	0.957	0.996	1.590	1.082	1.3
14	400	48.7	3.395	0.070	64	14.0	0.951	0.068	0.977	1.049	0.950	1.141	1.4
15	407	48.9	3.345	0.068	77	14.9	1.325	0.089	1.026	1.102	1.338	1.196	1.5
16	307	50.3	3.408	0.068	59	15.8	1.262	0.080	1.084	1.156	1.275	1.241	1.6
17	262	50.5	3.657	0.072	47	16.7	1.151	0.069	1.232	1.208	1.169	1.275	1.7
18	207	50.9	3.467	0.068	28	17.3	1.389	0.080	1.226	1.258	1.444	1.304	1.8
19	199	51.3	3.801	0.074	27	19.1	1.328	0.070	1.409	1.308	1.323	1.328	1.9
20	144	51.7	3.531	0.068	26	19.8	1.461	0.074	1.366	1.360	1.473	1.347	2
21	154	51.4	3.513	0.068	28	20.6	1.162	0.056	1.435	1.410	1.182	1.359	2.1
22	113	51.9	3.699	0.071	26	21.2	1.423	0.067	1.568	1.454	1.474	1.362	2.2
23	100	52.6	5.367	0.102	13	21.5	1.506	0.070	2.345	1.494	1.609	1.360	2.3
24	84	52.0	3.389	0.065	10	23.4	2.011	0.086	1.565	1.534	2.063	1.359	2.4
25	81	52.8	3.702	0.070	13	25.0	1.414	0.057	1.752	1.570	1.414	1.357	2.5
26	72	52.1	3.369	0.065	17	25.5	0.943	0.037	1.680	1.599	0.961	1.352	2.6
27	61	53.1	3.842	0.072	4	25.8	2.630	0.102	1.954	1.622	2.758	1.344	2.7
28	53	52.4	2.608	0.050	10	26.1	4.067	0.156	1.394	1.641	4.364	1.332	2.8
29	33	52.2	3.149	0.060	8	29.0	1.414	0.049	1.750	1.657	1.414	1.319	2.9
30	50	52.6	3.392	0.065	10	30.6	1.897	0.062	1.936	1.668	1.860	1.305	3
31	32	52.6	3.112	0.059	8	30.5	1.069	0.035	1.836	1.674	1.087	1.286	3.1
32	50	52.6	3.968	0.075	9	31.3	1.323	0.042	2.413	1.676	1.351	1.258	3.2
33	31	52.7	2.726	0.052	3	32.7	1.155	0.035	1.707	1.678	1.166	1.218	3.3
34	14	52.0	2.636	0.051	2	32.5	0.707	0.022	1.723	1.677	0.740	1.172	3.4
35	27	53.3	2.313	0.043	5	31.6	6.504	0.206	1.519	1.672	7.204	1.125	3.5
36	24	52.2	1.769	0.034	5	36.4	2.302	0.063	1.220	1.664	2.277	1.076	3.6
37	13	54.0	1.542	0.029	0	0.0	0	0.032	1.056	1.657	1.170	1.022	3.7
38	17	54.6	3.324	0.061	0	0.0	0	0.034	2.314	1.649	1.275	0.965	3.8
39	11	54.6	3.446	0.063	1	39.0	0.000	0.035	2.463	1.640	1.384	0.904	3.9
40	19	53.8	2.315	0.043	5	37.8	2.683	0.071	1.721	1.636	2.839	0.845	4
41	18	53.2	2.263	0.043	3	40.7	1.528	0.038	1.743	1.637	1.540	0.791	4.1
42	13	54.4	1.445	0.027	1	33.0	0.000	0.019	1.116	1.642	0.789	0.735	4.2
43	13	53.8	1.286	0.024	0	0.0	0	0.009	1.027	1.647	0.404	0.673	4.3
44	7	53.8	2.361	0.044	0	0.0	0	0.005	1.930	1.658	0.207	0.610	4.4
45	4	53.6	0.850	0.016	1	45.0	0	0.002	0.714	1.676	0.086	0.553	4.5
46	7	55.7	5.065	0.091	1	46.0	0	0.004	4.182	1.694	0.175	0.493	4.6
47	6	53.3	1.663	0.031	1	45.0	0	0.008	1.466	1.714	0.357	0.434	4.7
48	8	53.4	0.904	0.017	2	46.5	0.707	0.015	0.812	1.738	0.730	0.385	4.8
49	2	55.0	1.414	0.026	0	0.0	0	0.008	1.260	1.763	0.373	0.340	4.9
50	5	54.3	1.927	0.035	0	0.0	0	0.004	1.773	1.788	0.190	0.296	5
51	6	54.3	1.033	0.019	0	0.0	0	0.002	0.969	1.810	0.097	0.255	5.1
52	5	54.6	2.104	0.039	0	0.0	0	0.001	2.003	1.833	0.049	0.219	5.2
53	2	54.8	3.889	0.071	1	53.0	0	0.000	3.765	1.856	0.025	0.185	5.3
54	8	54.8	1.169	0.021	0	0.0	0	0.000	1.152	1.879	0.013	0.149	5.4
55	3	53.2	2.030	0.038	1	55.0	0	0.000	2.098	1.904	0.007	0.114	5.5
56	3	55.3	2.587	0.047	0	0.0	0	0.000	2.619	1.929	0.003	0.082	5.6
57	2	54.0	1.414	0.026	2	57.0	0.000	0.000	1.493	1.954	0.000	0.052	5.7
58	3	54.0	2.000	0.037	0	0.0	0	0.006	2.148	1.978	0.339	0.020	5.8
59	5	54.6	1.128	0.021	1	59.0	0	0.012	1.218	2.004	0.690	0.000	5.9
60	4	56.9	2.562	0.045	1	60.0	0	0.023	2.702	2.030	1.403	0.000	6
61	14	54.8	1.693	0.031	3	65.3	3.055	0.047	1.885	2.056	2.852	0.000	6.1

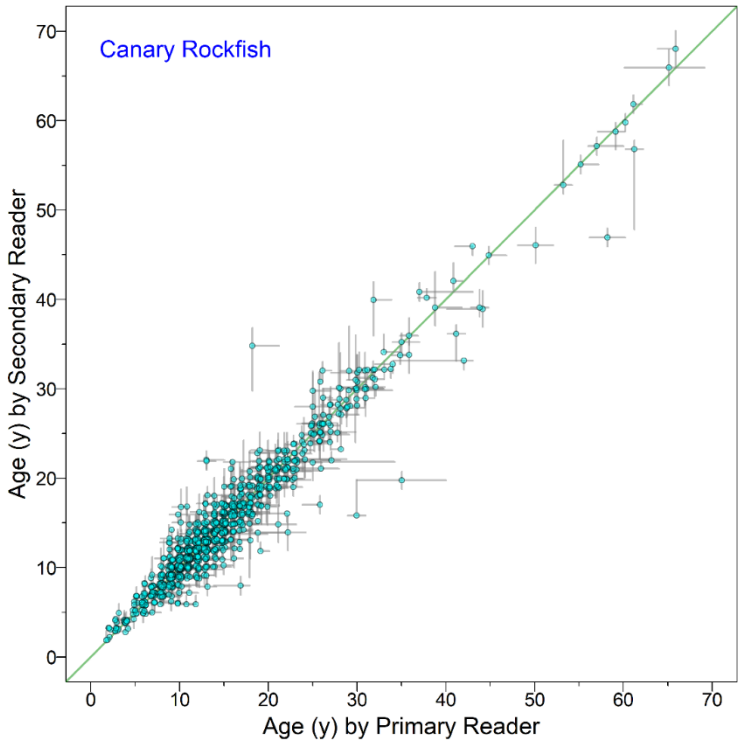

Figure D.15. Ageing error of CAR specified as the range between minimum and maximum age (grey bars) determined by primary and secondary readers for each accepted age (points). The data are jittered using a random uniform distribution between -0.25 and 0.25 y.

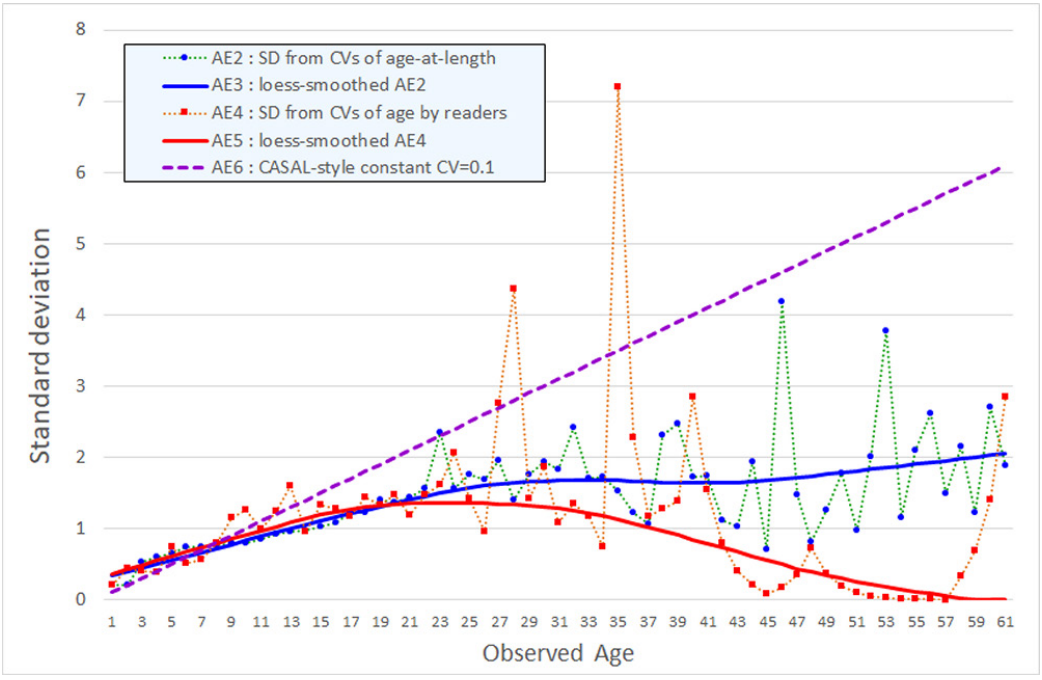

Figure D.16. Standard deviation of CAR ages used for model's ageing error – SDs calculated by age from SDs of length (AE2) and age-reader precision (AE4), and loess-smoothed series (AE3, AE5), respectively. CASAL-style (AE6) standard deviation simply uses CV=10%.

D.3. STOCK STRUCTURE

D.3.1. Stock Definition

At present, there is no genetic information to delineate separate stocks for CAR. The coastwide distribution of catch over 26 years suggests one continuous coastwide stock (Figure D.17).

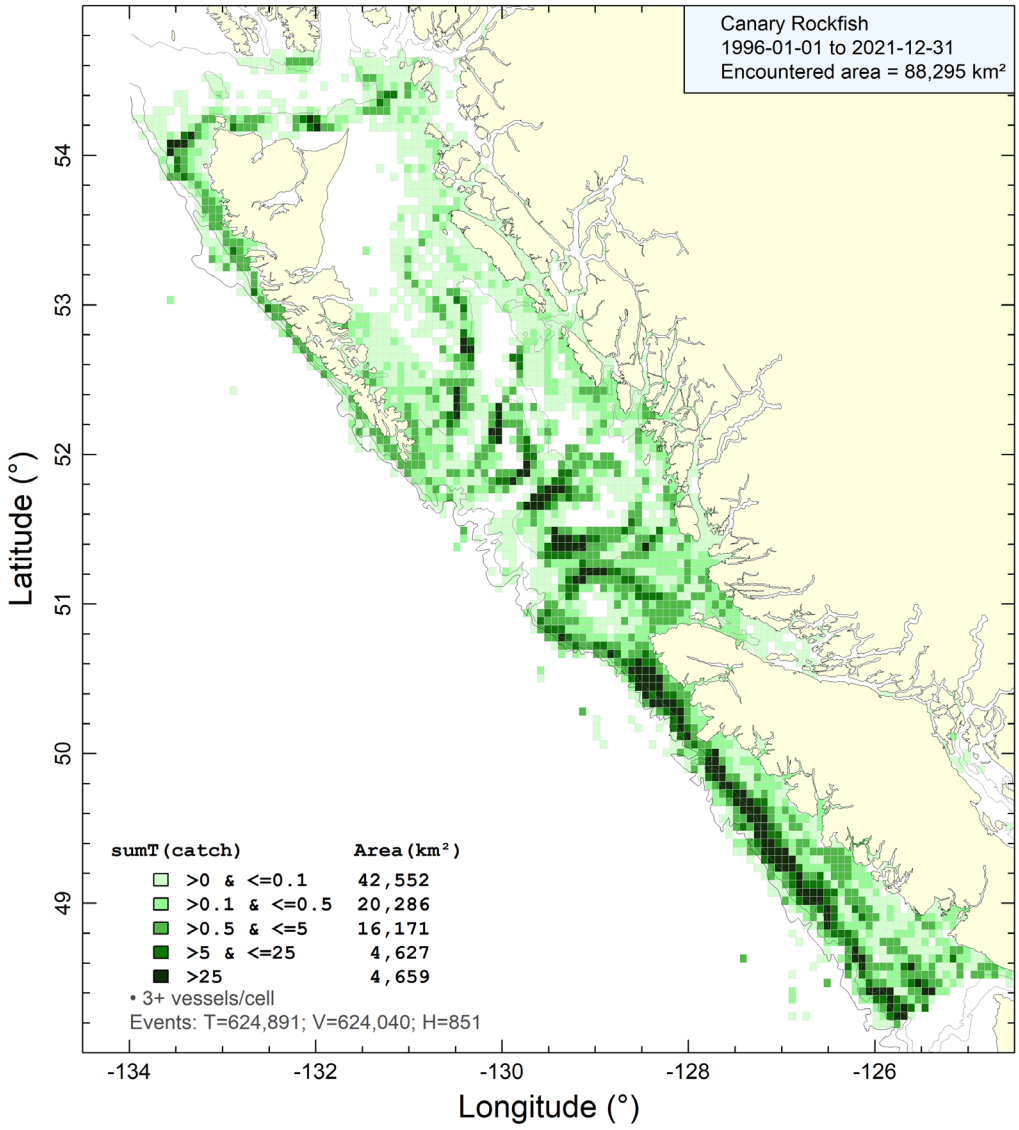

Figure D.17. Coastwide distribution of CAR catch by all fleets from 1996 to 2021.

Previous stock assessments of other rockfish (Starr and Haigh 2021a,b) have noted a physical separation of stocks between 5DE and more southerly PMFC areas. This separation may be caused by the North Pacific Current bifurcation (Pickard and Emery 1982; Freeland 2006; Cummins and Freeland 2006; Batten and Freeland 2007) whereby free-swimming larvae from the two regions are kept separated.

D.3.2. Fish Length Distributions

Simple comparisons of commercial length distributions by stock from the trawl fisheries show no evidence that length frequency distributions were markedly different by capture method when combined across all areas (Figure D.18). There is some evidence that midwater trawls catch older fish (Figure D.19). While these differences may be sufficient to treat midwater trawl as a separate fishery, there are inadequate data to characterise the midwater fishery as well as the observation that this fishery overall accounts for 13% of the annual catch of CAR from 1996 to 2021 coastwide. Consequently, we chose to combine the AF data from midwater trawl gear with the bottom trawl data.

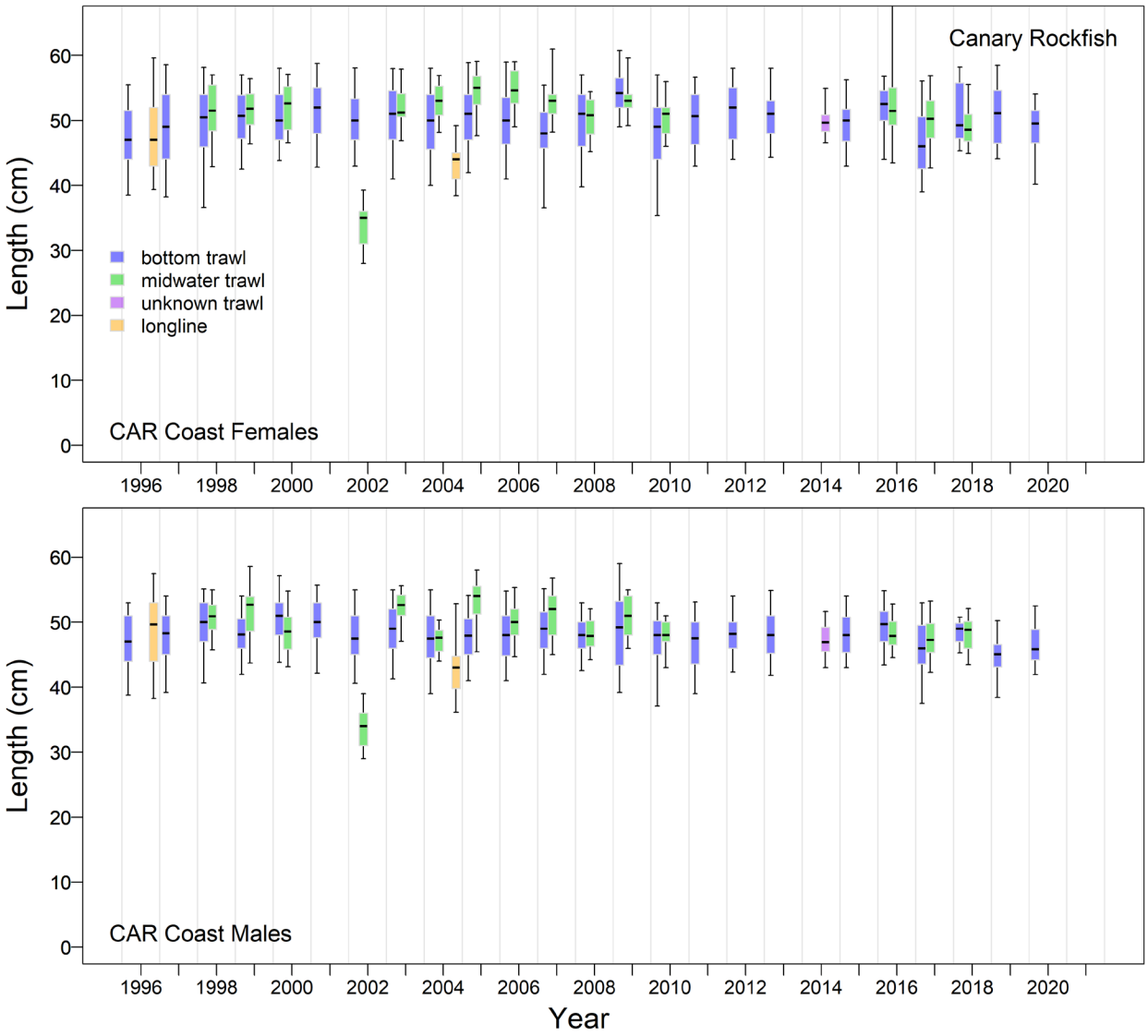

Figure D.18. Comparison of annual distributions of CAR length by sex among gear types in the commercial fisheries. Boxplot quantiles: 0.05, 0.25, 0.5, 0.75, 0.95.

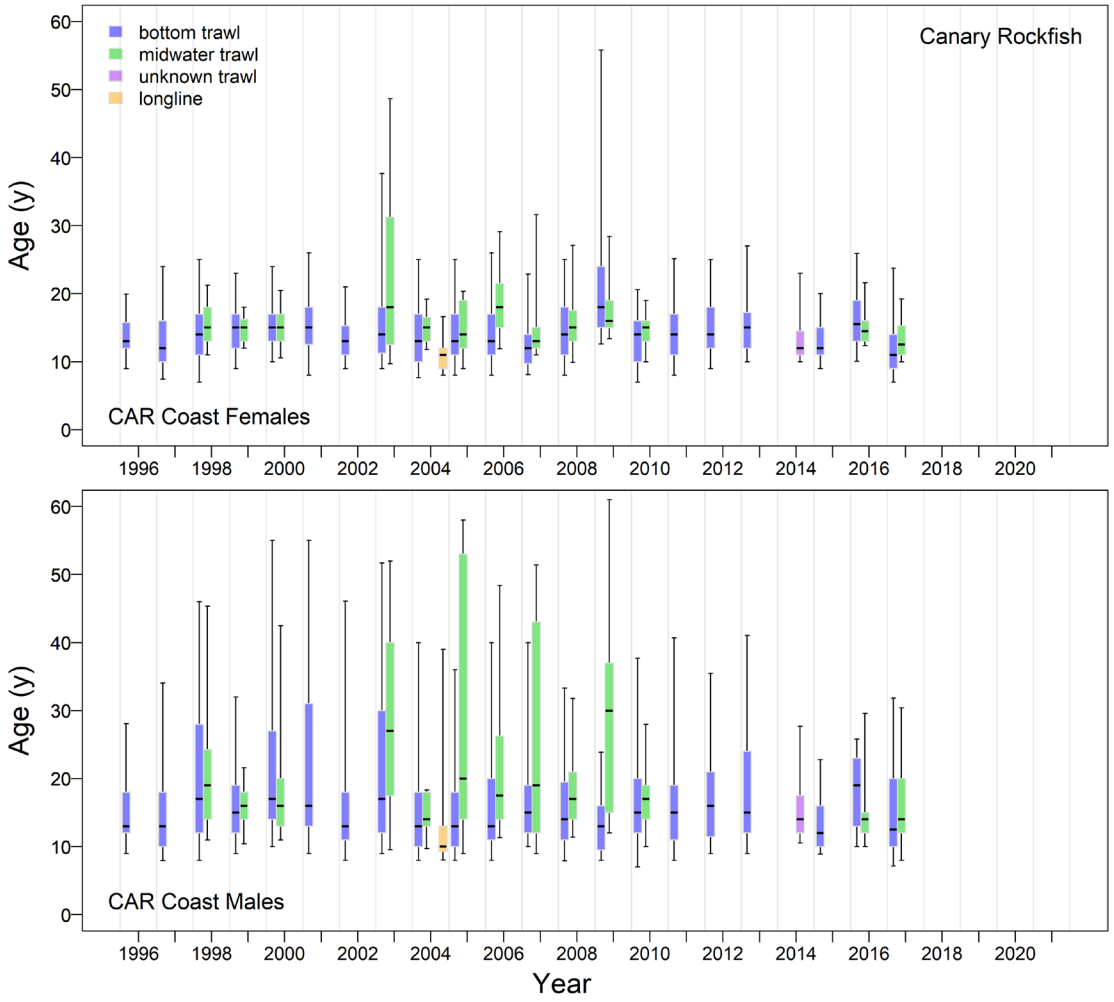

Figure D.19. Comparison of annual distributions of CAR age by sex among gear types in the commercial fisheries. Boxplot quantiles: 0.05, 0.25, 0.5, 0.75, 0.95.

The distributions of commercial lengths (Figure D.20) and ages (Figure D.21) for a northern subset (PMFC areas 5DE) show some differences by coastal region, with the northern (5DE) samples having older male fish than seen in the more southern fish. However, there are relatively few samples from 5DE and this combined area accounts for only a relatively small fraction of the annual CAR catch (about 3.5% over the period 1996–2021). We chose to go ahead with a single area model representing the entire coast because the differences among the two regions were not consistent in all years. There also were no 5DE age samples after 2011 (Figure D.21).

The distribution of lengths from a variety of surveys (Figure D.22) show inter-survey differences in mean length that likely stem from survey selectivity differences, perhaps influenced by depth:

- the WCHG synoptic survey appears to catch larger fish than most other surveys;
- the HS survey catches small fish consistently, and catches the greatest size range;
- the IPHC longline survey catches large fish while the HBLL surveys catch fish of similar sizes to most synoptic trawl surveys;
- the WCHG survey tends to catch the oldest fish, especially males.

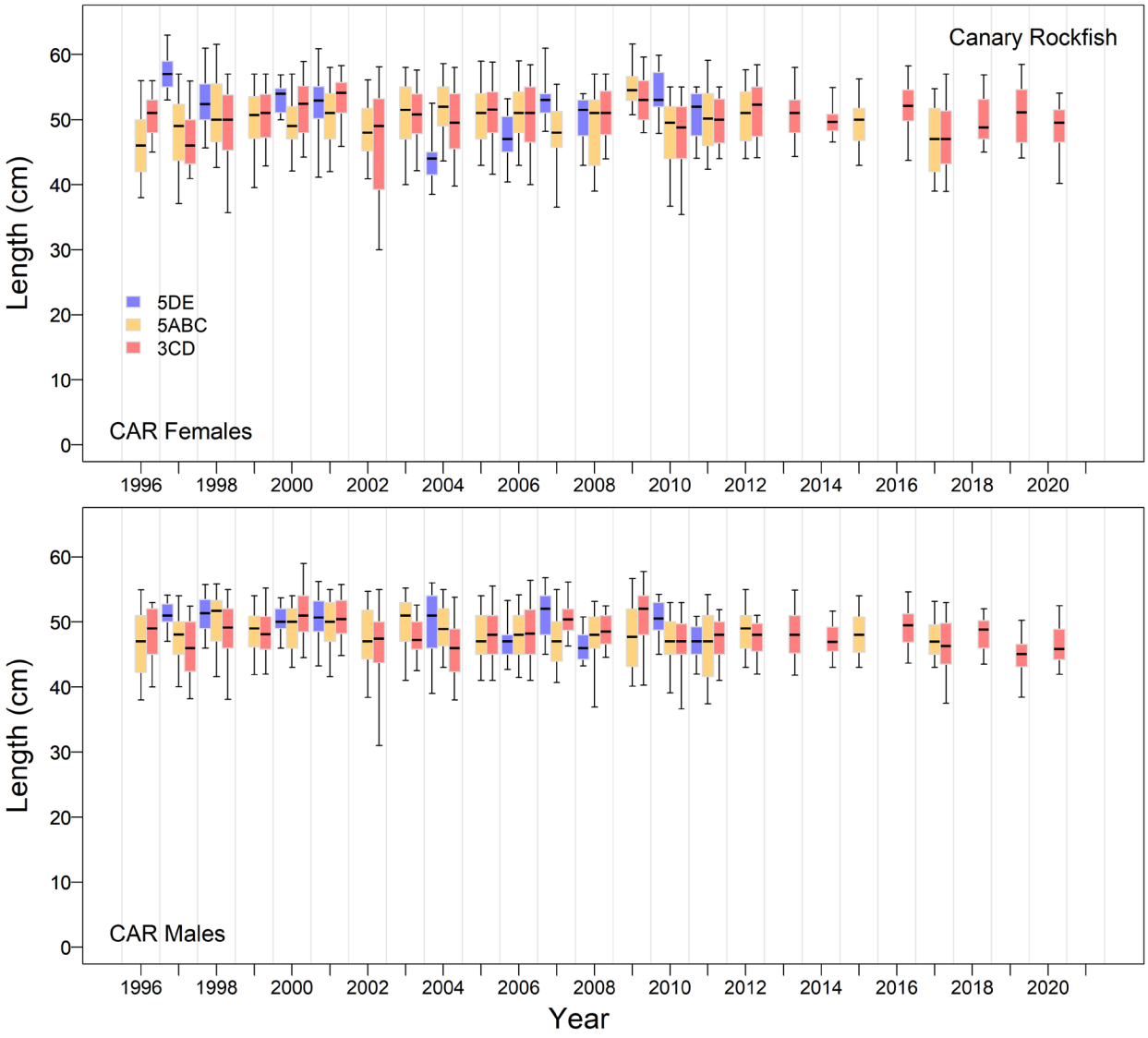

Figure D.20. Comparison of annual distributions of CAR length along the BC coast with northern (5DE) central (5ABC), and southern (3CD) areas in the commercial fisheries. Boxplot quantiles: 0.05, 0.25, 0.5, 0.75, 0.95.

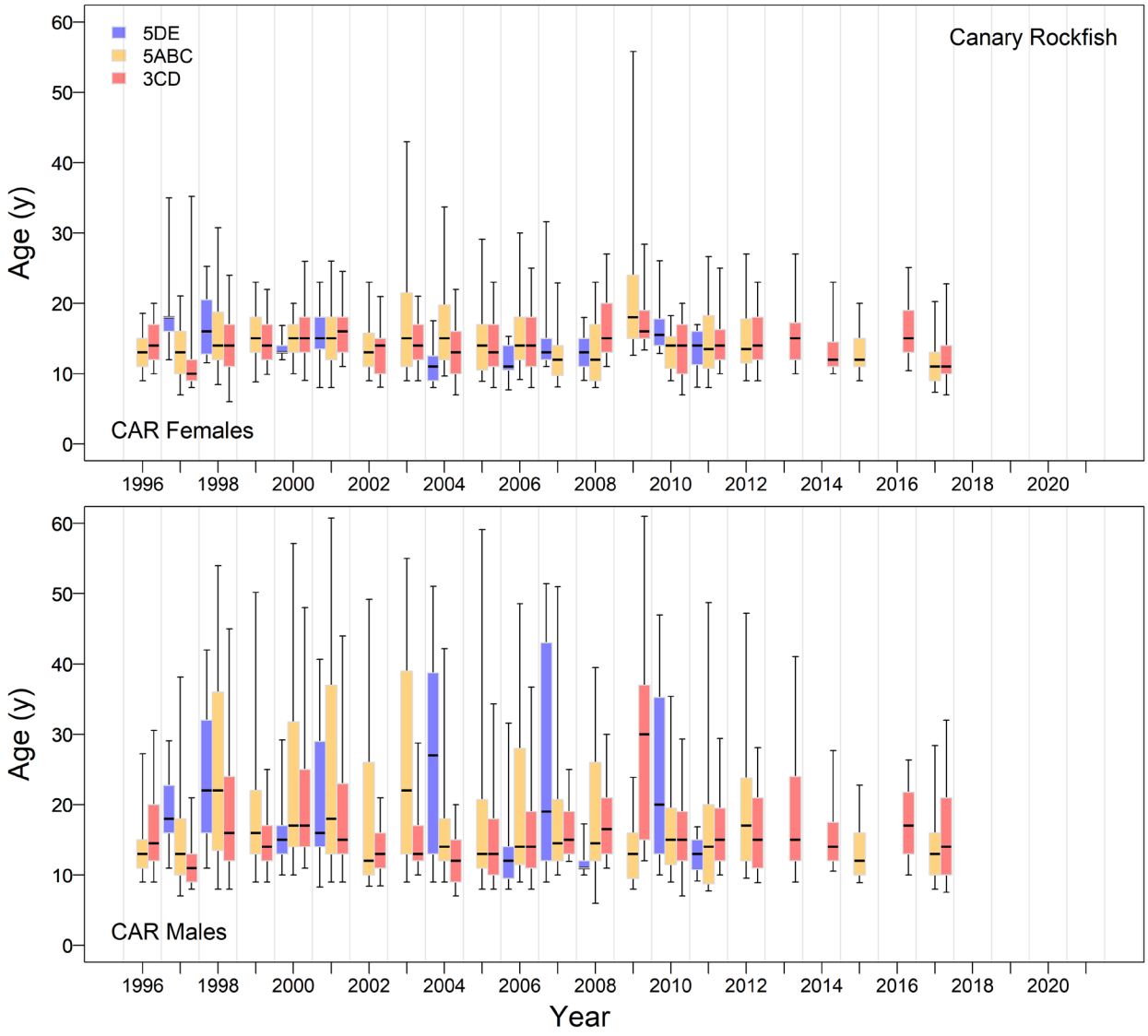

Figure D.21. Comparison of annual distributions of CAR age along the BC coast with northern (5DE), central (5ABC), and southern (3CD) areas in the commercial fisheries. Boxplot quantiles: 0.05, 0.25, 0.5, 0.75, 0.95.

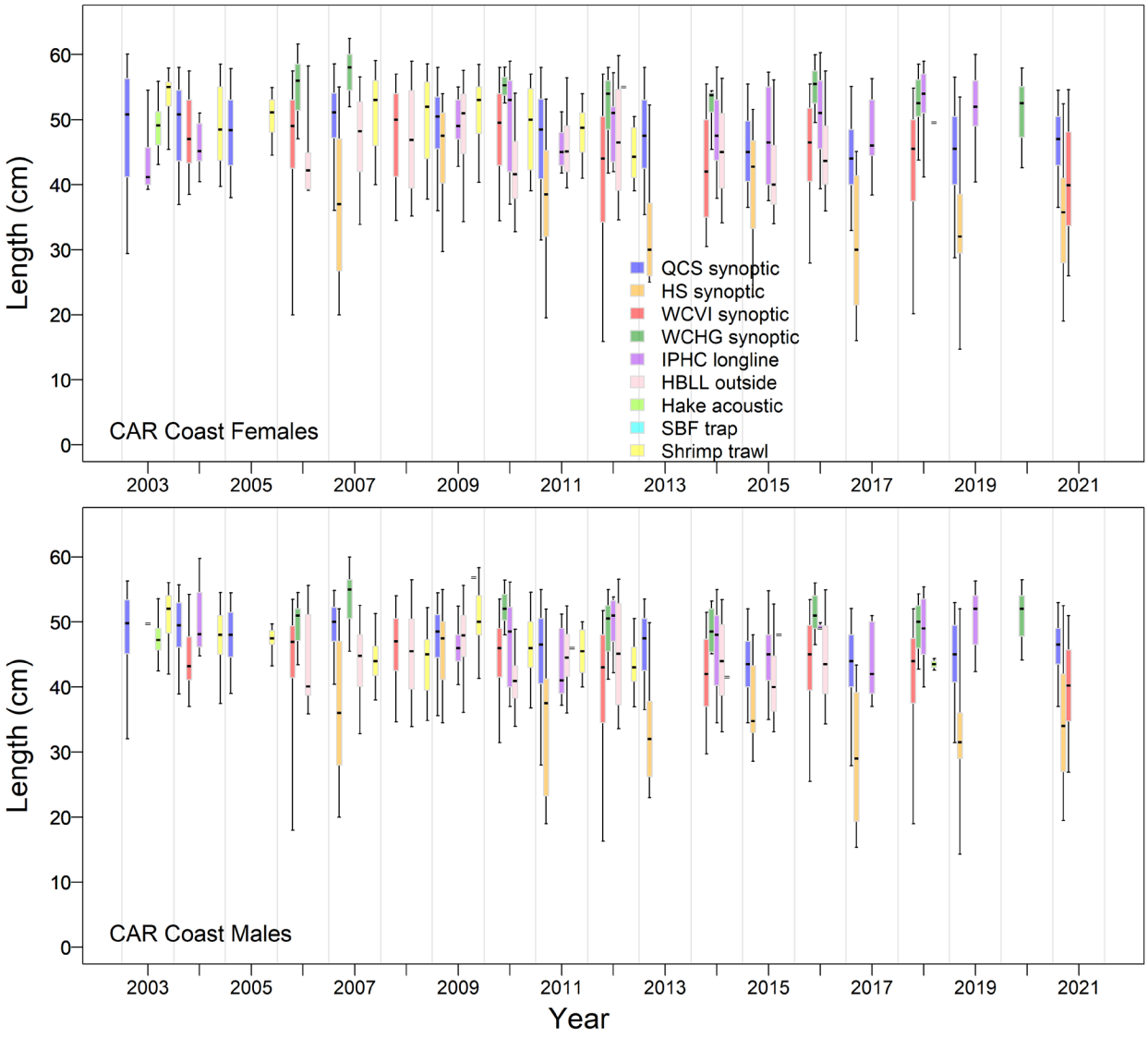

Figure D.22. Comparison of annual distributions of CAR length among nine surveys (five trawl, two longline, one trap, and one acoustic). Boxplot quantiles: 0.05, 0.25, 0.5, 0.75, 0.95.

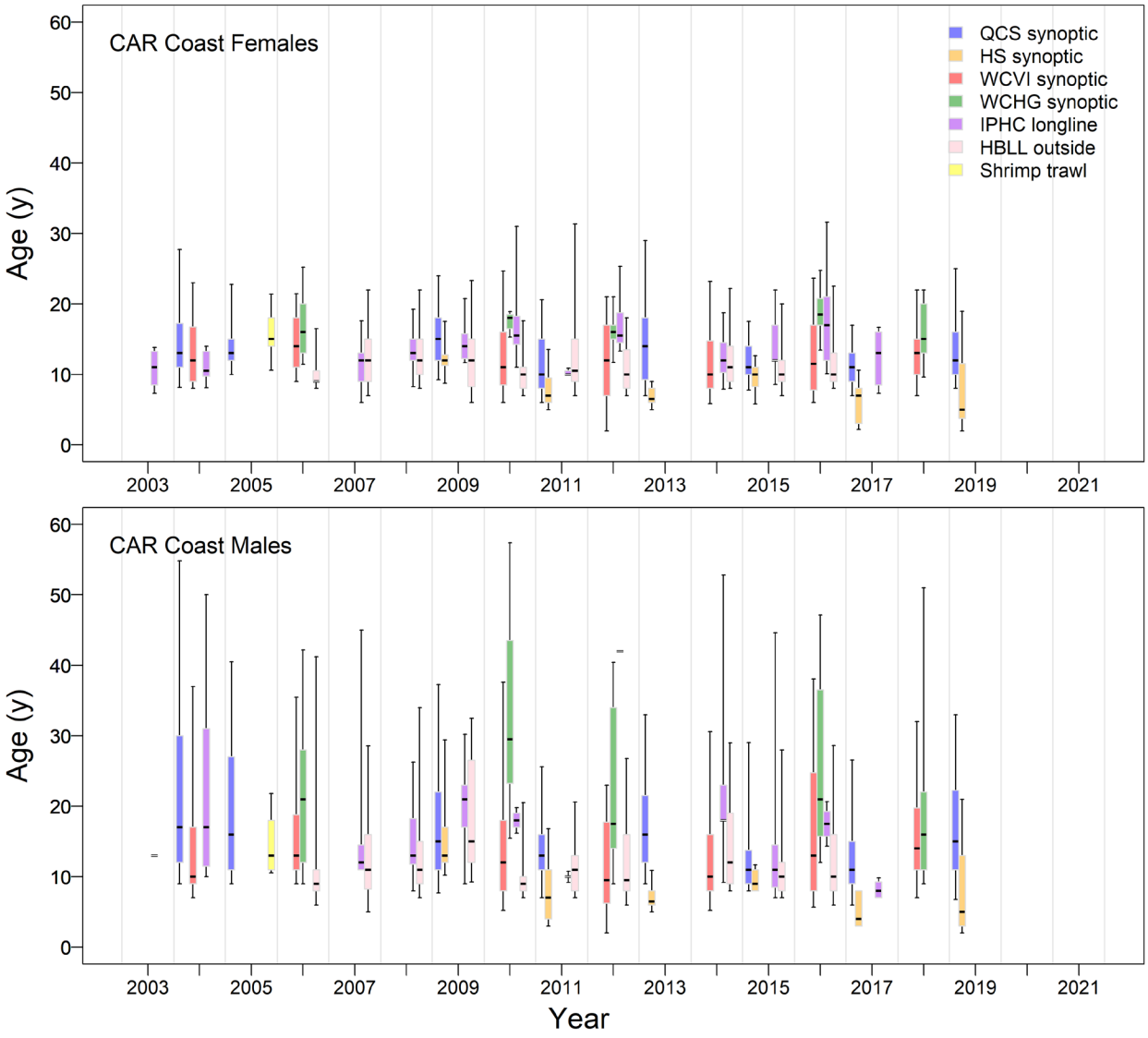

Figure D.23. Comparison of annual distributions of CAR age among surveys – four synoptic bottom trawl, one shrimp trawl, and two longline. Boxplot quantiles: 0.05, 0.25, 0.5, 0.75, 0.95.

D.3.3. Comparison of Growth Models

A comparison of growth models among various regions using survey length-age data (Figure D.24) shows the following trends:

- female estimates of L-infinity are larger than for males;
- northern males and females are slightly larger than their counterparts in central and southern BC regions.

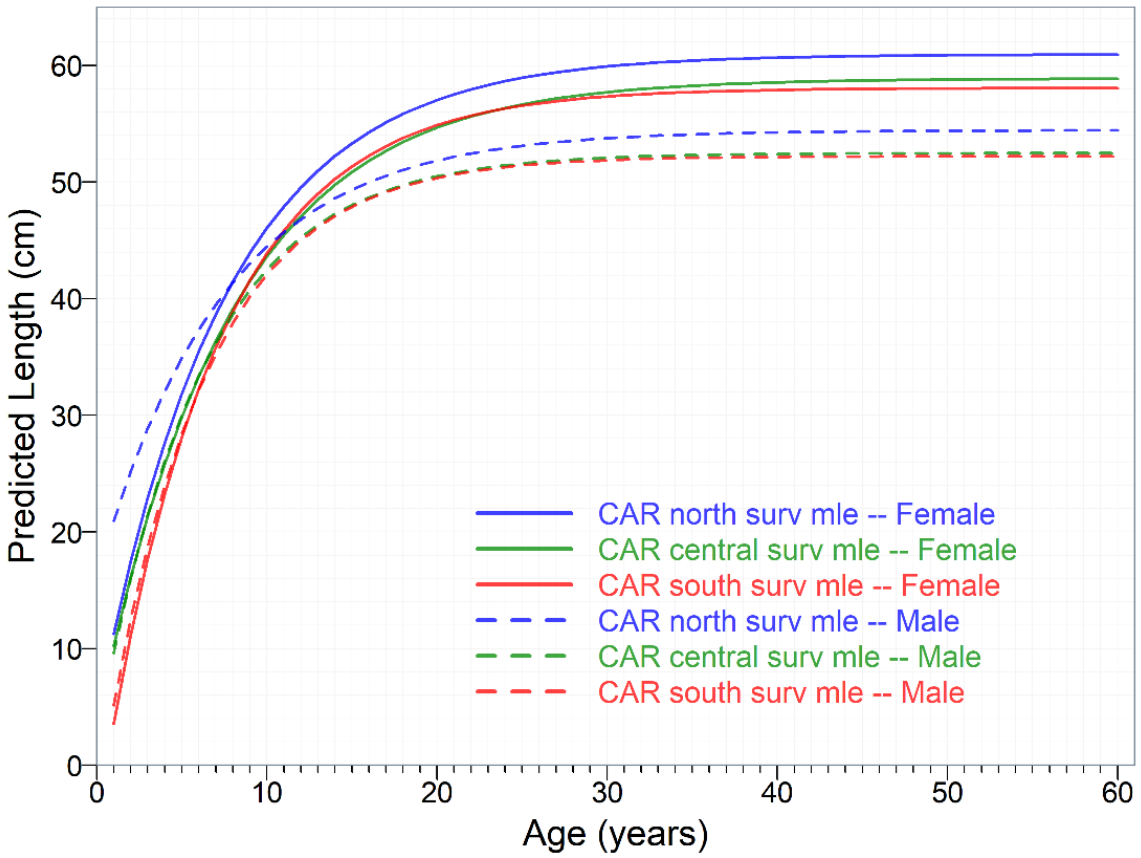

Figure D.24. von Bertalanffy MLE fits comparing growth among three BC regions: north (5DE), central (5ABC), and south (3CD) by sex from survey CAR length-age data. Line type indicates sex (solid=female, dashed=male). Line colour indicates region (blue=north, green=central, red=south).

D.4. REFERENCES – BIOLOGY

Batten, S.D. and Freeland, H.J. 2007. Plankton populations at the bifurcation of the North Pacific Current. Fisheries Oceanography 16(6): 536-546.

Bull, B., Francis, R.I.C.C., Dunn, A., McKenzie, A., Gilbert, D.J., Smith, M.H., Bian, R. and Fu, D. 2012. CASAL (C++ algorithmic stock assessment laboratory): CASAL User Manual v2.30-2012/03/21. NIWA Tech. Rep. 135. 280 p.

Cummins, P.F. and Freeland, H.J. 2007. Variability of the North Pacific Current and its bifurcation. Progress in Oceanography 75(2): 253-265.

DFO. 2022a. Proceedings of the Pacific regional peer review of the Redstripe Rockfish (*Sebastes proriger*) stock assessment for British Columbia in 2018; June 13-14, 2018. DFO Can. Sci. Advis. Sec. Proceed. Ser. 2022/014. iv + 13 p.

DFO. 2022b. Proceedings of the Pacific regional peer review on Yellowmouth Rockfish (*Sebastes reedi*) stock assessment for British Columbia in 2021; virtual meeting September 8-9, 2021. DFO Can. Sci. Advis. Sec. Proceed. Ser. 2022/033.

Freeland, H.J. 2006. What proportion of the North Pacific Current finds its way into the Gulf of Alaska? Atmosphere-Ocean 44(4): 321-330.

Haist, V., Breen, P.A. and Starr, P.J. 2009. A multi-stock, length-based assessment model for New Zealand rock lobster (*Jasus edwardsii*). N.Z. J. Mar. Freshw. Res. 43: 355-371.

Hamel, O.S. 2015. A method for calculating a meta-analytical prior for the natural mortality rate using multiple life history correlates. ICES J. Mar. Sci. 72(1): 62-69.

Hoenig, J.M. 1983. Empirical use of longevity data to estimate mortality rates. Fish. Bull. 82(1): 898-903.

IUCN Standards and Petitions Committee. 2022. Guidelines for using the IUCN Red List Categories and Criteria. Version 15.1. Prepared by the Standards and Petitions Committee of the IUCN Species Survival Commission. 114 p.

MacLellan, S.E. 1997. How to age rockfish (*Sebastes*) using *S. alutus* as an example – the otolith burnt section technique. Can. Tech. Rep. Fish. Aquat. Sci. 2146: 39 p.

Methot, R.D. and Stewart, I.J. 2005. Status of the U.S. canary rockfish resource in 2005. PFMC Technical Report, NWFSC, Seattle WA. 272 p. Revised Aug 31, 2005 Post-STAR review, Revised Oct 25, 2005 Post-SSC review.

Pickard, G.L. and Emery, W.J. 1982. Descriptive Physical Oceanography, an Introduction. Pergamon Press, Oxford UK, 4th (SI) enlarged ed.

Quinn, T.J.I. and Deriso, R.B. 1999. Quantitative Fish Dynamics. Oxford University Press, New York, NY.

Richards, L.J., Schnute, J.T., Kronlund, A.R. and Beamish, R.J. 1992. Statistical models for the analysis of ageing error. Can. J. Fish. Aquat. Sci. 49(9). 1801-1815.

Stanley, R.D., Starr, P. and Olsen, N. 2009. Stock assessment for Canary rockfish (*Sebastes pinniger*) in British Columbia waters. DFO Can. Sci. Advis. Sec. Res. Doc. 2009/013: xxii + 198 p.

Starr, P.J. and Haigh, R. 2021a. Redstripe Rockfish (*Sebastes proriger*) stock assessment for British Columbia in 2018. DFO Can. Sci. Advis. Sec. Res. Doc. 2021/014: vii + 340 p.

Starr, P.J. and Haigh, R. 2021b. Walleye Pollock (*Theragra chalcogramma*) stock assessment for British Columbia in 2017. DFO Can. Sci. Advis. Sec. Res. Doc. 2021/004. viii+294 p.

Then, A.Y., Hoenig, J.M., Hall, N.G. and Hewitt, D.A. 2015. Evaluating the predictive performance of empirical estimators of natural mortality rate using information on over 200 fish species. ICES J. Mar. Sci. 72(1): 82-92.

Westrheim, S. 1975. Reproduction, maturation, and identification of larvae of some *Sebastes* (Scorpaenidae) species in the northeast Pacific Ocean. J. Fish. Res. Bd. Can. 32: 2399-2411.

APPENDIX E. MODEL EQUATIONS

E.1. INTRODUCTION

The 2022 stock assessment of Canary Rockfish (CAR) adopted Stock Synthesis 3 (SS3), version 3.30.18 (Methot et al. 2021, downloaded Jan 11, 2022), which is a statistical age-structured population modelling framework (Methot and Wetzel 2013) that uses ADMB's power for Bayesian estimation of population trajectories and their uncertainties. The Stock Synthesis Development Team at NOAA (National Oceanic and Atmospheric Administration, U.S. Dept. Commerce) provides executables and documentation on how to run SS3, and the SS3 source code is available on GitHub.

Previously, CAR was assessed using a simpler age-structured model called 'Awatea', which is a version of Coleraine (Hilborn et al. 2003) that was modified and maintained by Allan Hicks (then at Univ. Washington, now at IPHC). Both Awatea and SS3 are platforms for implementing Automatic Differentiation Model Builder software (ADMB Project 2009), which provides (a) maximum posterior density estimates using a function minimiser and automatic differentiation, and (b) an approximation of the posterior distribution of the parameters using the Markov Chain Monte Carlo (MCMC) method, specifically using the Metropolis algorithm (Gelman et al. 2004).

SS3 has been used previously in age-structured assessments for ⟨ BC stocks ⟩ since 2021:

- 2021 – Yellowmouth Rockfish ⟨ YMR, BC coast ⟩ (Starr and Haigh 2022*c*)

Awatea has been used in age-structured assessments for ⟨ BC stocks ⟩ since 2007:

- 2021 – Bocaccio ⟨ BOR, BC coast ⟩ update of 2019 assessment (DFO 2022*a*);
- 2020 – Rougheye/Blackspotted Rockfish complex ⟨ REBS, 5DE and 3CD5AB ⟩ (Starr and Haigh 2022*b*);
- 2019 – Bocaccio ⟨ BOR, BC coast ⟩ (Starr and Haigh 2022*a*);
- 2019 – Widow Rockfish ⟨ WWR, BC coast ⟩ (Starr and Haigh 2021*a*);
- 2018 – Redstripe Rockfish ⟨ RSR, 5DE and 3CD5ABC ⟩ (Starr and Haigh 2021*b*);
- 2017 – Pacific Ocean Perch ⟨ POP, 5ABC ⟩ (Haigh et al. 2018);
- 2014 – Yellowtail Rockfish ⟨ YTR, BC coast ⟩ (DFO 2015);
- 2013 – Silvergray Rockfish ⟨ SGR, BC coast ⟩ (Starr et al. 2016);
- 2013 – Rock Sole ⟨ ROL, BC coast ⟩ (Holt et al. 2016);
- 2012 – Pacific Ocean Perch ⟨ POP, 3CD ⟩ (Edwards et al. 2014*b*);
- 2012 – Pacific Ocean Perch ⟨ POP, 5DE ⟩ (Edwards et al. 2014*a*);
- 2011 – Yellowmouth Rockfish ⟨ YMR, BC coast ⟩ (Edwards et al. 2012*a*),
- 2010 – Pacific Ocean Perch ⟨ POP, 5ABC ⟩ (Edwards et al. 2012*b*);
- 2009 – Canary Rockfish ⟨ CAR, BC coast ⟩ update of 2007 assessment (DFO 2009);
- 2007 – Canary Rockfish ⟨ CAR, BC coast ⟩ (Stanley et al. 2009).

The chief strength of Coleraine|Awatea is the use of a robust likelihood formulation proposed by Fournier et al. (1998) for the composition data by sex and age (or length). The robust normal model was used over the more traditional Multinomial error model because it reduced the influence of observations with standardised residuals > 3 standard deviations (Fournier et al. 1990). Fournier et al. (1990) identified two types of deviations:

- type I – occasional occurrence of an event of very low probability; and
- type II – probability of observing an event with higher frequency than normal in the population (e.g., school of young fish).

Their robustified likelihood function reduces both types of deviations.

SS3 offers two error models: the Multinomial and a compound Dirichlet-Multinomial. The latter can estimate effective sample sizes that are similar to iterative reweighting methods, but without requiring multiple iterations of running the assessment model (Thorson et al. 2017).

The data inputs to SS3 comprise four files – `'starter.ss'`, `'data.ss'`, `'control.ss'`, and `'forecast.ss'` – instead of a single file used by Awatea. Parameter control and priors appear in the `control.ss` file, and data appear in the `data.ss` file; these two files can be named anything the user wishes because the `starter.ss` file specifies their names. The names for the `starter.ss` and `forecast.ss` files must remain invariant. Unlike Awatea, which requires specifying an input file from the command line (e.g. `'awatea -ind fielname.txt'`), calling SS3 is done by typing only `'ss'` on the command line (assuming `'ss.exe'` occurs on the Windows system's PATH) because the software assumes the presence of the four files listed above. Additionally, this stock assessment used the optimized version of SS3 (`'ss_opt_win.exe'`), which is reportedly 'fast and optimized for speedy execution', rather than the 'safe' version (`'ss_win.exe'`), which performs bound checks. (The optimized version was renamed to `'ss.exe'` for convenience.) The options in SS3 for fitting the data are more complex than those for Awatea and offer a greater degree of flexibility; however, this flexibility requires a steep learning curve and increases opportunties for inadvertent errors.

In this assessment, the Dirichlet-Multinomial distribution was used for fitting age frequencies (AF). In a previous stock assessment (YMR, DFO 2022*b*), this distribution could not be used (see limitations in Section E.6.2.2.) and, instead, applied explicit reweighting using a harmonic mean ratio method based on McAllister and Ianelli (1997).

The running of SS3 was streamlined using custom R code (archived on the GitHub site 'PBS Software' in the repository '`PBSsynth`'), which relied heavily on code provided by the R packages '`PBSawatea`', '`r4ss`' (Taylor et al. 2020), and '`adnuts`' (Monnahan 2018). Figures and tables of output were automatically produced in R, an environment for statistical computing and graphics (R Core Team 2021). The R function `Sweave` (Leisch 2002) automatically collated, via LaTeX, the large amount of figures and tables into `'pdf'` files for model runs and Appendix F.

Methot and Wetzel (2013) provide mathematical notation of equations used in the SS3 model in their Appendix A. Below we present mathematical notation of selected equations used in the SS3 age-structured model (merged with notation used in previous DFO Awatea models), the Bayesian procedure, the reweighting scheme, the prior distributions, and the methods used for calculating reference points and performing projections.

E.2. MODEL ASSUMPTIONS

The **assumptions** of the model are:

1. The assessed BC population of Canary Rockfish (CAR) comprised a single stock in combined PMFC areas 3CD5ABCDE.
2. Annual catches were taken by two fisheries: 'Trawl', which included bottom and midwater gears, and 'Other', which denoted a combined fishery of non-trawl gears (halibut longline, sablefish trap, lingcod & salmon troll, and rockfish hook & line). The CAR fishery was dominated by trawl gear (~98% by catch in the last five years). The annual catch was known without error and occurred in the middle of each year.
3. The Beverton-Holt stock-recruitment relationship was time-invariant, with a log-normal error structure.

4. Selectivity was different among fleets (fishery and surveys), and remained invariant over time. Selectivity parameters were estimated when ageing data were available.
5. Natural mortality M was estimated using a normal prior, and held invariant over time. This parameter differed between the two sexes.
6. Growth parameters were fixed and invariant over time. These parameters differed between the two sexes.
7. Maturity-at-age parameters for females (and males) were fixed and invariant over time.
8. Recruitment at age 0 was 50% females and 50% males.
9. Recruitment standard deviation (σ_R) was fixed at 0.9.
10. Only fish ages determined using the preferred otolith break-and-burn methodology (MacLellan 1997) were used because ages determined by surface ageing methods (chiefly before 1978) were biased (Beamish 1979). Surface ageing was deemed suitable for very young rockfish (ages 1-3).
11. An ageing error (AE) vector based on CVs of observed lengths-at-age was used.
12. Commercial samples of catch-at-age in a given 3-month period within a year were representative of the fishery in that quarter-year if there were ≥2 samples in that year.
13. Relative abundance indices were proportional to the vulnerable biomass at the mid point of the year, after half the catch and half the natural mortality had been removed.
14. The age composition samples came from the middle of the year after half the catch and half the natural mortality had been removed.

E.3. MODEL NOTATION AND EQUATIONS

Model notation is given in Table E.1, the model equations in Tables E.2 and E.3, and description of prior distributions for estimated parameters in Table E.4. The model description is divided into the deterministic components, stochastic components and Bayesian priors. Full details of notation and equations are given after the tables.

The deterministic components in Table E.2 iteratively calculate numbers of fish in each age class (and of each sex) through time, while allowing for the commercial catch data, weight-at-age and maturity data, and known fixed values for all parameters.

Parameters not assumed to be fixed were estimated in the context of recruitment stochasticity. This is accomplished by the stochastic components given in Table E.3.

Incorporation of the prior distributions for estimated parameters is necessary for a full Bayesian implementation, the goal of which is to minimise the objective function $\mathcal{F}(\boldsymbol{\Theta})$ given by (E.52). This function is derived from sum of the negative log likelihoods from the the deterministic, stochastic and prior components of the model.

Table E.1. Notation for the SS3 catch-at-age model (continued overleaf). The assessment model uses only 'cohorts' (age-classes by year) even though SS3 recognises finer subdivisions of time called 'morphs' (seasons), which can be further characterised by 'platoons' (rates of growth).

Symbol	Description and units
	Indices (all subscripts)
a	▸ age class, where $a = 1, 2, 3, ...A$, and ▹ a' = reference age near youngest age well-represented in data; ▹ a'' = reference age near oldest age well-represented in data
l	▸ length bin, where $l = 1, 2, 3, ...\Lambda$, and Λ is the bin index of the largest length; ▹ L' = reference length for a'; ▹ L'' = reference length for a''; ▹ $\breve{L}_l$, $\mathring{L}_l$ = minimum and middle length of length bin l, respectively
t	▸ model year, where $t = 1, 2, 3, ...T$, corresponds to actual years: 1935, ..., 2023, and $t = 0$ represents unfished equilibrium conditions
g	▸ index for series (abundance|composition) data: 1 – Trawl Fishery|CPUE (commercial data) 2 – Other Fishery (commercial data) 3 – QCS Synoptic trawl survey series 4 – WCVI Synoptic trawl survey series 5 – NMFS Triennial trawl survey series 6 – HS Synoptic trawl survey series 7 – WCHG Synoptic trawl survey series 8 – GIG Historical trawl survey series
s	▸ sex, 1=females, 2=males
	Index ranges
A	▸ accumulator age-class, $A \in \{60\}$
G	▸ number of fleets (fisheries and surveys)
Λ	▸ number of length bins
T	▸ number of model years, $T = 89$
$\mathbf{T}_g$	▸ sets of model years for survey abundance indices from series g, listed here for clarity as actual years (subtract 1934 to give model year t): $\mathbf{T}_1$ = {1996, ..., 2021} $\mathbf{T}_3$ = {2003:2005, 2007, 2009, 2011, 2013, 2015, 2017, 2019, 2021} $\mathbf{T}_4$ = {2004, 2006, 2008, 2010, 2012, 2014, 2016, 2018, 2021} $\mathbf{T}_5$ = {1980, 1983, 1989, 1992, 1995, 1998, 2001} $\mathbf{T}_6$ = {2005, 2007, 2009, 2011, 2013, 2015, 2017, 2019, 2021} $\mathbf{T}_7$ = {2006:2008, 2010, 2012, 2016, 2018, 2020} $\mathbf{T}_8$ = {1967, 1969, 1971, 1973, 1976:1977, 1984, 1994}
$\mathbf{U}_g$	▸ sets of model years with proportion-at-age data for series g: $\mathbf{U}_1$ = {1977:1980, 1982:1985, 1988, 1990:2013, 2015:2017} $\mathbf{U}_3$ = {2004:2005, 2009, 2011, 2013, 2015, 2017, 2019, 2021} $\mathbf{U}_4$ = {2004, 2006, 2010, 2012, 2014, 2016, 2018, 2021} $\mathbf{U}_5$ = {1980, 1983, 1989, 1992, 1995, 2001}

Symbol	Description and units
	Data and fixed parameters
$\widetilde{a}_a$	▸ age after bias adjustment for age a (used in ageing error)
ξ_a	▸ standard deviation for age a (used in ageing error)
p_{atgs}	▸ observed weighted proportion of fish from series g in each year $t \in \mathbf{U}_g$ that are age-class a and sex s; so $\Sigma_{a=1}^{A}\Sigma_{s=1}^{2} p_{atgs} = 1$ for each $t \in \mathbf{U}_g$; in SS3: ▹ p_l = observed proportion in length bin l; ▹ p_a = observed proportion in age a; and ▹ p_z = observed proportion by size in length bin l; ▹ the CAR stock assessment only used p_a
n_{tg}	▸ specified sample size that yields corresponding p_{atgs}
$\widetilde{n}_{tg}$	▹ effective sample size based on $\widehat{p}_{atgs}$
C_{tg}	▸ observed catch biomass (tonnes) in year $t = 1, 2, ..., T-1$
τ_{tg}	▸ standard deviation of C_{tgs}
d_{tg}	▸ discarded catch biomass (tonnes) in year t
δ_{tg}	▸ standard deviation of d_{tg}
δ'_{tg}	▸ user-specified standard deviation offset to add to δ_{tg}
w_{as}	▸ average weight (kg) of individual of age-class a of sex s from fixed parameters
$\overline{w}_{tg}$	▸ mean body weight (kg) by year (t) and fleet (g)
ψ_{tg}	▸ standard deviation of $\overline{w}_{tg}$
ψ'_{tg}	▸ user-specified standard deviation offset to add to ψ_{tg}
m_a	▸ proportion of age-class a females that are mature, fixed from data
I_{tg}	▸ biomass estimates (tonnes) from surveys $g = 3, ..., 8$, for year $t \in \mathbf{T}_g$, tonnes
κ_{tg}	▸ standard deviation of I_{tg}
κ'_{tg}	▸ user-specified standard deviation offset added to κ_{tg}
σ_R	▸ standard deviation parameter for recruitment process error, $\sigma_R = 0.9$
ϵ_t	▸ recruitment deviations arising from process error
b_t	▸ recruitment bias adjustment parameter: ▹ ranges from 1 (data-rich years) to 0 (data-poor years)
$\widehat{x}$	▸ estimated values of observed data x (generalised)
	Estimated parameters
$\boldsymbol{\Theta}$	▸ set of estimated parameters:
R_0	▸ virgin recruitment of age-0 fish (numbers of fish, 1000s)
M_s	▸ natural mortality rate for sex $s = 1, 2$
h	▸ steepness parameter for Beverton-Holt recruitment
q_g	▸ catchability for fleets ($g = 1, 3, ..., 8$)
β_{itg}	▸ double-normal parameters for females ($s = 1$), where i=$1, ..., 6$ for the six β parameters that determine selectivity S_{atgs} for year t and series g=$1, 3, 4, 5$, using joiner functions j_{1atgs} and j_{2atgs} for ascending- and descending-limb functions π_{1atgs} and π_{2atgs}, respectively, where γ_{1tgs} and γ_{2tgs} describe exponential terms
Δ_{itg}	▸ shift in vulnerability for males ($s = 2$), where i=$1, ..., 5$ for the five Δ parameters and subscripts tg are the same as those for β

Symbol	Description and units
	Derived states
N_{ats}	▸ number of age-class a fish (1000s) of sex s at the start of year t
B_t	▸ spawning biomass (tonnes mature females) at the start of year t
B_0	▸ virgin spawning biomass (tonnes mature females) at the start of year 0
R_t	▸ recruitment of age-0 fish (numbers of fish, 1000s) in year t
ρ_t	▹ recruitment deviations (log thousands age-0 fish) in year t
V_{tg}	▸ vulnerable biomass (tonnes, females + males) in the middle of year t
$\mathcal{B}_{tg}$	▸ mid-season retained dead biomass (tonnes, females + males)
F_{tg}	▸ instantaneous fishing mortality rate for time period t by fishery g
	▹ hybrid method uses Pope's approximation and Baranov's equation
	▹ calculations facilitated by temporary variables $\mathcal{T}_{tg}$ and joiners $\mathcal{J}_{tg}$
Z_{ats}	▸ total mortality rate (natural & fishing) for time period t and sex s
	Likelihood components
$\mathcal{L}_{1g}(\boldsymbol{\Theta}\|\{\widehat{I}_{tg}\})$	▸ log-likelihood component: CPUE or abundance index
$\mathcal{L}_{2g}(\boldsymbol{\Theta}\|\{d_{tg}\})$	▸ log-likelihood component: discard biomass
$\mathcal{L}_{3g}(\boldsymbol{\Theta}\|\{\overline{w}_{tg}\})$	▸ log-likelihood component: mean body weight
$\mathcal{L}_{4g}(\boldsymbol{\Theta}\|\{l_{tg}\})$	▸ log-likelihood component: length composition
$\mathcal{L}_{5g}(\boldsymbol{\Theta}\|\{a_{tg}\})$	▸ log-likelihood component: age composition
$\mathcal{L}_{6g}(\boldsymbol{\Theta}\|\{z_{tg}\})$	▸ log-likelihood component: generalised size composition
$\mathcal{L}_{7g}(\boldsymbol{\Theta}\|\{C_{tg}\})$	▸ log-likelihood component: initial equilibrium catch
$\mathcal{L}_{R}(\boldsymbol{\Theta}\|\{R_{tg}\})$	▸ log-likelihood component: recruitment deviations
$\mathcal{L}_{\phi_j}(\boldsymbol{\Theta}\|\{\phi_j\})$	▸ log-likelihood component: parameter priors
$\mathcal{L}_{P_t}(\boldsymbol{\Theta}\|\{P_t\})$	▸ log-likelihood component: random parameter deviations (if time-varying)
$\mathcal{L}(\boldsymbol{\Theta})$	▸ total log-likelihood
	Prior distributions and objective function
$\phi_j(\boldsymbol{\Theta})$	▸ prior distribution for parameter j
$\phi(\boldsymbol{\Theta})$	▸ joint prior distribution for all estimated parameters
$\mathcal{F}(\boldsymbol{\Theta})$	▸ objective function to be minimised

Table E.2. Deterministic components. Using the catch, weight-at-age and maturity data, with fixed values for all parameters, the initial conditions are calculated from (E.1)-(E.6), and then state dynamics are iteratively calculated through time using the main equations (E.7), selectivity functions (E.8)-(E.14), and the derived states (E.15)-(E.33). Estimated observations for survey biomass indices and proportions-at-age can then be calculated using (E.36) and (E.37). In Table E.3, the estimated observations of these are compared to data.

Deterministic components

Initial conditions ($t = 0\,;\ s = 1, 2$)

$$N_{a0s} = 0.5R_0 e^{-aM_s}\ ; \quad 0 \le a \le 3A\text{-}1 \tag{E.1}$$

$$N_{A0s} = \sum_{a=A}^{3A-1} N_{a0s} + \left(N_{3A-1,0s}\, e^{-M_{as}}\right) / \left(1 - e^{-M_{as}}\right) \tag{E.2}$$

$$B_0 = B_1 = \sum_{a=1}^{A} w_{as} m_{as} N_{a0s}\ ; \quad s{=}1 \ \text{(female)} \tag{E.3}$$

$$L_{a0s} = \begin{cases} \breve{L}_1 + \left(a/a'\right)\left(L'_s - \breve{L}_1\right) & ;\ a \le a' \\ L_{\infty s} + \left(L'_s - L_{\infty s}\right) e^{-k_s(a-a')} & ;\ a' < a \le A\text{-}1 \end{cases} \tag{E.4}$$

$$\text{where}\ \ L_{\infty s} = L'_s + \left(L''_s - L'_s\right)\left[1 - e^{-k_s(a''-a')}\right] \tag{E.5}$$

$$L_{A0s} = \frac{\sum_{a=A}^{2A}\left[e^{-0.2(a-A-1)}\right]\left[L_{As} + (a/A-1)(L_{\infty s} - L_{A0s})\right]}{\sum_{a=A}^{2A} e^{-0.2(a-A-1)}} \tag{E.6}$$

State dynamics ($2 \le t \le T;\ s = 1, 2$)

$$N_{ats} = \begin{cases} cR_{0t} & ;\ a = 0, c = \text{proportion female} \\ N_{a-1,t-1,s}\, e^{-Z_{a,t-1,s}} & ;\ 1 \le a \le A\text{-}1 \\ N_{A-1,t-1,s}\, e^{-Z_{A-1,t-1,s}} + N_{A,t-1,s}\, e^{-Z_{A,t-1,s}} & ;\ a = A \end{cases} \tag{E.7}$$

Selectivity Pattern 20 ($g = 1, 3, 4, 5$)

$$S_{atgs} = \pi_{1atgs}\left(1 - j_{1atgs}\right) + j_{1atgs}\left[\left(1 - j_{2atgs}\right) + j_{2atgs}\pi_{2atgs}\right] \tag{E.8}$$

$$j_{1atgs} = 1 \Big/ \left[1 + e^{-20(a-\beta_{1tgs})/(1+|a-\beta_{1tgs}|)}\right]\ ; \quad \beta_{1tgs} = \text{first age when } S_{tgs}{=}1 \tag{E.9}$$

$$j_{2atgs} = 1 \Big/ \left[1 + e^{-20(a-a^{\star}_{tgs})/(1+|a-a^{\star}_{tgs}|)}\right]\ ; \quad a^{\star}_{tgs} = \text{last age when } S_{tgs}{=}1 \tag{E.10}$$

$$a^{\star}_{tgs} = \beta_{1tgs} + (0.99A - \beta_{1tgs})/(1 + \beta_{2tgs})\ ; \quad \text{assuming age bin = 1y} \tag{E.11}$$

$$\pi_{1atgs} = \left(\frac{1}{1 + e^{-\beta_{5tgs}}}\right)\left(\frac{1}{1 - \left(1 + e^{-\beta_{5tgs}}\right)}\right)\left(\frac{e^{-(a-\beta_{1tgs})^2/e^{\beta_{3tgs}}} - \gamma_{1tgs}}{1 - \gamma_{1tgs}}\right) \tag{E.12}$$

$$\pi_{2atgs} = 1 + \left[\left(\frac{1}{1 + e^{-\beta_{6tgs}}}\right) - 1\right]\left(\frac{e^{-(a-a^{\star}_{tgs})/e^{\beta_{4tgs}}} - 1}{\gamma_{2tgs} - 1}\right) \tag{E.13}$$

$$\gamma_{1tgs} = e^{-(1-\beta_{1tgs})^2/e^{\beta_{3tgs}}}\ ; \quad \gamma_{2tgs} = e^{-(A-a^{\star}_{tgs})^2/e^{\beta_{4tgs}}} \tag{E.14}$$

Deterministic components

Derived states ($1 \le t \le T-1$)

$$L_{ats} = L_{a-1,t-1,s} + \left(L_{a-1-k,t-1,s} - L_{\infty s} \right) \left(e^{-k_s} - 1 \right); \quad a < A \tag{E.15}$$

$$L_{Ats} = \frac{N_{A-1,ts}\bar{L}_{Ats} + N_{Ats}\left[L_{Ats} - \left(L_{Ats} + L_{\infty s} \right) \left(e^{-k_s} - 1 \right) \right]}{N_{A-1,ts} + N_{Ats}} \tag{E.16}$$

$$\bar{L}_{ats} = L_{ats} + \left(L_{ats} - L_{\infty s} \right) \left(e^{-0.5k_s} - 1 \right) \tag{E.17}$$

$$\alpha_{ats} = \begin{cases} \bar{L}_{ats}\nu'_s \,|\, a_{ts}\nu'_s & ; \ a \le a' \\ \bar{L}_{ats}\left[\nu'_s + (\bar{L}_{ats}\text{-}L'_s)/(L''_s\text{-}L'_s)(\nu''_s\text{-}\nu'_s) \right] \,| \\ \quad a_{ts}\nu'_s\left[\nu'_s + (a_{ts}\text{-}a'_s)/(a''_s\text{-}a'_s)(\nu''_s\text{-}\nu'_s) \right] & ; \ a' < a < a'' \\ \bar{L}_{ats}\nu''_s \,|\, a_{ts}\nu''_s & ; \ a'' \le a \end{cases} \tag{E.18}$$

$$\varphi_{lats} = \begin{cases} \Phi\left[(\breve{L}_l - \bar{L}_{ats})/\alpha_{ats} \right] & ; \ l = 1 \\ \Phi\left[(\breve{L}_{l+1} - \bar{L}_{ats})/\alpha_{ats} \right] - \Phi\left[(\breve{L}_l - \bar{L}_{ats})/\alpha_{ats} \right] & ; \ 1 < l < L \\ 1 - \Phi\left[(\breve{L}_l - \bar{L}_{ats})/\alpha_{ats} \right] & ; \ l = L \end{cases} \tag{E.19}$$

$w_{ls} = a_s \mathring{L}_l^{\,b_s}$; $\mathring{L}_l$ = mid-size of length bin l (E.20)

$f_a = \sum_{l=1}^{\Lambda} \varphi_{las}\, m_l o_l w_{ls}$; s=1, m=maturity, o=eggs/kg (E.21)

$Z_{ats} = M_{as} \sum_{g \in 1,\ldots,2} \left(S_{atgs} F_{tg} \right)$; F_{tg} = apical fishing mortality rate (E.22)

$$\mathcal{T}_{1tg} = C_{tg}/(\widehat{\mathcal{B}}_{tg} + 0.1C_{tg}) \ ; \ \mathcal{J}_{1tg} = 1/\left[1 + e^{30(\mathcal{T}_{1tg} - 0.95)}\right] \ ; \ \mathcal{T}_{2tg} = \mathcal{J}_{1tg}\mathcal{T}_{1tg} + 0.95(1 - \mathcal{J}_{1tg}) \tag{E.23}$$

$$F_{1tg} = -\log\left(1 - \mathcal{T}_{2tg} \right) \tag{E.24}$$

$$\widehat{C}_t = \sum_{g \in 1,\ldots,2} \sum_{s=1}^{2} \sum_{a=0}^{A} \frac{F_{1tg}}{Z_{ats}} w_{as} N_{ats} S_{atgs} \lambda_{ats} \ ; \quad \lambda_{ats} = \left(1 - e^{-Z_{ats}} \right)/\left(Z_{ats} \right) \tag{E.25}$$

$$\overrightarrow{Z}_t = C_t/(\widehat{C}_t + 0.0001) \ ; \ Z'_{ats} = M_{as} + \overrightarrow{Z}_t(Z_{ats} - M_{as}) \ ; \ \lambda'_{ats} = (1 - e^{-Z'_{ats}})/(Z'_{ats}) \tag{E.26}$$

$$\mathcal{T}_{3tg} = \sum_{s=1}^{2} \sum_{a=0}^{A} w_{as} N_{ats} S_{atgs} \lambda'_{ats} \tag{E.27}$$

$$F_{2tg} = C_{tg}/(\mathcal{T}_{3tg} + 0.0001) \ ; \quad \mathcal{J}_{2tg} = 1/\left[1 + e^{30(F_{2tg} - 0.95F_{\max})}\right] \tag{E.28}$$

$F_{tg} = \mathcal{J}_{2tg}F_{2tg} + (1 - \mathcal{J}_{2tg})F_{\max}$; updated estimate of F using hybrid method above (E.29)

$$C_{ats} = \sum_{g \in 1,\ldots,2} \frac{F_{tg}}{Z'_{ats}} w_{as} N_{ats} S_{atgs} \lambda'_{ats} \tag{E.30}$$

$B_t = \sum_{a=0}^{A} N_{ats} f_a$; s=1, f=fecundity (E.31)

$$V_{tg} = \sum_{s=1}^{2} \sum_{a=1}^{A} e^{-M_s/2} w_{as} N_{ats} S_{atgs} \ ; \quad g \in \{1, \ldots, 2\}, \ u_{tg} = C_{tg}/V_{tg}, \ u_{atgs} = u_{tg} S_{atgs} \tag{E.32}$$

Deterministic components

$$R_t = \frac{4hR_0B_{t-1}}{(1-h)B_0 + (5h-1)B_{t-1}} \quad \left(\equiv \frac{B_{t-1}}{\alpha + \beta B_{t-1}} \right) \tag{E.33}$$

Ageing error

$$\Phi(x|\mu,\sigma) = \frac{1}{\sqrt{2\pi}} \int_{-\infty}^{(x-\mu)/\sigma} e^{-(t^2/2)}\, dt \quad \text{cumulative normal distribution} \tag{E.34}$$

$$\Psi_a = \begin{cases} \Phi\left(\frac{a-\widetilde{a}_a}{\xi_a}\right) & ; \ a = 1 \\ \Phi\left(\frac{a+1-\widetilde{a}_a}{\xi_a}\right) - \Phi\left(\frac{a-\widetilde{a}_a}{\xi_a}\right) & ; \ 1 < a < A \\ 1 - \Phi\left(\frac{A-\widetilde{a}_a}{\xi_a}\right) & ; \ a = A \end{cases} \tag{E.35}$$

Estimated observations

$$\widehat{I}_{tg} = q_g \sum_{s=1}^{2} \sum_{a=1}^{A} e^{-M_s/2}(1 - u_{ats}/2) w_{as} S_{ags} N_{ats}\,; \quad t \in \mathbf{T}_g, \ g = 1, 3, ..., 8 \tag{E.36}$$

$$\widehat{p}_{atgs} = \frac{e^{-M_s/2}(1 - u_{ats}/2) S_{ags} N_{ats}}{\sum_{s=1}^{2} \sum_{a=1}^{A} e^{-M_s/2}(1 - u_{ats}/2) S_{ags} N_{ats}}; \ {\scriptstyle 1 \le a \le A, \ t \in \mathbf{U}_g, \ g=1,3,4,5, \ s=1,2} \tag{E.37}$$

Table E.3. Stochastic components. Calculation of likelihood function $\mathcal{L}(\boldsymbol{\Theta})$ for stochastic components of the model in Table E.2, and resulting objective function $f(\boldsymbol{\Theta})$ to be minimised.

Stochastic components

Estimated parameters

$$\boldsymbol{\Theta} = \{R_0; M_{1,2}; h; q_{1,3,\ldots,8}; \mu_{1,3,4,5}, \pi_{\mathsf{T}1,3,4,5}, v_{\mathsf{L}1,3,4,5L}, v_{\mathsf{R}1,3,4,5}, \pi_{\mathsf{F}1,3,4,5}, \theta_{1,3,4,5}\} \tag{E.38}$$

Recruitment deviations

$$\rho_{t+1} = \log R_{t+1} - \log B_t + \log(\alpha + \beta B_t) + 0.5 b_t \sigma_R^2 + \epsilon_t \; ; \quad \epsilon_t \sim \mathcal{N}(0, \sigma_R^2) \, , \; 1 \le t \le T\text{-}1 \tag{E.39}$$

$$\text{where } \; b_t = \begin{cases} 0 & ; \; t \le t_1^b \\ b_{\max}\left[1 - (t - t_1^b)/(t_2^b - t_1^b)\right] & ; \; t_1^b < t < t_2^b \\ b_{\max} & ; \; t_2^b \le t \le t_3^b \\ b_{\max}\left[1 - (t_3^b - t)/(t_4^b - t_3^b)\right] & ; \; t_3^b < t < t_4^b \\ 0 & ; \; t_4^b \le t \end{cases} \tag{E.40}$$

Log-likelihood components (⊛ active, ◁ inactive)

$$\circledast \; \mathcal{L}_{1g}(\boldsymbol{\Theta}|\{\widehat{I}_{tg}\}) = \sum_{t \in \mathbf{T}_g} \left[\frac{(\log I_{tg} - \log(q_g B_{tg}))^2}{2\kappa_{tg}^2} + \kappa'_{tg} \log \kappa_{tg} \right] \tag{E.41}$$

$$\triangleleft \; \mathcal{L}_{2g}(\boldsymbol{\Theta}|\{d_{tg}\}) = \sum_{t=1}^{T} 0.5(\mathsf{df}_g + 1) \log \left[\frac{1 + (d_{tg} - \widehat{d}_{tg})^2}{\mathsf{df}_g \delta_{tg}^2} \right] + \delta'_{tg} \log \delta_{tg} \tag{E.42}$$

$$\triangleleft \; \mathcal{L}_{3g}(\boldsymbol{\Theta}|\{\overline{w}_{tg}\}) = \sum_{t=1}^{T} 0.5(\mathsf{df}_{\overline{w}} + 1) \log \left[\frac{1 + (\overline{w}_{tg} - \widehat{\overline{w}}_{tg})^2}{\mathsf{df}_{\overline{w}} \psi_{tg}^2} \right] + \psi'_{tg} \log \psi_{tg} \tag{E.43}$$

$$\triangleleft \; \mathcal{L}_{4g}(\boldsymbol{\Theta}|\{l_{tg}\}) = \textstyle\sum_{t \in \mathbf{U}_g} \sum_{s=1}^{2} \sum_{l=1}^{L} n_{tgs} \, p_{ltgs} \, \log\left(p_{ltgs} / \widehat{p}_{ltgs}\right) \text{ ; composition option 1} \tag{E.44}$$

$$\circledast \; \mathcal{L}_{5g}(\boldsymbol{\Theta}|\{a_{tg}\}) = \textstyle\sum_{t \in \mathbf{U}_g} \sum_{s=1}^{2} \sum_{a=1}^{A} n_{tgs} \, p_{atgs} \, \log\left(p_{atgs} / \widehat{p}_{atgs}\right) \text{ ; composition option 2} \tag{E.45}$$

$$\triangleleft \; \mathcal{L}_{6g}(\boldsymbol{\Theta}|\{z_{tg}\}) = \textstyle\sum_{t \in \mathbf{U}_g} \sum_{s=1}^{2} \sum_{z=1}^{\Lambda} n_{tgs} \, p_{ztgs} \, \log\left(p_{ztgs} / \widehat{p}_{ztgs}\right) \text{ ; composition option 3} \tag{E.46}$$

$$\circledast \; \mathcal{L}_{7g}(\boldsymbol{\Theta}|\{C_{tg}\}) = \textstyle\sum_{t=1}^{T} \left[\log C_{tg} - \log(\widehat{C}_{tg} + 1\mathsf{e}\text{-}6)\right]^2 / \, 2\tau_{tg}^2 \tag{E.47}$$

$$\circledast \; \mathcal{L}_R(\boldsymbol{\Theta}|\{R_t\}) = 0.5 \textstyle\sum_{t=1}^{T} (\widetilde{R}_t^2 / \sigma_R^2) + b_t \log \sigma_R^2 \tag{E.48}$$

$$\circledast \; \mathcal{L}_{\phi_j}(\boldsymbol{\Theta}|\{\phi_j\}) = 0.5 \left[(\phi_j - \mu_{\phi_j})/\sigma_{\phi_j}\right]^2 \quad \text{; normal prior distributions for parameter } j \tag{E.49}$$

$$\circledast \; \mathcal{L}_{\phi_j}(\boldsymbol{\Theta}|\{\phi_j\}) = 0.5 \left[(\log \phi_j - \mu_{\phi_j})/\sigma_{\phi_j}\right]^2 \quad \text{; lognormal prior distributions for parameter } j \tag{E.50}$$

$$\triangleleft \; \mathcal{L}_{P_j}(\boldsymbol{\Theta}|\{P_{jt}\}) = (1/2\sigma_P^2) \textstyle\sum_{t=1}^{T} \widetilde{P}_{jt}^2 \quad \text{; for time-varing parameters, if any} \tag{E.51}$$

Objective function

$$\mathcal{F}(\boldsymbol{\Theta}) = \sum_{i=1}^{7} \sum_{g=1}^{G} \omega_{ig} \mathcal{L}_{ig} + \omega_R \mathcal{L}_R + \sum_{\phi} \omega_\phi \mathcal{L}_\phi + \sum_{P} \omega_P \mathcal{L}_P \quad ; \omega = \text{weighting factors for each } \mathcal{L} \tag{E.52}$$

Table E.4. Details for estimation of parameters, including prior distributions with corresponding means and standard deviations, bounds between which parameters are constrained, and initial values to start the minimisation procedure for the MPD (mode of the posterior density) calculations. For uniform prior distributions, the bounds completely parameterise the prior. In SS3, an analytical solution for q is calculated when the parameter is allowed to 'float'.

Parameter	Phase	Prior distribution	Mean, SD	Bounds	Initial value
CAR coastwide					
$\log R_0$	1	normal	7, 7	[1, 16]	7
M_2 (female)	4	normal	0.06, 0.018	[0.02, 0.2]	0.06
M_1 (male)	4	normal	0.06, 0.018	[0.02, 0.2]	0.06
h	5	beta	0.67, 0.17	[0.2, 1]	0.76
$\log q_{1,\ldots,8}$	-	analytic	-3, 6	[-15, 15]	-3
$\mu_{1,3,4,5}$	3	normal	14, 4.2	[5, 40]	14
$\mu_{2,6,7,8}$	-	fixed	14, 4.2	[5, 40]	14
$\log v_{\text{L}1,3,4,5}$	4	normal	2.5, 0.75	[-15, 15]	2.5
$\log v_{\text{L}2,6,7,8}$	-	fixed	2.5, 0.75	[-15, 15]	2.5
$\Delta_{1,3,4,5}$	4	normal	-0.4, 0.12	[-8, 10]	-0.4
$\Delta_{2,6,7,8}$	-	fixed	-0.4, 0.12	[-8, 10]	-0.4

E.4. DESCRIPTION OF DETERMINISTIC COMPONENTS

Notation (Table E.1) and set up of the deterministic components (Table E.2) are described below. Acronyms: SS3 = Stock Synthesis 3, AW = Awatea, AF = age frequencies|proportions, CAR = Canary Rockfish.

E.4.1. Age classes

Index (subscript) a represents age classes, going from 1 to the accumulator age class A of 60. Age class $a = 5$, for example, represents fish aged 4-5 years (which is the usual, though not universal, convention, Caswell 2001), and so an age-class 1 fish was born the previous year. The variable N_{ats} is the number of age-class a fish of sex s at the *start* of year t, so the model is run to year T which corresponds to the beginning of year 2023.

E.4.2. Years

Index t represents model years, going from 1 to $T = 89$, and $t = 0$ represents unfished equilibrium conditions. The actual year corresponding to $t = 1$ is 1935, and so model year $T = 89$ corresponds to 2023. The interpretation of year depends on the model's derived state or data input:

- beginning of year: N_{ats}, B_t, R_t
- middle of year: C_{tg}, V_{tg}, F_{tg}, u_{tg}, $\widehat{I}_{tg}$, $\widehat{p}_{atgs}$

E.4.3. Commercial Data

As described in Appendix A, the commercial catch was reconstructed back to 1918 for five fisheries – (1) trawl, (2) halibut longline, (3) sablefish trap|longline, (4) dogfish|lingcod|salmon troll, and (5) hook & line rockfish in outside (offshore) waters – all excluding PMFC area 4B (Strait of Georgia). In this assessment, two fisheries were used – 'Trawl' & 'Other' (comprising

the four non-trawl fisheries). Given the negligible catches in the early years, the model was started in 1935, with catches prior to 1935 not considered. The time series for catches by fishery are denoted C_{tg} and include retained and discarded catches (either observed or reconstructed). The set $\mathbf{U}_1$ (Table E.1) gives the years of available ageing data from the commercial fishery. The proportions-at-age values are given by p_{atgs} with observed sample size n_{tg}, where $g = 1$ corresponds to the commercial data source. The proportions are calculated using the stratified weighting scheme, described in Appendix D, that adjusts for unequal sampling effort across temporal and spatial strata.

E.4.4. Survey Data

Survey data from six 'fleets' (g=$3, ..., 8$) were used in the model, as described in detail in Appendix B. These surveys are indexed using g, with each subscript corresponding to a survey: g=3: Queen Charlotte Sound (QCS) Synoptic; g=4: West Coast Vancouver Island (WCVI) Synoptic; g=5: NMFS Triennial; g=6: Hecate Strait (HS) Synoptic; g=7: West Coast Haida Gwaii (WCHG) Synoptic; g=8: Goose Island Gully (GIG) Historical. The years for which data were available for each survey are given in Table E.1; $\mathbf{T}_g$ corresponds to years for the survey biomass estimates I_{tg} (and corresponding standard deviations κ_{tg}), and $\mathbf{U}_g$ corresponds to years for proportion-at-age data p_{atgs} (with observed sample sizes n_{tg}). Note that for surveys, sample size refers to the number of tows sampled, where each sample comprises specimens, typically ~5-50 fish.

E.4.5. Sex

A two-sex model was used, with subscript s=1 for females and s=2 for males (note that these subscripts are the reverse of the codes used in the GFBioSQL database). Ageing data were partitioned by sex, as were the weights-at-age inputs. Selectivities and natural mortality were specified by sex.

E.4.6. Weights-at-age

The weights-at-age w_{as} were assumed fixed over time and were based on sex-specific allometric (length-weight) and growth (age-length) model parameters derived from the biological data; see Appendix D for details.

E.4.7. Maturity of females

The proportion of age-class a females that are mature is m_a, and was assumed to be invariant over time; see Appendix D for details.

E.4.8. Initial conditions

An unfished equilibrium at the beginning of the reconstruction was assumed because there was no evidence of significant removals prior to 1935. The initial conditions (E.1) and (E.2) were obtained by setting $R_t = R_0$ (virgin recruitment), $N_{ats} = N_{a1s}$ (equilibrium condition) and $u_{ats} = 0$ (no fishing). The virgin spawning biomass B_0 was obtained from (E.3). The initial lengths were set using the growth equations of Schnute (1981) (E.4)-(E.6).

E.4.9. State dynamics

The core of the model is the set of dynamic equations (E.7) for the estimated number N_{ats} of age-class a fish of sex s at the start of year t. The proportion of female new recruits c in Equation (E.7) was set to 0.5. Equation (E.7) calculates the numbers of fish in each age class (and of each sex) that survive to the following year, where Z_{ats} represents the total mortality rate, which in this case comprises the sum of natural mortality M and fishing mortality F. The accumulator age class A retains survivors from this class in following years.

Natural mortality M_s was estimated separately for males and females. This parameter enters the equations in the form e^{-M_s} as the proportion of unfished individuals that survive the year.

E.4.10. Selectivities

Separate selectivities were estimated for each of the fleets with AF data (g=1 for the fishery, g=3 for QCS synoptic, g=4 for WCVI synoptic, and g=5 for NMFS triennial) using SS3's selectivity pattern 20 for females (Equations E.8-E.14) and selectivity option 3 for males. Note that 'log' herein refers to natural logarithms. Pattern 20 describes double normal selectivity for females where the parameters β_i ($i = 1, ..., 6$) for fleet g are:

1. β_{1g} – age at which selectivity first reaches maximum selectivity:
   - SS3: beginning age (year) for the plateau;
   - AW: age of full selectivity (μ_g) for females;
2. β_{2g} – (SS3 only) used to generate a logistic between peak (β_{1g}) and maximum age (A) that determines width of top plateau ($a_g^\star - \beta_{1g}$), where $a_g^\star$ is the final age of the top plateau;
3. β_{3g} – used to determine width of the ascending limb of double normal curve:
   - SS3: determines slope of ascending limb by tweaking its variance;
   - AW: log of variance for left limb ($v_{\mathsf{L}g}$) of selectivity curve;
4. β_{4g} – used to determine width of the descending limb of double normal curve:
   - SS3: determines slope of descending limb by tweaking its variance;
   - AW: log of variance for right limb ($v_{\mathsf{R}g}$) of selectivity curve;
5. β_{5g} – (SS3 only) determines initial selectivity by generating a logistic between 0 and 1 at first age;
   - where selectivity $S_{a=1,g} = 1/(1 + e^{-\beta_{5g}})$; however,
   - use -999 to ignore initial selectivity algorithm and decay small fish selectivity using β_{3g};
6. β_{6g} – (SS3 ony) determines final selectivity by generating a logistic between 0 and 1 at final age bin;
   - where selectivity $S_{Ag} = 1/(1 + e^{-\beta_{6g}})$.

Option 3 for pattern 20 describes male selectivity as offsets to female selectivity, where parameters Δ_i ($i = 1, ..., 5$) for fleet g are:

1. Δ_{1g} = male peak offset (Δ_g in AW) added to the first female selectivity parameter, β_{1g} (μ_g in AW);
2. Δ_{2g} = male width offset (log width) added to the third selectivity parameter, β_{3g} (same as female $v_{\mathsf{L}g}$ in AW);

3. Δ_{3g} = male width offset (log width) added to the fourth selectivity parameter, β_{4g} (same as female $v_{\mathrm{R}g}$ in AW);
4. Δ_{4g} = male plateau offset added to the sixth selectivity parameter, β_{6g} (not present in AW);
5. Δ_{5g} = apical selectivity for males (usually 1 but could be different than that for females; not present in AW).

Dome selectivity only occurs under three conditions:

- the width of the top plateau (between β_{1g} and $a_g^\star$) must be less than $A - \beta_{1g}$;
- the steepnees of the descending limb (controlled by β_{4g}) must not be too shallow; and
- the final selectivity (controlled by β_{6g}) must be less than peak selectivity (usually 1).

Generally for males, the same selectivity function is used except that some of the selectivity parameters (β_{ig} for $i \in \{1, 3, 4, 6\}$) may be shifted if male AF data are sufficiently different from female AF data.

E.4.11. Derived states

The spawning biomass (biomass of mature females, in tonnes) B_t at the start of year t is calculated in (E.31) by multiplying the numbers of females N_{at1} by fecundity f_a (E.21), which is a function of a length-age matrix φ_{lats} (E.19), the maturity ogive (m_l), egg production (o_l), and weights-at-length w_{l1} (E.20).

The fishing mortality rate F_{tg} (E.29) is derived through an iterative process to fit observed catches closely rather than removing the catches by subtraction. A mid-season harvest rate is calculated using Pope's approximation (Pope 1972), which is then converted to an instantaneous F using the Baranov equation (Baranov 1918). Each fleet's approximate F is repeated iteratively several times (usually three to four) using the Newton-Rhapson procedure until its value yields a close match to the observed catches by the fleet. Details can be found in Methot and Wetzel (2013).

Although SS3 does not report vulnerable biomass *per se*, equation (E.32) provides an equation from Awatea for V_{tg} mid-year. Assuming that C_{tg} is taken mid-year, the harvest rate is simply C_{tg}/V_{tg}. Further, for year t, the proportion u_{tg} of age-class a and sex s fish that are caught in fishery g can be calculated by multiplying the commercial selectivities S_{atgs} and the ratio u_t (E.32).

E.4.12. Stock-recruitment function

A Beverton-Holt recruitment function is used, parameterised in terms of steepness, h, which is the proportion of the long-term unfished recruitment obtained when the stock abundance is reduced to 20% of the virgin level (Mace and Doonan 1988; Michielsens and McAllister 2004). Awatea uses a prior on h taken from Forrest et al. (2010), where shape parameters for a beta distribution are $\alpha = (1-h)B_0/(4hR_0)$ and $\beta = (5h-1)/4hR_0$ (Hilborn et al. 2003; Michielsens and McAllister 2004). Substituting these into the Beverton-Holt equation, $R_t = B_{t-1}/(\alpha + \beta B_{t-1})$, where R_0 is the virgin recruitment, R_t is the recruitment in year t, B_t is the spawning biomass at the start of year t, and B_0 is the virgin spawning biomass. SS3 offers several recruitment options including Ricker, Beverton-Holt, and a three-parameter survivorship-based function suitable for low-fecundity species (Taylor et al. 2013).

E.4.13. Fitting to data

Model estimates of the survey biomass indices I_{tg} are denoted $\widehat{I}_{tg}$ and are calculated in (E.36). The estimated numbers N_{ats} are multiplied by the natural mortality term $e^{-M_s/2}$ (that accounts for half of the annual natural mortality), the term $1 - u_{ats}/2$ (that accounts for half of the commercial catch), weights-at-age w_{as} (to convert to biomass), and selectivity S_{ags}. The sum (over ages and sexes) is then multiplied by the catchability parameter q_g to give the model biomass estimate $\widehat{I}_{tg}$.

The estimated proportions-at-age $\widehat{p}_{atgs}$ are calculated in (E.37). For a particular year and gear type, the product $e^{-M_s/2}(1 - u_{ats}/2)S_{ags}N_{ats}$ gives the relative expected numbers of fish caught for each combination of age and sex. Division by $\sum_{s=1}^{2}\sum_{a=1}^{A} e^{-M_s/2}(1 - u_{ats}/2)S_{ags}N_{ats}$ converts these to estimated proportions for each age-sex combination, such that $\sum_{s=1}^{2}\sum_{a=1}^{A}\widehat{p}_{atgs} = 1$.

Ageing error (AE) in this stock assessment was applied using SS3's vector-style inputs of bias and precision. The bias vector used was 0.5 to 60.5 at increments of 1 year for ages 0 through 60, which in SS3 signifies no age bias. The precision vector for ages 0 through 60 was estimated as the standard deviation of ages 1 through 61 calculated from the CVs of lengths-at-age: $\sigma_a = a(\sigma_{L_a}/\mu_{L_a})$, where $a = 1, ..., 61$. Using these vectors, SS3 applies a cumulative normal distribution for each age to calculate the frequency of expected age given a mean assigned age and standard deviation (see E.35).

> *"SS3 never adjusts input data. Rather, it adjusts expected values for data to take into account known factors that influenced the creation of the observations. So, ageing error is applied to a modeled distribution of true ages (after selectivity has taken a subset from the population) to create a new distribution of ages that includes the influence of ageing error."*
>
> – Richard Methot, 2021, *pers. comm.*

E.5. DESCRIPTION OF STOCHASTIC COMPONENTS

E.5.1. Parameters

The set $\boldsymbol{\Theta}$ gives the parameters that are estimated. The estimation procedure is described in the Bayesian Computations section below.

E.5.2. Recruitment deviations

For recruitment, a log-normal process error is assumed, such that the stochastic version of the deterministic stock-recruitment function (E.33) is

$$R_t = \frac{B_{t-1}}{\alpha + \beta B_{t-1}} e^{-0.5 b_t \sigma_R^2 + \epsilon_t} \tag{E.53}$$

where $\epsilon_t \sim \mathcal{N}(0, \sigma_R^2)$, and the bias-correction term $-b_t\sigma_R^2/2$ term in (E.53) ensures that the mean of the recruitment deviations equals 0. This then gives the recruitment deviation equation (E.39) and log-likelihood function (E.48). In this assessment, the value of σ_R was fixed at 0.9 based on values used in recent BC rockfish stock assessments. Other assessments have used σ_R = 0.6 following an assessment of Silvergray Rockfish (Starr et al. 2016) in which the authors stated that the value was typical for marine 'redfish' (Mertz and Myers 1996). An Awatea model of Rock Sole used σ_R = 0.6 (Holt et al. 2016), citing that it was a commonly used default for finfish assessments (Beddington and Cooke 1983). In recent BC rockfish assessments, we have adopted σ_R = 0.9 based on an empirical model fit consistent with the age composition data for

5ABC POP (Edwards et al. 2012*b*). A study by Thorson et al. (2014) examined 154 fish populations and estimated σ_R = 0.74 (SD=0.35) across seven taxonomic orders; the marginal value for Scorpaeniformes was σ_R=0.78 (SD=0.32) but was only based on 7 stocks.

E.5.3. Log-likelihood functions

The objective funtion function $\mathcal{F}(\boldsymbol{\Theta})$ (E.52) comprises a weighted sum of individual likelihood components that include:

- $\mathcal{L}_{I_g}$ (E.41) – CPUE or abundance index by fleet
- $\mathcal{L}_{a_g}$ (E.45) – age composition by fleet
- $\mathcal{L}_{C_g}$ (E.47) – catch by fleet
- $\mathcal{L}_R$ (E.48) – recruitment deviations
- $\mathcal{L}_{\phi_j}$ (E.49) to (E.50) – parameter priors
- $\mathcal{L}_{P_j}$ (E.51) – random parameter deviations

See Methot and Wetzel (2013) and Methot et al. (2021) for more likelihood options and details.

E.6. BAYESIAN COMPUTATIONS

Estimation of parameters compares the estimated (model-based) observations of survey biomass indices and proportions-at-age with the data, and minimises the recruitment deviations. This is done by minimising the objective function $f(\boldsymbol{\Theta})$, which equation (E.52) shows is the negative of the sum of the total log-likelihood function comprising the logarithmic components (E.41)-(E.51).

The procedure for the Bayesian computations is as follows:

1. minimise the objective function $f(\boldsymbol{\Theta})$ to give estimates of the mode of the posterior density (MPD) for each parameter:
   a. this is done in phases,
   b. a reweighting procedure is performed;
2. generate samples from the joint posterior distributions of the parameters using Monte Carlo Markov Chain (MCMC) procedure, starting the chains from the MPD estimates.

E.6.1. Phases

The MPD estimates were obtained by minimising the objective function $f(\boldsymbol{\Theta})$, from the stochastic (non-Bayesian version) of the model. The resulting estimates were then used to initiate the chains for the MCMC procedure for the full Bayesian model.

Simultaneously estimating all the estimable parameters for complex nonlinear models is ill advised, and so ADMB allows some of the estimable parameters to be kept fixed during the initial part of the optimisation process ADMB Project (2009). Some parameters are estimated in phase 1, then some further ones in phase 2, and so on. The order (if estimated) typically used by the BC Offshore Rockfish assessment team is:

phase 1: virgin recruitment R_0 and survey catchabilities $q_{3,...,8}$
(although the q fit herein adopts a 'float' option, which calculates an analytical solution);
phase 2: recruitment deviations ϵ_t (held at 0 in phase 1);
phase 3: natural mortality M_s and age of full selectivity for females β_{1g} for g=$1, 3, 4, 5$;
phase 4: additional selectivity parameters β_{ng} for n=$2, ..., 6$ and g=$1, 3, 4, 5$;
phase 5: steepness h.

E.6.2. Reweighting

Sample sizes are used to calculate the variance for a data source and are useful to indicate the relative differences in uncertainty across years within each data source. However, sample size may not represent the relative difference in the variance between different data sources (usually abundance vs. composition). Therefore, the relative weights for each data source in an integrated stock assessment should be adjusted to reflect the information content of each, while retaining the relative differences across years. This can be accomplished by applying adjustment factors to abundance and composition data to weight either data source up or down relative to the other. Previous rockfish stock assessments using the Awatea platform (from 2011) adopted the Francis (2011) reweighting approach – adding series-specific process error to abundance index CVs on the first reweight, and iteratively reweighting age frequency (composition data) sample size by mean age on the first and subsequent reweights.

E.6.2.1. Abundance

For abundance data (survey indices, commercial CPUE indices), Francis (2011) recommends reweighting observed coefficients of variation, c_0, by first adding process error c_p ~ 0.2 to give a reweighted coefficient of variation

$$c_1 = \sqrt{c_0^2 + c_\mathrm{p}^2}\ . \tag{E.54}$$

Survey abundance indices for CAR exhibited high relative error, and so no additional error c_p was added to these indices.

A procedure was developed for estimating process error c_p to add to the commercial CPUE using a spline-smoother analysis. Francis (2011), citing Clark and Hare (2006), recommends using a smoothing function to determine the appropriate level of process error to add to CPUE data, with the goal of finding a balance between rigorously fitting the indices while not removing the majority of the signal in the data. An arbitrary sequence of length 50, comprising degrees of freedom (DF, ν_i), where $i = 2, ..., N$ and N = number of CPUE values U_t from $t = 1996, ..., 2021$, was used to fit the CPUE data with a spline smoother. At $i = N$, the spline curve fit the data perfectly and the residual sum of squares (RSS, ρ_N) was 0. Using spline fits across a range of trial DF ν_i, values of RSS ρ_i formed a logistic-type curve with an inflection point at $i = k$ (Figure E.1). The difference between point estimates of ρ_i (proxy for the slope δ_i) yielded a concave curve with a minimum δ_i, which occurred close to the inflection point k. At the inflection point k, ν_k= 5.4 for CAR coastwide, corresponding to ρ_k= 0.83, which was converted to c_p= 0.178 using:

$$c_\mathrm{p} = \sqrt{\frac{\rho_k}{N-2}}\ \left[\frac{1}{N}\sum_{t=1996}^{2021} U_t\right]^{-1}\ . \tag{E.55}$$

For each model run, the abundance index CVs were adjusted on the first reweight only using the process error c_p = 0.178, 0, 0, 0, 0, 0, and 0 along the BC coast (g=1,3,...,8).

E.6.2.2. Composition

In this stock assessment, composition data were reweighted using the Dirichlet-Multinomial distribution available in SS3 (Thorson et al. 2017). This approach adds an estimable parameter (θ) which automatically scales the input sample size as part of the likelihood.

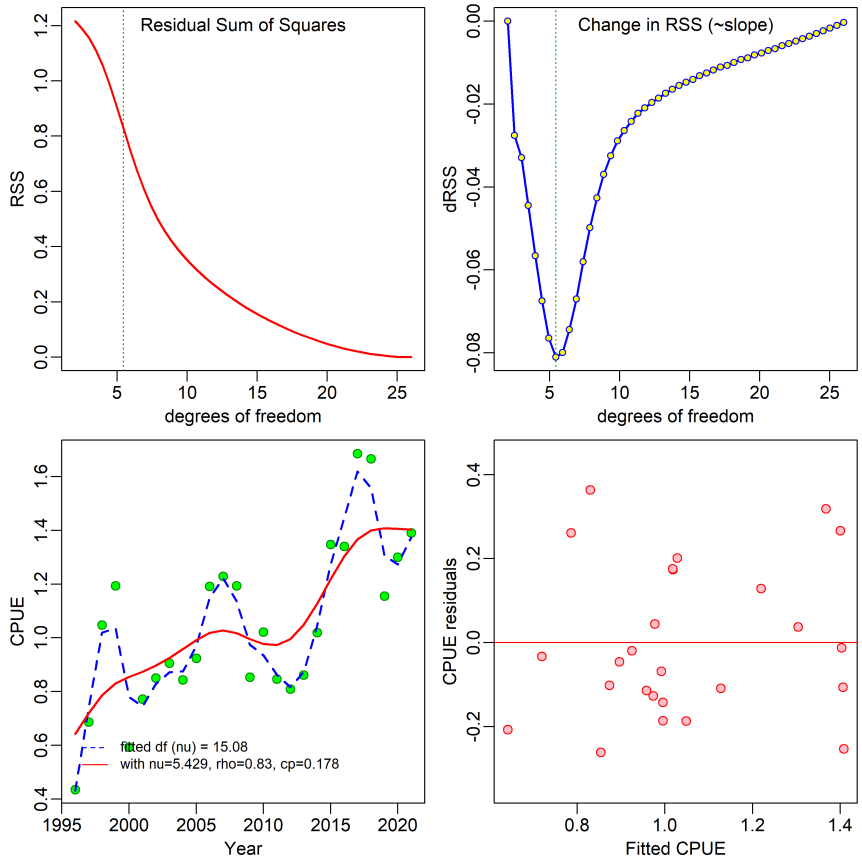

Figure E.1. Estimating process error to add to commercial CPUE data: top left – residual sum of squares (RSS) from spline-smoother at various degrees of freedom; top right – slope of RSS (~ first derivative), vertical dotted line at DF where slope is at a minimum; bottom left – CPUE index data with spline-fitted DF=15.1 (dashed blue curve) and optimised DF=5.4 (solid red curve); bottom right – standardised residual fit.

> *"In consultation with Jim Thorson, Ian Taylor proposed a normal $\mathcal{N}(0,1.813)$ prior for the* `ln(DM_parm)` *parameters to counteract the effect of the logistic transformation between this parameter and the data weighting. The 1.813 value was calculated as the standard deviation of the distribution of $\log(\theta)$ values derived from starting with a uniform distribution on the weights, weight = $\theta/(1+\theta) \sim \mathcal{U}(0,1)$, and solving for $\log(\theta)$."*
>
> – Methot et al. (2021), *Data Weighting*

If the calculated weight $\theta/(1+\theta)$ ratio is close to 1.0, the model is trying to tune the sample size as high as possible. In this case, Methot et al. (2021) suggest fixing the $\log$ DM θ parameter to a high value, like the upper bound of 20, which will result in 100% weight being applied to the input sample sizes. One caveat of using the $\log$ DM θ parameter is that it does not allow weights above 100% (by design).

E.6.3. Prior distributions

Descriptions of the prior distributions for the estimated parameters (without including recruitment deviations) are given in Table E.4. A wide normal prior $\mathcal{N}(7,7)$ was used for R_0; this provided

more stability in the model than using a uniform prior without affecting the estimation process. Steepness was estimated using a beta distribution, with priors generated by Forrest et al. (2010): β(0.67,0.17). Catchability parameters q_g were determined analytically by SS3 (using `float=1`). Selectivity was estimated using priors approximated from the MPD results in Table J.7 (p.157) of the 2007 CAR stock assessment (Stanley et al. 2009). The parameter estimates for commercial selectivity were very similar for Runs 8 to 17 so we chose μ=14, $\log v_{\text{L}}$=2.5, and Δ=-0.4 for means and CV=30% for standard deviations in the normal priors. Natural mortality was modelled using a normal prior with mean (M=0.06) based on the estimators of Hoenig (1983) and V. Gertseva (NWFSC, pers. comm., 2018) for the oldest age (84 years) and assumed a 30% CV.

E.6.4. MCMC properties

The MCMC procedure used the 'no U-turn sampling' (NUTS) algorithm (Monnahan and Kristensen 2018; Monnahan et al. 2019) to produce 8,000 (for base) / 4,000 (for sensitivities) iterations, parsing the workload into 8 parallel chains (using the R package `snowfall`, Knaus 2015) of 1,000 (base) / 500 (sens) iterations each, discarding the first 750 (base) / 250 (sens) iterations in each chain as a 'burn-in', leaving the final 250 samples per chain for use in the MCMC analysis. The parallel chains were then merged for a total of 2,000 samples to approximate the posterior distribution.

E.7. REFERENCE POINTS, PROJECTIONS, AND ADVICE TO MANAGERS

Advice to managers is given with respect to a suite of reference points. The first set is based on MSY (maximum sustainable yield) and includes the provisional reference points of the DFO Precautionary Approach (DFO 2006), namely 0.4B_{MSY} and 0.8B_{MSY} (and also provided are B_{MSY} and u_{MSY}, which denote the estimated equilibrium spawning biomass and harvest rate at MSY, respectively). A second set of reference points, based on the current spawning biomass B_{2023} and harvest rate u_{2022}, is used to show the probability of the stock size increasing from the current female spawning biomass or decreasing from the current harvest rate. A third set of reference points, based on B_0 (the estimated unfished equilibrium spawning biomass) is provided as an alternative to the B_{MSY} reference points. See main text for further discussion.

The probability P($B_{2023} > 0.4B_{\text{MSY}}$) is calculated as the proportion of the 2,000 MCMC samples for which $B_{2023} > 0.4B_{\text{MSY}}$ (and similarly for the other biomass-based reference points). For harvest rates, the probability P($u_{2022} < u_{\text{MSY}}$) is calculated so that both B- and u-based stock status indicators (and projections when $t = 2024, ..., 2033$) state the probability of being in a 'good' place.

Projections were made for 11 years starting with the biomass for the start of 2023. The user of SS3 should be aware that all derived values are for a start-of-year time period. Therefore, if the end year in the data file is specified as 2022, derived quantities like spawning biomass B_t are estimated to start of year 2022. By default, SS3 will project forward at least one year so that catch in 2022 can be applied and derived quantities will be generated for 2023 (one-year forecast). Therefore, in the file `forecast.ss`, a user needs to specify the current year plus any additional forecast years (e.g., a 10-yr forecast would need 11 specified catches from 2023 to 2034). Additionally, if a user needs generational forecasts (e.g, three CAR generations = 75 years), then 76 forecast years need to be specified before any MCMC runs are attempted.

A range of constant catch strategies were used, from 0 to 2000 t at 250 t increments (the average combined catch from 2017 to 2021 was 789 t along the BC coast). For each strategy, projections

were performed for each of the 2,000 MCMC samples (resulting in posterior distributions of future spawning biomass). Recruitments were randomly calculated using (E.33) (i.e. based on lognormal recruitment deviations from the estimated stock-recruitment curve), using randomly generated values of $\epsilon_t \sim \text{Normal}(0, \sigma_R^2)$. Unfortunately, SS3 calculates projected recruitment deviations at the time of the MCMC runs and so the user should be aware that changing the catch policy after the MCMCs had been performed is not possible. In Awatea, the `-mceval` switch can generate a user-specified time series of $\{\epsilon_t\}$ for each of the MCMC samples, which means that catch policies can vary in the number of years projected forward.

E.8. REFERENCES – MODEL EQUATIONS

ADMB Project. 2009. AD Model Builder: Automatic Differentiation Model Builder. Developed by David Fournier and freely available from admb-project.org.

Baranov, F.I. 1918. "On the question of the biological basis of fisheries: on the question of the dynamics of the fishing industry", (translated from Russian by W.E. Ricker 1945). Izvestiya Otdela Rybovodstva I Nauchno-promyslovykh Issledovanii 1. 81–128.

Beamish, R.J. 1979. New information on the longevity of Pacific ocean perch (*Sebastes alutus*). Can. J. Fish. Aquat. Sci. 36(11). 1395–1400.

Beddington, J.R. and Cooke, J.G. 1983. The potential yield of fish stocks. FAO Fish. Tech. Paper 242. v + 47 p.

Caswell, H. 2001. Matrix Population Models: Construction, Analysis and Interpretation. Sinauer Associates, Massachusetts.

Clark, W.G. and Hare, S.R. 2006. Assessment and management of Pacific halibut: data, methods, and policy. Sci. Rep. 83, International Pacific Halibut Commission, Seattle, WA.

DFO. 2006. A harvest strategy compliant with the precautionary approach. DFO Can. Sci. Advis. Sec. Sci. Advis. Rep. 2006/023. 7 p.

DFO. 2009. Stock assessment update for British Columbia Canary Rockfish. DFO Can. Sci. Advis. Sec. Sci. Resp. 2009/019. 39 p.

DFO. 2015. Yellowtail Rockfish (*Sebastes flavidus*) stock assessment for the coast of British Columbia, Canada. DFO Can. Sci. Advis. Sec. Sci. Advis. Rep. 2015/010. 14 p.

DFO. 2022*a*. Update of the 2019 Bocaccio (*Sebastes paucispinis*) stock assessment for British Columbia in 2021. DFO Can. Sci. Advis. Sec. Sci. Resp. 2022/001. 33 p.

DFO. 2022*b*. Yellowmouth Rockfish (*Sebastes reedi*) stock assessment for British Columbia in 2021. DFO Can. Sci. Advis. Sec. Sci. Advis. Rep. 2022/001. 18 p.

Edwards, A.M., Haigh, R. and Starr, P.J. 2014*a*. Pacific Ocean Perch (*Sebastes alutus*) stock assessment for the north and west coasts of Haida Gwaii, British Columbia. DFO Can. Sci. Advis. Sec. Res. Doc. 2013/092. vi + 126 p.

Edwards, A.M., Haigh, R. and Starr, P.J. 2014*b*. Pacific Ocean Perch (*Sebastes alutus*) stock assessment for the west coast of Vancouver Island, British Columbia. DFO Can. Sci. Advis. Sec. Res. Doc. 2013/093. vi + 135 p.

Edwards, A.M., Haigh, R. and Starr, P.J. 2012*a*. Stock assessment and recovery potential assessment for Yellowmouth Rockfish (*Sebastes reedi*) along the Pacific coast of Canada. DFO Can. Sci. Advis. Sec. Res. Doc. 2012/095. iv + 188 p.

Edwards, A.M., Starr, P.J. and Haigh, R. 2012*b*. Stock assessment for Pacific ocean perch (*Sebastes alutus*) in Queen Charlotte Sound, British Columbia. DFO Can. Sci. Advis. Sec. Res. Doc. 2011/111. viii + 172 p.

Forrest, R.E., McAllister, M.K., Dorn, M.W., Martell, S.J.D. and Stanley, R.D. 2010. Hierarchical Bayesian estimation of recruitment parameters and reference points for Pacific rockfishes (*Sebastes* spp.) under alternative assumptions about the stock-recruit function. Can. J. Fish. Aquat. Sci. 67. 1611–1634.

Fournier, D.A., Hampton, J. and Sibert, J.R. 1998. MULTIFAN-CL: a length-based, age-structured model for fisheries stock assessment, with application to South Pacific albacore, *Thunnus alalunga*. Can. J. Fish. Aquat. Sci. 55(9). 2105–2116.

Fournier, D.A., Sibert, J.R., Majkowski, J. and Hampton, J. 1990. MULTIFAN a likelihood-based method for estimating growth parameters and age composition from multiple length frequency data sets illustrated using data for southern bluefin tuna (*Thunnus maccoyii*). Can. J. Fish. Aquat. Sci. 47(2). 301–317.

Francis, R.I.C.C. 2011. Data weighting in statistical fisheries stock assessment models. Can. J. Fish. Aquat. Sci. 68(6). 1124–1138.

Gelman, A., Carlin, J.B., Stern, H.S. and Rubin, D.B. 2004. Bayesian Data Analysis, 2nd edition. Chapman and Hall/CRC, New York.

Haigh, R., Starr, P.J., Edwards, A.M., King, J.R. and Lecomte, J.B. 2018. Stock assessment for Pacific Ocean Perch (*Sebastes alutus*) in Queen Charlotte Sound, British Columbia in 2017. DFO Can. Sci. Advis. Sec. Res. Doc. 2018/038. v + 227 p.

Hilborn, R., Maunder, M., Parma, A., Ernst, B., Payne, J. and Starr, P. 2003. Coleraine: A generalized age-structured stock assessment model. User's manual version 2.0. University of Washington Report SAFS-UW-0116. Tech. rep., University of Washington.

Hoenig, J.M. 1983. Empirical use of longevity data to estimate mortality rates. Fish. Bull. 82(1). 898–903.

Holt, K.R., Starr, P.J., Haigh, R. and Krishka, B. 2016. Stock assessment and harvest advice for Rock Sole (*Lepidopsetta* spp.) in British Columbia. DFO Can. Sci. Advis. Sec. Res. Doc. 2016/009. ix + 256 p.

Knaus, J. 2015. snowfall: Easier cluster computing (based on snow). R package version 1.84-6.1.

Leisch, F. 2002. Sweave: dynamic generation of statistical reports using literate data analysis. In W. Härdle and B. Rönz, eds., Compstat 2002 - Proceedings in Computational Statistics, p. 575–580. Physica Verlag, Heidelberg.

Mace, P.M. and Doonan, I.J. 1988. A generalized bioeconomic simulation for fish population dynamics. NZ Fish. Assess. Res. Doc. 88/4. 51 p.

MacLellan, S.E. 1997. How to age rockfish (*Sebastes*) using *S. alutus* as an example – the otolith burnt section technique. Can. Tech. Rep. Fish. Aquat. Sci. 2146. 39 p.

McAllister, M.K. and Ianelli, J.N. 1997. Bayesian stock assessment using catch-age data and the sampling – importance resampling algorithm. Can. J. Fish. Aquat. Sci. 54(2). 284–300.

Mertz, G. and Myers, R. 1996. Influence of fecundity on recruitment variability of marine fish. Can. J. Fish. Aquat. Sci. 53(7). 1618–1625.

Methot, R.D., Wetzel, C.R., Taylor, I.G., Doering, K.L. and Johnson, K.F. 2021. Stock Synthesis: User Manual Version 3.30.18. Tech. rep., NOAA Fisheries, Seattle WA, USA, October 1, 2021.

Methot, R.D. and Wetzel, C.R. 2013. Stock Synthesis: A biological and statistical framework for fish stock assessment and fishery management. Fish. Res. 142. 86–99.

Michielsens, C.G.J. and McAllister, M.K. 2004. A Bayesian hierarchical analysis of stock-recruit data: quantifying structural and parameter uncertainties. Can. J. Fish. Aquat. Sci. 61(6). 1032–1047.

Monnahan, C.C. 2018. adnuts: No-U-Turn MCMC Sampling for ADMB Models. R package ver. 1.1.2.

Monnahan, C.C., Branch, T.A., Thorson, J.T., Stewart, I.J. and Szuwalski, C.S. 2019. Overcoming long Bayesian run times in integrated fisheries stock assessments. ICES J. Mar. Sci. 76(6). 1477–1488.

Monnahan, C.C. and Kristensen, K. 2018. No-U-turn sampling for fast Bayesian inference in ADMB and TMB: Introducing the adnuts and tmbstan R packages. PLoS ONE 13(5). e0197,954.

Pope, J.G. 1972. An investigation of the accuracy of virtual population analysis using cohort analysis. Int. Comm. Northwest Atl. Fish. Res. Bull. 9. 65–74.

R Core Team. 2021. R: A Language and Environment for Statistical Computing. R Foundation for Statistical Computing, Vienna, Austria.

Schnute, J.T. 1981. A versatile growth model with statistically stable parameters. Can. J. Fish. Aquat. Sci. 38(9). 1128–1140.

Stanley, R.D., Starr, P. and Olsen, N. 2009. Stock assessment for Canary Rockfish (*Sebastes pinniger*) in British Columbia waters. DFO Can. Sci. Advis. Sec. Res. Doc. 2009/013. xxii + 198 p.

Starr, P.J. and Haigh, R. 2021*a*. Widow Rockfish (*Sebastes entomelas*) stock assessment for British Columbia in 2019. DFO Can. Sci. Advis. Sec. Res. Doc. 2021/039. vi + 238 p.

Starr, P.J. and Haigh, R. 2022*a*. Bocaccio (*Sebastes paucispinis*) stock assessment for British Columbia in 2019, including guidance for rebuilding plans. DFO Can. Sci. Advis. Sec. Res. Doc. 2022/001. vii + 292 p.

Starr, P.J. and Haigh, R. 2022*b*. Rougheye/Blackspotted Rockfish (*Sebastes aleutianus / melanostictus*) stock assessment for British Columbia in 2020. DFO Can. Sci. Advis. Sec. Res. Doc. 2022/20. vii + 385 p.

Starr, P.J. and Haigh, R. 2021*b*. Redstripe Rockfish (*Sebastes proriger*) stock assessment for British Columbia in 2018. DFO Can. Sci. Advis. Sec. Res. Doc. 2021/014. vii + 340 p.

Starr, P.J. and Haigh, R. 2022*c*. Yellowmouth Rockfish (*Sebastes reedi*) stock assessment for British Columbia in 2021. DFO Can. Sci. Advis. Sec. Res. Doc. 2022/10. viii + 288 p.

Starr, P.J., Haigh, R. and Grandin, C. 2016. Stock assessment for Silvergray Rockfish (*Sebastes brevispinis*) along the Pacific coast of Canada. DFO Can. Sci. Advis. Sec. Res. Doc. 2016/042. vi + 170 p.

Taylor, I.G., Gertseva, V., Methot., R.D. and Maunder, M.N. 2013. A stock-recruitment relationship based on pre-recruit survival, illustrated with application to spiny dogfish shark. Fish. Res. 142. 15–21.

Taylor, I.G., Stewart, I.J., Hicks, A.C., Garrison, T.M., Punt, A.E., Wallace, J.R., Wetzel, C.R., Thorson, J.T., Takeuchi, Y., Ono, K., Monnahan, C.C., Stawitz, C.C., A'mar, Z.T., Whitten, A.R., Johnson, K.F., Emmet, R.L., Anderson, S.C., Lambert, G.I., Stachura, M.M., Cooper, A.B., Stephens, A., Klaer, N.L., McGilliard, C.R., Mosqueira, I., Iwasaki, W.M., Doering, K., Havron, A.M., Vaughan, N. and Denson, L.S. 2020. r4ss: R Code for Stock Synthesis. R package ver. 1.40.1.

Thorson, J.T., Jensen, O.P. and Zipkin, E.F. 2014. How variable is recruitment for exploited marine fishes? A hierarchical model for testing life history theory. Can. J. Fish. Aquat. Sci. 71(7). 973–983.

Thorson, J.T., Johnson, K.F., Methot, R.D. and Taylor, I.G. 2017. Model-based estimates of effective sample size in stock assessment models using the Dirichlet-multinomial distribution. Fish. Res. 192. 84–93.

APPENDIX F. MODEL RESULTS

F.1. INTRODUCTION

All model runs were performed using the Stock Synthesis 3 (SS3) platform, v.3.30.18 (Methot et al. 2021, see also Appendix E for model details). This appendix describes results for a coastwide stock of Canary Rockfish (CAR, *Sebastes pinniger*) that spans the outer BC coast in PMFC areas 3CD5ABCDE. These results include:

- mode of the posterior distribution (MPD) calculations to compare model estimates to observations;
- Markov chain Monte Carlo (MCMC) simulations to derive posterior distributions for the estimated parameters for a base run;
- MCMC diagnostics for the base run; and
- a range of sensitivity model runs, including MCMC diagnostics.

MCMC diagnostics are evaluated using the following subjective criteria:

- Good – no trend in traces and no spikes in $\log R_0$, split-chains align, no autocorrelation;
- Fair – trace trend temporarily interrupted, occasional spikes in $\log R_0$, split-chains somewhat frayed, some autocorrelation;
- Poor – trace trend fluctuates substantially or shows a persistent increase/decrease, split-chains differ from each other, substantial autocorrelation;
- Unacceptable – trace trend shows a persistent increase/decrease that has not levelled, split-chains differ markedly from each other, persistent autocorrelation.

The final advice consists of a single base run that estimates natural mortality (M) and steepness (h), and provides the primary guidance. A range of sensitivity runs are presented to show the effect of the important modelling assumptions. Estimates of major quantities and advice to management (decision tables) are presented here and in the main text.

F.2. CANARY ROCKFISH COASTWIDE

The base run for CAR BC was selected after running a range of preliminary model runs. This base run included the following decisions and assumptions:

- assumed two sexes (females, males);
- estimated a single mortality M per sex to represent all ages;
- set plus-age class A to 60 years;
- assumed two commercial fisheries: 'Trawl' (predominant with ~97% of catch) and 'Other';
  - Trawl fishery comprised bottom and midwater trawl gear;
  - Other fishery included non-trawl gear (halibut longline, sablefish trap/longline, dogfish/lingcod troll, and hook & line rockfish);
  - age frequency (AF) data were only available from the Trawl fishery;
- used one commercial bottom trawl fishery abundance index series (bottom trawl CPUE index, 1996–2021);
- used six survey abundance index series (QCS Synoptic, WCVI Synoptic, NMFS Triennial, HS Synoptic, WCHG Synoptic, and GIG Historical), with age frequency (AF) data for the first three surveys;
- assumed a wide (weak) normal prior $\mathcal{N}(7, 7)$ on $\log R_0$ to help stabilise the model;
- used informed normal priors for the three primary selectivity parameters (μ_g, $v_{g\text{L}}$, Δ_g, see Appendix E) for all fleets (fishery and surveys) derived from Table J.7 in Stanley et al. (2009);

- estimated recruitment deviations from 1950 to 2012;
- applied abundance reweighting: added CV process error to index CVs, c_{p}=0.178 for the commercial CPUE series and c_{p}=0 for the surveys (see Appendix E);
- used SS3's Dirichlet-Multinomial error distribution to fit AF data instead of applying composition reweighting;
- fixed the standard deviation of recruitment residuals (σ_R) to 0.9;
- used an ageing error vector based on the CV of observed lengths at age, described in Appendix D, Section D.2.3 and plotted in Figure D.26 (left panel).

The base run (Run24: estimate M and h, CPUE c_{p}=0.178) was used as a reference run against fourteen sensitivity runs taken to MCMC; four additional sensitivity runs taken to the MPD were compared.

All model runs were reweighted once for abundance, by adding process error c_{p} to the commercial CPUE (no additional error was added to the survey indices because observed error was already high). The process error added to the commerical CPUE was based on a spline analysis (Appendix E). There was no weighting applied for composition as the AF data were fit using the Dirichlet-Multinomial distribution.

F.2.1. Base Run

F.2.1.1. MPD fits

The modelling procedure first determined the best fit (MPD = mode of posterior distribution) to the data by minimising the negative log likelihood. The MPD was used as the starting point for the MCMC simulations.

The following plot references apply to the base run.

- Figure F.2 – model fits to the CPUE and survey indices across observed years;
- Figures F.3-F.10 – model fits (lines=predicted) to the female and male age frequency data (bars=observed) for the fishery and three survey data sets along with respective standardised residuals of model fits;
- Figure F.11 – model estimates of mean age compared to the observed mean ages;
- Figure F.12 – estimated gear selectivities, together with the ogive for female maturity;
- Figure F.13 – spawning biomass time series and depletion;
- Figure F.14 – the recruitment time series and recruitment deviations;
- Figure F.15 – the stock-recruitment curve.

In this CAR stock assessment, both natural mortality (M) and steepness (h) were estimated without difficulty, there being only weak correlation between these two parameters (Figure F.1). This eliminated the procedure used in previous assessments where multiple runs using fixed M values were needed to build a composite base case that covered a plausible range of values for this parameter. The MPD for female natural mortality (M=0.093) shifted much higher than the prior mean value (M=0.06), while the male MPD remained close to the prior mean (M=0.065). This divergence between the estimates by sex was driven by the difference in the age frequency data by sex amd was required to fit the AF data credibly. Steepness was also estimated to be higher (h=0.88) than the prior mean (h=0.76). The selectivity parameter estimates did not move far from the prior means; however, the estimated age at full selectivity (μ_g) was lower for the surveys than for the commercial fishery, which is consistent with the surveys using smaller mesh codends. The WCVI μ value was estimated to be near 10 while the QCS and Triennial survey

estimates for this parameter were 12.4 and 12.3, respectively, compared to age 13.3 in the commercial fishery, reflecting the presence of younger fish in the survey data. There was little information in the data to move the male shift parameter (Δ_{1g}) away from its initial prior mean of -0.4.

Only the commercial CPUE indices were downweighted by adding process error to the index CVs (CPUE c_{p}); this was because the GLM model-estimated standard errors were extraordinarily small (see Table C.9). The bootsrap survey index relative errors were already high so no additional process error was added. Model fits to the survey abundance indices were generally satisfactory (Figure F.2), although various index points were missed entirely (e.g., 1996 CPUE, 2009 QCS, 2006 WCVI, 1980 NMFS, 2011 and 2021 HS, 2016 WCHG). The fit to the commercial CPUE indices was flat from 1996 to 2002 followed by an upward trend from 2003 to 2021.

Neither Francis (2011) reweighting (using mean ages) nor McAllister and Ianelli (1997) reweighting (using harmonic mean ratios) were used in this stock assessment, a departure from previous stock assessments. Instead, the Dirichlet-Multinomial distribution, as implemented in SS3, was used as a model-based method for estimating effective sample size (Thorson et al. 2017). This distribution incorporates an additional parameter per 'fleet' ($\log$ DM θ_g), which governs the ratio of nominal ('input') and effective ('output') sample size.

Fits to the commercial trawl fishery age frequency data were good, with the model tracking year classes consistently across the 41-year time span represented by the commercial AF data (Figure F.3). Standardised residuals rarely exceeded 1 for the various age classes (Figure F.4), although there were many small negative residuals, which may indicate that there was a tendency to underestimate the age proportions. Residuals by sample year showed that standardised residuals exceeded 1 only in several years (e.g., 2001, 2004, and 2017). Fits to the survey AFs from the three surveys were fair, with some residuals exceeding 2 (Figures F.5–F.10). As with the commercial AF fits, the survey AF fits also tended to show small negative residuals, again indicating that the model tended to underestimate the age proportions.

Mean ages appeared to be well tracked (Figure F.11), suggesting that the Dirichlet-Multinomial θ_g parameters were re-weighting effectively (although, see caveats in Appendix E). The maturity ogive, generated from an externally fitted model (see Appendix D), was situated to the left of the commercial selectivity fits for all ages up to 11, indicating that younger mature fish were not being heavily harvested by the commercial fishery. This was also true of the QCS and Triennial surveys, while the WCVI survey selectivity ogive sat well to the left of the female maturity ogive, indicating that this survey selected all mature and sub-mature CAR.

Biomass trajectories (Figure F.13) partition total biomass into various components (total male, total female, and spawning female). Spawing biomass is relatively small compared to total biomass (by approximately one third) because there is a considerable amount of biomass that is not mature females, including all males. The biomass trajectories declined from 1935 to 1995. The year 1996 marked the introduction of the 100% onboard observer program followed by the implementation of an individual vessel quota system in 1997. Biomass, beginning with 1996, ceased to decline, and, beginning in the early 2000s, began to increase. Prior to 1996, spawning biomass levels remained below $0.4B_0$ for a decade.

Recruitment was below average until the late 1990s (Figure F.14), when there followed a long period with above average recruitment punctuated by a number of solid recruitment events. There was at least one notable recruitment event in 2010 (Figure F.15). Although the cohort continuity patterns presented in Appendix D were not as persuasive as those for other offshore

rockfish species (e.g., POP), the stock assessment model was capable of fitting these data credibly.

The likelihood profile analysis indicated that the age frequency data were the primary contributors of information for the female M parameter, while both the age data and the biomass data precluded low estimates of $\log\ R_0$ (Figure F.16). There was not a great deal of information in any of the data sets to constrain the upper bound of $\log\ R_0$.

A retrospective analysis was undertaken using the base run as the initial model. The upper panel of Figure F.17 shows the model adjusting its fit to the CPUE index series as more years were added to the series, while the lower panel shows an increase in the level of the biomass trajectory as some year classes with strong recruitment entered the fishery. This retrospective analysis did not reveal any underlying problems in the model, with between-year shifts explained through the introduction of new information into the model.

The size of the recruitment events can be gauged from Figures F.17 to F.18 (upper panel) while the differences in the model runs look smaller in a relative sense when the stock is plotted in terms of B_0 (Figure F.18, lower panel). The overall conclusion from the retrospective analysis was that there were no apparent pathologies associated with this stock assessment. Observed changes in the stock assessments were directly attributable to changes in the available data, not to underlying structural issues associated with the model assumptions.

F.2.1.1.1. Tables MPD base run

Table F.1. CAR BC: Priors and MPD estimates for estimated parameters. Prior information – distributions: 0=uniform, 2=beta, 6=normal. Acronyms: LN = natural logarithm, BH = Beverton-Holt, QCS = Queen Charlotte Sound, WCVI = west coast Vancouver Island, NMFS = National Marine Fisheries Service (USA), DM =Dirichlet-Multinomial.

Parameter	Phase	Range	Type	(Mean,SD)	Initial	MPD
M Female	4	(0.02, 0.2)	6	(0.06, 0.018)	0.06	0.093
M Male	4	(0.02, 0.2)	6	(0.06, 0.018)	0.06	0.065
LN(R0)	1	(1, 16)	6	(7, 7)	7	7.913
BH h	5	(0.2, 1)	2	(0.67, 0.17)	0.76	0.877
mu(1) TRAWL	3	(5, 40)	6	(14, 4.2)	14	13.321
varL(1) TRAWL	4	(-15, 15)	6	(2.5, 0.75)	2.5	2.395
delta1(1) TRAWL	4	(-8, 10)	6	(-0.4, 0.12)	-0.4	-0.391
mu(3) QCS	3	(5, 40)	6	(14, 4.2)	14	12.416
varL(3) QCS	4	(-15, 15)	6	(2.5, 0.75)	2.5	2.677
delta1(3) QCS	4	(-8, 10)	6	(-0.4, 0.12)	-0.4	-0.390
mu(4) WCVI	3	(5, 40)	6	(14, 4.2)	14	10.427
varL(4) WCVI	4	(-15, 15)	6	(2.5, 0.75)	2.5	2.786
delta1(4) WCVI	4	(-8, 10)	6	(-0.4, 0.12)	-0.4	-0.391
mu(5) NMFS	3	(5, 40)	6	(14, 4.2)	14	12.272
varL(5) NMFS	4	(-15, 15)	6	(2.5, 0.75)	2.5	2.620
delta1(5) NMFS	4	(-8, 10)	6	(-0.4, 0.12)	-0.4	-0.400
ln(DM theta) 1	2	(-5, 10)	6	(0, 1.813)	0	6.855
ln(DM theta) 3	2	(-5, 10)	6	(0, 1.813)	0	5.720
ln(DM theta) 4	2	(-5, 10)	6	(0, 1.813)	0	5.540
ln(DM theta) 5	2	(-5, 10)	6	(0, 1.813)	0	4.873

Table F.2. CAR BC: Likelihood components reported in `likelihoods_used`.

Likelihood Component	values	lambdas
TOTAL	374.8	—
Equilibrium catch	0	—
Survey	40.14	—
Age composition	302.1	—
Recruitment	0.05506	1
Initial equilibrium regime	0	1
Forecast recruitment	0.3411	1
Parameter priors	32.08	1
Parameter softbounds	0.002910	—
Parameter deviations	0	1
Crash Penalty	0	1

F.2.1.1.2. Figures MPD base run

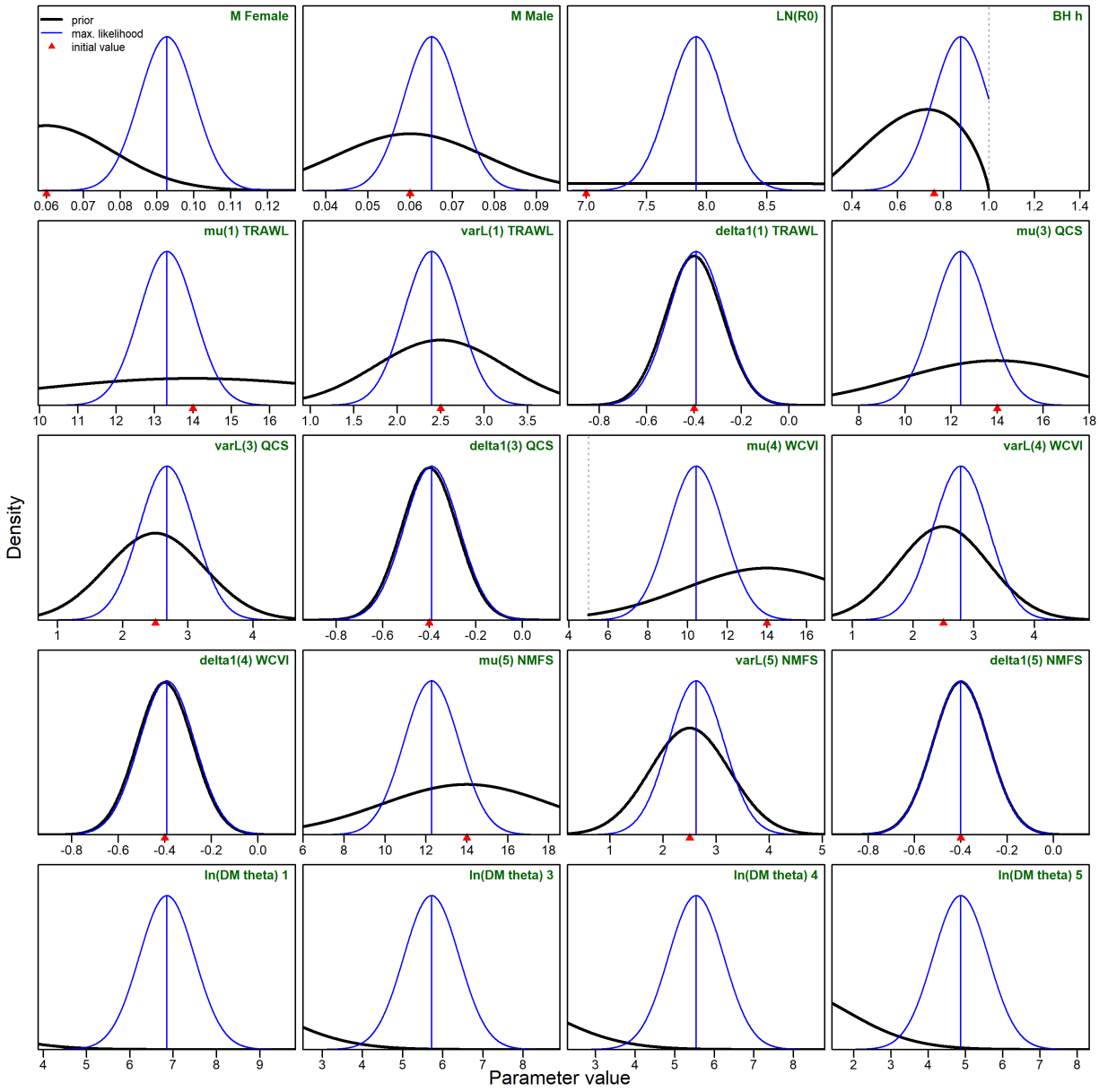

Figure F.1. CAR BC: likelihood profiles (thin blue curves) and prior density functions (thick black curves) for the estimated parameters. Vertical lines represent the maximum likelihood estimates; red triangles indicate initial values used in the minimization process.

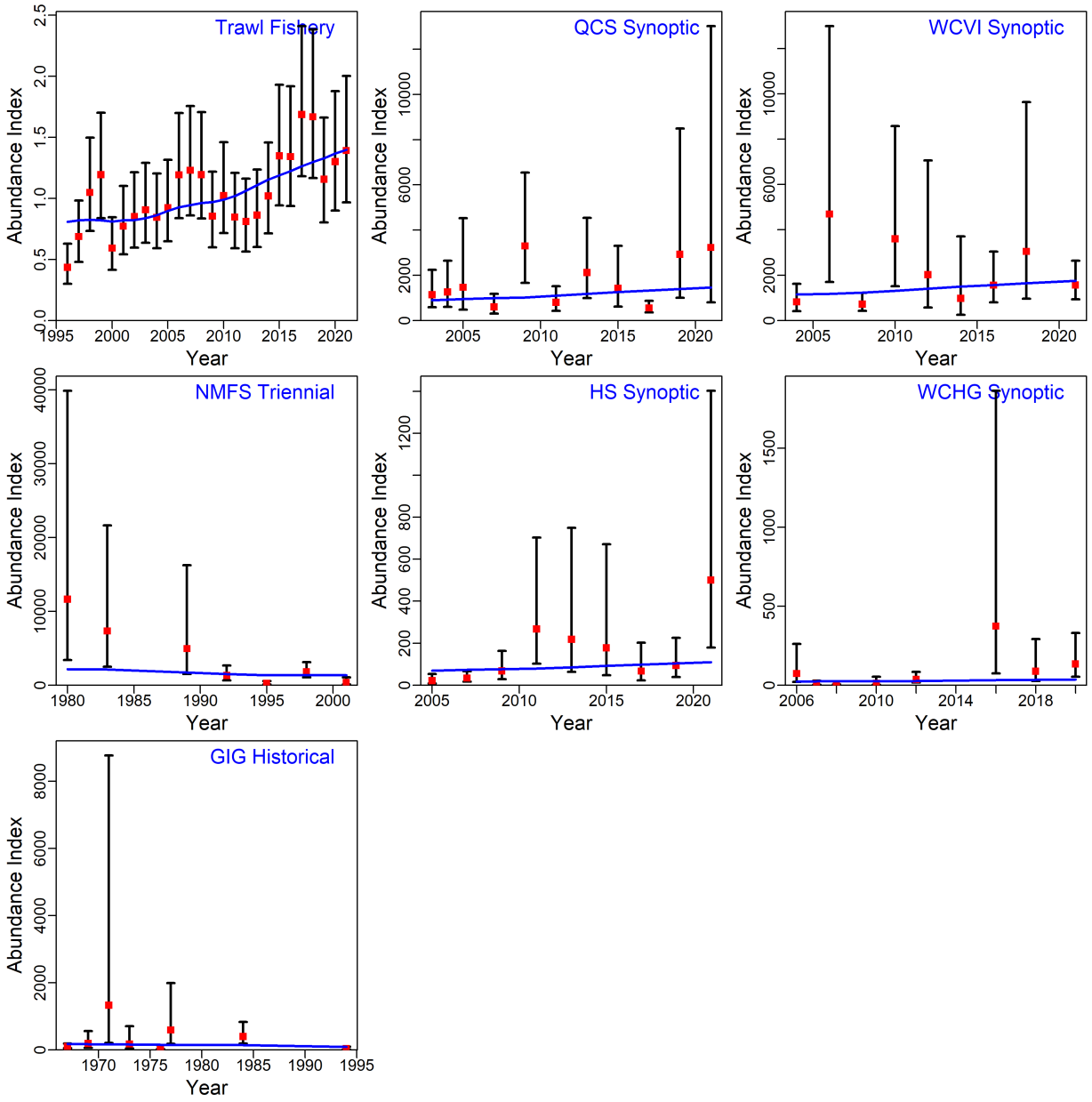

Figure F.2. CAR BC: survey index values (points) with 95% confidence intervals (bars) and MPD model fits (curves) for the fishery-independent survey series.

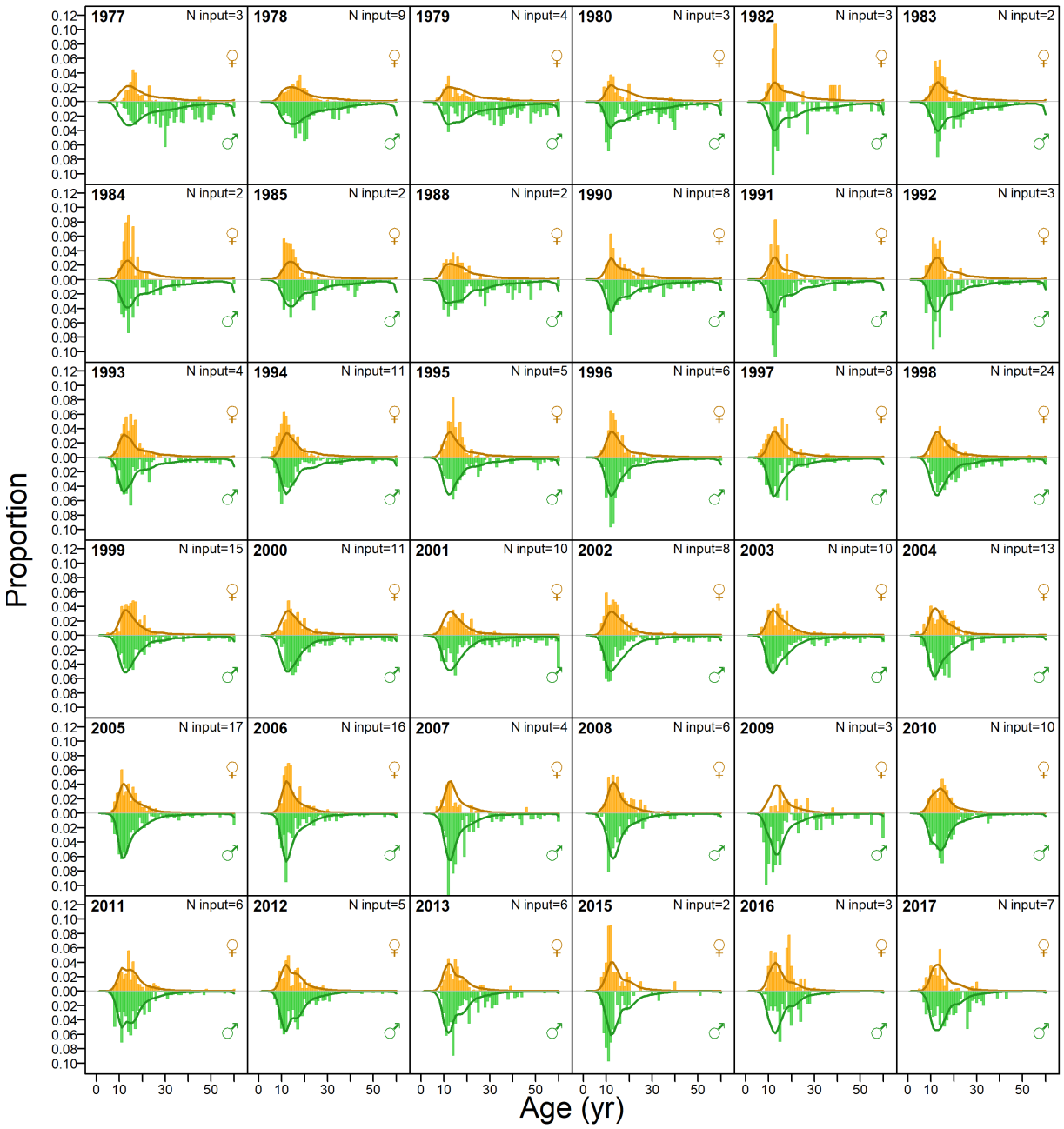

Figure F.3. CAR BC: Trawl fishery proportions-at-age (bars=observed, lines=predicted) for females and males combined.

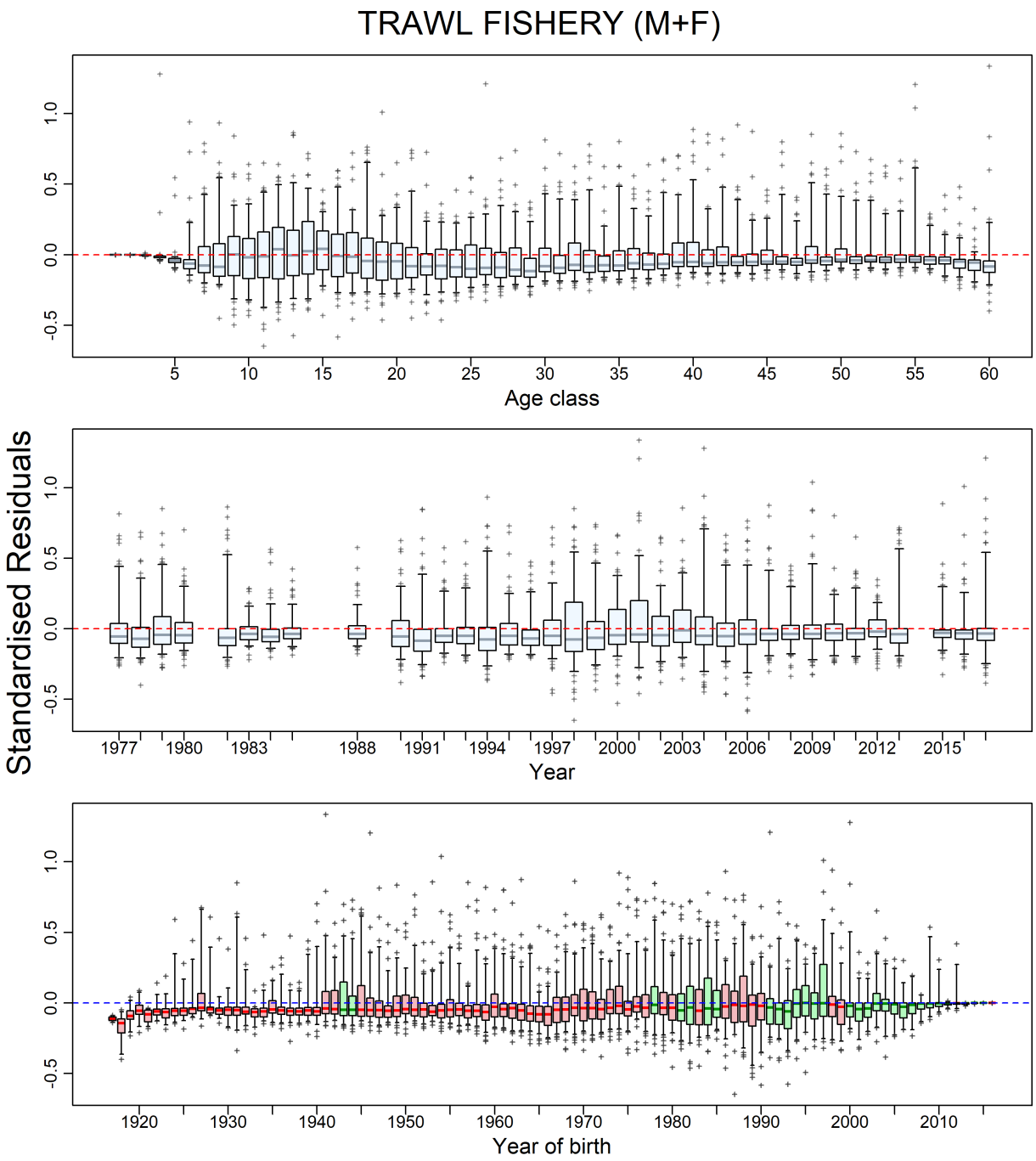

Figure F.4. CAR BC: Trawl fishery residuals of model fits to proportion-at-age data. Vertical axes are standardised residuals. Boxplots in the three panels show residuals by age class, by year of data, and by year of birth (following a cohort through time). Cohort boxes are coloured green if recruitment deviations in birth year are positive, red if negative. Boxes give quantile ranges (0.25-0.75) with horizontal lines at medians, vertical whiskers extend to the the 0.05 and 0.95 quantiles, and outliers appear as plus signs.

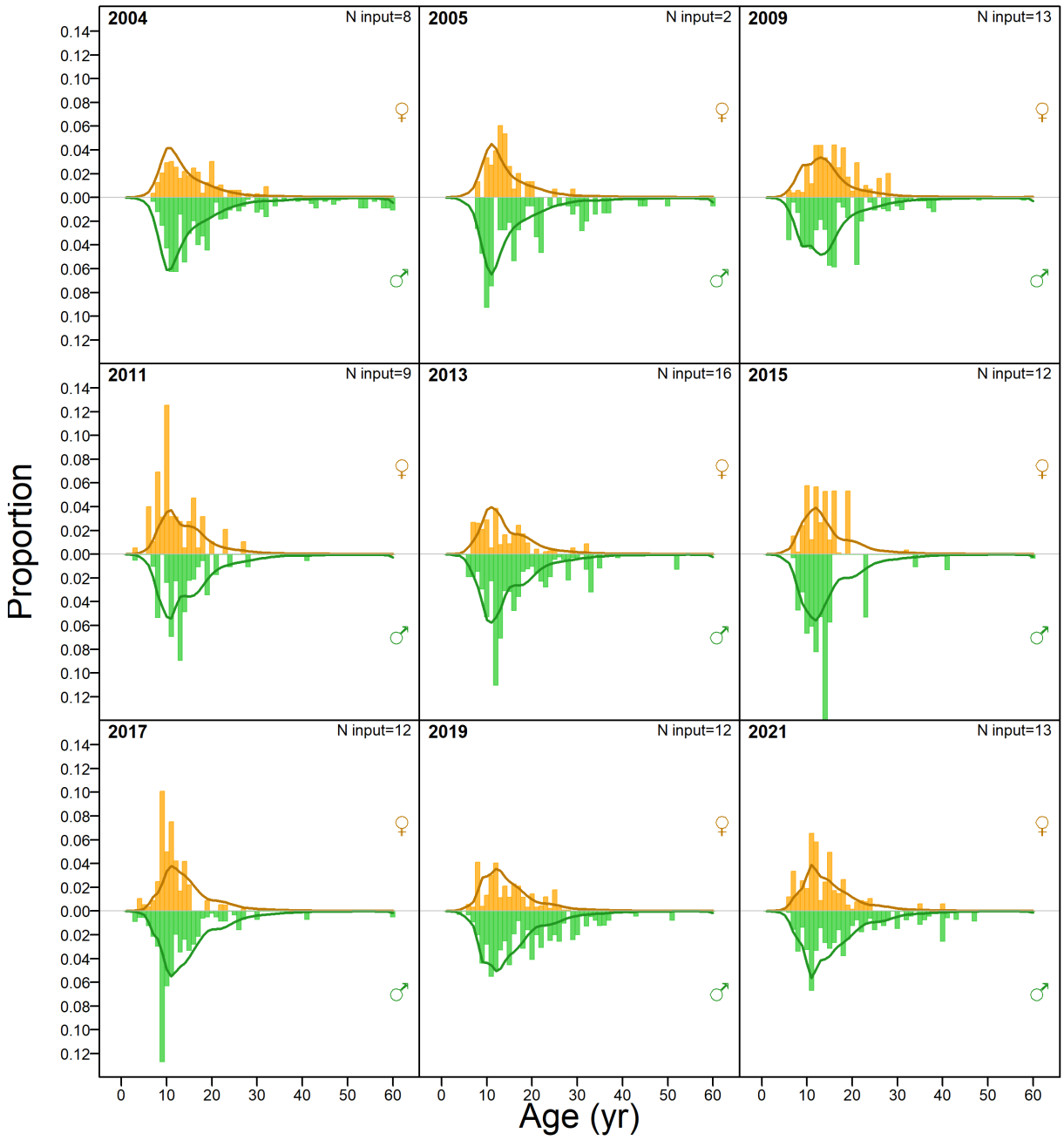

Figure F.5. CAR BC: QCS Synoptic survey proportions-at-age (bars=observed, lines=predicted) for females and males combined.

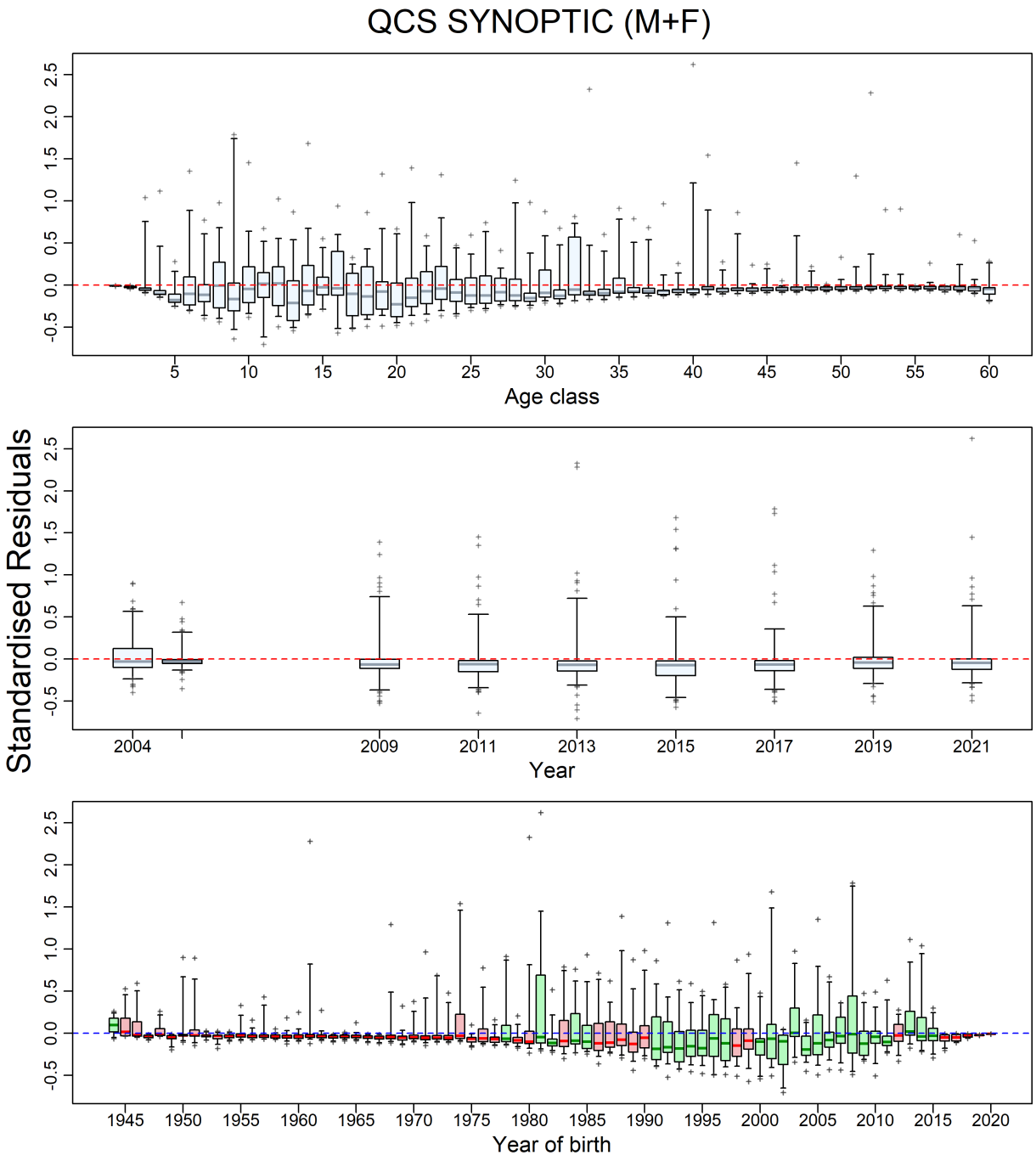

Figure F.6. CAR BC: QCS Synoptic survey residuals of model fits to proportion-at-age data. See Fig. F.4 caption for plot details.

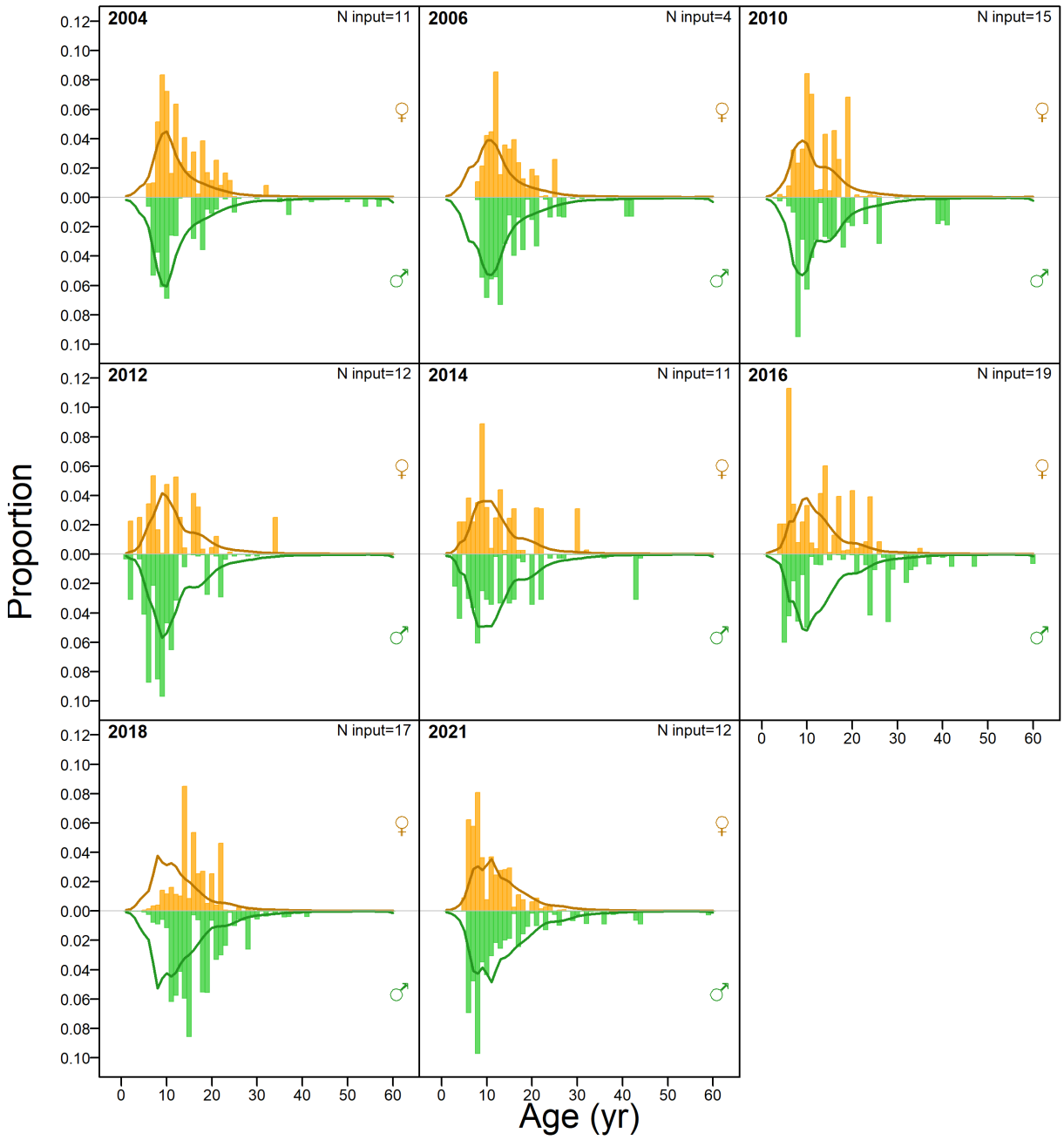

Figure F.7. CAR BC: WCVI Synoptic survey proportions-at-age (bars=observed, lines=predicted) for females and males combined.

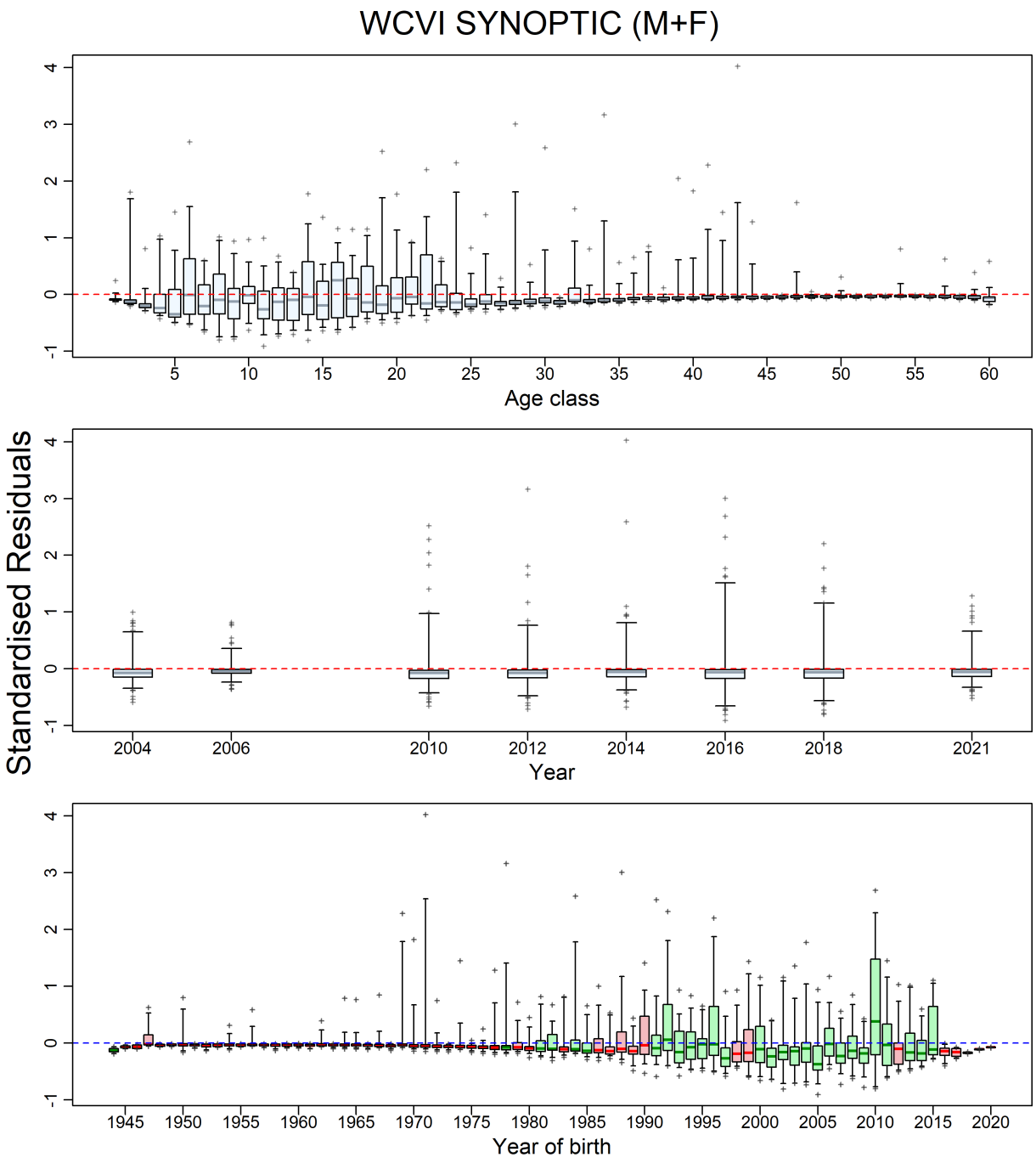

Figure F.8. CAR BC: WCVI Synoptic survey residuals of model fits to proportion-at-age data. See Fig. F.4 caption for plot details.

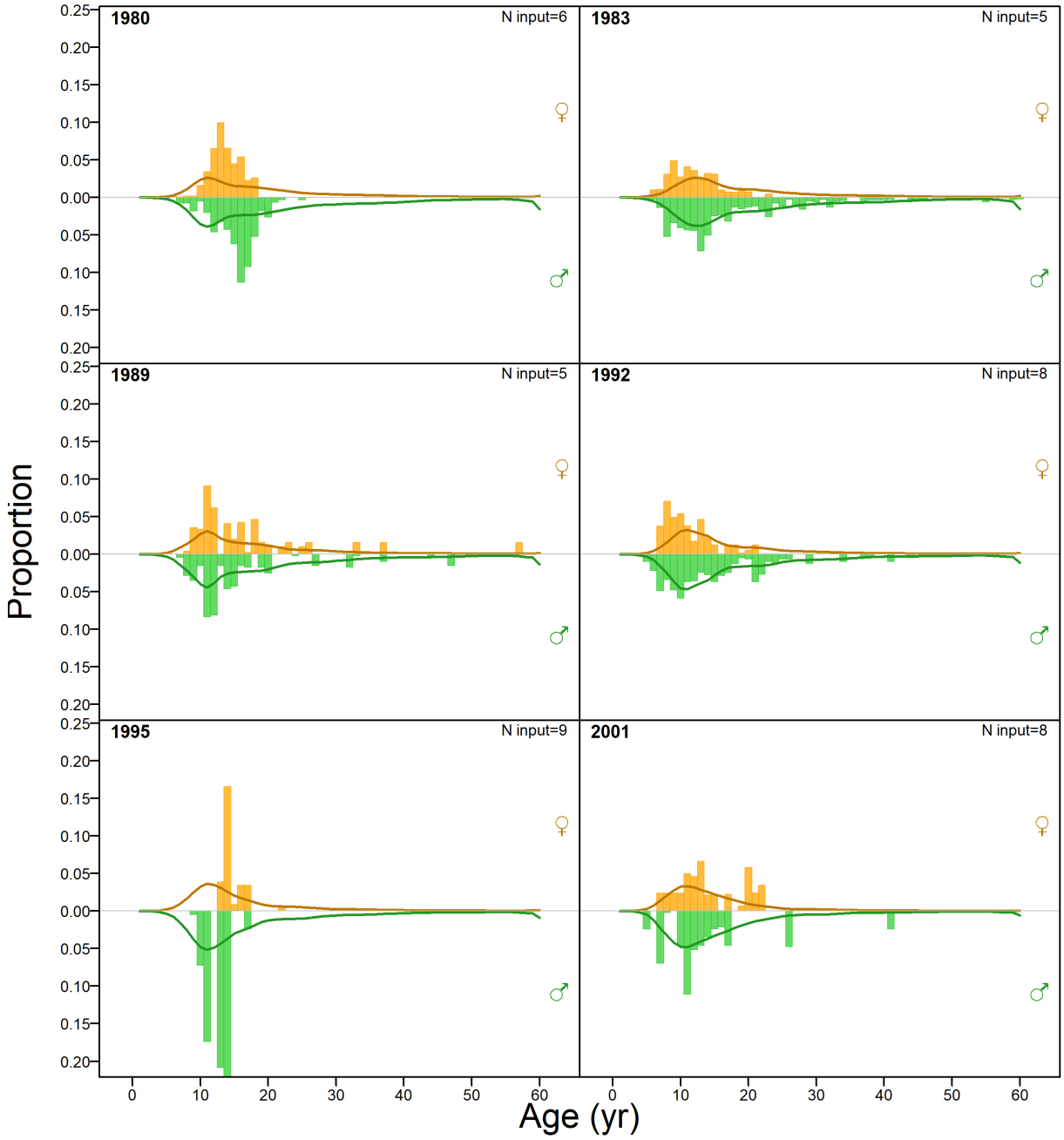

Figure F.9. CAR BC: NMFS Triennial survey proportions-at-age (bars=observed, lines=predicted) for females and males combined.

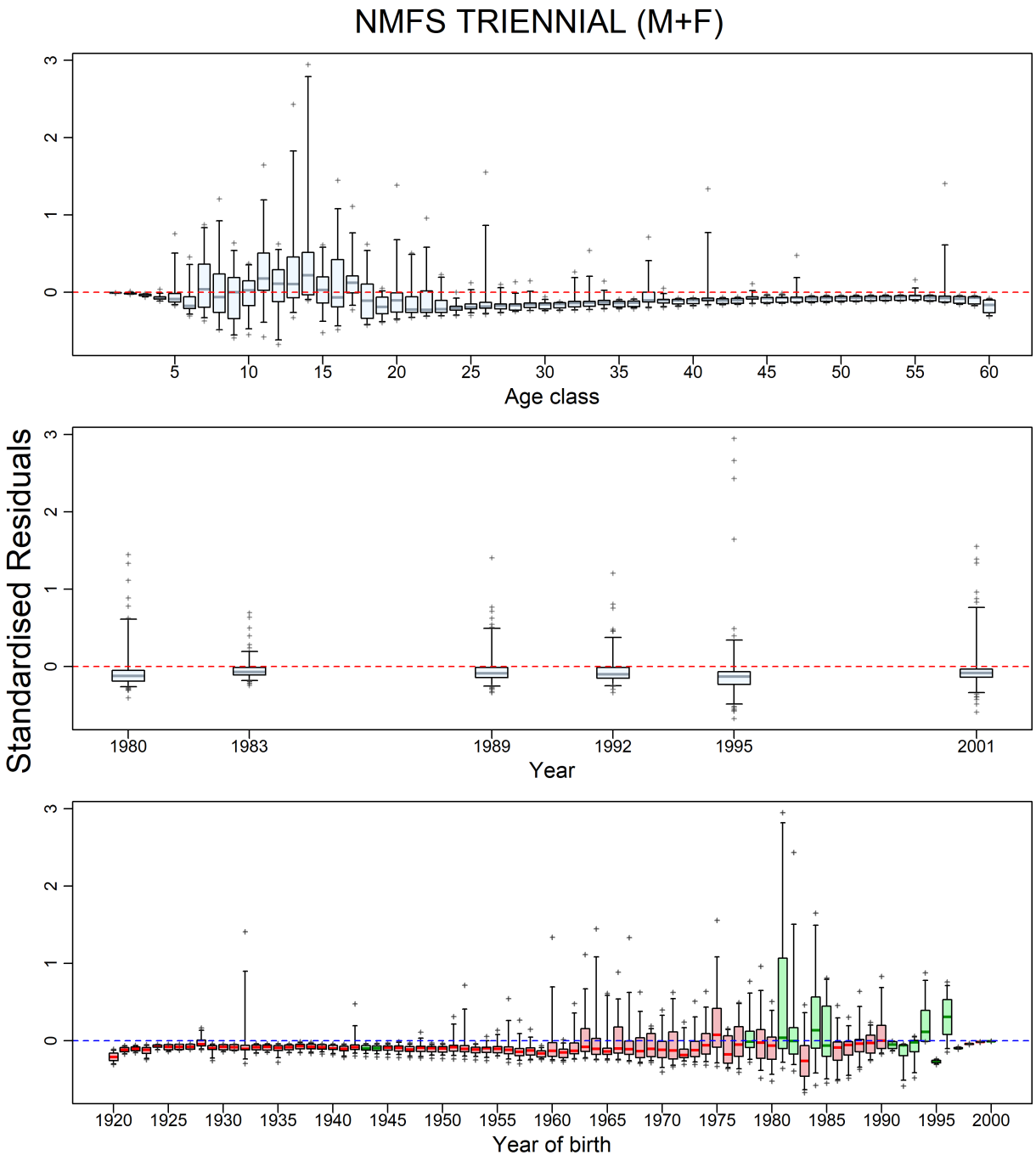

Figure F.10. CAR BC: NMFS Triennial survey residuals of model fits to proportion-at-age data. See Fig. F.4 caption for plot details.

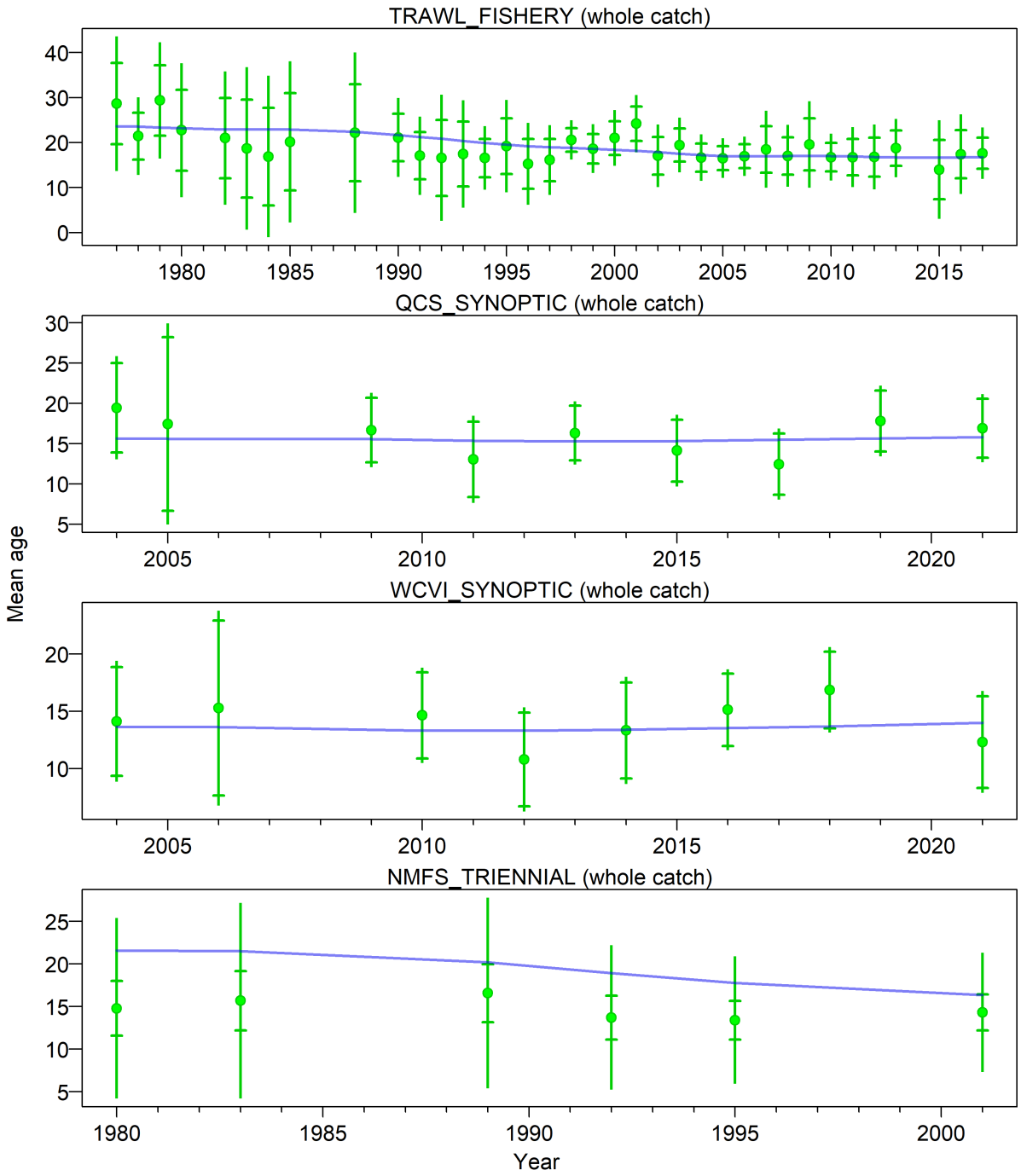

Figure F.11. CAR BC: mean ages each year for the weighted data (solid circles) with 95% confidence intervals and model estimates (blue lines) for the commercial and survey age data.

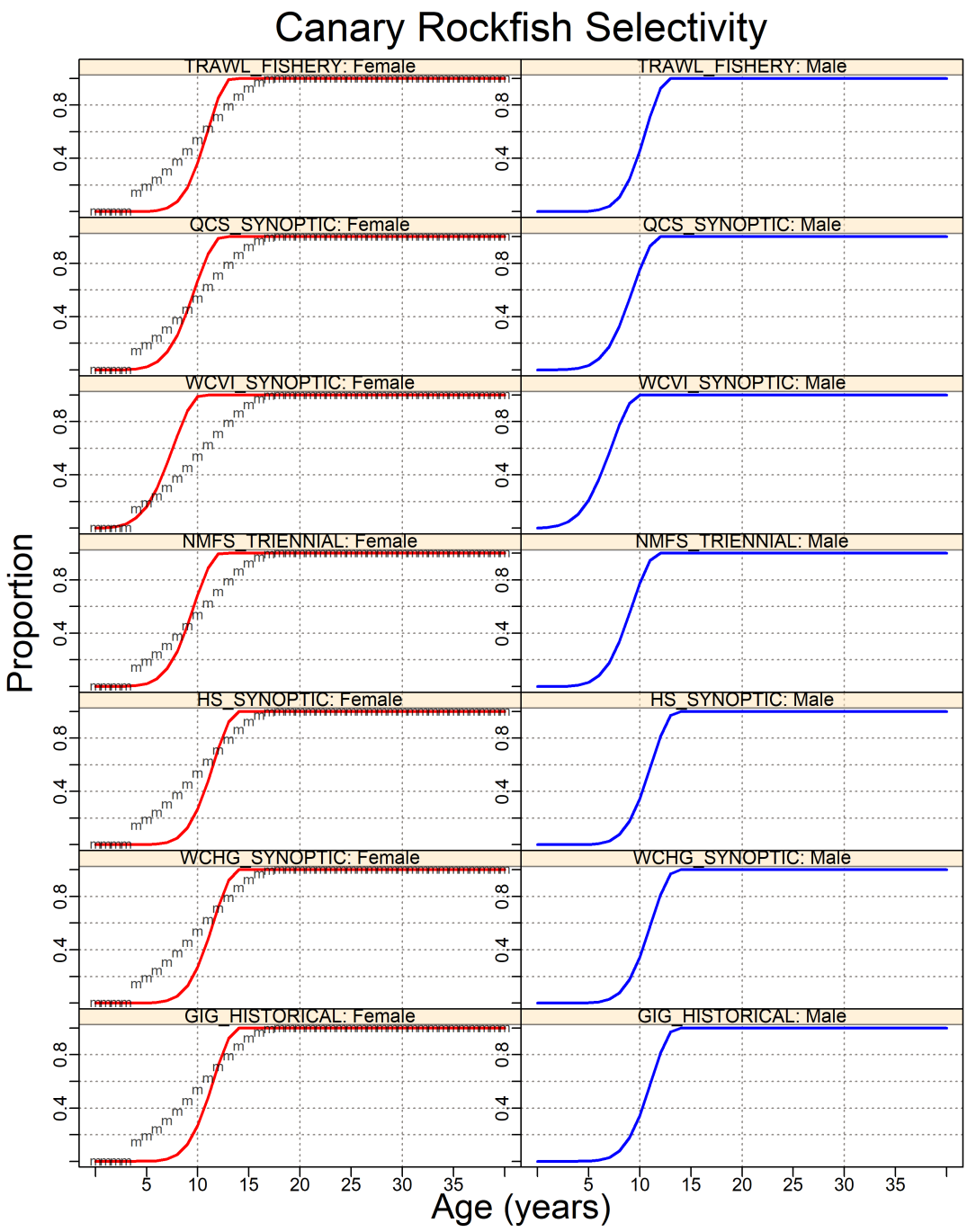

Figure F.12. CAR BC: selectivities for commercial fleet catch and surveys (all MPD values), with maturity ogive for females indicated by 'm'.

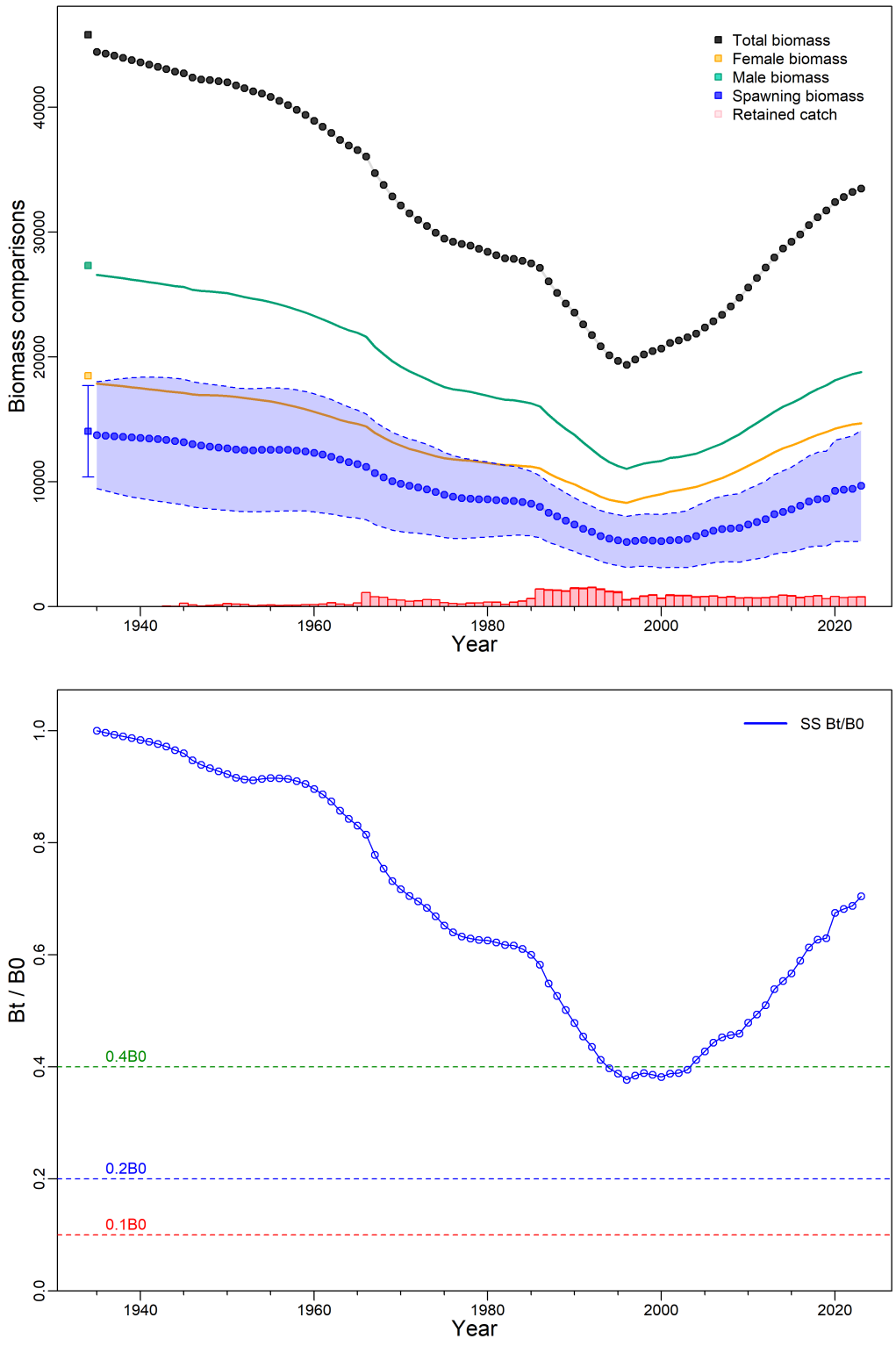

Figure F.13. CAR BC: [Top] time series of biomass (spawning, female, male, total) in tonnes (bottom). Uncertainty envelope generated by SS is provided for spawning female biomass. Pink bars along the bottom show catch biomass (tonnes) for both fisheries predominant). [Bottom] spawning biomass B_t relative to unfished equilbrium spawning biomass B_0.

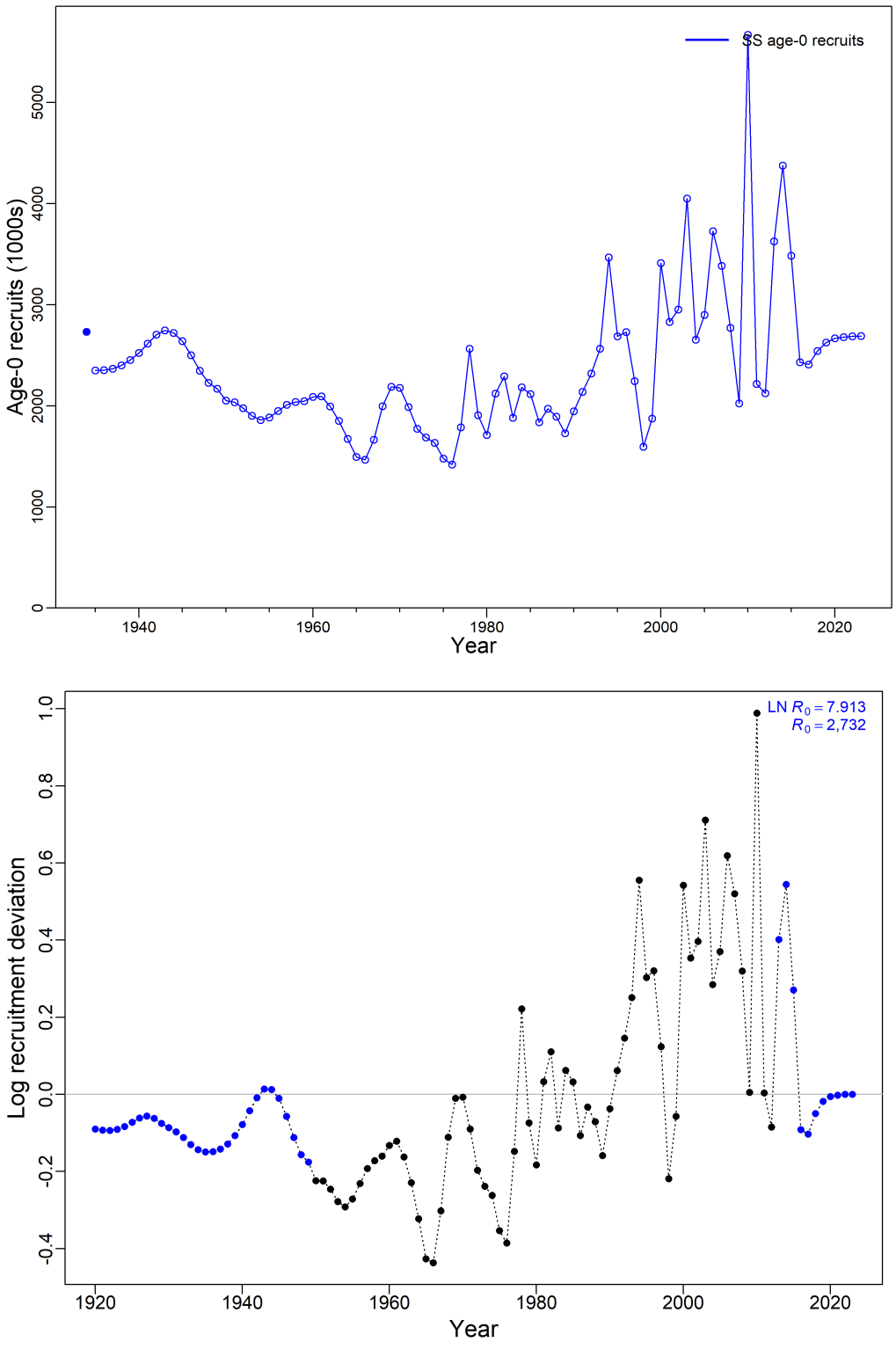

Figure F.14. CAR BC: recruitment (thousands of fish) over time (top) and log of annual recruitment deviations (bottom), ϵ_t, where bias-corrected multiplicative deviation is $e^{\epsilon_t - \sigma_R^2/2}$ and $\epsilon_t \sim$ Normal$(0, \sigma_R^2)$. Blue line designates 2023 SS fit for age-0 fish.

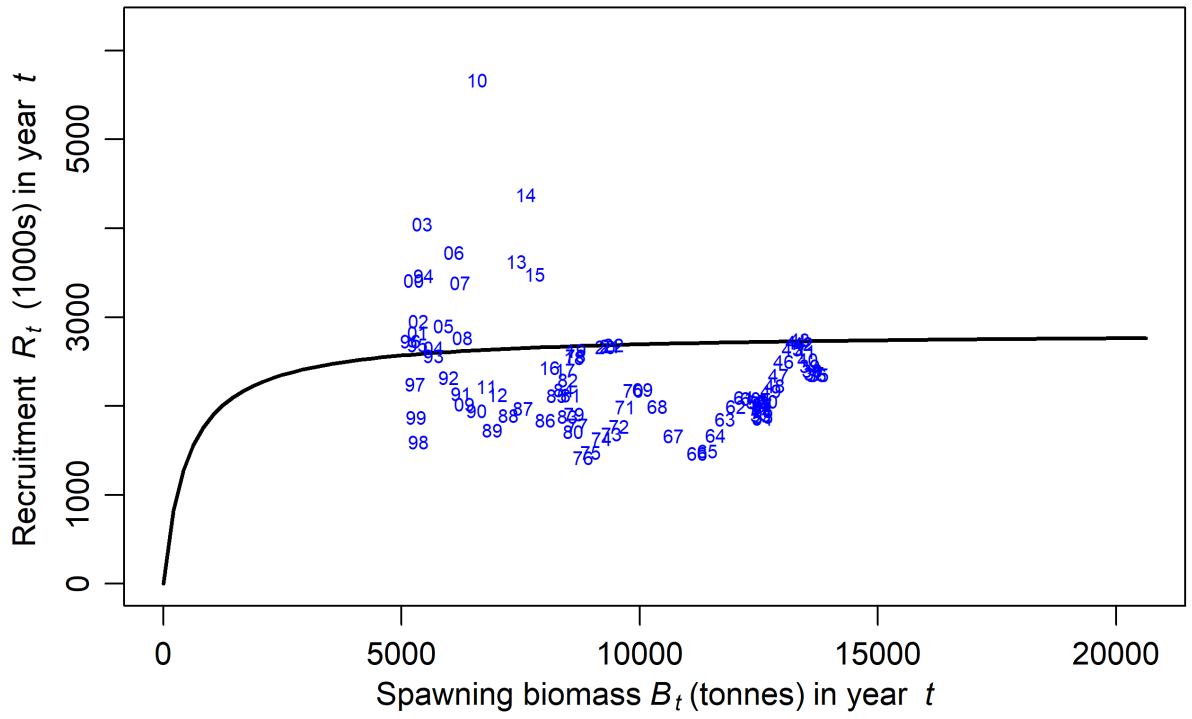

Figure F.15. CAR BC: deterministic stock-recruit relationship (black curve) and observed values (labelled by year of spawning).

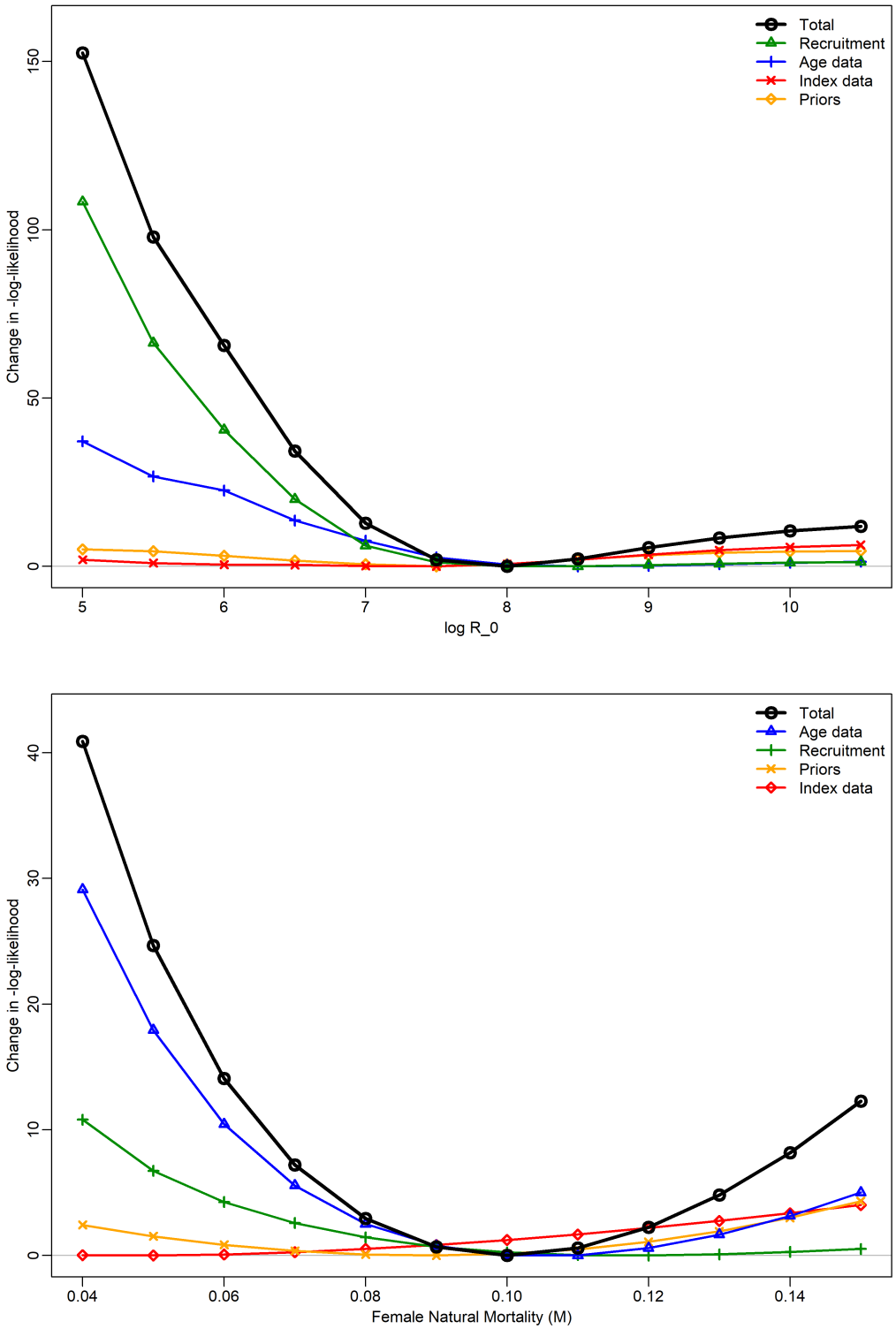

Figure F.16. CAR BC: likelihood profiles for $\log R_0$ *and* M_2 *(female).*

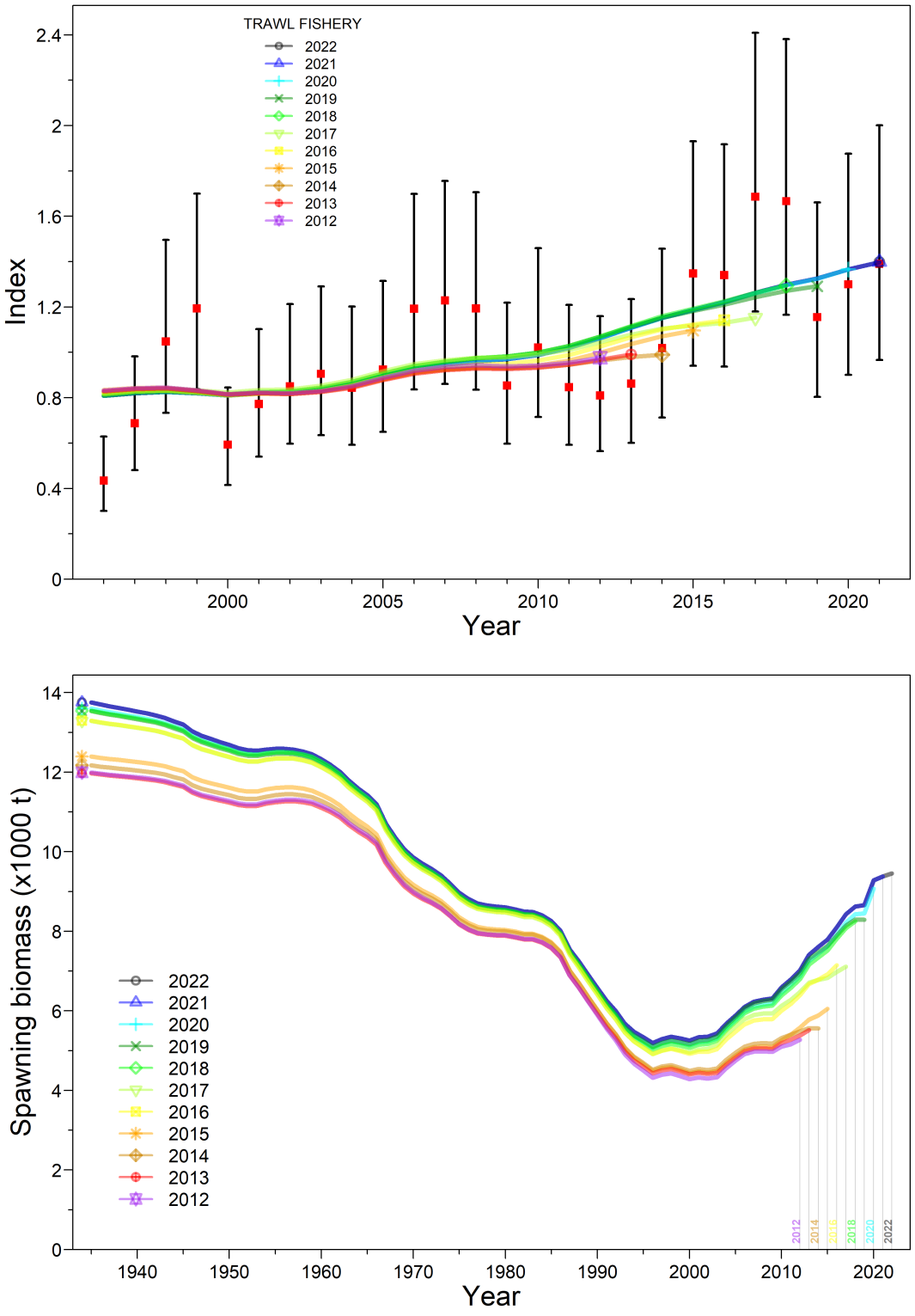

Figure F.17. CAR BC: retrospective analysis showing results for fits to the CPUE index (top) and spawning stock biomass (bottom).

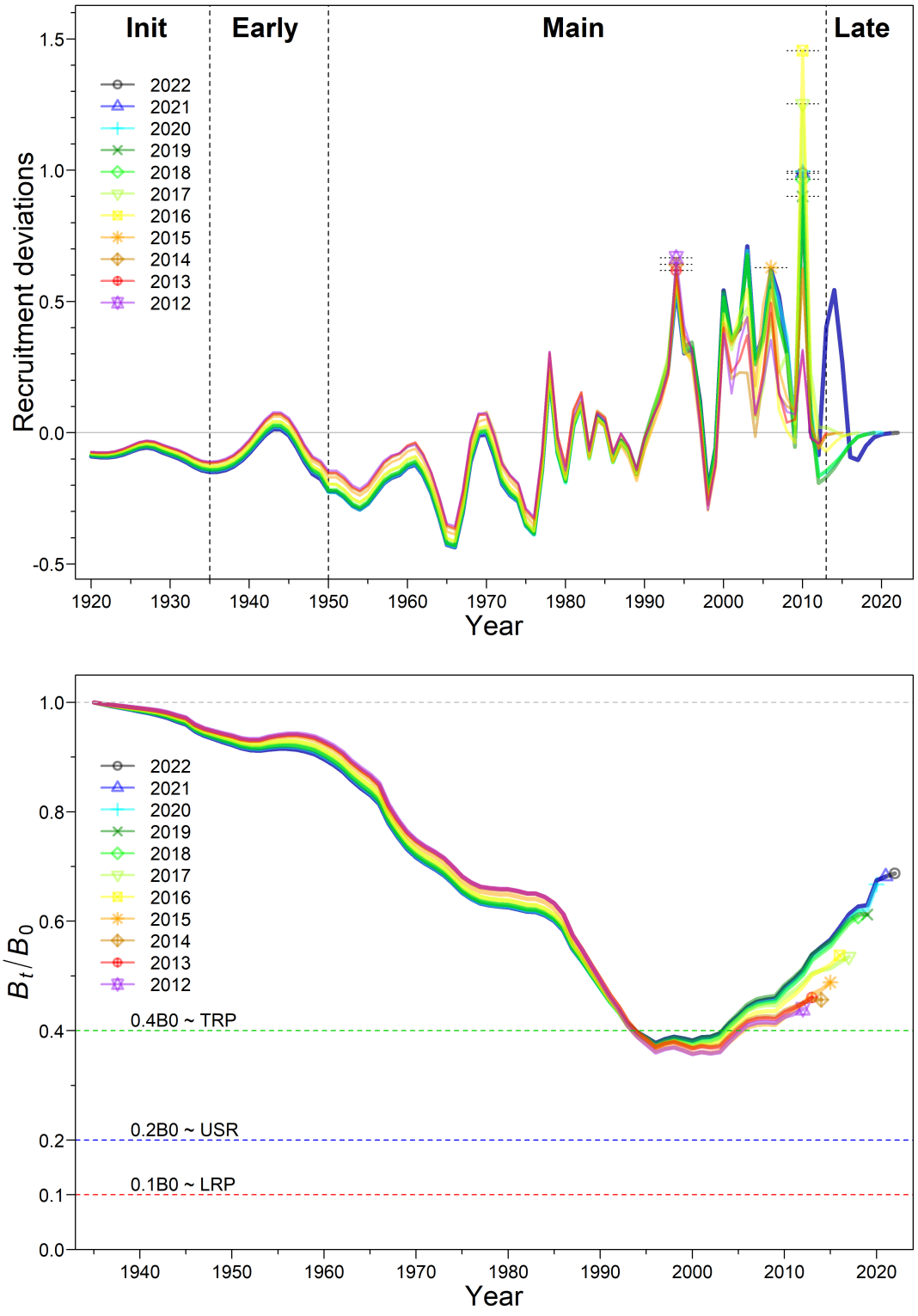

Figure F.18. CAR BC: retrospective analysis showing results for fits to the recruitment deviations (top) and spawning stock depletion (bottom).

F.2.1.2. MCMC fits

The MCMC procedure used the 'no U-turn sampling' (NUTS) algorithm (Monnahan and Kristensen 2018; Monnahan et al. 2019) to produce 4,000 iterations, parsing the workload into 8 parallel chains (Knaus 2015) of 1,000 iterations each, discarding the first 750 iterations and saving the last 250 samples per chain. The parallel chains were then merged for a total of 2,000 samples for use in the MCMC analysis.

For the primary estimated parameters, MCMC plots show:

- Figure F.19 – traces for 2,000 samples;
- Figure F.20 – split-chain diagnostics;
- Figure F.21 – auto-correlation diagnostics;
- Figure F.22 – marginal posterior densities compared to their respective prior density functions.

MCMC traces for the base run showed good diagnostics (no trend with increasing sample number) for the estimated parameters (Figure F.19). In particular, a desired feature for good fit is the lack of high-excursion events for the parameter LN(R0). When this excursion occurs, it indicates samples with poor convergence. The split-chain diagnostic plots (that split posterior samples into three equal consecutive segments, Figure F.20), were largely consistent (overlaying each other), with some minor fraying in the LN(R0) parameter. Autocorrelation out to 60 lags showed no large spikes or predictable patterns (Figure F.21). Most of the parameter medians did not move far from their maximum likelihood estimates from the MPD fits, with the possible exception of steepness (Figure F.22).

In this stock assessment, projections extended 10 years to 2033. Projections out to three generations (75 years), where one generation was determined to be 25 years (see Appendix D), were not computed because the stock status of CAR fell unambiguously into the Healthy zone. Various model trajectories and final stock status for the base run appear in the figures:

- Figure F.23 – estimated spawning biomass B_t (tonnes) from model posteriors spanning 1935-2033;
- Figure F.24 – estimated spawning biomass relative to B_0 (top panel) and B_{MSY} (bottom panel) from model posteriors;
- Figure F.25 – estimated exploitation rate u_t (top panel) and u_t/u_{MSY} (bottom panel) from model posteriors;
- Figure F.26 – estimated recruitment R_t (1000s age-0 fish, top panel) and recruitment deviations (bottom panel) from model posteriors;
- Figure F.27 – phase plot through time of median B_t/B_{MSY} and u_{t-1}/u_{MSY} relative to DFO's Precautionary Approach (PA) default reference points;
- Figure F.28 – CAR BC stock status at beginning of 2023.

Female natural mortality appeared to be the most important component of uncertainty in this stock assessment because older females disappeared from the samples. Either they remained hidden from the gear (e.g., occurred in non-trawlable areas) or their natural mortality increased after a certain age. Previous stock assessments of CAR in BC and Washington used a stepped mortality function to model this change. This stock assessment chose to model this observation in the base run by estimating a higher female natural mortalitiy relative to male natural mortality because including a stepped-mortality function did not improve the fit to the data or change management advice, but required an additional assumption and more parameters. This stock

assessment also explored a range of other model uncertainties in sensitivity runs relative to the base run 24.

The base run was used to calculate a set of parameter estimates (Table F.3) and derived quantities at equilibrium and those associated with MSY (Table F.4). The base run population trajectory from 1935 to 2023 (Figure F.23), estimated median spawning biomass B_t in t=1935, 2023, and 2033 (assuming a constant catch of 750 t/y) to be 13,908, 10,760, and 11,010 tonnes, respectively. Figure F.24 indicates that the median stock biomass will remain above the USR for the next 10 years at annual catches equal to all catches (up to 2,000 t/y) used in catch projections. Exploitation rates largely stayed below u_{MSY} for much of the fishery's history (Figure F.25). Recruitment of age-0 fish showed fairly even recruitment, with the top four recruitment years being 2010, 2003, 2014, and 2006 (Figure F.26).

A phase plot of the time-evolution of spawning biomass and exploitation rate by the modelled fisheries in MSY space (Figure F.27) suggested that the stock was in the Healthy zone, with a current position at B_{2023}/B_{MSY} = 3.043 (1.924, 4.886) and u_{2022}/u_{MSY} = 0.27 (0.151, 0.474). (Four samples were dropped because estimated MSY was 0 t, and subsequently u_{MSY}=0, rendering division by zero errors in u_{t-1}/u_{MSY}.) The current-year stock status figure (Figure F.28) shows that the position of the base run lay in the DFO Healthy zone.

F.2.1.2.1. Tables MCMC base run

Table F.3. Base run: the 0.05, 0.25, 0.5, 0.75, and 0.95 quantiles for model parameters (defined in Appendix E) from MCMC estimation of one base run of 2,000 samples.

	5%	25%	50%	75%	95%
$\log R_0$	7.534	7.754	7.933	8.137	8.432
M (Female)	0.08094	0.08841	0.09329	0.09839	0.1063
M (Male)	0.05471	0.06086	0.06543	0.07057	0.07748
BH (h)	0.5659	0.7025	0.7958	0.8750	0.9508
μ_1 (TRAWL)	12.05	12.78	13.24	13.75	14.55
$\log v_{\text{L1}}$ (TRAWL)	1.783	2.160	2.382	2.588	2.884
$\Delta 1_1$ (TRAWL)	-0.5866	-0.4681	-0.3963	-0.3242	-0.2078
μ_3 (QCS)	10.41	11.47	12.25	13.06	14.36
$\log v_{\text{L3}}$ (QCS)	1.875	2.357	2.647	2.930	3.307
$\Delta 1_3$ (QCS)	-0.5892	-0.4712	-0.3931	-0.3124	-0.2022
μ_4 (WCVI)	8.284	9.445	10.33	11.30	13.15
$\log v_{\text{L4}}$ (WCVI)	2.014	2.478	2.791	3.100	3.545
$\Delta 1_4$ (WCVI)	-0.5812	-0.4702	-0.3926	-0.3132	-0.2028
μ_5 (NMFS)	9.901	11.15	12.06	13.04	14.52
$\log v_{\text{L5}}$ (NMFS)	1.642	2.224	2.584	2.926	3.363
$\Delta 1_5$ (NMFS)	-0.5904	-0.4790	-0.4029	-0.3208	-0.2002
$\log$ [DM θ_1]	6.088	6.619	6.998	7.480	8.265
$\log$ [DM θ_3]	4.873	5.405	5.881	6.393	7.310
$\log$ [DM θ_4]	4.636	5.254	5.697	6.267	7.203
$\log$ [DM θ_5]	4.048	4.648	5.123	5.716	6.572

Table F.4. Base run: the 0.05, 0.25, 0.5, 0.75, and 0.95 quantiles of MCMC-derived quantities from 2,000 samples from a single base run. Definitions are: B_0 – unfished equilibrium spawning biomass (mature females), B_{2023} – spawning biomass at the beginning of 2023, u_{2022} – exploitation rate (ratio of total catch to vulnerable biomass) in the middle of 2022, u_{max} – maximum exploitation rate (calculated for each sample as the maximum exploitation rate from 1935-2022), B_{MSY} – equilibrium spawning biomass at MSY (maximum sustainable yield), u_{MSY} – equilibrium exploitation rate at MSY, All biomass values (and MSY) are in tonnes. For reference, the average catch over the last 5 years (2017-2021) was 775 t by Trawl and 13.5 t by Other.

	5%	25%	50%	75%	95%
B_0	10,354	12,218	13,908	15,994	20,295
B_{2023}	7,275	9,071	10,761	12,886	17,637
B_{2023}/B_0	0.5703	0.6848	0.7780	0.8757	1.045
u_{2022}	0.01335	0.01814	0.02170	0.02555	0.03226
u_{max}	0.04564	0.05719	0.06530	0.07269	0.08360
MSY	947.5	1,152	1,305	1,496	1,886
B_{MSY}	2,149	2,886	3,580	4,475	5,964
$0.4B_{\text{MSY}}$	859.8	1,154	1,432	1,790	2,385
$0.8B_{\text{MSY}}$	1,720	2,309	2,864	3,580	4,771
B_{2023}/B_{MSY}	1.924	2.468	3.043	3.744	4.886
B_{MSY}/B_0	0.1670	0.2170	0.2593	0.3019	0.3652
u_{MSY}	0.05108	0.06828	0.08124	0.09485	0.1141
u_{2022}/u_{MSY}	0.1514	0.2128	0.2700	0.3419	0.4744

Table F.5. Log likelihood (LL) values reported by the single base run for survey indices, age composition (AF), recruitment, and total (not all LL components reported here)

LL value	24.01
Run	24
CPUE Bottom Trawl	-25.0
QCS Synoptic	7.93
WCVI Synoptic	2.00
NMFS Triennial	13.9
HS Synoptic	8.63
WCHG Synoptic	23.9
GIG Historical	8.77
Abundance Index	40.1
Age Frequency	302
Recruitment	0.0551
Total	375

Table F.6. Base run: model parameter MPDs (delimited by '|') and MCMC medians (with 0.05 and 0.95 quantile limits) for the base model run of 2,000 samples.

	B1 (R24)
$\log R_0$	|7.91| 7.93 (7.53,8.43)
M (Female)	|0.0927| 0.0933 (0.0809,0.106)
M (Male)	|0.0651| 0.0654 (0.0547,0.0775)
BH (h)	|0.877| 0.796 (0.566,0.951)
μ_1	|13.3| 13.2 (12.0,14.6)
$\log v_{\text{L1}}$	|2.40| 2.38 (1.78,2.88)
$\Delta 1_1$	|-0.391| -0.396 (-0.587,-0.208)
μ_3	|12.4| 12.3 (10.4,14.4)
$\log v_{\text{L3}}$	|2.68| 2.65 (1.88,3.31)
$\Delta 1_3$	|-0.390| -0.393 (-0.589,-0.202)
μ_4	|10.4| 10.3 (8.28,13.1)
$\log v_{\text{L4}}$	|2.79| 2.79 (2.01,3.54)
$\Delta 1_4$	|-0.391| -0.393 (-0.581,-0.203)
μ_5	|12.3| 12.1 (9.90,14.5)
$\log v_{\text{L5}}$	|2.62| 2.58 (1.64,3.36)
$\Delta 1_5$	|-0.400| -0.403 (-0.590,-0.200)
$\log$ [DM θ_1]	|6.85| 7.00 (6.09,8.27)
$\log$ [DM θ_3]	|5.72| 5.88 (4.87,7.31)
$\log$ [DM θ_4]	|5.54| 5.70 (4.64,7.20)
$\log$ [DM θ_5]	|4.87| 5.12 (4.05,6.57)

Table F.7. Base run: MCMC median (with 0.05 and 0.95 quantile limits) for derived model quantities for the base model run of 2,000 samples.

	B1 (R24)
B_0	13,908 (10,354,20,295)
B_{2023}	10,761 (7,275,17,637)
B_{2023}/B_0	0.78 (0.57,1.0)
u_{2022}	0.022 (0.013,0.032)
u_{max}	0.065 (0.046,0.084)
MSY	1,305 (947,1,886)
B_{MSY}	3,580 (2,149,5,964)
$0.4B_{\text{MSY}}$	1,432 (860,2,385)
$0.8B_{\text{MSY}}$	2,864 (1,720,4,771)
B_{2023}/B_{MSY}	3.0 (1.9,4.9)
B_{MSY}/B_0	0.26 (0.17,0.37)
u_{MSY}	0.081 (0.051,0.11)
u_{2022}/u_{MSY}	0.27 (0.15,0.47)

F.2.1.2.2. Figures MCMC base run

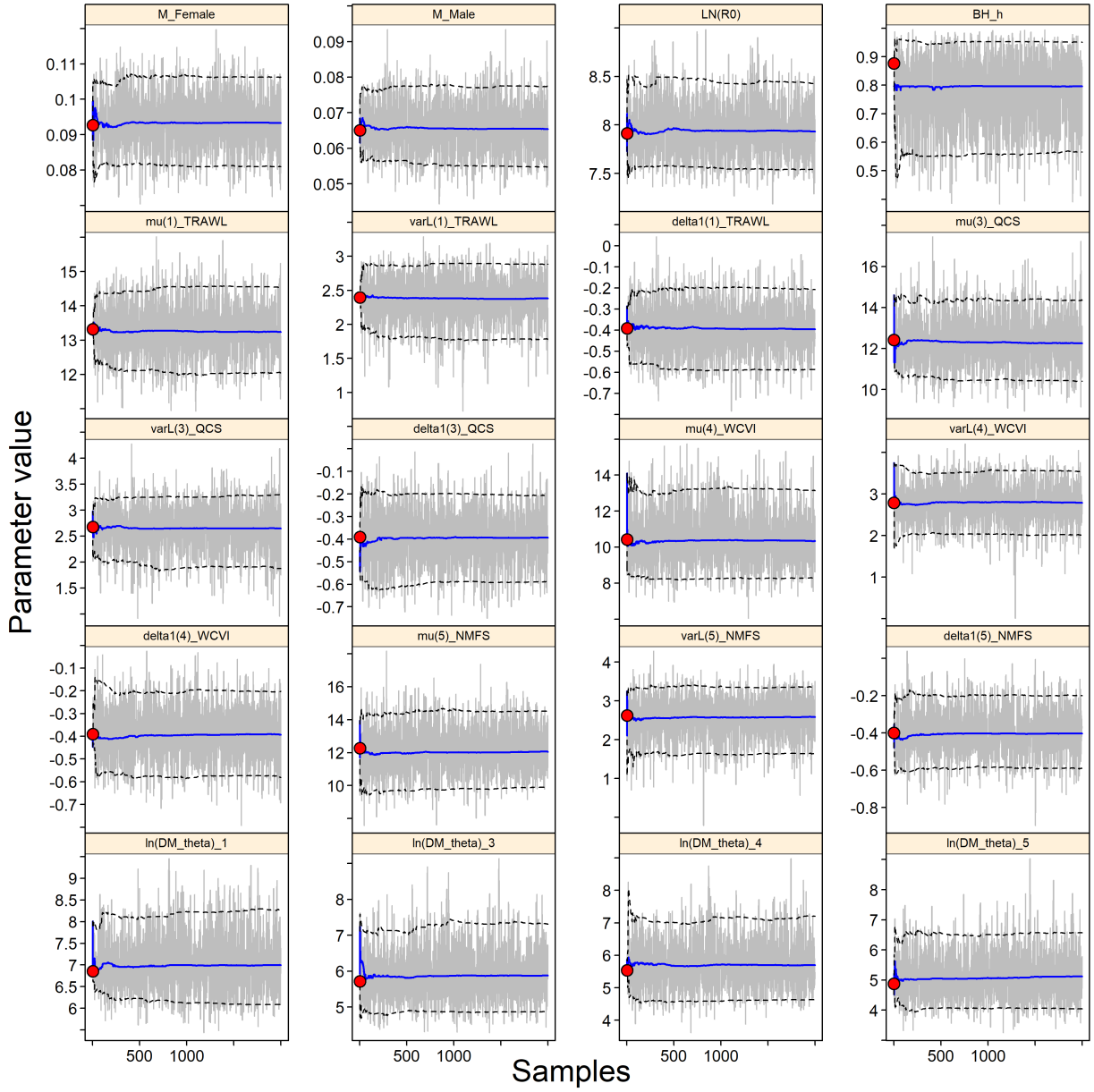

Figure F.19. CAR BC: MCMC traces for the estimated parameters. Grey lines show the 2,000 samples for each parameter, solid lines show the cumulative median (up to that sample), and dashed lines show the cumulative 0.05 and 0.95 quantiles. Red circles are the MPD estimates. For parameters other than `delta1`*, numbers (1, 3-5) correspond to fleets (fisheries and surveys).*

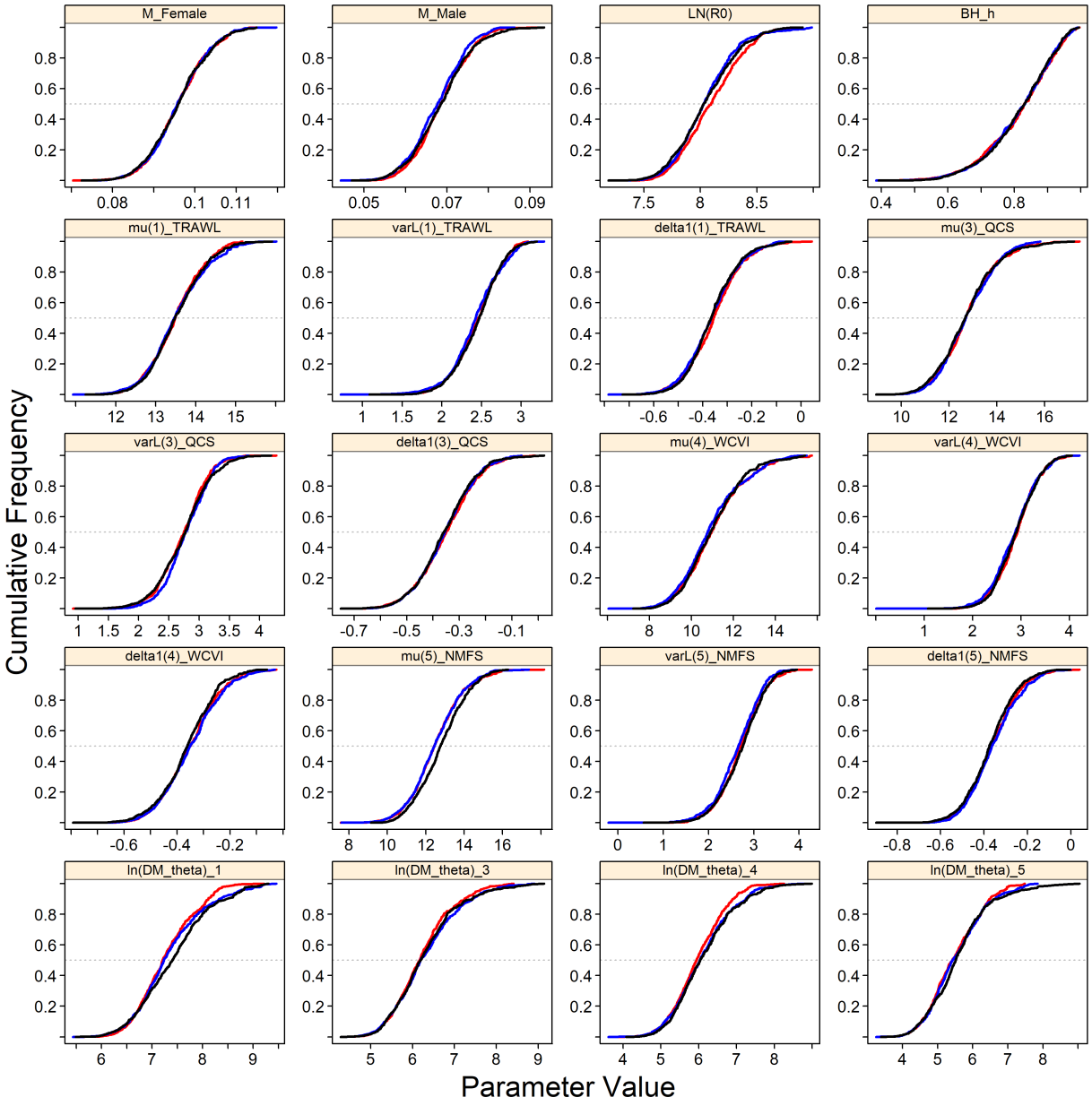

Figure F.20. CAR BC: diagnostic plot obtained by dividing the MCMC chain of 2,000 MCMC samples into three segments, and overplotting the cumulative distributions of the first segment (red), second segment (blue) and final segment (black).

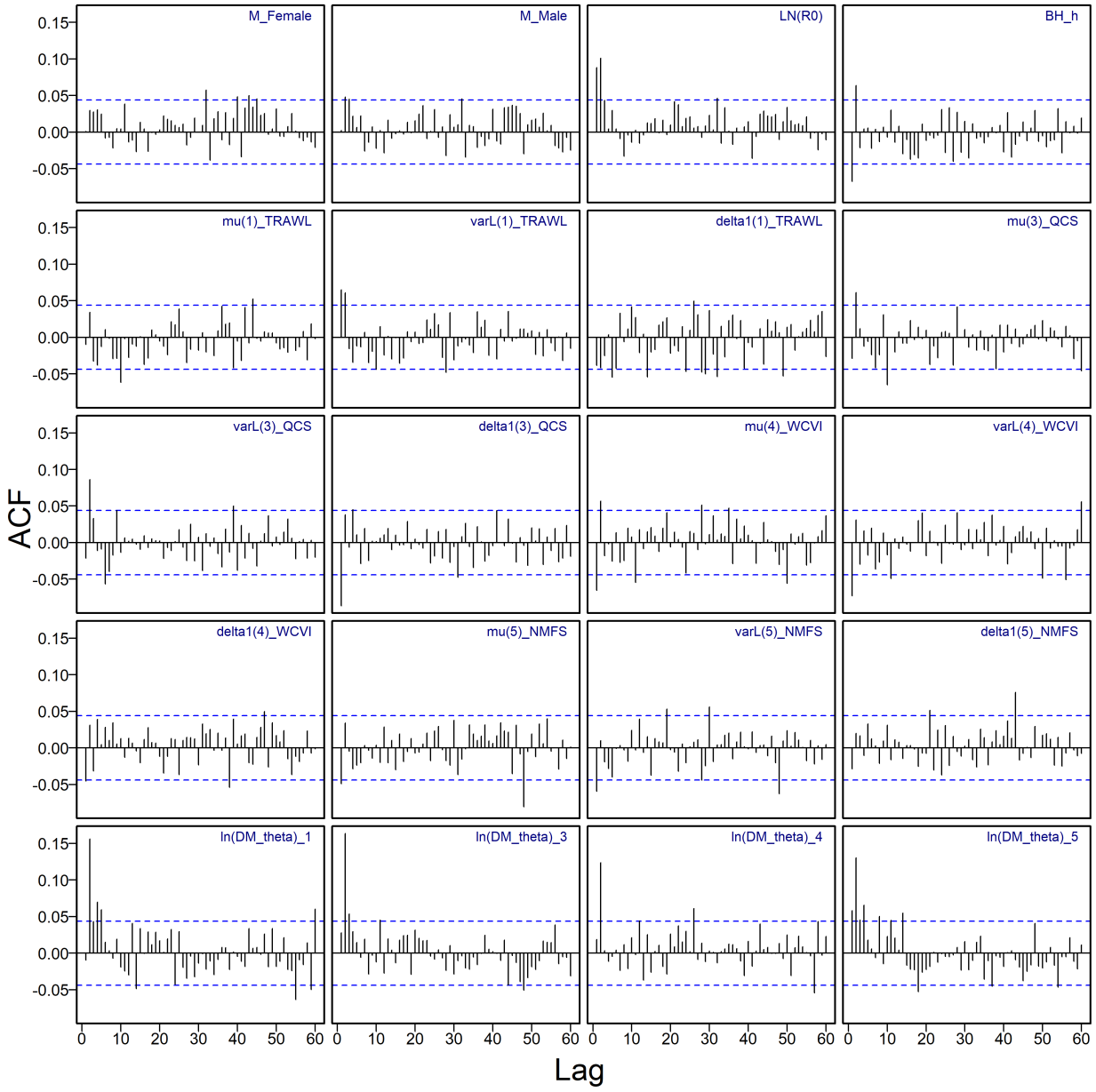

Figure F.21. CAR BC: autocorrelation plots for the estimated parameters from the MCMC output. Horizontal dashed blue lines delimit the 95% confidence interval for each parameter's set of lagged correlations.

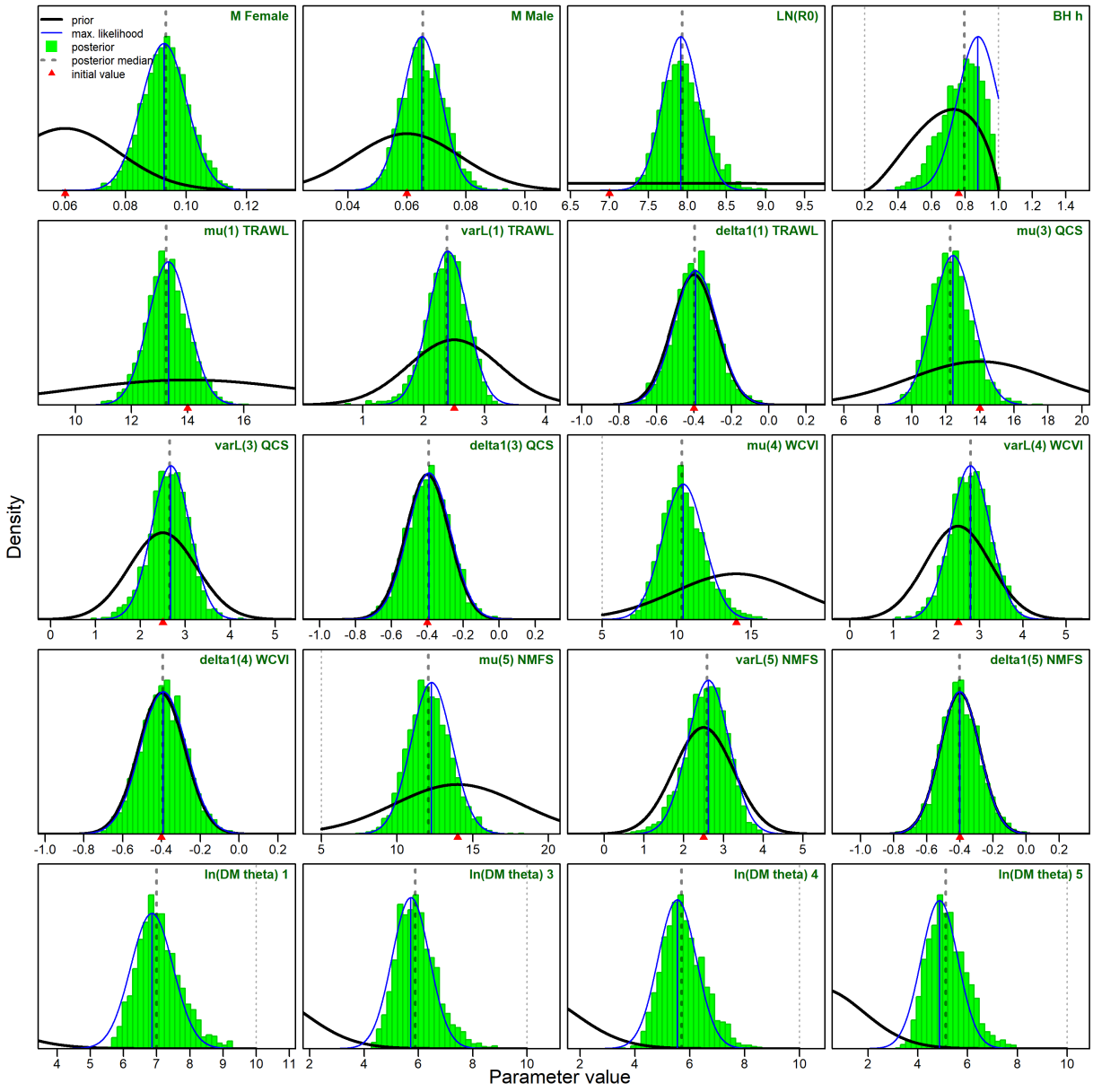

Figure F.22. CAR BC: posterior distribution (vertical green bars), likelihood profile (thin blue curve), and prior density function (thick black curve) for estimated parameters. Vertical dashed line indicates the MCMC posterior median; vertical blue line represents the MPD; red triangle indicates initial value for each parameter.

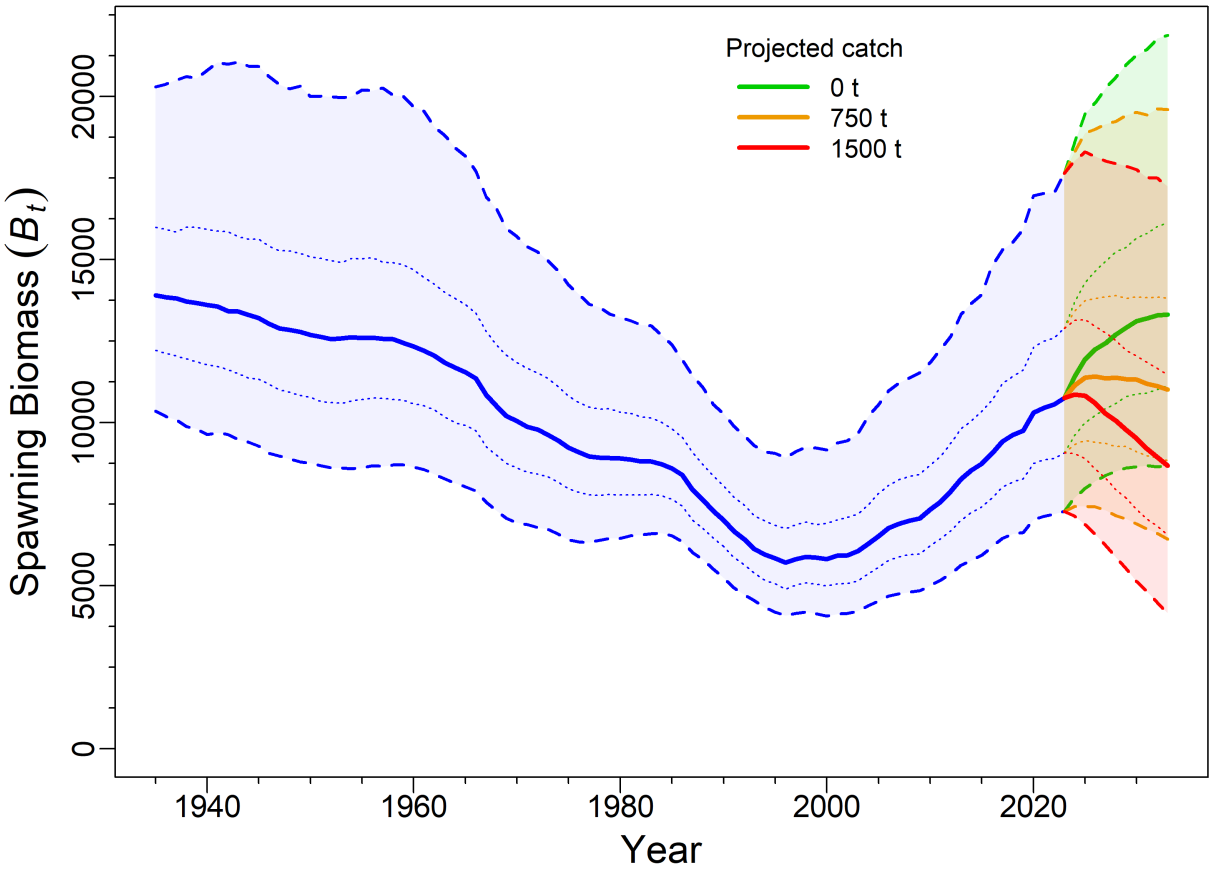

Figure F.23. CAR base run: estimates of spawning biomass B_t (tonnes) from model posteriors. The median biomass trajectory appears as a solid curve surrounded by a 90% credibility envelope (quantiles: 0.05-0.95) in light blue and delimited by dashed lines for years t=1935:2023; projected biomass for years t=2024:2033 appear in green for no catch, orange for average catch (750 t/y), and red for high catch (1500 t/y). Also delimited is the 50% credibility interval (quantiles: 0.25-0.75) delimited by dotted lines. The horizontal dashed lines show the median LRP and USR.

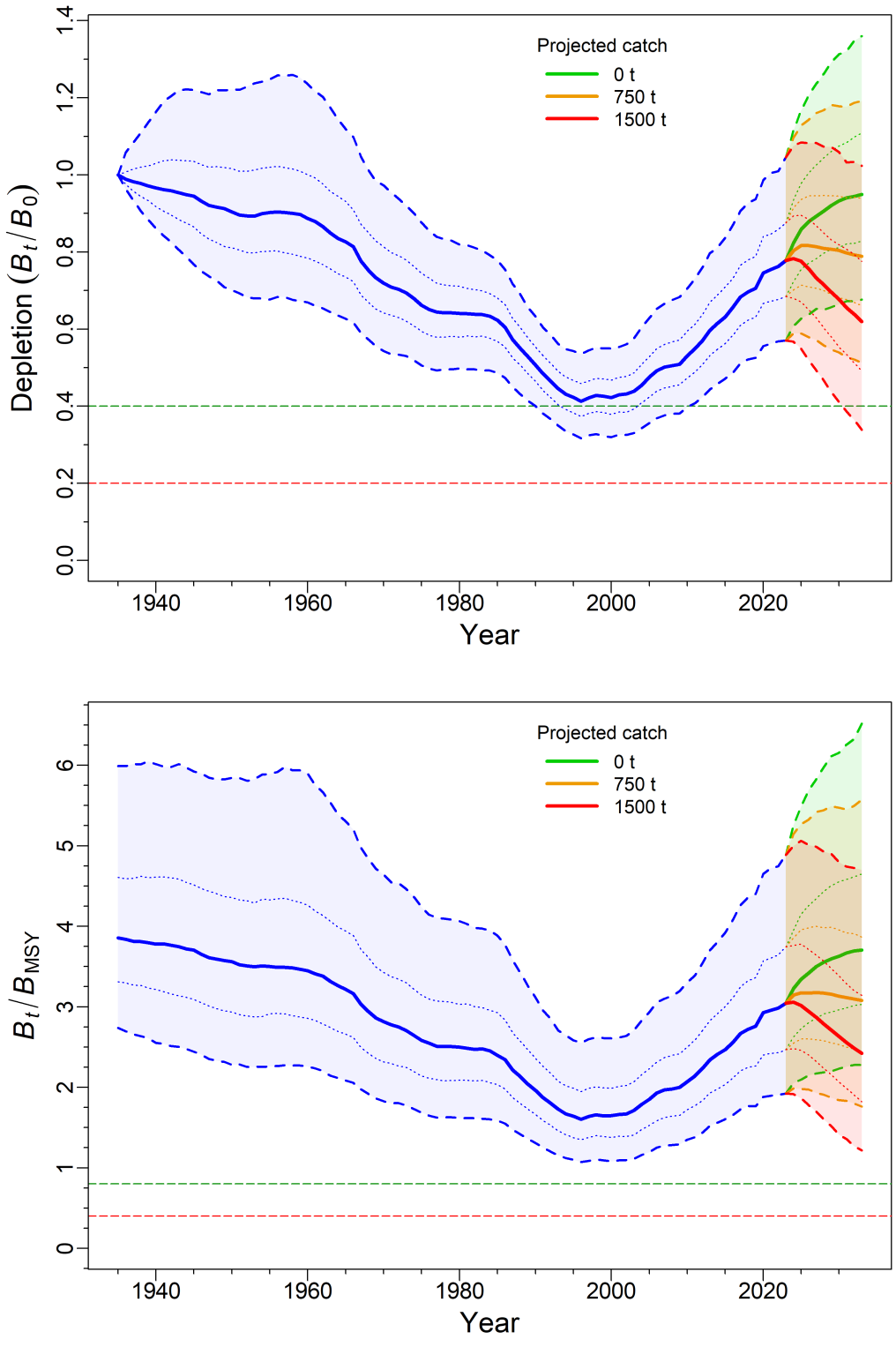

Figure F.24. CAR base run: estimates of spawning biomass B_t relative to (top) B_0 and (bottom) B_{MSY} from model posteriors. The horizontal dashed lines show $0.2B_0$ & $0.4B_0$ (top) and $0.4B_{MSY}$ & $0.8B_{MSY}$ (bottom). See Fig. F.23 caption for envelope details.

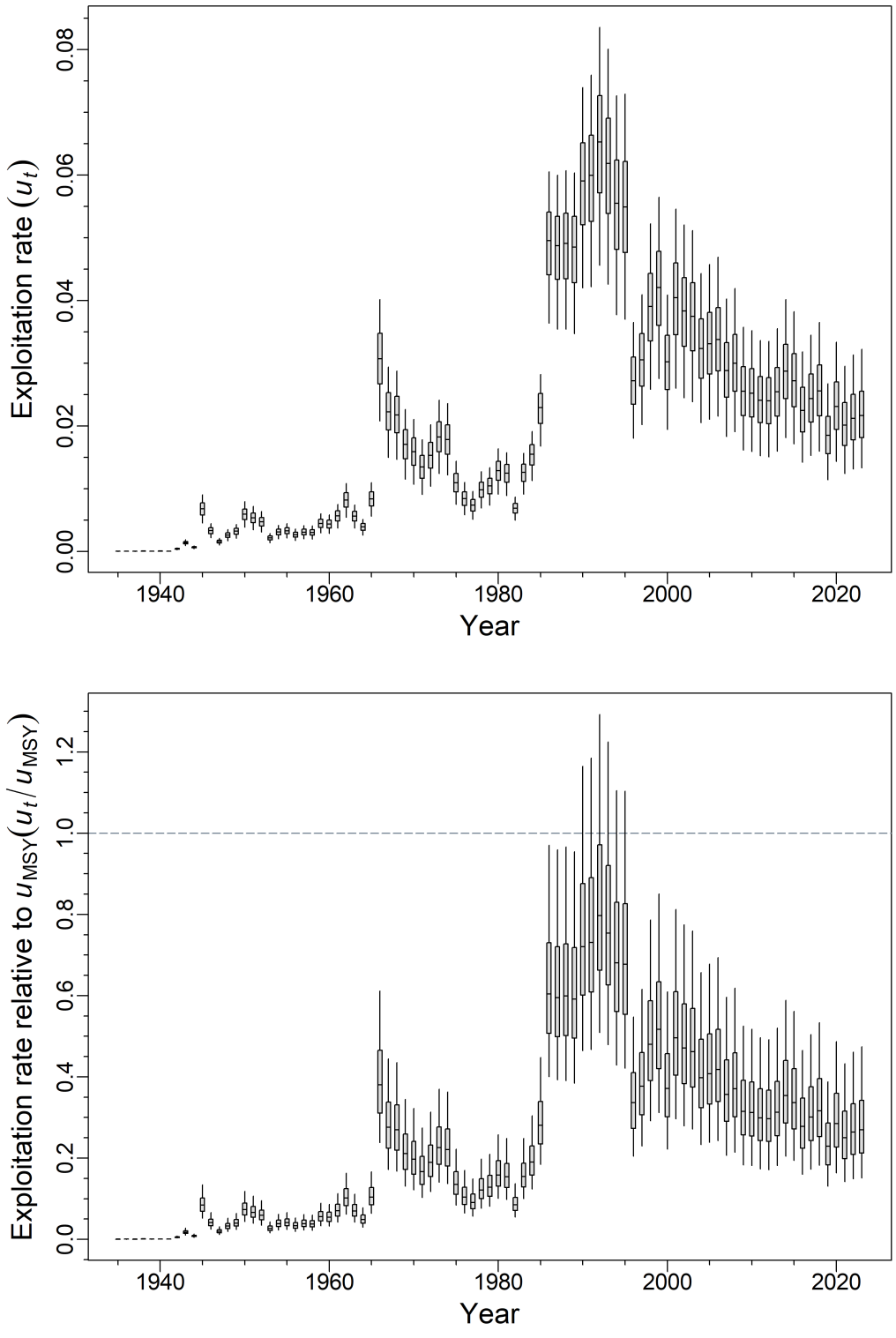

Figure F.25. CAR base run: posterior distribution of (top) exploitation trajectory u_t and (bottom) exploitation relative to u_{MSY}.

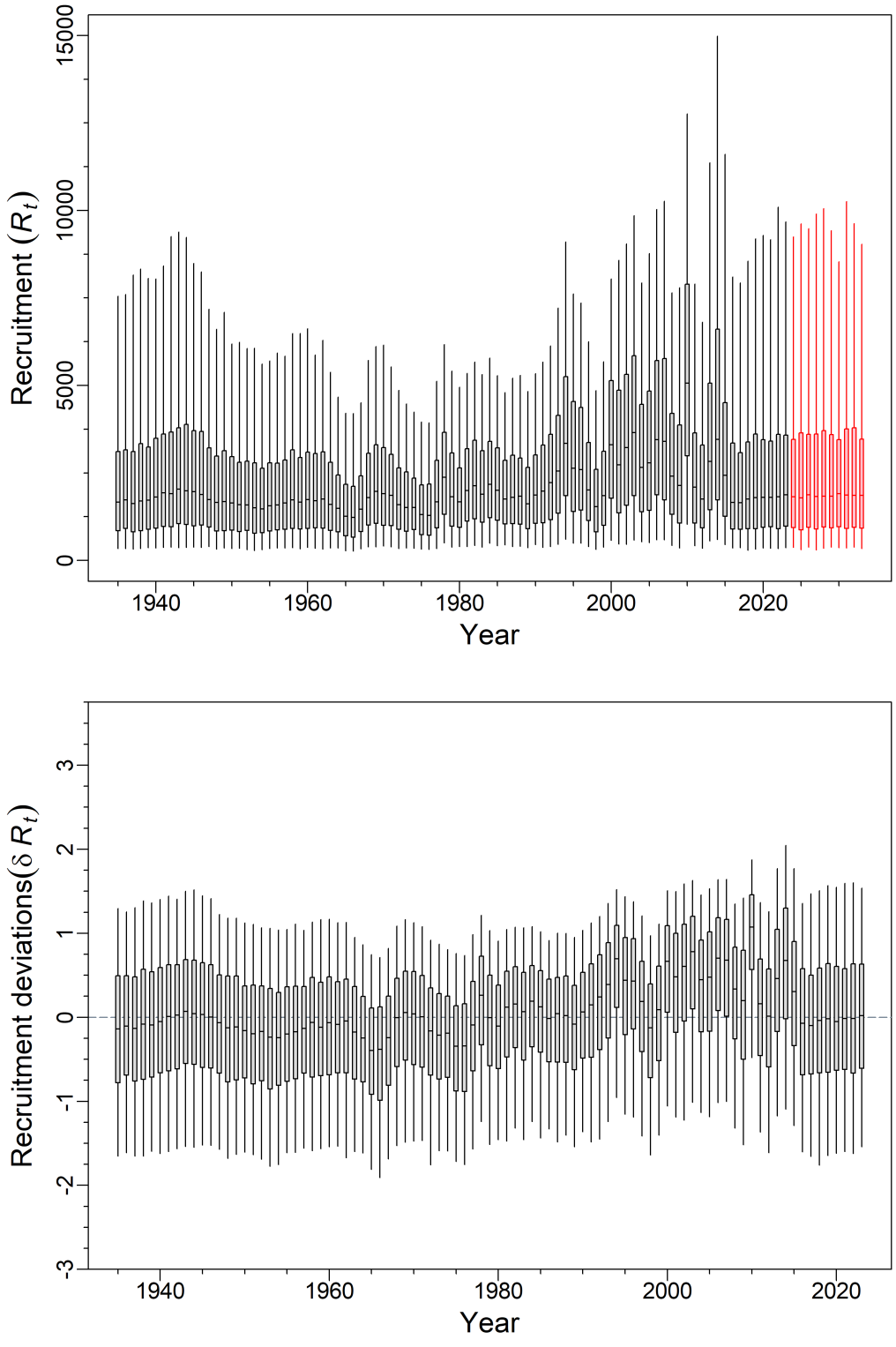

Figure F.26. CAR base run: posterior distribution of (top) recruitment trajectory (1000s of age-0 fish) and (bottom) recruitment deviation trajectory.

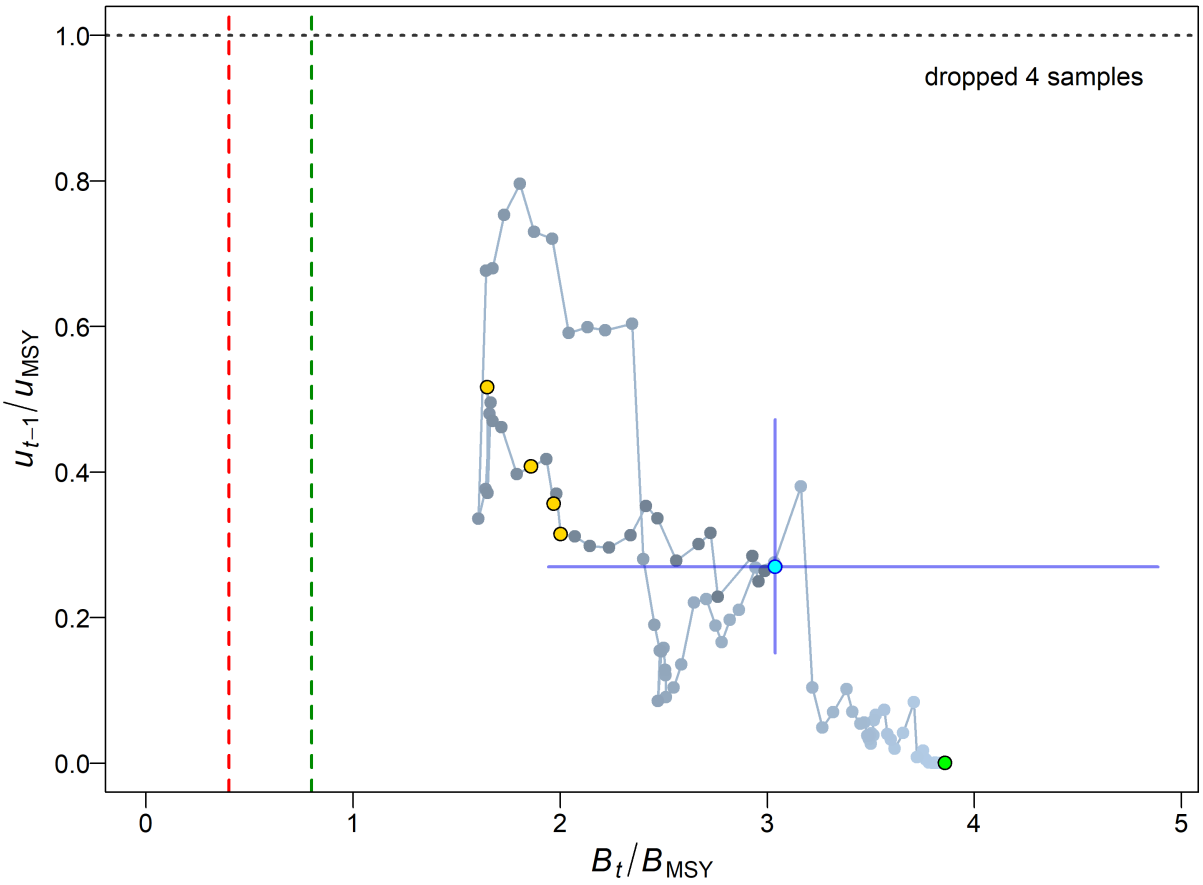

Figure F.27. CAR base run: phase plot through time of the medians of the ratios B_t/B_{MSY} (the spawning biomass in year t relative to B_{MSY}) and u_{t-1}/u_{MSY} (the exploitation rate in year $t-1$ relative to u_{MSY}) for the combined fishery (trawl+other). The filled green circle is the equilibrium starting year (1935). Years then proceed along lines gradually darkening from light grey, with the final year (2023) as a filled cyan circle, and the blue cross lines represent the 0.05 and 0.95 quantiles of the posterior distributions for the final year. Red and green vertical dashed lines indicate the PA limit and upper stock reference points (0.4, 0.8 B_{MSY}), and the horizontal grey dotted line indicates u at MSY.

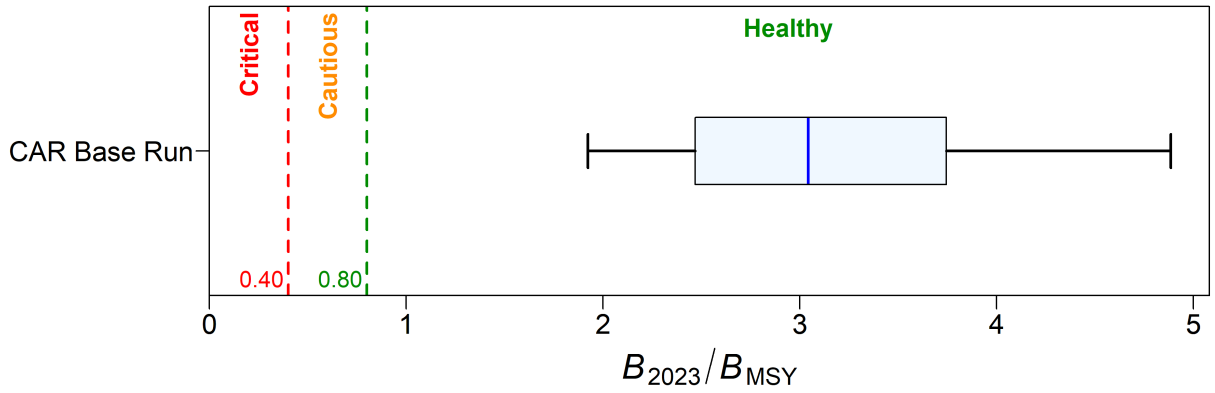

Figure F.28. CAR base run: stock status at beginning of 2023 relative to the PA reference points of $0.4B_{MSY}$ and $0.8B_{MSY}$ for the base run. Quantile plots show the 0.05, 0.25, 0.5, 0.75, and 0.95 quantiles from the MCMC posteriors.

F.2.2. GMU – Guidance for setting TACs

Decision tables for the base run provide advice to managers as probabilities that current and projected biomass B_t ($t = 2023, ..., 2033$) will exceed biomass-based reference points (or that projected exploitation rate u_t will fall below harvest-based reference points) under constant catch (CC) policies. Note that years for biomass-based reference points refer to the start of years, whereas years for harvest-based reference points refer to years prior to the start ($\sim$mid-year). Four suspicious samples were dropped before constructing the decision tables because the estimated MSY was 0 t, h was <0.4, and B_{MSY} was > 12,000 t, well outside the posterior distribution of B_{MSY}. Additionally, forecast values for these samples were not all finite.

Decision tables in the document (all under a constant catch policy):

- Table F.8 – probability of B_t exceeding the LRP, P$(B_t > 0.4B_{\text{MSY}})$;
- Table F.9 – probability of B_t exceeding the USR, P$(B_t > 0.8B_{\text{MSY}})$;
- Table F.10 – probability of B_t exceeding biomass at MSY, P$(B_t > B_{\text{MSY}})$;
- Table F.11 – probability of u_t falling below harvest rate at MSY, P$(u_t < u_{\text{MSY}})$;
- Table F.12 – probability of B_t exceeding current-year biomass, P$(B_t > B_{2023})$;
- Table F.13 – probability of u_t falling below current-year harvest rate, P$(u_t < u_{2022})$;
- Table F.14 – probability of B_t exceeding a non-DFO 'soft limit', P$(B_t > 0.2B_0)$;
- Table F.15 – probability of B_t exceeding a non-DFO 'target' biomass, P$(B_t > 0.4B_0)$;

MSY-based reference points estimated within a stock assessment model can be highly sensitive to model assumptions about natural mortality and stock recruitment dynamics (Forrest et al. 2018). As a result, other jurisdictions use reference points that are expressed in terms of B_0 rather than B_{MSY} (e.g., N.Z. Min. Fish. 2011) because B_{MSY} is often poorly estimated as it depends on estimated parameters and a consistent fishery (although B_0 shares several of these same problems). Therefore, the reference points of $0.2B_0$ and $0.4B_0$ are also presented here. These are default values used in New Zealand respectively as a 'soft limit', below which management action needs to be taken, and a 'target' biomass for low productivity stocks, a mean around which the biomass is expected to vary. The 'soft limit' is equivalent to the upper stock reference (USR, $0.8B_{\text{MSY}}$) in the DFO Sustainable Fisheries Framework while a 'target' biomass is not specified by the DFO SFF. Additionally, results are provided comparing projected biomass to B_{MSY} and to current spawning biomass B_{2023}, and comparing projected harvest rate to current harvest rate u_{2022}.

COSEWIC indicator A1 is reserved for those species where the causes of the reduction are clearly reversible, understood, and ceased. Indicator A2 is used when the population reduction may not be reversible, may not be understood, or may not have ceased. Under A2, a species is considered Endangered or Threatened if the decline has been >50% or >30% below B_0, respectively.

Additional short-term tables for COSEWIC's A2 criterion:

- Table F.16 – probability of B_t exceeding 'Endangered' status (P$(B_t > 0.5B_0)$;
- Table F.17 – probability of B_t exceeding 'Threatened' status (P$(B_t > 0.7B_0)$.

F.2.2.1. Decision Tables

*Table F.8. CAR BC: decision table for the limit reference point $0.4B_{MSY}$ featuring current- and 10-year projections for a range of **constant catch** strategies (in tonnes). Values are P($B_t > 0.4B_{MSY}$), i.e. the probability of the spawning biomass (mature females) at the start of year t being greater than the limit reference point. The probabilities are the proportion (to two decimal places) of the 1996 MCMC samples for which $B_t > 0.4B_{MSY}$. For reference, the average catch over the last 5 years (2017-2021) was 789 t.*

CC	2023	2024	2025	2026	2027	2028	2029	2030	2031	2032	2033
0	1	1	1	1	1	1	1	1	1	1	1
250	1	1	1	1	1	1	1	1	1	1	1
500	1	1	1	1	1	1	1	1	1	1	1
750	1	1	1	1	1	1	1	1	1	1	1
1000	1	1	1	1	1	1	1	1	1	1	1
1250	1	1	1	1	1	1	1	1	1	1	1
1500	1	1	1	1	1	1	1	1	1	1	1
1750	1	1	1	1	1	1	1	1	1	1	>0.99
2000	1	1	1	1	1	1	1	1	>0.99	>0.99	>0.99

*Table F.9. CAR BC: decision table for the upper stock reference point $0.8B_{MSY}$ featuring current- and 10-year projections for a range of **constant catch** strategies (in tonnes), such that values are P($B_t > 0.8B_{MSY}$). For reference, the average catch over the last 5 years (2017-2021) was 789 t.*

CC	2023	2024	2025	2026	2027	2028	2029	2030	2031	2032	2033
0	1	1	1	1	1	1	1	1	1	1	1
250	1	1	1	1	1	1	1	1	1	1	1
500	1	1	1	1	1	1	1	1	1	1	1
750	1	1	1	1	1	1	1	1	1	1	1
1000	1	1	1	1	1	1	1	1	1	1	1
1250	1	1	1	1	1	1	1	1	1	1	1
1500	1	1	1	1	1	1	1	1	>0.99	>0.99	>0.99
1750	1	1	1	1	1	1	>0.99	>0.99	>0.99	0.99	0.98
2000	1	1	1	1	1	>0.99	>0.99	0.99	0.99	0.97	0.95

*Table F.10. CAR BC: decision table for the reference point B_{MSY} featuring current- and 10-year projections for a range of **constant catch** strategies (in tonnes), such that values are P($B_t > B_{MSY}$). For reference, the average catch over the last 5 years (2017-2021) was 789 t.*

CC	2023	2024	2025	2026	2027	2028	2029	2030	2031	2032	2033
0	1	1	1	1	1	1	1	1	1	1	1
250	1	1	1	1	1	1	1	1	1	1	1
500	1	1	1	1	1	1	1	1	1	1	1
750	1	1	1	1	1	1	1	1	1	1	1
1000	1	1	1	1	1	1	1	1	>0.99	>0.99	1
1250	1	1	1	1	1	1	1	>0.99	>0.99	>0.99	>0.99
1500	1	1	1	1	1	1	>0.99	>0.99	0.99	0.99	0.98
1750	1	1	1	1	1	>0.99	>0.99	0.99	0.98	0.97	0.95
2000	1	1	1	1	>0.99	>0.99	0.99	0.97	0.96	0.92	0.89

*Table F.11. CAR BC: decision table for the reference point u_{MSY} featuring current- and 10-year projections for a range of **constant catch** strategies, such that values are P($u_t < u_{MSY}$). For reference, the average catch over the last 5 years (2017-2021) was 789 t.*

CC	2022	2023	2024	2025	2026	2027	2028	2029	2030	2031	2032
0	1	1	1	1	1	1	1	1	1	1	1
250	1	1	1	1	1	1	1	1	1	1	1
500	1	1	1	1	1	1	1	1	1	1	1
750	1	1	1	1	1	1	1	1	1	1	1
1000	1	>0.99	>0.99	>0.99	>0.99	>0.99	>0.99	>0.99	>0.99	>0.99	>0.99
1250	1	0.99	0.99	0.99	0.99	0.99	0.98	0.98	0.97	0.97	0.96
1500	1	0.97	0.97	0.96	0.95	0.93	0.92	0.91	0.90	0.88	0.87
1750	1	0.93	0.91	0.89	0.87	0.85	0.83	0.81	0.78	0.75	0.73
2000	1	0.86	0.83	0.79	0.77	0.73	0.70	0.66	0.63	0.60	0.57

*Table F.12. CAR BC: decision table for the reference point B_{2023} featuring current- and 10-year projections for a range of **constant catch** strategies, such that values are P($B_t > B_{2023}$). For reference, the average catch over the last 5 years (2017-2021) was 789 t.*

CC	2023	2024	2025	2026	2027	2028	2029	2030	2031	2032	2033
0	0	0.95	0.97	0.96	0.95	0.94	0.93	0.91	0.91	0.90	0.89
250	0	0.88	0.92	0.91	0.88	0.86	0.84	0.82	0.81	0.80	0.79
500	0	0.78	0.83	0.81	0.77	0.74	0.73	0.70	0.69	0.67	0.64
750	0	0.67	0.72	0.68	0.64	0.61	0.58	0.56	0.54	0.51	0.50
1000	0	0.56	0.61	0.55	0.51	0.47	0.46	0.43	0.40	0.38	0.37
1250	0	0.50	0.50	0.44	0.39	0.38	0.34	0.31	0.29	0.27	0.26
1500	0	0.43	0.42	0.34	0.32	0.27	0.25	0.23	0.21	0.19	0.17
1750	0	0.37	0.34	0.29	0.24	0.20	0.18	0.16	0.13	0.13	0.12
2000	0	0.32	0.28	0.23	0.18	0.14	0.12	0.10	0.09	0.09	0.08

*Table F.13. CAR BC: decision table for the reference point u_{2022} featuring current- and 10-year projections for a range of **constant catch** strategies, such that values are P($u_t < u_{2022}$). For reference, the average catch over the last 5 years (2017-2021) was 789 t.*

CC	2022	2023	2024	2025	2026	2027	2028	2029	2030	2031	2032
0	0	1	1	1	1	1	1	1	1	1	1
250	0	1	1	1	1	1	1	1	1	1	1
500	0	1	1	1	1	1	1	1	1	1	1
750	0	1	0.99	0.93	0.85	0.78	0.72	0.68	0.64	0.61	0.59
1000	0	0	0	<0.01	<0.01	0.01	0.02	0.03	0.04	0.04	0.05
1250	0	0	0	0	0	0	<0.01	<0.01	<0.01	<0.01	<0.01
1500	0	0	0	0	0	0	0	0	0	0	0
1750	0	0	0	0	0	0	0	0	0	0	0
2000	0	0	0	0	0	0	0	0	0	0	0

*Table F.14. CAR BC: decision table for an alternative reference point $0.2B_0$ featuring current- and 10 year projections for a range of **constant catch** strategies, such that values are P$(B_t > 0.2B_0)$. For reference, the average catch over the last 5 years (2017-2021) was 789 t.*

CC	2023	2024	2025	2026	2027	2028	2029	2030	2031	2032	2033
0	1	1	1	1	1	1	1	1	1	1	1
250	1	1	1	1	1	1	1	1	1	1	1
500	1	1	1	1	1	1	1	1	1	1	1
750	1	1	1	1	1	1	1	1	1	1	1
1000	1	1	1	1	1	1	1	1	1	1	1
1250	1	1	1	1	1	1	1	1	1	1	1
1500	1	1	1	1	1	1	1	1	1	>0.99	>0.99
1750	1	1	1	1	1	1	1	>0.99	>0.99	>0.99	0.99
2000	1	1	1	1	1	1	>0.99	>0.99	0.99	0.98	0.96

*Table F.15. CAR BC: decision table for an alternative reference point $0.4B_0$ featuring current- and 10 year projections for a range of **constant catch** strategies, such that values are P$(B_t > 0.4B_0)$. For reference, the average catch over the last 5 years (2017-2021) was 789 t.*

CC	2023	2024	2025	2026	2027	2028	2029	2030	2031	2032	2033
0	1	1	1	1	1	1	1	>0.99	1	1	1
250	1	>0.99	1	1	>0.99	>0.99	>0.99	>0.99	>0.99	1	1
500	1	>0.99	1	>0.99	>0.99	>0.99	>0.99	>0.99	>0.99	1	1
750	1	>0.99	>0.99	>0.99	>0.99	>0.99	>0.99	>0.99	>0.99	>0.99	>0.99
1000	1	>0.99	>0.99	>0.99	>0.99	>0.99	>0.99	0.99	0.99	0.98	0.98
1250	1	>0.99	>0.99	>0.99	>0.99	0.99	0.99	0.98	0.97	0.96	0.95
1500	1	>0.99	>0.99	>0.99	0.99	0.99	0.98	0.96	0.94	0.92	0.88
1750	1	>0.99	>0.99	0.99	0.99	0.97	0.95	0.92	0.88	0.84	0.80
2000	1	>0.99	>0.99	0.99	0.98	0.95	0.91	0.86	0.80	0.76	0.70

*Table F.16. CAR BC: decision table for COSEWIC reference criterion A2 'Endangered' featuring current- and 10-year projections and for a range of **constant catch** strategies, such that values are P$(B_t > 0.5B_0)$. For reference, the average catch over the last 5 years (2017-2021) was 789 t.*

CC	2023	2024	2025	2026	2027	2028	2029	2030	2031	2032	2033
0	0.99	0.99	>0.99	>0.99	>0.99	>0.99	>0.99	>0.99	>0.99	>0.99	>0.99
250	0.99	0.99	0.99	>0.99	>0.99	>0.99	>0.99	>0.99	>0.99	0.99	0.99
500	0.99	0.99	0.99	0.99	0.99	0.99	0.99	0.99	0.99	0.99	0.99
750	0.99	0.99	0.99	0.99	0.99	0.98	0.99	0.97	0.97	0.97	0.96
1000	0.99	0.99	0.99	0.98	0.98	0.97	0.96	0.95	0.94	0.92	0.91
1250	0.99	0.99	0.98	0.98	0.97	0.95	0.93	0.91	0.88	0.86	0.83
1500	0.99	0.98	0.98	0.96	0.94	0.92	0.89	0.84	0.80	0.77	0.74
1750	0.99	0.98	0.97	0.95	0.91	0.87	0.82	0.77	0.72	0.67	0.63
2000	0.99	0.98	0.96	0.93	0.88	0.82	0.76	0.69	0.63	0.57	0.52

*Table F.17. CAR BC: decision table for COSEWIC reference criterion A2 'Threatened' featuring current- and 10-year projections and for a range of **constant catch** strategies, such that values are P($B_t > 0.7B_0$). For reference, the average catch over the last 5 years (2017-2021) was 789 t.*

CC	2023	2024	2025	2026	2027	2028	2029	2030	2031	2032	2033
0	0.71	0.80	0.86	0.88	0.90	0.91	0.92	0.92	0.93	0.93	0.93
250	0.71	0.79	0.83	0.85	0.86	0.87	0.87	0.87	0.87	0.87	0.87
500	0.71	0.77	0.81	0.81	0.82	0.82	0.81	0.80	0.80	0.79	0.78
750	0.71	0.75	0.78	0.77	0.76	0.75	0.73	0.71	0.70	0.69	0.67
1000	0.71	0.74	0.75	0.72	0.71	0.68	0.65	0.62	0.60	0.58	0.56
1250	0.71	0.72	0.71	0.68	0.65	0.60	0.57	0.54	0.50	0.48	0.45
1500	0.71	0.71	0.68	0.64	0.58	0.53	0.49	0.45	0.42	0.38	0.35
1750	0.71	0.69	0.64	0.59	0.52	0.46	0.42	0.38	0.33	0.31	0.28
2000	0.71	0.67	0.61	0.54	0.46	0.40	0.35	0.30	0.27	0.24	0.21

F.2.3. Sensitivity Analyses

Fourteen sensitivity analyses were run (with full MCMC simulations) relative to the base run (Run24: M and h estimated, CPUE c_{p}=0.178). The MCMC procedure used for sensitivity runs followed the same procedure (NUTS algortihm) as that for the base run but differed in the number of simulations (2,000 iterations, parsing the workload into 8 parallel chains of 500 iterations each, discarding the first 250 iterations and saving the last 250 samples per chain for a total of 2,000 samples). The sensitivity analyses were run to test the sensitivity of the outputs to alternative model assumptions:

- **S01** (Run25) – split M between ages 13 and 14 (label: "split M ages(13,14)");
- **S02** (Run26) – apply no ageing error (label: "AE1 no age error");
- **S03** (Run27) – use smoothed ageing error from age-reader CVs (label: "AE5 age reader CV");
- **S04** (Run28) – use constant-CV ageing error (label: "AE6 CASAL CV=0.1");
- **S05** (Run29) – reduce commercial catch (1965-95) by 30% (label: "reduce catch 30%");
- **S06** (Run30) – increase commercial catch (1965-95) by 50% (label: "increase catch 50%");
- **S07** (Run31) – reduce σ_R to 0.6 (label: "sigmaR=0.6");
- **S08** (Run32) – increase σ_R to 1.2 (label: "sigmaR=1.2");
- **S09** (Run33) – use female dome-shaped selectivity (label: "female dome select");
- **S10** (Run34) – use AF data from HS & WCHG synoptic surveys (label: "use AF HS WCHG");
- **S11** (Run35) – add HBLL North & South surveys (label: "add HBLL surveys");
- **S12** (Run36) – use CPUE fitted by Tweedie distribution (label: "use Tweedie CPUE");
- **S13** (Run37) – remove commercial CPUE series (label: "remove comm CPUE");
- **S14** (Run49) – use Francis mean-age reweighting (label: "use Francis reweight");

All sensitivity runs were reweighted once for abundance, by adding process error to the commercial CPUE (except for S12 Tweedie because error was already high). The process error added to the commercial CPUE for all sensitivities (except S12) was the same as that adopted in the base run B1 (R24) (CPUE=0.178), based on a spline analysis (Appendix E). No additional process error was added to survey indices because observed error was already high. As relative error on the Hard-bottom Longline (HBLL) surveys was lower than that for the synoptic surveys, we ran an MPD with added process error of 25%, but the MPD parameter estimates were very similar to those with no added process error; therefore, the MCMC results for the original run in

S11 were used. No explicit composition reweighting was applied; instead the parameters $\log$ DM θ_g, which govern the ratio of nominal and effective sample size (Appendix E), were estimated.

The differences among the sensitivity runs (including the base run) are summarised in tables of median parameter estimates (Tables F.18-F.19) and median MSY-based quantities (Table F.20). Sensitivity plots appear in:

- Figure F.29 – trace plots for chains of $\log\ R_0$ MCMC samples;
- Figure F.30 – diagnostic split-chain plots for $\log\ R_0$ MCMC samples;
- Figure F.31 – diagnostic autocorrelation plots for $\log\ R_0$ MCMC samples;
- Figure F.32 – trajectories of median B_t/B_0;
- Figure F.33 – trajectories of median B_t (tonnes);
- Figure F.34 – trajectories of median recruitment deviations;
- Figure F.35 – trajectories of median recruitment R_t (1000s age-0 fish);
- Figure F.36 – trajectories of median exploitation rate u_t;
- Figure F.37 – quantile plots of selected parameters for the sensitivity runs;
- Figure F.38 – quantile plots of selected derived quantities for the sensitivity runs;
- Figure F.39 – stock status plots of $B_{2023}/B_{\mathsf{MSY}}$.

F.2.3.1. Sensitivity diagnostics

The diagnostic plots (Figures F.29 to F.31) show that seven sensitivity runs exhibited good MCMC behaviour and seven were fair. None were in the poor or unacceptable categories.

- Good – no trend in traces and no spikes in $\log R_0$, split-chains align, no autocorrelation:
  - S01 (split M ages(13,14))
  - S03 (AE5 age reader CV)
  - S04 (AE6 CASAL CV=0.1)
  - S06 (increase catch 50%)
  - S08 (sigmaR=1.2)
  - S11 (add HBLL surveys)
  - S14 (use Francis reweight)
- Fair – trace trend temporarily interrupted, occasional spikes in $\log R_0$, split-chains somewhat frayed, some autocorrelation:
  - S02 (AE1 no age error)
  - S05 (reduce catch 30%)
  - S07 (sigmaR=0.6)
  - S09 (female dome select)
  - S10 (use AF HS WCHG)
  - S12 (use Tweedie CPUE)
  - S13 (remove comm CPUE)

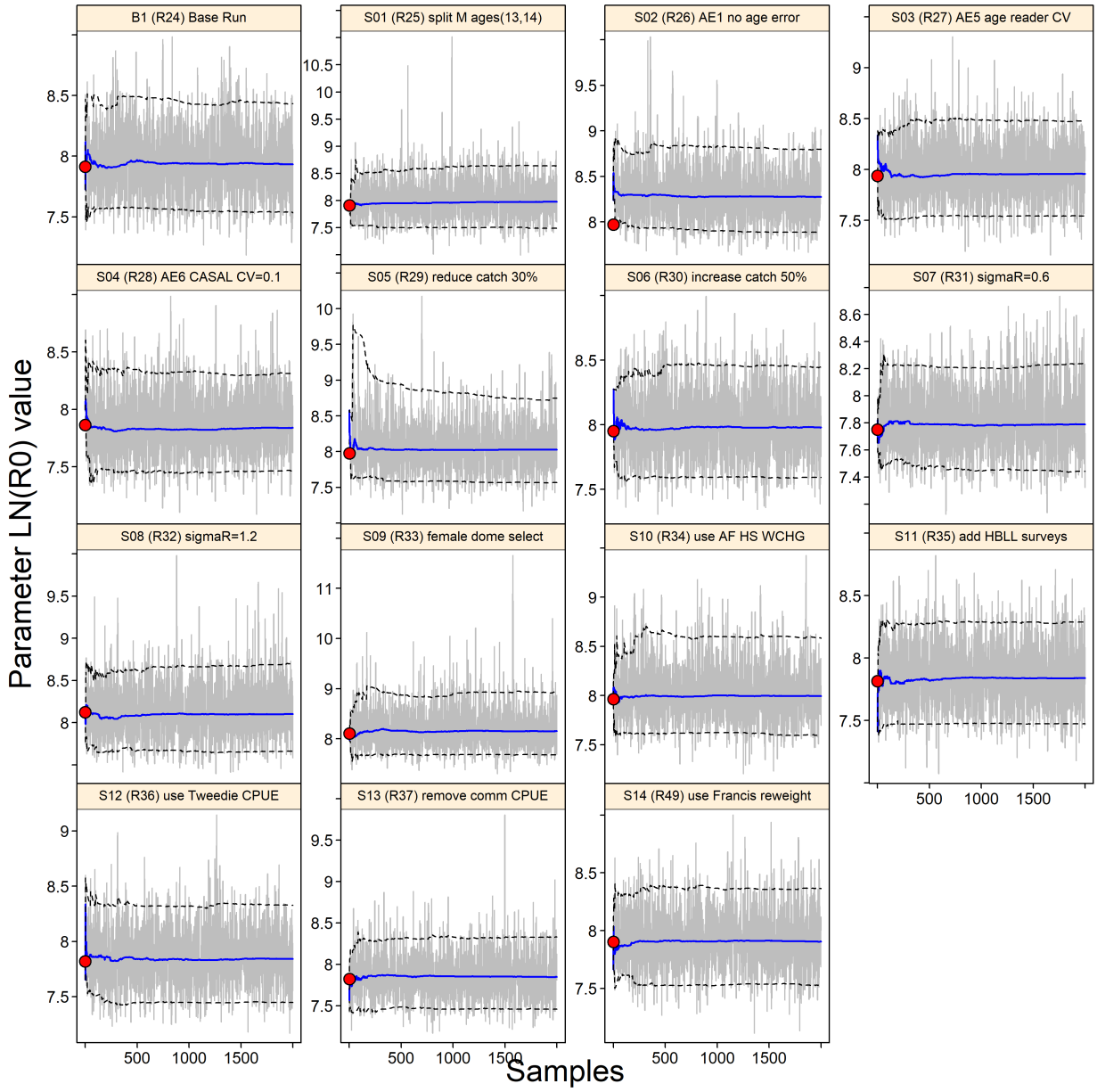

Figure F.29. CAR sensitivity R_0: MCMC traces for the estimated parameters. Grey lines show the 2,000 samples for each parameter, solid blue lines show the cumulative median (up to that sample), and dashed lines show the cumulative 0.05 and 0.95 quantiles. Red circles are the MPD estimates.

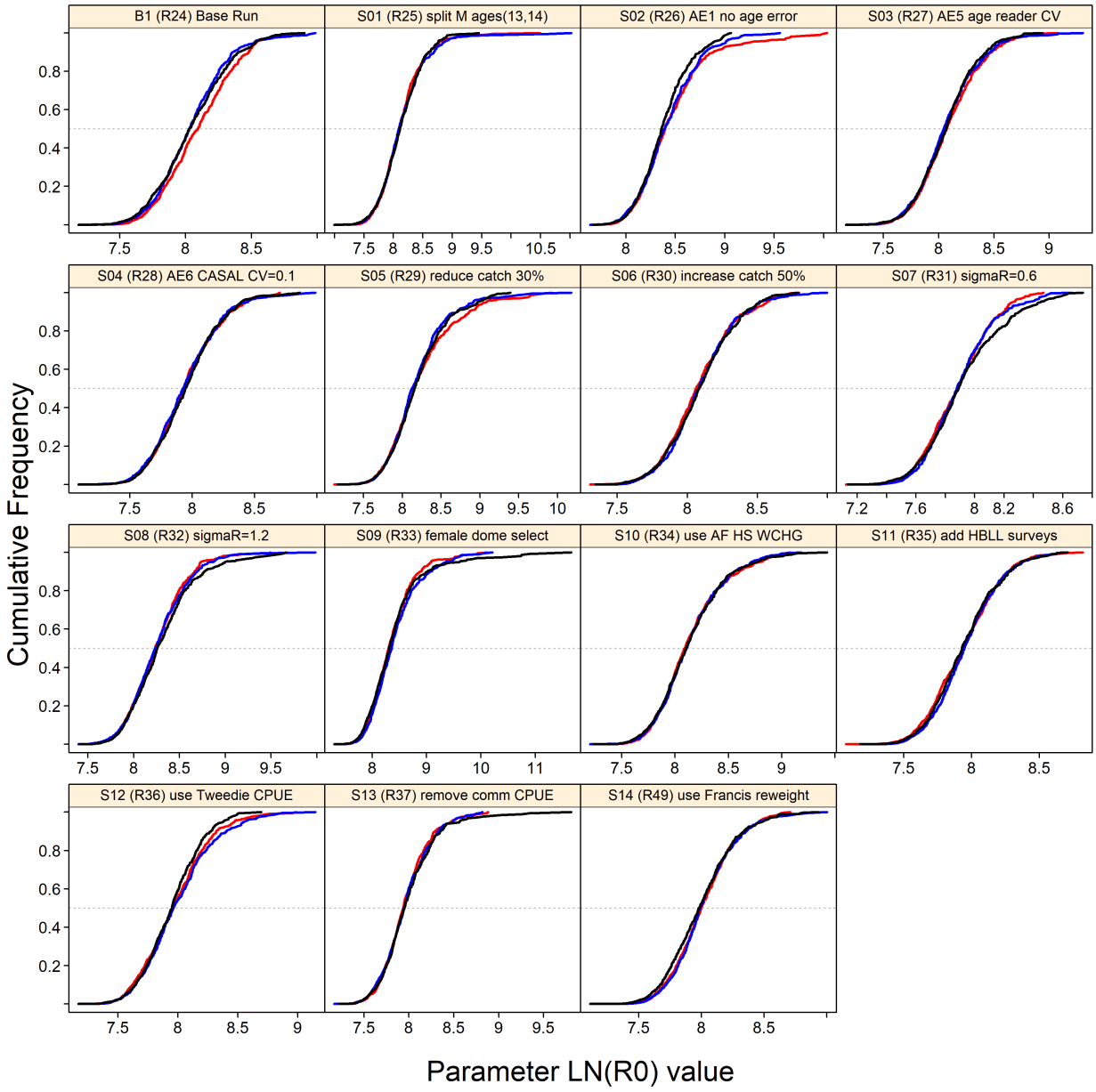

Figure F.30. CAR sensitivity R_0: diagnostic plots obtained by dividing the MCMC chain of 2,000 MCMC samples into three segments, and overplotting the cumulative distributions of the first segment (red), second segment (blue) and final segment (black).

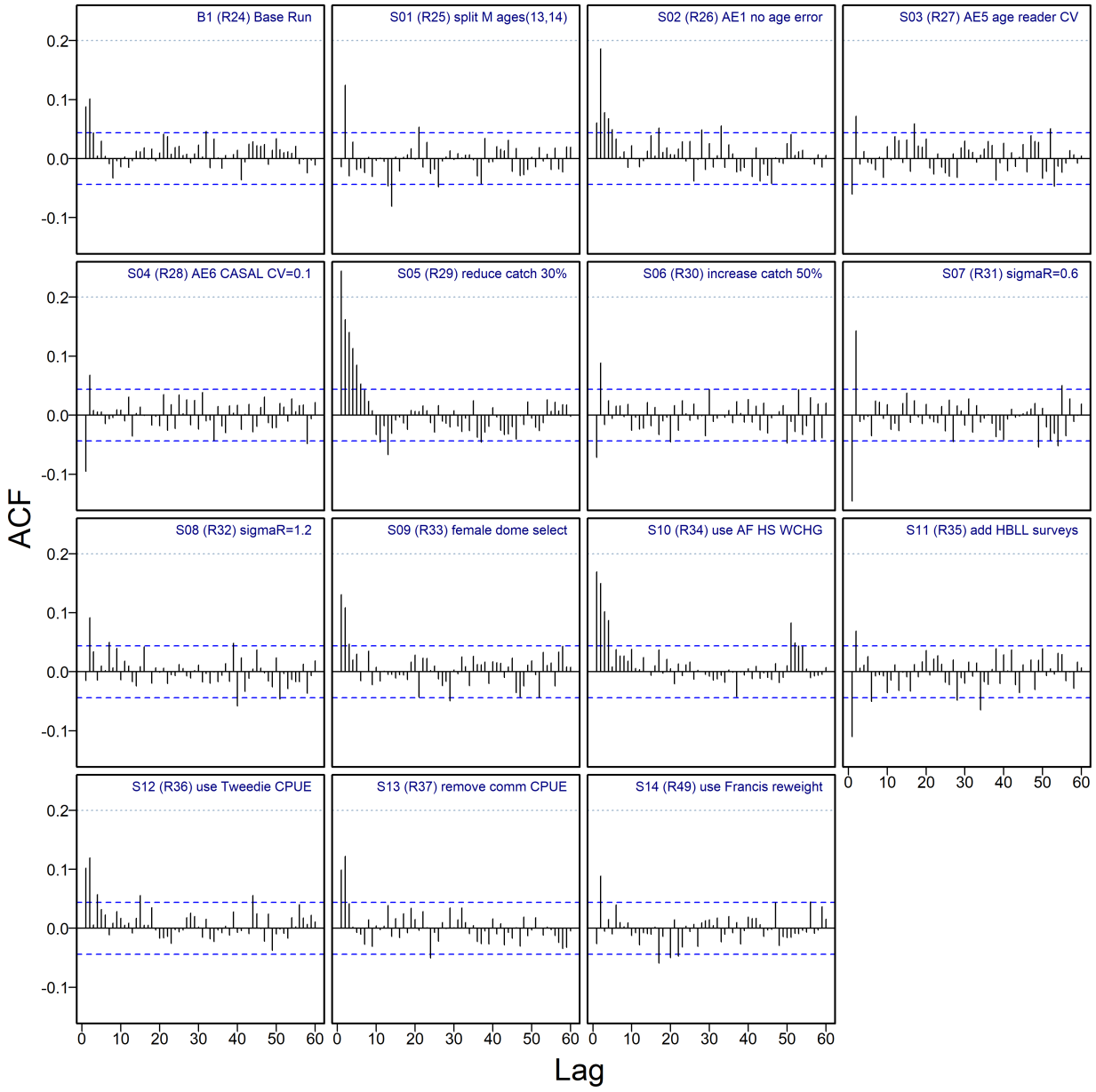

Figure F.31. CAR sensitivity R_0: autocorrelation plots for the estimated parameters from the MCMC output. Horizontal dashed blue lines delimit the 95% confidence interval for each parameter's set of lagged correlations.

F.2.3.2. Sensitivity comparisons

The trajectories of the B_t medians relative to B_0 (Figure F.32) indicate that all sensitivities followed a similar trajectory to the base run trajectory with some variation. The median final-year depletion ranged from a low of 0.622 by S11 (add HBLL) to a high of 0.973 by S01 (split M). As the split-M scenario was the most optimistic, with respect to depletion in 2023, the selected base run (first natural mortality hypothesis: single M) was considered to be a conservative choice.

Sensitivity S01 (second M hypothesis), which emulated the previous CAR stock assessment (Stanley et al. 2009; DFO 2009) by estimating a lower M for both males and females and then allowing M to increase for females after age 14, resulted in a much more optimistic stock depletion than the base run (median estimate B_{2023}/B_0=0.97 vs. 0.78 in the base run).

The third M hypothesis to explain the lack of older females in this population, represented in sensitivity (S09), which used female dome-shaped selectivity to explain this, resulted in larger biomass and a more optimistic stock depletion (median estimate B_{2023}/B_0=0.84) than the base run (Figure F.32). The larger B_0 estimate stemmed from the cryptic biomass that was created by this model run, acting as a reservoir of additional female spawners.

Two of the sensitivity runs resulted in less optimistic estimates of stock depletion. These were S11 (adding the HBLL surveys) and S12 (using Tweedie CPUE). Both these runs provided good MCMC diagnostics and could be considered alternative interpretations for the CAR stock. These runs used different data inputs, either additional survey data or an alternative interpretation of CPUE data. The Tweedie CPUE analysis (without interaction effects) was credible and represented an alternative interpretation of the catch/effort data. A second Tweedie analysis, using a full interaction model between DFO locality and year, finished quite closely to the delta-lognormal model used in the base run (Figure C.20) and would have returned a model with intermediate results between the base run and run S12.

Both CPUE series may have been compromised through changes in the collection procedure of catch/effort data as a result of administrative responses to the COVID-19 pandemic. The observer programme was suspended in March 2020 and was replaced by an audited electronic monitoring logbook programme in April 2020. Although individual landings were audited, there has been no overall audit of the post-March 2020 data collection process.

The sensitivity run which omitted the CPUE data entirely (S13) resulted in a less optimistic stock depletion estimate than in the base run, but greater than the Tweedie sensitivity run (S12) (median estimate B_{2023}/B_0=0.67 compared to 0.78 for the base run and 0.63 for S12).

An interesting sensitivity run was S10, adding the AF data for the HS and WCHG surveys, data that were not included in the base run because the model could not fit to these data very well. However, the HS survey observed younger ages and sizes (see Figure D.6) compared to the other synoptic surveys. When the model was offered the HS AF data, it estimated a very large year class for 2014 compared to the base run (Figures F.34 and F.35). While this year class may have been as large as the run S10 estimate, it seemed prudent to investigate this possibility as a sensitivity run without including such an optimistic estimate in the base run projections.

Three of the sensitivity runs addressed ageing error issues: S02 dropped ageing error entirely; S03 used an alternative ageing error vector based on the error between alternative reads of the same otolith; and S04 implemented a constant 10% error term for every age. These alternative ageing error vectors are shown concurrently in Figure D.9. The sensitivity runs employing the alternative ageing error vectors (S03 and S04) resulted in model runs that were almost identical

to the base run when plotted as a percentage of B_0 (Figure F.32). When plotted as absolute biomass (Figure F.33), sensitivity S04 lay slightly below the base run while sensitivity S03 lay on top of the base run. Sensitivity S02, which dropped ageing error entirely, was less optimistic in terms of percentage B_0 and was considerably larger in terms of absolute B_t than the base run.

The two sensitivity runs which adjusted early (1965-1995) catches downward (S05) and upward (S06) provided predictable results relative to the base run, with S05 returning a similar B_0 while S06 resulted in a much larger stock. In terms of percent B_0, S05 returned more optimistic results compared to the base run (especially after about 1990), while S06 was consistently below the base run, returning one of the least optimistic trajectories.

The two sensitivity runs that varied the σ_R parameter showed mixed results. Run S07 (sigmaR=0.6) was nearly identical to the base run, apart from estimating a smaller stock (about 10% smaller) but with no difference in terms of stock depletion. Run S08 (sigmaR=1.2) did the opposite: stock size increased (by about 15%) but stock depletion, and consequently the advice, changed very little. The SS3 platform calculates an alternative sigmaR based on the estimated variance of the recruitment deviations. This value was 0.81 for the base run, which aligned well with the sigmaR assumption made by the base run.

The sensitivity run that used Francis reweighting (S14) had good MCMC diagnostics and estimated similar parameter medians as those for the base run, with some divergence in the median estimates for natural mortality: M_1=0.097 vs. 0.093 and M_2=0.071 vs. 0.065. Estimated age at full selectivity for the trawl fishery was also slightly higher at μ_1=14.0 vs. 13.2. The derived parameters showed more variation with S14 estimating a 12% lower B_0 than that for the base run and a current spawning stock size (B_{2023}) 16% lower. However depletion was very similar between the runs: S14 B_{2023}/B_0 = 0.75, base run B_{2023}/B_0 = 0.78.

Apart from $\log R_0$, there was little variation in the key leading parameter estimates among the fourteen sensitivity runs (Figure F.37) The one exception was sensitivity run S01 (split M) because only the M for young (ages 0-13) fish was plotted. The M parameters for young and mature (ages 14+) fish were not comparable to the M values estimated for the other sensitivity runs. Another exception was S14 where the posterior for age at full selectivity for the trawl fishery shifted higher than for all other runs. Derived quantities based on MSY (Figure F.38) exhibited divergences that were consistent with the sensitivity, e.g., high B_0 for S09 (female dome-shaped selectivity) and high u_{max} for S06 (increased catch in 1965-95).

The stock status (B_{2023}/B_{MSY}) for the sensitivities (Figure F.39) were all in the DFO Healthy zone, including the most pessimistic S12 run that used the Tweedie distribution for fitting CPUE index data.

Table F.18. CAR BC: median values of MCMC samples for the primary estimated parameters, comparing the base run to 14 sensitivity runs (2,000 samples each). R = Run, S = Sensitivity. Numeric subscripts other than those for R_0 and M indicate the following gear types g: 1 = Bottom Trawl CPUE, 3 = QCS Synoptic, 4 = WCVI Synoptic, 5 = NMFS Triennial, 6 = HS Synoptic, 7 = WCHG Synoptic, and 8 = GIG Historical. Sensitivity runs: S01 = split M ages(13,14), S02 = AE1 no age error, S03 = AE5 age reader CV, S04 = AE6 CASAL CV=0.1, S05 = reduce catch 30%, S06 = increase catch 50%, S07 = sigmaR=0.6, S08 = sigmaR=1.2, S09 = female dome select, S10 = use AF HS WCHG, S11 = add HBLL surveys, S12 = use Tweedie CPUE, S13 = remove comm CPUE, S14 = use Francis reweight

	B1(R24)	S01(R25)	S02(R26)	S03(R27)	S04(R28)	S05(R29)	S06(R30)	S07(R31)	S08(R32)	S09(R33)	S10(R34)	S11(R35)	S12(R36)	S13(R37)	S14(R49)
$\log R_0$	7.933	7.977	8.275	7.959	7.839	8.028	7.979	7.789	8.104	8.153	7.994	7.839	7.841	7.848	7.905
M_1	0.09329	0.06097	0.09727	0.09392	0.09184	0.09808	0.08959	0.09272	0.09415	0.08609	0.09487	0.08737	0.09266	0.09264	0.09738
M_2	0.06543	0.05393	0.06988	0.06603	0.06380	0.07082	0.06152	0.06500	0.06627	0.06870	0.06721	0.06921	0.06466	0.06481	0.07052
BH h	0.7958	0.7547	0.8224	0.7982	0.7942	0.7767	0.7969	0.8271	0.7829	0.7608	0.7946	0.7928	0.7768	0.7901	0.8029
μ_1 (TRAWL)	13.24	13.30	13.48	13.21	13.24	13.16	13.32	13.27	13.30	13.21	13.08	13.19	13.20	13.21	13.99
$\log\ v_{\text{L1}}$ (TRAWL)	2.382	2.432	2.556	2.334	2.312	2.346	2.413	2.380	2.396	2.524	2.327	2.351	2.396	2.387	2.576
$\Delta 1_1$ (TRAWL)	-0.3963	-0.4116	-0.3931	-0.3938	-0.3876	-0.3927	-0.3903	-0.3909	-0.3912	-0.3905	-0.3902	-0.4108	-0.3934	-0.3921	-0.3905
μ_3 (QCS)	12.25	12.23	12.34	12.25	12.31	12.25	12.19	12.21	12.30	11.86	12.33	12.46	12.20	12.43	12.31
$\log\ v_{\text{L3}}$ (QCS)	2.647	2.680	2.730	2.640	2.635	2.647	2.636	2.669	2.654	2.631	2.624	2.712	2.629	2.677	2.622
$\Delta 1_3$ (QCS)	-0.3931	-0.3967	-0.3912	-0.3898	-0.3899	-0.3930	-0.3922	-0.3941	-0.3887	-0.4022	-0.3899	-0.3936	-0.3893	-0.3941	-0.3901
μ_4 (WCVI)	10.33	10.03	10.41	10.29	10.49	10.32	10.29	10.22	10.39	9.823	10.59	10.44	10.34	10.54	10.61
$\log\ v_{\text{L4}}$ (WCVI)	2.791	2.758	2.849	2.756	2.831	2.782	2.788	2.794	2.776	2.726	2.810	2.836	2.772	2.823	2.841
$\Delta 1_4$ (WCVI)	-0.3926	-0.3991	-0.3902	-0.3891	-0.3910	-0.3919	-0.3897	-0.3916	-0.3908	-0.3990	-0.3935	-0.3956	-0.3899	-0.3912	-0.3960
μ_5 (NMFS)	12.06	12.01	12.32	12.12	12.11	12.07	12.15	12.11	12.20	—	12.07	12.14	12.00	12.00	12.13
$\log\ v_{\text{L5}}$ (NMFS)	2.584	2.594	2.713	2.577	2.556	2.584	2.613	2.604	2.612	—	2.577	2.604	2.583	2.585	2.488
$\Delta 1_5$ (NMFS)	-0.4029	-0.4048	-0.4008	-0.3988	-0.4000	-0.4010	-0.4058	-0.3979	-0.3965	—	-0.4062	-0.4028	-0.3983	-0.3990	-0.4048
$\log$ (DM $\theta)_1$	6.998	7.111	7.201	7.178	6.983	6.998	7.024	7.023	7.009	7.230	7.036	7.059	7.044	7.068	—
$\log$ (DM $\theta)_3$	5.881	5.946	5.978	6.011	5.849	5.841	5.915	5.882	5.913	5.923	5.853	5.957	5.809	5.856	—
$\log$ (DM $\theta)_4$	5.697	5.733	5.766	5.783	5.715	5.627	5.688	5.674	5.716	5.597	5.646	5.744	5.669	5.688	—
$\log$ (DM $\theta)_5$	5.123	5.318	5.243	5.197	5.094	5.084	5.087	5.054	5.111	5.308	5.109	5.079	5.084	5.111	—

Table F.19. CAR BC: median values of MCMC samples for remaining estimated parameters for 4 sensitivity runs (2,000 samples each). R = Run, S = Sensitivity. Numeric subscripts other than those for $M2$ indicate the following gear types g: 1 = Trawl, 3 = QCS Synoptic, 4 = WCVI Synoptic, 6 = HS Synoptic, 7 = WCHG Synoptic, 9 = HBLL North, and 10 = HBLL South. Sensitivity runs: S01 = split M ages(13,14), S09 = female dome select, S10 = use AF HS WCHG, S11 = add HBLL surveys

	S01(R25)	S09(R33)	S10(R34)	S11(R35)
$M2_1$	0.1454	—	—	—
$M2_2$	0.06902	—	—	—
$\log\ v_{R1}$ (TRAWL)	—	2.648	—	—
$\beta 6_1$ (TRAWL)	—	10.00	—	—
$\Delta 2_1$ (TRAWL)	—	-0.3502	—	—
$\Delta 3_1$ (TRAWL)	—	2.358	—	—
$\Delta 4_1$ (TRAWL)	—	-14.06	—	—
$\log\ v_{R3}$ (QCS)	—	2.590	—	—
$\beta 6_3$ (QCS)	—	10.00	—	—
$\Delta 2_3$ (QCS)	—	-0.2002	—	—
$\Delta 3_3$ (QCS)	—	1.907	—	—
$\Delta 4_3$ (QCS)	—	-10.23	—	—
$\log\ v_{R4}$ (WCVI)	—	2.591	—	—
$\beta 6_4$ (WCVI)	—	10.00	—	—
$\Delta 2_4$ (WCVI)	—	-0.1616	—	—
$\Delta 3_4$ (WCVI)	—	1.468	—	—
$\Delta 4_4$ (WCVI)	—	-5.215	—	—
μ_6 (HS)	—	—	6.963	—
$\log\ v_{L6}$ (HS)	—	—	2.662	—
$\Delta 1_6$ (HS)	—	—	-0.4069	—
μ_7 (WCHG)	—	—	16.24	—
$\log\ v_{L7}$ (WCHG)	—	—	2.728	—
$\Delta 1_7$ (WCHG)	—	—	-0.3937	—
μ_9 (HBLLN)	—	—	—	8.978
$\log\ v_{L9}$ (HBLLN)	—	—	—	1.610
$\Delta 1_9$ (HBLLN)	—	—	—	-0.3715
μ_{10} (HBLLS)	—	—	—	9.488
$\log\ v_{L10}$ (HBLLS)	—	—	—	2.042
$\Delta 1_{10}$ (HBLLS)	—	—	—	-0.3686
$\log$ (DM $\theta)_6$	—	—	4.916	—
$\log$ (DM $\theta)_7$	—	—	5.322	—
$\log$ (DM $\theta)_9$	—	—	—	4.884
$\log$ (DM $\theta)_{10}$	—	—	—	5.202

Table F.20. CAR BC: medians of MCMC-derived quantities from the base run and 14 sensitivity runs (2,000 samples each) from their respective MCMC posteriors. Definitions are: B_0 – unfished equilibrium spawning biomass (mature females), B_{2023} – spawning biomass at the end of 2023, u_{2023} – exploitation rate (ratio of total catch to vulnerable biomass) in the middle of 2023, u_{max} – maximum exploitation rate (calculated for each sample as the maximum exploitation rate from 1935 - 2023), MSY – maximum sustainable yield at equilibrium, B_{MSY} – equilibrium spawning biomass at MSY, u_{MSY} – equilibrium exploitation rate at MSY. All biomass values (and MSY) are in tonnes. Sensitivity runs: S01 = split M ages(13,14), S02 = AE1 no age error, S03 = AE5 age reader CV, S04 = AE6 CASAL CV=0.1, S05 = reduce catch 30%, S06 = increase catch 50%, S07 = sigmaR=0.6, S08 = sigmaR=1.2, S09 = female dome select, S10 = use AF HS WCHG, S11 = add HBLL surveys, S12 = use Tweedie CPUE, S13 = remove comm CPUE, S14 = use Francis reweight

	B1(R24)	S01(R25)	S02(R26)	S03(R27)	S04(R28)	S05(R29)	S06(R30)	S07(R31)	S08(R32)	S09(R33)	S10(R34)	S11(R35)	S12(R36)	S13(R37)	S14(R49)
B_0	13,908	14,816	17,659	13,915	13,212	13,666	15,816	12,327	15,882	20,873	14,321	14,528	12,773	12,852	12,168
B_{2023}	10,761	14,220	11,806	10,862	10,185	12,001	10,691	9,478	11,664	17,235	11,224	9,059	7,996	8,571	9,007
B_{2023}/B_0	0.778	0.973	0.674	0.774	0.775	0.890	0.677	0.772	0.747	0.837	0.788	0.622	0.626	0.672	0.748
u_{2022}	0.0217	0.0170	0.0195	0.0217	0.0231	0.0197	0.0216	0.0251	0.0196	0.0160	0.0188	0.0282	0.0284	0.0265	0.0260
u_{max}	0.0653	0.0537	0.0599	0.0652	0.0682	0.0437	0.0905	0.0674	0.0631	0.0474	0.0620	0.0722	0.0683	0.0681	0.0753
MSY	1,305	1,712	1,798	1,319	1,214	1,302	1,441	1,189	1,528	1,550	1,358	1,188	1,163	1,192	1,210
B_{MSY}	3,580	4,579	4,310	3,588	3,392	3,608	4,090	2,961	4,276	5,605	3,665	3,576	3,356	3,347	3,054
$0.4B_{\text{MSY}}$	1,432	1,832	1,724	1,435	1,357	1,443	1,636	1,184	1,711	2,242	1,466	1,430	1,343	1,339	1,222
$0.8B_{\text{MSY}}$	2,864	3,663	3,448	2,870	2,714	2,886	3,272	2,369	3,421	4,484	2,932	2,861	2,685	2,678	2,443
B_{2023}/B_{MSY}	3.04	3.22	2.77	3.04	3.04	3.39	2.62	3.22	2.80	3.10	3.08	2.51	2.40	2.57	2.97
B_{MSY}/B_0	0.259	0.307	0.245	0.260	0.257	0.265	0.261	0.241	0.272	0.271	0.256	0.248	0.266	0.261	0.254
u_{MSY}	0.0812	0.0915	0.0869	0.0818	0.0806	0.0795	0.0802	0.0863	0.0796	0.0742	0.0818	0.0798	0.0778	0.0802	0.0843
u_{2022}/u_{MSY}	0.270	0.187	0.224	0.268	0.286	0.245	0.276	0.292	0.242	0.217	0.231	0.357	0.362	0.334	0.307

Table F.21. Log likelihood (LL) values reported by base and sensitivity runs for survey indices, age composition (AF), recruitment, and total (not all LL components reported here)

Sen.Run	Label	QCS	WCVI	NMFS	HS	WCHG	GIG	HBLLN	HBLLS	Index	AF	Recruit	Total
B1 (R24)	base run	7.933	2.003	13.86	8.634	23.92	8.773	—	—	40.14	302.1	0.05506	374.8
S01 (R25)	split M ages(13,14)	7.936	2.022	14.22	8.739	24.06	8.841	—	—	40.64	296.0	-0.4476	367.8
S02 (R26)	AE1 no age error	7.821	2.019	14.05	8.567	23.94	8.898	—	—	40.69	299.6	-0.2411	372.8
S03 (R27)	AE5 age reader CV	7.956	2.000	13.82	8.647	23.92	8.796	—	—	40.13	302.5	0.04441	375.4
S04 (R28)	AE6 CASAL CV=0.1	7.996	1.998	13.68	8.703	23.95	8.670	—	—	39.70	302.3	0.05653	374.3
S05 (R29)	reduce catch 30%	7.897	1.994	15.54	8.735	24.03	9.336	—	—	42.87	302.4	1.213	379.4
S06 (R30)	increase catch 50%	7.995	2.022	11.87	8.496	23.79	8.170	—	—	36.98	301.7	-1.148	369.5
S07 (R31)	sigmaR=0.6	7.710	2.002	13.70	8.872	24.23	8.578	—	—	40.64	303.5	-13.01	363.5
S08 (R32)	sigmaR=1.2	8.035	2.040	13.93	8.522	23.78	8.944	—	—	40.12	301.4	9.574	383.6
S09 (R33)	female dome select	7.826	2.028	14.55	8.978	24.58	9.131	—	—	41.76	294.5	-0.4393	368.3
S10 (R34)	use AF HS WCHG	8.107	2.139	13.95	8.012	23.78	8.808	—	—	39.69	364.5	-0.04880	447.1
S11 (R35)	add HBLL surveys	7.741	1.989	13.18	8.632	24.24	8.629	-4.816	1.126	37.02	149.7	-0.3935	227.8
S12 (R36)	use Tweedie CPUE	6.956	2.145	13.62	9.503	25.19	8.695	—	—	45.99	301.6	-1.296	378.4
S13 (R37)	remove comm CPUE	7.263	2.064	13.54	8.977	24.44	8.689	—	—	64.97	302.2	-1.050	398.3
S14 (R49)	use Francis reweight	8.049	1.967	13.92	8.642	23.80	8.527	—	—	39.59	190.1	0.6417	242.8

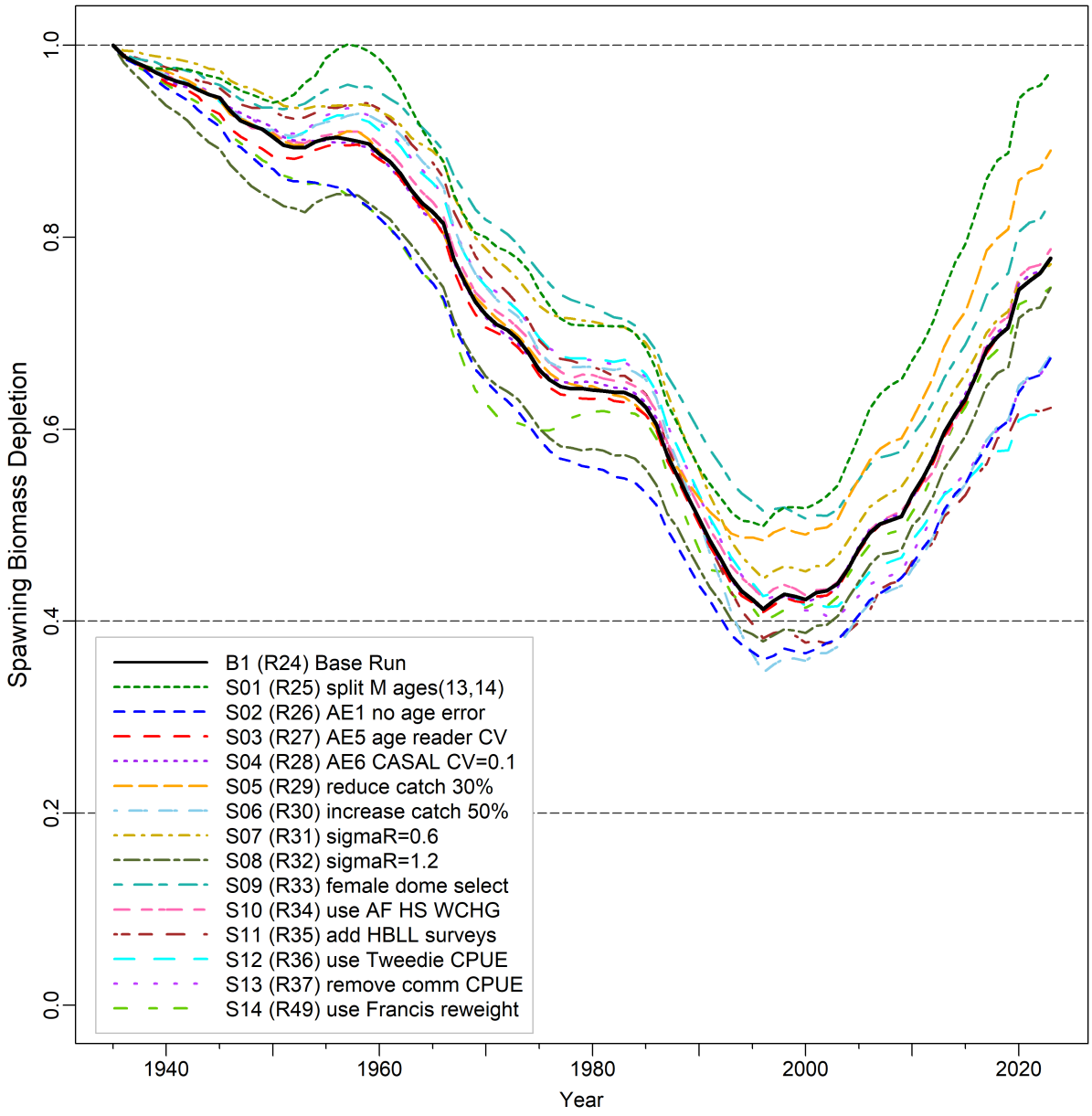

Figure F.32. CAR sensitivity: model trajectories of median spawning biomass as a proportion of unfished equilibrium biomass (B_t/B_0) for the base run and 14 sensitivity runs. Horizontal dashed lines show alternative reference points used by other jurisdictions: 0.2B_0 (~DFO's USR), 0.4B_0 (often a target level above B_{MSY}), and B_0 (equilibrium spawning biomass).

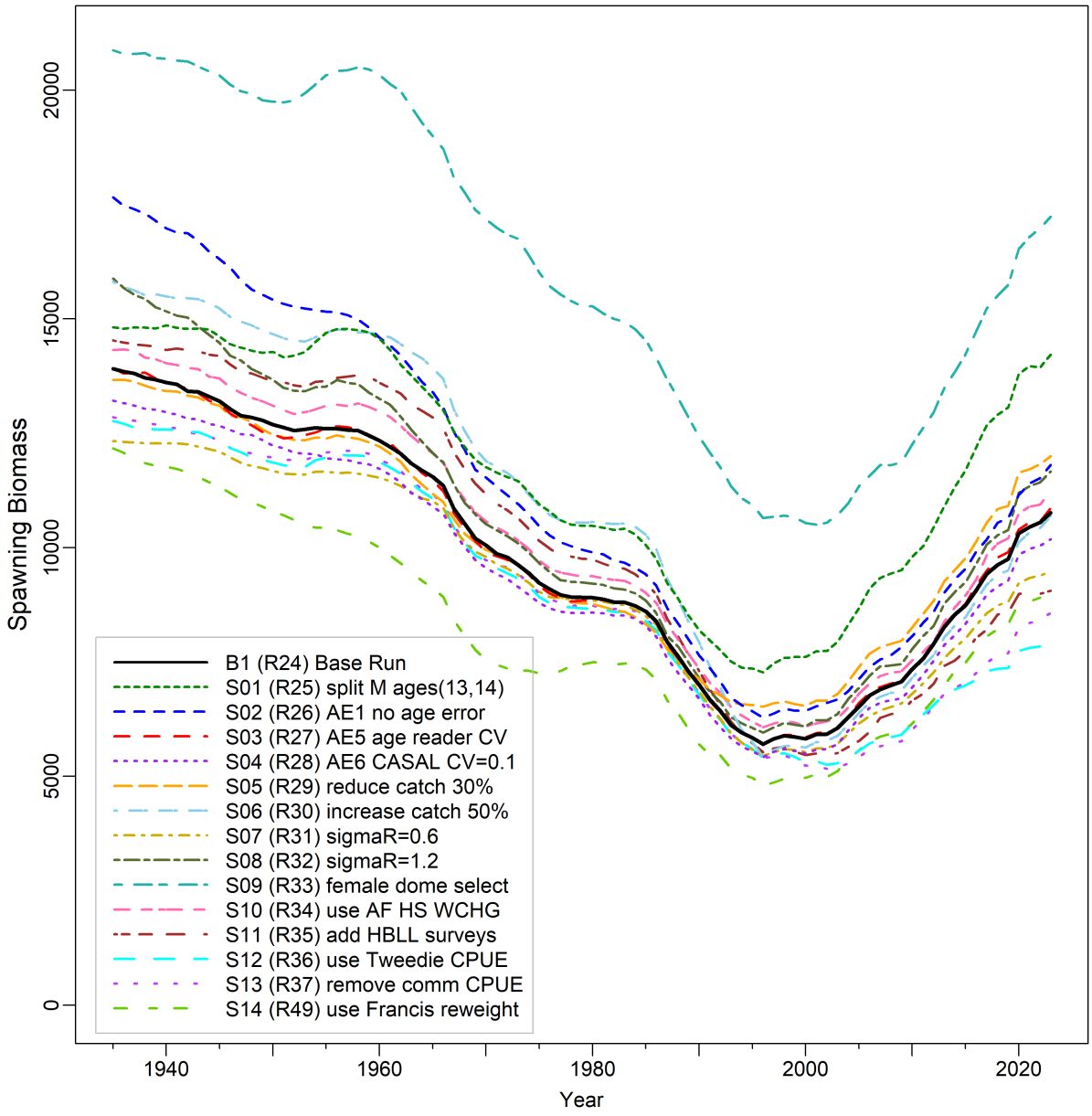

Figure F.33. CAR sensitivity: model trajectories of median spawning biomass (tonnes) for the base run and 14 sensitivity runs.

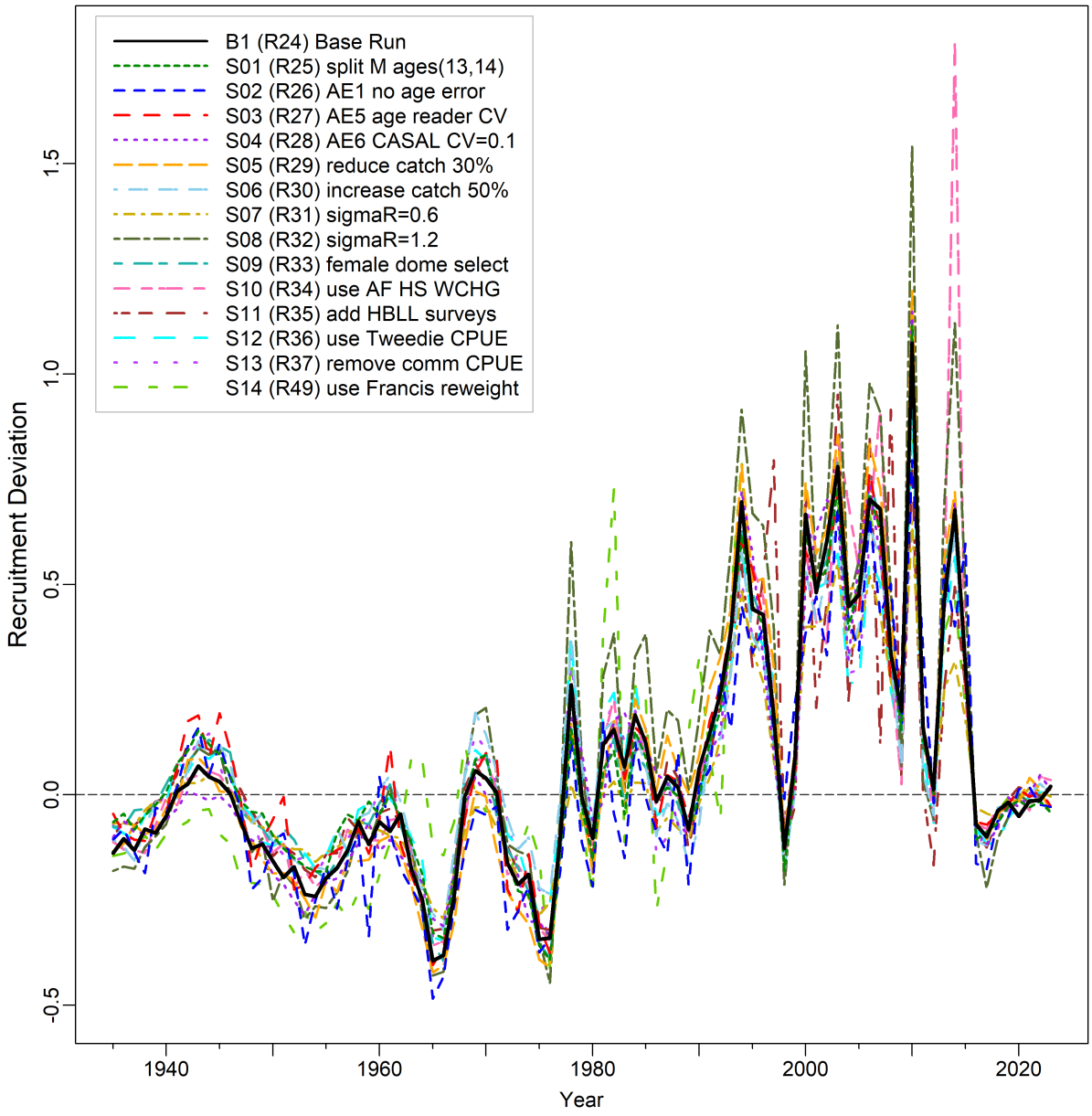

Figure F.34. CAR sensitivity: model trajectories of median recruitment deviations for the base run and 14 sensitivity runs.

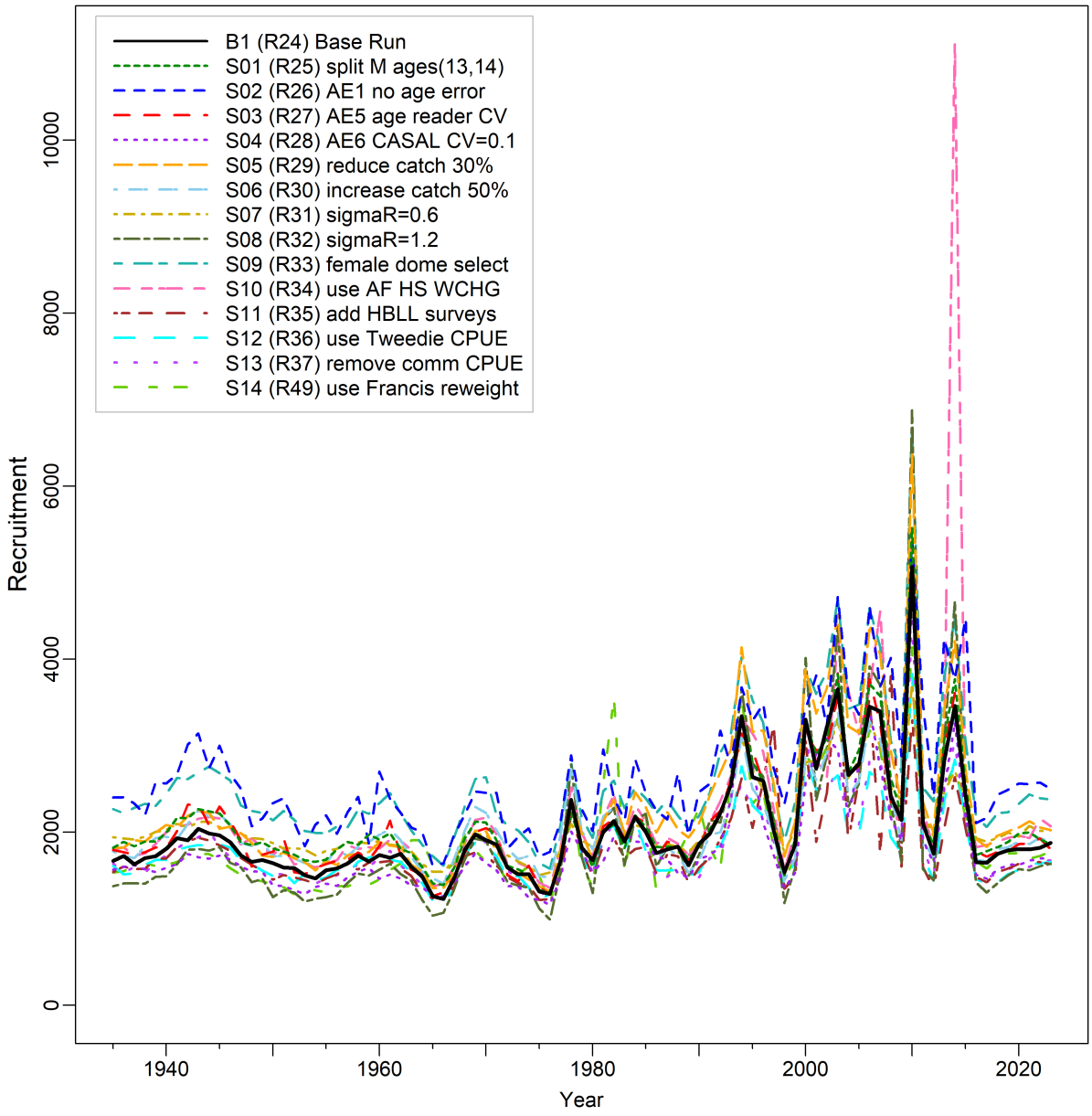

Figure F.35. CAR sensitivity: model trajectories of median recruitment of one-year old fish (R_t, 1000s) for the base run and 14 sensitivity runs.

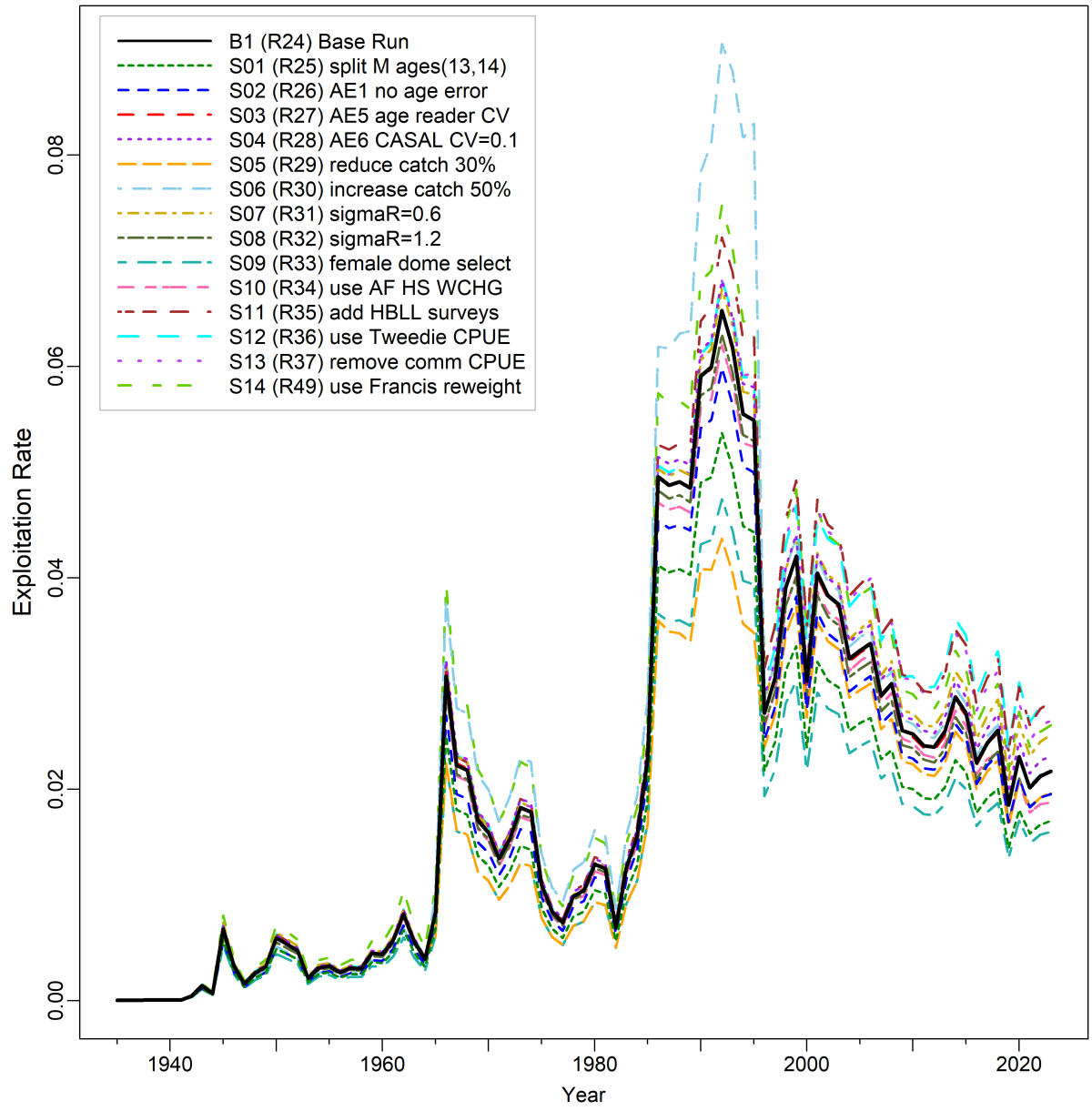

Figure F.36. CAR sensitivity: model trajectories of median exploitation rate of vulnerable biomass (u_t) for the base run and 14 sensitivity runs.

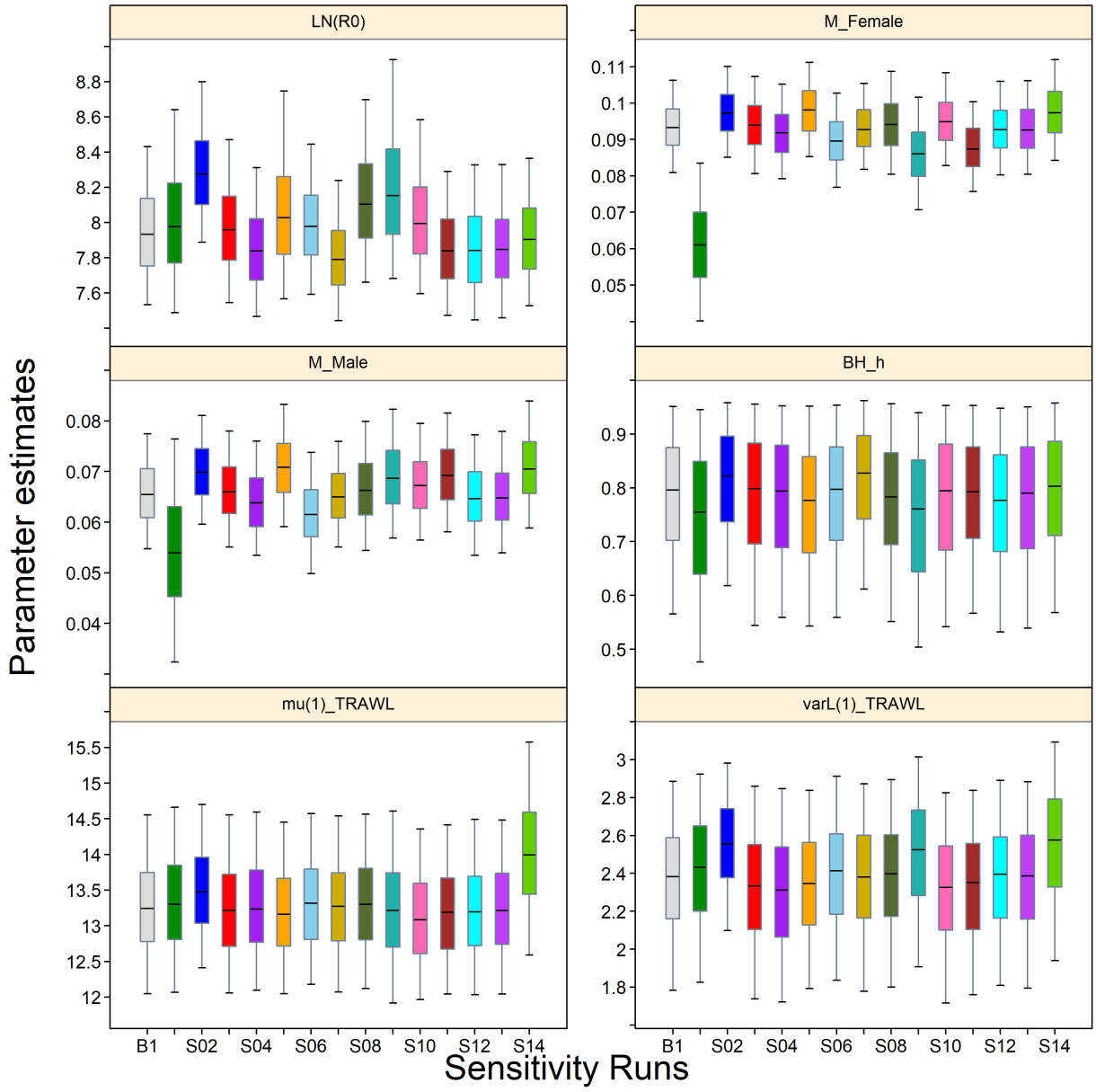

Figure F.37. CAR sensitivity: quantile plots of selected parameter estimates ($\log R_0$, $M_{s=1,2}$, h, $\mu_{g=1}$, $\log v_{Lg=1}$) comparing the base run with 14 sensitivity runs. See text on sensitivity numbers. The boxplots delimit the 0.05, 0.25, 0.5, 0.75, and 0.95 quantiles; outliers are excluded.

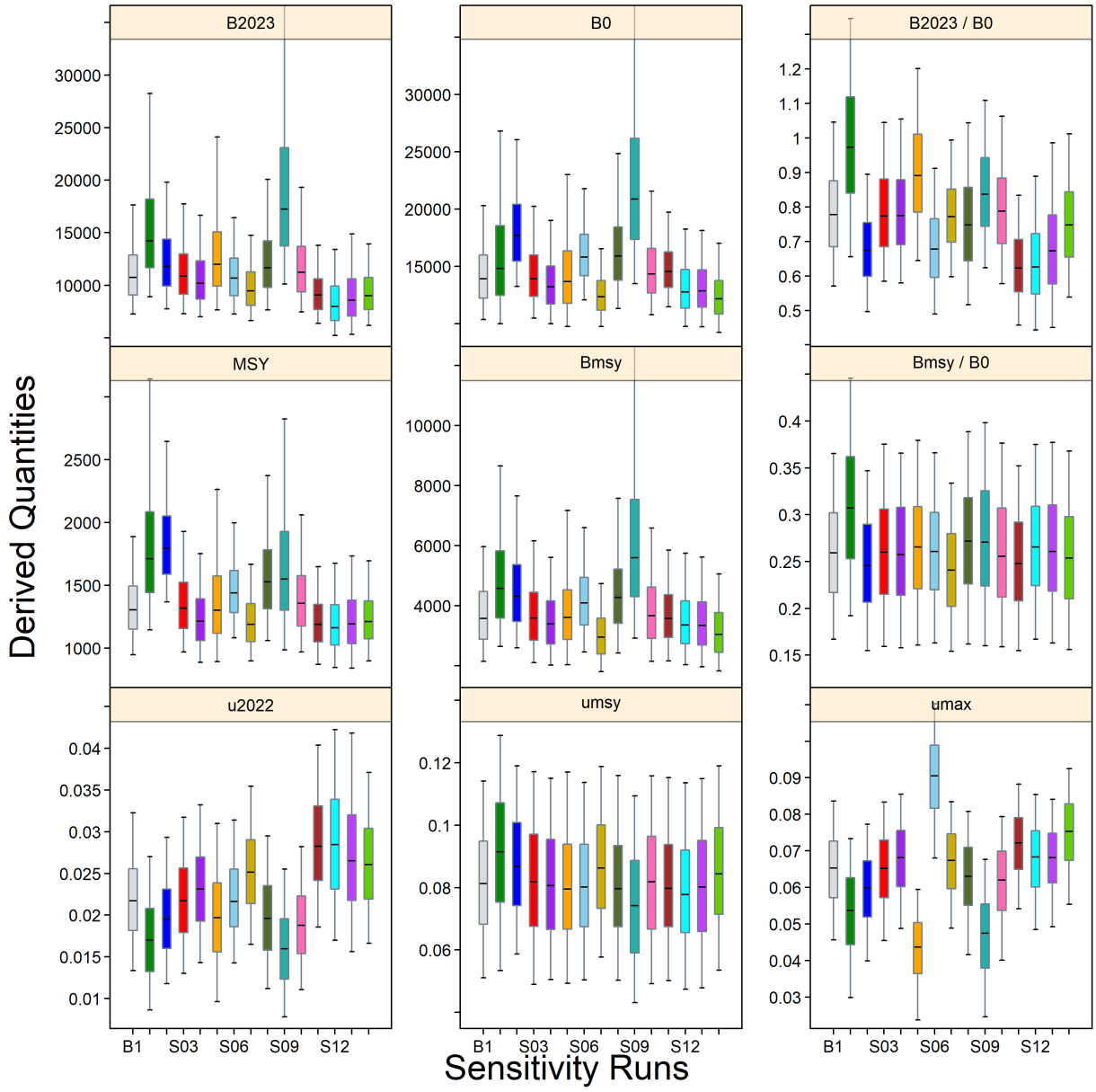

Figure F.38. CAR sensitivity: quantile plots of selected derived quantities (B_{2023}, B_0, B_{2023}/B_0, MSY, B_{MSY}, B_{MSY}/B_0, u_{2022}, u_{MSY}, u_{max}) comparing the base run with 14 sensitivity runs. See text on sensitivity numbers. The boxplots delimit the 0.05, 0.25, 0.5, 0.75, and 0.95 quantiles; outliers are excluded.

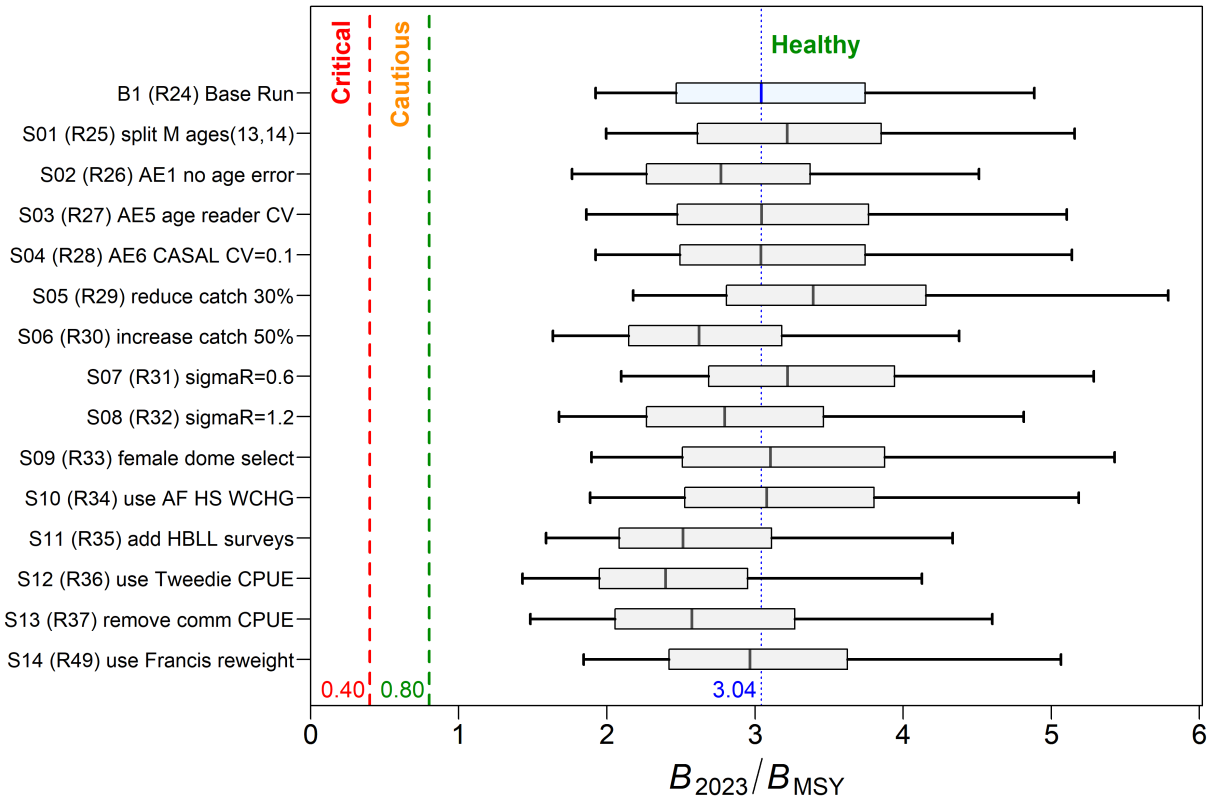

Figure F.39. CAR sensitivity: stock status at beginning of 2023 relative to the DFO PA reference points of $0.4B_{MSY}$ and $0.8B_{MSY}$ for the base run (Run24) and 14 sensitivity runs. Vertical dotted line uses median of the base run to faciliate comparisons with sensitivity runs. Boxplots show the 0.05, 0.25, 0.5, 0.75, and 0.95 quantiles from the MCMC posterior.

F.3. REFERENCES – MODEL RESULTS

DFO. 2009. Stock assessment update for British Columbia Canary Rockfish. DFO Can. Sci. Advis. Sec. Sci. Resp. 2009/019. 39 p.

Forrest, R.E., Holt, K.R. and Kronlund, A.R. 2018. Performance of alternative harvest control rules for two Pacific groundfish stocks with uncertain natural mortality: bias, robustness and trade-offs. Fish. Res. 206. 259–286.

Francis, R.I.C.C. 2011. Data weighting in statistical fisheries stock assessment models. Can. J. Fish. Aquat. Sci. 68(6). 1124–1138.

Knaus, J. 2015. snowfall: Easier cluster computing (based on snow). R package version 1.84-6.1.

McAllister, M.K. and Ianelli, J.N. 1997. Bayesian stock assessment using catch-age data and the sampling – importance resampling algorithm. Can. J. Fish. Aquat. Sci. 54(2). 284–300.

Methot, R.D., Wetzel, C.R., Taylor, I.G., Doering, K.L. and Johnson, K.F. 2021. Stock Synthesis: User Manual Version 3.30.18. Tech. rep., NOAA Fisheries, Seattle WA, USA, October 1, 2021.

Monnahan, C.C., Branch, T.A., Thorson, J.T., Stewart, I.J. and Szuwalski, C.S. 2019. Overcoming long Bayesian run times in integrated fisheries stock assessments. ICES J. Mar. Sci. 76(6). 1477–1488.

Monnahan, C.C. and Kristensen, K. 2018. No-U-turn sampling for fast Bayesian inference in ADMB and TMB: Introducing the adnuts and tmbstan R packages. PLoS ONE 13(5). e0197,954.

N.Z. Min. Fish. 2011. Operational Guidelines for New Zealand's Harvest Strategy Standard. Ministry of Fisheries, New Zealand.

Stanley, R.D., Starr, P. and Olsen, N. 2009. Stock assessment for Canary Rockfish (*Sebastes pinniger*) in British Columbia waters. DFO Can. Sci. Advis. Sec. Res. Doc. 2009/013. xxii + 198 p.

Thorson, J.T., Johnson, K.F., Methot, R.D. and Taylor, I.G. 2017. Model-based estimates of effective sample size in stock assessment models using the Dirichlet-multinomial distribution. Fish. Res. 192. 84–93.

APPENDIX G. ECOSYSTEM INFORMATION

This appendix describes ecosystem information relevant to Canary Rockfish (CAR, GFBioSQL code '437') along the British Columbia (BC) coast. Some of these analyses compare three regions: northern (PMFC areas 5DE), central (PMFC areas 5ABC), and southern (PMFC areas 3CD); however, the stock assessment treats the coastwide population of CAR as a single stock. The information in this appendix provides information that might be useful to other agencies and supports the interpretation of CAR spatial and biological information.

G.1. SPATIAL DISTRIBUTION

Data for spatial analyses of CAR were extracted from the SQL DFO databases 'PacHarvest[1]' and 'GFFOS[2]' on Nov 25, 2021. Some of the analyses below are designed to facilitate the reporting of findings to COSEWIC (Committee on the Status of Endangered Wildlife in Canada), regardless of its assessed status.

Canary Rockfish is ubiquitous along the BC coast, with CPUE hotspots along the west coast of Vancouver Island and in the shallower head regions of the three gullies of Queen Charlotte Sound (Figure G.1). Broadly, the 'extent of occurrence' (EO) for CAR covers 124,097 km^2 (on water and excluding seamounts data) using historical fishing events (1987-2021) to determine a convex hull envelope (Figure G.2). Of the bottom trawl tows capturing CAR, 98% of the tows have starting depths between 68 m and 391 m (Figure G.3). By region, these boundaries are shallower in the north (5DE, 54-351 m, Figure G.4) and in the central region (5ABC, 64-305 m, Figure G.5), whereas they deepen in the south (3CD, 74-448 m, Figure G.6). Using the coastwide CAR bottom-tow depth range as a proxy for suitable CAR benthic habitat, a refined estimate of EO is 68,327 km^2 in BC's Exclusive Economic Zone (Figure G.7). To estimate the 'area of occupancy' (AO), the catch of CAR was located within a grid comprising 4 km^2 cells (2 km × 2 km), and the cells occupied by CAR were summed to estimate an AO of 42,016 km^2 along the BC coast spanning 26 years (Figure G.8). An alternative depiction of CAR catch is summarised by fishery in DFO fishing localities – Trawl (Figure G.9), Halibut (Figure G.10), Sablefish (Figure G.11), Dogfish/Lingcod (Figure G.12), and H&L Rockfish (Figure G.13).

[1] PacHarvest (or PacHarv) was the DFO database, managed by the Pacific region's Groundfish Section, housing the trawl fishery's observer data from 1996 to 2007. Fisherlogs were also added to PacHarvest and all records (observer and fisher) were reconciled with the official landings from the dockside monitoring program.

[2] GFFOS is the Groundfish interface to DFO's current database platform for catch statistics called 'Fishery Operation System'. Groundfish catch records from the H&L fisheries were switched to GFFOS in 2006 while those from the trawl fisheries were switched to GFFOS in 2007.

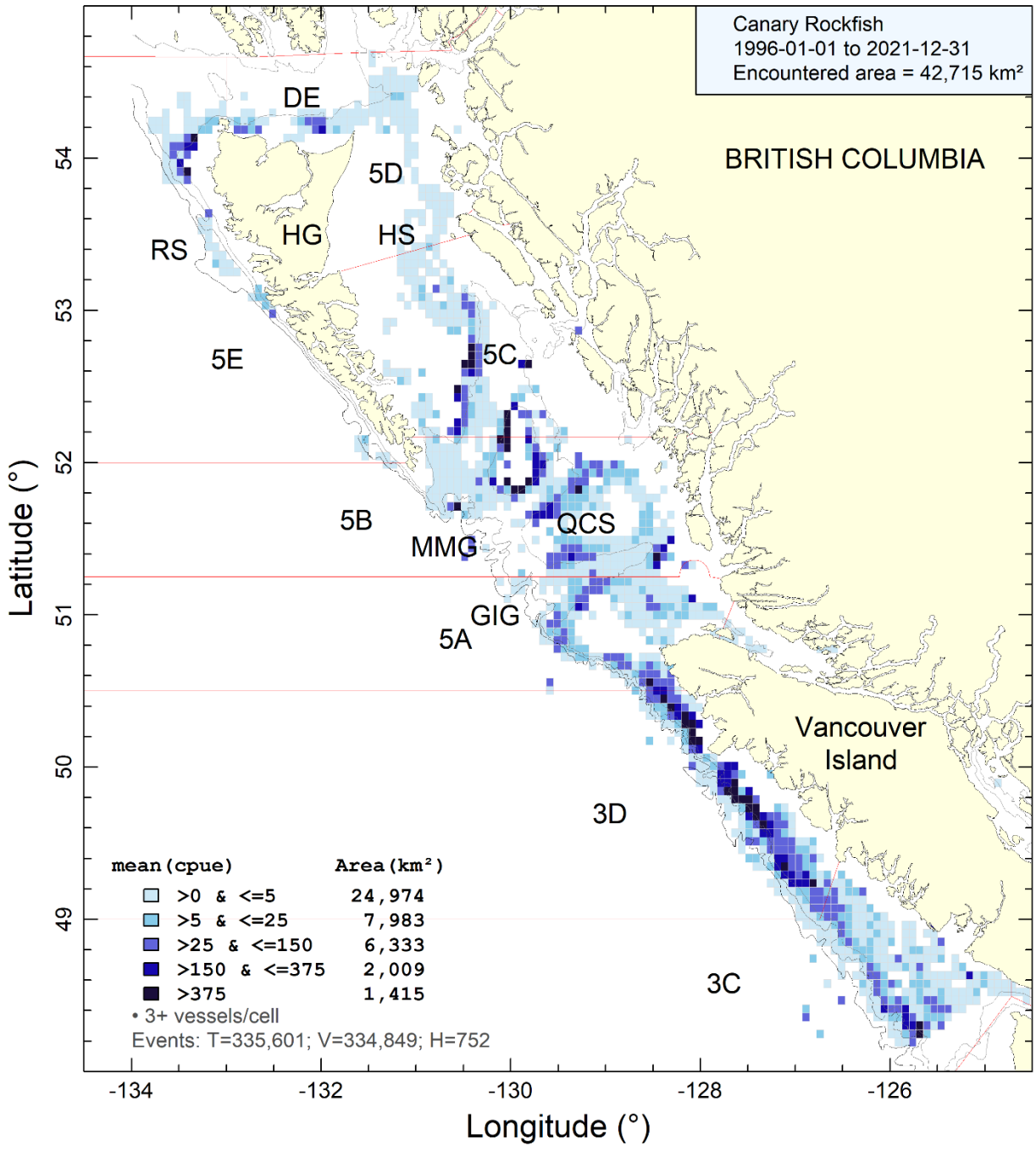

Figure G.1. CPUE density of CAR from trawl tows (bottom and midwater) occurring from 1996 to 2021. DE = Dixon Entrance, GIG = Goose Island Gully, HG = Haida Gwaii, HS = Hecate Strait, MMG = Moresby and Mitchell's Gullies, QCS = Queen Charlotte Sound, RS = Rennell Sound.

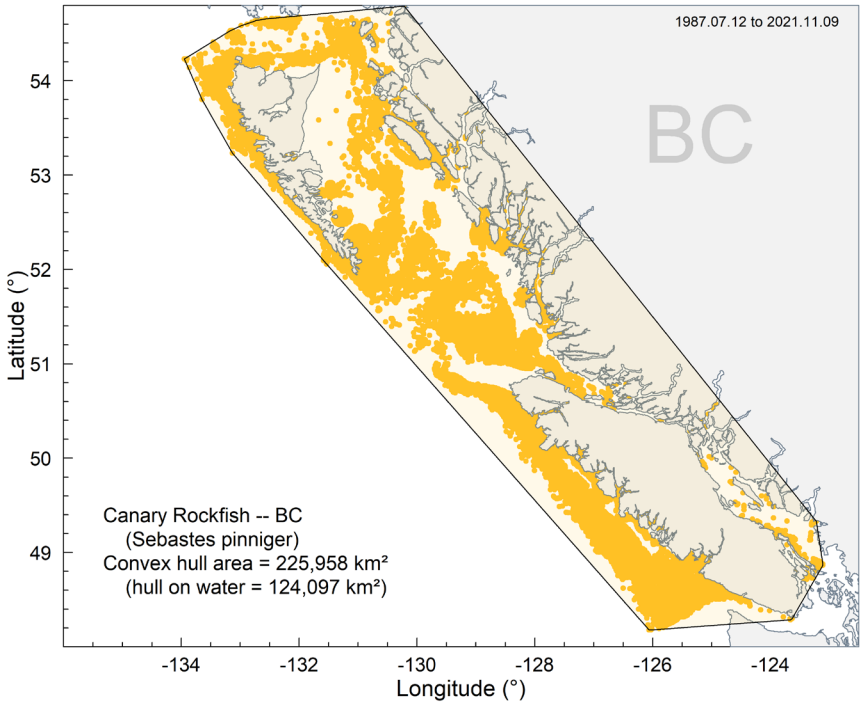

Figure G.2. Extent of Occurrence as a convex hull surrounding fishing events that caught CAR along the BC coast; the shading within the hull on water covers 124,097 km².

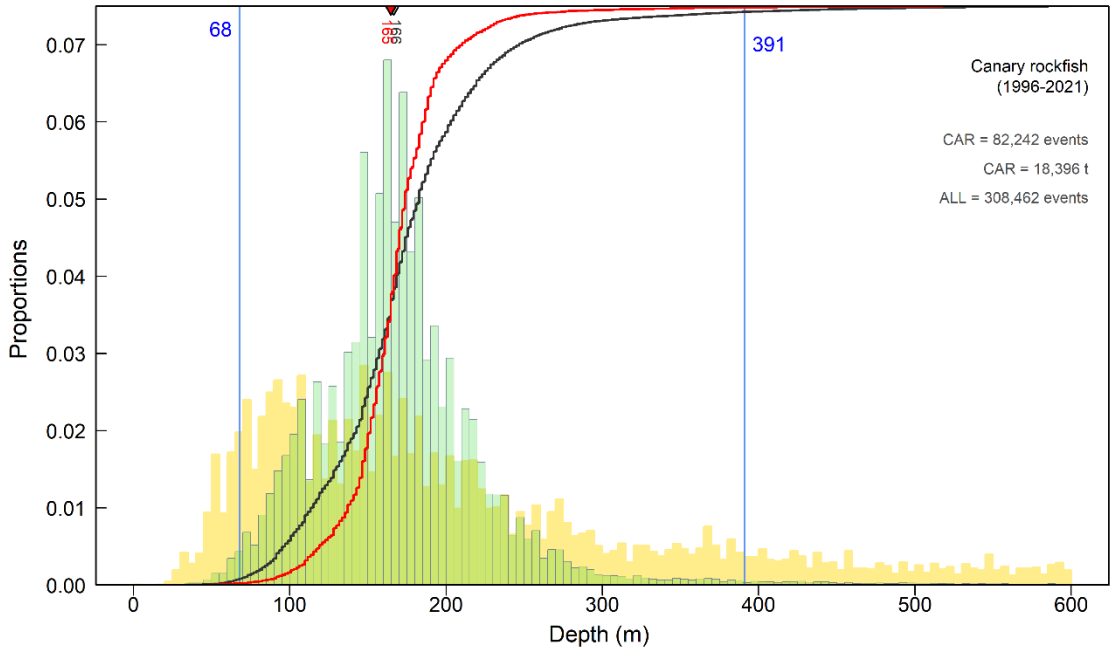

Figure G.3. CAR coastwide – Depth frequency of bottom trawl tows (green histogram) that captured CAR from commercial logs (1996-2021 in PacHarvest and GFFOS) in PMFC areas 3CD5ABCDE. The vertical solid lines denote the 0.01 and 0.99 quantiles. The black curve shows the cumulative frequency of tows that encounter CAR while the red curve shows the cumulative catch of CAR at depth (scaled from 0 to 1). The median depths of CAR encounters (inverted grey triangle) and of cumulative catch (inverted red triangle) are indicated along the upper axis. The yellow histogram in the background reports the relative trawl effort on all species offshore down to 600 m.

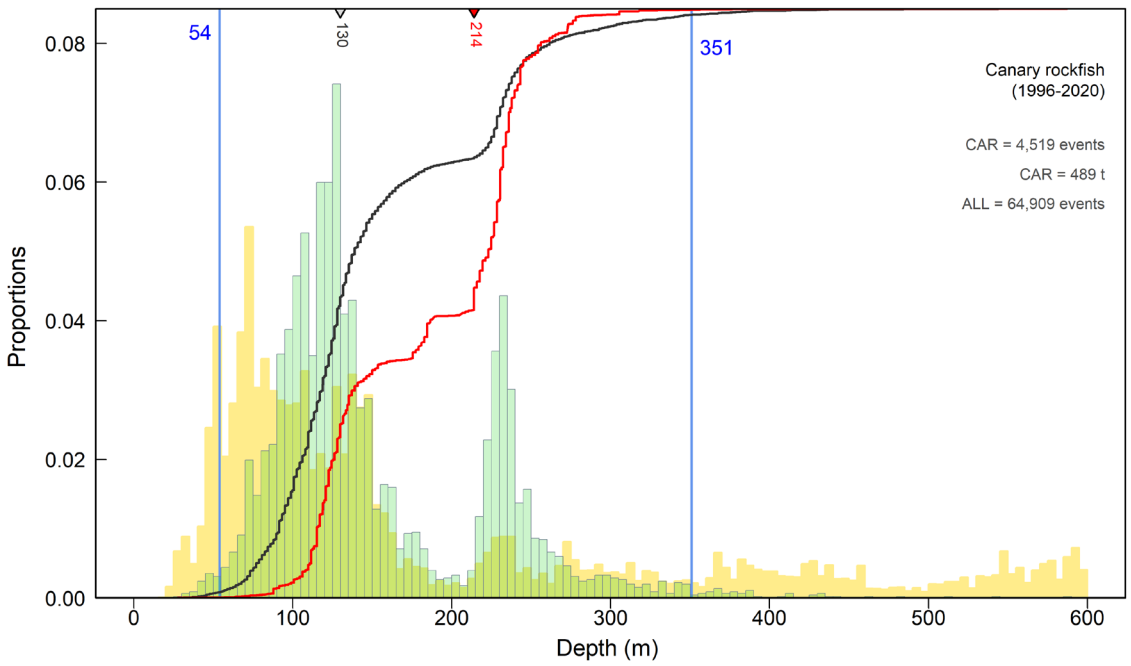

Figure G.4. CAR north – Depth frequency of bottom trawl tows (green histogram) that captured CAR from commercial logs (1996-2020 in PacHarvest and GFFOS) in PMFC areas 5DE. See Figure G.2 caption for additional details.

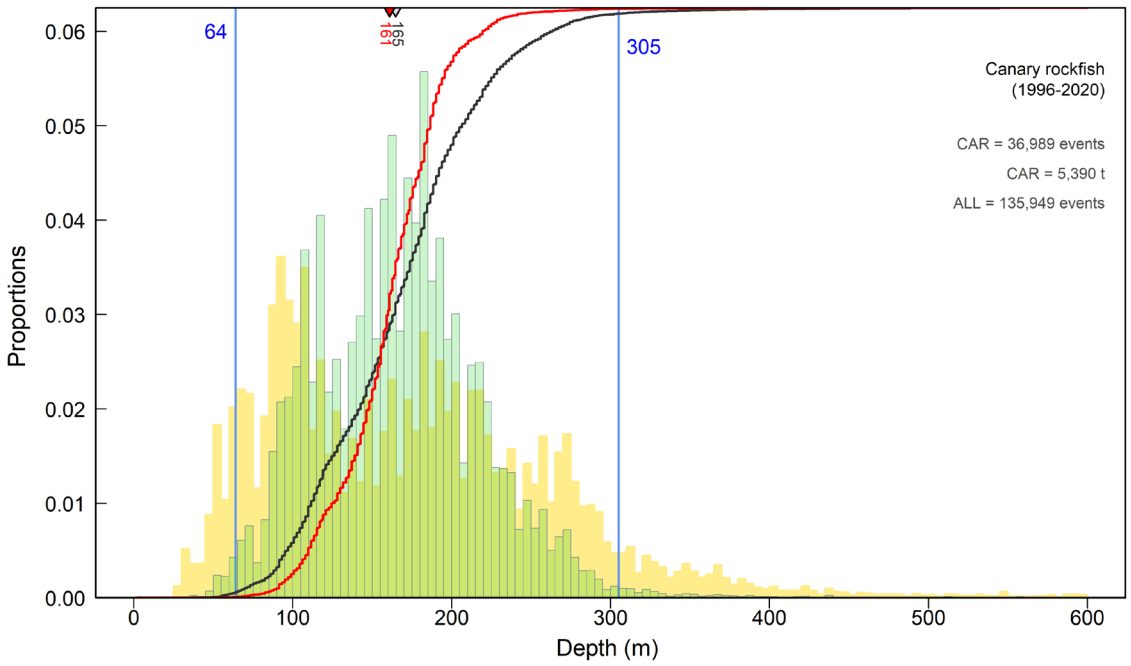

Figure G.5. CAR central – Depth frequency of bottom trawl tows (green histogram) that captured CAR from commercial logs (1996-2020 in PacHarvest and GFFOS) in PMFC areas 5ABC. See Figure G.2 caption for additional details.

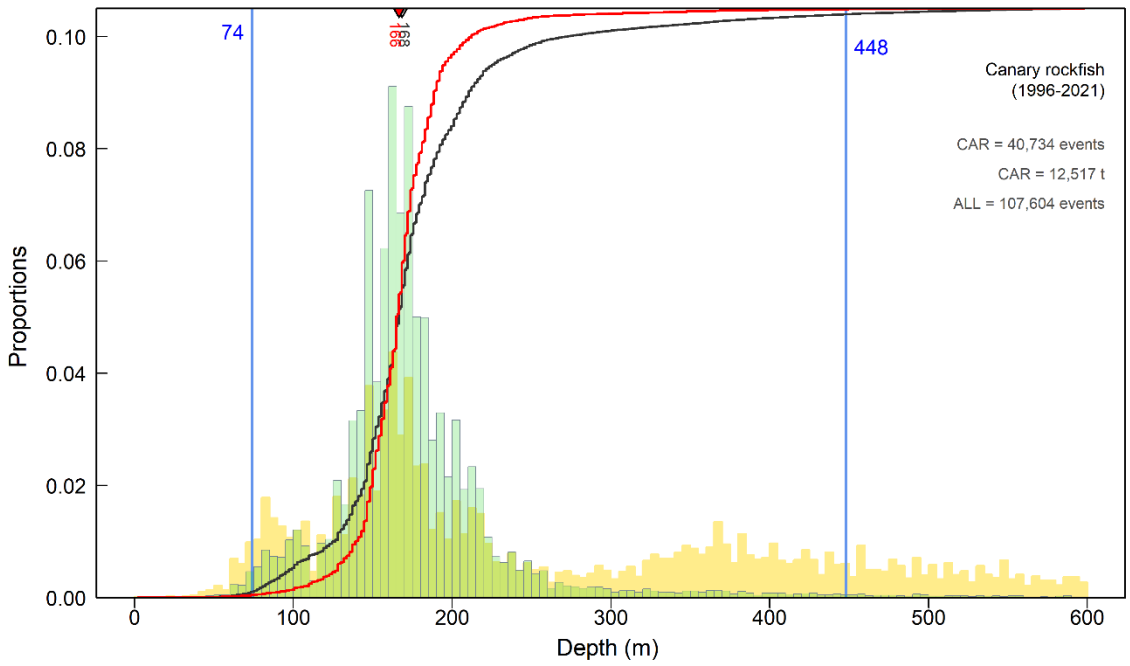

Figure G.6. CAR south – Depth frequency of bottom trawl tows (green histogram) that captured CAR from commercial logs (1996-2021 in PacHarvest and GFFOS) in PMFC areas 3CD. See Figure G.2 caption for additional details.

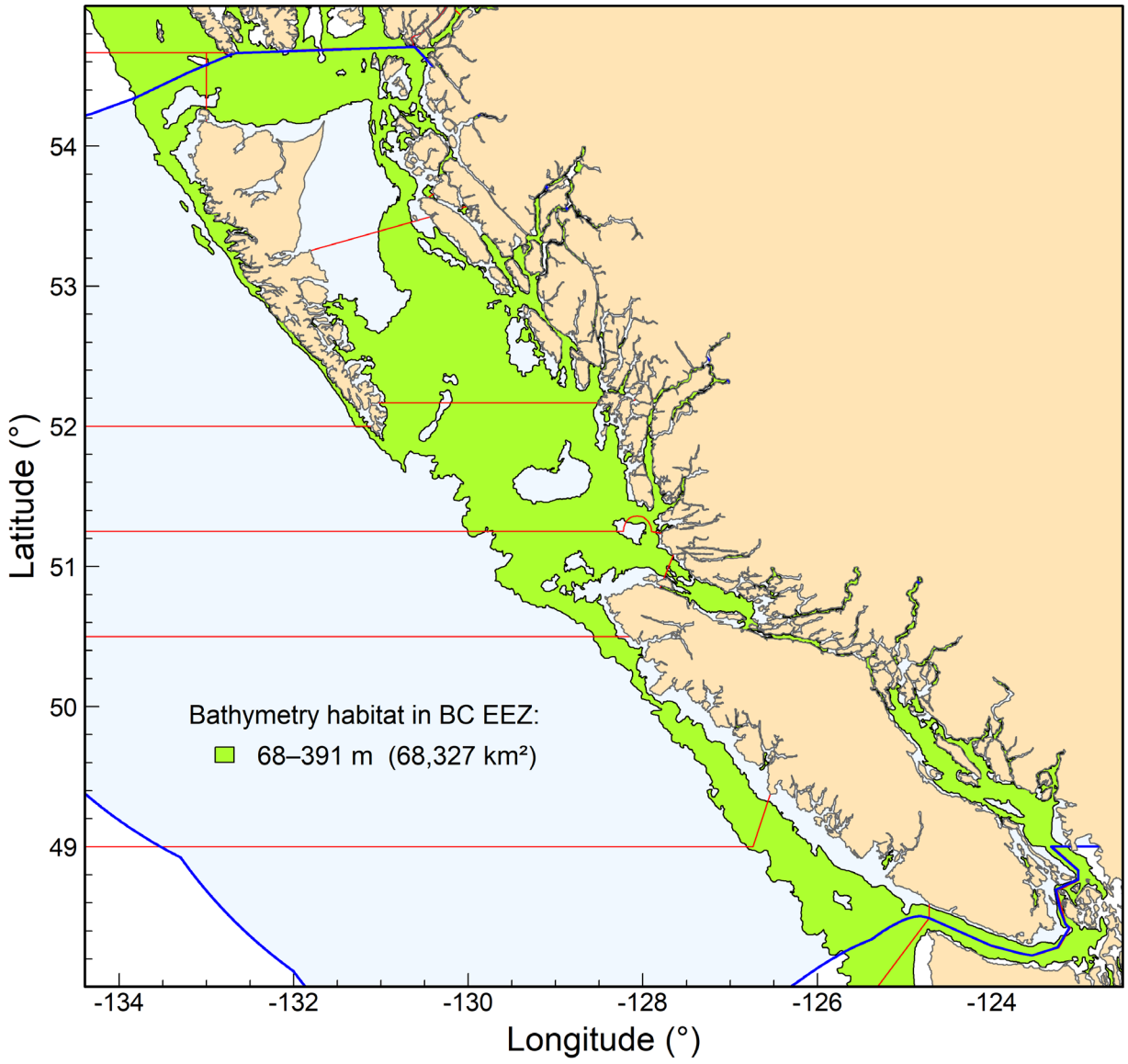

Figure G.7. Highlighted bathymetry (green) between 68 and 391 m serves as a proxy for benthic habitat along the BC coast for CAR. The green highlighted region within Canada's exclusive economic zone (EEZ, blue highlighted area) covers 68,327 km². The boundaries in red delimit PMFC areas.

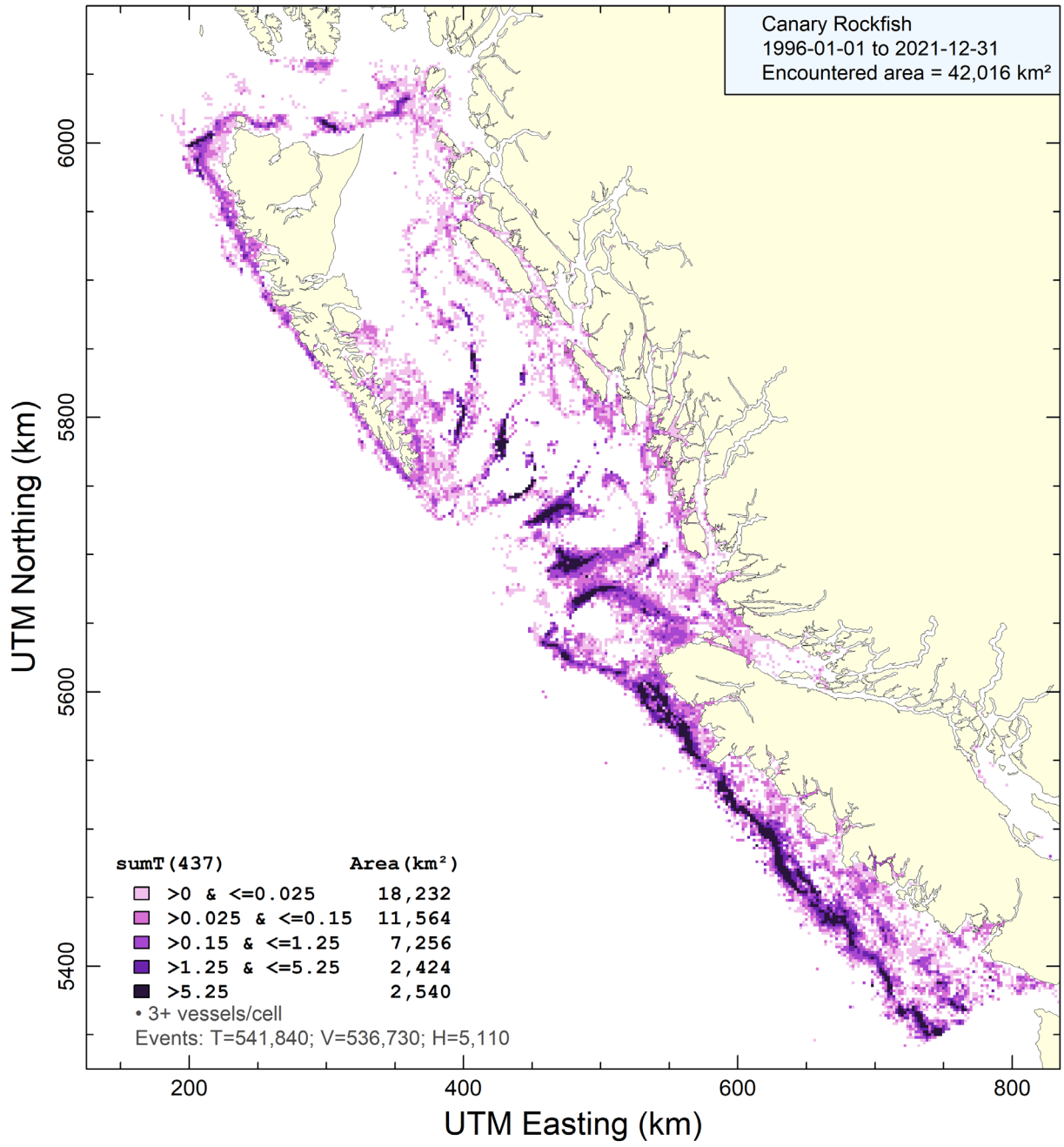

Figure G.8. Area of Occupancy (AO) determined by all-gear capture of CAR in grid cells 2km × 2km. Cells with fewer than three fishing vessels are excluded. The estimated AO is 42,016 km² along the BC coast.

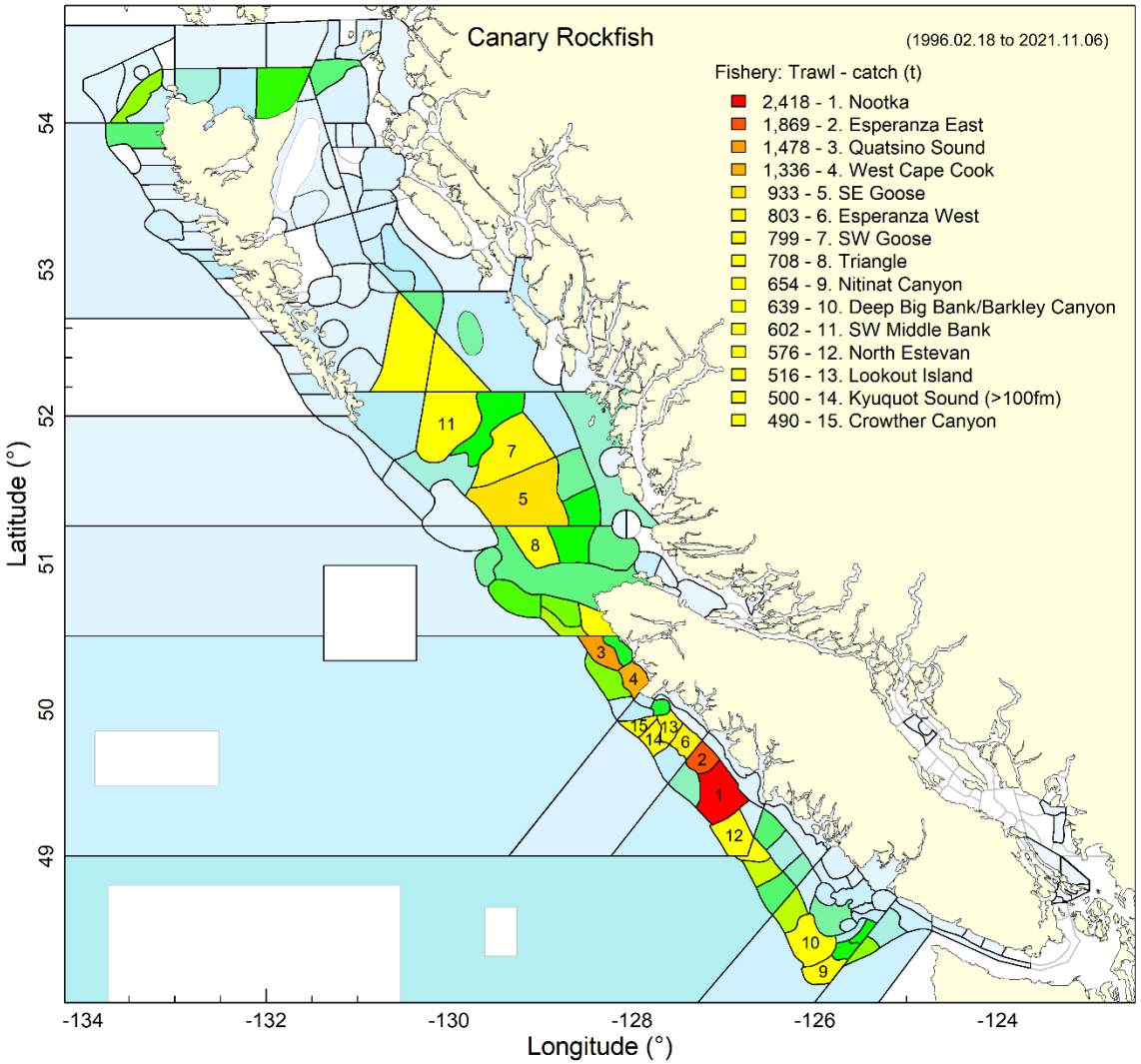

Figure G.9. CAR Trawl – Top 15 fishing localities by total catch (tonnes) where CAR was caught by the trawl fishery. All shaded localities indicate areas where CAR was encountered from 1996 to 2021, ranging from relatively low numbers in cool blue, through the spectrum, to relatively high catches in red. Seamount catches are excluded.

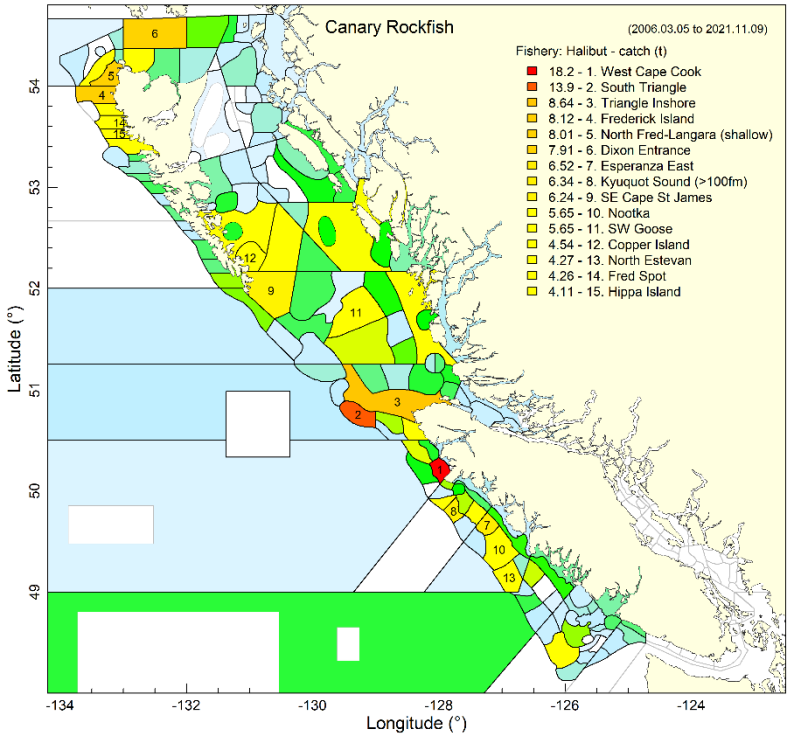

Figure G.10. CAR Halibut – Top 15 fishing localities by total catch (tonnes) where CAR was caught by the halibut fishery. See Figure G.9 caption for further details.

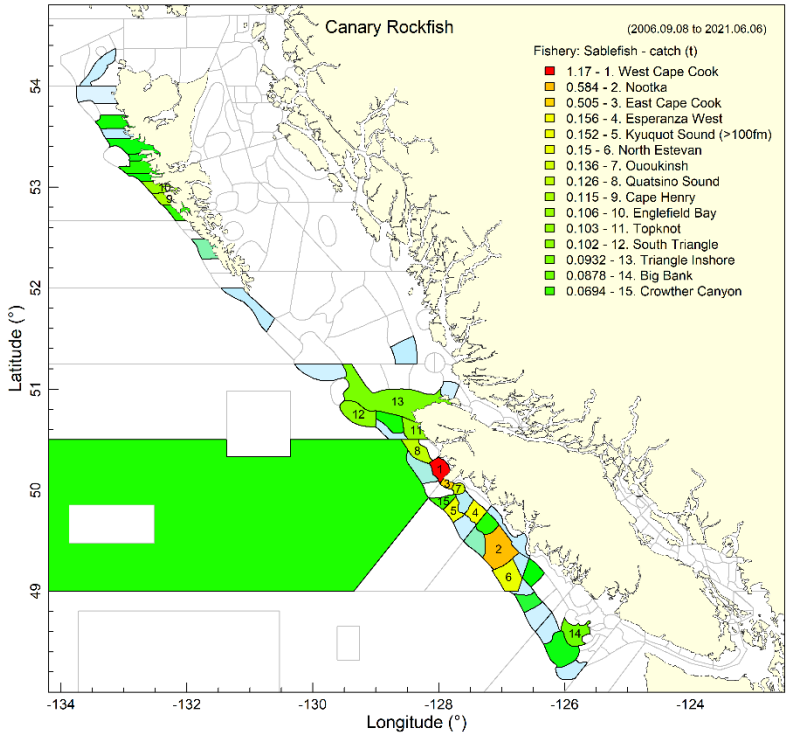

Figure G.11. CAR Sablefish – Top 15 fishing localities by total catch (tonnes) where CAR was caught by the sablefish fishery. See Figure G.9 caption for further details.

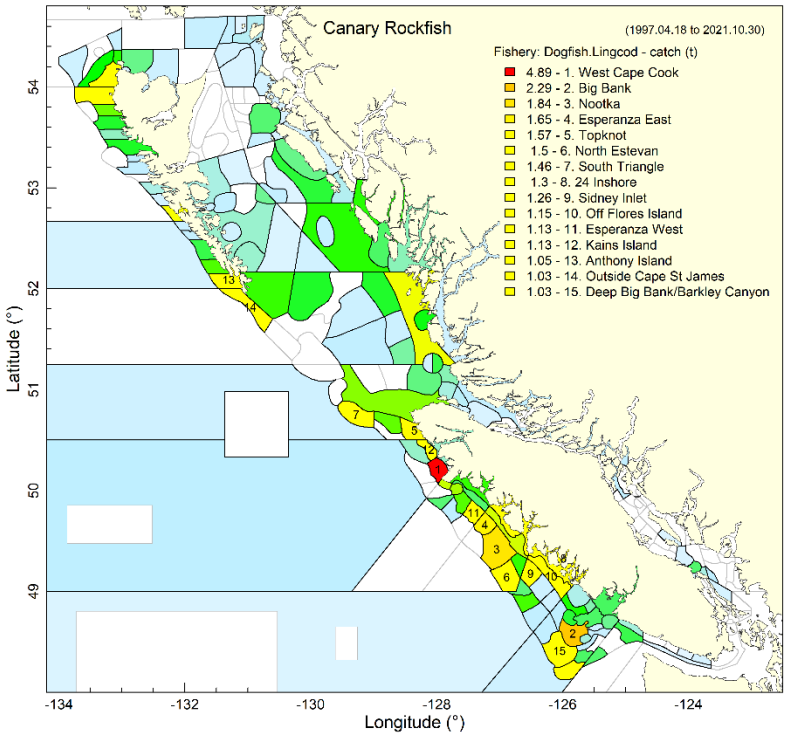

Figure G.12. CAR Dogfish/Lingcod – Top 15 fishing localities by total catch (tonnes) where CAR was caught by the dogfish/lingcod (formerly Schedule II) fishery. See Figure G.9 caption for further details.

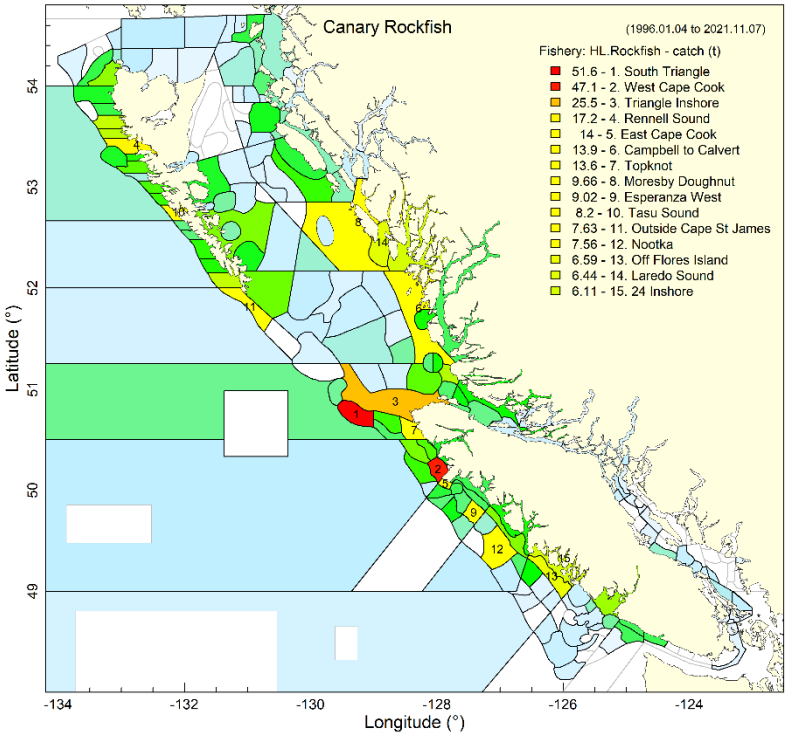

Figure G.13. CAR H&L Rockfish – Top 15 fishing localities by total catch (tonnes) where CAR was caught by the hook and line rockfish (Outside H&L, formerly ZN) fishery. See Figure G.9 caption for further details.

G.2. CONCURRENT SPECIES

Species caught concurrently in coastwide bottom trawl tows that captured at least one CAR specimen comprised, by region:

- Coastal BC (3CD+5ABCDE):
  21% Arrowtooth Flounder, 17% Pacific Ocean Perch, 8% Yellowtail Rockfish,
  5% Dover Sole, and 5% Silvergray Rockfish by weight (Table G.1, Figure G.14);
- North (5DE):
  23% Arrowtooth Flounder, 13% POP, 9% Dover Sole,
  8% English Sole, and 6% Pacific Cod (Table G.2, Figure G.15);
- Central (5ABC):
  25% POP, 14% Arrowtooth Flounder, 9% Yellowmouth Rockfish,
  7% Yellowtail Rockfish, and 7% Silvergray Rockfish (Table G.3, Figure G.16);
- South (3CD):
  25% Arrowtooth Flounder, 14% Yellowtail Rockfish, 7% Dover Sole,
  6% Lingcod, and 6% POP (Table G.4, Figure G.17);

The other gear types that intercept CAR (midwater, hook and line) are shown in Tables G.1-G.4 and Figures G.14-G.17).

Table G.1. CAR coastwide – Top 10 species by catch weight (sum of landed + discarded 1996-2021) that co-occur in CAR fishing events by gear type in PMFC areas 3CD5ABCDE (Figure G.14). Rockfish species of interest to COSEWIC appear in red font, target species (occur in every tow) appear in blue font.

Code*	Species	Latin Name	Catch (tonnes)	Catch (%)	∑Catch (%)
Gear:	**Bottom Trawl**				
602	Arrowtooth Flounder	*Atheresthes stomias*	142,003	20.8	20.8
396	Pacific Ocean Perch	*Sebastes alutus*	116,502	17.1	37.9
418	Yellowtail Rockfish	*Sebastes flavidus*	54,352	7.98	45.9
626	Dover Sole	*Microstomus pacificus*	34,794	5.11	51.0
405	Silvergray Rockfish	*Sebastes brevispinis*	33,257	4.88	55.9
440	Yellowmouth Rockfish	*Sebastes reedi*	32,970	4.84	60.8
467	Lingcod	*Ophiodon elongatus*	29,142	4.28	65.0
222	Pacific Cod	*Gadus macrocephalus*	22,790	3.35	68.4
044	Spiny Dogfish	*Squalus acanthias*	18,909	2.78	71.2
437	Canary Rockfish	*Sebastes pinniger*	17,030	2.50	73.7
Gear:	**Midwater Trawl**				
225	Pacific Hake	*Merluccius productus*	651,433	81.5	81.5
418	Yellowtail Rockfish	*Sebastes flavidus*	50,829	6.36	87.9
417	Widow Rockfish	*Sebastes entomelas*	40,961	5.13	93.0
228	Walleye Pollock	*Theragra chalcogramma*	27,591	3.45	96.5
439	Redstripe Rockfish	*Sebastes proriger*	6,658	0.83	97.3
440	Yellowmouth Rockfish	*Sebastes reedi*	5,302	0.66	98.0
396	Pacific Ocean Perch	*Sebastes alutus*	4,898	0.61	98.6
437	Canary Rockfish	*Sebastes pinniger*	2,441	0.31	98.9
044	Spiny Dogfish	*Squalus acanthias*	1,641	0.21	99.1
405	Silvergray Rockfish	*Sebastes brevispinis*	1,254	0.16	99.3
Gear:	**Hook and Line****				
614	Pacific Halibut	*Hippoglossus stenolepis*	66,053	53.4	53.4
455	Sablefish	*Anoplopoma fimbria*	11,873	9.6	63.0
044	Spiny Dogfish	*Squalus acanthias*	11,531	9.32	72.3
467	Lingcod	*Ophiodon elongatus*	9,614	7.77	80.0
394	Rougheye Rockfish	*Sebastes aleutianus*	5,855	4.73	84.8
059	Longnose Skate	*Raja rhina*	4,358	3.52	88.3
401	Redbanded Rockfish	*Sebastes babcocki*	3,780	3.05	91.3
442	Yelloweye Rockfish	*Sebastes ruberrimus*	3,731	3.01	94.4
405	Silvergray Rockfish	*Sebastes brevispinis*	1,153	0.93	95.3
403	Shortraker Rockfish	*Sebastes borealis*	893	0.72	96.0
Gear:	**Trap*****				
455	Sablefish	*Anoplopoma fimbria*	5,015	95.9	95.9
614	Pacific Halibut	*Hippoglossus stenolepis*	81	1.55	97.5
394	Rougheye Rockfish	*Sebastes aleutianus*	71	1.36	98.8
602	Arrowtooth Flounder	*Atheresthes stomias*	27	0.52	99.3
044	Spiny Dogfish	*Squalus acanthias*	12	0.22	99.6
401	Redbanded Rockfish	*Sebastes babcocki*	8	0.15	99.7
467	Lingcod	*Ophiodon elongatus*	7	0.14	99.9
442	Yelloweye Rockfish	*Sebastes ruberrimus*	1	0.02	99.9
059	Longnose Skate	*Raja rhina*	1	0.02	99.9
403	Shortraker Rockfish	*Sebastes borealis*	1	0.02	99.9

*COSEWIC species in {‘027’, ‘034’, ‘394’, ‘410’, ‘424’, ‘435’, ‘437’, ‘440’, ‘442’, ‘453’}
**CAR with 14th highest catch in CAR hook and line events, representing 0.4% by catch weight.
***CAR does not appear in the top 20 species for trap events.

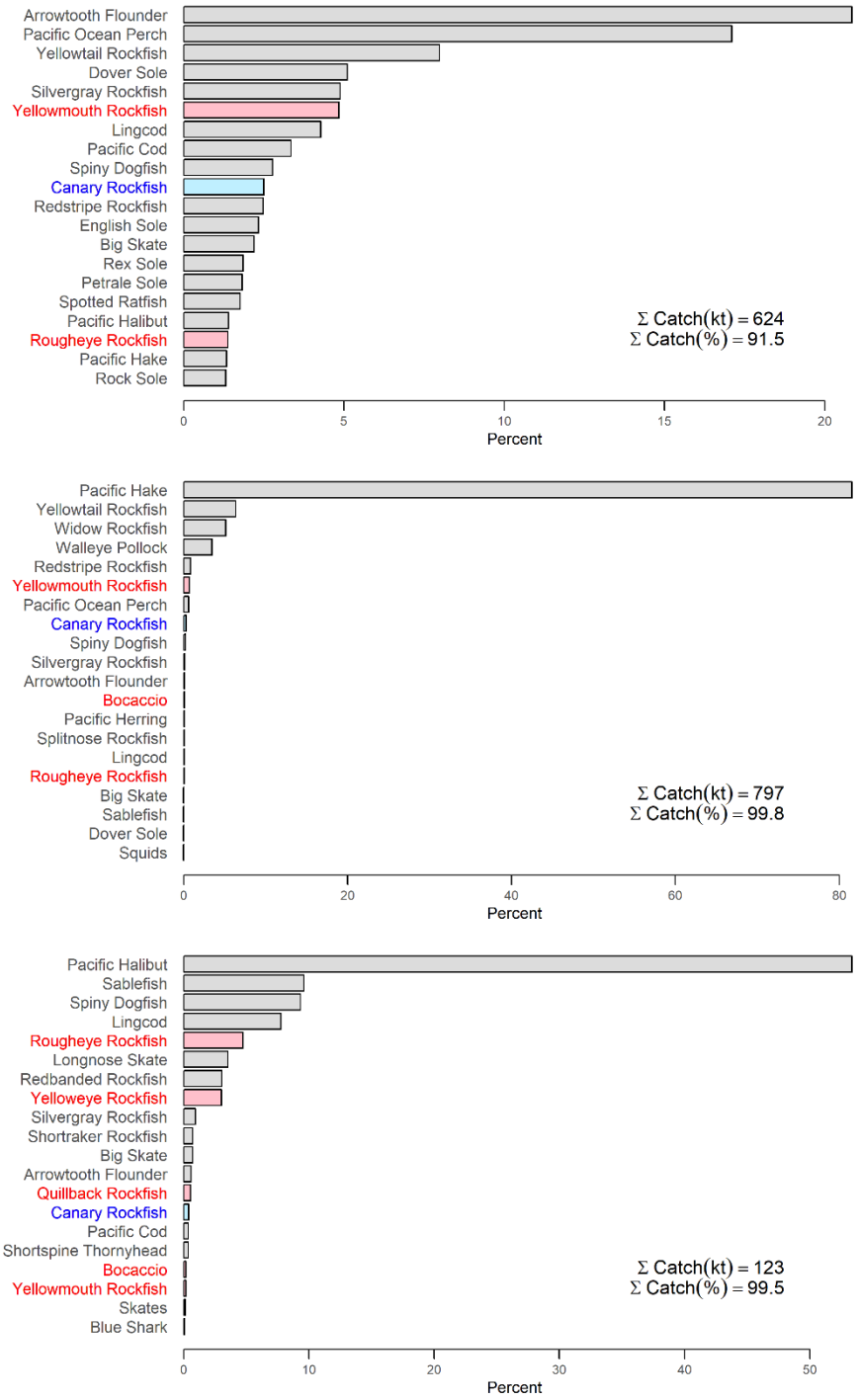

Figure G.14. CAR coastwide – Distribution of catch weights summed over the period Feb 1996 to Dec 2021 for important finfish species from fishing events in GFFOS (includes PacHarv) that caught at least one CAR in PMFC areas 3CD5ABCDE. The four panels correspond to various gear types – bottom trawl (top), midwater trawl (middle), and hook and line (bottom). Fishing events were selected over a depth range between 68 and 391 m (the 0.01 and 0.99 quantile range, see Figure G.3). Relative concurrence is expressed as a percentage by species relative to the total catch weight summed over all finfish species in the specified period. Assessment species appear in blue; COSEWIC species appear in red.

Table G.2. CAR north – Top 10 species by catch weight (sum of landed + discarded from 1996 to 2021) that co-occur in CAR fishing events by gear type in PMFC areas 5DE (Figure G.15). Rockfish species of interest to COSEWIC appear in red font, target species (which occur in every tow) appear in blue font.

Code*	Species	Latin Name	Catch (tonnes)	Catch (%)	∑Catch (%)
Gear:	**Bottom Trawl****				
602	Arrowtooth Flounder	*Atheresthes stomias*	39,124	23.0	23.0
396	Pacific Ocean Perch	*Sebastes alutus*	22,771	13.4	36.3
626	Dover Sole	*Microstomus pacificus*	16,151	9.48	45.8
628	English Sole	*Parophrys vetulus*	13,243	7.77	53.6
222	Pacific Cod	*Gadus macrocephalus*	10,851	6.37	59.9
056	Big Skate	*Raja binoculata*	9,673	5.68	65.6
066	Spotted Ratfish	*Hydrolagus colliei*	8,495	4.99	70.6
405	Silvergray Rockfish	*Sebastes brevispinis*	6,632	3.89	74.5
610	Rex Sole	*Errex zachirus*	5,830	3.42	77.9
440	Yellowmouth Rockfish	*Sebastes reedi*	4,318	2.53	80.5
Gear:	**Midwater Trawl****				
228	Walleye Pollock	*Theragra chalcogramma*	14,268	45.8	45.8
225	Pacific Hake	*Merluccius productus*	10,366	33.3	79.1
417	Widow Rockfish	*Sebastes entomelas*	2,839	9.1	88.2
418	Yellowtail Rockfish	*Sebastes flavidus*	2,588	8.31	96.6
602	Arrowtooth Flounder	*Atheresthes stomias*	181	0.58	97.1
396	Pacific Ocean Perch	*Sebastes alutus*	119	0.38	97.5
439	Redstripe Rockfish	*Sebastes proriger*	110	0.35	97.9
405	Silvergray Rockfish	*Sebastes brevispinis*	105	0.34	98.2
056	Big Skate	*Raja binoculata*	95	0.30	98.5
628	English Sole	*Parophrys vetulus*	73	0.23	98.7
Gear:	**Hook and Line****				
614	Pacific Halibut	*Hippoglossus stenolepis*	19,352	60.1	60.1
394	Rougheye Rockfish	*Sebastes aleutianus*	3,183	9.9	70.0
467	Lingcod	*Ophiodon elongatus*	2,729	8.47	78.4
442	Yelloweye Rockfish	*Sebastes ruberrimus*	1,316	4.08	82.5
455	Sablefish	*Anoplopoma fimbria*	1,206	3.74	86.3
059	Longnose Skate	*Raja rhina*	782	2.43	88.7
401	Redbanded Rockfish	*Sebastes babcocki*	754	2.34	91.0
044	Spiny Dogfish	*Squalus acanthias*	619	1.92	93.0
405	Silvergray Rockfish	*Sebastes brevispinis*	519	1.61	94.6
056	Big Skate	*Raja binoculata*	384	1.19	95.8
Gear:	**Trap****				
455	Sablefish	*Anoplopoma fimbria*	513	93.1	93.1
394	Rougheye Rockfish	*Sebastes aleutianus*	24	4.42	97.6
614	Pacific Halibut	*Hippoglossus stenolepis*	7	1.27	98.8
602	Arrowtooth Flounder	*Atheresthes stomias*	3	0.55	99.4
467	Lingcod	*Ophiodon elongatus*	1	0.17	99.5
442	Yelloweye Rockfish	*Sebastes ruberrimus*	1	0.15	99.7
059	Longnose Skate	*Raja rhina*	0	0.03	99.7
10A	Gastropods	Gastropoda	0	0.03	99.7
044	Spiny Dogfish	*Squalus acanthias*	0	0.03	99.8
3G0	Jellyfish	Scyphozoa	0	0.02	99.8

*COSEWIC species in {‘027’, ‘034’, ‘394’, ‘410’, ‘424’, ‘435’, ‘437’, ‘440’, ‘442’, ‘453’}
**CAR does not appear in the top 20 species for any gear type.

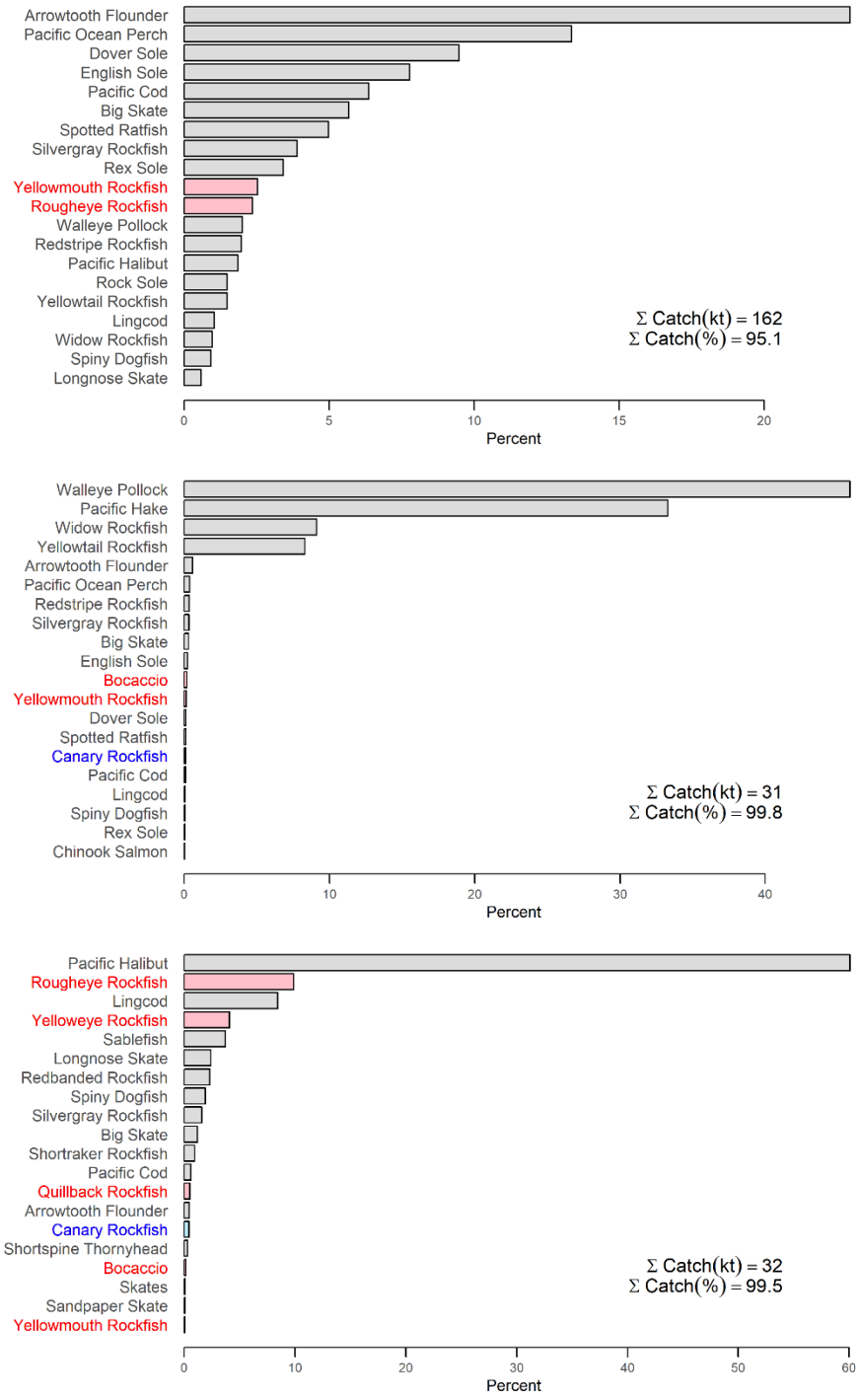

Figure G.15. CAR north – Distribution of catch weights summed over the period Feb 1996 to Dec 2021 for important finfish species from fishing events in GFFOS (includes PacHarv) that caught at least one CAR in PMFC areas 5DE between 54 and 351 m for gears bottom trawl (top), midwater trawl (middle), and hook and line (bottom). See Figure G.14 caption for further details.

Table G.3. CAR central – Top 10 species by catch weight (sum of landed + discarded from 1996 to 2021) that co-occur in CAR fishing events by gear type in PMFC areas 5ABC (Figure G.16). Rockfish species of interest to COSEWIC appear in red font, target species (which occur in every tow) appear in blue font.

Code*	Species	Latin Name	Catch (tonnes)	Catch (%)	∑Catch (%)
Gear:	**Bottom Trawl****				
396	Pacific Ocean Perch	*Sebastes alutus*	69,123	24.5	24.5
602	Arrowtooth Flounder	*Atheresthes stomias*	39,974	14.2	38.6
440	Yellowmouth Rockfish	*Sebastes reedi*	25,938	9.2	47.8
418	Yellowtail Rockfish	*Sebastes flavidus*	21,091	7.47	55.3
405	Silvergray Rockfish	*Sebastes brevispinis*	20,641	7.31	62.6
467	Lingcod	*Ophiodon elongatus*	13,466	4.77	67.3
621	Rock Sole	*Lepidopsetta bilineatus*	9,577	3.39	70.7
626	Dover Sole	*Microstomus pacificus*	8,307	2.94	73.7
222	Pacific Cod	*Gadus macrocephalus*	8,077	2.86	76.5
439	Redstripe Rockfish	*Sebastes proriger*	7,483	2.65	79.2
Gear:	**Midwater Trawl*****				
225	Pacific Hake	*Merluccius productus*	130,243	74.6	74.6
417	Widow Rockfish	*Sebastes entomelas*	19,029	10.9	85.5
418	Yellowtail Rockfish	*Sebastes flavidus*	9,048	5.18	90.7
440	Yellowmouth Rockfish	*Sebastes reedi*	4,716	2.70	93.4
439	Redstripe Rockfish	*Sebastes proriger*	4,155	2.38	95.8
396	Pacific Ocean Perch	*Sebastes alutus*	2,723	1.56	97.3
228	Walleye Pollock	*Theragra chalcogramma*	1,679	0.96	98.3
405	Silvergray Rockfish	*Sebastes brevispinis*	652	0.37	98.6
602	Arrowtooth Flounder	*Atheresthes stomias*	374	0.21	98.9
435	Bocaccio	*Sebastes paucispinis*	226	0.13	99.0
Gear:	**Hook and Line******				
614	Pacific Halibut	*Hippoglossus stenolepis*	30,931	64.1	64.1
467	Lingcod	*Ophiodon elongatus*	4,107	8.52	72.6
044	Spiny Dogfish	*Squalus acanthias*	2,606	5.40	78.0
401	Redbanded Rockfish	*Sebastes babcocki*	2,156	4.47	82.5
442	Yelloweye Rockfish	*Sebastes ruberrimus*	1,998	4.14	86.7
455	Sablefish	*Anoplopoma fimbria*	1,756	3.64	90.3
059	Longnose Skate	*Raja rhina*	1,642	3.41	93.7
424	Quillback Rockfish	*Sebastes maliger*	627	1.30	95.0
405	Silvergray Rockfish	*Sebastes brevispinis*	535	1.11	96.1
056	Big Skate	*Raja binoculata*	355	0.74	96.9
Gear:	**Trap*******				
455	Sablefish	*Anoplopoma fimbria*	515	96.3	96.3
614	Pacific Halibut	*Hippoglossus stenolepis*	14	2.64	98.9
602	Arrowtooth Flounder	*Atheresthes stomias*	2	0.32	99.3
401	Redbanded Rockfish	*Sebastes babcocki*	1	0.21	99.5
394	Rougheye Rockfish	*Sebastes aleutianus*	1	0.21	99.7
467	Lingcod	*Ophiodon elongatus*	0	0.08	99.8
044	Spiny Dogfish	*Squalus acanthias*	0	0.07	99.8
059	Longnose Skate	*Raja rhina*	0	0.06	99.9
442	Yelloweye Rockfish	Sebastes ruberrimus	0	0.03	99.9
403	Shortraker Rockfish	*Sebastes borealis*	0	0.03	100.0

*COSEWIC species in {‘027’, ‘034’, ‘394’, ‘410’, ‘424’, ‘435’, ‘437’, ‘440’, ‘442’, ‘453’}
**CAR with 13th highest catch in CAR bottom trawl events, representing 1.9% by catch weight.
***CAR with 11th highest catch in CAR midwater trawl events, representing 0.1% by catch weight.
****CAR with 12th highest catch in CAR hook and line events, representing 0.4% by catch weight.
*****CAR does not appear in the top 20 species for trap events.

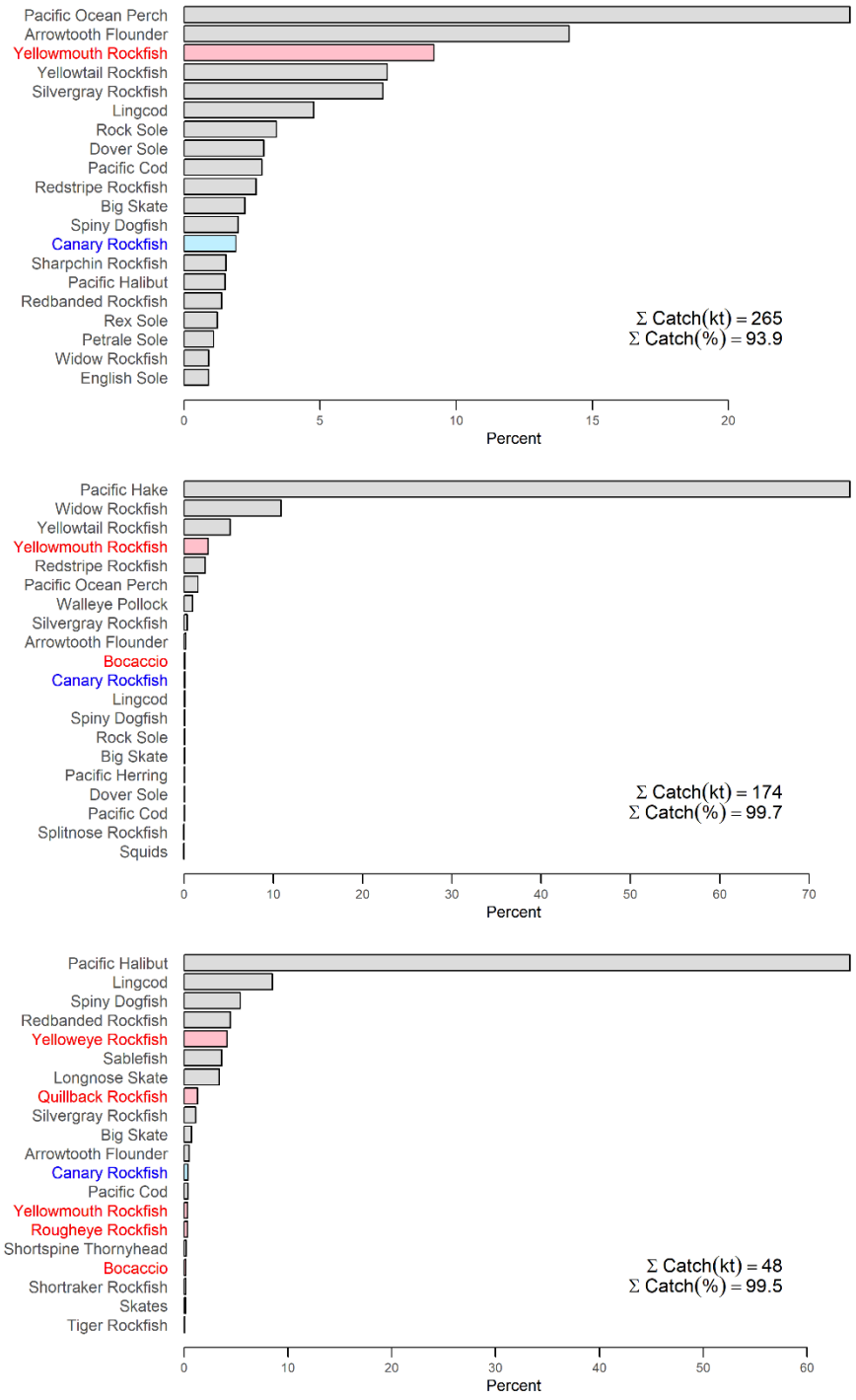

Figure G.16. CAR central – Distribution of catch weights summed over the period Feb 1996 to Dec 2021 for important finfish species from fishing events in GFFOS (includes PacHarv) that caught at least one CAR in PMFC areas 5ABC between 64 and 305 m for gears bottom trawl (top), midwater trawl (middle), and hook and line (bottom). See Figure G.14 caption for further details.

Table G.4. CAR south – Top 10 species by catch weight (sum of landed + discarded from 1996 to 2021) that co-occur in CAR fishing events by gear type in PMFC areas 3CD (Figure G.16). Rockfish species of interest to COSEWIC appear in red font, target species (which occur in every tow) appear in blue font.

Code*	Species	Latin Name	Catch (tonnes)	Catch (%)	∑Catch (%)
Gear:	**Bottom Trawl**				
602	Arrowtooth Flounder	*Atheresthes stomias*	54,847	25.1	25.1
418	Yellowtail Rockfish	*Sebastes flavidus*	30,725	14.1	39.2
626	Dover Sole	*Microstomus pacificus*	14,600	6.7	45.8
467	Lingcod	*Ophiodon elongatus*	14,040	6.43	52.3
396	Pacific Ocean Perch	*Sebastes alutus*	13,464	6.16	58.4
044	Spiny Dogfish	*Squalus acanthias*	11,605	5.31	63.7
437	Canary Rockfish	*Sebastes pinniger*	11,172	5.11	68.9
607	Petrale Sole	*Eopsetta jordani*	8,694	3.98	72.8
225	Pacific Hake	*Merluccius productus*	7,483	3.42	76.3
439	Redstripe Rockfish	*Sebastes proriger*	5,988	2.74	79.0
Gear:	**Midwater Trawl**				
225	Pacific Hake	*Merluccius productus*	566,090	87.5	87.5
418	Yellowtail Rockfish	*Sebastes flavidus*	39,376	6.1	93.6
417	Widow Rockfish	*Sebastes entomelas*	19,039	2.94	96.5
228	Walleye Pollock	*Theragra chalcogramma*	9,761	1.51	98.0
439	Redstripe Rockfish	*Sebastes proriger*	2,354	0.36	98.4
437	Canary Rockfish	*Sebastes pinniger*	2,221	0.34	98.7
396	Pacific Ocean Perch	*Sebastes alutus*	2,194	0.34	99.1
044	Spiny Dogfish	*Squalus acanthias*	1,439	0.22	99.3
602	Arrowtooth Flounder	*Atheresthes stomias*	577	0.09	99.4
394	Rougheye Rockfish	*Sebastes aleutianus*	573	0.09	99.5
Gear:	**Hook and Line****				
455	Sablefish	*Anoplopoma fimbria*	8,402	28.0	28.0
044	Spiny Dogfish	*Squalus acanthias*	7,251	24.16	52.2
614	Pacific Halibut	*Hippoglossus stenolepis*	5,612	18.70	70.9
467	Lingcod	*Ophiodon elongatus*	2,879	9.60	80.5
394	Rougheye Rockfish	*Sebastes aleutianus*	1,653	5.51	86.0
059	Longnose Skate	*Raja rhina*	1,484	4.94	90.9
401	Redbanded Rockfish	*Sebastes babcocki*	610	2.03	93.0
442	Yelloweye Rockfish	*Sebastes ruberrimus*	537	1.79	94.7
403	Shortraker Rockfish	*Sebastes borealis*	350	1.17	95.9
602	Arrowtooth Flounder	*Atheresthes stomias*	231	0.77	96.7
Gear:	**Trap*****				
455	Sablefish	*Anoplopoma fimbria*	3,580	97.2	97.2
614	Pacific Halibut	*Hippoglossus stenolepis*	39	1.05	98.3
394	Rougheye Rockfish	*Sebastes aleutianus*	20	0.54	98.8
602	Arrowtooth Flounder	*Atheresthes stomias*	16	0.44	99.3
044	Spiny Dogfish	*Squalus acanthias*	14	0.37	99.6
467	Lingcod	*Ophiodon elongatus*	5	0.15	99.8
401	Redbanded Rockfish	*Sebastes babcocki*	4	0.12	99.9
403	Shortraker Rockfish	*Sebastes borealis*	1	0.03	99.9
97A	Octopus	Octopoda	1	0.02	99.9
451	Shortspine Thornyhead	*Sebastolobus alascanus*	1	0.01	99.9

*COSEWIC species in {'027', '034', '394', '410', '424', '435', '437', '440', '442', '453'}
**CAR with 12th highest catch in CAR hook and line events, representing 0.6% by catch weight.
***CAR does not appear in the top 20 species for trap events.

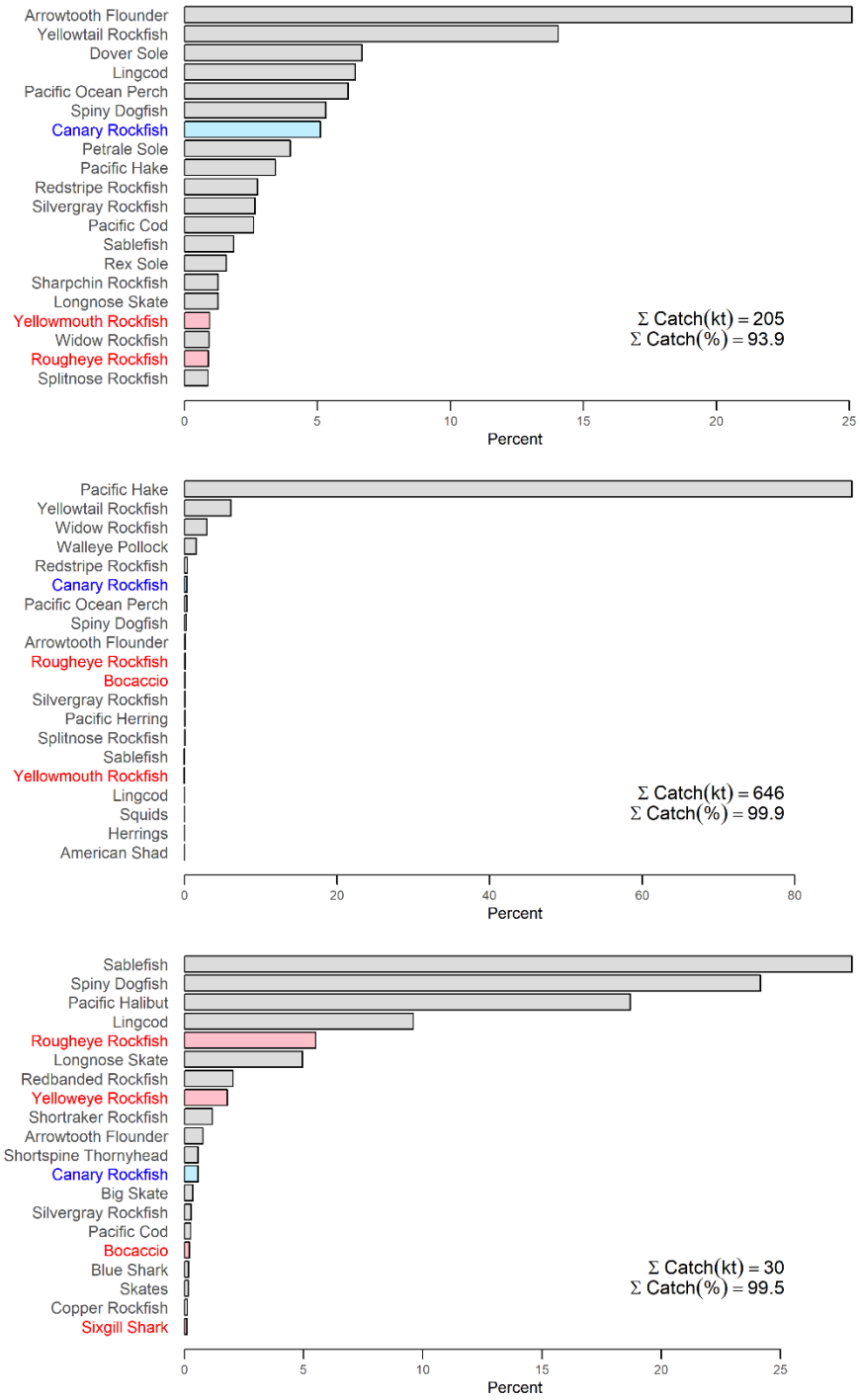

Figure G.17. CAR south – Distribution of catch weights summed over the period Feb 1996 to Dec 2021 for important finfish species from fishing events in GFFOS (includes PacHarv) that caught at least one CAR in PMFC areas 3CD between 74 and 448 m for gears bottom trawl (top), midwater trawl (middle), and hook and line (bottom). See Figure G.14 caption for further details.

G.3. TROPHIC INTERACTIONS

Fu et al (2017) used an ecosystem model (OSMOSE: Object-oriented Simulator of Marine Ecosystems Exploitation) to explore predator-prey interactions in a previously-defined ecosystem called PNCIMA[3]. The study used 10 key populations and 19 background taxa, one of which included CAR in the shelf rockfish category; POP was treated as a separate background taxon. The OSMOSE model focused on a pelagic group of species that included Pacific Herring, Walleye Pollock, and Pacific Cod; however, the model could be applied to other functional groups.

GFBioSQL only reports one instance of shrimp and one of other fish in the stomach contents of CAR. Love et al. (2002) reported that CAR pelagic juveniles eat copepods, amphipods, and krill eggs and larvae, while CAR adults prey on krill and small fish (lanternfish, anchovies, sanddabs, etc.); CAR are preyed upon by other fish, marine birds and mammals.

G.4. ENVIRONMENTAL EFFECTS

Various environmental indices were explored by Edwards et al. in Appendix F of Haigh et al. (2018) for Pacific Ocean Perch (POP). The working hypothesis was that the release of POP larvae in February-March (also true for Canary, see Figure D.7) would be influenced by winter environmental conditions (e.g., eddy movement, upwelling, wind circulation, water transport). They adopted the period December to March to represent winter in the various environmental indices explored, and we do likewise.

One of the most commonly used indices is the Pacific Decadal Oscillation (PDO), which was defined in Haigh et al. (2018) as 'the first mode of an Empirical Orthogonal Function (EOF) analysis of gridded sea surface temperature in the North Pacific (Zhang et al. 1997 and reported in Mantua et al. 1997). The PDO represents sea surface temperature and sea surface height anomalies in the North Pacific and is connected to the El Niño Southern Oscillation (ENSO, Alexander et al. 2002; Newman et al. 2003).' A negative phase of the PDO is associated with cold temperatures in the eastern North Pacific (Mantua et al. 1997) and a weak Aleutian Low (Di Lorenzo et al. 2010, 2013). NOAA Fisheries often refer to cooler waters with higher dissolved oxygen as 'minty', and associate these conditions with strong recruitment events (Schroeder et al. 2019).

While the PDO index series has shown congruity with marine populations on the scale of the NE Pacific basin (e.g., Alaskan salmon, Mantua et al. 1997), other indices are perhaps more relevant to populations that occupy smaller scales. For instance, the Aleutian Low Pressure Index was used to identify a regime shift in 1977 that increased the recruitment success of BC Sablefish (King et al. 2000). At lower trophic levels, an upwelling index at 54°N was better correlated than PDO with primary production along the BC shelf (Preikshot 2005).

[3] Pacific North Coast Integrated Management Area – encompasses Queen Charlotte Sound, Hecate Strait, Dixon Entrance , and the west coast of Haida Gwaii.

Table G.5. Annual winter PDO values calculated as the mean from December (of previous year) to March (n=4). Standard deviations calculated from the n values and SE calculated as SD/sqrt(n). Negative PDO indices can loosely be called 'minty' and correspond to cooler sea temperatures in the eastern North Pacific Ocean.

Year	PDO	SD	SE	Year	PDO	SD	SE	Year	PDO	SD	SE
1855	-0.648	0.746	0.373	1911	-0.595	0.791	0.396	1967	-0.375	0.284	0.142
1856	-0.095	0.655	0.328	1912	-0.410	0.411	0.205	1968	-0.360	0.369	0.185
1857	-0.800	0.731	0.366	1913	-0.078	0.189	0.094	1969	-0.858	0.447	0.224
1858	-1.200	0.549	0.274	1914	-0.108	0.213	0.106	1970	1.100	0.083	0.041
1859	-1.638	0.601	0.301	1915	-0.168	0.397	0.198	1971	-1.313	0.282	0.141
1860	-1.263	0.098	0.049	1916	-1.308	0.347	0.173	1972	-1.843	0.253	0.126
1861	-0.923	0.357	0.179	1917	-1.955	0.340	0.170	1973	-0.488	0.309	0.154
1862	-0.508	0.796	0.398	1918	-0.293	0.579	0.289	1974	-1.085	0.253	0.126
1863	-0.175	0.215	0.107	1919	0.083	0.550	0.275	1975	-0.595	0.603	0.301
1864	-0.388	0.439	0.219	1920	-0.785	0.292	0.146	1976	-1.223	0.220	0.110
1865	-0.200	0.480	0.240	1921	-1.045	0.375	0.187	1977	1.143	0.375	0.187
1866	-1.890	0.754	0.377	1922	-0.705	0.868	0.434	1978	0.608	0.500	0.250
1867	-0.300	0.139	0.070	1923	-0.265	0.724	0.362	1979	-0.715	0.403	0.201
1868	0.508	0.438	0.219	1924	-0.515	0.222	0.111	1980	0.330	0.312	0.156
1869	-0.370	0.562	0.281	1925	-0.618	0.270	0.135	1981	0.985	0.457	0.229
1870	-0.098	0.296	0.148	1926	1.083	0.249	0.125	1982	0.035	0.420	0.210
1871	-0.390	0.409	0.204	1927	1.310	0.571	0.285	1983	0.815	0.698	0.349
1872	-0.358	0.150	0.075	1928	0.500	0.427	0.213	1984	1.483	0.208	0.104
1873	-1.985	0.211	0.106	1929	0.428	0.355	0.177	1985	0.373	0.509	0.255
1874	-0.755	0.390	0.195	1930	0.978	0.556	0.278	1986	1.130	0.596	0.298
1875	-1.315	0.191	0.096	1931	1.103	0.181	0.090	1987	1.498	0.152	0.076
1876	-0.625	0.499	0.249	1932	-1.085	0.434	0.217	1988	0.533	0.296	0.148
1877	-0.133	0.075	0.038	1933	-0.668	0.578	0.289	1989	-1.018	0.593	0.297
1878	0.515	0.455	0.227	1934	-0.023	0.680	0.340	1990	-0.760	0.592	0.296
1879	0.468	0.563	0.282	1935	0.520	0.774	0.387	1991	-1.555	0.553	0.276
1880	-0.430	0.812	0.406	1936	1.623	0.407	0.203	1992	0.040	0.171	0.085
1881	-0.178	0.209	0.104	1937	0.213	0.897	0.449	1993	0.078	0.272	0.136
1882	-1.580	0.695	0.348	1938	0.605	0.872	0.436	1994	0.530	0.277	0.138
1883	-0.758	0.963	0.482	1939	0.395	0.904	0.452	1995	-0.650	1.182	0.591
1884	-1.703	0.221	0.111	1940	1.670	0.208	0.104	1996	0.828	0.269	0.135
1885	1.915	0.697	0.348	1941	2.660	0.176	0.088	1997	0.273	0.211	0.106
1886	-0.180	0.539	0.269	1942	1.940	0.593	0.296	1998	1.213	0.243	0.121
1887	-1.543	0.484	0.242	1943	-0.733	0.803	0.402	1999	-1.028	0.173	0.086
1888	-0.515	0.596	0.298	1944	0.820	1.165	0.582	2000	-1.515	0.688	0.344
1889	0.260	0.234	0.117	1945	-0.243	0.202	0.101	2001	0.015	0.364	0.182
1890	-0.850	0.571	0.286	1946	-0.423	1.346	0.673	2002	-1.080	0.468	0.234
1891	-0.913	0.335	0.167	1947	-0.320	0.915	0.458	2003	1.315	0.247	0.124
1892	-0.928	0.533	0.266	1948	-0.183	0.697	0.349	2004	-0.378	0.230	0.115
1893	-0.810	0.275	0.137	1949	-2.415	0.685	0.342	2005	-0.025	0.554	0.277
1894	-2.070	0.826	0.413	1950	-1.650	0.532	0.266	2006	0.020	0.575	0.288
1895	-0.830	0.248	0.124	1951	-1.373	0.302	0.151	2007	-0.730	0.280	0.140
1896	0.020	0.284	0.142	1952	-1.665	0.375	0.187	2008	-1.273	0.288	0.144
1897	-0.080	0.459	0.229	1953	-0.680	0.479	0.240	2009	-1.740	0.313	0.156
1898	-0.180	0.207	0.104	1954	-0.853	0.457	0.229	2010	-0.093	0.325	0.162
1899	-0.335	0.835	0.418	1955	-0.498	0.788	0.394	2011	-1.645	0.340	0.170
1900	0.485	0.277	0.138	1956	-2.418	0.343	0.172	2012	-1.815	0.441	0.221
1901	0.618	0.664	0.332	1957	-1.245	0.307	0.153	2013	-1.328	0.167	0.084
1902	0.715	0.442	0.221	1958	0.713	0.214	0.107	2014	-0.433	0.555	0.278
1903	0.078	0.269	0.135	1959	0.598	0.604	0.302	2015	1.553	0.222	0.111
1904	0.818	0.402	0.201	1960	0.525	0.374	0.187	2016	0.965	0.568	0.284
1905	2.155	0.953	0.477	1961	0.613	0.427	0.214	2017	0.160	0.300	0.150
1906	0.535	1.081	0.540	1962	-1.165	0.385	0.192	2018	-0.103	0.457	0.229
1907	-0.838	0.708	0.354	1963	-0.060	0.226	0.113	2019	-0.400	0.223	0.112
1908	1.460	0.644	0.322	1964	0.073	0.531	0.265	2020	-1.160	0.787	0.394
1909	0.955	0.276	0.138	1965	-0.588	0.320	0.160	2021	-1.095	0.443	0.221
1910	-1.513	0.572	0.286	1966	-0.463	0.529	0.265	2022	-2.173	0.470	0.235

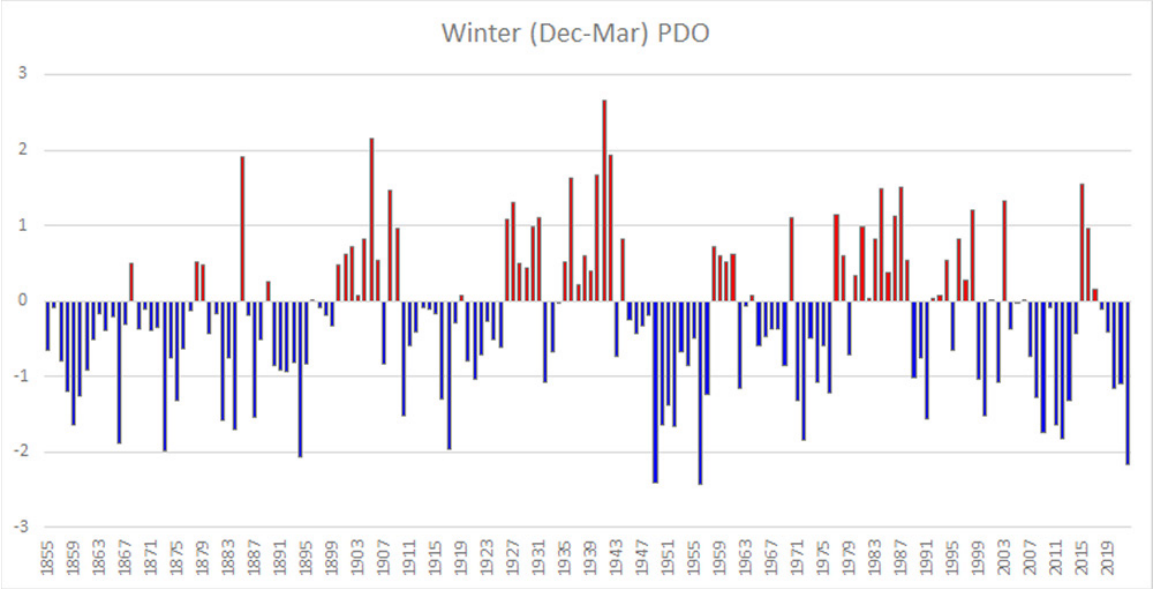

Figure G.18. Mean of monthly (Dec-Mar) Pacific Decadal Oscillation indices by year from 1855 to 2022 (data source: National Centers for Environmental Information, NOAA). Along the western coast of North America, positive (red) values correspond to 'spicy' conditions while negative (blue) values denote 'minty' conditions (Schroeder et al. 2019).

G.5. ADVICE FOR MANAGERS

There is potential for environmental indicators to be incorporated into stock assessment models. Andrew Edwards (DFO, pers. comm. 2021) secured three years funding for a project entitled '*Incorporating environmental information into management advice by understanding historical declines of Pacific Herring and recent increases of Bocaccio*'. It will build on work in Edwards et al. (2017) and Haigh et al. (2018) while using the framework of the Gulf of St. Lawrence Ecosystem Approach project.

The modelling platform Stock Synthesis 3 (SS3) has a few methods for including environmental effects into the recruitment estimation process function (Methot et al. 2021). However, the SS3 authors provide the following advice: '*The preferred approach to including environmental effects on recruitment is not to use the environmental effect in the direct calculation of the expected level of recruitment. Instead, the environmental data would be used as if it were a survey observation of the recruitment deviation.* (Methot, pers. comm. 2021)' We tried both methods, focusing on the latter, and found that the influence of the environmental index depended on how much weight was applied to the series (through adding various levels of process error to the index). This outcome is presented in detail in Section 8.2.3 of the Main document.

In future stock assessments, adding environmental data can be explored, but will be necessarily constrained by the modelling platform implementation. Alternatively, geospatial indices for the synoptic surveys are being developed to include more environmental factors (specifically, temperature and perhaps oxygen, Sean Anderson, DFO, pers. comm. 2022). The factors are largely limited by data that are collected by instruments deployed alongside trawl tows, but might also include measurements derived from satellites or oceanic/atmospheric models. This work could be used to inform analysts of the covariates that affect the distribution or apparent catchability of the species. This highlights the other major limitation to this type of analysis which is the lack of supporting work to identify environmental covariates that would be expected to affect recruitment or catchability, rather than selecting series without real understanding of their potential impact.

G.6. REFERENCES – ECOSYSTEM

Alexander, M.A., Bladé, I., Newman, M., Lanzante, J.R., Lau, N.C. and Scott, J.D. 2002. The atmospheric bridge: the influence of ENSO teleconnections on air-sea interaction over the global oceans. J. Clim. 15(16). 2205–2231.

Di Lorenzo, E., Cobb, K.M., Furtado, J.C., Schneider, N., Anderson, B.T., Bracco, A., Alexander, M.A. and Vimont, D.J. 2010. Central Pacific El Niño and decadal climate change in the North Pacific Ocean. Nat. Geosci. 3(11). 762–765.

Di Lorenzo, E., Mountain, D., Batchelder, H.P., Bond, N. and Hofmann, E.E. 2013. Advances in marine ecosystem dynamics from US GLOBEC: the horizontal-advection bottom-up forcing paradigm. Oceanogr. 26(4). 22–33.

Edwards, A.M., Haigh, R., Tallman, R., Swain, D.P., Carruthers, T.R., Cleary, J.S., Stenson, G. and Doniol-Valcroze, T. 2017. Proceedings of the Technical Expertise in Stock Assessment (TESA) National Workshop on 'Incorporating an ecosystem approach into single-species stock assessments', 21-25 November 2016, Nanaimo, British Columbia. Can. Tech. Rep. Fish. Aquat. Sci. 3213. vi + 53 p.

Fu, C., Olsen, N., Taylor, N., Grüss, A., Batten, S., Liu, H., Verley, P. and Shin, Y.J. 2017. Spatial and temporal dynamics of predator-prey species interactions off western Canada. ICES J. Mar. Sci. 74(8). 2107-2119.

Haigh, R., Starr, P.J., Edwards, A.M., King, J.R. and Lecomte, J.B. 2018. Stock assessment for Pacific Ocean Perch (*Sebastes alutus*) in Queen Charlotte Sound, British Columbia in 2017. DFO Can. Sci. Advis. Sec. Res. Doc. 2018/038: v + 227 p.

King, J.R., Mcfarlane, G.A. and Beamish, R.J. 2000. Decadal-scale patterns in the relative year class success of sablefish (*Anoplopoma fimbria*). Fish. Oceanogr. 9(1). 62–70.

Love, M.S., Yoklavich, M. and Thorsteinson, L. 2002. The Rockfishes of the Northeast Pacific. University of California Press, Berkeley and Los Angeles, California.

Mantua, N., Hare, S., Zhang, Y., Wallace, J. and Francis, R. 1997. A Pacific interdecadal climate oscillation with impacts on salmon production. Bull. Am. Meteorol. Soc. 78(6). 1069–1080.

Methot, R.D., Wetzel, C.R., Taylor, I.G., Doering, K.L. and Johnson, K.F. 2021. Stock Synthesis: User Manual Version 3.30.18. Tech. rep., NOAA Fisheries, Seattle WA, USA, October 1, 2021.

Newman, M., Compo, G.P. and Alexander, M.A. 2003. ENSO-forced variability of the Pacific Decadal Oscillation. J. Clim. 16(23). 3853–3857.

Preikshot, D. 2005. Data sources and derivation of parameters for generalised Northeast Pacific Ocean Ecopath with Ecosim models. UBC Fish. Cent. Res. Rep. 13(1). 179–237.

Schroeder, I.D., Santora, J.A., Bograd, S.J., Hazen, E.L., Sakuma, K.M., Moore, A.M., Edwards, C.A., Wells, B.K. and Field, J.C. 2019. Source water variability as a driver of rockfish recruitment in the California Current Ecosystem: implications for climate change and fisheries management. Can. J. Fish. Aquat. Sci. 76(6). 950–960.

Zhang, Y., Wallace, J.M. and Battisti, D.S. 1997. ENSO-like interdecadal variability: 1900-93. J. Clim. 10(5). 1004–1020.